Université du Québec

INRS Institut national de la recherche scientifique

Centre Armand-Frappier Santé Biotechnologie

MODIFICATIONS MORPHOLOGIQUES ET METABOLIQUES DU RETICULUM ENDOPLASMIQUE ET DES MITOCHONDRIES PAR LES *FLAVIVIRUS*

Par

Wesley Freppel

Thèse présentée pour l'obtention

du grade de Philosophiae Doctor (Ph.D.) en sciences de virologie et immunologie

Jury d'évaluation

Président du jury et examinateur interne	Patrick Labonté INRS – Centre Armand-Frappier Santé Biotechnologie
Examinateur externe	Gilles Gouspillou Université du Québec à Montréal Département des Sciences de l'activité physique
Examinateur interne	Benoit Barbeau Université du Québec à Montréal Département des Sciences biologiques
Directeur de recherche	Laurent Chatel-Chaix INRS – Centre Armand-Frappier Santé Biotechnologie

« Best thing I can do is go,
experience life and live my dream»
Josh Sirlin

« Freeeeeddooooommmm »
William Wallace, Braveheart, 1995

REMERCIEMENTS

J’exprime en premier lieu mes sincères reconnaissances à mon directeur de thèse, Laurent Chatel-Chaix qui m’a offert l’opportunité de réaliser ce doctorat. Alors que mes espoirs de trouver un sujet de thèse en maladies infectieuses après deux ans de recherche commençaient à s’effondrer, j’ai eu la surprise en octobre 2016 d’avoir été choisi pour travailler sur ce projet. Cette nouvelle changea ma vie bien que je n’eusse à ce moment-là aucune expertise en virologie. Je le remercie profondément de m’avoir offert sa confiance, son soutien, sa gentillesse, ses connaissances et de m’avoir ouvert la porte à ce fameux et incroyable monde de la virologie. Malgré des moments difficiles et de doutes, Laurent a toujours su trouver les mots pour remotiver l’équipe et mettre en avant nos points forts en recherche. J’espère vraiment être digne de l’enseignement qu’il m’a apporté.

Je remercie le professeur Patrick Labonté, président et examinateur interne, et les professeurs Gilles Gouspillou et Benoit Barbeau, examinateurs externes d’avoir accepté d’être membres de mon jury de thèse et ainsi de prendre part à la finalisation de cette longue aventure.

Je remercie également tous les professeurs de l’INRS pour leurs conseils, leurs réponses aux questions et leurs encadrements qui ont participé à ma formation durant mon doctorat. Je remercie Jessy Tremblay, responsable de la plateforme de microscopie en qui j’ai une confiance absolue dans la prise et traitement d’images au microscope confocal et qui m’a plus d’une fois aidé à résoudre mes problèmes de microscopie. Je remercie également Michel Courcelles, notre bibliothécaire qui, toujours de bonne humeur, nous connait tous par nos prénoms et projets.

Cette thèse aurait été beaucoup plus difficile sans le financement des organismes subventionnaires. Je remercie les Instituts de Recherche en Santé du Canada pour les fonds de recherche accordés à mon directeur de thèse qui ont principalement financer le projet. Je remercie également les Fonds de Recherche du Québec en Santé et la fondation Armand-Frappier pour les bourses doctorales.

Evidemment, je remercie tous les membres du laboratoire pour leur soutien et amitié tout le long de ce doctorat. Anaïs et Clément, on a fondé le laboratoire ensemble et je vous dois énormément pour la réussite de ce projet. Anaïs, ce fut un plaisir de t’avoir formé à ton arrivée en tant que stagiaire. Tu as rapidement évolué en passant par une maitrise puis en étant assistante de recherche et je ne pourrais jamais te remercier assez pour tout ton travail dévoué, efficace et de qualité. Je te dois ce doctorat et tu en mérites bien la moitié. Ce fut également un plaisir d’être ta calculatrice humaine et de résoudre tes problèmes de dilution. Clément, mon frère de thèse. Sans

toi, tes conneries, tes blagues, tes fotes d'aurtaugraf, mes journées auraient souvent été plus sombres avec les hivers interminables du Québec. Merci pour ta bonne humeur peu importe les moments difficiles. Merci pour tout ton travail apporté en aide à mon projet. Merci pour ton soutien psychologique et nos longues conversations lors de tes pauses cigarettes. Cette image, c'était nous trois à nos début en 2017, et j'en garde un excellent souvenir.

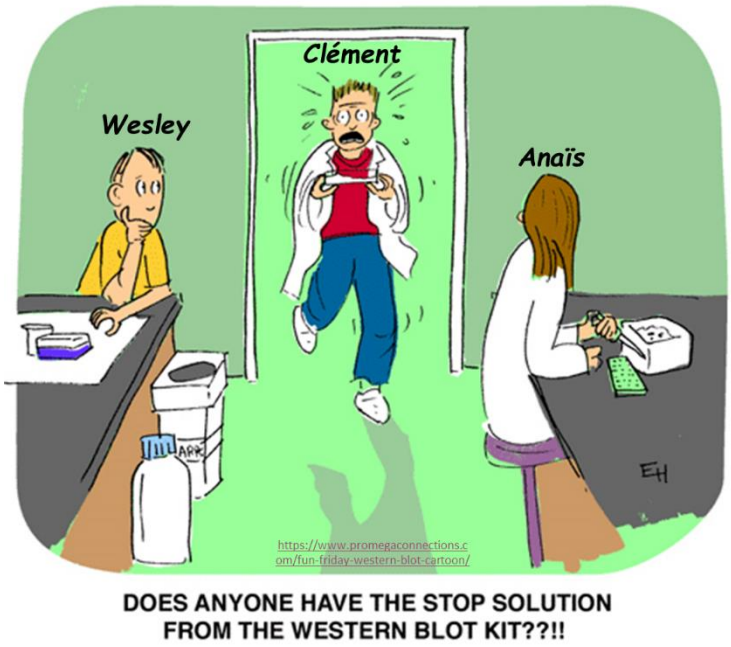

Aïcha, tu es peut-être arrivée plus tard, mais tu t'es rapidement intégrée à notre petite équipe en apportant une petite touche exotique au labo, je parle évidement de ton poisson zèbre. Merci pour toutes nos longues conversations à propos de tout et de rien. Merci pour tes biscuits après une journée longue et frustrante. Merci pour tes conseils dans les moments difficiles. Merci pour nos petits échanges bourgeois en anglais, « shall we ? ». Et bravo d'avoir gagné tous les prix lors des congrès même quand il n'y en a pas à gagner ! Laisses-en pour les autres aussi voyons. Je remercie également tous les autres membres du labo qui ont agrandi l'équipe durant ces dernières années, Nicolas, Behnam, Alexandrine, Marie, Hélène, Geneviève, Viviana, Olus, et tous les stagiaires.

Je remercie les membres du laboratoire de Ian-Gaël avec qui on a partagé le laboratoire et le bureau étudiant. Paulin, Claudia I, Gaëlle, chacun après l'autre, vous avez partagé le bureau derrière moi et je vous remercie pour les discussions et les blagues durant nos après-midi fainéantes. Merci également à Claudia II, pour son aide et ses conseils au sein du laboratoire.

Le PRF et ses horizons par ordre alphabétique, Adeline, Alex, Bélinda (+ Francis et Liam la croquette), Gab, Guillaume, Josianne, Juliette (+ William), Laurie (+ Guillaume), Léa, Léna (+ Georges), Melany, Mustapha, Richard, Rita, Vincent, Zoé et tous ceux que je n'ai pas cité, comment résumer 5 ans avec vous ? Merci pour tous les moments ensemble, les discussions de 3h sur des pauses lunch de 1h ou entre des manipes, les soirées belote, les après-midi/soirs au parc, pétanque, les rando, les chalets, les resto, les ciné, les congrès, et j'en passe. Merci d'avoir partagé vos lunch ou au moins de m'avoir laissé goûter vos petits plats préparés soigneusement. Mais surtout, merci d'avoir été présent lorsque j'en avais le plus besoin après mon accident. Merci d'avoir cuisiné, lavé la vaisselle, fait le ménage et l'épicerie durant ma période de rétablissement. C'était un moment vraiment difficile que j'ai pu surmonter facilement grâce à vous tous et votre soutien. Le Québec était une aventure incroyable et je suis heureux de l'avoir fait avec vous tous, ma famille québécoise. Je termine ce doctorat et quitte le Québec avec beaucoup de magnifiques souvenirs.

Je remercie également toutes les personnes que j'ai croisé au Québec que ce soit à l'institut ou non avec qui j'ai passé d'incroyables et d'inoubliables moments.

Pour terminer, je remercie mes parents, mes sœurs, mon frère, toute ma famille et mes amis de France et d'ailleurs qui ont su me soutenir et m'encourager pendant les moments difficiles avant et après mon départ pour accomplir ce doctorat.

RÉSUMÉ

En l'absence de traitements ou de vaccins, les infections par les virus de la dengue (VDEN) et Zika (VZIK), constituent un enjeu majeur de santé publique dans le monde. Lors de l'infection, les VDEN et VZIK remodèlent le réticulum endoplasmique (ER) pour former des usines de réplication virale (URv) qui incluent les convolutions de membrane (CM). De plus, ils induisent l'élongation des mitochondries (par NS4B pour VDEN) en faveur de la réplication virale suggérant une modulation des fonctions mitochondriales. Des observations antérieures ont identifié des contacts physiques entre les mitochondries et les CM en même temps qu'une diminution des contacts de l'interface réticulo-mitochondriale (IRM). Par conséquent, nous avons étendu nos recherches au niveau moléculaire, par comment les VDEN et VZIK exploitent l'IRM pour leur réplication, et si cela modifie le métabolisme respiratoire mitochondriale et l'apoptose.

Des analyses en microscopie électronique à transmission démontrent que les VDEN et VZIK altèrent l'IRM. Celle-ci repose sur plusieurs interactions entre des protéines situées à la surface des deux organites, telles que PTPIP51-VAPB, SYNJ2BP-RRBP1 ou VDAC1-IP3R1. L'infection par les VDEN et VZIK induit une altération globale de ces interactions. Simultanément, l'infection virale altère le profil d'expression de RRBP1 et SYNJ2BP, suggérant qu'ils ciblent spécifiquement cette interaction protéine-protéine. Par ailleurs, l'inhibition de l'expression des protéines de l'IRM augmente la réplication virale, ce qui soutient que l'IRM est altérée au bénéfice de la réplication virale. De plus, l'infection par VDEN/VZIK et l'expression de NS4B modulent de manière significative la phosphorylation oxydative mitochondriale. Nos analyses métabolomiques et mitoprotéomiques révèle que cela est corrélé à une diminution de l'abondance de plusieurs métabolites du cycle de Krebs et à des changements dans la stœchiométrie des protéines de la chaîne de transport d'électrons. Par ailleurs, la déstabilisation de l'IRM par diminution de l'expression de protéines lors de l'infection virale entraîne une diminution drastique de l'apoptose, démontrant l'importance de l'altération de l'IRM par VDEN et VZIK pour leur réplication.

Dans l'ensemble, nos données suggèrent fortement que les perturbations morphologiques des mitochondries par les VDEN et VZIK modulent leur activité métabolique via NS4B pour répondre aux besoins énergétiques du cycle de réplication virale. Cette étude soutient également un modèle selon lequel ces virus perturbent l'IRM afin de s'approprier des facteurs spécifiques de l'hôte nécessaires à la morphogenèse des CM et de diminuer ou retarder des mécanismes cellulaires importants défavorables au cycle de vie des *Flavivirus.*

Mots-clés : Virus de la dengue, virus Zika, réticulum endoplasmique, mitochondrie, métabolisme.

ABSTRACT

With no available treatments or vaccines, infections with dengue virus (DENV) or Zika virus (ZIKV constitute an important public health concern worldwide. During infection, DENV and ZIKV remodel the endoplasmic reticulum (ER) to form viral replication organelles (vRO) that include convoluted membranes (CM). In addition, these pathogens induce the elongation of mitochondria (via NS4B for DENV) in favour of viral replication suggesting a modulation of mitochondria functions. Previous observations identified physical contacts between mitochondria and CM concomitantly with a decrease of ER-mitochondria contacts (ERMC). In this project, we have extended our study to investigate at the molecular level how DENV and ZIKV take advantage of ERMC structures to their replication and whether this modulates the respiratory metabolism and apoptosis.

Extensive transmission electron microscopy-based analysis demonstrated that both DENV and ZIKV alter ERMCs. Stable ERMCs rely on specialized tethering protein complexes located at the surface of both organelles, such as VAPB-PTPIP51, RRBP1-SYNJ2BP and IP3R1-VDAC1. DENV and ZIKV infection induced an overall alteration of ERMCs protein-protein interactions. Interestingly, flaviviral infection altered the expression profile of both RRBP1 and SYNJ2BP, suggesting that they specifically target this tethering complex. Importantly, expression knockdown of ERMC proteins increased virus replication, supporting that ERMCs are altered for the benefit of viral replication. Furthermore, DENV or ZIKV infection as well as NS4B expression markedly modulated mitochondrial oxygen consumption rate. Our metabolomic and mitoproteomic analyses revealed that this correlated with a decrease in the abundance of several metabolites of the Krebs cycle and with changes in the stoichiometry of the proteins of the electron transport chain. Most importantly, ERMC destabilization by protein knockdown showed a decrease in virus-induced apoptosis demonstrating the importance of ERMC alteration by DENV and ZIKV for a sustained replication.

Overall, our data strongly suggest that the morphological perturbations of mitochondria by DENV and ZIKV modulate their metabolic activity via NS4B to sustain the energetic needs of the viral replication cycle. This study further supports a model in which these viruses perturb ERMCs to hijack specific host factors that are required for CM morphogenesis and decrease or delay important cellular mechanisms unfavourable for flaviviruses life cycle.

Keywords : Dengue virus, Zika virus, endoplasmic reticulum, mitochondria, metabolism

TABLE DES MATIÈRES

LISTE DES FIGURES

LISTE DES TABLEAUX

LISTE DES ABRÉVIATIONS

25HC :	25-hydroxycholesterol
ADE :	facilitation de l'infection par des anticorps
ADN :	acide désoxyribonucléique
ADNm :	ADN mitochondrial
ARN :	acide ribonucléique *(RNA : ribonucleic acid)*
ARNdb :	ARN double brin *(dsRNA : double-strand RNA)*
ARNi :	ARN d'interférence
ARNm :	ARN messager *(mRNA : messenger RNA)*
ARNsb+ :	ARN simple brin à polarité positive *(dsRNA+ : double-strand positive RNA)*
ARNsf :	ARN sous-génomique flaviviral
ARNv :	ARN viral *(vRNA : viral RNA)*
ATP :	adénosine triphosphate
Ca^{2+} :	calcium
CCCP :	carbonyl cyanide m-chlorophenylhydrazone
cGAS :	cyclic GMP-AMP synthase
CL :	cardiolipine
CM :	convolution de membrane
CMV :	cytomégalovirus
CNP :	cellules neuronales progénitrices
CoQ_{10} :	coenzyme Q_{10}
CTE :	chaine de transport d'électrons *(ETC : electron transport chain)*
D1 et D2 :	domaines ATPase de VCP
DAPI :	4'6-diamidino-2-phenylindole
DMEM :	dulbecco's modified eagle medium

DRP1 :	dynamin-related protein 1
EIM :	espace intermembranaire
ERAD :	dégradation associé au réticulum endoplasmique
ERMC :	ER-mitochondria contacts (voir IRM)
ERMES :	ER-mitochondria encounter structure
FIS1 :	mitochondrial fission 1 protein
GL :	gouttelette lipidique
GRP75 :	glucose-regulated protein 75
GTPase :	guanosyltransférase
HA :	hémagglutinine
Huh :	lignée cellulaire d'hépatocarcinome humain
IFN :	interféron
IP3R :	inositol 1,4,5-triphosphate
IRF3 :	interferon regulatory factor 3
IRM :	interface réticulo-mitochondriale
LATV :	vaccin tétravalent chimérique vivant atténué
MAD :	dégradation associée aux mitochondries
MAVS :	mitochondrial antiviral-signaling protein
MCU :	mitochondrial calcium uniporter
MDA5 :	melanoma differentiation-associated protein 5
MEM :	membrane externe mitochondriale
MFF :	mitochondrial fission factor
MFN1/2 :	mitofusines 1 et 2
MID49 :	mitochondrial dynamics protein 49
MID51 :	mitochondrial dynamics protein 51
MIM :	membrane interne mitochondriale

MOI :	multiplicité d'infection (*multiplicity of infection)*
MTase :	méthyltransférase
mTOR :	mammalian target of rapamycin
NS :	protéines non structurales
NTPase :	nucléotide triphosphatase
OPA1 :	optic atrophy 1
ORF :	cadre de lecture
OST :	complexe oligosaccharyltransférase
OXPHOS :	phosphorylation oxydative ou phosphorylation oxydative
PA :	acide phosphatidique
PABP :	poly-A binding protein
PBS :	Tampon Phosphate Salin
PC :	phosphatidylcholine
PCR :	Réaction en chaine par polymérase
PE :	phosphatidyléthanolamine
PEI :	Polyéthylénimine
PERK :	protéine réticulum endoplasmique kinase-like 1
PG :	phoshatidylglycérol
PI :	phosphatidylinositol
PI3K :	phosphoinositide 3-kinase
PINK1 :	protéine PTEN-induced putative kinase 1
PKB :	protein kinase B
PLA :	essai de proximité par ligation *(proximity ligation assay)*
PLXD :	interface Peroxysome – Gouttelette lipidique
PS :	phosphatidylsérine
PTPIP51 :	protein tyrosine phosphatase-interacting protein 51

PV :	paquets vésiculaires
RdRp :	ARN polymérase ARN-dépendante
RE :	reticulum endoplasmique
RIG-I :	retinoic acid-inducible gene I
Rluc :	renilla luciferase
ROS :	dérivés réactifs d'oxygène *(Reactive oxygen specie)*
RRBP1 :	ribosome binding protein
RTPase :	ARN-triphosphatase
SDHA/B/C/D :	complexe succinate déhydrogénase sous unités A, B, C ou D
SDS :	dodécylsulfate de Sodium *(Sodium dodecyl sulfate)*
shRNA :	petit ARN en épingle à cheveux *(short hairpin RNA)*
SNC :	système nerveux centrale
STING :	protéine stimulatrice des gènes d'interféron
SV :	sac de virus
SYNJ2BP :	synaptojanin 2 binding protein
T7 pol :	polymérase T7
TBK1 :	TANK-binding kinase 1
TCA :	cycle de Krebs ou de l'acide citrique
TIM :	translocase inner membrane
TLR :	récepteurs de type Toll
TNF-α :	tumor necrosis factor
TOM :	translocase outer membrane
TRIM25 :	tripartite motif-containing protein 25
URv :	usines de réplication virale *(vRO : viral replication organelle)*
UTR :	extrémités des régions 3' et 5' non traduites
VAPB :	vesicle-associated membrane protein-associated protein B

VCMH :	cytomégalovirus humain
VCP :	valosin-containing protein/97
VDAC1 :	voltage-dependant annion channel 1
VDEN :	virus de la dengue *(DENV : Dengue virus)*
VEJ :	virus de l'encéphalite japonaise
VFJ :	virus de la fièvre jaune
VHC :	virus de l'hépatite C
VMET :	virus de la méningoencéphalite à tique
VNO :	virus du Nil occidental
VZIK :	virus Zika
WT :	souche sauvage *(Wild-Type)*
YFV-17D :	vaccin 17D du virus de la fièvre jaune

1 INTRODUCTION GENERALE

1.1 Les *Flavivirus*

« Dans le règne des virus, la famille des *Flaviviridae* est un groupe de virus enveloppés à ARN simple brin de polarité positive qui englobe beaucoup de pathogènes causants des maladies graves chez l'humain. Cette famille est sous-divisée en quatre genres, soit *Flavivirus*, *Hepacivirus*, *Pestivirus* et *Pegivirus*. Au cours des dernières décennies, les deux premiers groupes ont été plus étudiés que les deux autres puisqu'ils incluent des virus pathogènes pour les humains. Les infections par les *Flavivirus* tels que le virus de la dengue (VDEN) le virus Zika (VZIK), le virus du Nil occidental (VNO), le virus de la fièvre jaune (VFJ), le virus de la méningoencéphalite à tique (VMET) ou encore le virus de l'encéphalite japonaise (VEJ) représentent un enjeu majeur de santé publique dans le monde. » (Freppel *et al.*, 2022). Cette thèse discutera des *Flavivirus* en général avec une préférence pour le VZIK et le VDEN, les deux *Flavivirus* qui ont été étudiés lors de mon doctorat.

1.1.1 Epidémiologie et histoire

Les infections par le VDEN ne sont pas nouvelles puisque des traces de premières infections ont été découvertes en Asie, Afrique et en Amérique du Nord datant du 18ème siècle (Guzman *et al.*, 2010). Cependant, ce n'est seulement qu'à partir des années quarante que différents sérotypes du VDEN ont réellement été découvert et on en dénombre actuellement quatre (Holmes *et al.*, 2003). Le VDEN1 a été isolé pour la première fois en 1943 au Japon et en Polynésie Française, le VDEN2 en 1944 en Indonésie et Papouasie-Nouvelle-Guinée, le VDEN3 et VDEN4 en 1953 respectivement aux Philippines et Thaïlande (Hotta, 1952). Suivant la globalisation et l'urbanisation au cours du dernier siècle, le VDEN a rapidement conquis les quatre coins du globe emporté par le déplacement de son vecteur principal qui est le moustique *Aedes* et est maintenant principalement retrouvé dans les régions tropicales (figure 1.1) (Gubler, 2011; Mousson *et al.*, 2005; Weaver, 2013). Avec une estimation aujourd'hui de plus de 390 millions de personnes infectées et de 22,000 décès par an (Bhatt *et al.*, 2013; Shepard *et al.*, 2016), le VDEN est responsable de la maladie arbovirale la plus prévalente dans le monde.

Beaucoup plus récent que le VDEN, le VZIK est un virus découvert par l'écossais Alexander Haddow et isolé d'un macaque rhésus (numéro 766) en 1947 dans la forêt Ziika (ou Zika) en Ouganda (Dick *et al.*, 1952). La forêt Zika est connue pour être un nid à maladies infectieuses par son environnement favorable. En effet, on y retrouve une faune dangereuse mais surtout

une flore tropicale abritant plus de 70 espèces de moustiques qui regroupent plus d'une douzaine de pathogènes dangereux pour l'humain (Vidal, 2016). Cependant, ce n'est qu'en 1952 que ce virus a été caractérisé comme une nouvelle espèce virale connu aujourd'hui comme la souche ancestrale ou africaine, la souche MR766 (Dick *et al.*, 1952).

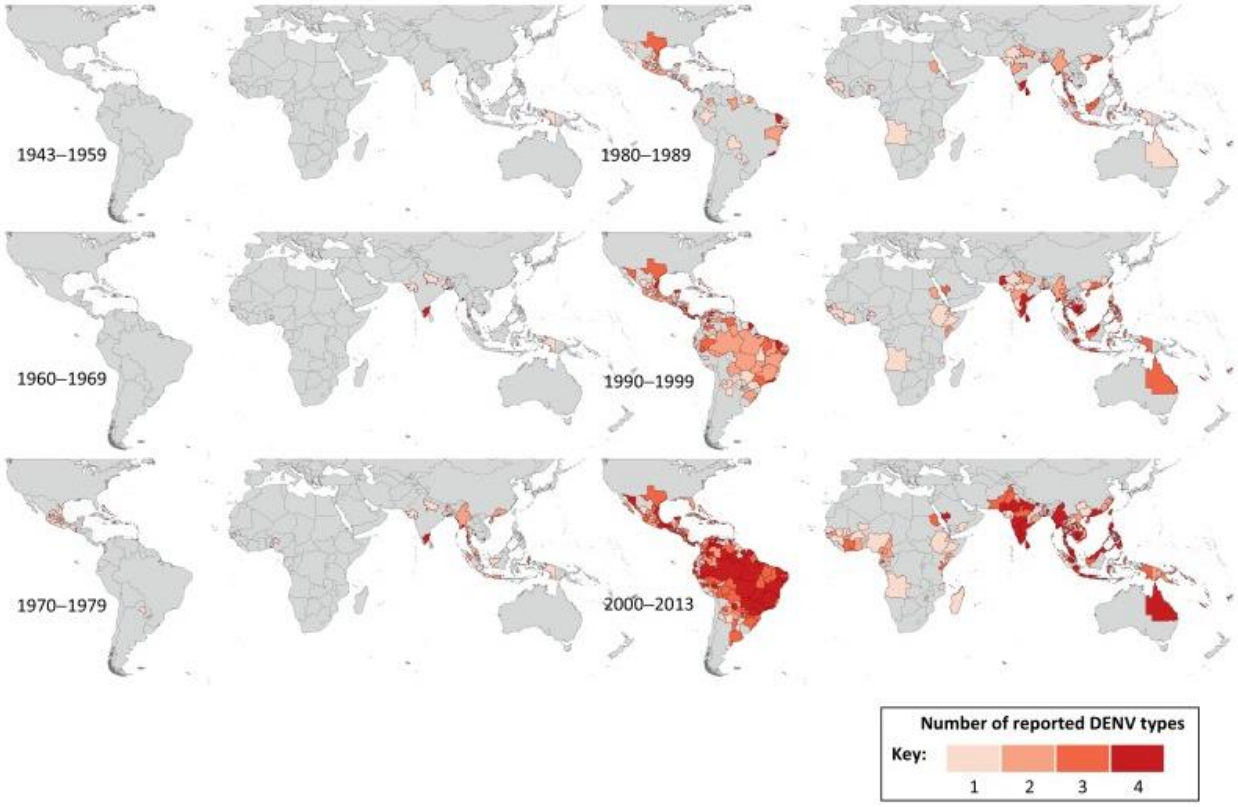

Figure 1.1 Codistribution des quatre VDEN au cours du temps

Rose pâle : un seul type de VDEN recensé ; rose foncé : 2 types de VDEN recensés ; rouge pâle : 3 types de VDEN recensés ; rouge foncé : 4 types de VDEN recensés. (Messina *et al.*, 2014)

La première identification du virus hors Afrique a été découverte en Malaisie en 1966 chez le moustique *Aedes* (Marchette *et al.*, 1969). Issu de la souche africaine, la nouvelle souche asiatique possédant moins de 4% de différence en séquences d'amino-acides s'est ensuite répandue à travers l'Asie pendant des décennies (figure 1.2). Ce n'est seulement qu'au début des années 2000 que le VZIK a beaucoup attiré l'attention lors de son émergence soudaine à travers le globe (Haddow *et al.*, 2012; Lanciotti *et al.*, 2016). En effet, la souche asiatique est responsable de plusieurs épidémies telles que sur les îles Yap en Micronésie en 2007, en Polynésie française en 2013, en Nouvelle Calédonie en 2014 et depuis 2015 sur le continent

américain avec plus d'un million de cas détectés (Chang *et al.*, 2016; Liu *et al.*, 2019). En date de décembre 2022, le VZIK est présent dans 89 pays (World Health Organisation, 2022).

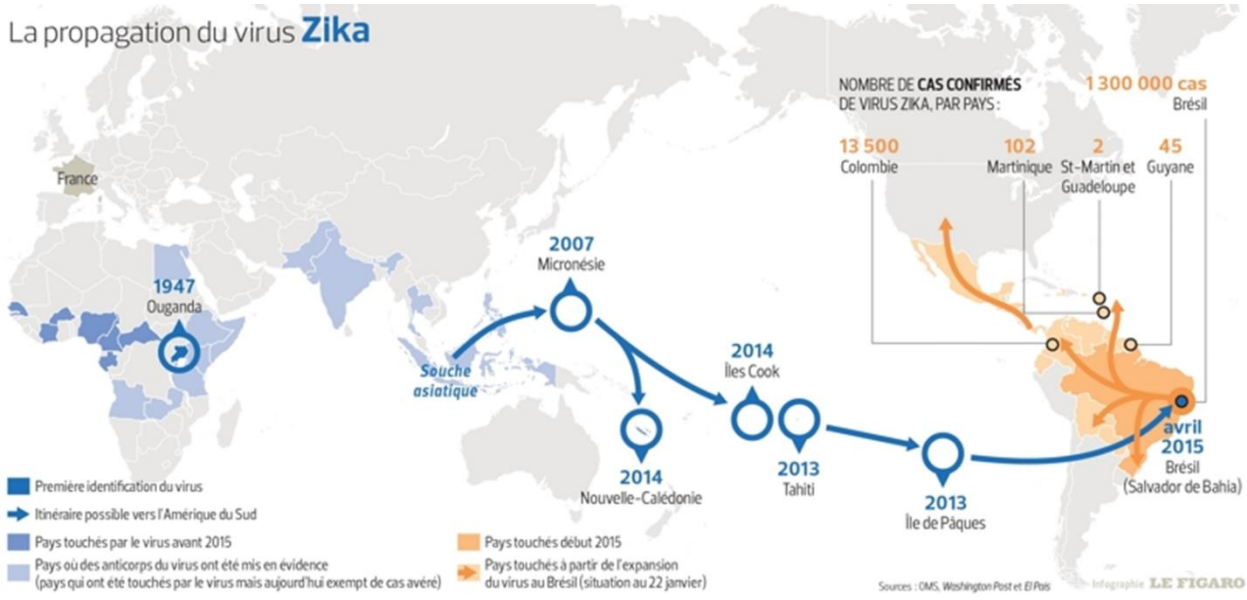

Figure 1.2 Évolution et propagation du VZIK

Les flèches bleues indiquent la propagation du VZIK au cours du temps à travers le globe. Les flèches oranges indiquent la propagation du VZIK après son éclosion en Amérique. (Roy, 2016)

1.1.2 Transmission

1.1.2.1 Vectorielle

Les *Flavivirus* responsables d'infections des mammifères peuvent être classés en deux catégories, ceux transmis par piqûre de moustique de type *Aedes* pour le VDEN, le VZIK et le VFJ, ou de type *Culex* pour le VNO et le VEJ (Pandit *et al.*, 2018), et ceux transmis par morsure de tique de type *Ixodes* pour le VMET ou d'autres *Flavivirus* plus rares tels que le virus Powassan (Grabowski *et al.*, 2017; Pierson *et al.*, 2013). Puisque ces virus sont essentiellement transmis par vecteurs de type insecte, les *Flavivirus* font partie des *Arbovirus,* mot issue de la combinaison du terme anglais « arthropod-borne virus », c'est-à-dire les virus ayant pour vecteur un insecte.

Dans notre cas, le VDEN et le VZIK sont transmis par deux espèces différentes d'*Aedes.* En effet l'*Aedes albopictus (*connu sous le nom de moustique tigre dans un langage familier*)* et l'*Aedes aegypti* sont les deux vecteurs clés de la transmission de ces deux virus. Principalement présent aux zones tropicales (figure 1.3), le moustique *A. albopictus* migre de plus en plus vers

les pôles à cause du réchauffement climatique que la Terre subit depuis quelques décennies dû à l'activité humaine (Iwamura *et al.*, 2020). En effet, l'Europe fait face depuis quelques années à l'apparition de premiers cas autochtones d'infections aux *Flavivirus* (Brady *et al.*, 2019a; La Ruche *et al.*, 2010; Lazzarini *et al.*, 2020). Par ailleurs, ce moustique transporte non seulement les VDEN et VZIK (Effler *et al.*, 2005; Ramchurn *et al.*, 2009), mais également d'autres virus tel que le virus Chikungunya, un *Alphavirus* (Paupy *et al.*, 2009). De plus, des études expérimentales ont démontré la forte capacité du moustique à pouvoir transporter une vingtaine d'autres arbovirus, tels que le VFJ, le VEJ ou encore le VNO pour n'en citer que quelques-uns (Medlock *et al.*, 2015; Schaffner *et al.*, 2013).

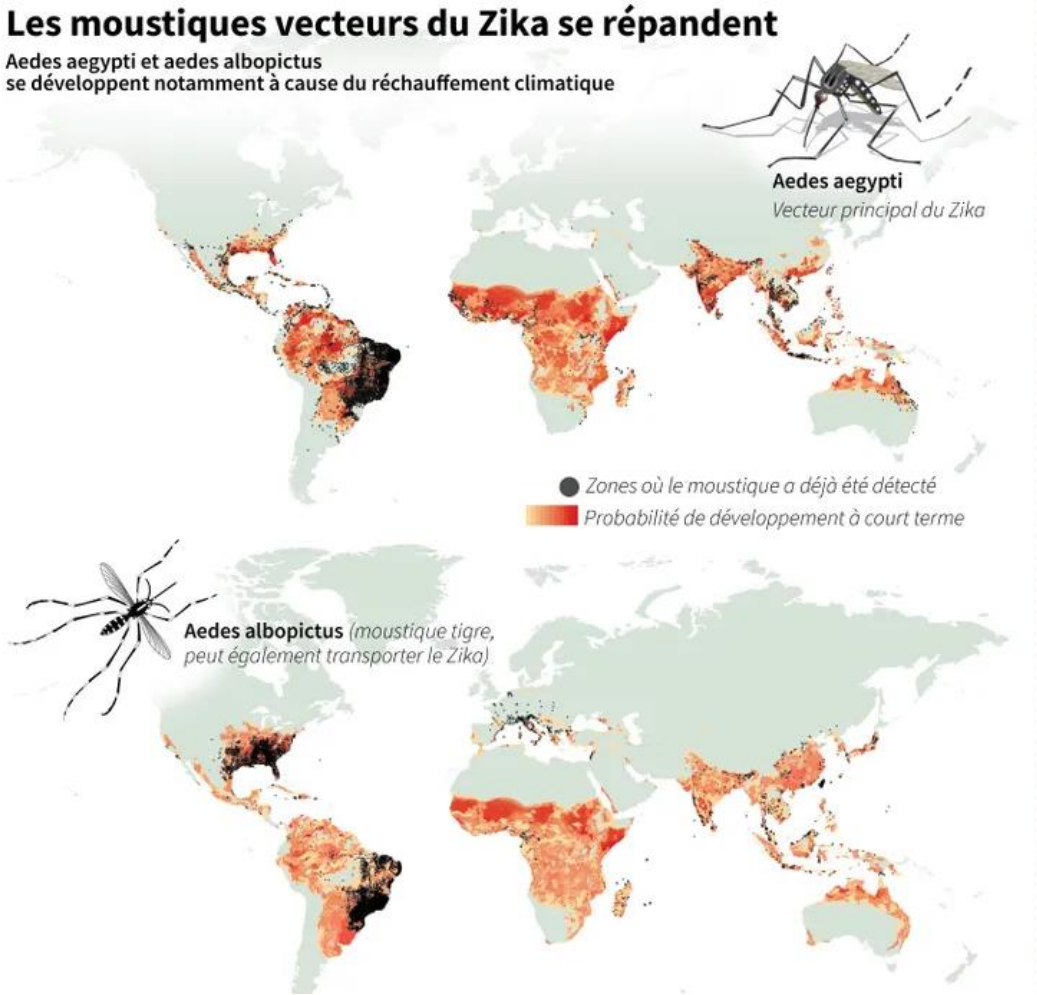

Figure 1.3 Répartition globales des moustiques Aedes

Représentation de la distribution des deux types de moustique *Aedes* en fonction de leur recensement et de la probabilité de leur apparition dépendante de l'environnement. Modifié de (Kraemer *et al.*, 2015)

Dans un moustique femelle infecté, le VDEN et le VZIK vont se répliquer dans l'intestin, lieu de digestion du sang préalablement infecté. Les virus vont ensuite atteindre des tissus secondaires tels que les glandes salivaires, lieu de stockage des virus et porte de sortie lors de la transmission à l'humain. La période d'incubation extrinsèque, c'est-à-dire la période entre l'ingestion du virus par le moustique et la transmission du virus à l'humain lors d'une piqûre est d'environ de 8 à 12 jours si les conditions climatiques avoisinent les 28°C (Tjaden *et al.*, 2013; Watts *et al.*, 1987). Une fois infecté, le moustique ne guérira jamais du virus et le portera à vie (durée de vie d'environ deux semaines).

1.1.2.2 Non-vectorielle

Allant à l'encontre de nos précédentes connaissances des *Flavivirus* et leur transmission dépendante d'un vecteur arthropode, le VZIK est également capable d'être transmis par voie interhumaine ajoutant un enjeu de santé publique plus important encore. Ceci implique la voie sexuelle, la voie congénitale ou la voie sanguine.

En effet, depuis son éclosion récente, et l'apparition de microcéphalie chez les nouveau-nés (discuté dans la section 1.1.3.1), de nombreuses études dirigées vers la reproduction ont montré de nombreux cas de transmission sexuelle (Kim *et al.*, 2018). Notamment, il semblerait que les testicules et le mucus vaginale serviraient de réservoir expliquant ainsi la charge virale élevée retrouvée dans le sperme ou les secrétions vaginales (Atkinson *et al.*, 2016; Tang *et al.*, 2016b).

La transmission congénitale ou verticale, c'est-à-dire de la mère au fœtus pendant la grossesse a été démontrée par analyse du liquide amniotique, de l'urine et du sérum des mères enceintes dont le fœtus présentait des malformations cérébrales (Tabata *et al.*, 2018). En effet, la présence d'ARN viral (ARNv) suggère fortement la capacité du VZIK à traverser la barrière placentaire et à infecter le fœtus (Brasil *et al.*, 2016). De plus, malgré qu'aucun cas de transmission n'ait été découvert par l'allaitement de l'enfant, la présence élevé d'ARNv dans le lait maternel ouvre la porte à une possible voie de transmission de la mère à l'enfant (Dupont-Rouzeyrol *et al.*, 2016; Mann *et al.*, 2018).

Bien que la possibilité d'une contamination au VZIK soit élevée due à une virémie asymptomatique (Beau *et al.*, 2020), Il n'y a à ce jour aucune contamination recensée par transfusion sanguine interhumaine. Cependant, le Brésil a confirmé le 16 janvier 2016 avoir eu deux cas de contamination après une transfusion interhumaine de plaquette (Motta *et al.*, 2016).

Ces données confirment que les transferts sanguins doivent être supervisés, améliorés et contrôlés pour éviter d'éventuels accidents de contamination.

1.1.3 Sémiologie

1.1.3.1 Manifestations cliniques

Suivant l'infection de l'humain par piqûre de moustique, le VDEN infecte premièrement les cellules épidermiques kératinocytes puis les cellules de Langherans (Palucka, 2000). Les cellules de Langherans vont alors se déplacer avec le virus dans les nœuds lymphatiques pour présenter les antigènes du VDEN aux cellules immunitaires tels que les macrophages ou les monocytes. Malheureusement, au lieu de neutraliser le VDEN en le ciblant, les macrophages et les monocytes vont également être infectés par le VDEN et répandre ainsi le virus à travers l'organisme. Les premiers symptômes se déclenchent généralement après 3 à 10 jours d'incubation et durent environ 5 à 7 jours dépendamment de la gravité de la maladie (World Health Organization, 2016).

Plusieurs manifestations cliniques ont été répertoriées dont notamment la plus fréquente (environ 75%) étant une fièvre de type grippale appelée fièvre classique de la dengue. Cette fièvre (40^{o}C) est souvent accompagnée de maux de tête, douleurs articulaires et musculaires, de nausées, de vomissements et d'éruptions cutanées (Whitehorn *et al.*, 2011). Bien que 25% environ des infections présentent des symptômes pouvant être sévères, tels que la fièvre hémorragique ou le syndrome de choc, moins de 1% aboutissent au décès du patient (World Health Organization, 2022). La fièvre hémorragique (figure 1.4) est caractérisée par des hémorragies profuses, l'apparition d'une thrombocytopénie, de fuite plasmatique et de détresse respiratoire pouvant évoluer en syndrome de choc et au décès du patient.

Le VZIK est différent puisqu'il s'agît d'un virus neurotrope, c'est-à-dire qu'il infecte particulièrement les cellules du cerveau, telles que les cellules neuronales progénitrices (CNP), les astrocytes, les microglies ou encore les oligodendrocytes (Gaburro *et al.*, 2018; Wen *et al.*, 2017). Des études ont également montré que le VZIK infecte différents autres types cellulaires appartenant par exemple au placenta (cellules Hofbauer, trophoblastes, cellules endothéliales fœtal), organes reproducteurs ou encore les fluides corporels (Miner *et al.*, 2017). Les mécanismes par lesquels le VZIK provoque des complications neurologiques sont encore peu connus. En revanche, nous savons que le VZIK interfère dans la myélinogénèse des neurones pouvant alors provoquer de graves séquelles (Schultz *et al.*, 2021). Par exemple chez l'adulte,

le syndrome de Guillain-Barré est caractérisé par la dégradation progressive des gaines de myéline enveloppant les axones (van den Berg *et al.*, 2014). À ce jour, quelques autres complications neurologiques ont été rapportées avec une infection par le VZIK, tels qu'une méningite encéphalite ou des symptômes neuropsychiatriques (Carteaux *et al.*, 2016; da Silva *et al.*, 2017; Zucker *et al.*, 2017).

Chez les nouveau-nés après une transmission verticale, le VZIK est bien connu pour causer une microcéphalie, c'est-à-dire un développement anormal du cerveau associé à un retard mental et des troubles à l'apprentissage (figure 1.5) (de Araujo *et al.*, 2016; Moura da Silva *et al.*, 2016). Les chances de développer une microcéphalie sont plus grandes lors d'une infection virale pendant les deux premiers trimestres de grossesse (Brady *et al.*, 2019b). D'après les données de l'Organisation Mondiale de la Santé, le VZIK cause environ 160 microcéphalies par an (World Health Organisation, 2018). Dans ce symptôme, il a été montré que le VZIK cible les CNP, altère leur différenciation, leur prolifération et favorise leur élimination par mort cellulaire par voie apoptotique (Li *et al.*, 2016; Tang *et al.*, 2016a). Notamment, le VZIK inhibe la voie Akt-mTOR et p53, réduisant la différentiation des CNP (El Ghouzzi *et al.*, 2018; Liang *et al.*, 2016).

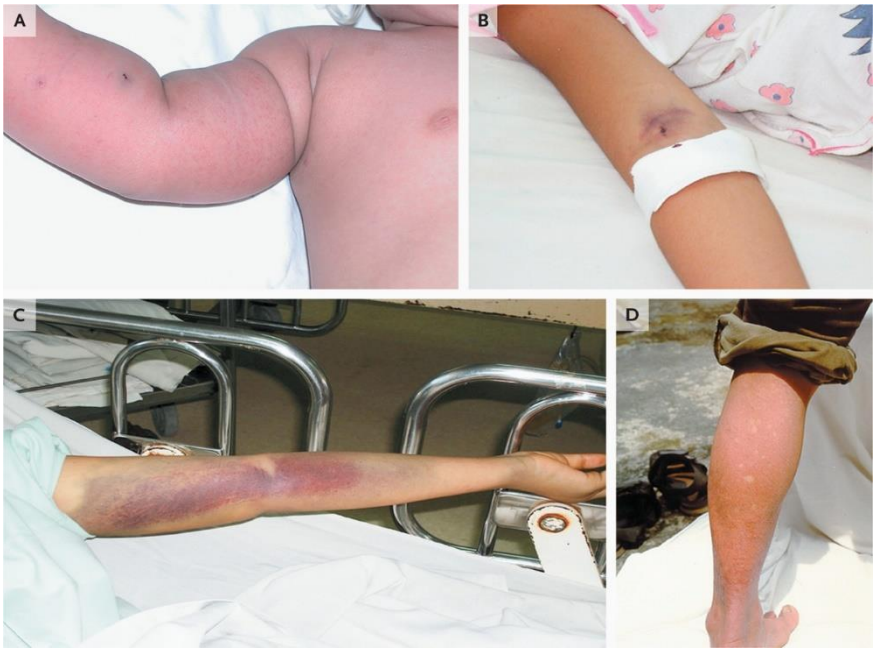

Figure 1.4 Manifestation hémorragique de l'infection par le VDEN

(A) Typique pétéchie observée chez l'enfant. (B) Saignement au niveau d'une piqure intraveineuse dû à l'infection virale. (C) Large hématome, caractéristique de l'hémorragie causée par le VDEN. (D) Éruption maculopapuleuse typique suivant une guérison chez l'adulte d'une infection non sévère au VDEN. (Simmons *et al.*, 2012)

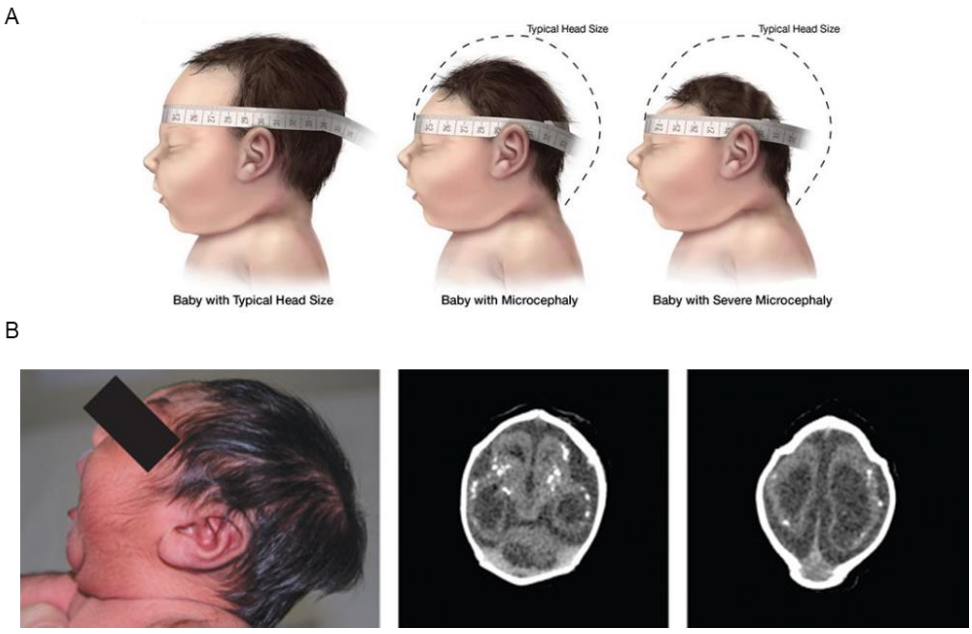

Figure 1.5 Microcéphalie chez le nouveau-né

(A) Représentation schématique de la taille du cerveau chez le nouveau-né. Gauche, cerveau normal. Milieu, microcéphalie. Droite, microcéphalie sévère. (CDC, 2020) (B) Nouveau-né avec une microcéphalie. Gauche, photo montrant le phénotype de profil. Milieu et droite, scan du cerveau montrant une réduction du volume cérébral. Modifié (de Araujo *et al.*, 2016)

1.1.3.2 Facilitation de l'infection par des anticorps

La facilitation de l'infection par des anticorps, « antibody-dependent enhancement (ADE) » est un phénomène paradoxal puisque les anticorps supposés être de puissants alliés face aux pathogènes sont dans ce cas nos ennemis en facilitant l'entrée des pathogènes dans les cellules, tel un cheval de Troie. L'ADE a été découvert pour la première fois dans les années 60-70 chez les *Flavivirus*, en étudiant des cas de dengue sévère après une deuxième infection (Halstead *et al.*, 1967).

Dans un monde idéal, les anticorps provenant de la réponse adaptative ciblent les pathogènes pour provoquer une opsonisation afin de les éliminer. Brièvement, les récepteurs Fc vont ensuite se lier aux anticorps pour activer la destruction par phagocytose médiée par les cellules phagocytaires. Cependant une ADE se produit lorsque les anticorps se liant au pathogène ne permettent pas la neutralisation de ce dernier (Halstead, 2003). Dans le cas des *Flavivirus*, les virus peuvent être assez proches génétiquement pour que les anticorps dirigés contre un *Flavivirus* en particulier puissent également reconnaitre d'autres *Flavivirus*. En revanche, malgré

la reconnaissance, l'anticorps n'est pas assez spécifique pour neutraliser le virus. Ce sont des anticorps non-neutralisants ayant une réactivité croisée. C'est le cas des quatre sérotypes du VDEN ou encore entre le VDEN et le VZIK. Des études ont montré que les protéines de surface E et prM du VDEN sont les principales causes de l'ADE (Crill *et al.*, 2004; Serafin *et al.*, 2001). Malheureusement, l'ADE peut causer beaucoup de déficiences dans l'immunité innée, telles que la reconnaissance de l'ARNv dans le cytosol par des senseurs d'ARN cytosolique (Ubol *et al.*, 2010) ou encore la réduction de la voie dépendante des récepteurs de type Toll (TLR) (Modhiran *et al.*, 2010). En effet, l'interaction entre les anticorps non neutralisant et les récepteurs Fc réduit la régulation des TLR en favorisant leur régulation négative par la voie NF-κB. Finalement, l'ADE provoquerait une accumulation de virus non éliminés ce qui aboutirait à une réponse immunitaire excessive caractérisée par une expression accrue de cytokines pro-inflammatoires.

1.1.4 Structure des *Flavivirus*

Les *Flavivirus* sont des virus à ARN simple brin à polarité positive (ARNsb+) appartenant au groupe IV dans la classification de Baltimore. Ils sont composés d'une bicouche lipidique (dérivée des membranes de la cellule hôte) entourant la nucléocapside (figure 1.6). Cette dernière inclue une copie du génome viral sous forme d'ARNv et de 180 copies de la protéine capside C (Zhang *et al.*, 2007). L'enveloppe virale est composée de 180 copies de la protéine M (clivée à partir de son précurseur prM) et de 90 copies de la protéine d'enveloppe E dimérisée.

Les *Flavivirus* immatures ont une taille d'environ 60 nm de diamètre possédant 60 pics à la surface. Chaque pic est fait de 3 protéines E et prM homodimérisées (Zhang *et al.*, 2003). Lorsque le virus subit sa maturation à travers l'appareil de Golgi, le diamètre du virus est de 53 nm dû au réarrangement de la protéine E en trimère parallèle et au clivage de prM en M (Yu *et al.*, 2008). Finalement, la forme mature des *Flavivirus* possède une surface lisse et un diamètre de 50 nm (Kuhn *et al.*, 2002). La structure de l'enveloppe est composée à l'extérieur de protéines E, parallèles aux protéines M à l'intérieur.

1.1.5 Le génome des *Flavivirus*

Le génome des *Flavivirus*, long de 10 à 11 kb, est composé d'un seul cadre de lecture, « Open Reading Frame (ORF) », codant pour les 3 protéines structurales C, prM et E et les sept protéines non structurales NS1, NS2A, NS2B, NS3, NS4A, NS4B et NS5 (figure 1.7). L'ORF possède à ses extrémités des régions 3' et 5' non traduites, « Untranslated Transcribed Region (UTR) » (Ng *et al.*, 2017; Selisko *et al.*, 2014).

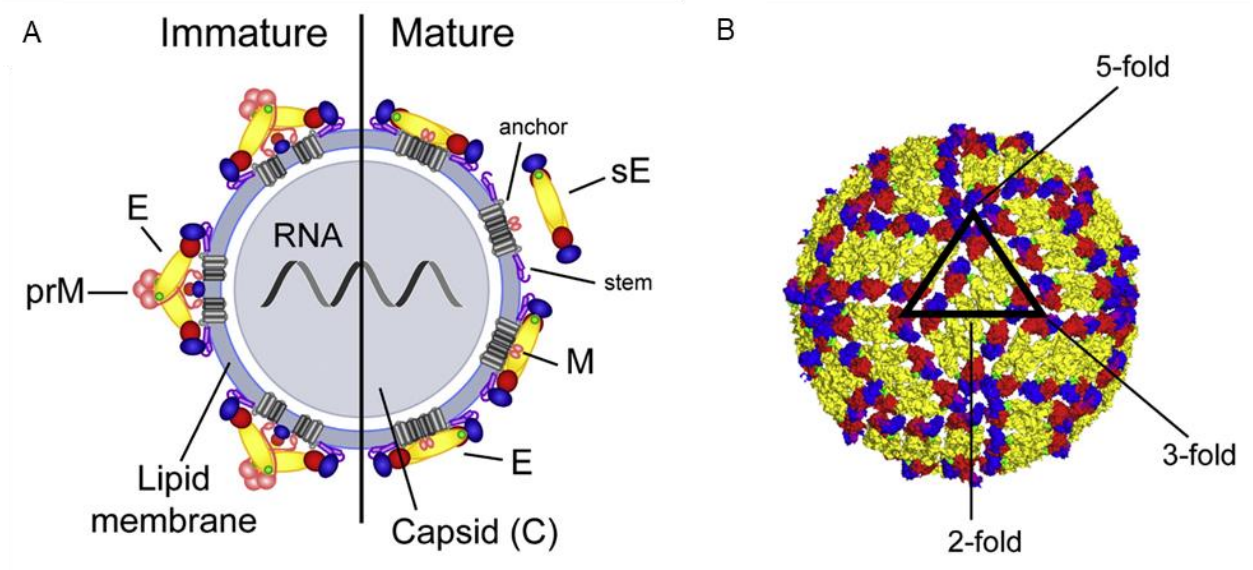

Figure 1.6 Structure des *Flavivirus*

(A) Représentation schématique des *Flavivirus* immature et mature. (B) Représentation schématique de axes de la structure des particules virales. (Heinz *et al.*, 2012)

L'extrémité 5'UTR possède une coiffe de type I (m7 GpppAm2) permettant la traduction de l'ARNv en imitant les ARM messager (ARNm) cellulaires (Garcia-Blanco *et al.*, 2016). L'extrémité 3'UTR est composée de 3 sous structures bien définies dans la littérature. En effet, on peut citer la région hyper variable qui se trouve juste en aval du codon STOP suivi de la région semi variable et finalement la région hautement conservée (Villordo *et al.*, 2015). Bien que l'ARNv ne possède pas de queue poly-A comme les ARNm cellulaires, l'extrémité 3'UTR est riche en A, permettant la liaison avec le « poly-A binding protein (PABP) » afin d'initier la traduction. Finalement, pour permettre la réplication du génome, celui-ci doit subir une circularisation. Ceci est possible grâce à une grande capacité de plasticité de l'ARNv qui entreprend des changements de conformation. La circularisation de l'ARNv se fait principalement par l'interaction ARN-ARN longue distance entre des structures spécifiques du 3'UTR et du 5'UTR, notamment par l'interaction de PABP avec le « cap-binding complex eIF4F » (Mazeaud *et al.*, 2018).

Les *Flavivirus* ont également la capacité à produire des ARN flaviviraux sous-génomiques ne codant pour aucunes protéines virales (Hamilton *et al.*, 1999). Il existe actuellement trois classes décrites dans la littérature, les petits ARN viraux « viral small RNAs », les génomes interférant défectueux « defective interfering genomes » et les ARN flaviviraux sous-génomiques,

« subgenomic *Flavivirus* RNA (ARNsf) » (Li *et al.*, 2001; Pijlman *et al.*, 2008). Seuls les ARNsf ont vraiment bien été étudiés ces dernières décennies. Brièvement, les ARNsf sont des structures génomiques de 0.3 à 0.7 kb et représentent la majorité des ARN viraux présents dans une cellule infectée (Pijlman *et al.*, 2008). Les ARNsf sont produits par la dégradation incomplète de l'ARNv à partir de son extrémité 5'UTR par l'exonucléase cellulaire XRN1/Pacman (Funk *et al.*, 2010; Pijlman *et al.*, 2008). L'exonucléase XRN1/Pacman avance le long de l'ARNv en le dégradant mais est bloquée au niveau de l'extrémité 3'UTR par sa structure en nœud. Notamment, les ARNsf jouent un rôle important dans l'interférence de l'immunité innée et de l'apoptose (discuté respectivement dans les sections 1.7.3.1 et 1.8.1.1).

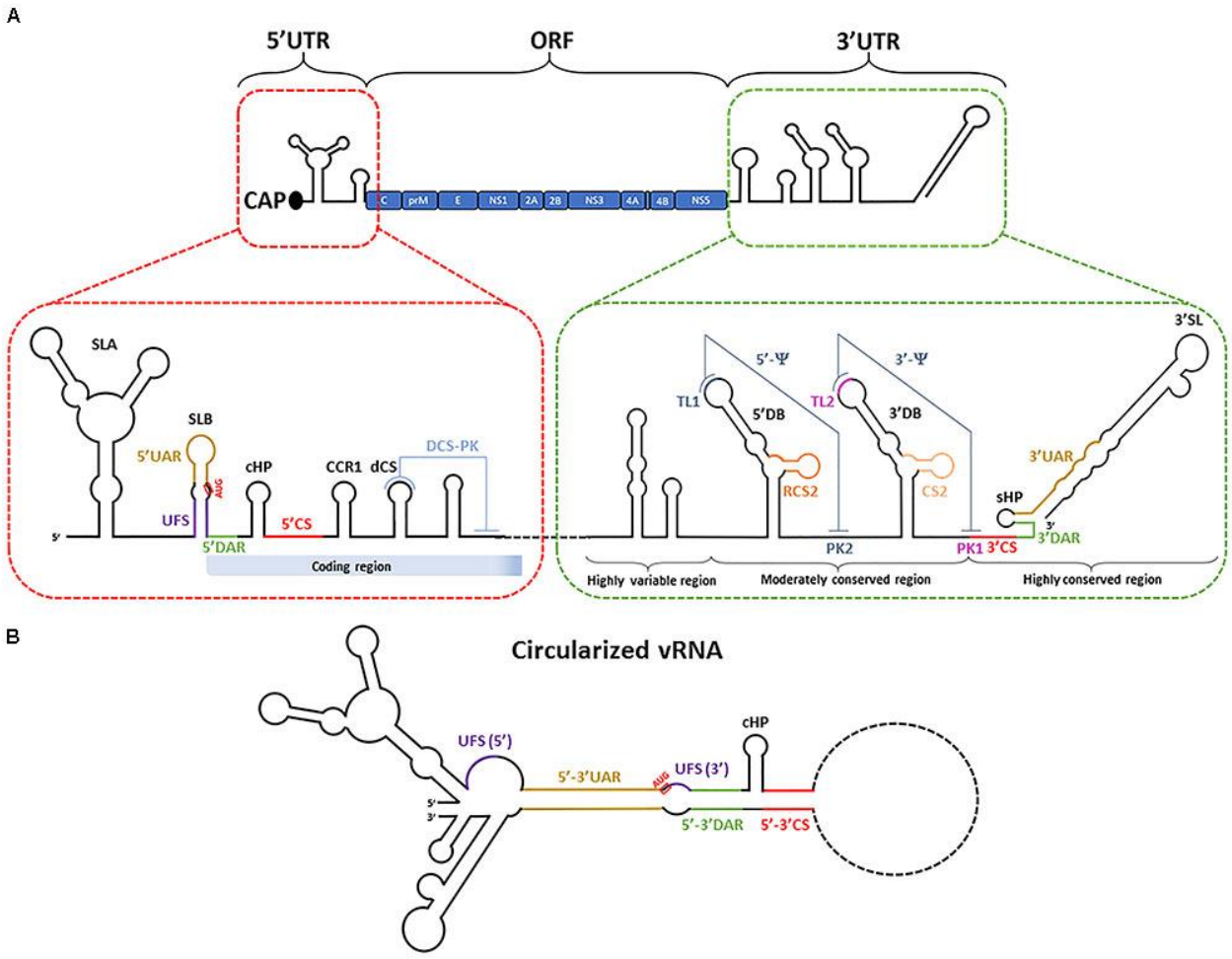

Figure 1.7 Structure du génome des *Flavivirus*

(A) Représentation schématique du génome viral sur un plan linéaire. (B) Représentation du génome virale après circularisation. (Mazeaud *et al.*, 2018)

1.1.6 Cycle des *Flavivirus*

En général, les *Flavivirus* partage un cycle viral conservé à partir de l'entrée jusqu'à la sortie du virus infectieux, c'est-à-dire dans l'entrée du virus, la fusion des membranes libérant l'ARNv, la réplication et traduction au niveau du réticulum endoplasmique (RE), l'assemblage / maturation et la sortie du virus nouvellement formé hors de la cellule hôte (figure 1.8).

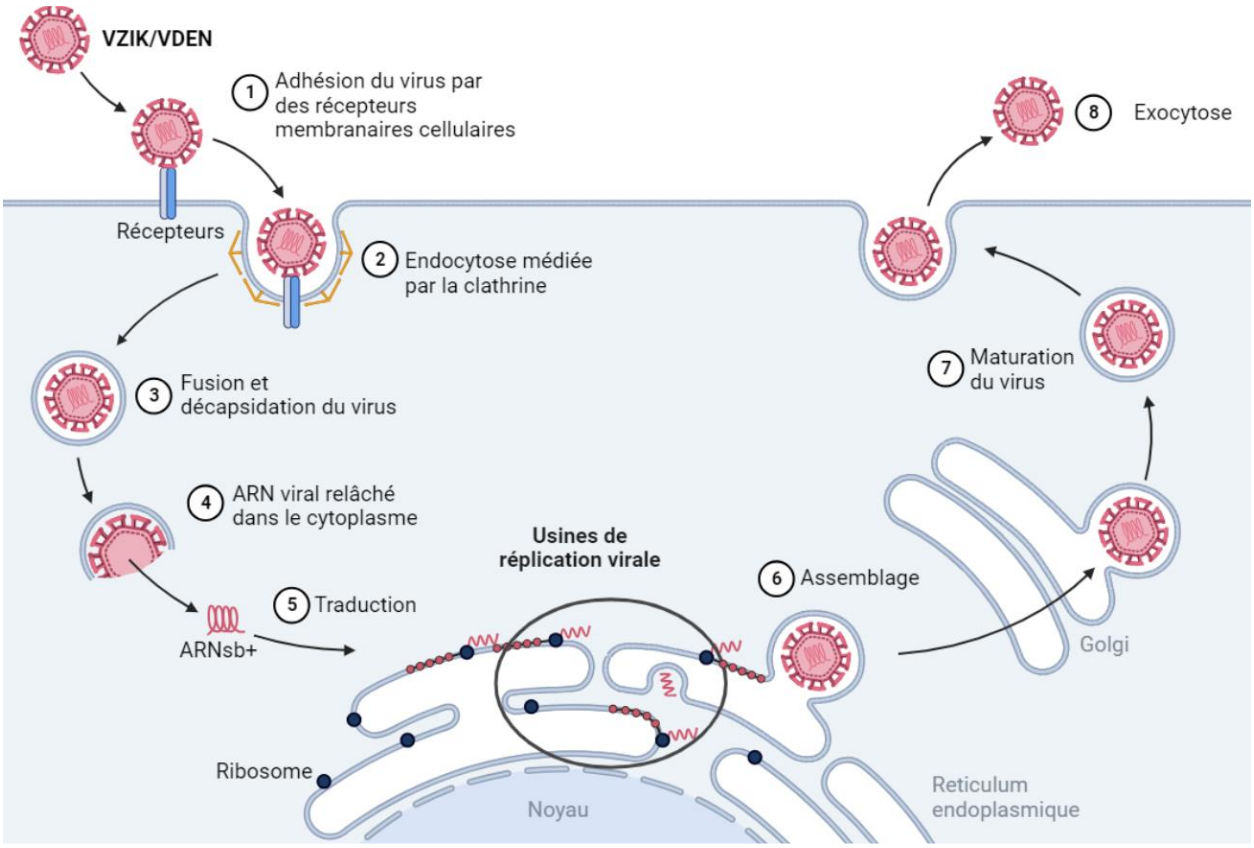

Figure 1.8 Représentation schématique du cycle des *Flavivirus*

(1) Attachement des *Flavivirus* par des récepteurs cellulaires. (2) Endocytose des *Flavivirus* par clathrine. (3 et 4) Fusion et libération de l'ARNv dans le cytosol. (5) Traduction de l'ARNv en polyprotéine virale. (6) Assemblage et accumulation des virions dans les sacs de virus. (7 et 8) Maturation des virions à travers l'appareil de Golgi et exocytose des virus mature infectieux. Schéma réalisé à l'aide de la ressource en ligne BioRender (**https://biorender.com/**).

1.1.6.1 Adhésion / Endocytose

La première étape du cycle des *Flavivirus* consiste en l'attachement du virus sur la membrane cellulaire. Ceci se fait à l'aide de la protéine virale E et des récepteurs cellulaires de surface tels que des tyrosines kinase de la famille TAM et TIM, des lectines type C tel que DC-SIGN, des

intégrines, des protéines heat-shock 70/90, des récepteurs laminine, ou encore des héparates sulfates (Chu *et al.*, 2004; Germi *et al.*, 2002; Meertens *et al.*, 2012; Miller *et al.*, 2008b; Niu *et al.*, 2018; Pereira *et al.*, 2019; Reyes-Del Valle *et al.*, 2005; Richard *et al.*, 2017; Tio *et al.*, 2005; Zhang *et al.*, 2022). L'interaction entre la protéine E et des récepteurs cellulaires de surface vont activer la deuxième étape qui est l'entrée du virus par endocytose médiée par clathrine (Acosta *et al.*, 2008; van der Schaar *et al.*, 2008). L'endocytose par clathrine chez les *Flavivirus* fait intervenir une réorganisation de facteurs d'internalisation en structure type tubulaire. C'est le cas par exemple de LY6E qui est indispensable à l'endocytose du VDEN et du VZIK (Hackett *et al.*, 2018).

1.1.6.2 Fusion / Relâche / Traduction

À la suite de l'endocytose des *Flavivirus*, la troisième étape consiste à fusionner l'enveloppe des *Flavivirus* avec la membrane de l'endosome. La diminution du pH interne de l'endosome, réalisée par la pompe à proton V-ATPase (Kozik *et al.*, 2013; Lafourcade *et al.*, 2008) modifie la conformation de la protéine E permettant son insertion dans la membrane de l'endosome et formant un pore dans lequel l'ARNv peut être relâché dans le cytosol, quatrième étape du cycle flaviviral (Allison *et al.*, 1995; Chao *et al.*, 2015).

L'ARNv cytosolique est ensuite dirigé au niveau des membranes du RE pour y subir la cinquième étape du cycle flaviviral, la traduction. L'ARNv est traduit par la machinerie ribosomique cellulaire en une seule polyprotéine virale (figure 1.9). Cette polyprotéine est clivée de manière co- et post-traductionnelle par des protéases virales et cellulaires, générant ainsi les protéines structurales C, prM et E et non-structurales NS1, NS2A, NS2B, NS3, NS4A, NS4B et NS5 (Bartenschlager *et al.*, 2013; Mazeaud *et al.*, 2018).

« Les protéines non structurales, incluant deux types d'enzymes virales, contrôlent la réplication du génome viral tout en établissant un environnement cytoplasmique favorable à la pathogénèse virale. La néosynthèse de l'ARN viral est catalysée par une ARN polymérase dépendante de l'ARN, soit NS5. Cette étape du cycle viral est assistée par l'activité hélicase de la protéine virale NS3 qui déroulent les ARN double-brins générés lors de la réplication. NS3 possède également une activité protéase qui, avec le cofacteur NS2B est requise pour cliver la polyprotéine virale en protéines virales matures. Les autres protéines non structurales ne possèdent pas d'activité enzymatique mais sont néanmoins indispensables à la réplication virale (Bartenschlager *et al.*, 2013; Mazeaud *et al.*, 2018) Notamment, ces dernières induisent le remodelage du RE en

ultrastructures membranaires appelées organites ou usines de réplication virale. » (Freppel *et al.*, 2022)

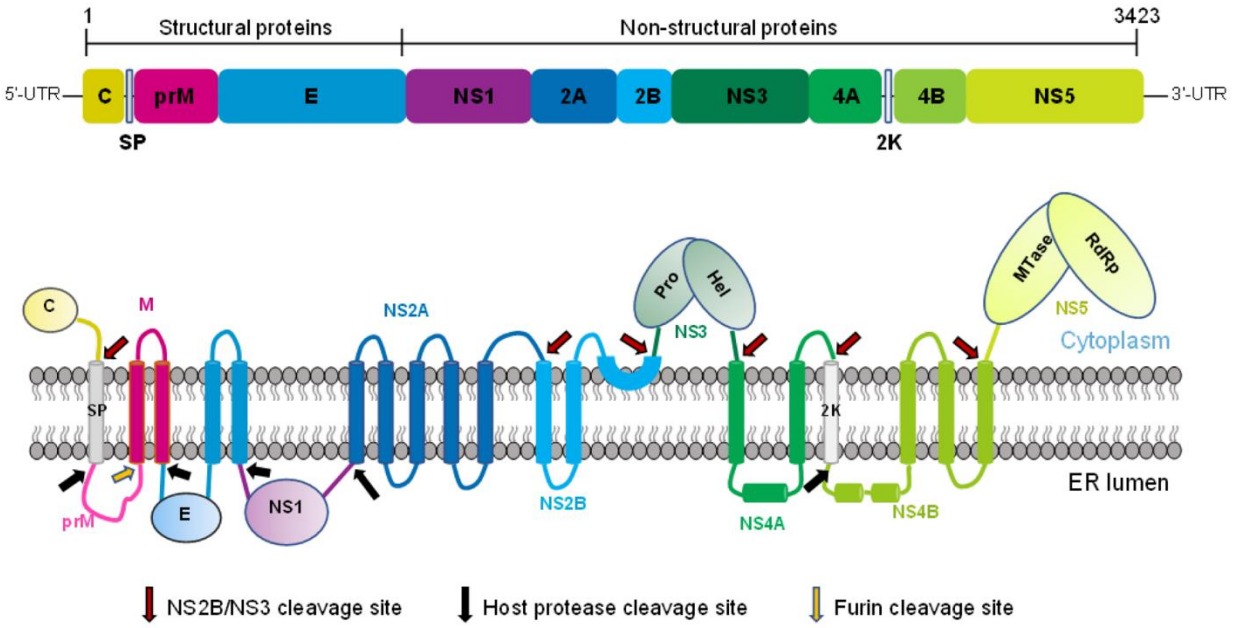

Figure 1.9 Topologie de la polyprotéine flavivirale

Le génome flaviviral est traduit en une seule polyprotéine transmembranaire au niveau du RE et est clivée à l'aide de protéases virale et cellulaire. (Qin *et al.*, 2022)

1.1.6.3 Assemblage / Maturation / Exocytose

La sixième étape du cycle flaviviral consiste à assembler les protéines virales structurales nouvellement synthétisées en virions prêt à devenir infectieux. À la suite d'une interaction entre l'ARNv et la protéine capside C, les protéines structurales s'assemblent en nouveaux virions au niveau des sacs de virus. Les virions sont ensuite relâchés des sacs de virus et vont traverser l'appareil de Golgi. À ce stade, les virions vont entreprendre leur septième étape de leur voyage pour subir une maturation par la protéase cellulaire furine qui va cliver prM (Elshuber *et al.*, 2003). Les nouveaux virus matures et donc infectieux avec la protéine E située à la surface sont relâchés par exocytose, dernière étape du cycle flaviviral, à l'extérieur de la cellule, et peuvent recommencer le cycle flaviviral.

1.1.6.4 Les usines de réplication flavivirales

« Les usines de réplication flavivirales (URv) se forment à partir des membranes du RE et incluent trois sous-structures singulières et facilement observables en microscopie électronique (figure 1.10) (Cortese *et al.*, 2017; Gillespie *et al.*, 2010; Welsch *et al.*, 2009; Westaway *et al.*, 1997) : 1- les paquets vésiculaires, résultant de l'invagination de la membrane du RE et dont l'intérieur est suspecté d'être le site où la réplication du génome viral s'effectue ; 2- les sacs de virus qui sont de larges citernes de RE où les virions assemblés s'accumulent de façon ordonnée, voire géométrique ; et 3- les convolutions de membranes dont les fonctions sont peu caractérisées. » (Freppel *et al.*, 2022)

Les paquets vésiculaires

Les paquets vésiculaires (PV) de forme sphérique alignée sont des invaginations du RE ayant pour diamètre une moyenne de 90 nm (Welsch *et al.*, 2009). Les PV sont retrouvés non seulement chez les mammifères, mais également chez les moustiques indiquant des mécanismes de formation conservés au cours de l'évolution (Junjhon *et al.*, 2014; Welsch *et al.*, 2009). On suppose que ces sous structures sont le lieu de réplication de l'ARNv. En effet, ils ont été montrés riche en NS1, NS2B3, NS4A, NS4B, NS5 et en ARN double-brin (Junjhon *et al.*, 2014; Welsch *et al.*, 2009). Etant donnée la taille minime du pore connectant les PV au cytoplasme (10 nm), ils pourraient également jouer un rôle dans la protection de l'ARNv face aux facteurs cytosoliques antiviraux tels que RIG-I ou MDA5, deux senseurs d'ARN impliqués dans la réponse précoce immunitaire antivirale (discuté dans la section 1.7.3.1). Le mécanisme par lequel les *Flavivirus* forment les VP est encore peu connu. NS4A pourrait être impliquée puisque cette protéine virale est essentielle dans la réplication de l'ARNv et le remodelage de la membrane du RE (Chatel-Chaix *et al.*, 2015; Miller *et al.*, 2007; Miller *et al.*, 2006; Roosendaal *et al.*, 2006; Zou *et al.*, 2015a).

Les sacs de virus

Les sacs de virus (SV) sont des structures organisées dans les membranes du RE (Welsch *et al.*, 2009). Dans des cellules infectées par le VDEN, les virus, des particules denses de 45 nm s'accumulent à l'intérieur des SV observable au microscope à transmission électronique. De plus, des expériences d'immunogold ont montré une accumulation de la protéine E à l'intérieur des SV (Welsch *et al.*, 2009). Le rôle des SV serait possiblement d'entreposer les virions immatures nouvellement formés avant d'entreprendre leur étape de maturation à travers l'appareil de Golgi. De plus, une autre hypothèse suggère que les SV serviraient également de contrôle/qualité des

virions immatures avant de les éliminer, une hypothèse qui reste à confirmer par d'éventuelles études.

Les convolutions de membranes

Les convolutions de membranes (CM) sont une accumulation de membranes du RE en forme de spaghetti ou en pelote de laine. Leurs fonctions sont encore peu connues aujourd'hui, mais nous avons plusieurs évidences qui pourraient expliquer leurs rôles. Bien que la biogénèse des CM ne soit pas encore correctement élucidée, la surexpression de NS4A induit partiellement la formation des CM (Miller *et al.*, 2007). De plus, l'accumulation de la protéase virale NS2B3 dans les CM suggère éventuellement un rôle de dégradation ou de la traduction de la polyprotéine virale (Chatel-Chaix *et al.*, 2016; Welsch *et al.*, 2009; Westaway *et al.*, 1997). Néanmoins, l'absence de l'ARNv dans les CM contredit cette hypothèse. De plus, les CM ne sont pas retrouvés chez le moustique, ce qui implique que la réplication de l'ARNv n'a pas lieu dans les CM (Junjhon *et al.*, 2014). Le fait que les CM ne soient retrouvés que chez les mammifères implique également que le mécanisme de la biogénèse des CM soit spécifique et implique des facteurs ou des processus cellulaires qui ne sont pas retrouvés chez le moustique. Notamment, l'immunité innée chez le moustique est différente des mammifères. Par exemple, le RE et les mitochondries font intervenir le complexe protéiques MAVS impliqué dans l'expression des interférons (discuté dans la section 1.7.3.1). Le complexe MAVS est absent chez le moustique, on pourrait alors supposer que les *Flavivirus* enroulent les membranes du RE en CM afin de bloquer l'activité de MAVS et potentiellement en le séquestrant dans les CM par l'intermédiaire de NS4B. En effet, plus récemment, la protéine virale NS4B a été montrée en grande présence dans les CM (Chatel-Chaix *et al.*, 2016). Puisque NS4B possède une grande capacité interactomique avec de nombreuses autres protéines virales et cellulaires (discuté dans la section 1.3.1), les CM pourraient jouer un rôle de séquestration de protéines néfastes à la réplication virale, telles que des protéines impliquées dans l'immunité innée antivirale.

Puisque l'origine des CM provient des membranes du RE, il n'est pas surprenant que les membranes du RE en contact avec d'autres organites soient également détournées. En effet, les contacts entre le RE et les mitochondries appelés l'interface réticulo-mitochondriale (IRM) serait diminués lors d'une infection au VDEN au bénéfice de la biogénèse des CM (discuté dans la section 1.7.3.1) (Chatel-Chaix *et al.*, 2016). Puisque l'IRM est connue pour intervenir dans l'immunité innée antivirale par l'intermédiaire de RIG-I, les *Flavivirus* auraient tout intérêt à détacher le RE des mitochondries pour en faire des CM.

Finalement, bien que le rôle des CM ne soit pas encore correctement compris, il est évident qu'ils contribueraient à la mise en place d'un environnement favorable à la réplication permettant aux *Flavivirus* d'échapper aux processus cellulaires néfastes pour le virus tels que l'immunité innée antivirale.

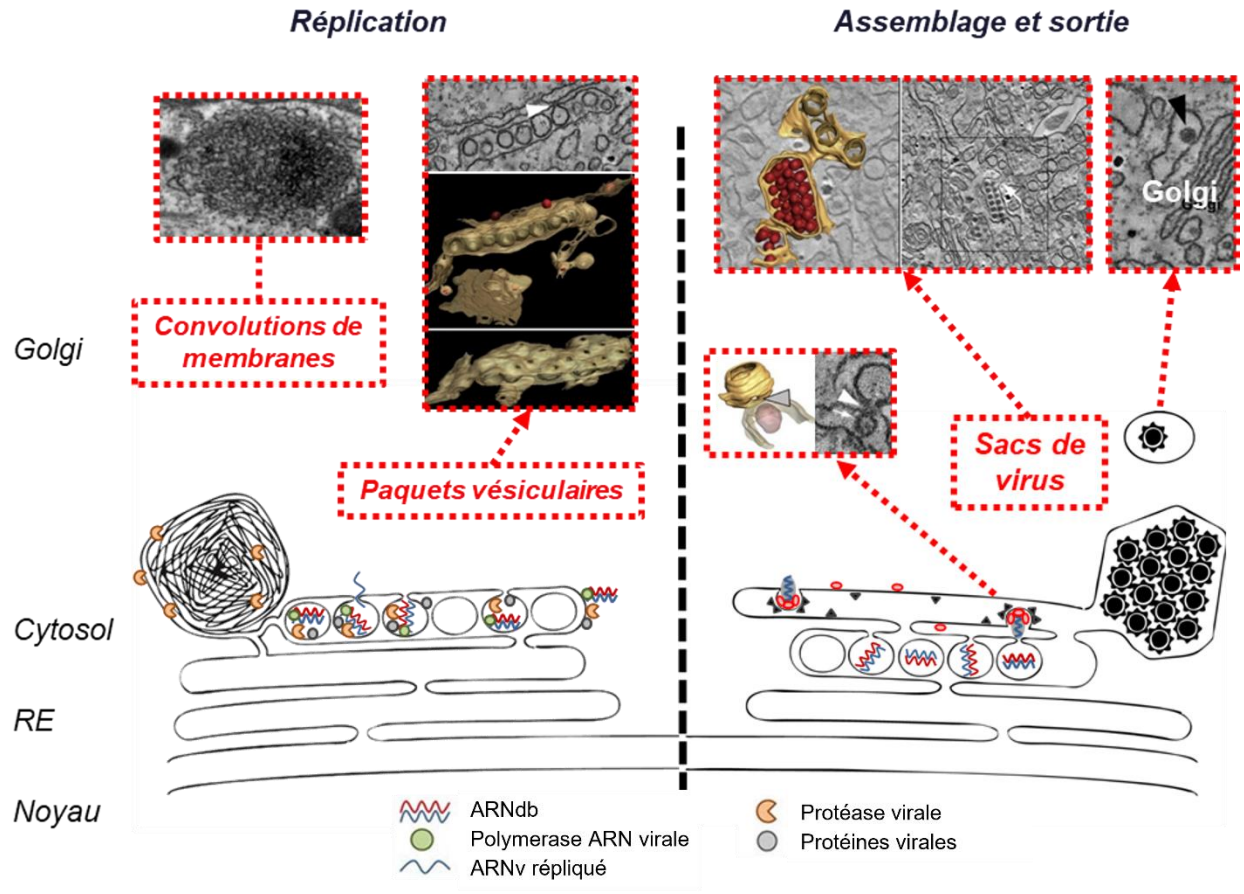

Figure 1.10 Réorganisation membranaire des usines de réplication flavivirales

Les *Flavivirus* remodèlent la membrane du RE en paquets vésiculaires, en sacs de virus et en convolutions de membranes. Modifié de (Chatel-Chaix *et al.*, 2014; Welsch *et al.*, 2009)

1.2 Traitements

Durant la dernière décennie, les VDEN et VZIK sont devenus des menaces à l'échelle mondiale par leur rapidité à se répandre à travers le monde dans des zones habituellement non touchées et notamment VZIK avec ses complications neurologiques. Bien qu'il existe des vaccins contre certains *Flavivirus*, il n'y a à ce jour aucuns traitements thérapeutiques ou vaccinaux efficaces

contre ces deux virus (Araujo *et al.*, 2020). Néanmoins, cette section discutera des stratégies actuellement en place contre les *Flavivirus* en général d'un point de vue thérapeutique ou vaccinale et également les nouvelles découvertes actuellement en étude.

1.2.1 Approche thérapeutique

Développer un composé clinique peut prendre jusqu'à une quinzaine d'années d'études incluant la découverte de la molécule à sa mise en vente sur le marché (Van Norman, 2016). La stratégie actuelle est de tester des composés déjà connus sur les infections virales *in vitro* / *in vivo* afin de gagner du temps en évitant les phases cliniques I et II puisque ces phases ont déjà été étudiées. Dans cette section, des exemples de deux types d'antiviraux seront discutés en fonction de leur mode d'action : les antiviraux ciblant les protéines virales et les antiviraux ciblant le cycle viral.

1.2.1.1 Les antiviraux ciblant les protéines virales

Protéine d'enveloppe E

Le peptide Z2 dérivé de la région conservée de la protéine E est efficace contre le VDEN, VZIK et le VFJ. En effet, chez la souris, une administration péritonéale de Z2 confère une protection d'environ 75% contre le VZIK avec aucunes complications neurologiques observées. (Yu *et al.*, 2017). Un autre peptide, le P5, dérivé cette fois de la région en hélice de la protéine E du VEJ est efficace contre le VEJ et le VZIK. Chez la souris, un traitement de faible dose permet de réduire les dommages causés au cerveau. Bien que les mécanismes de ces deux composés soient encore inconnus, il se pourrait que la région en hélice permette de bloquer l'interaction de la protéine E lors de la fusion des membranes virale et cellulaire (Schmidt *et al.*, 2010).

Les cyanohydrazones, une autre classe d'inhibiteurs de la protéine E du VDEN sont également efficaces contre VDEN, VZIK et VEJ *in vitro*. En particulier, le composé JBJ-01-162-04, réduit la virémie chez la souris (Li *et al.*, 2019). Il semblerait que le composé interagit avec une partie conservée de la protéine E appelée « pocket n-octyl-β-D-glucoside » bloquant ainsi la fusion des membranes virale et cellulaire contrôlée par la protéine E (de Wispelaere *et al.*, 2018; Li *et al.*, 2019).

Autres que des composés chimiques, des anticorps ont également été développés contre la protéine E dû à son exposition sur la surface externe. Par exemple, l'anticorps ab513 liant le domaine III de la protéine E (EDIII) du VDEN a montré une neutralisation avec une grande affinité contre les quatre sérotypes du VDEN (Robinson *et al.*, 2015). L'anticorps ab153 confère chez la

souris une réduction de la charge virale, une augmentation de la survie et une protection contre les dommages cérébraux. Finalement, le 2D22, un anticorps humain spécifique au VDEN réduit également la virémie chez la souris dans le plasma sanguin, et la moelle osseuse (Fibriansah *et al.*, 2015). Le 2D22 se lie aux trois domaines de la protéine E et empêche ainsi la fusion des membranes virale et cellulaire lors de la fusion.

Protéase virale NS2B3

Un inhibiteur contre la protéase virale NS2B3, le NSC157058 est très efficace contre le VZIK (Shiryaev *et al.*, 2017). Ce composé inhibe l'infection au VZIK dans des cellules précurseurs neuronales fœtales et réduit la charge virale chez la souris. Il semblerait que le composé interfère dans le repliement du cofacteur NS2B avec NS3 bloquant ainsi l'activité protéase de NS2B3.

L'antibiotique Novobiocin inhibe fortement le VDEN et le VZIK en culture cellulaire mais également chez la souris en conférant une survie de 100% et une diminution significative de la charge virale dans le sang (Yuan *et al.*, 2017). Cet antibiotique se lie au domaine de liaison NS2B-NS3 bloquant ainsi son activité protéase. Par un mécanisme similaire, le Temoporfin inhibe la protéase NS2B3 réduisant ainsi l'infection au VZIK des cellules de placenta humain ou des cellules progénitrices neuronales humaines (Xu *et al.*, 2016). *In vitro,* le Temoporfin est également efficace contre le VDEN et autres *Flavivirus,* tels que le VEJ, le VFJ et le VNO. Chez la souris, un traitement réduit la présence d'ARNv et protège à 83% contre le VZIK et ses complications neurologiques.

Protéine virale NS4B

La protéine virale NS4B est une composante majeure de cette thèse et la section 1.3 y est complètement consacrée. Notamment, la figure 1.11 montre les sites d'inhibitions des inhibiteurs discutés dans cette section.

Le NITD-618 supprime la synthèse de l'ARNv chez le VDEN en liant directement NS4B aux acides aminés P104 et A119. Ces deux acides aminés étant conservés chez les quatre sérotypes du VDEN et non retrouvés chez d'autres *Flavivirus*, cela expliquerait pourquoi le NITD-618 est inefficace contre le VNO ou le VFJ (Xie *et al.*, 2011b).

Le NITD-688 est un composé très puissant contre le VDEN en liant directement la protéine virale NS4B. En effet, chez la souris, le NITD-688 réduit la virémie après 3 jours de traitement seulement (Moquin *et al.*, 2021). Lorsque NS4B est mutée, l'effet du NITD-688 est encore plus fort. En revanche, des mutations spécifiques de NS4B (T215A et A222V) empêchent l'interaction du

NITD-688 avec NS4B et réduisent son efficacité. Chez le rat et le chien, cette drogue est très bien tolérée et facilement éliminée par l'organisme.

Le JNJ-A07 bloque l'interaction NS3-NS4B du VDEN par un possible changement dans la conformation de la boucle cytosolique (Kaptein *et al.*, 2021). Chez la souris, un traitement prophylactique oral réduit la charge virale et les symptômes reliés à une infection au VDEN. Très similaire, le JNJ-1802 bloque également l'interaction NS3-NS4B puisqu'il s'agît d'une optimisation du JNJ-A07 (Goethals *et al.*, 2023). Ce composé est très efficace contre les DENV1 et DENV2 chez des sujets primates non humains et a réussi avec succès une première étude clinique de phase I avec une haute tolérance. Ces deux composés sont très prometteurs car ils sont efficaces à de très basses concentrations (picomolaire à nanomolaire) et visent les 4 sérotypes de VDEN. Le SDM25N est un antagoniste des récepteurs opiacés δ. Ce composé cible l'acide aminé F164 de la protéine NS4B. Une mutation de NS4B en F164L confère au VDEN2 une résistance contre cet inhibiteur (van Cleef *et al.*, 2013). *In vitro*, le SDM25N montre une activité antivirale contre le VDEN dans des cellules de mammifères, mais pas dans des cellules C6/36 de moustique.

Le JNJ-1A, un inhibiteur d'un autre virus appartenant à la famille des *Flaviviridae*, le virus de l'hépatite C (VHC), montre une efficacité *in vitro* contre les sérotypes 1, 2 et 4 du VDEN (Hernandez-Morales *et al.*, 2017). Des virus résistant à JNJ-1A montrent une mutation en T108I dans NS4B confirmant l'action de ce composé spécifiquement sur NS4B.

Protéine virale NS5

La protéine virale NS5 est une des protéines les plus importantes des *Flavivirus* puisque celle-ci possède différentes activités enzymatiques, telles que l'ARN polymérase ARN-dépendante (RdRp), la méthyltransférase (MTase) ou encore la guanosyltransférase (GTPase) permettant la réplication de l'ARNv (Davidson, 2009; Issur *et al.*, 2009; Kroschewski *et al.*, 2008). L'analogue BCX4430 connu aussi sous le nom de Galidesivir est un inhibiteur de l'ARN polymérase du VHC. L'analogue réduit les effets cytopathiques du VMET, du VNO et de différentes souches du VZIK que ce soit *in vitro* ou *in vivo* (Eyer *et al.*, 2017; Julander *et al.*, 2017; Taylor *et al.*, 2016). De plus, chez la souris, une administration intramusculaire de 8 jours réduit la charge virale et augmente la survie à 87.5%.

Le NITD008 cible la RdRp pour inhiber la réplication virale du VDEN et du VZIK aboutissant à la réduction des titres viraux *in vitro* de différentes souches du VZIK (Yin *et al.*, 2009). Chez la souris, un traitement NITD008 réduit la virémie et protège à 50% de la mort et des complications neurologiques causées par le VZIK (Deng *et al.*, 2016).

Un autre exemple prometteur d'inhibiteur de la protéine NS5 est l'analogue 7-deaza-2'-C-methyladenosine. Celui-ci réduit la présence d'ARNv du VNO et du VZIK dans des cellules Vero (Zmurko *et al.*, 2016). Chez la souris infectée au VZIK, le traitement diminue la virémie et retarde la progression de la maladie.

1.2.1.2 Les antiviraux ciblant le cycle viral

L'endocytose des Flavivirus

Le Sunitinib/Erlotinib agît sur l'entrée du VDEN, du VNO et du VZIK *in vitro* en ciblant spécifiquement la protéine kinase 1 associée à la kinase AP2 et à la kinase associée à la cycline G, toutes deux impliquées dans la modulation du trafic membranaire intracellulaire médié par protéines adaptatrices (Bekerman *et al.*, 2017). Chez la souris, le traitement réduit la charge virale, la mortalité et modifie la réponse cytokine à la suite d'une infection au VDEN.

Le Prochlorpérazine est un autre inhibiteur de l'endocytose (Simanjuntak *et al.*, 2015). Celui-ci altère la distribution de chlatrine par l'inhibition des récepteurs dopamine D2, interférant ainsi sur l'endocytose médiée par chlatrine. Chez la souris infectée par le VDEN ou VEJ, le traitement immédiat protège de la mort tandis qu'un traitement tardif retarde la mort et améliore la survie.

La fusion des Flavivirus

La chloroquine est un composé bien connu dans la littérature et déjà utilisé dans la lutte anti paludique (Uhlemann *et al.*, 2005). Chez le singe avec une infection au VDEN, la chloroquine réduit la virémie, le niveau d'interféron gamma et le niveau du facteur nécrotique tumoral TNFα (Farias *et al.*, 2015). Il semblerait que la chloroquine inhibe l'acidification des endosomes empêchant la fusion des membranes virale et cellulaire (Delvecchio *et al.*, 2016). Chez la souris, la chloroquine réduit également une infection au VZIK en bloquant l'internalisation du virus diminuant ainsi la virémie (Li *et al.*, 2017b). De plus, un traitement chez des souris en gestation réduit l'apoptose des cellules du cerveau fœtal.

Le 25-hydroxycholesterol (25HC) est un dérivé du cholestérol qui possède une activité antivirale contre le VZIK, le VNO, le VFJ et le VDEN (Li *et al.*, 2017a). Le 25HC régule le métabolisme lipidique et interfère alors l'étape de fusion entre la membrane virale et la membrane cellulaire. Un traitement avec le 25HC chez des souris infectées au VZIK réduit la virémie, la mortalité et la charge virale dans le cerveau.

La réplication des Flavivirus

L'Ivermectin est un composé réduisant le niveau de la polymérase NS5 dans le noyau des cellules infectées par le VZIK se traduisant en la diminution du niveau d'infection (Ji *et al.*, 2020). Il semblerait dans ce cas que l'Ivermectin inhibe l'IMPα/β1 (importine de l'hôte) ainsi empêchant le trafic des protéines vers le noyau (Crump, 2017; Ji *et al.*, 2020). En revanche, chez la souris, aucune amélioration n'a été observée dans la mortalité ou la morbidité (Ketkar *et al.*, 2019).

Un autre composé approuvé est actuellement en investigation, le AR-12, un dérivé du Celecoxib (Abdulrahman *et al.*, 2017). A l'échelle cellulaire, le traitement réduit la réplication virale en diminuant la voie PI3/AKT. Chez la souris, le traitement réduit l'expression des protéines non structurales et des virions diminuant ainsi la mortalité.

L'assemblage et l'exocytose des Flavivirus

Le UV-12, un imminosaccharide, inhibe l'activité des deux α-glucosidase I et II, impliquées dans la glycosylation de la protéine E des *Flavivirus* lors de la maturation des virions (Warfield *et al.*, 2015). Chez la souris infectée au VDEN, le traitement aboutit à 100% de survie, une drastique diminution de la charge virale et des niveaux élevés de cytokines et chémokines synthétisées.

L'imminosaccharide UV-4B partage le même mécanisme que le UV-12 (Warfield *et al.*, 2016). Un traitement à l'UV-4B abouti également à la diminution de la charge virale lors d'une infection au VDEN *in vitro*. Chez la souris, le traitement confère une protection même si le traitement est commencé tardivement, c'est-à-dire 2 jours après l'infection.

1.2.2 Approche vaccinale

Avec l'apparition de pandémies virales de plus en plus fréquentes, la course au développement de vaccin à fait un bon et la recherche vaccinale a beaucoup évolué ces dernières années, notamment dans la vaccination anti-flaviviral. Cependant, la proximité génétique des *Flavivirus* et le phénomène d'ADE donnent à la science vaccinale un défi difficile dans le développement de vaccins. Cette section discutera de quelques exemples importants de différentes stratégies de vaccination actuellement disponibles ou en études cliniques.

Virus de la fièvre jaune

Le vaccin 17D (YFV-17D) actuel ou connu sous le nom commercial Stamaril® (Lutmer *et al.*, 2022) dérive directement du premier vaccin contre le VFJ développé en 1936 utilisant la souche 17D (Ferguson *et al.*, 2010). Ce vaccin très fiable peut éventuellement déclencher de rares complications, comme aux États-Unis, avec un indice de 0.4 cas pour 100 000 personnes au-

dessus de 60 ans (Lindsey *et al.*, 2008; Miller *et al.*, 2008a). Le YFV-17D provoque une réponse immunitaire forte, robuste, rapide et durable contre la protéine virale E (Monath *et al.*, 2002; Vratskikh *et al.*, 2013). Etant donné la qualité de ce vaccin contre le VFJ, il a été utilisé comme vecteur pour le développement de possibles autres vaccins contre les *Flavivirus* tel que le VEJ, le VNO, le VDEN et le VZIK.

Le virus de l'encéphalite japonaise

Le premier vaccin contre le VEJ est un vaccin inactivé dérivé de cerveau de souris et commercialisé dans les années 30 par Sanofi Pasteur sous le nom de JE-VAX pour être finalement retiré du marché en 2005 (Hoke *et al.*, 1988; Hsu *et al.*, 1971; Kurane *et al.*, 2000; Paulke-Korinek *et al.*, 2008). La recherche de vaccin vivant atténué a abouti au développement du vaccin SA-14-14-2 (Yu, 2010). Ce vaccin est actuellement le principal utilisé en Chine depuis plus de 30 ans (Schioler *et al.*, 2007). Deux vaccins recombinants, le ALVAC-JEV (base virale canarypox) et le NYVAC-JEV (base virale vaccinia atténué) ont montré une bonne efficacité et tolérance lors des phases cliniques (Kanesa-thasan *et al.*, 2000). Le vaccin JE-CV, dérivé du YFV-17D montre une efficacité similaire à celle du SA-14-14-2 (Kim *et al.*, 2014a).

Le virus du Nil occidental

Il n'y a malheureusement aucun vaccin disponible pour l'humain. En revanche, quatre vaccins sont disponibles principalement pour les chevaux. Le West-Nile Innovator, le Vetera WNV, le Recombitek Equine WNV et le Equi-Nile (Ishikawa *et al.*, 2014). Ces vaccins ne confèrent une immunité que pour une année environ, ce qui implique une vaccination annuelle. Différents prototypes de vaccin chez l'humain ont été étudié en phase clinique I et II, néanmoins aucuns n'a été validées par la suite (Kaiser *et al.*, 2019).

Le virus de la dengue

En 2015, un vaccin développé sous le nom de Dengvaxia® (CYD-TDV) par Sanofi Pasteur a été approuvé pour la vente dans des zones à haut risque (Thomas *et al.*, 2019). Ce vaccin, un tétravalent chimérique vivant atténué « live-attenuated tetravalent vaccine (LATV) » fait à partir du YFV-17D dont les protéines prM et E ont été remplacées, possède une plus grande affinité pour les sérotypes 3 et 4 que les sérotypes 1 et 2 (Hadinegoro *et al.*, 2015; Malisheni *et al.*, 2017). Le CYD-TDV confère une immunité d'environ quatre ans. (Guy *et al.*, 2017). Cependant, très tôt en 2018, plus d'une dizaine d'enfants sont décédés à la suite d'une campagne vaccinale désastreuse aux Philippines. Finalement, en 2021, ce vaccin a été approuvé par l'Union Européenne seulement pour les personnes entre 9 et 45 ans qui ont déjà été infectées par le

VDEN ou pré-vaccinées, ce qui rend ce vaccin peu utile. D'autres vaccins ont ensuite été étudiés en essais cliniques.

Le LATV rDEN∆30 par exemple, est un vaccin vivant atténué avec une délétion de 30 nucléotides dans l'extrémité 3'UTR pour chacun des sérotypes du VDEN (Blaney *et al.*, 2006; Durbin *et al.*, 2001). Ce vaccin, très immunogène chez l'humain et le singe, est beaucoup moins virulent chez le moustique limitant ainsi la transmission de l'humain au moustique (Blaney *et al.*, 2004; Blaney *et al.*, 2008; Durbin *et al.*, 2001; Durbin *et al.*, 2011). Le TV003 est un vaccin mélangeant les quatre LATV rDEN∆30, c'est-à-dire le rDEN1∆30, le rDEN2∆30, le rDEN3∆30 et le rDEN4∆30 et est actuellement en étude clinique de phase III (Kirkpatrick *et al.*, 2015; Nivarthi *et al.*, 2021). Après vaccination, environ 92% des patients présentaient des anticorps dirigés contre les quatre sérotypes du VDEN avec une plus forte réponse contre VDEN2 que le Dengvaxia® (Kirkpatrick *et al.*, 2016). Le TV005, qui est une mise à jour du TV003 en rajoutant plus de LATV rDEN2∆30 possède une plus grande réponse immunitaire observée en étude clinique de phase I après une seule vaccination (90% de patients avec le TV005 contre 76% avec le TV003) (Kirkpatrick *et al.*, 2015).

Plus récemment, le LATV TAK-003 aussi connu sous le nom de DENVax ou Qdenga, a montré une très grande efficacité et est très prometteur pour l'avenir (George *et al.*, 2015; Jackson *et al.*, 2018; Osorio *et al.*, 2014; Rupp *et al.*, 2015). Ce vaccin est un recombinant chimérique du VDEN1, 3 et 4 construit sur la base du VDEN2 (Huang *et al.*, 2013). Les études cliniques en phase III menées sur une cohorte de patients de 4 à 16 ans montrent une performance dépendante du sérotype avec une plus faible efficacité pour le DENV3 (Biswal *et al.*, 2020). Un suivi de cette étude deux ans plus tard montre que le TAK-003 confère une immunité continue avec une légère diminution de l'efficacité dans la deuxième année chez les patients de 4 à 16 ans (Lopez-Medina *et al.*, 2022). Finalement, une autre étude confirme l'efficacité de ce vaccin après 3 ans de vaccination bien que l'efficacité continue de diminuer (Rivera *et al.*, 2022). Un booster serait éventuellement requis pour maintenir une immunité efficace contre les quatre sérotypes du VDEN. En août 2022, le vaccin TAK-003 a été approuvé pour les patients de 6 à 45 ans par l'Agence fédérale indonésienne des produits alimentaires et médicamenteux (Becker, 2022).

Le virus Zika

Le VRC5283 et le VRC5288, des vaccins à ADN, sont composés d'un plasmide circulaire d'ADN codant pour les protéines virales prM et E de la souche polynésienne H/PF/2013 du VZIK. Chez le singe, ces vaccins procurent une immunité robuste et efficace contre VZIK (Van Rompay *et al.*,

2019). En date du 5 décembre 2022, le VRC5283 a complété deux études cliniques chez l'humain tandis que le VRC5288 est toujours en phase I (Gaudinski *et al.*, 2018).

L'ARNm-1325 et l'ARNm-1893 sont des vaccins à ARNm codant pour les protéines virales prM-E de la souche polynésienne H/PF/2013 du VZIK. Ces deux vaccins confèrent une immunité efficace et robuste chez la souris contre le VZIK (Pardi *et al.*, 2017; Richner *et al.*, 2017). Ils sont depuis 2019 en étude clinique de phase I.

Le rZIKV/D4Δ30-713 est un vaccin vivant atténué recombiné à partir du VDEN4 ayant une délétion de 30 nucléotides à l'extrémité 3'UTR du génome viral. Le vaccin exprime les protéines virales prM-E du VZIK FSS13025. Chez la souris, la vaccination aboutit à une immunité efficace avec un titre élevé d'anticorps neutralisants (Chin *et al.*, 2021). Le vaccin a complété son étude clinique de phase I en juin 2022. Un autre exemple de vaccin vivant atténué est le ChAdOx1 Zika. Bien qu'il ait été montré chez la souris que ce vaccin est peu efficace (Lopez-Camacho *et al.*, 2020), il est malgré tout rentré en étude clinique de phase I d'octobre 2019 à mars 2022.

1.3 La protéine virale NS4B

Chez les *Flavivirus*, les protéines non structurales sont essentielles à la réplication du génome virale, mais également à la création d'un environnement favorable à la réplication. Une en particulier a montré au cours des dernières décennies sont importance. En effet, la protéine virale NS4B, très conservée chez les *Flavivirus* représente un intérêt particulier dans la poursuite de thérapie antivirale (Blaney *et al.*, 2003) (Zmurko *et al.*, 2015). Bien qu'elle ne possède aucune activité enzymatique, cette protéine possède un rôle essentiel dans la réplication virale (Chatel-Chaix *et al.*, 2016; Zou *et al.*, 2014). Notamment, NS4B s'est montrée être une cible thérapeutique par différents composés en étude clinique depuis quelques années (discuté dans la section 1.2.1.1) (Wang *et al.*, 2015; Xie *et al.*, 2015). Pour autant, les mécanismes d'action ne sont toujours pas élucidés.

1.3.1 Structure topologique

Comme son nom l'indique, NS4B est la 4ème protéine non structurale du génome viral. Sa forme finale et donc mature d'un poids moléculaire de 28kDa et de 248 acides aminés est composée de deux domaines associés à la membrane intra RE (PM1 et PM2) et de trois domaines transmembranaires (PTM3, PTM4 et PTM5) ce qui en fait d'elle une protéine membranaire hydrophobe (figure 1.11) (Miller *et al.*, 2006). Cependant, NS4B n'est pas toujours retrouvée sous cette forme puisqu'elle doit au préalable subir une maturation enzymatique (Cahour *et al.*, 1992).

En effet, la forme immature de NS4B (46kDa) est toute d'abord liée à NS4A par un peptide signal 2K (2kDa). La première réaction enzymatique réalisée par la protéase virale NS2B3 permet d'obtenir la forme pseudo mature (30kDa) libérée de NS4A et détachée de NS5 mais toujours liée à 2K. Le peptide signal 2K, la partie carboxy-terminale de NS4A permet la translocation de NS4B du côté transmembranaire intra RE. Une fois la translocation terminée, le peptide 2K subit un clivage enzymatique par une signal peptidase.

Très intéressant, une région ultra conservée entre PTM3 et PTM4, la boucle cytosolique, présente dans le cytosol, possède un rôle important puisque c'est elle qui permet l'interaction protéine-protéine avec NS3. En effet, étudié par la méthode de substitution à l'alanine, les résidus Q134, G140 et M140, important dans l'interaction avec NS3, abolissent la réplication virale démontrant la valeur essentielle de cette très petite structure de NS4B (Chatel-Chaix *et al.*, 2015; Zou *et al.*, 2015a).

Finalement, bien que l'importance de NS4B dans sa globalité ait principalement été étudié chez le VDEN, la proximité génétique entre le VDEN et le VZIK pourrait suggérer des mécanismes conservés impliqués dans la mise en place d'un environnement favorable à la réplication.

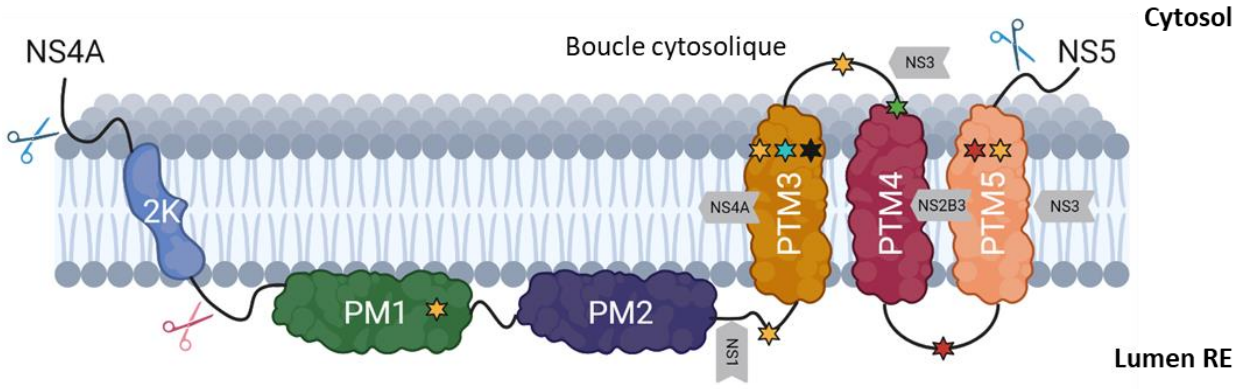

Figure 1.11 Topologie de la protéine virale NS4B des *Flavivirus*

Représentation schématique de la topologie, des interactions et des inhibitions de NS4B. Ciseaux bleus : NS2B3 ; ciseaux rouges : signal peptidase ; étoiles jaunes : site d'inhibition par JNJ-A07 ; étoile bleue : site d'inhibition par JNJ-1A ; étoile rouge : site d'inhibition par NITD-688 ; étoile verte : site d'inhibition par SDM25N ; étoile noire : site d'inhibition par NITD-618 ; flèches grises : site d'interaction protéine-protéine. Schéma réalisé à l'aide de la ressource en ligne BioRender (**https://biorender.com/**).

1.3.2 Le rôle de NS4B dans les usines de réplication

Malgré qu'il n'y ait pas d'évidence à ce jour d'une modulation des URv par NS4B, cette dernière pourrait tout de même jouer un rôle important dans la mise en place des URv. En effet la topologie spécifique de NS4B (et de NS4A) entièrement membranaire force la courbure de la membrane du RE vers le lumen induisant des invaginations (Miller *et al.*, 2007; Miller *et al.*, 2006; Roosendaal *et al.*, 2006). Ceci est dû aux structures en hélices présent parallèlement du côté luminal du RE. Comme déjà mentionné dans la section 1.1.2.2, l'expression seule de NS4A du VDEN est capable de partiellement former les CM à partir des membranes du RE (Miller *et al.*, 2007). Cependant il y'a une différence structurale observée entre les CM formés par surexpression de NS4A seule et une infection avec le VDEN démontrant que NS4A seule n'est pas suffisant à réaliser un tel processus. Lors de la maturation de NS4B, la protéine virale est d'abord transloquée au niveau de la membrane du RE à l'aide de son peptide signal 2K. Cette translocation pourrait forcer la courbure de la membrane lors du clivage protéolytique du 2K et la maturation de NS4B (Miller *et al.*, 2007). Il faut aussi prendre en compte que l'oligomérisation de ces deux protéines virales pourrait également jouer un rôle dans la mise en place des usines de réplication (Stern *et al.*, 2013).

1.3.3 Le rôle de NS4B dans l'immunité

Pour contrer le système immunitaire antivirale, les *Flavivirus* ont beaucoup évolué pour développer des stratégies leurs permettant de survivre dans les cellules des mammifères et réaliser leur cycle viral. La protéine virale NS4B est un facteur important dans l'évasion de la réponse immunitaire de la cellule hôte.

L'expression des interférons de type I et III (IFN I et IFN III) fait partie de la réponse innée précoce antivirale en réponse à une intrusion. Démontré chez le VDEN et le VZIK, NS4B interfère par différents mécanismes dans l'expression des IFN. En effet, NS4B empêche l'induction des gènes de réponse aux interférons en inhibant la phosphorylation activatrice de STAT1/STAT2 bloquant ainsi sa translocation nucléaire (Fanunza *et al.*, 2021; Munoz-Jordan *et al.*, 2005). En addition, NS4B inhibe également la voie principale de reconnaissance des ARN étrangers par les senseurs cytosoliques RIG-I et MDA5. En effet, NS4B inhibe une fois de plus la phosphorylation mais cette fois de IRF3 et TBK1 bloquant l'expression des IFN-β (Dalrymple *et al.*, 2015). La voie cGAS-STING, senseur d'ADN, n'échappe pas non plus à NS4B car l'activité de STING est également inhibée par une possible interaction directe protéine-protéine (Ishikawa *et al.*, 2009). Finalement,

l'élongation mitochondriale causée par NS4B du VDEN accompagnée de l'altération de l'IRM jouent également un rôle important dans l'immunité antivirale (discuté à la section 1.7.3.1).

1.3.4 NS4B et ses interactions protéine-protéine

L'importance de NS4B dans la réplication virale repose essentiellement sur sa capacité à se lier à d'autres protéines. En effet, de nombreuses interactions protéine-protéine ont été démontrées jusqu'à présent impliquant NS4B et des protéines virales ou cellulaires. On peut citer par exemple les cas de NS4B-NS1, NS4B-NS2B, NS4B-NS3 ou encore NS4B-NS4A dans le cas d'une interaction entre protéines virales et de NS4B-VCP dans le cas d'une interaction entre protéines virales et cellulaires parmi tant d'autres. Eventuellement, cette capacité incroyable à lier de nombreuses protéines différentes servirait à séquestrer des protéines néfastes pour le virus.

1.3.4.1 Interactions avec des protéines virales

NS1 est une protéine virale importante dans la réplication virale ou dans l'interférence du système immunitaire (Muller *et al.*, 2013). Chez le VNO, une étude de spectrométrie de masse montre que NS1 interagit par l'intermédiaire de ces résidus R10 et Q11 avec NS4B à son résidus F86 entre les domaines PM2 et PTM3 (figure 1.11) (Youn *et al.*, 2012). Il semblerait que son interaction avec NS4B favorise sa localisation au niveau des membranes cellulaires lors de l'infection permettant par la suite son homodimèrisation (Giraldo *et al.*, 2018). De plus, l'interaction de NS1 avec la forme immature de NS4B, c'est-à-dire NS4A-2K-NS4B, semble essentielle dans la réplication de l'ARNv (Plaszczyca *et al.*, 2019).

Toujours chez le VNO, la colocalisation de NS4B et de NS2B au niveau de la membrane du RE suggère une interaction entre les deux protéines virales (figure 1.11) (Yu *et al.*, 2013). En effet, l'étude confirme leur proximité d'environ 10nm par la technique de transfert d'énergie par résonance de fluorescence (FRET). Cette interaction serait impliquée dans le recrutement de la protéine virale NS3 au niveau de la membrane du RE et permettrait de la lier au domaine cofacteur NS3 de NS2B formant ainsi la protéase virale NS2B3.

La protéine NS3 qui avec NS2B forme la protéase virale a également été identifiée dans les protéines interagissant avec NS4B. En effet, la colocalisation de NS4B, NS3 et de l'ARNv double brin active l'activité hélicase de NS3 permettant la séparation de l'ARNv double brin (Umareddy *et al.*, 2006). Une récente étude suggère également que les résidus 51 à 83 de NS4B améliorent l'activité hélicase de NS3 (Lu *et al.*, 2021). Cette interaction est rendue possible par la boucle

cytosolique entre PTM3 et PTM4 qui interagit avec les résidus I190 et P319 de NS3 (figure 1.11) (Chatel-Chaix *et al.*, 2015; Lu *et al.*, 2021).

L'interaction entre NS4B et NS4A chez le VDEN a été montrée par des études de biophysique et déterminée par utilisation de protéines virales recombinantes (Zou *et al.*, 2015b). Les résidus impliqués dans l'interaction sont L48, T54 et L60 de NS4A (Zou *et al.*, 2015a; Zou *et al.*, 2015b). Une mutation de ces résidus affecte l'interaction NS4B-NS4A et abolit la réplication virale. Chez le VEJ, il semblerait que les résidus impliqués dans l'interaction soient A97 pour NS4A et Y3 pour NS4B (Tajima *et al.*, 2011). Une mutation de ces résidus aboutit à une diminution de la réplication virale montrant l'importance de l'interaction NS4B-NS4A dans le cycle viral des *Flavivirus* (Li *et al.*, 2015b).

Finalement, NS4B interagit avec lui-même par homodimèrisation. En effet, une étude *in vitro* chez le VNO par mutagénèse a montré que l'homodimèrisation est réalisée par l'interaction entre les régions contenant les résidus 129 à 165 de la boucle cytosolique et les résidus 166 à 248 de la région C-terminal (figure 1.11) (Zou *et al.*, 2014). Bien que la fonction de l'homodimèrisation de NS4B soit encore inconnue, il semblerait que son homodimèrisation soit importante pour la réplication virale.

1.3.4.2 Interactions avec des protéines de l'hôte

Outre les interactions de NS4B avec des protéines virales, cette protéine est également connue pour interagir avec diverses protéines cellulaires dans le but d'atténuer ou d'activer des processus cellulaires dans le bénéfice de la réplication virale. Par exemple, le complexe oligosaccharyltransférase (OST), une composante intégrale de la membrane du RE ayant pour rôle la glycosylation post-traductionnelle des protéines, interagit avec NS4B (Lin *et al.*, 2017a). Alors que les fonctions catalytiques d'OST (STT3A et STT3B) ne sont pas nécessaires pour le VDEN, la sous-unité MAGT1, en particulier le motif CXXC de son site d'oxydoréductase, est en revanche essentielle pour la réplication du virus. Il semblerait que NS4B soit recrutée par le motif CXXC d'OST au niveau de la membrane du RE.

Un autre exemple d'interaction avec NS4B est celui de la protéine réticulum endoplasmique kinase-like 1 (PERK). PERK est un facteur pro-apoptotique qui est suractivé par NS4B du VEJ ainsi permettant l'apoptose des neurones et le stress lié au RE aboutissant aux complications neurologiques associées à une infection au VEJ (Wang *et al.*, 2019). Fait très intéressant, l'interaction implique une seule protéine NS4B et deux protéines PERK, suggérant que NS4B

joue éventuellement un rôle dans la dimérisation de PERK, cette dernière étant la forme activatrice de l'apoptose.

Un dernier exemple important dans les interactions de NS4B avec des protéines de l'hôte est celui de la valosin-containing protein/p97 (VCP), une protéine qui a beaucoup été étudié ces dernières années. Chez le VEJ, une étude récente montre que NS4B interagit avec VCP via son domaine de liaison avec son cofacteur NLP4 (Arakawa *et al.*, 2022). En effet, NS4B recrute le complexe VCP/NLP4 au site de réplication de l'ARNv pour inhiber les réponses de stress cellulaires et faciliter la synthèse des protéines virales. Dans cette étude, l'expression de NS4B ou de VCP seule permet d'annuler la formation de granule de stress. Ceci suggère fortement un rôle important du recrutement de VCP par NS4B pour faciliter la réplication virale. De plus, nous avons récemment montré que NS4B s'associe avec VCP dans les CM induites par le virus (Anton *et al.*, 2021). En effet, nos travaux ont permis d'identifier l'interaction protéine-protéine entre VCP et NS4B du VZIK. Dans des cellules infectées, l'inhibition de l'activité de VCP cause une diminution de la stabilité de NS3, sans altérer l'interaction NS3-NS4B ni l'expression d'autres protéines virales. Cela conduit à une réduction de l'abondance et de la taille des CM, à une inhibition de l'élongation mitochondriale et à une augmentation de l'apoptose. De ce fait, cette étude révèle VCP comme un facteur cellulaire nécessaire à la réplication du VZIK, en particulier pour maintenir l'intégrité des URv.

Pour conclure sur cette protéine, NS4B est essentielle à la réplication virale, à l'évasion du système immunitaire, et est également la cible thérapeutique de molécules actuellement en études clinique. Ainsi, NS4B est une protéine qui mérite plus d'attention et une meilleure compréhension dans ses différents rôles au sein du cycle flaviviral et ses interférences dans les processus cellulaires tels que l'immunité innée par exemple. Mon directeur de thèse s'est particulièrement intéressé à cette protéine durant les dernières années et a étudié son interactome au niveau cellulaire (Chatel-Chaix *et al.*, 2016). Les données en spectrométrie de masse ont montré plus d'une dizaine de protéines interagissant avec NS4B dont la plupart étant des protéines mitochondriales.

1.4 La mitochondrie

« Il y a environ 1,5 à 2 milliards d'années, la vie unicellulaire a connu un tournant majeur grâce à l'intégration par endosymbiose d'une α-protéobactérie dans une protocellule eucaryote. Ce phénomène est à l'origine d'une composante intracellulaire complexe qui, au cours de l'évolution, est devenue un organite jouant un rôle central dans la vie des cellules eucaryotes : la

mitochondrie. De taille avoisinant quelques micromètres, cet organite est capable de se déplacer dans le cytoplasme le long du cytosquelette par des kinésines (transport antérograde) et des dynéines (transport rétrograde) (Pilling *et al.*, 2006). Généralement présent en grande quantité dans la plupart des cellules eucaryotes supérieures, cet organite contribue au métabolisme énergétique de la cellule, notamment par l'intermédiaire de la β-oxydation, du cycle de Krebs ou encore de la phosphorylation oxydative (Spinelli *et al.*, 2018). Source principale d'ATP dans la cellule, la mitochondrie s'est vue attribuée le surnom de « centrale énergétique de la cellule ». Pourtant, depuis quelques décennies, nous savons qu'au-delà des fonctions métaboliques et respiratoires, les mitochondries jouent également des rôles importants dans l'apoptose et la sénescence cellulaire, le contrôle du cycle cellulaire ou encore la réponse antivirale pour n'en citer que quelques-uns (Antico Arciuch *et al.*, 2012; McBride *et al.*, 2006; Weinberg *et al.*, 2015). » (Freppel *et al.*, 2022)

1.4.1 Structure

Les mitochondries ont une longueur allant de 1 à 10 µm en moyenne pour un diamètre de 1 à 3 µm et sont isolées du cytoplasme par une membrane externe (MEM), un espace intermembranaire (EIM) et d'une membrane interne (MIM) en crête renfermant la matrice mitochondriale.

1.4.1.1 La membrane externe mitochondriale

La MEM est la première barrière séparant les composantes cytoplasmiques des composantes mitochondriales. D'une épaisseur d'environ 6 à 7.5 nm, cette membrane est composée principalement de phospholipides retrouvés dans la plupart des membranes cellulaires avec un enrichissement en phosphatidylcholine (PC), en phosphatidyléthanolamine (PE), en phosphatidylinositol (PI), en phosphatidylsérine (PS) et en acide phosphatidique (PA) (Osman *et al.*, 2011; Tamura *et al.*, 2020; Zinser *et al.*, 1991). De plus, la MEM possède une signature particulière en possédant également des phosphatidylglycérol (PG) et des cardiolipines (CL) (Houtkooper *et al.*, 2008).

La MEM est également caractérisée par la présence de nombreuses protéines membranaires impliquées dans les échanges cytoplasmiques / mitochondriaux. En effet, les porines formant des canaux dans la membrane permettent le transport de petites molécules hydrophiles, telles que les anions ou des cations (Ellenrieder *et al.*, 2019). La porine « voltage-dependent annion channel 1 (VDAC1) » permet le transport de potassium, sodium ou de calcium (Bayrhuber *et al.*, 2008;

Camara *et al.*, 2017). Dans le cas de molécules de taille plus importante, des translocases sont nécessaires telles que la « translocase outer membrane 40 (TOM40) » ou encore la TOM 22 (Endo *et al.*, 2010).

1.4.1.2 L'espace intermembranaire mitochondriale

Dans un contexte évolutif, l'EIM est aux mitochondries ce que le périplasme est aux bactéries, c'est-à-dire un espace séparant les deux membranes externe et interne. D'une épaisseur de 20 nm environ, l'EIM possède une composition similaire à celle du cytosol en partie dû à la présence élevée de porines dans la MEM (Yartsev, 2019). Cependant, l'EIM est caractérisé par la présence importante de cytochrome C, qui joue un rôle dans le transport des électrons et dans l'interaction avec la cardiolipine (Garrido *et al.*, 2006). L'EIM est une étape intermédiaire dans le transport des molécules du cytosol à la matrice mitochondriale ou vice versa.

1.4.1.3 La membrane interne mitochondriale

La MIM est la barrière séparant l'espace intermembranaire de la matrice mitochondriale. Celle-ci forme des invaginations dans la matrice, appelées crête, permettant une surface de la MIM plus importante que la MEM. La dynamique des cristaes varie en fonction de l'état physiologique de la cellule, c'est-à-dire des stress, tels que l'apoptose ou des besoins énergétiques. En termes de composition, la signature lipidique est similaire à la MEM, cependant, la MIM est caractérisée par la présence de protéines transmembranaires impliquées dans la chaîne respiratoire mitochondriale (Osman *et al.*, 2011; Tamura *et al.*, 2020; Zinser *et al.*, 1991). Cette particularité confère à la MIM un rôle important dans la production d'ATP et dans la survie cellulaire expliquant ainsi la raison d'une surface imposante par rapport à la MEM. Notamment, le transport de molécules de part et d'autre de la MIM est réalisé par la présence de « translocase inner membrane (TIM) » (Bauer *et al.*, 2000).

1.4.1.4 La matrice mitochondriale

La matrice mitochondriale est le cœur de la mitochondrie et est composée d'ADN mitochondriale (ADNm), de ribosomes, d'enzymes solubles et de nombreux autres métabolites intervenant dans des processus métaboliques propres à la mitochondrie. En effet, la matrice mitochondriale est le site du cycle de Krebs qui permet de nourrir la chaine respiratoire mitochondriale (Murphy *et al.*, 2016). Par ces diverses fonctions impliquées dans le métabolisme, la matrice mitochondriale est

une importante composante de la mitochondrie lui conférant son célèbre surnom d'usine énergétique.

1.4.2 Dynamique : fusion et fission

« Outre leur mobilité intracellulaire, lorsque l'on observe des mitochondries dans des cellules vivantes, il est évident que leur forme est en constante évolution. En effet, les mitochondries changent de longueur et peuvent se présenter sous forme allongée ou sphérique selon l'état de stress ou de croissance de la cellule. D'une manière générale, elles oscillent entre ces deux états très rapidement par un mécanisme de régulation dynamique qui permet de répondre rapidement aux besoins de la cellule. Plus généralement, la forme des mitochondries repose sur un équilibre entre leur fusion (menant à leur élongation) et leur fission (résultant en un aspect fragmenté). Par exemple, l'aspect allongé des mitochondries peut résulter soit d'une stimulation de leur fusion, soit d'une altération de leur fragmentation. Cette morphodynamique mitochondriale est régulée dans le temps et dans l'espace par des facteurs de fusion et de fission (figure 1.13). » (Freppel *et al.*, 2022)

« Les mitofusines MFN1 et MFN2 sont responsables de la fusion des membranes mitochondriales externes, et OPA1 (« *optic atrophy 1* ») de celles des membranes mitochondriales internes. Brièvement, lors de la fusion, l'ancrage de deux mitochondries est contrôlé par l'interaction entre deux molécules MFN1 ou MFN2 par l'intermédiaire de leur domaine HR2 et la fusion membranaire dépend de leur activité GTPase (Ishihara *et al.*, 2004; Koshiba *et al.*, 2004). » (Freppel *et al.*, 2022)

« Le transfert aux mitochondries du facteur de fission DRP1 (« *dynamin-related protein 1* ») par l'interaction avec ses récepteurs mitochondriaux MFF (« *mitochondrial fission factor* »), FIS1 (« *mitochondrial fission 1 protein* »), MID49 (« *mitochondrial dynamics protein 49* ») et MID51 (« *mitochondrial dynamics protein 51* ») régule la fragmentation des mitochondries (Westermann, 2010). Lors de la fission, la phosphorylation de DRP1 sur la sérine 616 active son transfert aux mitochondries et la formation d'une structure en hélice au niveau de sites de pré-constriction formés par le RE (Friedman *et al.*, 2011; Yoon *et al.*, 2001). Ainsi, l'IRM maintenue par des interactions protéine-protéine gardant une distance d'environ 10 à 25 nm entre les deux organites implique que le RE contrôle également la morphologie mitochondriale (Giacomello *et al.*, 2016). À l'inverse, la phosphorylation de la sérine 637 de DRP1 inhibe le transfert de DRP1 favorisant ainsi indirectement la fusion (Chang *et al.*, 2007). Les mitochondries fusionnent ou se fragmentent constamment selon l'état fonctionnel et les besoins métaboliques de la cellule. En effet, il y a

fusion si les mitochondries sont très mobiles avec une augmentation de la consommation en O_2, de la production d'ATP et du potentiel de membrane tandis qu'une situation inverse provoque la fission mitochondriale (Westermann, 2012). » (Freppel *et al.*, 2022)

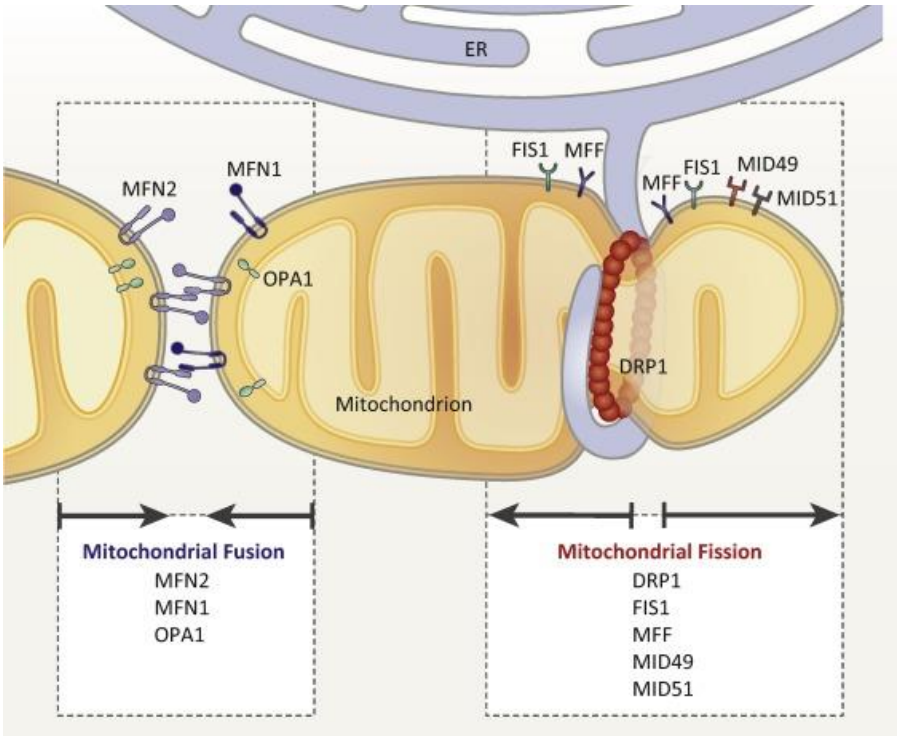

Figure 1.12 Dynamique morphologique de la mitochondrie

Les facteurs de fusion MFN1 et MFN2 participent à la fusion des membranes mitochondriales externes tandis que OPA1 fusionne les membranes mitochondriales internes. Les récepteurs FIS1, MFF, MID49 et MID51 recrute DRP1 au niveau des sites de constrictions par le RE pour fragmenter la mitochondrie. (Sebastian *et al.*, 2017)

1.4.3 Fonctions

1.4.3.1 Métabolisme énergétique

La respiration cellulaire mitochondriale est la principale voie de production d'ATP regroupant différents processus se passant dans plusieurs compartiments cellulaires. Dans le cytosol, la glycolyse métabolise le glucose en pyruvate suivi par sa décarboxylation en acétyl-CoA (Li *et al.*, 2015a). Ce dernier (également produit par la β-oxydation mitochondriale) est pris en charge par le cycle de Krebs qui s'effectue dans la matrice mitochondriale. Au sein de la membrane interne de la mitochondrie, le processus général de la phosphorylation oxydative nourrit par le cycle de

Krebs et la β-oxydation permet la phosphorylation de molécules d'ADP en ATP (Papa *et al.*, 2012). La respiration cellulaire aérobique peut théoriquement produire 38 molécules d'ATP par molécule de glucose. Cependant, en raison de diverses pertes, notamment le coût de transport du pyruvate, du phosphate et de l'ADP vers les mitochondries, la réelle production atteint 30 à 32 ATP par cycle (Chaudhry *et al.*, 2021).

La β-oxydation

La β-oxydation est une voie métabolique mitochondriale permettant la dégradation des acides gras à la suite de leur activation en acyl-CoA par l'enzyme acyl-CoA synthétase (figure 1.14). En effet, cette voie permet par l'intermédiaire de différentes étapes enzymatiques de nourrir le TCA en acétyl-CoA et la phosphorylation oxydative en NADH et $FADH_2$ (Bartlett *et al.*, 2004). Cette voie peut également être réalisée par les péroxysomes (Poirier *et al.*, 2006).

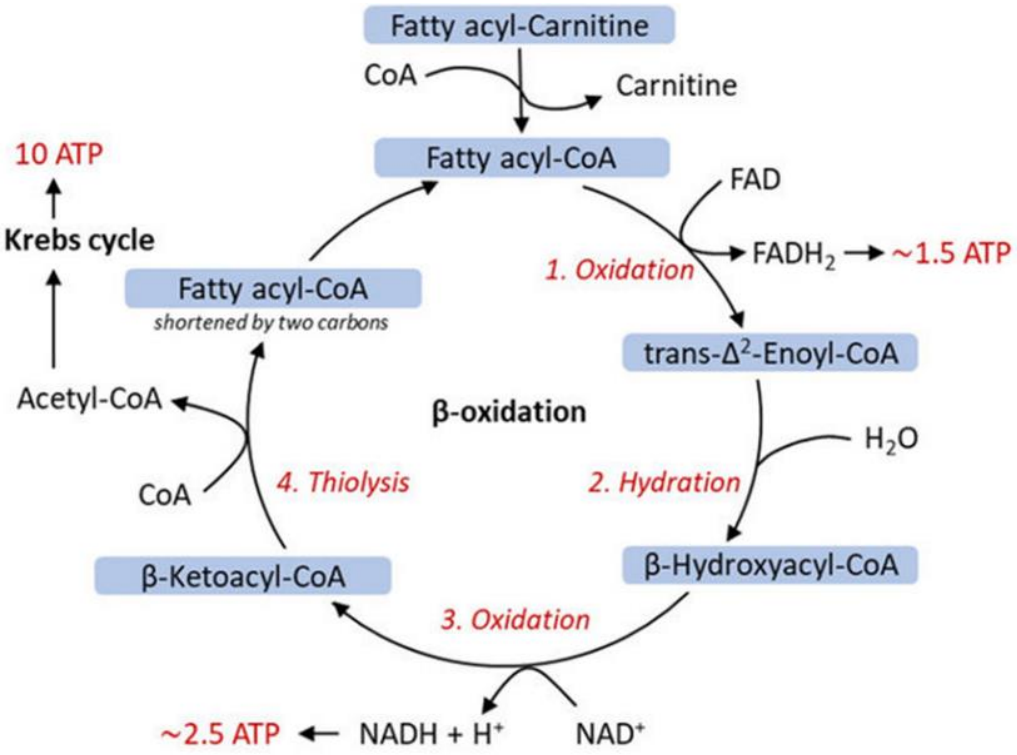

Figure 1.13 La β-oxydation

La bêta-oxydation est un processus métabolique essentiel qui dégrade les acides gras pour produire de l'énergie. Elle se déroule dans les mitochondries et se compose de plusieurs étapes enzymatiques. L'acyl-CoA, formé à partir de l'acide gras, est dégradé en acétyl-CoA par élimination de groupes de deux atomes de carbone successifs. Ce processus génère de l'énergie sous forme de NADH et FADH2. Modifiée de (Kloska *et al.*, 2020)

Dans la matrice mitochondriale, l'acyl-CoA subit une déshydrogénation par le FAD pour produire du trans-Δ^2-énoyl-CoA et du $FADH_2$ grâce à la catalysation par l'enzyme acyl-CoA déshydrogénase. La deuxième étape hydrate réversiblement le trans-Δ^2-énoyl-CoA en L-β-hydroxyacyl-CoA par l'énoyl-CoA hydratase. Le L-β-hydroxyacyl-CoA est ensuite oxydé par le NAD^+ en β-cétoacyl-CoA par l'action enzymatique de la 3-hydroxyacyl-CoA déshydrogénase et génère du $NADH+H^+$. Finalement, la dernière étape réalisée par l'enzyme acétyl-CoA C-acyltransférase génère à partir du β-cétoacyl-CoA une molécule de acyl-CoA et une molécule de acétyl-CoA. La β-oxydation se poursuit sur un acide gras tant que la chaine carbonée n'est pas entièrement découpée. En effet, chaque cycle retire deux atomes de carbone et une molécule d'acétyl-CoA de l'acyl-CoA généré à partir d'un acide gras. Le bilan énergétique est finalement aléatoire dépendamment de la taille des acides gras dégradés par la β-oxydation.

Le cycle de Krebs

Le cycle de Krebs ou le cycle de l'acide citrique (TCA) est une voie complexe mitochondriale permettant d'oxyder l'acétyl-CoA provenant de la glycolyse cytoplasmique ou de la β-oxydation en huit étapes afin de générer de l'énergie sous forme de GTP mais également des substrats permettant l'activité de la phosphorylation oxydative, tels que le NADH ou le succinate (figure 1.15) (Alabduladhem *et al.*, 2022).

Au sein de la matrice mitochondriale, l'enzyme citrate synthase catalyse irréversiblement dans la première étape du cycle, l'acétyl-CoA et l'oxaloacétate en acide citrique. Ce dernier est catalysé dans la deuxième étape en cis-aconitate puis en isocitrate par l'enzyme aconitase. La décarboxylation oxydative de l'isocitrate par l'isocitrate déhydrogénase lors de la troisième étape produit l'α-cétoglutarate, génère une molécule de CO_2 et réduit une molécule de NAD^+ en NADH et un proton H^+. Cette étape est la première à produire un coenzyme important dans la respiration mitochondriale. La quatrième étape convertit l'α-cétoglutarate en succinyl-CoA par l'intermédiaire de l'enzyme α-cétoglutarate déhydrogénase et réduit également une molécule de NAD+ en $NADH+H^+$ et une molécule de CO_2. Le succinyl-CoA est ensuite transformé par l'enzyme succinyl-CoA synthétase en succinate. Cette cinquième étape est la première à générer une molécule de GTP à partir de la phosphorylation d'une molécule de GDP. L'oxydation du succinate en fumarate est réalisée lors de la sixième étape par l'enzyme succinate déshydrogénase et réduit l'ubiquinone aussi connu sous le nom de coenzyme Q_{10} (CoQ_{10}) en ubiquinol, coenzyme $Q_{10}H_2$ ($CoQ_{10}H_2$). L'enzyme succinate s'avère être le complexe II de la chaine respiratoire. La septième étape hydrate le fumarate en malate par l'action de l'enzyme fumarase en consommant une molécule d'H_2O. L'enzyme malate déshydrogénase oxyde le malate lors de la dernière étape du

cycle en oxaloacétate en produisant à nouveau une molécule de $NADH+H^+$. L'oxaloacétate nouvellement produit peut ainsi recommencer un nouveau cycle. Finalement, le TCA produit deux molécules de CO_2, trois molécules de $NADH+H^+$, une molécule de $CoQ_{10}H_2$, une molécule de $FADH_2$ et une molécule de GTP. Les molécules $NADH+H^+$ et $CoQ_{10}H_2$ sont ensuite utilisées par la phosphorylation oxydative.

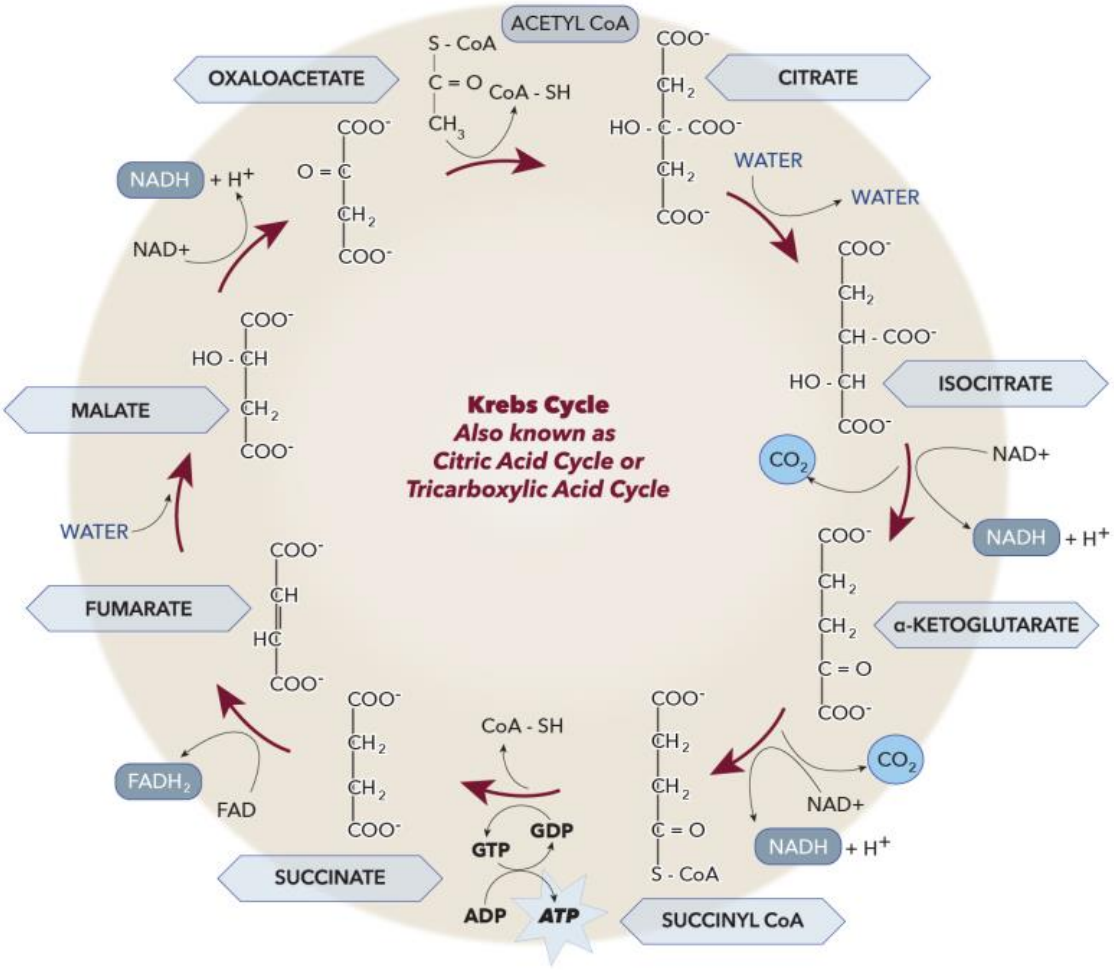

Figure 1.14 Le cycle de Krebs

Le cycle de Krebs est une voie complexe mitochondriale permettant d'oxyder l'acétyl-CoA provenant de la glycolyse cytoplasmique en huit étapes afin de générer de l'énergie sous forme d'ATP mais également des substrats permettant l'activité de la phosphorylation oxydative tels que le NADH ou le succinate (Alabduladhem *et al.*, 2022).

La phosphorylation oxydative

La respiration oxydative ou la phosphorylation oxydative (OXPHOS) est la principale source d'ATP dans la cellule. Cette voie, réalisée au niveau de la membrane interne mitochondriale par l'intermédiaire de différents complexes enzymatiques, consomme les substrats produits par le TCA et consomme de l'oxygène (figure 1.16). L'OXPHOS est composée de quatre complexes intervenant dans la chaine de transport d'électrons (CTE) et de la chimiosmose composée uniquement d'un seul complexe, l'ATP synthase (Cooper, 2000).

Le complexe I ou NADH déshydrogénase est la première enzyme de la CTE. L'enzyme est composée de 45 sous-unités protéiques membranaires dont sept sont codées par l'ADNm (Carroll *et al.*, 2006). Cette enzyme oxyde le NADH en NAD^+ libérant 2 électrons qui réduisent le CoQ_{10} en $CoQ_{10}H_2$. Cette réaction permet la sortie de quatre protons dans l'EIM en échange de deux électrons libérés dans la CTE. Le complexe I peut être inhibé par l'action de la roténone en agissant sur son site de liaison à la CoQ_{10} ainsi bloquant le transfert d'électrons (Lambert *et al.*, 2004).

Le complexe II ou succinate déhydrogénase est composé de quatre sous-unités, la succinate déhydrogénase (SDHA), la « succinate dehydrogenase ubiquinone iron–sulfur subunit mitochondrial (SDHB) », la « succinate dehydrogenase complex subunit C (SDHC) » et la « succinate dehydrogenase complex subunit D (SDHD) ». Cette enzyme catalyse l'oxydation du succinate en fumarate et réduit également le CoQ_{10} en $CoQ_{10}H_2$ (sixième étape du TCA). Cette étape transfert 2 électrons du succinate au CoQ_{10} et ne possède pas d'échange de H^+.

Le complexe III ou cytochrome C réductase est composé de onze sous-unités : trois sous-unités à groupe prosthétique ; deux sous-unités cytochrome b, une sous-unité cytochrome c et de six sous-unités de faible poids moléculaires (Zhang *et al.*, 1998). Le complexe III libère deux électrons lors de l'oxydation du $CoQ_{10}H_2$ en CoQ_{10}. Ces deux électrons sont transférés à deux molécules cytochrome C permettant leur réduction. Cette réaction permet de libérer quatre protons dans l'EIM par un gradient de proton. Le complexe III peut être inhibé par l'action de l'antimycine A en agissant sur le site Q_1 de l'enzyme cytochrome C réductase ainsi bloquant l'oxydation du $CoQ_{10}H_2$ (Kim *et al.*, 1999).

Le complexe IV ou cytochrome C oxidase est composé de quatorze sous-unités, dont trois transcrits codés par l'ADNm, et de plusieurs sites aux hèmes (Zong *et al.*, 2018). Le complexe IV finalise le transport d'électrons à travers la CTE. En effet, il retire quatre électrons de quatre molécules de cytochrome C et les transfère à des molécules d'oxygène. Le dyoxygène est alors

réduit en deux molécules d'H_2O libérant quatre protons H^+ dans l'EIM par le complexe IV générant un gradient proton.

Le complexe V ou ATP synthase est composé de deux régions membranaires, une étant ancrée dans la MIM (région F_o) et l'autre en contact direct avec la matrice mitochondriale (région F_1) (Jonckheere *et al.*, 2012). Le complexe V fonctionne par chimiosmose, c'est-à-dire en la phosphorylation de l'ADP en ATP par l'intermédiaire d'un gradient proton H^+. Le gradient proton crée un gradient électrochimique utilisé par la région F_o permettant le transfert de proton H^+ dans la matrice mitochondriale. L'énergie libérée lors du passage des protons H^+ déclenche la rotation de la région F_o, activant la phosphorylation de l'ADP en ATP. Le complexe V peut être inhibé par l'action de l'oligomycine en bloquant le canal à protons présent sur la région F_o ainsi empêchant la phosphorylation de l'ADP en ATP (Jastroch *et al.*, 2010).

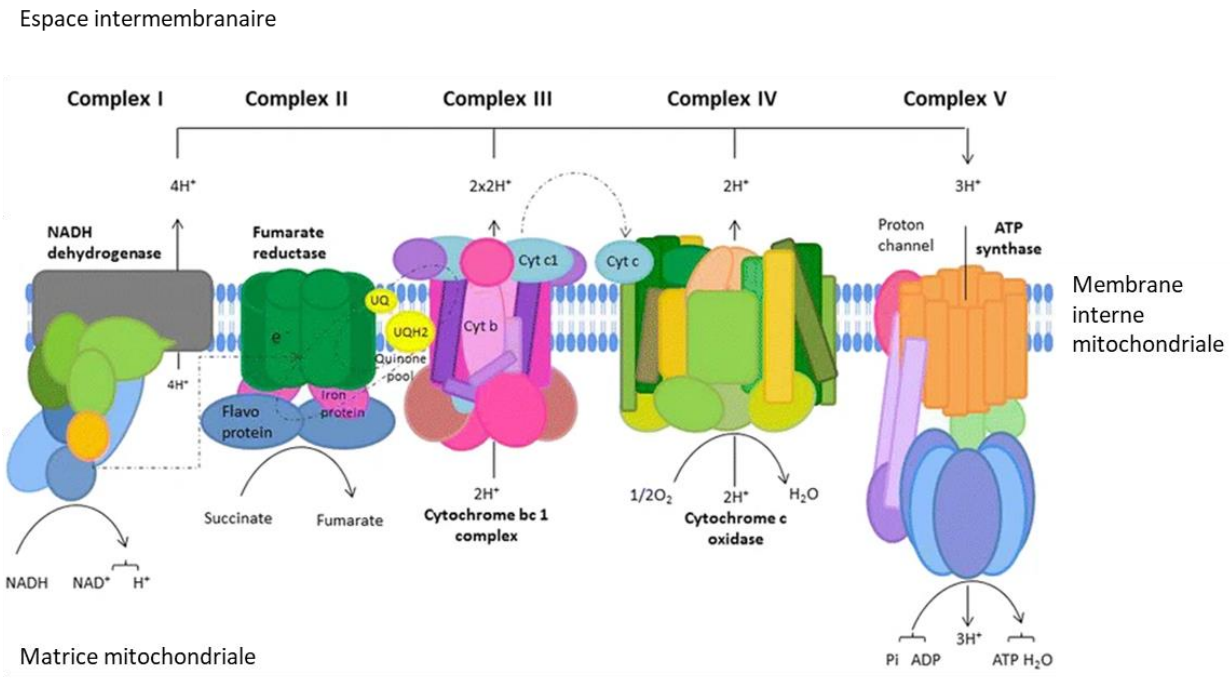

Figure 1.15 La phosphorylation oxydative

Le complexe I oxyde le NADH en NAD^+ libérant 2 électrons qui seront transportés du complexe I au III par la coenzyme Q_{10}. Les électrons sont ensuite transférés au cytochrome c (complexe III) puis au cytochrome b (complexe IV) en réduisant l'O_2. Le complexe V permet la phosphorylation de l'ADP en ATP par l'intermédiaire du gradient à protons généré par la chaine de transport d'électrons. (Granata *et al.*, 2015)

1.4.3.2 Apoptose

« L'apoptose est une mort cellulaire programmée à la suite d'un stress permettant à la cellule de s'auto-détruire. Elle peut être activée par 2 voies possibles, la voie extrinsèque impliquant des récepteurs de la superfamille des facteurs de croissance tumorale et la voie intrinsèque faisant intervenir la mitochondrie par le biais des protéines de la famille BCL-2 (Elmore, 2007). » (Freppel *et al.*, 2022)

En effet, cette dernière est notamment activée lorsque les cellules sont soumises à un stress modifiant la perméabilité membranaire des mitochondries provoquée par les facteurs pro-apoptotiques. Ces stress peuvent être divers tels que des dommages directs à l'ADN, hypoxie, une surcharge en calcium ou des oncogènes, par exemple. Premièrement, la voie p53 est activée par phosphorylation par des facteurs réagissant aux différents stress cellulaires, tels que ATM ou Chk2 (Cheng *et al.*, 2010; Lahav, 2008). La protéine p53 activée initialise ensuite la voie apoptotique par transcription de facteurs pro-apoptotiques de la famille des Bcl2, tels que BAK et BAX et en réprimant les facteurs opposés, c'est-à-dire anti-apoptotique, tel que Bcl2 et Bcl-xL (Shen *et al.*, 2001). Ceci a pour effet de libérer dans le cytosol le cytochrome C et MCL1 (« *induced myeloid leukemia cell differentiation protein* »), ce qui conduit à l'activation de APAF1 (« *apoptotic protease-activating factor 1* ») puis des caspases 9 et 3 qui en retour, activent des facteurs apoptotiques et engagent la phase d'exécution de l'apoptose.

L'impact de la morphologie mitochondriale a récemment été également mis en évidence dans la voie apoptotique (Jenner *et al.*, 2022). En effet, La protéine DRP1 impliquée dans la fission mitochondriale est recrutée par BAX et interagit physiquement avec sa partie N-terminale. Cette interaction active la translocation de DRP1 au niveau des membranes mitochondriales lorsque la voie apoptotique est engagée. Ceci a pour but de moduler la perméabilisation membranaire et la fragmentation mitochondriale par DRP1 afin de favoriser l'apoptose ou la mitophagie.

1.4.3.3 Mitophagie

« La mitophagie consiste en la dégradation sélective des mitochondries par autophagie. Cette dernière est la conséquence de différents types de stress tels que l'hypoxie (Bellot *et al.*, 2009; Zhang *et al.*, 2008), la dépolarisation mitochondriale (Matsuda *et al.*, 2010; Narendra *et al.*, 2008) ou l'accumulation des ROS (Xiao *et al.*, 2017a; Xiao *et al.*, 2017b) permettant le recyclage des mitochondries par voie lysosomale (Galluzzi *et al.*, 2017; Kroemer *et al.*, 2010; Mizushima, 2018). La voie d'activation de la mitophagie impliquant les protéines PINK1 (« *PTEN-induced putative*

kinase 1 ») et Parkin est la mieux caractérisée (Jin *et al.*, 2010; Lazarou *et al.*, 2015; Meissner *et al.*, 2011). Brièvement, PINK1 détecte le dommage des mitochondries, souvent fragmentées, par l'entremise de la phosphorylation de l'ubiquitine. Cela conduit au transfert mitochondrial et à l'activation de Parkin, une ligase d'ubiquitine de type E3. Le complexe PINK1/Parkin mitochondrial va alors induire le recrutement du phagophore, la membrane isolée à l'origine de la formation de l'autophagosome. » (Freppel *et al.*, 2022)

1.5 L'interface réticulo-mitochondriale

Bien connue dans la littérature depuis quelques années maintenant, l'IRM, c'est-à-dire l'interaction membrane-membrane du RE et des mitochondries a été mise en avant pour son implication dans divers processus cellulaires, tels que l'homéostasie lipidique et calcique ou encore dans l'immunité innée précoce antivirale (Anastasia *et al.*, 2021; Horner *et al.*, 2011; Jacobs *et al.*, 2013; Ma *et al.*, 2021; Patergnani *et al.*, 2011). Dans cette thèse, nous parlerons de sa structure, ses fonctions et son potentiel détournement par les virus.

1.5.1 Structure

Les observations de l'IRM en microscopie électronique montrent une étroite proximité entre les membranes du RE et la MEM sans pour autant qu'elles soient en direct contact. En effet, cette distance est maintenue par des interactions protéine-protéine qui permettent également des échanges moléculaires. Dépendamment du type membranaire du RE, c'est-à-dire lisse ou rugueux, la distance séparant les deux organites est différente (Giacomello *et al.*, 2016). Dans le cas d'une interaction RE lisse, la distance est d'environ de 10 à 20 nm tandis que l'interaction avec du RE rugueux est plutôt de l'ordre de 50 à 80 nm (figure 1.17). Ce phénomène pourrait être expliqué par la présence des ribosomes à la surface du RE rugueux qui rajouterait une distance supplémentaire.

Puisque la distance est vraiment très minime, il est évident que des protéines soient impliquées dans le maintien de l'intégrité de l'IRM (figure 1.17). Ces interactions protéine-protéine ont été bien étudiées jusqu'à présent. Bien que l'IRM possède de nombreuses interactions, telles que l'interaction entre la protéine membranaire du RE « Inverted formin-2 (INF2) » avec la protéine membranaire externe des mitochondries « Spire Type Actin Nucleation Factor 1c (SPIRE1c) » (Manor *et al.*, 2015) ou encore entre la protéine membranaire du RE « oxysterol-binding protein (OSBP)-related proteins 5/8 (ORP5 et ORP8) » avec la protéine membranaire externe des mitochondries « ATPase Family AAA Domain Containing 3A (ATAD3A) » (Galmes *et al.*, 2016),

cette thèse discutera essentiellement de 3 interactions protéiques en particulier qui ont montré leur importance dans l'intégrité de l'IRM. La protéine du RE « vesicle-associated membrane protein-associated protein B (VAPB) » interagit avec la protéine mitochondriale « protein tyrosine phosphatase-interacting protein 51 (PTPIP51) or (RMDN3) » formant le couple VAPB-PTPIP51 (De Vos *et al.*, 2012). La protéine du RE « ribosome binding protein 1 (RRBP1) » interagit avec la protéine mitochondriale « synaptojanin 2 binding protein (SYNJ2BP) » formant le couple RRBP1-SYNJ2BP (Hung *et al.*, 2019). La protéine du RE « inositol 1,4,5-triphosphate (IP3R) » interagit avec la protéine mitochondriale « voltage-dependant anion-selective channel 1 (VDAC1) » par l'intermédiaire d'une protéine chaperonne cytosolique « glucose-regulated protein 75 (GRP75) » formant le couple IP3R-VDAC1 (Hartmann *et al.*, 1998).

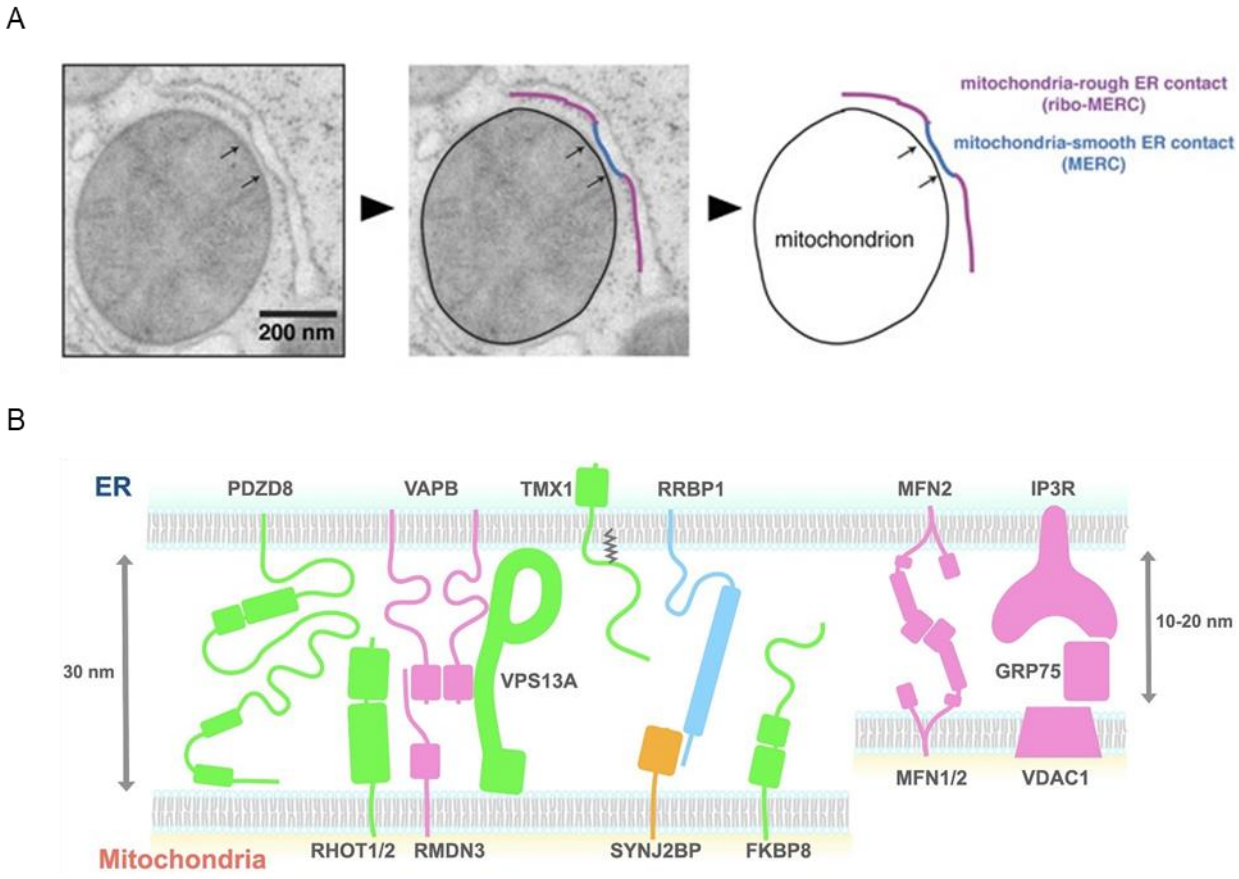

Figure 1.16 Structure de l'interface réticulo-mitochondriale

(A) Observation microscopique de l'IRM. Violet : Contact entre RE rugueux et une mitochondrie. Bleu : Contact entre RE lisse et une mitochondrie. Modifié de (Giacomello *et al.*, 2016). (B) Représentation schématique des interactions protéines-protéines impliquées dans l'IRM. Les couples protéines ER-mitochondriales : VAPB-PTPIP51, RRBP1-SYN2BP, MFN2-MFN1/2 et IPR3-VDAC1 maintiennent l'intégrité de l'interface réticulo-mitochondriale. (Aoyama-Ishiwatari *et al.*, 2021)

1.5.2 Fonctions

D'un point de vue de biologie cellulaire, l'interaction entre deux organites est rarement anodine. En effet, si une interaction se créée, c'est sans aucun doute pour permettre l'échange de molécules ou pour favoriser un processus cellulaire. Nous discuterons dans cette partie essentiellement de quatre importantes fonctions de l'IRM dans ses généralités : la dynamique mitochondriale, l'homéostasie lipidique, l'homéostasie calcique et l'immunité innée précoce antivirale.

1.5.2.1 La dynamique mitochondriale dépendante du RE

La fusion ou fragmentation mitochondriale est importante pour qu'une cellule fonctionne correctement et une perturbation dans la dynamique mitochondriale peut aboutir à des maladies neurodégénératives (Cho *et al.*, 2010). La morphodynamique mitochondriale dépend principalement d'un équilibre entre facteurs de fusion et de fission (discuté dans la section 1.5.2). Cependant, le RE joue un rôle important également dans la fission mitochondriale en créant des sites de constrictions qui permettent le recrutement des facteurs de fission DRP1 et MFF (Friedman *et al.*, 2011). En effet, les tubules du RE entourent les mitochondries en anneaux et serrent les mitochondries pour passer d'une circonférence initiale de 190-200nm à une circonférence de 138 à 146 nm (Ingerman *et al.*, 2005; Legesse-Miller *et al.*, 2003; Mears *et al.*, 2011). Puisque la circonférence de DRP1 sous forme d'hélice oligomérisée est d'environ 110 à 130 nm, il se pourrait que la constriction des mitochondries par le RE permet de faciliter le recrutement de DRP1 et MFF pour aboutir à la fission. Bien que le mécanisme permettant cette constriction soit encore peu connu, le RE dans cette fission est dans ce cas un participant passif déclenchant uniquement la fission en recrutant DRP1 et MFF. En effet, il a été démontré que, bien que la suppression d'expression de DRP1 et de MFF favorise l'élongation mitochondriale, le RE se trouve toujours aux niveaux des sites de constrictions sans être capable de fragmenter les mitochondries, ce qui suggère fortement que le RE resserre les mitochondries bien avant le recrutement des facteurs de fission (Friedman *et al.*, 2011).

Outre la fission, l'IRM possède également un rôle important dans la fusion mitochondriale. La fusion par mitofusine (discuté dans la section 1.5.2) est la principale voie qui permet de fusionner les mitochondries entre elles. Cependant, la mitofusine 2 (MFN2) présente à la MEM est capable de maintenir l'IRM en se liant au RE. Une étude chez des fibroblastes d'embryon de souris a montré que la déficience en MFN2 réduit l'IRM (de Brito *et al.*, 2008). Puisque MFN2 est requis

dans la fusion mitochondriale et affecte l'intégrité de l'IRM, il est possible que l'IRM soit nécessaire pour la fusion mitochondriale aux niveaux de la présence membranaire de MFN2.

1.5.2.2 L'homéostasie lipidique

L'homéostasie lipidique dans l'IRM implique principalement trois classes de phospholipides, la PS, la PE et la PC. Chez les mammifères, le RE possède la plupart des enzymes permettant la synthèse de ces phospholipides bien que quelques-unes soient également présentes dans les mitochondries. Premièrement, la PS est synthétisée par deux enzymes au niveau du RE, la PS synthase 1 et la PS synthase 2 (Vance *et al.*, 2013). La PS est ensuite transloquée du RE à la MEM puis à la MIM (Osman *et al.*, 2011). La PE obtenue par la conversion du PS grâce à l'intervention de l'enzyme PS décarboxylase PSD1 et PSD2 est envoyée par le chemin inverse au RE (Trotter *et al.*, 1995; Vance, 2014). Ensuite, une portion du PE nouvellement obtenue est rendue au RE pour subir une conversion en PC ou pour être distribuée à d'autres compartiments cellulaires dans le besoin de PC.

Evidemment, ces échanges lipidiques entre le RE et les mitochondries font intervenir des complexes protéiques de connexions entre le RE et les mitochondries. Chez la levure, l'IRM a été particulièrement bien étudié et un complexe en particulier, « l'ER-mitochondria encounter structure (ERMES) » est responsable de la coordination de la synthèse des phospholipides entre les deux organites. En effet, ERMES est un complexe protéique formant un pont au niveau membranaire du RE et de la MEM et est composé de 4 protéines distinctes, la « maintenance of mitochondrial morphology protein 1 (Mmm1) » et la Mmm12 au RE, la « mitochondrial distribution and morphology protein 10 (Mdm10) », et la Mdm34 au niveau de la MEM (Kornmann *et al.*, 2009). Une déficience en ERMES aboutit à une réduction de conversion de PC à partir de PS montrant l'importance le rôle de ERMES dans les échanges lipidiques (Kornmann *et al.*, 2009). Chez les mammifères, un homologue de ERMES a récemment été proposé, le PDZD8. PDZD8 est une protéine contenant un domaine « Synaptotagmin-like Mitochondrial lipid-binding (SMP) » (Hirabayashi *et al.*, 2017). Elle est principalement retrouvée à l'IRM ; cependant sa fonction a été corrélée aux échanges calciques et non lipidiques.

1.5.2.3 L'homéostasie du calcium

« Le calcium (Ca^{2+}) intracellulaire, impliqué dans de nombreux processus moléculaires, est un élément essentiel de la cellule. Il peut notamment servir de second messager dans plusieurs

voies de signalisation, notamment celles impliquant la calmoduline (Clapham, 2007). » (Freppel *et al.*, 2022)

« Les mitochondries ont une capacité de stockage du Ca^{2+} intracellulaire allant de 50 à 500 nM et en échangent avec le RE au niveau de l'IRM par l'intermédiaire des récepteurs de IP3R de la membrane du RE, et de VDAC1, une protéine transmembranaire de la membrane mitochondriale externe (Hartmann *et al.*, 1998). Ces protéines, avec l'aide de la chaperonne GRP75, forment un canal permettant le transfert direct du Ca^{2+} du RE vers l'espace intermembranaire des mitochondries (Bartok *et al.*, 2019). Ce cation est ensuite transporté vers la matrice mitochondriale par la protéine transmembranaire MCU (« mitochondrial calcium uniporter ») (Boyman *et al.*, 2020). » (Freppel *et al.*, 2022)

On observe actuellement trois différentes fonctions du rôle du transfert de Ca^{2+} du RE vers les mitochondries. Premièrement, et la plus évidente est de maintenir une concentration très élevée accessible aux protéines membranaires mitochondriales qui interagissent avec le Ca^{2+} pour activer leur fonctions Ca^{2+} dépendante (Berridge, 2002). Deuxièmement, la fragmentation mitochondriale réalisée par la présence de RE aux sites de constrictions et par le recrutement de DRP1 et MFF nécessite une stimulation précoce par les échanges en Ca^{2+} (Friedman *et al.*, 2011). DRP1 possède un rôle essentiel dans la perméabilisation de la membrane externe mitochondriale en facilitant l'oligomérisation de BAX sur la MEM. Ceci est nécessaire pour un relargage de cytochrome C pendant l'apoptose (Cassidy-Stone *et al.*, 2008; Montessuit *et al.*, 2010). De plus, ceci ne concerne non seulement DRP1 ou MFF, mais également la plupart des facteurs moléculaires impliqués dans la morphodynamique mitochondriale. Par exemple, la « Mitochondrial rho GTPase (MIRO) », protéine essentielle au transport des mitochondries joue un rôle clé dans la régulation du Ca^{2+}, dans la morphodynamique mitochondriale et également dans la mitophagie (Kittler, 2015). Cette dernière possède deux domaines GTPases et deux domaines hélice-boucle-hélice se liant au Ca^{2+} appelés plus généralement « EF-hand ». EF-hand se lie au Ca^{2+} pour être relocalisé avec ERMES (Kornmann *et al.*, 2011). La troisième fonction concerne l'activation Ca^{2+} dépendant de l'apoptose (Scorrano *et al.*, 2003). En effet, l'accumulation de Ca^{2+} au niveau mitochondrial stimule la perméabilisation membranaire ouvrant des pores mitochondriaux, les « mitochondrial permeability transition pore (mPTP) » (Orrenius *et al.*, 2003). L'ouverture de ces pores permet de relâcher dans le cytosol des facteurs pro-apoptotiques, comme le cytochrome C. De plus, le couple IP3R-VDAC1 ajoute un transfert de Ca^{2+} pendant que l'apoptose est déjà en place (Jayaraman *et al.*, 1997; Khan *et al.*, 1996).

1.5.2.1 L'immunité innée antivirale

« Outre les fonctions métaboliques décrites ci-dessus, la mitochondrie possède un rôle primordial dans la réponse immunitaire innée précoce. Notamment, sa surface, et plus précisément l'IRM constituent un carrefour permettant à de nombreux facteurs de l'immunité de déclencher une cascade de réactions aboutissant à l'activation de facteurs de transcription qui contrôlent l'expression d'interférons de type I et III. Par exemple, la protéine transmembranaire mitochondriale de signalisation antivirale (MAVS pour « *mitochondrial antiviral-signaling protein* »), sert de protéine adaptatrice pour les récepteurs cytosoliques de type RIG-I (RIG-I pour « *retinoic acid-inducible gene I* », et MDA5 pour « *melanoma differentiation-associated protein 5* »). À la suite de la reconnaissance par ces derniers d'un motif d'ARN étranger par leurs domaines hélicases « *DExD/H box* » (Loo *et al.*, 2011; Refolo *et al.*, 2020), ces détecteurs se déplacent vers l'IRM grâce à la liaison de leur motif CARD (« *caspase activation and recruitment domains* ») à MAVS. Il s'en suit alors la stimulation des voies de signalisation IKKα/β/γ (« *inhibitor of nuclear factor kappa-B kinase subunits α, β, and γ* ») ou IKKε/TBK1 (« *TANK-binding kinase 1* ») qui vont phosphoryler et activer les facteurs de transcription IRF3 (« *interferon regulatory factor 3* »), IRF7 et NF-κB (« *nuclear factor-kappa-B* »). À la suite de leur import nucléaire, ces derniers induisent la transcription d'interférons (IFN) de type I et III. RIG-I et MDA5 sont les récepteurs cytosoliques les plus étudiés dans la littérature. Ils jouent un rôle important dans la reconnaissance de génomes viraux sous forme d'ARN simple brin non coiffés, d'ARN double brin courts, d'ARN riches en U/A (poly U/A) et d'ARN double brin longs (Brisse *et al.*, 2019; Said *et al.*, 2018). » (Freppel *et al.*, 2022)

1.6 La mitochondrie et l'interface réticulo-mitochondriale face aux *Flavivirus*

« Considérant les différents rôles de la mitochondrie et de l'IRM dans les processus cellulaires qui peuvent influencer de façon positive ou néfaste les infections de la cellule hôte, il n'est pas surprenant que la mitochondrie et l'IRM constituent pour les virus des cibles de prédilection à contrôler en priorité pour maximiser leur réplication intracellulaire. Les *Flavivirus* ne font pas exception puisqu'ils interfèrent avec ces organites à plusieurs niveaux. » (Freppel *et al.*, 2022)

1.6.1 Morphodynamique mitochondriale

« En considérant les besoins énergétiques requis par la réplication et la production virale, il n'est pas étonnant que les virus aient développé des moyens de réguler la morphologie des

mitochondries afin d'interférer avec les fonctions cellulaires qui y sont associées. » (Freppel *et al.*, 2022)

« Bien que le RE soit l'organite le plus étudié en ce qui concerne les altérations morphologiques du cytoplasme par les *Flavivirus,* la morphodynamique mitochondriale est également une cible de ces pathogènes. En effet, lors d'une infection par le VDEN ou le VZIK, ces deux virus induisent une élongation mitochondriale marquée (Figure 1.18) (Barbier *et al.*, 2017; Chatel-Chaix *et al.*, 2016). Dans le cas du VDEN, cette élongation est attribuée à une inhibition de la phosphorylation du facteur de fission DRP1 sur la sérine 616 par la protéine virale NS4B empêchant ainsi son transfert aux mitochondries (Chatel-Chaix *et al.*, 2016). Une diminution de l'expression de DRP1 stimule la réplication du VDEN et du VZIK alors que celle du facteur de fusion MFN2 provoque le phénotype inverse. Cela supporte le modèle dans lequel les *Flavivirus* induisent l'élongation au profit de la réplication virale. Cette étude montre également que l'IRM est largement altérée, suggérant une déstabilisation des sites de pré-fission des mitochondries par le RE, ce qui favoriserait en retour la fusion mitochondriale. Dans les cellules infectées par le VDEN, le peu de tubules de RE encore en contact avec les mitochondries est connecté avec les CM. Ceci suggère fortement que la morphogenèse des CM est responsable de l'altération de l'IRM et donc contribue à l'élongation mitochondriale. En parfait accord avec ce modèle, nous avons récemment démontré que la déstabilisation des CM du VZIK par l'inhibition pharmacologique de l'activité ATPase de la protéine cellulaire VCP, une composante de cette ultrastructure, induit une perte rapide de la morphologie allongée des mitochondries (Anton *et al.*, 2021). Puisque la biogénèse des CM est réalisée à partir de la membrane du RE, il se pourrait qu'indirectement, VCP favorise la fusion mitochondriale par le biais de l'altération des contacts RE-mitochondries tel qu'observé avec le VDEN. De façon réciproque, l'élongation des mitochondries stimule la formation des CM puisque l'invalidation génique de DRP1 augmente leur taille. De plus, une fragmentation mitochondriale subite causée par la dépolarisation des mitochondries à la suite d'un traitement avec du CCCP (carbonyl cyanide m-chlorophenylhydrazone) provoque la disparition des CM. Finalement, la réplication du VDEN est diminuée dans des cellules traitées avec du Mito-C, un inhibiteur hétérocyclique ciblant les protéines de la famille des NEET, qui induit une augmentation des contacts RE-mitochondries et de la fragmentation mitochondriale dépendante de DRP1 (Molino *et al.*, 2020). » (Freppel *et al.*, 2022)

« Malgré les évidences d'un lien morphologique et fonctionnel entre les URv et les mitochondries allongées, une autre étude a montré récemment l'inverse, avec une induction de la fragmentation

des mitochondries dans des cellules neuronales par le VZIK (Yang *et al.*, 2020). Dans ce type cellulaire, le VZIK modulerait la morphologie mitochondriale en favorisant la fission par la diminution de MFN2. De plus, l'inhibition pharmacologique de la fission avec la molécule Mdivi-1 (« *mitochondrial division inhibitor 1* ») réduit la mort cellulaire induite par le VZIK, indiquant l'importance de la fusion mitochondriale dans la diminution de l'apoptose et la réplication du VZIK. Les cellules neuronales sont en général sensibles aux infections virales et vont rapidement induire l'apoptose en réponse à l'infection, et ce même à des niveaux faibles de réplication. La fragmentation observée dans ce cas, serait plutôt une conséquence de l'induction de la mort cellulaire, les deux processus étant généralement fonctionnellement reliés. Dans un autre contexte expérimental, une étude antérieure montre que le VDEN peut interférer avec la fusion mitochondriale dans une certaine mesure par l'intermédiaire du clivage des deux facteurs de fusion MFN1/2 par la protéase virale NS2B/3 lorsque cette dernière est surexprimée (Yu *et al.*, 2015). Cependant, la fragmentation observée avec le VZIK et le VDEN dans cette étude a été étudié à des temps précoces de l'infection dans des systèmes artificiels d'hétérocaryons et d'hyperfusion mitochondriale alors que l'élongation rapportée dans d'autres études est plutôt très marquée à des temps plus tardifs correspondant au pic de réplication. Par ailleurs, cette étude n'a pas rapporté que l'infection virale dans la lignée cellulaire d'étude (soit les cellules épithéliales pulmonaires humaines A549) induit une fragmentation mitochondriale, ce qui questionne l'impact d'un tel clivage des mitofusines sur la morphologie générale des mitochondries. Considérant ces résultats contradictoires en apparence, il est possible que la capacité de certains *Flavivirus* à moduler la morphodynamique mitochondriale varie selon le temps d'infection, la souche utilisée, le type cellulaire et la sensibilité des cellules au stress produit par les infections. Il est d'ailleurs à souligner que le VNO ne semble pas induire l'élongation mitochondriale dans les hépatocytes humains Huh7, à l'inverse du VZIK et du VDEN lorsque ces derniers sont testés en parallèle (Chatel-Chaix *et al.*, 2016). Ceci suggère donc qu'il y a des différences parmi les *Flavivirus* en ce qui concerne la régulation de la morphologie des mitochondries. » (Freppel *et al.*, 2022)

« Globalement, toutes ces données mettent en lumière l'impact des infections par les *Flavivirus* sur le remodelage morphologique des mitochondries. Considérant que de nombreuses fonctions des mitochondries sont intimement liées à la morphologie de cet organite, ces altérations architecturales pourraient contribuer à leur contrôle fonctionnel par les *Flavivirus* au profit de la réplication virale. » (Freppel *et al.*, 2022)

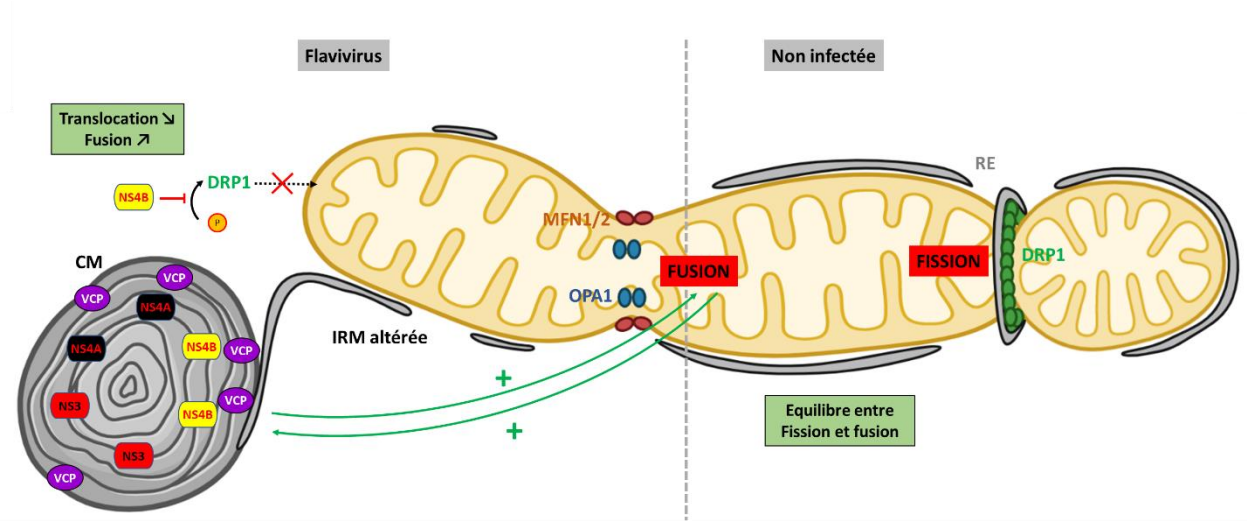

Figure 1.17 Altérations morphologiques de la mitochondrie par les *Flavivirus*

Partie gauche : représentation schématique de la fusion mitochondriale provoquée par les *Flavivirus* par l'entremise de l'inhibition de l'activation du facteur de fission DRP1 (« *dynamin-related protein 1* ») par phosphorylation. Les convolutions de membranes (CM) riches en protéines flavivirales NS3, NS4B et NS4A sont connectées aux mitochondries par un tubule de réticulum endoplasmique (RE) alors que l'interface réticulo-mitochondriale (IRM) est altérée. Partie droite : représentation schématique de l'équilibre entre fusion et fission à l'état normal de la cellule. Modifié de (Freppel *et al.*, 2022)

1.6.2 Métabolisme mitochondrial

1.6.2.1 Homéostasie calcique

Bien que le RE soit le principal réservoir de Ca^{2+}, les mitochondries en contiennent également et jouent donc un rôle important dans cette homéostasie. Les échanges de Ca^{2+} dans l'IRM permettent de maintenir un équilibre en fonction des besoins cellulaires.

« Une surcharge en Ca^{2+} dans les mitochondries induit l'apoptose tandis qu'une diminution excessive conduit à la mort cellulaire par nécrose (Orrenius *et al.*, 2003). Ainsi, une altération de l'interface entre le RE et les mitochondries impacte directement les fonctions mitochondriales et plus généralement l'homéostasie cellulaire du Ca^{2+} (Lee *et al.*, 2018). La maitrise du flux calcique par un pathogène donné permet en théorie de contrôler indirectement des processus cellulaires qui pourraient nuire ou favoriser la multiplication de l'agent infectieux et contribuer à sa pathogenèse. » (Freppel *et al.*, 2022)

« D'un point de vue général, puisque la biogenèse des URv impliquent le remodelage du RE, qui est le réservoir principal du Ca^{2+}, il est possible que ce processus soit associé à un contrôle par le virus de l'homéostasie du Ca^{2+}. Par la suite, le maintien des URv et l'altération de l'IRM

pourraient influencer les échanges de Ca^{2+} entre le RE et les mitochondries et contrôler indirectement les différents processus qui en dépendent, comme l'apoptose. Dans le cas des *Flavivirus*, il n'y a pas d'évidences qui montrent un lien direct entre le contrôle des concentrations calciques mitochondriales et l'infection virale. Cependant, la protéine E du VDEN ou du VZIK interagit avec des composants structuraux de l'IRM tels que GRP78 *(« glucose-regulated protein 78 »)* au niveau du RE, qui elle-même lie VDAC à la surface des mitochondries (Jitobaom *et al.*, 2016; Khongwichit *et al.*, 2021). VDAC1 normalement distribuée de façon périnucléaire serait relocalisée de façon diffuse à la suite d'une infection par VDEN sans être dégradée. Une autre étude a rapporté que VDAC1 est également relocalisée de l'IRM vers le cytosol par le complexe protéase NS2B3 sans pour autant modifier le niveau d'expression de VDAC1 (Tangsongcharoen *et al.*, 2019). Bien que ces données soient contradictoires avec une localisation mitochondriale de VDAC1, elles ouvrent la porte à l'hypothèse d'une altération par le virus de l'intégrité du module de transit calcique IP3R1-VDAC1 bien que cela n'ait pas été testé. Par ailleurs, une étude d'interactome a identifié VDAC2 comme partenaire de la protéine NS4B du VDEN dans les cellules infectées (Chatel-Chaix *et al.*, 2016). Cependant, il reste à démontrer si ces interactions sont spécifiques ou si elles résultent plutôt d'une co-purification de mitochondries entières avec les URv, les VDAC étant des composantes abondantes des mitochondries. » (Freppel *et al.*, 2022)

« Finalement, en activant la voie SOCE (« *store operated calcium entry* »), le VDEN perturbe la perméabilité de la membrane plasmique et augmente la concentration en Ca^{2+} cytoplasmique (Dionicio *et al.*, 2018). Ceci corrèle avec une diminution de la capacité du RE à relâcher le Ca^{2+}. De façon similaire, cet influx calcique dans la cellule est également observé lors des premières heures de l'infection par le VNO (Scherbik *et al.*, 2010). Ces changements de concentration cytoplasmique en Ca^{2+} sont importants pour le cycle viral puisque des traitements avec des inhibiteurs du flux calcique réduisent la réplication du VDEN et du VNO. Au-delà de ces changements généraux sur VDAC1 et sur les flux de calcium au niveau du RE et de la membrane plasmique lors de l'infection par les *Flavivirus*, il serait important d'évaluer dans le futur si cela induit des changements spécifiques du transport du calcium vers les mitochondries et dans quelle mesure cela influence la réplication et la pathogenèse. » (Freppel *et al.*, 2022)

1.6.2.2 Homéostasie lipidique

« Les *Flavivirus* possèdent des mécanismes pour contrôler l'homéostasie lipidique afin de favoriser le remodelage morphologique des organites membranaires, mais aussi pour contrôler certains processus cellulaires dépendants des acides gras. » (Freppel *et al.*, 2022)

« Une étude de spectrométrie de masse à haute résolution de cellules de moustique a permis de déterminer qu'au moins 15% du répertoire lipidique est modifié à la suite d'une infection par le VDEN (Perera *et al.*, 2012). L'ajout de C75, un inhibiteur de la distribution lipidique intracellulaire réduit la réplication virale. Cette étude montre aussi que l'abondance de plusieurs acides gras, tels que les sphingolipides ou la phosphatidylcholine qui sont impliqués dans le dynamisme mitochondrial de fusion/fission et dans la régulation du cytosquelette est augmentée lors d'une infection virale, illustrant ainsi l'importance des lipides dans le cycle viral du VDEN, mais également dans celui du VNO et du VZIK (Diamond *et al.*, 2010; Martin-Acebes *et al.*, 2014 ; Melo *et al.*, 2016). D'autre part, le VDEN et le VNO augmentent la production locale de la synthèse des acides gras libres en recrutant FASN, la synthétase d'acides gras, vers les complexes de réplication du génome viral (Heaton *et al.*, 2010b ; Martin-Acebes *et al.*, 2011 ; Mohamed *et al.*, 2020; Tang *et al.*, 2014). Dans le cas du VDEN, cette redistribution s'effectue par l'intermédiaire de la protéase virale NS3 et de la protéine Rab18, une GTPase (Heaton *et al.*, 2010a; Tang *et al.*, 2014). Chez le VNO, des traitements avec deux inhibiteurs pharmacologiques de la synthèse des acides gras, soit la cérulénine et le C75, diminuent la réplication virale, ce qui démontre que la réplication du VNO dépend de la synthèse des acides gras. Dans le cas du VDEN et du VZIK, la synthèse des lipides à longue chaine est importante pour la réplication, puisque la diminution de l'expression ou l'inhibition de l'hydrostéroide β17 déhydrogénase de type 2 (HSD17B12) diminue l'abondance des gouttelettes lipidiques (GL) et la production de particules infectieuses (Mohamed *et al.*, 2020). » (Freppel *et al.*, 2022)

« Ainsi, les mécanismes moléculaires divergents employés par les *Flavivirus* pour moduler les niveaux d'acides gras pourraient illustrer que les URv requièrent des classes de lipides différentes lors de leur morphogenèse du remodelage à partir du RE. Par ailleurs, la régulation de la β-oxydation influence indirectement le rendement en ATP fourni par la respiration cellulaire et pourrait également atténuer des processus potentiellement antiviraux qui dépendent des lipides. Finalement, l'infection par le VZIK et la surexpression de NS4B induisent une diminution des niveaux de cardiolipine (Leier *et al.*, 2020). Considérant le rôle de ce lipide « mito-spécifique » dans la fission mitochondriale et l'apoptose (Ott *et al.*, 2007; Paradies *et al.*, 2019), il est possible qu'une telle perturbation de l'homéostasie lipidique des mitochondries favorise

leur élongation viro-induite ainsi que l'atténuation des effets cytopathiques. » (Freppel *et al.*, 2022)

1.6.2.3 Respiration cellulaire

« Les différentes étapes de la respiration cellulaire constituent des cibles de choix pour les virus, afin de contrôler l'apport d'énergie sous forme d'ATP requis pour les différentes étapes du cycle viral. Bien que la glycolyse n'implique pas directement la mitochondrie, elle n'en reste pas moins la voie de synthèse clé nourrissant le cycle de Krebs en acétyl-CoA. Plusieurs études ont démontré que la glycolyse est stimulée par plusieurs *Flavivirus* par divers mécanismes moléculaires et que ce processus métabolique est requis pour une réplication virale optimale (Allonso *et al.*, 2015; Duan *et al.*, 2018; Fontaine *et al.*, 2015; Jung *et al.*, 2016; Kumar *et al.*, 2019; Ramière *et al.*, 2014). » (Freppel *et al.*, 2022)

« Les *Flavivirus* ont évolué pour s'approprier le cœur de la production d'énergie mitochondriale de masse (figure 1.19). En effet, des augmentations de la consommation en oxygène ont été observées dans des cellules hépatiques HepG2 infectées par le VDEN (El-Bacha *et al.*, 2007). Ces modifications bioénergétiques sont accompagnées d'une modification ultrastructurale des mitochondries où elles apparaissent gonflées, un phénotype typique de l'initiation du processus apoptotique. La technologie Seahorse mesurant la consommation en oxygène en temps réel et sans marquage dans les cellules vivantes ont confirmé ces résultats (Barbier *et al.*, 2017). Cette étude montre que les cellules infectées par le VDEN ayant des mitochondries allongées présentent une consommation cellulaire en oxygène augmentée. En effet, l'infection par le VDEN augmente la respiration basale (soit la consommation « normale » d'oxygène des cellules à l'équilibre), la respiration maximale et la production en ATP. Ces résultats corrèlent avec une morphologie allongée des mitochondries dans les cellules infectées, suggérant que le virus favorise la fusion mitochondriale, ce qui augmente la production en ATP. À l'inverse des observations faites dans le cas des infections avec le VDEN, le VZIK inhibe les consommations basale et maximale en oxygène dans les trophoblastes infectés (Chen *et al.*, 2020). De plus, cette étude rapporte une fragmentation mitochondriale à la suite d'une infection par le VZIK confirmant le lien fonctionnel entre la respiration et la morphologie mitochondriale. Une étude récente dans des cellules astrocytaires a montré une augmentation dans la consommation en oxygène et en production d'ATP suivant une infection précoce avec le VZIK (Ledur *et al.*, 2020). Cependant, à partir de 36 heures d'infection, la tendance s'inverse et la consommation diminue ce qui suggère un besoin massif en énergie dans les phases précoces de l'infection, durant lesquelles la

biogenèse des URv s'effectue. Tel que mentionné plus haut pour la morphologie, la perturbation de la respiration mitochondriale pourrait également dépendre du type cellulaire, du temps d'infection, ou encore de l'état de stress, tel que l'apoptose qui modifie la perméabilisation de la membrane externe mitochondriale et provoque l'arrêt de la phosphorylation oxydative. De plus, on ignore toujours quelles protéines virales régulent ce processus métabolique. » (Freppel *et al.*, 2022)

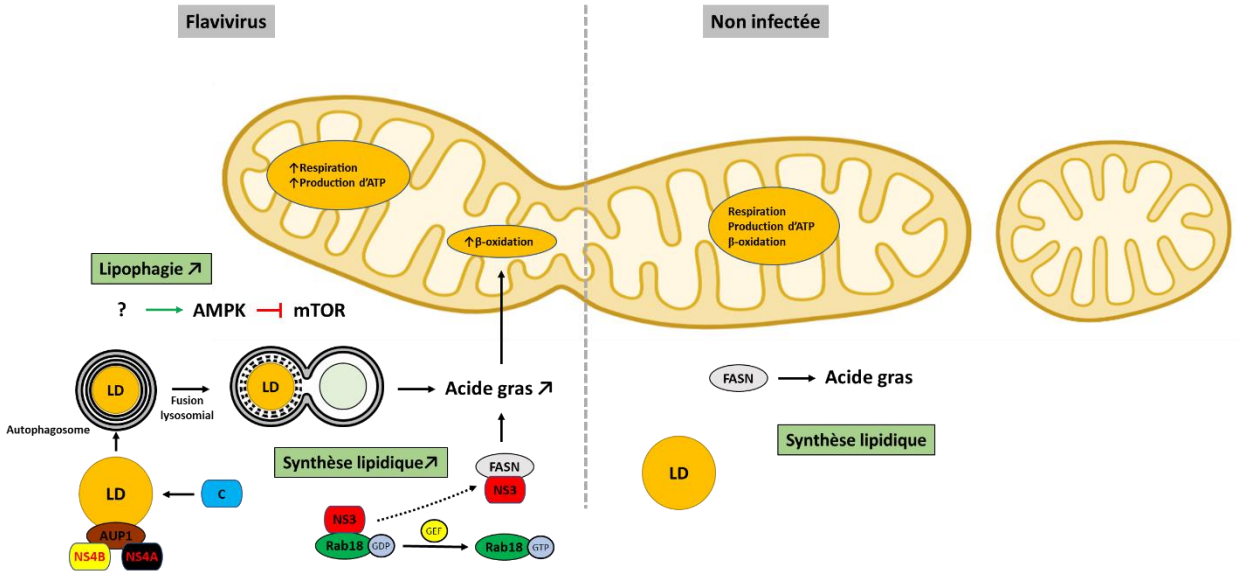

Figure 1.18 Impact des *Flavivirus* sur le métabolisme mitochondrial

Partie gauche : représentation schématique de la perturbation du métabolisme mitochondrial par les *Flavivirus*. Les protéines virales stimulent la lipophagie des gouttelettes lipidiques (GL) et la synthèse des acides gras par la « *fatty acid synthase* » (FASN), aboutissant à l'augmentation de la β-oxydation et de la respiration mitochondriale. Partie droite : représentation schématique du métabolisme mitochondrial dans des conditions « normales » en l'absence d'infection. AUP1: « *ancient ubiquitous protein 1* »; AMPK: « *AMP-activated protein kinase* »; mTOR: « *mammalian target of rapamycin* ». Modifié à partir de (Freppel *et al.*, 2022)

1.6.3 Réponse immunitaire antivirale

1.6.3.1 La surface mitochondriale, un carrefour de la réponse immunitaire innée

« RIG-I et MDA5 sont des facteurs-clés de la détection intracellulaire de la plupart des *Flavivirus* tels que le VDEN, le VNO, le VZIK, le VFJ, et le VEJ (Beauclair *et al.*, 2020; Bowen *et al.*, 2017; Chang *et al.*, 2006; Fredericksen *et al.*, 2008; Hamel *et al.*, 2015; Jiang *et al.*, 2014; Kato *et al.*,

2006; Mukherjee *et al.*, 2015; Nazmi *et al.*, 2011; Qin *et al.*, 2011; Saito *et al.*, 2008). Cependant, d'un point de vue coévolutif, ces virus sont capables d'atténuer l'induction de cette réponse antivirale par des mécanismes moléculaires variés (figure 1.20). Par exemple, l'ubiquitination de RIG-I par TRIM25 (« *tripartite motif-containing protein 25* »), une ligase d'ubiquitine de type E3, est requise pour son transfert vers les mitochondries (Gack *et al.*, 2007). Dans le cas du VDEN, des petits ARN flaviviraux sous-génomiques (ARNsf) qui sont des sous-produits non codants issus de la dégradation intracellulaire de l'ARN viral (Finol *et al.*, 2019; Pijlman *et al.*, 2008), inhibent l'activation de RIG-I en se liant à TRIM25, empêchant ainsi l'activation de RIG-I par ubiquitination (Manokaran *et al.*, 2015). 14-3-3ε, une autre protéine impliquée dans le recrutement de RIG-I et de MDA5 par MAVS par la reconnaissance de motifs sérine ou thréonine phosphorylés, est également ciblée par le VDEN et le VZIK (Chan *et al.*, 2016b; Liu *et al.*, 2012; Riedl *et al.*, 2019). Au cours des infections avec ces deux *Flavivirus*, la protéine virale NS3 inhibe le transfert mitochondrial de RIG-I en séquestrant 14-3-3ε par compétition grâce à un motif phosphomimétique conservé de type RxEP dans la protéine NS3 (Chan *et al.*, 2016b; Riedl *et al.*, 2019). » (Freppel *et al.*, 2022)

« Finalement, la régulation de la morphodynamique mitochondriale par les *Flavivirus* joue également un rôle significatif dans l'interférence de l'immunité innée antivirale en régulant la voie dépendante de MAVS (Castanier *et al.*, 2010; Horner *et al.*, 2011; Jacobs *et al.*, 2013). En effet, l'altération de l'IRM ou la perturbation de la dynamique fusion/fission mitochondriale peuvent avoir un impact sur les protéines pro-immunologiques présentes à l'IRM. Comme déjà mentionné plus haut, la stimulation de l'élongation mitochondriale dans les cellules infectées avec le VDEN joue également un rôle dans l'atténuation de l'immunité innée précoce puisqu'elle régule négativement l'expression des IFN-λ et -β (Chatel-Chaix *et al.*, 2016). De plus, ceci corrèle avec une réduction du transfert de RIG-I vers l'IRM et une augmentation de la réplication virale. Des phénotypes inverses sont observés lorsque l'on favorise la fission mitochondriale par l'invalidation de MFN2. Finalement, l'IRM est altérée dans les cellules infectées par le VDEN, ce qui est consistant avec le fait que la voie de signalisation RIG-I/MAVS n'est pas activée de façon optimale. Dans l'ensemble, toutes ces données illustrent que les *Flavivirus* exploitent la morphodynamique mitochondriale et l'IRM à leur avantage pour atténuer la réponse immunitaire innée et ainsi éviter un état cellulaire antiviral potentiellement préjudiciable à la réplication virale. » (Freppel *et al.*, 2022)

1.6.3.2 La mitochondrie et son matériel génétique, une boite de Pandore cellulaire

« Une des particularités de la mitochondrie est de contenir son propre génome sous forme d'ADN mitochondrial (ADNmt). Ce dernier possède de nombreux sites CpG et est hautement méthylé de façon similaire à l'ADN des procaryotes (Patil *et al.*, 2019). L'ADNmt peut être libéré dans le cytoplasme à la suite d'un stress, tel qu'une infection virale. Dans une telle situation, cet acide nucléique est reconnu comme un ADN étranger par TLR9 (« *Toll-like receptor 9* ») (Zhang *et al.*, 2010) ou par cGAS (« *cyclic GMP-AMP synthase* ») (Cai *et al.*, 2014; Guo *et al.*, 2020) aboutissant à la stimulation de la voie de signalisation dépendante de NF-κB, et donc à l'expression de protéines pro-inflammatoires (Zhang *et al.*, 2014). Par exemple, dans des cellules dendritiques, le VDEN induit la libération de l'ADNmt dans le cytosol à la suite de la production excessive de dérivés réactifs d'oxygène (ROS pour « *reactive oxygen species* ») et à l'activation de l'inflammasome, ce qui résulte en l'activation des TLR9 (Lai *et al.*, 2018). Par ailleurs, à la suite de la détection de l'ADNmt par cGAS, cette protéine via la protéine adaptatrice STING (« *stimulator of interferon genes protein* »), partage l'information aux cellules voisines non infectées à travers les jonctions serrées intercellulaires (Sun *et al.*, 2017). Un mécanisme d'interférence développé par le VDEN est d'induire la dégradation de cGAS par les lysosomes par la protéine virale NS2B (figure 1.20) (Aguirre *et al.*, 2017). Un tel mode d'évasion est aussi retrouvé pendant l'infection par le VZIK. En effet, le VZIK, par l'intermédiaire de la protéine virale NS1, recrute la deubiquitinase U8 pour cliver les chaines de poly-ubiquitine sur la caspase 1, ce qui la stabilise. Ceci favorise le clivage de cGAS par cette dernière, empêchant ainsi la reconnaissance de l'ADNmt libéré (Zheng *et al.*, 2018). De plus, STING est également soumis à un clivage par la protéase virale NS3 (avec son co-facteur NS2B). Ce mécanisme d'interférence est retrouvé lors de l'infection par plusieurs *Flavivirus* tels que le VDEN, le VZIK et le VNO, mais pas par le VFJ (Ding *et al.*, 2018). Tous ces mécanismes d'échappement développés par les *Flavivirus* montrent l'ingéniosité de l'évolution de ces virus en parallèle de l'évolution du système immunitaire chez l'humain. » (Freppel *et al.*, 2022)

« Fait intéressant, lorsque des erreurs se produisent lors de la réplication de l'ADNmt à la suite de stress externes, l'ADNmt peut subir des cassures double-brin pour former des ADNmt fragmentés (Moretton *et al.*, 2017). Ces ADNmt fragmentés sont encore peu connus, mais leur production active la voie IFN de type I par la phosphorylation de STAT1 (« *signal transducer and activator of transcription 1* ») et l'activation des gènes stimulés par les interférons (Tigano *et al.*, 2021). Ces ADNmt fragmentés peuvent également provoquer la perméabilisation des

membranes mitochondriales par BAX (« *Bcl-2–associated X protein* ») et BAK (« *Bcl-2 homologous antagonist/killer* protein») permettant l'échappement de l'ARN mitochondrial de la matrice et la reconnaissance par RIG-I et MAVS activant l'expression des IFN de type I et III. Cependant, un tel processus reste à démontrer expérimentalement lors d'infections par les *Flavivirus*. » (Freppel *et al.*, 2022)

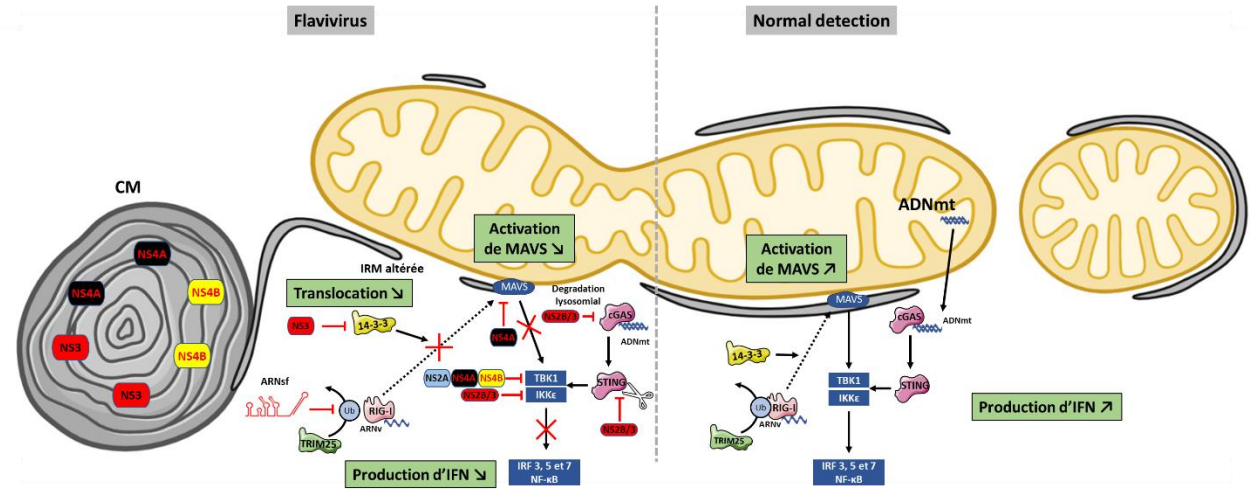

Figure 1.19 Interférence de l'immunité innée par les *Flavivirus*

Partie gauche : représentation schématique de l'interférence des voies de signalisation de l'immunité innée précoce par les *Flavivirus*. Partie droite : représentation schématique des voies de signalisation de l'immunité innée précoce en condition classique d'infection avec un virus à ARN reconnu par « *retinoic acid-inducible gene I* » (RIG-I) sans interférence. L'effet indirect de l'infection sur la voie interféron (IFN) par l'entremise de la libération d'ADN mitochondrial (ADNmt) par les mitochondries et sa reconnaissance par la « *cyclic GMP-AMP synthase* » (cGAS) est également illustré. Ciseaux : clivage protéolytique ; MAVS : « *mitochondrial antiviral-signaling protein* »; STING : « *stimulator of interferon genes protein* »; TRIM25 : « *tripartite motif-containing protein 25* »; TBK1 : « *TANK-binding kinase 1* »; IKKε : « *Inhibitor of nuclear factor kappa-B kinase subunit epsilon* »; IRF3, 7: « *Interferon regulatory factor 3 and 7* »; ARNsf: petits ARN flaviviraux sous-génomiques; Ub: ubiquitine; CM: convolutions de membranes; IRM: interface réticulo-mitochondriale. RE : réticulum endoplasmique. Modifié à partir de (Freppel *et al.*, 2022)

1.7 La mort cellulaire face aux *Flavivirus*

La mort cellulaire est un processus permettant d'éliminer les cellules défectueuses, néfastes ou inutiles. En fonctions du stress rencontrée par la cellule, on retrouve différentes voies de la mort cellulaire telles que l'apoptose ou l'autophagie (Galluzzi *et al.*, 2018). Cette section discute de l'induction positive ou négative de la mort cellulaire par les *Flavivirus* en faveur de leur réplication.

1.7.1 Apoptose

Il y a beaucoup d'évidence que les *Flavivirus* modulent les deux voies de l'apoptose *in vivo* comme *in vitro* (Deng *et al.*, 2008; Fischer *et al.*, 2007; Ghosh Roy *et al.*, 2014; Ghouzzi *et al.*, 2016; Li *et al.*, 2016; Liu *et al.*, 2014; Souza *et al.*, 2016).

1.7.1.1 Voie intrinsèque

Modulation directe

« Les protéines virales NS2, NS3, C, E et M des virus VDEN, VNO et VEJ activent individuellement la voie intrinsèque (Bhuvanakantham *et al.*, 2010; Catteau *et al.*, 2003). De plus, l'apoptose résultant du stress oxydatif, du stress du RE et/ou de la dérégulation des homéostasies du Ca^{2+} et des lipides contribue aux effets cytopathiques observés en culture cellulaire à la suite de l'infection (Okamoto *et al.*, 2017). Face à cette réponse cellulaire, ces pathogènes possèdent des mécanismes d'atténuation qui vont retarder la mort cellulaire et maximiser la production virale (figure 1.21). La voie PI3K/PKB/mTOR (« *phosphoinositide 3-kinase* »/ « *protein kinase B* », appelée aussi AKT / « *mammalian target of rapamycin* »), particulièrement importante dans la régulation de la croissance et la survie cellulaire a un rôle central dans le contrôle de l'apoptose induite par les infections aux *Flavivirus* (Hemmings *et al.*, 2012). En effet, une fois PKB phosphorylée, cette dernière inhibe les facteurs pro-apoptotiques, tels que BAD (« *Bcl2-associated agonist of cell death* ») et la caspase 9, ainsi que le relargage du cytochrome C par les mitochondries. Lors de l'infection par les virus VDEN, VEJ, et VNO, cette voie est stimulée, ce qui favorise la survie cellulaire et retarde l'apoptose. Par exemple, la voie PI3K/PKB/mTOR impliquée dans l'inhibition de l'apoptose est soit activée lors d'une infection par le VDEN ou VEJ favorisant ainsi le relargage de Bcl-2 (Lee *et al.*, 2005), soit intervient dans l'inhibition des caspases 3 et 8 suite à son activation par la protéine C du VNO (Urbanowski *et al.*, 2013). L'infection par le VZIK entraîne également un retard de l'apoptose, ce qui favorise sa réplication. En effet, le virus contrôle la voie anti-apoptotique au moyen d'une stabilisation de Bcl-2 (Turpin *et al.*, 2019). » (Freppel *et al.*, 2022)

« Fait très intéressant, les ARNsf régulent l'apoptose et ce, de façon divergente selon l'espèce. En effet, des souches de VZIK mutées qui ne produisent pas d'ARNsf, induisent de l'apoptose dans des moustiques infectés, à l'inverse de la souche sauvage (Slonchak *et al.*, 2020). Cette étude démontre donc un rôle anti-apoptotique de l'ARNsf, soulevant l'hypothèse que cet ARN non-codant constituerait un facteur clé dans la transmission du VZIK du moustique à l'humain.

Pourtant à l'inverse, dans les cellules de mammifères, l'ARNsf joue également un rôle stimulateur dans l'activation de l'apoptose et des effets cytopathiques, notamment en inhibant la phosphorylation de PKB et l'activation de Bcl-2, ce qui promeut au final le relargage de cytochrome C (Liu *et al.*, 2014; Pijlman *et al.*, 2008). » (Freppel *et al.*, 2022)

Modulation indirecte

« D'un point de vue morphologique, la dynamique mitochondriale joue également un rôle dans l'apoptose. En effet, la fragmentation altère la morphologie des crêtes de la membrane mitochondriale interne et rend les membranes de cet organite plus perméables, résultant en un relargage accru de cytochrome C et à la potentialisation de l'apoptose (Liesa *et al.*, 2009; Montessuit *et al.*, 2010; Oettinghaus *et al.*, 2016; Park *et al.*, 2015; Sheridan *et al.*, 2010; Suen *et al.*, 2008). Même si cela reste débattu, la fragmentation augmenterait la surface membranaire des mitochondries, permettant ainsi d'accommoder plus de pores relarguant des molécules pro-apoptotiques. Ce modèle est soutenu par le fait que l'infection de neurones par le VZIK induit l'apoptose neuronale à la suite de la fragmentation des mitochondries par une réduction de l'abondance du facteur de fusion MFN2 dans ce type cellulaire (Yang *et al.*, 2020). Un traitement avec le Mdivi-1, un inhibiteur de DRP1 et donc, de la fragmentation mitochondriale, atténue la mort cellulaire lors d'une infection au VZIK, suggérant que la dynamique mitochondriale a un impact direct sur l'apoptose. À l'opposé, certains types cellulaires tolèrent mieux le stress de l'infection virale et les effets cytopathiques apparaissent à des temps tardifs de l'infection. La production virale dans ces conditions est généralement élevée et corrèle avec un aspect allongé des mitochondries. Notamment, l'activité ATPase de VCP est requise pour maintenir l'élongation mitochondriale et la formation des CM. Ceci corrèle avec une atténuation des effets cytopathiques puisque l'inhibition de VCP induit une apoptose prématurée dépendante du VZIK (Anton *et al.*, 2021). Ceci suggère que la diminution de l'apoptose par VCP serait accompagnée par la fusion mitochondriale et l'altération de l'IRM lors de la biogénèse des CM (Anton *et al.*, 2021). L'activité du facteur de fission DRP1, une cible inhibée par le VDEN, est intimement liée à la régulation de l'apoptose. En effet, à la suite de sa déplétion par interférence par l'ARN, on constate un délai dans la fission mitochondriale, la sortie du cytochrome C et dans l'activation des caspases ce qui décroît l'induction de l'apoptose (Breckenridge *et al.*, 2003; Frank *et al.*, 2001; Lee *et al.*, 2004). L'hypothèse la plus probable serait donc que les *Flavivirus* modulent la morphodynamique mitochondriale ce qui retarderait la mort cellulaire due au stress de l'infection et maximiserait la réplication du génome et la production de virions. » (Freppel *et al.*, 2022)

« Enfin, on ne peut pas exclure que la diminution des niveaux de cardiolipine dans les cellules infectées par le VZIK (Leier *et al.*, 2020) contribue aux effets cytopathiques, puisque ce lipide mitochondrial lie le cytochrome C au sein de la membrane mitochondriale interne et limite donc son relargage lors de l'apoptose (Choi *et al.*, 2007; Kagan *et al.*, 2005; Ott *et al.*, 2002). À l'inverse, et de façon paradoxale (et controversée), la cardiolipine serait requise pour la perméabilisation de la membrane mitochondriale externe et donc, pour la libération du cytochrome C. Il serait très intéressant d'évaluer comment cette altération des niveaux de cardiolipine influence la réplication et surtout, si cela potentialise ou atténue l'apoptose induite par le VZIK. » (Freppel *et al.*, 2022)

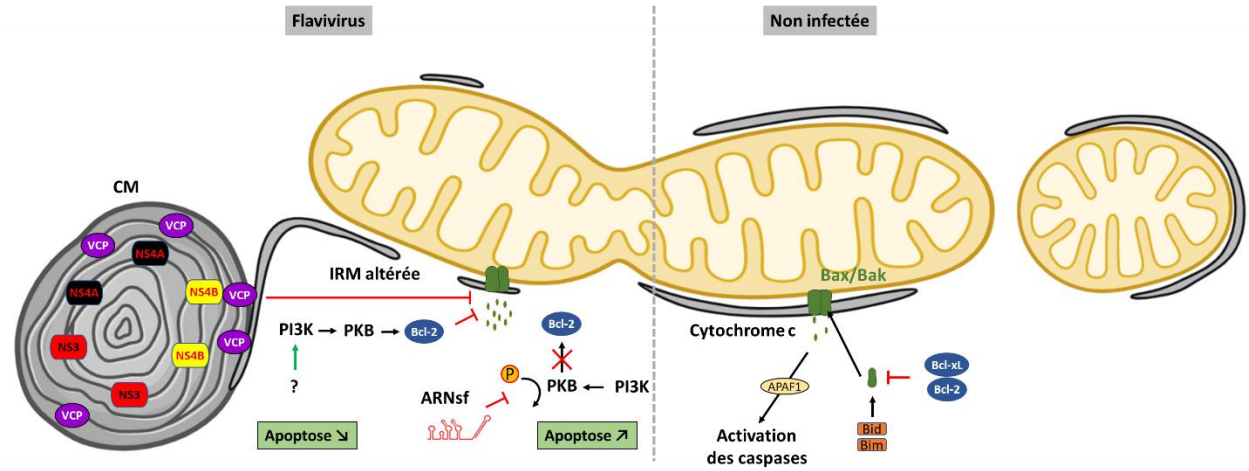

Figure 1.20 Perturbations de l'apoptose par les *Flavivirus*

Partie de gauche : représentation schématique de la perturbation négative ou positive de l'induction de l'apoptose par les *Flavivirus*. Partie de droite : représentation de la voie intrinsèque d'induction de l'apoptose dans des conditions sans infection. IRM : Interface réticulo-mitochondriale ; CM : convolutions de membranes ; RE : réticulum endoplasmique. PI3K : « *Phosphatidylinositol 3-kinase* » ; ARNsf : petits ARN flaviviraux sous-génomiques ; VCP : « *valosin-containing protein* ». Modifié à partir de (Freppel *et al.*, 2022)

1.7.1.1 Voie extrinsèque

La voie extrinsèque est activée par des facteurs ne faisant pas intervenir la mitochondrie directement, telle que la voie intrinsèque. Brièvement, elle est activée par la liaison de facteurs de mort (death ligand) tels que « tumor necrosis factor- α (TNF-α) », « Fas ligand (FasL) ou « TNF-related apoptosis-inducing ligand (TRAIL) » sur les récepteurs de mort (death receptor) à la surface cellulaire externe, tels que TNFR1 par exemple (Elmore, 2007). La liaison déclenche

l'activation du complexe protéique DISC qui à son tour provoque une réaction en chaine de clivages et d'activations des caspases 8, suivi de 7 et 10, puis 3, aboutissant à la mort cellulaire.

Dans une infection au VDEN, les protéines NS2, NS3, NS5, E et C sont impliquées dans l'induction de l'apoptose et de cytokines pro-inflammatoires dans des cellules endothéliales, hépatiques ou encore de l'immunité (Avirutnan *et al.*, 1998). Par exemple, la localisation nucléaire de la protéine C ou de NS5 est nécessaire dans l'activation de l'apoptose par liaison direct avec la protéine DAXX associée à FAS (Khunchai *et al.*, 2012; Netsawang *et al.*, 2010). De plus, par un mécanisme encore inconnu, une infection au VDEN provoque la surexpression de la protéine « apoptosis protein (XIAP)-associated factor-1 (XAF1) » induisant l'apoptose par surexpression de la caspase 3 (Long *et al.*, 2013). XAF1 est un facteur pro-apoptotique qui peut être induit par les IFN et TNF-α (Leaman *et al.*, 2002). À l'opposé, la répression de l'apoptose par le VDEN a également été observée. Par exemple la protéine phosphatase 1 activatrice de la voie AKT interagit avec la capside C bloquant ainsi la phosphorylation de AKT et donc l'apoptose (Airo *et al.*, 2018).

Chez le VNO, la protéine C active l'apoptose par son interaction avec l'importine-α suivi de la phosphorylation de la protéine kinase C (Bhuvanakantham *et al.*, 2010). De plus, l'infection active les récepteurs Toll-like 3 et augmente la perméabilité de la barrière hémato-encéphalique par l'action de TNF-α causant ainsi des dommages au système cérébral (Wang *et al.*, 2004). La protéine NS2A du VNO a également été impliquée dans l'induction de l'apoptose. En effet, une mutation de NS2A en A30P diminue l'effet cytopathique suggérant son rôle nécessaire dans l'activation de l'apoptose (Liu *et al.*, 2006).

La protéine virale NS3 du *Flavivirus* Langat active l'apoptose en se liant directement à la caspase 8 par l'intermédiaire de ses domaines protéase et hélicase (Prikhod'ko *et al.*, 2002). Chez le même *Flavivirus*, la protéine E active la voie apoptotique en induisant l'activation de protéase de type caspase 3 (Prikhod'ko *et al.*, 2001).

Le VZIK peut activer l'apoptose en modulant la caspase 3 *in vivo* et *in vitro* (Huang *et al.*, 2016; Lin *et al.*, 2017b). De plus, des études ont montré la possible relation entre l'apoptose induite et les problèmes neurologiques causés par le VZIK. En effet, chez le singe rhésus, une infection au VZIK active l'apoptose des cellules progénitrices neuronales (Martinot *et al.*, 2018). Cette étude est soutenue par de nombreuses autres impliquant l'augmentation de l'apoptose dans des cellules neuronales (Ghouzzi *et al.*, 2016; Huang *et al.*, 2016; Li *et al.*, 2016; Qian *et al.*, 2016; Souza *et al.*, 2016). Il semblerait que l'un des mécanismes impliqués par le VZIK dans l'induction

de l'apoptose par la voie extrinsèque soit l'activation des caspases 3, 7, 8 et 9 par l'augmentation de l'expression de TRAIL (Jungmann *et al.*, 2017; Tang *et al.*, 2016a).

Finalement, toutes ces études montrent clairement que les *Flavivirus* peuvent directement ou indirectement contrôler positivement ou négativement les deux voies de l'apoptose en faveur de la réplication virale.

1.7.2 Autophagie

L'autophagie est un processus cellulaire permettant la dégradation sélective de différents constituants de la cellule par voir lysosomale (Yorimitsu *et al.*, 2005). En effet, à la suite d'un stress cellulaire ou pour maintenir une homéostasie saine, les constituants défectueux sont ciblés et isolés dans un autophagosome, c'est-à-dire une vésicule à double membrane lipidique. Celle-ci fusionne avec un lysosome afin de dégrader et recycler le contenu. De nombreuses études ont montré que la réplication des *Flavivirus* dépend des protéines impliquées dans l'autophagie induite dans les cellules infectées (Paul *et al.*, 2016). Par exemple, les *Flavivirus* peuvent induire l'autophagie pour retarder le déclenchement de l'apoptose. En effet, la protéine virale NS4A induit l'autophagie dans des cellules épithéliales par la voie de signalisation de PI3K protégeant le virus de la mort cellulaire (McLean *et al.*, 2011). Au stade d'infection précoce avec le VDEN, la protéine virale NS1 interagit avec Beclin-1 pour initier l'autophagie et retarder l'apoptose (Lu *et al.*, 2020).

1.7.2.1 Lipophagie

La lipophagie est l'autophagie sélective des gouttelettes lipidiques afin de libérer des acides gras nécessaires au bon fonctionnement de la cellule (Shin, 2020). « En aval des détournements des facteurs intervenant dans la lipogenèse (discuté dans la section 1.7.2.2), les *Flavivirus* interfèrent également avec le catabolisme des acides gras au niveau des mitochondries (figure 1.19). En effet, le VDEN stimule la β-oxydation et la libération des acides gras libres provenant de l'autophagie des GL. La stimulation de cette lipophagie par le VDEN dépend de l'activation d'AMPK qui en retour inhibe mTOR, le répresseur principal de l'autophagie (Jordan *et al.*, 2017). Par ailleurs, la lipophagie est induite par les protéines virales C, NS4A et NS4B, ces deux dernières interagissant avec AUP1, une protéine membranaire de type-III associée aux GL. L'interaction avec AUP1 a pour effet de détourner son activité acyltransférase et de cibler les GL vers la machinerie autophagique (Byk *et al.*, 2016; Heaton *et al.*, 2010b; Samsa *et al.*, 2009; Zhang *et al.*, 2018). » (Freppel *et al.*, 2022)

1.7.2.2 Mitophagie

Un autre type d'autophagie modulé par les *Flavivirus* est la mitophagie qui est simplement l'autophagie sélective des mitochondries. « Chez les *Flavivirus*, il semblerait que la mitophagie ne soit pas induite. En effet, l'inhibition du transfert de Ajuba aux mitochondries, une protéine cellulaire impliquée dans l'activation de PINK1, par la protéine virale NS5 du VZIK bloque la mitophagie (Ponia *et al.*, 2021). De plus, le fait que la fusion mitochondriale soit favorisée lors d'une infection avec le VDEN et VZIK favorise le modèle selon lequel la mitophagie n'a pas lieu dans les cellules infectées (Barbier *et al.*, 2017; Chatel-Chaix *et al.*, 2016). En effet, la majorité des mitochondries prises en charge par la machinerie autophagique sont fragmentées dans la plupart des cas. L'élongation mitochondriale, à l'inverse, est plutôt associée à une protection de ces organites vis-à-vis de l'autophagie, ce qui favoriserait la production d'énergie et la survie cellulaire lors d'un stress de privation en sérum (Wu *et al.*, 2020). Finalement, on ne peut pour l'instant pas exclure l'hypothèse que la réplication des *Flavivirus* dépende aussi de perturbations des processus mitophagiques indépendants de Parkin, tels que ceux impliquant la cardiolipine ou les ligases d'ubiquitine Gp78 et SIAH1 (Chu *et al.*, 2013; Fu *et al.*, 2013; Szargel *et al.*, 2016; von Stockum *et al.*, 2018). Notamment, le fait que les niveaux de cardiolipine diminuent dans les cellules infectées par le VZIK laisse supposer que cela contribuerait à inhiber la mitophagie (Leier *et al.*, 2020). » (Freppel *et al.*, 2022)

2 HYPOTHESES DE RECHERCHE

« La compréhension du rôle de la mitochondrie dans la cellule s'est considérablement complexifiée dans les quinze dernières années. Cet organite est passé du simple statut de « centrale énergétique de la cellule » à celui de carrefour fonctionnel où convergent de nombreux processus cellulaires importants au maintien de l'homéostasie, à la survie et à la réponse à divers stress (pathogéniques ou non). Il n'est donc pas surprenant que, lors d'infections par des pathogènes tels que les *Flaviviridae,* cet organite soit ciblé, ce qui favorise leur multiplication et contribue à la pathogenèse que ce soit en régulant la production d'énergie ou en s'évadant du système immunitaire. Il reste encore beaucoup d'énigmes à résoudre dans la plupart des cas, notamment au niveau des mécanismes moléculaires impliqués dans ces détournements fonctionnels, incluant l'identification des déterminants viraux impliqués. Dans le cas des *Flavivirus*, il apparaît que les usines de réplication virales dérivées du RE sont impliquées dans ce détournement par l'intermédiaire de contacts physiques. » (Freppel *et al.*, 2022)

En effet, à la suite de l'entrée du VDEN ou du VZIK dans la cellule et à la synthèse des protéines virales, ces dernières avec l'aide de facteurs cellulaires induisent la biogenèse des usines de réplication virales à partir du RE. Par ailleurs, mon directeur de thèse, Laurent Chatel-Chaix a démontré que la protéine virale NS4B du VDEN induit une élongation drastique des mitochondries dans les cellules infectées, lesquelles font des contacts avec les usines de réplication (Chatel-Chaix *et al.*, 2016). Notamment, des évidences préliminaires en microscopie montrent que le VDEN réduirait l'IRM qui est impliqué, entre autres, dans les voies de signalisation précoces de l'immunité innée.

On ignore si NS4B est impliquée dans le remodelage de cette interface inter-organite et comment ce processus est régulé au niveau moléculaire. De façon frappante, la modulation de la morphodynamique mitochondriale par le VDEN favorise la réplication virale tout en atténuant la signalisation de l'immunité innée diminuant ainsi la production d'interférons de type I et de type III. La plupart de ces phénotypes ont aussi été observés dans les cellules infectées par le VZIK suggérant que ces deux virus partagent la même stratégie afin de créer un environnement cytoplasmique propice à la réplication virale.

Nous faisons l'hypothèse que NS4B possède un rôle important dans le remodelage morphologique du RE et des mitochondries, et notamment joue un rôle important dans l'altération de l'IRM afin de réduire certains processus cellulaires qui y sont reliés, tels que l'apoptose ou la phosphorylation oxydative en faveur de la réplication virale. Dans cette thèse, nous avons étudié

à l'échelle moléculaire la relation entre le VDEN, le VZIK et l'IRM. En effet, nous avons regardé l'impact des deux virus et notamment de NS4B sur l'intégrité de l'IRM mais aussi à l'inverse, l'impact de l'IRM sur la réplication virale. Nous avons également étudié son rôle et celui des deux virus dans la phosphorylation oxydative et comment une altération de l'IRM en condition d'infection agît sur la mort cellulaire par apoptose. Ce travail représente mon projet de doctorat et est alors le chapitre principal de cette thèse.

3 FLAVIVIRUS ALTER ENDOPLASMIC RETICULUM-MITOCHONDRIA CONTACTS TO REGULATE RESPIRATION AND APOPTOSIS

Les *Flavivirus* altèrent l'interface réticulo-mitochondriale pour réguler la respiration et l'apoptose

Auteurs :

Wesley Freppel[1,*], Anaïs Anton[1], Zaynab Nouhi[2], Clément Mazeaud[1], Claudia Gilbert[1], Nicolas Tremblay[1], Viviana Andrea Barragan Torres[1], Aïssatou Aïcha Sow[1], Xavier Laulhé[1], Alain Lamarre[1], Ian Gaël Rodrigue-Gervais[1], Andreas Pichlmair[3,4], Pietro Scaturro[3,5], Laura Hulea[2,6] and Laurent Chatel-Chaix[1,7,8#]

[1] Centre Armand-Frappier Santé Biotechnologie, Institut National de la Recherche Scientifique, Laval, Québec, Canada

[2] Maisonneuve-Rosemont Hospital Research Center, Montréal, Québec, Canada

[3] Institute of Virology, Technical University of Munich, School of Medicine, Munich, Germany

[4] German Center of Infection Research (DZIF), Munich partner site, Munich, Germany

[5] Leibniz Institute of Virology, Hamburg, Germany

[6] Department of Medicine, University of Montréal, Montréal, Québec, Canada

[7] Center of Excellence in Orphan Diseases Research-Fondation Courtois, Québec, Canada

[8] Regroupement Intersectoriel de Recherche en Santé de l'Université du Québec, Québec, Canada

[*] Current address: Institute for Glycomics, Gold Coast Campus, Griffith University, Southport, QLD 4222, Australia

Titre de la revue ou de l'ouvrage :

- Soumis dans BioRxiv le 10 mars 2023 : https://doi.org/10.1101/2023.03.09.531853
- Soumis dans Cell Report (IF : 9.995) le 17 mars 2023

Contribution des auteurs :

W.F: Exécution de la majorité des expériences (essais de ligation de proximité, essais de phosphorylation oxydative par la technologie Seahorse, essais en apoptose, titration virale par essais de plaque, immunobuvardages, microscopie confocale, knockdown des protéines de l'IRM) analyses des données et de la rédaction du manuscrit ; A.A: PLA and TEM, préparation des échantillons pour le GC-MS; A.A.S: Optimisation des essais en apoptose; C.M: Caractérisation primaire de RRBP1; N.T and V.A.B.T: Purification mitochondriale; C.G, X.L, I.G.R.G and A.L: Acquisition et analyses des données en FACS; P.S and A.P: Masse spectrométrie et analyse des données ; Z.N and L.H: Extraction des métabolites, GC-MS et analyses des données. L.C.C: Conceptualisation du projet, financement, analyses des données, correction du manuscrit. Tous les auteurs ont lu, corrigé et approuvé la version finale du manuscrit.

3.1 Abstract

With no therapeutics available, there is an urgent need to better understand the pathogenesis of flaviviruses which constitute a threat to public health worldwide. During infection, dengue virus (DENV) and Zika virus (ZIKV), two flaviviruses induce alterations of mitochondria morphology to favor viral replication, suggesting a viral co-opting of mitochondria functions. Here, we performed an extensive transmission electron microscopy-based quantitative analysis to demonstrate that both DENV and ZIKV alter endoplasmic reticulum-mitochondria contacts (ERMC). This correlated at the molecular level with an impairment of ERMC tethering protein complexes located at the surface of both organelles. Furthermore, virus infection, as well as NS4B expression modulated the mitochondrial oxygen consumption rate. Consistently, metabolomic and mitoproteomic analyses revealed a decrease in the abundance of several metabolites of the Krebs cycle and changes in the stoichiometry of the electron transport chain. Most importantly, ERMC destabilization by protein knockdown increased virus replication while dampening ZIKV-induced apoptosis. Overall, our results support the notion that flaviviruses hijack ERMCs to generate a cytoplasmic environment beneficial for sustained and efficient replication.

3.2 Introduction

Flavivirus infections constitute a major public health concern worldwide. With an estimation of 390 million people infected per year, dengue virus (DENV) causes the most prevalent arthropod-borne viral disease (Bhatt *et al.*, 2013). Although DENV mainly circulates in (sub-)tropical regions, it has also now reached Europe and North America because of vector colonization of these areas (Liu-Helmersson *et al.*, 2016; Ryan *et al.*, 2019). Upon infection through the bite of an *Aedes*-type mosquito, symptoms associated with dengue fever can manifest as severe fevers which may be haemorrhagic and eventually lead to shock syndrome and death (World Health Organization, 2022). In 2015, Zika virus (ZIKV), another flavivirus closely related to DENV, has quickly emerged in South America causing unexpected symptoms such as microcephaly in newborns following congenital transmission, in addition to other neurological complications in adults such as Guillain-Barré syndrome (Carod-Artal, 2018; Moore *et al.*, 2017). Unfortunately, no treatments against DENV and ZIKV are currently available, partly due to our limited knowledge of the cellular and molecular mechanisms involved in flavivirus life cycle and pathogenesis, which could constitute therapeutic targets.

DENV and ZIKV are single positive-stranded RNA viruses belonging to the *Flavivirus* genus within the *Flaviviridae* family. Following entry into the host cell, the viral RNA genome (vRNA) is translated into a single polyprotein at the membrane of the endoplasmic reticulum (ER). This viral protein product is cleaved by host and viral proteases, generating three structural proteins (C, prM and E) which assemble with the vRNA to form new viral particles, and into 7 non-structural proteins (NS1, NS2A, NS2B, NS3, NS4A, NS4B, NS5) which are involved in the replication of the viral genome (Mazeaud *et al.*, 2018). The viral replication takes place in cytoplasmic substructures called viral replication organelles (vRO) that are derived from ER membrane alterations induced by the virus (Chatel-Chaix *et al.*, 2014; Cortese *et al.*, 2017; Gillespie *et al.*, 2010; Junjhon *et al.*, 2014; Miorin *et al.*, 2013; Paul *et al.*, 2015; Welsch *et al.*, 2009). vROs comprise: 1- vesicle packets, believed to be the site of vRNA replication; 2- virus bags, ER cisternae in which immature assembled virions accumulate; and 3- convoluted membranes (CM), that are enriched in NS3, NS4B, and NS4A (Chatel-Chaix *et al.*, 2016; Miller *et al.*, 2007; Welsch *et al.*, 2009) whose functions are poorly understood. It was proposed that CMs dampen antiviral cellular processes, such as early innate immunity response and apoptosis to favor viral replication.

In DENV- and ZIKV-infected cells, mitochondria make physical contacts with CMs and exhibit an elongated morphology, which stimulates viral replication (Barbier *et al.*, 2017; Chatel-Chaix *et al.*,

2016). This regulation of mitochondrial morphodynamics was attributed to NS4B which partly resides in CMs. The pharmacological destabilization of CMs induces mitochondria fragmentation and correlates with a stimulation of virus-induced apoptosis (Anton *et al.*, 2021). Conversely, mitochondria elongation positively influences the size and abundance of CMs and dampens the RIG-I-dependent type-I and -III interferon induction (Chatel-Chaix *et al.*, 2016). This supports a model in which flaviviruses regulate mitochondrial functions through their contacts with CMs for the benefit of replication.

ER-mitochondria contacts (ERMC) rely on protein-protein connections maintaining a 10-25 nm-wide interface between the ER and the mitochondria that allows molecular transfers between both organelles (Csordas *et al.*, 2006; Fujimoto *et al.*, 2011; Vance, 2015). This ultrastructure contributes to several cellular processes such as calcium homeostasis, lipid transport, autophagy regulation, mitochondrial morphodynamics, apoptosis induction and early innate immunity (Cohen *et al.*, 2018; Friedman *et al.*, 2011; Hamasaki *et al.*, 2013; Pourcelot *et al.*, 2014; Schwarz *et al.*, 2016). Illustrating their important roles in cellular processes, ERMC are a target of viruses for interfering with mitochondrial-mediated antiviral responses (Horner *et al.*, 2011; Horner *et al.*, 2015). Recently, we have shown that DENV-induced mitochondria elongation positively regulates the biogenesis of CM (Chatel-Chaix *et al.*, 2016). This is accompanied with a decrease in colocalization between the ER and mitochondria at the cellular level in confocal microscopy. However, it is still unclear whether flaviviruses globally alter ERMC and what the resulting impacts are regarding cellular processes such as oxidative respiration and apoptosis.

In this study, we show an overall alteration of the ERMC compartment following DENV and ZIKV infections. Concomitantly, reducing expression of several ERMC proteins responsible for tethering mitochondria and the ER increased DENV and ZIKV replication, supporting that both viruses alter ERMC to stimulate viral replication. Interestingly, the expression profile of several ERMC proteins was changed with a drastic decrease in the levels of RRBP1 over the course of the infection and the appearance of an alternative ZIKV-specific SYNJ2BP protein product. This suggests that both viruses destabilize ERMC by targeting tethering proteins. Furthermore, both DENV and ZIKV modulated mitochondrial respiratory metabolism in living cells. This correlated with a decrease in the abundance of several metabolites of the Krebs cycle and changes in the stoichiometry of the electron transport chain. Most importantly, targeting ERMC by silencing either RRBP1 or SYNJ2BP increased respiration and dampened ZIKV-induced apoptosis supporting the importance of ERMC alteration by DENV and ZIKV for attenuating antiviral cellular processes and for maintaining a cytoplasmic environment favorable to the viral replication.

3.3 Results

3.3.1 DENV and ZIKV alter ERMCs

Previous observation of DENV-infected Huh7 cells at the ultrastructural level suggested that ERMCs were altered. Although this was not quantified, this correlated with a decrease of 3D colocalization between mitochondria and ER in a limited number of analyzed cells in confocal microscopy, *i.e.*, at a resolution which is too low to precisely measure heterotypic organelle contacts (Chatel-Chaix *et al.*, 2016). The molecular mechanisms underlying this phenotype was not described and it was also not established whether this phenotype is specific for DENV or also expands to other relevant flaviviruses, such as ZIKV. To clearly address whether DENV and ZIKV infections induce a global alteration of ERMCs, we performed a comprehensive quantitative ultrastructural analysis of DENV- and ZIKV-infected Huh7.5 hepatoma cells using transmission electron microscopy. The Huh7.5 cell line was chosen as a model because these cells are defective in RIG-I-dependent interferon induction, warranting that any observed phenotype is not caused by early innate immunity, a process that relies on mitochondrial protein MAVS (Loo *et al.*, 2011). More than two hundred mitochondria per conditions (n=215-351) were analyzed for ERMCs following 48 hrs of infection with the ZIKV H/PF/2013 contemporary strain or serotype 2 DENV 16681s strain. In uninfected conditions, 74.7% of mitochondria were surrounded by ER tubules with up to 75% of the mitochondrial perimeter being in contact with these ER membranes (median at 31.4%; Fig. 3.1a-c). In stark contrast, both DENV and ZIKV-infected cells exhibited a reduced proportion of mitochondria in contact with ER membranes, with a phenotype more pronounced for DENV than for ZIKV. In addition, when the two organelles were still physically associated, only 19% of the mitochondria perimeter in average were in contact with ER following both ZIKV and DENV infections, compared to 35% in uninfected condition (Fig 3.1c). Consistent with the previous observation, mitochondria showed an elongated morphology and were often located in the vicinity of CMs (Fig. 3.1a).

To examine the impact of both virus infections on ERMCs at a molecular level in a larger cell population, we analyzed the extent of protein-protein interactions involved in tethering mitochondria and ER using proximity ligation assay (PLA). This technique allows the detection of the proximity between two proteins at a maximum distance of 40 nm and the analysis of the intracellular localization of protein complexes using confocal microscopy. We focused our PLA analysis on three ERMC tethering complexes known to contribute to ERMC formation and/or stability, namely the interactions between: 1- ER -resident vesicle-associated membrane protein-associated protein B (VAPB) and the mitochondrial outer membrane protein, protein tyrosine

phosphatase-interacting protein 51 (PTPIP51) (De Vos *et al.*, 2012); 2- ER-resident, ribosome-binding protein 1 (RRBP1) and the mitochondrial protein, synaptojanin 2-binding protein (SYNJ2BP) (Duan *et al.*, 2022; Hung *et al.*, 2019); and 3- the ER protein, inositol 1,4,5-trisphosphate receptor 1 (IP3R1) and mitochondrial voltage-dependent anion-selective channel 1 (VDAC1) via the chaperone glucose-regulated protein 75 (GRP75) (Hartmann *et al.*, 1998) (Fig. 3.2a). First, we confirmed that PLA signals detected for these three different tethering complexes mostly colocalized with the mitochondria network in Huh7.5 cells stably expressing the mitochondria-localized mito-mTurquoise2 fluorophore (Suppl. Fig. 3.1a). PLAs were then performed for VAPB-PTPIP51, RRBP1-SYNJ2PB and IP3R1-VDAC1 interactions in uninfected- or DENV/ZIKV infected-Huh7.5 cells at 48 and 72 hrs post-infection and combined with immunostaining of NS3 viral protein to identify infected cells. As expected, we detected a high amount of RRBP1-SYNJ2BP (Fig. 3.2b), IP3R1-VDAC1 (Suppl. Fig. 3.1b) and VAPB-PTPIP51 (Suppl. Fig. 3.1c) interactions in the uninfected condition in confocal microscopy. The signal was specific to the targeted protein-protein interactions since omitting either primary antibody gave very little, if any, PLA signal (Fig. 3.2c, Ab alone controls). Strikingly, when comparing ZIKV- or DENV-infected (green) and uninfected cells in the same images, it was obvious that the RRBP1-SYNJ2BP PLA signal was less abundant in infected cells (Fig 3.2b). Subsequent quantification of the PLA dots per cell demonstrated an overall decrease in PLA signal in NS3-positive cells *(i.e.*, infected) in all three assays (Fig. 3.2c, Suppl. Fig. 3.1b-c). This demonstrates a decrease in the abundance of the RRBP1-SYNJ2BP, IP3R1-VDAC1 and VABP-PTPIP51 ERMC tethering complexes and confirms an alteration of ERMCs by DENV and ZIKV at the molecular level. Interestingly, this decrease was particularly prominent for RRBP1-SYNJ2BP and IP3R1-VDAC1 at 72 hrs post-infection.

To examine the impact of DENV and ZIKV infection on the expression of ERMC proteins, we performed western blotting on extracts from uninfected or infected Huh7.5 cells at 48 and 72hrs post-infection. The expression levels of GRP75, VDAC1, VAPB and PTPIP51 were unchanged upon ZIKV and DENV infections (Suppl. Fig. 3.2a-b). In contrast, the expression of RRBP1 was reduced at 48 hrs post-infection with a further decrease of its levels at 72hrs post-infection (Fig. 3.2d and Suppl. Fig. 3.2a). Moreover, an alternative SYNJ2BP product exhibiting a higher molecular weight was detected in ZIKV-infected cells at 48 and 72 hrs post-infection (Fig. 3.2d and Suppl. Fig. 3.2a). Finally, our immunofluorescence-based confocal microscopy analysis of DENV- and ZIKV-infected cells did not reveal any changes in the sub-cellular distribution of IP3R1, VDAC1, RRBP1, SYNJ2BP and PTPIP51 in DENV/ZIKV infection (Suppl. Fig. 3.3). Interestingly, viral infection induced a drastic relocalization of ER-resident VAPB into large NS3-

positive foci reminiscent of CMs, suggesting that DENV and ZIKV alter VAPB/PTPIP51-dependent ERMC by physically sequestering VAPB. Altogether, these data strongly support that DENV and ZIKV target ERMC tethering complexes.

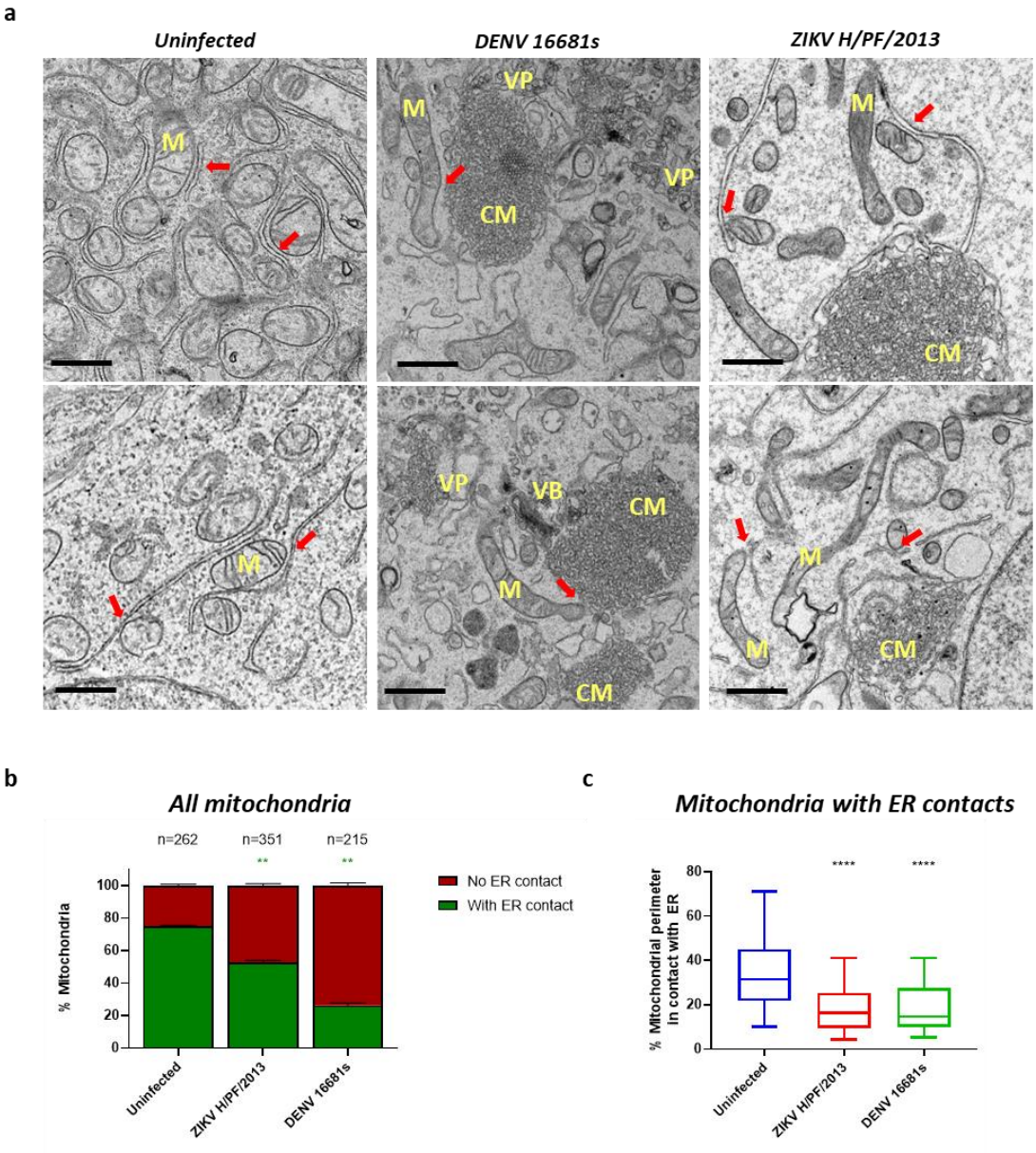

Figure 3.1 DENV and ZIKV infection alter endoplasmic reticulum-mitochondria contact sites

Huh7.5 cells were infected with DENV2 16681s (multiplicity of infection (MOI)=1), or ZIKV H/PF/2013 (MOI=10) or left uninfected. Forty-eight hours later, cells were processed for transmission electron microscopy. (a) Electron micrographs of uninfected and infected cells. Red arrows indicate ER-mitochondria contact sites. CM: convoluted membranes; VP: vesicle packets; M: mitochondria; VB: virus bags. Scale bar = 1 µm. (b) Proportion of mitochondria with or without contacts with the ER; n: number of analyzed mitochondria. (c) Percentage of the mitochondrial perimeter in contact with ER. The mitochondria of (b) which were not in contact with ER were excluded from this quantification. Values in the 5%-95% percentile range are shown. Analyses were made with micrographs from 2 independent experiments.

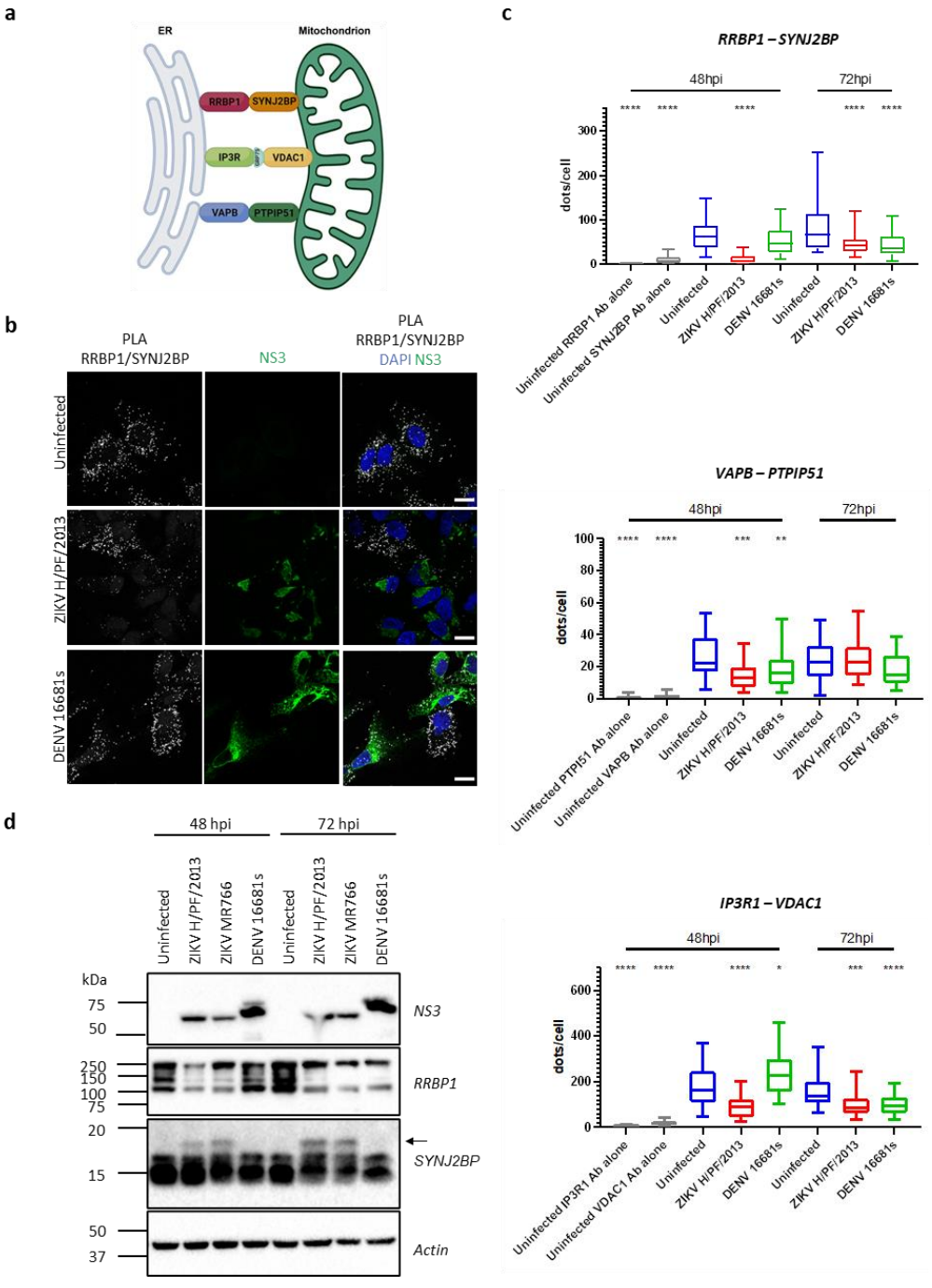

Figure 3.2 Impact of DENV and ZIKV infection on the expression of ERMC proteins

(a) Schematic representation of ERMC tethering complexes. Generated with BioRender. (b) Huh7.5 cells were infected with DENV 16681s (MOI=1) or ZIKV H/PF/2013 (MOI=10) or left uninfected. Two or three days later, cells were fixed and subjected to proximity ligation assays (PLA) to detect SYNJ2BP-RRBP1 interactions, and immunostained for NS3 viral protein to identify infected cells. Cells were imaged using confocal microscopy. Representative images are shown. Scale bar=20 µm. (c) Quantification of PLA dot abundance for RRBP1-SYNJ2BP, VAPB-PTPIP51 and IP3R1-VDAC1 interactions in uninfected- and infected-cells from two independent experiments. Values in the 5%-95% percentile range are shown. (d) Cells were prepared as in (b). Two- or three-days post-infection, cell extracts were prepared, and the expression levels of the indicated proteins were analyzed by western blotting. The arrow indicates the ZIKV-induced SYNJ2BP protein product.

3.3.2 DENV and ZIKV perturb mitochondrial respiration

The remodelling of organelles such as ER or mitochondria by flaviviruses and maintaining vROs is presumably highly energy-consuming while being a source of cellular stress. Considering that mitochondria is the powerhouse of the cell, we investigated the impact of flaviviral infection on the oxidative respiration process in mitochondria, which is the main source of energy in the form of adenosine triphosphate (ATP) in cells. Briefly, we analyzed mitochondrial respiration properties in uninfected- and infected-living Huh7.5 cells at 24, 48 and 72hrs post-infection by measuring the oxygen consumption rate (OCR) while sequentially adding oligomycin (ATP synthase inhibitor), FCCP (protonophore) and rotenone/antimycin A (complex I and III inhibitors, respectively) that directly act on the electron transport chain of the inner mitochondrial membrane (Fig. 3.3a). The OCR profile, an indicator of mitochondrial respiration, slightly increased at 24hrs post-infection with both viral infections compared to the uninfected condition (Fig. 3.3b, e). Very interestingly, the OCR profiles were shifted down at later time points of the infection at levels attributed to the non-mitochondrial oxygen consumption (Fig. 3.3c-e) suggesting that mitochondria are no longer able to efficiently perform oxidative respiration. Analyzing the OCR profiles revealed significant increases of the basal respiration, the ATP-linked respiration, and the maximal respiration at 24hrs post-infection whereas a drastic significant shut-off of these indicators was observed at 72hrs post-infection demonstrating a time-dependent modulation of the oxidative respiration by flaviviruses. (Fig. 3.3e).

To gain more insight about the causes of this respiration alteration at the late time points of flaviviral infection, we analyzed the mitochondrial levels of proteins involved in the Krebs cycle and the electron transport chain (ETC) by performing quantitative mass spectrometry on mitochondria purified from uninfected and ZIKV- and DENV-infected-Huh7.5 cells 48 hrs post-infection (Fig 3.3f). We have included in the analysis a second ZIKV strain from the African lineage, namely MR766. This mitoproteomic analysis identified changes in the stoichiometry of several proteins of the ETC proteins compared to uninfected cells (Fig. 3.3f, Suppl. Table 3.1, Suppl. Fig. 3.4a). Most notably, the composition of the complex II (succinate dehydrogenase), which is a component of both the Krebs cycle and the ETC was changed upon infection. Indeed, mitochondrial levels of sub-units D and C of SDH were increased upon DENV and ZIKV MR766 infections, respectively, compared to other subunits. Interestingly, the SDH assembly factor SDHAF2 was less abundant in mitochondria from DENV-infected cells and this phenotype was confirmed by western blotting on purified mitochondria (Suppl. Fig. 3.4b).

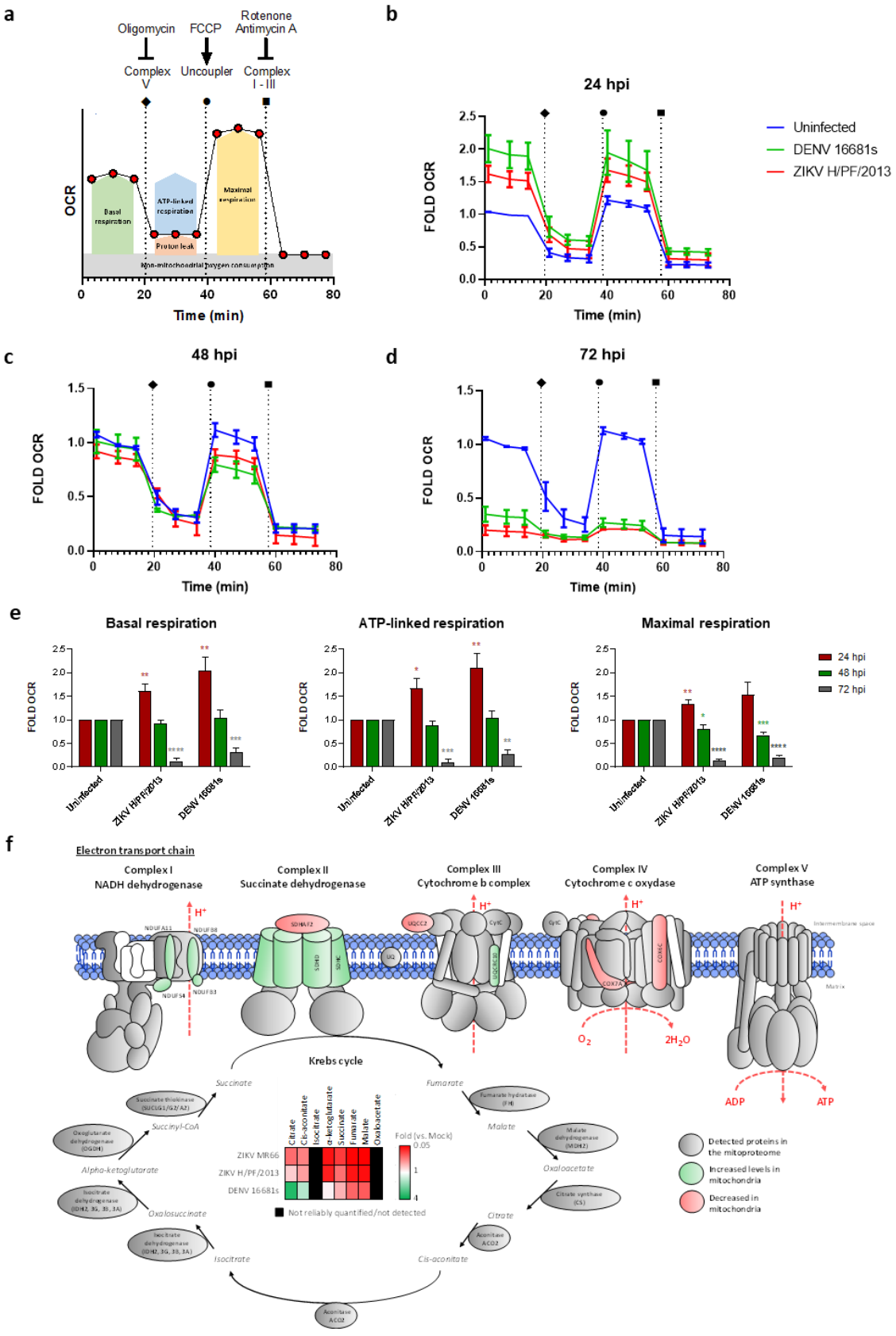
a
Oligomycin
FCCP
Rotenone
Antimycin A
Complex V
Uncoupler
Complex I - III
OCR
Basal respiration
ATP-linked respiration
Maximal respiration
Proton leak
Non-mitochondrial oxygen consumption
Time (min)
b
24 hpi
FOLD OCR
Time (min)
Uninfected
DENV 16681s
ZIKV H/PF/2013
c
48 hpi
FOLD OCR
Time (min)
d
72 hpi
FOLD OCR
Time (min)
e
Basal respiration
ATP-linked respiration
Maximal respiration
FOLD OCR
Uninfected
ZIKV H/PF/2013
DENV 16681s
24 hpi
48 hpi
72 hpi
f
Electron transport chain
Complex I
NADH dehydrogenase
Complex II
Succinate dehydrogenase
Complex III
Cytochrome b complex
Complex IV
Cytochrome c oxydase
Complex V
ATP synthase
Krebs cycle
Succinate
Fumarate
Malate
Oxaloacetate
Citrate
Cis-aconitate
Isocitrate
Alpha-ketoglutarate
Oxalosuccinate
Succinyl-CoA
ZIKV MR66
ZIKV H/PF/2013
DENV 16681s
Not reliably quantified/not detected
Fold (vs. Mock)
Detected proteins in the mitoproteome
Increased levels in mitochondria
Decreased in mitochondria
ADP
ATP

Figure 3.3 DENV and ZIKV perturb mitochondrial respiration

Huh7.5 cells were infected with DENV 16681s (MOI=1) or ZIKV H/PF/2013 (MOI=10), or left uninfected for 24, 48 and 72hr before analysis. (a) Schematic representation of the respiration profile in living cells generated with the Seahorse technology. The ATP synthase inhibitor oligomycin, the proton ionophore carbonyl cyanide p-trifluoromethoxyphenylhydrazone (FCCP), and a mixture of mitochondrial complex III inhibitor antimycin A / mitochondrial complex I inhibitor rotenone are sequentially added to analyze various parameters of the respiration. (b-d) The oxygen consumption rates (OCR) of uninfected and infected cells were analyzed at the indicated time points (N=5). (e) Based on the data of (3b-d), basal respiration, ATP production and maximal respiration were determined. (f) DENV/ZIKV-infected and control cells were analyzed two days post-infection for their mitochondrial protein composition following mass spectrometry on purified mitochondria (N=4), as well as for the abundance of the Krebs cycle metabolites measured by GC-MS in 4 independent experiments. Schematic representation of the mitochondrial electron transport chain coupled to the Krebs cycle is shown. Red elements indicate proteins/metabolites which were downregulated upon DENV/ZIKV infection. In contrast, green elements highlight upregulated proteins/metabolites. The expressions of the proteins in grey were not significantly impacted by flaviviral infections. All values were normalized to the uninfected condition. Isocitrate and oxaloacetate were not detected using GC-MS in these experiments.

However, in contrast to SDH, the mitochondrial levels of all other enzymes of the Krebs cycle remained unchanged (Fig 3.3f, Suppl. Table 3.1). The changes in SDH composition correlated with a drastic decrease of several metabolites of the Krebs cycle (i.e., α-ketoglutarate, succinate, fumarate and malate) as measured by gas chromatography-coupled mass spectrometry (GC-MS) (Fig. 3.3f, Suppl. Fig. 3.4c). Interestingly, in the case of DENV infection, the levels of citrate and cis-aconitate were specifically increased, which suggests a dysfunction of the Krebs cycle downstream aconitase activity. In addition to complex II, the stoichiometries of complexes I, III and IV were also altered in DENV- and ZIKV-infected cells with COX6C, COX7A2, COA4 and NDUFS4 being modulated by all three tested flaviviruses (Fig. 3.3f, Suppl. Fig. 3.4a, Suppl. Table 3.1). In contrast, some modulated ETC proteins were specific to either virus (Suppl. Fig. 3.4a). Flow cytometry analysis of infected cells with MitoTracker Orange showed that DENV and ZIKV did not induce a notable decrease in the mitochondrial potential at 48hrs post infection (Suppl. Fig 3.4d). This strongly supports that the observed respiration and mitoproteome phenotypes were not the result of a loss of mitochondrial integrity at that time point. Altogether, these data combining respirometric, proteomic and metabolomic approaches clearly demonstrate that ZIKV and DENV interfere with the mitochondrial respiratory metabolism.

3.3.3 ERMC alteration increases mitochondrial respiration

Since DENV and ZIKV infections induce a shut-off of the mitochondrial oxygen consumption over time and disrupt ERMCs, we investigated the impact of this sub-cellular compartment alteration on respiration. To that aim, we analyzed the oxygen consumption of living cells following expression knockdown of ERMC tethering proteins by transducing cells with shRNA-expressing lentiviruses. Indeed, it is well established that knockdown of ERMC proteins destabilizes physical

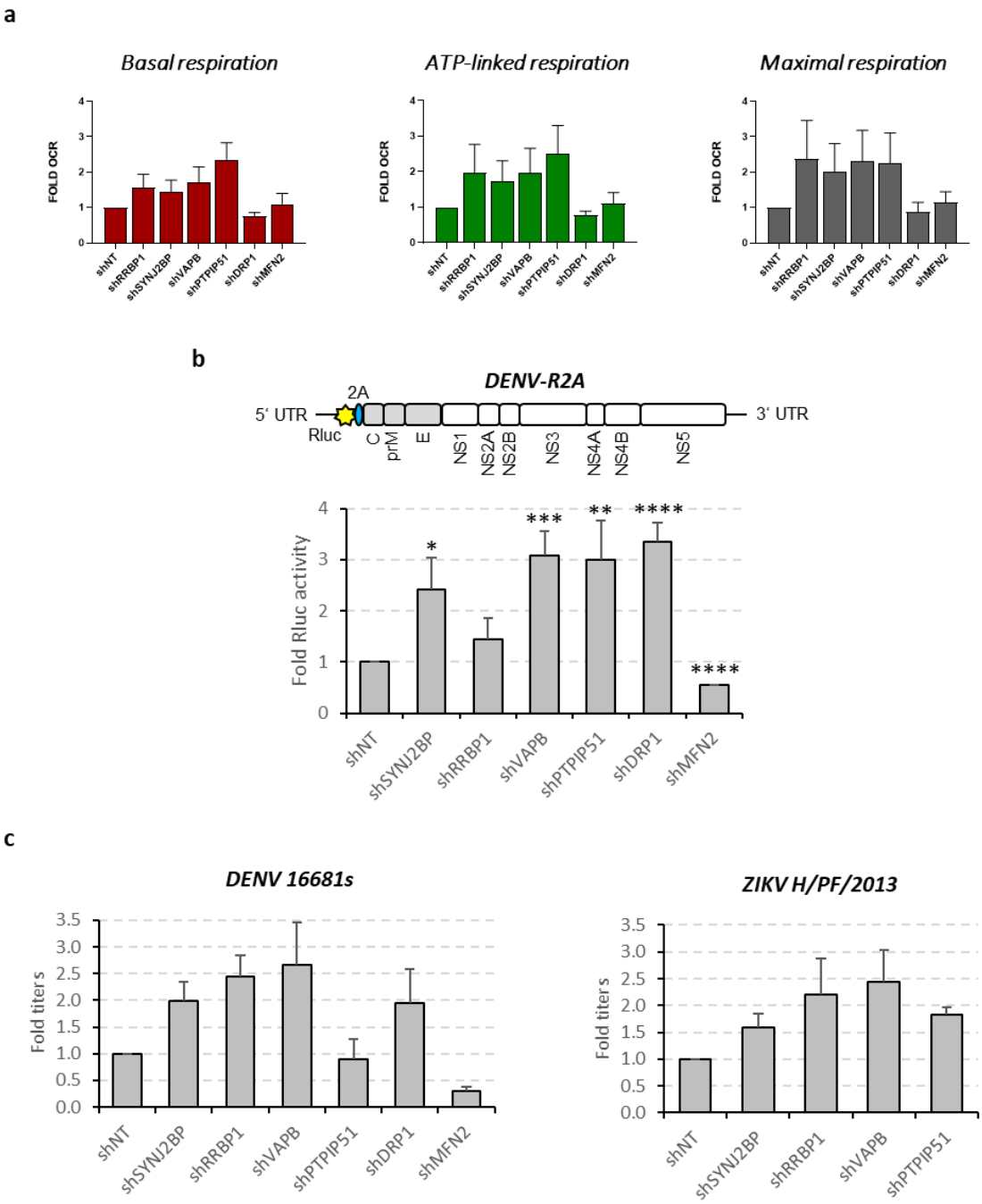

Figure 3.4 ERMC proteins negatively regulate mitochondrial respiration and viral replication

(a) Huh7.5 cells were transduced with lentiviruses expressing shRNAs which target the indicated proteins (MOI=4). Four days later, cells were trypsinized, counted and processed for measurements of various parameters of the oxygen consumption rate using the Seahorse technology as described in the Material and Methods section. (N=6). Data were normalized to the non-target shRNA (shNT) control condition. (b) Cells were transduced as in (a). Two days post transduction, cells were infected with DENV-R2A reporter viruses which express *Renilla reniformis* luciferase (Rluc) at a MOI of 0.01. Two days post-infection, the luciferase activity was measured as a read-out of viral replication and normalized to the shNT control condition. (c) Two days post-transduction, cells were infected with wildtype DENV 16681s or ZIKV H/PF/2013 (MOI=0.1). Two days post-infection, the infectious titers of extracellular viral particles were determined by plaque assays. All values were normalised to the shNT condition.

contacts between ER and mitochondria organelles (Anastasia *et al.*, 2021; Deng *et al.*, 2008; Duan *et al.*, 2018; Stoica *et al.*, 2014). We identified shRNAs whose expression led to efficient silencing of SYNJ2BP, RRBP1, VAPB and PTPIP51 without reducing cellular viability 4 days post-transduction (Suppl. Fig. 3.5a-b). The IP3R1-GRP75-VDAC1 tethering complex was voluntarily omitted from the analysis because we reasoned that knocking these factors down may induce pleiotropic effects related to their ion channel activity and their role in calcium homeostasis and not to the contacts *per se* (Hartmann *et al.*, 1998). To exclude that potential phenotypes would be due to changes in mitochondrial morphodynamics (which can influence viral replication), we used confocal microscopy to control that ERMC protein knockdown did not change the morphology of the mitochondrial network compared to the non-target shRNA (shNT) control condition (Suppl. Fig. 3.5d). As control, knockdown of fission factor DRP1 and fusion factor MFN2 led to mitochondrial elongation and fragmentation, respectively (Suppl. Fig. 3.5a, d). Moreover, flow cytometry analysis of ERMC protein-depleted cells showed no impact of ERMC alteration on the mitochondrial potential (Suppl. Fig. 3.5c). Interestingly, the mitochondrial oxygen consumption in Huh7.5 cells in which ERMC proteins were knocked down generally increased as compared to the shNT control condition (Fig. 3.4a). In contrast, no obvious changes in the OCR parameters were observed when mitochondrial morphodynamics was modulated upon DRP1 and MFN2 knockdown. These data show that ERMC alteration by DENV and ZIKV stimulates respiration independently of mitochondria morphodynamics and may explain why respiration is increased at early time points. Such a viral regulation also might attenuate the respiratory stress induced later in the infection.

3.3.4 ERMC protein knockdown increases viral replication

We next investigated the impact of RNAi-mediated alteration of ERMC on viral replication. Huh7.5 cells in which ERMC proteins were knocked down were infected with a DENV reporter virus (DENV-R2A) expressing *Renilla reniformis* luciferase (Rluc), allowing us to evaluate DENV replication levels by measuring bioluminescence in cells at 2 days post-infection. We observed an increase in DENV-R2A replication upon ERMC protein knockdown, which was most pronounced when VAPB and PTPIP51 were depleted (Fig. 3.4b). Consistently, comparable phenotypes were obtained when cells were infected with either wild-type DENV2 16681s or ZIKV H/PH/2013 since the production of infectious viral particles was increased upon knockdown of ERMC proteins as measured by plaque assays (Fig. 3.4c). As controls and in line with previous observations (Chatel-Chaix *et al.*, 2016), the modulation of mitochondrial morphodynamics showed the expected phenotypes. Indeed, the silencing of DRP1, which results in enhanced

mitochondrial elongation, stimulated DENV replication while reduction of MFN2 expression impaired it (Fig. 3.4b-c). Overall, these data indicate that ERMC proteins restrict viral replication and further support that the DENV- and ZIKV-induced modulation of the physical contacts between mitochondria and ER is proviral.

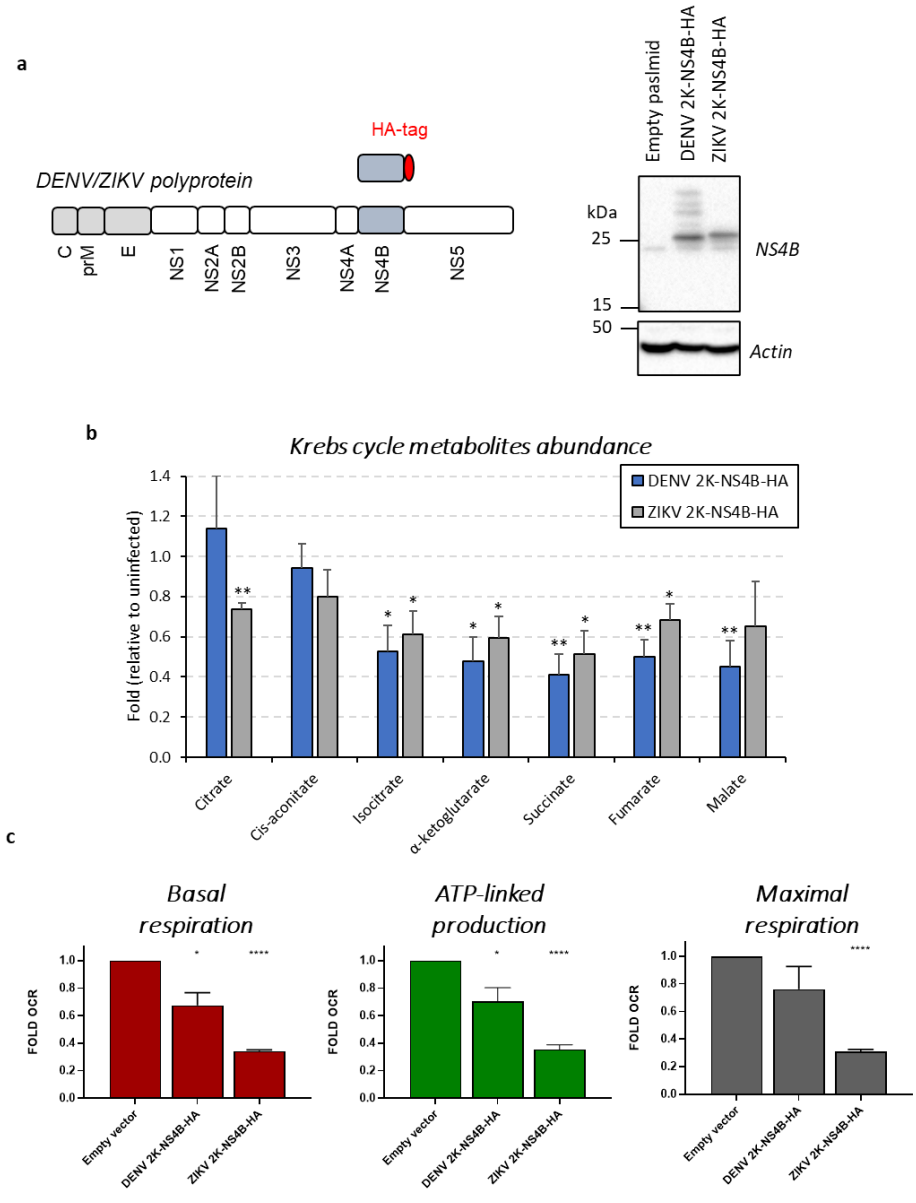

Figure 3.5 NS4B viral protein inhibit the mitochondrial respiratory metabolism

Huh7.5 cells were transduced with lentiviruses expressing HA-tagged DENV or ZIKV NS4B proteins including the N-terminal 2K signal peptide (MOI= 2-4). Transduced cells were selected with puromycin and analyzed 4 days post-transduction for: (a) NS4B expression using western blotting, (b) the abundance of Krebs cycle metabolites using GC-MS in 3 independent experiments, and (c) their basal respiration, ATP production and maximal respiration using the Seahorse technology (N=3). All values were normalised to the empty vector control condition. For (b) and (c) an equal number of cells for all conditions was used.

3.3.5 NS4B viral protein inhibits the mitochondrial respiratory metabolism

The conserved flaviviral NS4B protein is essential for viral replication and is a component of vROs (Chatel-Chaix *et al.* ; Grant *et al.*, 2011; Kelly *et al.*, 2010; Welsch *et al.*, 2009; Zou *et al.*, 2014). Since it was shown that DENV NS4B expression induces mitochondria elongation (Chatel-Chaix *et al.*, 2016), we hypothesized that this viral protein was at least in part responsible for the observed alteration of mitochondrial respiration in DENV- and ZIKV-infected cells. First, we showed that the transient expression of ZIKV NS4A-2K-NS4B precursor and 2K-NS4B pseudo-mature proteins (2K serving as a signal peptide for NS4B) in Huh7.5-T7 cells induced mitochondria elongation as DENV NS4B, suggesting that ZIKV and DENV NS4B proteins modulate mitochondria functions via similar molecular mechanisms. (Suppl. Fig. 3.6a-b).

We next investigated the impact of NS4B expression on mitochondrial respiratory functions. To ensure that all cells stably expressed this viral protein, we transduced Huh7.5 cells using lentiviruses expressing ZIKV or DENV HA-tagged NS4B and conferring resistance to puromycin. Following selection with this antibiotic, we verified the proper expression of NS4B by western blotting (Fig. 3.5a) and subsequently measured the abundance of the Krebs cycle metabolites by GC-MS. As in infected cells, the overexpression of both DENV and ZIKV NS4B significantly reduced the levels of α-ketoglutarate, succinate and fumarate (Fig 3.5b). Consistently, this correlated with a decrease in basal respiration, ATP-linked respiration and maximal respiration (Fig. 3.5c) which was more pronounced for ZIKV NS4B-HA. Comparable phenotypes on oxygen consumption rates were observed when DENV and ZIKV NS4B proteins were expressed as NS4A-2K-NS4B precursors (Suppl. Fig 3.6c-d). Altogether, these data demonstrate that NS4B is one of the main viral determinants contributing to the decrease of the oxidative respiration observed at the late time points of DENV and ZIKV infections.

3.3.6 RRBP1 and SYNJ2BP regulate ZIKV-induced apoptosis

We have previously shown that CM integrity relies on VCP ATPase activity which is required to dampen ZIKV-induced apoptosis (Anton *et al.*, 2021). Since CMs are physically connected to mitochondria through residual associated ER membranes and considering that ERMC were reported to regulate mitochondria-dependent cell death (Carpio *et al.*, 2021; Giamogante *et al.*, 2021; Suresh, 2019; Verfaillie *et al.*, 2012), we hypothesized that the alteration of ERMC integrity dampens apoptosis during flaviviral infection. To test this, we measured the activity of caspase 3 (the major regulator of the execution phase of apoptosis) in Huh7.5 cells upon RRBP1 or SYNJ2BP silencing. We chose this ERMC tethering couple because it was the one that was the

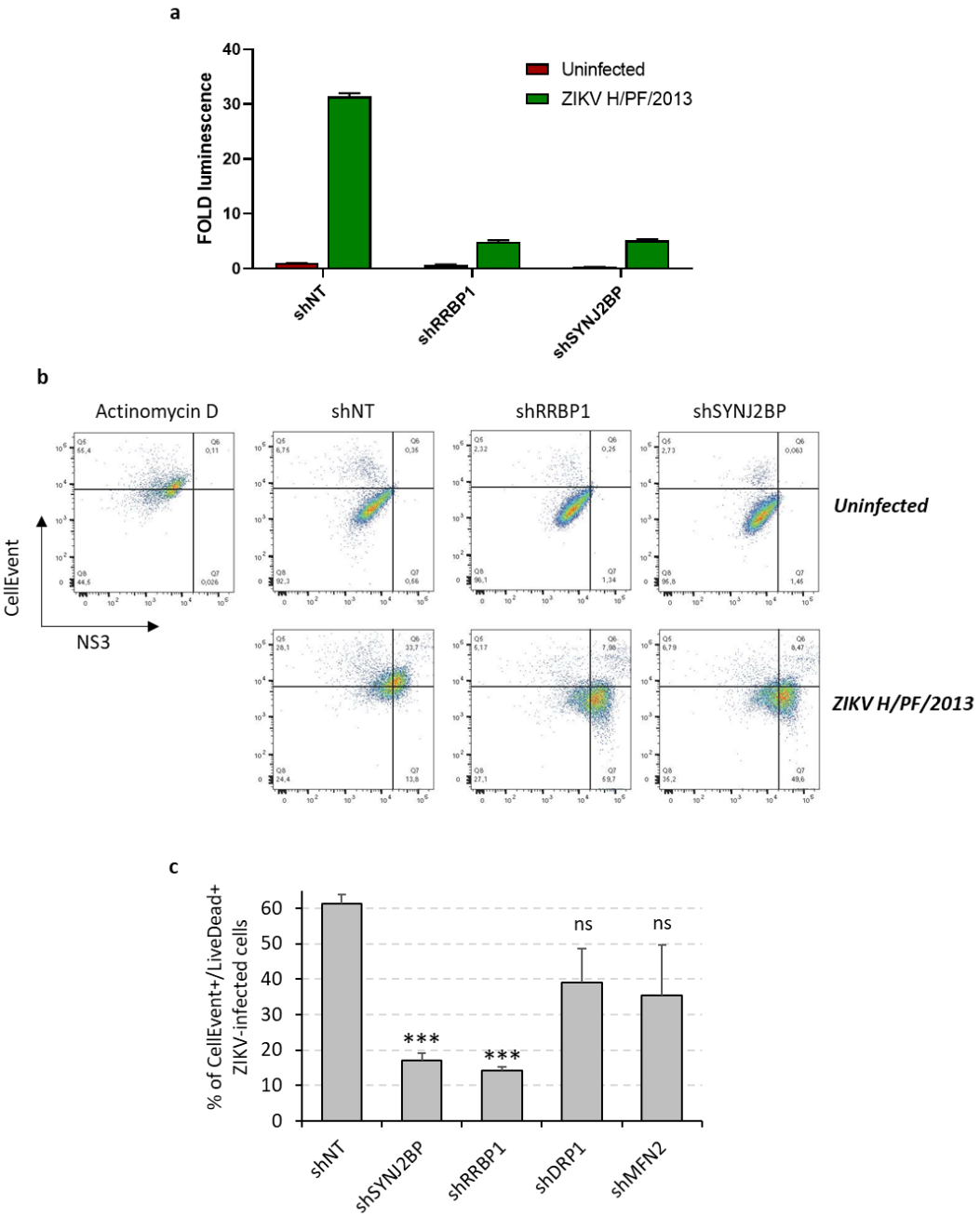

Figure 3.6 ERMC alteration dampens ZIKV-induced apoptosis

(a) Huh7.5 cells were transduced with lentiviruses expressing shRNAs which target the indicated proteins (MOI=4). Two days post-transduction, cells were infected with ZIKV H/PF/2013 (MOI=20) or left uninfected. Two days post-infection, cell lysates were prepared, and apoptosis induction was measured by measuring bioluminescence using the Caspase-Glo 3/7 assay kit. (b) Cells were transduced and infected as in (a). Two days post-infection (*i.e.*, 4 days post-transduction), apoptosis induction, cell death and ZIKV infection were detected by flow cytometry using the CellEvent caspase-3/7 green reagent, the amine reactive viability dye LIVE/DEAD aqua fixable stain, and anti-NS3 antibodies, respectively. Actinomycin D treatment (2.5 µM, 24 hours) was used as a positive control of apoptosis induction. The plots show representative results of the caspase activity in function of NS3 expression. (c) Gated ZIKV-infected cells (*i.e.*, NS3+ cells) were analyzed for apoptosis induction and cell viability using the CellEvent caspase-3/7 green and LIVE/DEAD biosensors, respectively (N=3). All values were normalised to the shNT condition.

most impacted by ZIKV infection (Fig. 3.2b-c). Very interestingly, upon RRBP1 or SYNJ2BP depletion, the activity of caspase 3/7 was reduced in lysates of ZIKV-infected cells as measured using a bioluminescence-based assay (Fig. 3.6a). We confirmed these phenotypes by flow cytometry using the CellEvent caspase-3/7 green reagent, a fluorescent biosensor of caspase 3/7 activity, and anti-NS3 antibodies to detect ZIKV-infected cells (Fig. 3.6b). While 61.2% of the cells were apoptotic (*i.e.*, CellEvent-positive) in control infected conditions (shNT), this proportion was reduced to 13.2% and 15.3% when RRBP1 and SYNJ2BP were knocked down, respectively. Moreover, the proportion of ZIKV infected cells which were non-apoptotic (*i.e.*, NS3-positive/CellEvent-negative cells) drastically increased under these conditions (13.8% for shNT versus 59.7% and 49.6% for shRRBP1 and shSYNJ2BP, respectively). Furthermore, by combining these markers with the amine reactive viability dye LIVE/DEAD aqua fixable stain (Fig. 3.6c), we showed that the silencing of RRBP1 and SYNJ2BP decreased the proportion of dead ZIKV-infected cells, namely cells that were apoptotic and exhibited a ruptured plasma membrane (% of NS3-gated CellEvent-positive and LIVE/DEAD-positive cells). Finally, as expected, no apoptosis was observed in any uninfected conditions demonstrating that ERMC destabilization *per se* does not induce apoptosis (Fig. 3.6b). In contrast, as positive control, treatment of the cells with actinomycin D robustly induced apoptosis. Altogether, these data support that ZIKV alters ERMC integrity to dampen infection-induced apoptosis and promote replication.

3.4 Discussion

In this study, we demonstrate that DENV and ZIKV modulate the mitochondrial oxidative respiration and virus-induced apoptosis in favor of viral replication notably by altering the physical contacts between mitochondria and the ER. Our observations are consistent with the fact that ERMC were reported to play a crucial role in the induction of the apoptosis pathway, as explained below (Carpio *et al.*, 2021; Giamogante *et al.*, 2021; Suresh, 2019; Verfaillie *et al.*, 2012). Such morphological remodeling allows flaviviruses to create a proviral cytoplasmic environment. Although there is reported evidence that mitochondrial fission is initiated at sites where the ER tubules wrap mitochondria and constrict mitochondria prior to DRP1 recruitment (Friedman *et al.*, 2011), we did not observe any changes in mitochondria morphology upon ERMC protein knockdown in Huh7.5 cells (Suppl. Fig. 3.5d) supporting that the phenotypes reported here are independent of DRP1-mediated fission regulation by flaviviruses (Barbier *et al.*, 2017; Chatel-Chaix *et al.*, 2016).

Flaviviruses induce membranous replication factories from the ER membranes (Chatel-Chaix *et al.*, 2014; Paul *et al.*, 2015). More recently, it was shown that DENV and ZIKV induce the elongation of mitochondria in the vicinity of CMs (Barbier *et al.*, 2017; Chatel-Chaix *et al.*, 2016). As it was already observed (Chatel-Chaix *et al.*, 2016), we noticed that mitochondria remain connected to CMs via residual associated ER membranes. This raises the hypothesis that the morphogenesis of CMs uses the reticulo-mitochondrial interface as a source of ER membranes via the destabilization of this specific cytoplasmic compartment. In addition, we show that DENV and ZIKV alter ERMC by decreasing the abundance of three different tethering protein complexes (RRBP1-SYNJ2BP, IP3R1-VDAC1 and VAPB-PTPIP51). We did not observe any difference in the expression level of VDAC1, VAPB and PTPIP51. Interestingly, RRBP1 levels were reduced after 48 hours of infection with both viruses while a ZIKV-specific SYNJ2BP product exhibiting a higher molecular weight was detected. Whether these results from a flavivirus-specific regulation of alternative splicing or of posttranslational modifications will be explored in future studies. While VAPB-PTPIP51 and IP3R1-VDAC1 were reported to contribute to calcium homeostasis, autophagy or in phospholipid transfer (Colombini, 2016; De Vos *et al.*, 2012; Gomez-Suaga *et al.*, 2017; Yeo *et al.*, 2021), the contribution of the RRBP1-SYNJ2BP complex to specific cellular function beyond contributing to ERMCs is unknown. This could explain why DENV and ZIKV target specifically this protein-protein couple to separate ER and mitochondria without affecting essential cellular processes. Very interestingly, a recent mass spectrometry-based study has shown that in human fibroblasts, herpes simplex virus type 1, influenza A virus and betacoronavirus HCoV-OC43 decrease the abundance of mitochondrial proteins involved in ERMC whereas the human cytomegalovirus (HCMV) mostly positively regulates them (Cook *et al.*, 2022). Increasing the abundance of ERMC proteins such as VAPB, MFN1/2 fusion proteins, fission-associated proteins DRP1 and MFF, and ER-mediated calcium transfer proteins PTPIP51 and VDAC1 occurred very early during the infection (8 hours post-infection). This HCMV-mediated regulation of ERMCs favors cellular processes such as ER-to-mitochondria calcium flux, mitochondrial fragmentation, and reshaping of cristae for the benefit of HCMV viral particle production. This highlights that viruses from other families than *Flaviviridae* have evolved to co-opt mitochondrial functions via diverse strategies.

The biogenesis of vROs occurs early in infection and their maintenance presumably requires high energy needs in the form of ATP. Consistently, we show here that in the first 24 hours of infection, DENV and ZIKV significantly increase the oxidative respiration followed by a near complete shut-down of this bioenergetic process later in the infection, which correlated with a decrease in the levels of several metabolites of the Krebs cycle (Fig. 3.3). This might result from the mitochondrial

stress and the onset of cytopathic effects generated by the infection. The close analysis of oxygen consumption rate profiles using the Seahorse technology with different inhibitors of the ETC revealed that global respiration was impacted by DENV and ZIKV rather than for instance only the maximal respiration. In line with our data, a recent study showed increases in oxygen consumption and ATP production in astrocytes at the early time points of the infection (*i.e.*, 18 to 24 hrs post-infection) (Ledur *et al.*, 2020). In contrast, later in the infection, the phenotype was reversed with an observed decrease of the oxygen consumption at 48 hrs post-infection. These data support our model of high energy needs when DENV and ZIKV establish the infection notably during the biogenesis of vROs. It is worth mentioning that some studies reported contrasting phenotypes. For instance, it was reported that DENV infection increases oxidative respiration in Huh7 and HepG2 liver cells at 2 days post-infection (Barbier *et al.*, 2017; El-Bacha *et al.*, 2007). Another study showed an inhibition of the basal and maximal oxygen consumption in first-trimester primary trophoblasts infected with ZIKV, that correlated with the fragmentation of the mitochondrial network (Chen *et al.*, 2020). In neurons, ZIKV infection also induced mitochondrial fission by decreasing the expression of the fusion factor MFN2 despite low levels of viral replication (Yang *et al.*, 2020). Pharmacological inhibition of DRP1 (and hence, of fission) reduced ZIKV-induced cell death in this model. This suggests a functional interplay between mitochondrial morphodynamics, the respiratory metabolism and virus-induced apoptosis, which dictates the fate of the infected cell and would be regulated by flaviviruses. While some of these results may seem contradictory and might be explained by the used viral strains and/or cell types more prone to cell death induction (and metabolism suppression) upon infection/stress (*e.g.*, neurons, immune competent cells), we believe that our kinetic analysis described here showing that the time of infection (and most probably the extent of viral protein and remodeled organelles accumulation) is an important determinant of the flaviviral impact on the respiratory metabolism and partly explains these discrepancies. Furthermore, we used here the Huh7.5 cell line which is deficient for the RIG-I-dependent signaling and interferon production. Thus, we can rule out that the observed phenotypes are due to the activation of antiviral innate immunity. The fact that ERMC protein knockdown increased the oxygen consumption rate (Fig. 3.4a) supports the model in which DENV and ZIKV alter ERMCs to stimulate mitochondrial activity to favor vRO formation and delay cell death at the late time points of infection. Very interestingly, we demonstrate that NS4B viral protein is at least partly responsible for the observed decreases in the oxygen consumption rate and the levels of Krebs cycle metabolites. While it remains unknown how NS4B can interfere with mitochondrial respiration, it is noteworthy that this protein is absolutely required for viral RNA replication and is the target of highly potent direct-acting antivirals including one

currently challenged in clinical trial (Chatel-Chaix *et al.*, 2015; Kaptein *et al.*, 2021; Moquin *et al.*, 2021; van Cleef *et al.*, 2013; Xie *et al.*, 2011b; Zou *et al.*, 2015a; Zou *et al.*, 2014).

Apoptosis is a programmed cell death that is induced by both extrinsic and intrinsic pathways. The intrinsic pathway relies on the activation of the caspase 3 via the release of BCL-2 family proteins from mitochondria (Elmore, 2007). Given that ERMC were reported to regulate this cell death pathway, we investigated whether their alteration could influence ZIKV-induced apoptosis. In this study, we demonstrate that the alteration of ERMCs by knocking down RRBP1 and SYNJ2BP decreases apoptosis in ZIKV-infected cells. ERMCs notably regulate this cell death induction pathway through IP3R1 and VDAC1 which interact and act as calcium channels to directly transfer calcium from the ER to mitochondria. Since an overload of calcium in mitochondria leads to apoptosis (Orrenius *et al.*, 2003), it is tempting to speculate that the loss of ERMCs reduces the amounts of mitochondrial calcium and thus, delays the induction of apoptosis. Mitochondria fission positively regulates the activation of apoptosis, notably through the interaction between DRP1 and BAX, a pro-apoptotic factor (Jenner *et al.*, 2022; Montessuit *et al.*, 2010; Oettinghaus *et al.*, 2016; Park *et al.*, 2015). However, RRBP1 and SYN2JBP knockdown did not result in apparent changes in mitochondria morphology, thus allowing us to conclude that these phenotypes were not related to the mitochondria elongation induced by DENV and ZIKV. Interestingly, we have already shown that the integrity of CMs during ZIKV infection is required to both dampen apoptosis and maintain the elongated morphology of mitochondria (Anton *et al.*, 2021). This suggests that both DENV/ZIKV-induced mitochondria elongation and ERMC alteration independently regulate apoptosis. It is interesting to note that in our cell culture system, mitochondria integrity appeared to be preserved upon DENV/ZIKV infection and ERMC protein knockdown since we did not detect any notable changes in the mitochondrial membrane potential (Suppl. Fig. 3.4d, 3.5c), implying that these cells are quite resistant to the cytopathic effects induced by mitochondrial stress.

Finally, the ERMC compartment also serves as a signalling platform during early antiviral innate immunity leading to the induction of type I and III interferons (IFN). When RIG-I senses a foreign RNA, it is translocated to the surface of the mitochondria and binds mitochondrial antiviral-signalling protein adaptor (MAVS) which is located at the ERMC (Horner *et al.*, 2011). Several inhibition mechanisms of RIG-I activation by flaviviruses have been discovered in the last decade (Chatel-Chaix *et al.*, 2016; Gack *et al.*, 2016; Gack *et al.*, 2007; Liu *et al.*, 2012; Manokaran *et al.*, 2015; Riedl *et al.*, 2019; Serman *et al.*, 2019; Tremblay *et al.*, 2019). Thus, perturbing the reticulo-mitochondrial interface may constitute another strategy to inhibit or delay cellular processes that

could be harmful for viruses. While we can rule out that our phenotypes in RIG-I-deficient Huh7.5 cells are due to interferon induction, it will be interesting to evaluate in the future whether the alteration of the reticulo-mitochondrial interface by flaviviruses contributes to countering antiviral immunity in immune-competent cells.

Overall, our data demonstrate that the morphological perturbations of the reticulo-mitochondrial interface by DENV and ZIKV modulate mitochondrial respiratory metabolism to sustain the energetic needs of flaviviral life cycle. This study further supports a model in which these viruses perturb ERMC to hijack specific host factors that are required for CM morphogenesis, and vice-versa. More studies are required to better understand these mechanisms at a molecular level, including the specific viral determinants involved in the alteration of ERMCs and the mitochondrial functions regulated by this sub-cellular compartment. It will be also interesting to evaluate how this impacts ERMC function other than apoptosis and innate immunity, such as calcium homeostasis or lipid metabolism.

3.5 Material and methods

Cell lines and virus strains

Huh7.5, HEK293T, VeroE6, and HeLa cells were cultured in Dulbecco's modified Eagle medium (DMEM, Life Technologies) supplemented with 10% fetal bovine serum (Wisent), 1% non-essential amino acids (Life Technologies) and 1% penicillin-streptomycin (Life Technologies). The generation of the Huh7.5-T7 cell line expressing the T7 RNA polymerase was reported elsewhere (Anton *et al.*, 2021). These cells were cultured in the presence of 5 µg/mL blasticidin (Thermo-Fisher). Huh7.5 cells stably expressing mito-mTurquoise2 were produced exactly as before using lentiviral transduction (Chatel-Chaix *et al.*, 2016) and were maintained in 5 µg/mL zeocin (Life Technologies). ZIKV H/PF/2013 and ZIKV MR766 strains were provided by the European Virus Archive Global (EVAg). Virus stocks were generated by amplification in VeroE6 cells following inoculation with a multiplicity of infection (MOI) of 0.001. Virus aliquots were stored at 80°C until use. Infectious titers were determined by plaque assays exactly as reported before (Freppel *et al.*, 2018). DENV2 16681s and reporter Rluc-expressing DENV-R2A particles were generated using a reverse genetics system (a kind gift of Ralf Bartenschlager) (Fischl *et al.*, 2013) and by electroporating VeroE6 cells with *in vitro*-transcribed DENV RNA genomes as reported before *(Mazeaud et al., 2021).*

Antibodies

Rabbit anti-DENV NS4B (GTX124250; cross-reactive for ZIKV), rabbit anti-ZIKV NS4B (GTX133311), rabbit anti-ZIKV NS3 (GTX133309) and mouse monoclonal anti-DENV NS3 (GTX629477; cross-reactive for ZIKV) were obtained from Genetex. Rat polyclonal antibodies against DENV2 16681 NS3 which are cross-reactive with ZIKV NS3 were generated by Medimabs (Montreal, Canada) as reported before (Anton *et al.*, 2021). Mouse anti-VDAC1 (ab14734) and mouse anti-GRP75 (ab2799) were obtained from Abcam. Rabbit anti-IP3R1 (NBP2-22458) antibodies were obtained from Novus Biologicals. Mouse anti-VAPB (66191-1-Ig) was obtained from ProteinTech. Mouse anti-RRBP1 (MA5-18302) was obtained from Invitrogen. Rabbit anti-PTPIP51 (HPA009975) and rabbit anti-SYNJ2BP (HPA000866) were obtained from Sigma-Millipore.

DNA cloning

The cloning of the constructs expressing DENV/ZIKV NS4B proteins in a T7 RNA polymerase-dependent manner was previously described (Anton *et al.*, 2021; Chatel-Chaix *et al.*, 2015). For generating the lentiviral plasmids expressing HA-tagged 2K-NS4B or NS4A-2K-NS4B proteins, corresponding coding sequences were amplified using the plasmids above as templates (Fischl *et al.*, 2013; Shan *et al.*, 2016). DNA fragments were cloned into the AscI/SpeI or BamHI/SpeI cassettes of the pWPI lentiviral plasmid for ZIKV and DENV proteins, respectively (Chatel-Chaix *et al.*, 2016).

Lentivirus production, titration, and transduction

Knockdowns of ERMC proteins were achieved by transduction with lentiviruses expressing MISSION shRNA from MilliporeSigma (shSYNJ2BP: TRCN0000121988; shRRBP1: TRCN0000117408; shVAPB: TRCN0000152520; shPTPIP51: TRCN0000135580). Constructs expressing shDRP1 and shMFN2 were already described (Chatel-Chaix *et al.*, 2016). For lentivirus production, HEK293T cells were transfected with packaging plasmids pCMV-Gag-Pol, pMD2-VSV-G and pLKO-shRNA or pWPI expressing NS4B using 25 kDa linear polyethylenimine (Polysciences Inc.) exactly as before (Anton *et al.*, 2021; Chatel-Chaix *et al.*, 2016; Mazeaud *et al.*, 2021). Two days post-transfection, lentivirus-containing medium was collected, filtered and stored at -80°C until use. Lentivirus titration was performed in HeLa cells. Cells were seeded at 50,000 cells/well in 24-well plates and lentivirus-containing medium was titrated in 10-fold serial dilution 10^{-1} to 10^{-3} in duplicate. Transduced cells were selected by antibiotic selection one-day post-transduction treatment with 1 µg/mL puromycin. Six days post-transduction, cells were

washed once in PBS, and then fixed and stained with 1% crystal violet/10% ethanol for 20 minutes. Stained cells were washed with tap water. Colony-forming unit were counted, and titers were determined taking into consideration the dilution factor. Huh7.5 cells were transduced with lentiviruses at a MOI of 5-10 in the presence of 8 µg/mL polybrene.

Cell viability assays

7,500 Huh7.5 cells/well in 100µl-DMEM were seeded in 96-well plates and transduced as indicated above. Four days post transduction, 20 µL of 3-(4,5-dimethylthiazol-2-yl)-2,5-diphenyltetrazolium bromide (MTT) at 5 mg/mL were added to the medium for 1 to 4 hr at 37°C. Medium was removed and 150 µL of 2% (v/v) of 0.1 M glycine in DMSO (pH 11) were added to dissolve the MTT precipitates. Absorbance at 570 nm was read with Spark multimode microplate reader (Tecan).

Renilla luciferase assay

1.10^5 Huh7.5 cells/well were plated in 12-well plates in triplicates and transduced as indicated above. The day after, the culture medium was replaced. Two days post-transduction, cells were infected with virus DENV-R2A reporter virus (MOI~0.01). 2 days later, the medium was removed, and cells were lysed in 200 µl of luciferase lysis buffer (1% Triton-X-100; 25 mM Glycyl-Glycine, pH7.8; 15 mM MgSO4; 4 mM EGTA; 1 mM DTT added directly prior to use). 30 µl of lysates were transferred into a white 96-well plate. Luminescence was read with a Spark multimode microplate reader (Tecan) after injection of 150 µl of assay buffer (25 mM Glycyl-Glycine pH7.8; 15 mM KPO_4 buffer pH7.8; 15 mM $MgSO_4$; 4 mM EGTA; 1 mM coelenterazine freshly added before the assay). All values were normalized to the shNT control condition.

Virus production assay

2.10^5 Huh7.5 cells/well were plated in 6-well plates and transduced in the presence of 8 µg/mL polybrene. The day after, culture medium was changed. Two days post-transduction, cells were infected with DENV2 16681s or ZIKV H/PF/2013 (MOI = 0.1). Three hours later, culture medium was changed. Two days post-infection, cell supernatants were collected, filtered at 0.45 µm, and kept at -80ºC until use. 2.10^5 VeroE6 cells/well were seeded in 24-well plates. The day after, cells were infected in 10-fold serial virus dilutions (10^{-1} to 10^{-6}) in duplicate in complete DMEM. Three hours post-infection, the medium was removed, and replaced with serum-free MEM (Life Technologies) containing 1.5% carboxymethylcellulose (MilliporeSigma). Five (ZIKV) or seven (DENV) days post-infection, cells were fixed for 2 hours in 5% formaldehyde. Cells were washed vigorously with tap water and stained with 1% crystal violet/10% ethanol for 20 minutes. Cells

were washed with tap water. Plaques were counted, and infectious titers in particles forming unit (PFU/mL) were calculated.

Immunofluorescence-based confocal microscopy

For immunofluorescence of transiently expressed NS4B proteins, 50,000 Huh7.5-T7 cells/well in 24-well plates were seeded on sterile glass coverslips. The next day, cells were transfected with 0.5 µg of NS4B-encoding plasmids using TransIT-LT1 Transfection Reagent (Mirus) according to the manufacturer's instructions. Four hours post-transfection, culture media were changed. Eighteen hours post transfection, cells were rinsed twice in PBS and fixed in PBS containing 4% paraformaldehyde for 20 minutes.

For confocal microscopy of infected cells, Huh7.5 cells were seeded on coverslips before immunofluorescence assay and infected the day after with DENV2 16681s (MOI = 1-5) or ZIKV H/PF/2013 (MOI=5-10) 2- or 3-days post-infection, cells were washed three times with PBS and fixed for 20 minutes with PBS containing 4% PFA. Coverslips were rinsed 3 times with PBS and kept at 4^{o}C in PBS until use. Prior immunostaining, cells were permeabilized for 15 min in PBS containing 0.2% Triton X-100, and then blocked for 1hr with PBS containing 5% bovine serum albumin (BSA) and 10% goat serum (Thermo-Fisher). Coverslips were incubated 2hrs with primary antibodies at room temperature diluted in PBS/5% BSA. Coverslips were washed three times in PBS and incubated for 1hr at room temperature and in the dark with Alexa Fluor (488, 568 or 647)-conjugated secondary antibodies (Life Technologies) diluted in PBS/5% BSA. Coverslips were washed three times in PBS and incubated 15 min in PBS containing 4', 6'-diamidino-2-phenylindole (DAPI; Life Technologies) diluted 1/10,000 for nuclei staining. Coverslips were washed three times in PBS, and once in water before being mounted on slides with FluoromountG (Southern Biotechnology Associates). Cells were observed and imaged using a LSM780 confocal microscope (Carl Zeiss Microimaging) at the Confocal Microscopy Core Facility of the INRS-Centre Armand-Frappier Santé Biotechnologie. Images were processed with the Fiji software.

Proximity ligation assay

Huh7.5 cells were cultured on coverslips and infected as above. Coverslips were washed three times with PBS and fixed for 20 min with PBS/4% paraformaldehyde. Coverslips were rinsed 3 times with PBS and kept at 4 ^{o}C in PBS until use. Prior to the assay, cells were permeabilized with 0.2% Triton X-100 for 15 min. Proximity ligation assays were performed using the Duolink PLA Kit (Millipore-Sigma) according to the manufacturer's protocol. Briefly, cells were blocked

with the kit buffer for 1 hr at 37ºC in prior incubation with the indicated mouse and rabbit primary antibodies for 2 hours at room temperature. Coverslips were washed three times with the buffer A from the kit and incubated for 1 hr at 37 ºC with PLUS and MINUS PLA probes. Coverslips were washed three times in buffer A and incubated for 30 min at 37ºC with the ligation solution. Coverslips were washed three times with buffer A and incubated 100 min at 37ºC with the kit amplification solution. After final washes with buffer B, coverslips were stained as above with rat anti-NS3 antibodies and Alexa Fluor488 anti-rat antibodies (see immunofluorescence-base confocal microscopy). Cells were then incubated for 15 min in 0.01% buffer B and a 1/10,000 dilution of DAPI (Life Technologies) for nuclei staining. Coverslips were washed three times in buffer B, then once in 0.01% buffer B and mounted on slides with FluoromountG (Southern Biotechnology Associates). Cells were observed and imaged using a LSM780 confocal microscope (Carl Zeiss Microimaging) at the Confocal Microscopy Core Facility of the INRS-Centre Armand-Frappier Santé Biotechnologie. The quantifications of the intracellular PLA dots were performed with the Fiji software. Briefly, 8-bit format images were processed for each channel. We increased the signal for NS3 to saturation in order to delineate the entire cell area. The threshold of PLA signal was adjusted to eliminate the non-specific background. A given PLA signal was considered positive when bigger than 0.02µm^2 and having a circularity between 0.02 and 1.00. PLA dots were counted in each cell. Same acquisition and counting settings were applied to all data for each experiment.

Transmission electron microscopy

Infected cells were prepared for transmission electron microscopy exactly as previously reported (Anton *et al.*, 2021; Mazeaud *et al.*, 2021). Briefly, Huh7.5 cells were seeded on Lab-tech chambers Slide™ (Thermo Fisher) and infected with DENV 16681s MOI 1 or ZIKV H/PF/2013 MOI of 10. Two days later, cells were fixed in 2.5% glutaraldehyde in 0.1M sodium cacodylate buffer pH 7.4 overnight at 4°C and washed three times with washing buffer. Cells were postfixed for 1 hour with the washing buffer containing 1% aqueous OsO_4 and 1.5% aqueous potassium ferrocyanide. Following three washes in washing buffer, samples were dehydrated in sequential dipping into a series of ethanol-dH_2O solutions of increasing concentration up to 70% followed by a 1 hour-long staining with 2% uranyl acetate in 70% ethanol. Samples were washed twice in 70% ethanol and subjected to a progressive dehydration with up to 100% ethanol. A Graded Epon-ethanol series (1:1, 3:1) was used to infiltrate the samples before embedding in 100% Epon and polymerizing in an oven at 60 °C for 48hrs. A Diatome diamond knife using a Leica Microsystems EM UC7 ultramicrotome was used to cut serial sections (90-100 nm thick) from the

polymerized blocks. Ultrathin sections were then transferred into 200-mesh copper grids and stained during 6 minutes with 4% uranyl acetate and 5 minutes in Reynold's lead. Image acquisitions of TEM grids were performed with a FEI Tecnai G2 Spirit 120 kV TEM equipped with a Gatan Ultrascan 4000 CCD Camera Model 895 (Gatan, Pleasanton, CA) located at McGill University Facility for Electron Microscopy Research. TEM images were analyzed using the Fiji software for measurements of mitochondria perimeter and ERMC length. Ultrastructures were considered as ERMCs when the measured distance between ER and mitochondria was below 50nm. The ratio between these two values indicated the percentage of the mitochondrial perimeter in contact with ER.

Oxygen consumption rate measurements

The day prior the assay, Seahorse 96-well sensor cartridges (Agilent) were hydrated overnight at 37ºC in a non-CO_2 incubator with 200 µl/well of the Seahorse XF calibrant (Agilent). The day of the assay, living cells were trypsinized and counted with Trypan blue. 50,000 cells/well were seeded into a Seahorse XF 96-well cell culture microplate (Agilent) in DMEM and incubated for at least 4 hours at 37 ºC with 5% CO_2. Culture medium was changed for 180 µl of Seahorse XF DMEM which was supplemented with 1 mM pyruvate, 2 mM glutamine and 10 mM glucose. Cells were incubated for 1 hour in a non-CO_2 incubator at 37 ºC. For measurements of the oxygen consumption rates, we used the Seahorse XF Cell Mito Stress Test kit (Agilent) according to the manufacturer's instructions. Briefly, 20 µl oligomycin 10 µM, 22 µl FCCP 10 µM and 25 µl rotenone/antimycin A 5 µM were loaded into the ports of the sensor cartridges. Sensor cartridges were placed on top of the Seahorse XF cell culture microplate. Sequential drug addition (10-fold dilution) and time-lapse oxygen consumption rate measurements were achieved with a Seahorse XFe96 analyzer (Agilent). Data were analyzed using Wave 2.6.1 software to determine the basal respiration, the maximal respiration and the ATP production in each sample.

Mitochondria affinity purification and quantitative LC-MS/MS

For the determination of mitochondrial proteome, four independent affinity purifications were performed for each experimental condition as follows. Huh7.5 cells were infected with DENV2 16681s (MOI=2), ZIKV H/PF/2013 (MOI=10) or ZIKV MR766 (MOI=2) to achieve 100% of infection. Forty hours later, cells were prepared, and mitochondria were purified with the Human Mitochondria Isolation Kit (Miltenyi Biotec) according to the manufacturer's instructions. Briefly, were washed twice with cold PBS and counted. Ten million cells were then lysed with a Dounce homogenizer on ice in the kit lysis buffer supplemented with EDTA-free protease inhibitors (Roche). Cell homogenates were subjected to immunoprecipitation using magnetic beads-

coupled anti-TOMM22 antibodies. Isolated mitochondria were centrifuged at 13,000xg for 2 minutes at 4 ^{o}C and resuspended in in 40 µl U/T buffer (6 M urea, 2 M thiourea, 10 mM Hepes (pH 8.0)), and reduction and alkylation carried out with 10 mM DTT and 55 mM iodoacetamide in 50 mM ABC buffer (50 mM NH4HCO3 in water pH 8.0), respectively. For the determination of the whole proteome, 5 x 10^6 washed cells were lysed in a buffer containing 6 M guanidium chloride and 10 mM Tris(2-carboxyethyl) phosphine (TCEP), 0.1M Tris/HCl (pH 8). Fifty micrograms of cleared protein lysates were reduced/alkylated, and peptides were purified on stage tips as described above After digestion with 1 µg LysC (WAKO Chemicals USA) at room temperature for 3 h, the suspension was diluted in ABC buffer, and the protein solution was digested with trypsin (Promega) overnight at room temperature. Peptides were purified on self-assembled stage tips with three C18 Empore filter discs (3M) and analyzed by liquid chromatography coupled to mass spectrometry on a QExactive HF instrument (Thermo Fisher Scientific) as previously described (Scaturro *et al.*, 2018).

Raw mass-spectrometry data were processed with MaxQuant software versions 1.5.6.2 using the built-in Andromeda search engine to search against the human proteome (*Homo sapiens*; UniprotKB #UP0000005684; release 2012_02) containing forward and reverse sequences concatenated with the DENV (UniprotKB #P29990) and ZIKV (UniprotKB #KU955593) viral proteins, and the label-free quantitation (LFQ) algorithm as described previously (Holze *et al.*, 2018; Tyanova *et al.*, 2016a). Additionally, the intensity-based absolute quantification (iBAQ) algorithm and “Match Between Runs” option were used. In MaxQuant, carbamidomethylation was set as fixed and methionine oxidation and N-acetylation as variable modifications, using an initial mass tolerance of 6 ppm for the precursor ion and 0.5 Da for the fragment ions. Search results were filtered with a false discovery rate (FDR) of 0.01 for peptide and protein identifications.

Perseus software version 1.6.10.43 was used to further process the affinity-purification and global proteome dataset. Protein tables were filtered to eliminate the identifications from the reverse database and common contaminants. In analyzing mass spectrometry data, only proteins identified on the basis of at least one peptide and a minimum of 3 quantitation events in at least one experimental group were considered. Significant interactors were determined by Welch’s paired T-tests with permutation-based false discovery rate statistics on LFQ intensities (Global proteomes) or the relative abundance of Mitochondria-enriched proteins after normalization against the corresponding cellular lysates (Mitoproteome) (n=4, (|Log2(fold-change))| ≥ 1.58), -Log10(P-value) ≥ 2.). We performed 250 permutations, and the FDR threshold was set at 0.05. The parameter S0 was set at 1 to separate background from specifically enriched interactors

(mitoproteome), or to define significantly up- or down-regulated proteins in pairwise comparisons (global proteome). (Tyanova *et al.*, 2016b) UniprotKB accession codes of protein groups and proteins associated with Krebs cycle and electron transport chain identified by mass spectrometry, and their respective LFQ intensities, normalized ratios and significance values are provided in Suppl. Table 1. The complete list of identified proteins will be published alongside a different study.

GC-MS metabolomic analyses

For infection experiments, Huh7.5 cells were infected with DENV2 16681s (MOI=2), ZIKV H/PF/2013 (MOI=10) or ZIKV MR766 (MOI=2) to achieve 100% of infection and collected two days post-infection for metabolite preparation. For 2K-NS4B overexpression experiments, Huh7.5 cells were transduced with NS4B-expressing lentiviruses (MOI=2). The day after, the medium was replaced and puromycin was added to a final concentration of 1 µg/mL. Three days later (i.e., 4 days post-transduction), selected transduced cells were washed on ice three times with a cold and filtered isotonic solution (0.9% NaCl). Cells were then quickly collected with 800 µL of 80% MS-grade methanol which was stored at -80 ºC. Samples were stored at -80 ºC until metabolite extraction. In parallel, additional replicate samples were generated for cell counting after trypsinization, and quality controls using western blotting to ensure that the infection and NS4B overexpression were successful. Experiments were design so that between 0.75 x 10^6 and 2 x 10^6 cells were used for subsequent processing for GC-MS.

Membranes disruption was carried by sonication at 4 °C (2x10 min, 30 sec on, 30 sec off, high setting, Diagenode Bioruptor). Extracts were cleared by centrifugation (15,000 rpm, 10 min, 4 °C) and supernatants were transferred into new tubes containing 1µl 800 ng/µl myristic acid-D27 (Sigma; dissolved in pyridine). Next, they were dried in a cold trap (Labconco) overnight at − 4 °C. Pellets were solubilized in 30 µl pyridine containing methoxyamine-HCl (10 mg/mL, Sigma) by sonication and vortex, and were incubated at RT for 20 min (methoximation). Samples were centrifuged (15,000 rpm, 10 min, RT) and the supernatants were transferred into glass vials containing MTBSTFA (70 µl, Sigma) for derivatization at 70 °C for 1 h. One µL was injected per sample for GC–MS analysis. GC–MS instrumentation and software were all from Agilent. GC–MS methods and analyses are as previously described (Hulea *et al.*, 2018). Data analyses were performed using the Chemstation and MassHunter software (Agilent, Santa Clara, USA). Three replicates per experiment for each condition were processed. The included data show the mean and SEM obtained from the analysis of 4 and 3 ©ndependent experiments for virus infection and 2K-4B expression studies, respectively.

Caspase-Glo 3/7 assay

300,000 Huh7.5 cells were seeded in 6-well plates and transduced with shRNA-expressing lentivirus at a MOI of 4 with 8µg/mL polybrene. Two days post transduction, cells were infected with ZIKV H/PF/2013 (MOI of 20) or left uninfected. Two days post infection, cells were scraped in culture medium, collected, and centrifuged for 1 min at 10,000 rpm. Cell pellets were resuspended in 70 µL of a 50/50% mixture containing PBS and the Caspase-Glo 3/7 reagent (Promega). Lysates were incubated at least 2 hours protected from the light at room temperature. Luminescence was measured in duplicates in white 96-well plates (30 µl/well) with a Spark multi-mode microplate reader (Tecan). All values were background-subtracted and normalized to the shNT-transduced uninfected condition.

Flow cytometry

300,000 Huh7.5 cells were prepared exactly as in Caspase-Glo 3/7 assays Two days post-infection, cells were detached by trypsin treatment and stained with 25 nM MitoTracker® Orange CM-H_2 TMRos (Thermo-Fisher) for 30 min at 37 °C followed by a treatment with 4µM CellEvent caspase 3/7 green (Thermo-Fisher) and the amine reactive viability dye LIVE/DEAD aqua fixable stain (Thermo-Fisher) for 30min in the dark at room temperature. Cells were fixed with 2% formaldehyde and permeabilized with 0.1% Triton X-100. To identify ZIKV-infected cells, total cells were stained for ZIKV using a rat polyclonal anti-NS3 antibodies and subsequently with goat anti-rat cross-adsorbed AlexaFluor 647-conjugated secondary antibodies. Cells were stored at 4°C in the dark until flow cytometry processing (performed within 24 hr) and data acquisition with a BD LSRFortessa instrument at the Flow Cytometry Core Facility of INRS. Data analysis was performed using FlowJo version 10.0 software. After setting of singlets, infected Huh7.5 were defined as NS3+ cells and analyzed for active caspase 3/7 expression and LIVE/DEAD signal.

Statistical analyses

Statistical significance was evaluated by multiple *t*-test using GraphPad Prism 8.0 software. p values < 0.05 were considered significant: ****: $p < 0.0001$; ***: $p < 0.001$; **: $p < 0.01$; * $p < 0.05$; ns: not significant.

3.6 Acknowledgements

We are grateful to Jessy Tremblay at the Confocal Microscopy and Flow Cytometry Facility of INRS-Centre Armand-Frappier for excellent technical assistance during imaging and data acquisition, and Jeannie Mui and Kelly Sears at the McGill University Facility for Electron

Microscopy Research for sample preparation and precious assistance with imaging. We thank the GCRC Metabolomics Core Facility (led by Dr. Daina Avizonis), which is supported by the Canada Foundation for Innovation, the Dr. John R. and Clara M. Fraser Memorial Trust, the Terry Fox Foundation (TFF Oncometabolism Team Grant 1048 in partnership with the Fondation du Cancer du Sein du Quebec), and McGill University. We thank Dr. Ralf Bartenschlager (University of Heidelberg) for providing the DENV reverse genetics system, and Dr. Frédérick Antoine Mallette (University of Montréal), Dr. Tom Hobman (University of Alberta), Dr. Patrick Labonté (Institut National de la Recherche Scientifique) and Dr. Anil Kumar (University of Saskatchewan) for generously providing cell lines. We are grateful to the European Virus Archive Global (EVAg) and Dr. Xavier de Lamballerie (Emergence des Pathologies Virales, Aix-Marseille University, France) for providing ZIKV original stocks.

3.7 Conflict of interest

The authors declare that they have no conflicts of interest.

3.8 Funding statement

W.F received PhD fellowships from the Armand-Frappier Foundation and Fonds de la Recherche du Québec-Santé (FRQS). A.A was a recipient of a master's training fellowship from FRQS. C.M and A.A.S received PhD fellowships from the Armand-Frappier Foundation and the Center of Excellence in Research on Orphan Diseases-Courtois Foundation (CERMO-FC). A.A.S is receiving a PhD fellowship from the Fonds de la Recherche du Québec-Nature et Technologies (FRQNT). L.C.C has received a research scholar (Junior 2) salary support from FRQS. L.H. is the recipient of a research scholar salary support from FRQS (Junior 1) and the L.H. laboratory is supported by a project grant from the Canadian Institutes of Health Research (CIHR; PJT165901) and an operating grant from the Cancer Research Society (CRS; #25350). Work in A.P's laboratory was funded by an ERC Consolidator grant (ERC-CoG ProDAP, 817798), the German research foundation (PI 1084/4, PI 1084/5 and TRR179/TP10 and TRR237/A07) and KA1-Co-02 "COVIPA" (Helmholtz Association's Initiative and Networking Fund). Work in P.S laboratory was founded by the Free and Hanseatic City of Hamburg, the German research foundation (SC314/2-1) and the German Federal Ministry of Education and Research (VirMScan). This research was supported by a project grant from the CIHR (PJT153020), awarded to L.C.C.

3.9 Supplemental information

Suppl Figure 3.1 *DENV and ZIKV infection decrease the abundance of ERMC tethering complexes*

(a) Fixed Huh7.5 cells stably expressing mito-mTurquoise2 (exhibiting fluorescent mitochondria) were subjected to PLAs detecting VDAC1-IP3R1, SYNJ2BP-RRBP1 and VAPB-PTPIP51 interactions. Scale bar = 10 µm. (b,c) Huh7.5 cells were infected with DENV 16681s (MOI=1) or ZIKV H/PF/2013 (MOI=10), or left uninfected. Two days later, cells were fixed and subjected to proximity ligation assays (PLA) to detect (b) VDAC1/IP3R1 or (c) PTPIP51/VAB interactions, and immunostained for NS3 viral protein to identify infected cells. Cells were imaged using confocal microscopy. Representative images are shown.

Suppl Figure 3.2 *DENV and ZIKV modulates ERMC proteins*

(a, b) Huh7.5 cells were infected with DENV 16681s (MOI=1) or ZIKV H/PF/2013 (MOI=10) or left uninfected. Two- or three-days post-infection, cell extracts were prepared, and the expression levels of the indicated proteins were analyzed by western blotting. The arrow indicates the ZIKV-induced SYNJ2BP protein product.

Suppl Figure 3.3 *ERMC protein cellular localization in DENV and ZIKV-infected cells*

Uninfected and DENV/ZIKV-infected Huh7.5 cells were imaged at two days post-infection by confocal microscopy using antibodies detecting the indicated ERMC proteins. Infected cells were detected with anti-NS3 antibodies.

Suppl Figure 3.4 *NS4B DENV and ZIKV perturb mitochondrial respiratory metabolism*

(a) A Venn diagram illustrating the electron transport chain proteins whose mitochondrial abundance is significantly changed when cells are infected with DENV 16681s, ZIKV H/PF/2013 or ZIKV MR766. (b) Huh7.5 cells were infected with DENV 16681s (MOI=2) or ZIKV H/PF/2013 (MOI=10) or left uninfected. Two days later, mitochondria were purified and analyzed by western blotting for their content in SDHAF2 and TOMM20 as control. (c) DENV/ZIKV-infected and control cells were analyzed two days post-infection for the abundance of the Krebs cycle metabolites measured by GC-MS. All values were normalized to the uninfected condition. (d) Cells we treated

as in (b) and the mitochondrial potential in uninfected and DENV/ZIKV-infected cells was measured by FACS following staining with MitoTracker Orange CM-H2 TMRos and anti-NS3 antibodies.

Suppl Figure 3.5 *ERMC protein knockdown does not impact mitochondria morphology and integrity*

(a-b) Huh7.5 cells were transduced with lentiviruses expressing shRNAs which target the indicated proteins (MOI=5) and selected with puromycin 1 µg/mL. Four days later, cells were either collected for (a) assessing shRNA-mediated knockdown efficiency by western blotting or (b) evaluating the impact of protein depletion on cell viability using MTT assays. (c) Mitochondrial potential upon ERMC protein knockdown was measured by FACS following staining with MitoTracker Orange CM-H2 TMRos. (d) The mitochondrial morphology was analyzed in knocked down cells using confocal microscopy following staining with the MitoTracker Red CMXRos dye. Quantification was made with data from two independent experiments and 75-100 cells per condition per experiment.

Suppl Figure 3.6 *ZIKV NS4B induces mitochondria elongation and DENV/ZIKV NS4B precursors inhibit the mitochondrial respiratory metabolism.*

(a) Huh7.5/T7 cells expressing the T7 RNA polymerase were transfected with plasmids expressing DENV or ZIKV NS4B constructs. Sixteen hours post-transfection, the mitochondrial morphology was analyzed using confocal microscopy following staining with the MitoTracker Red CMXRos dye and anti-HA antibodies. (b) Quantification of elongated, normal, and fragmented mitochondria in transfected cells from two independent experiments. (c) Huh7.5 cells were transduced with lentiviruses expressing DENV and ZIKV NSA-2K-NS4B which were HA-tagged (MOI=4) and submitted to puromycin selection. Three days post-transduction, cells were analyzed for NS4B expression by western blotting. (d) Huh7.5 cells were transduced with lentiviruses and selected as in (c). Three days post-transduction, equal amounts of transduced living cells were analyzed for their basal respiration, ATP production and maximal respiration using the Seahorse technology. All values were normalised to the control empty vector condition.

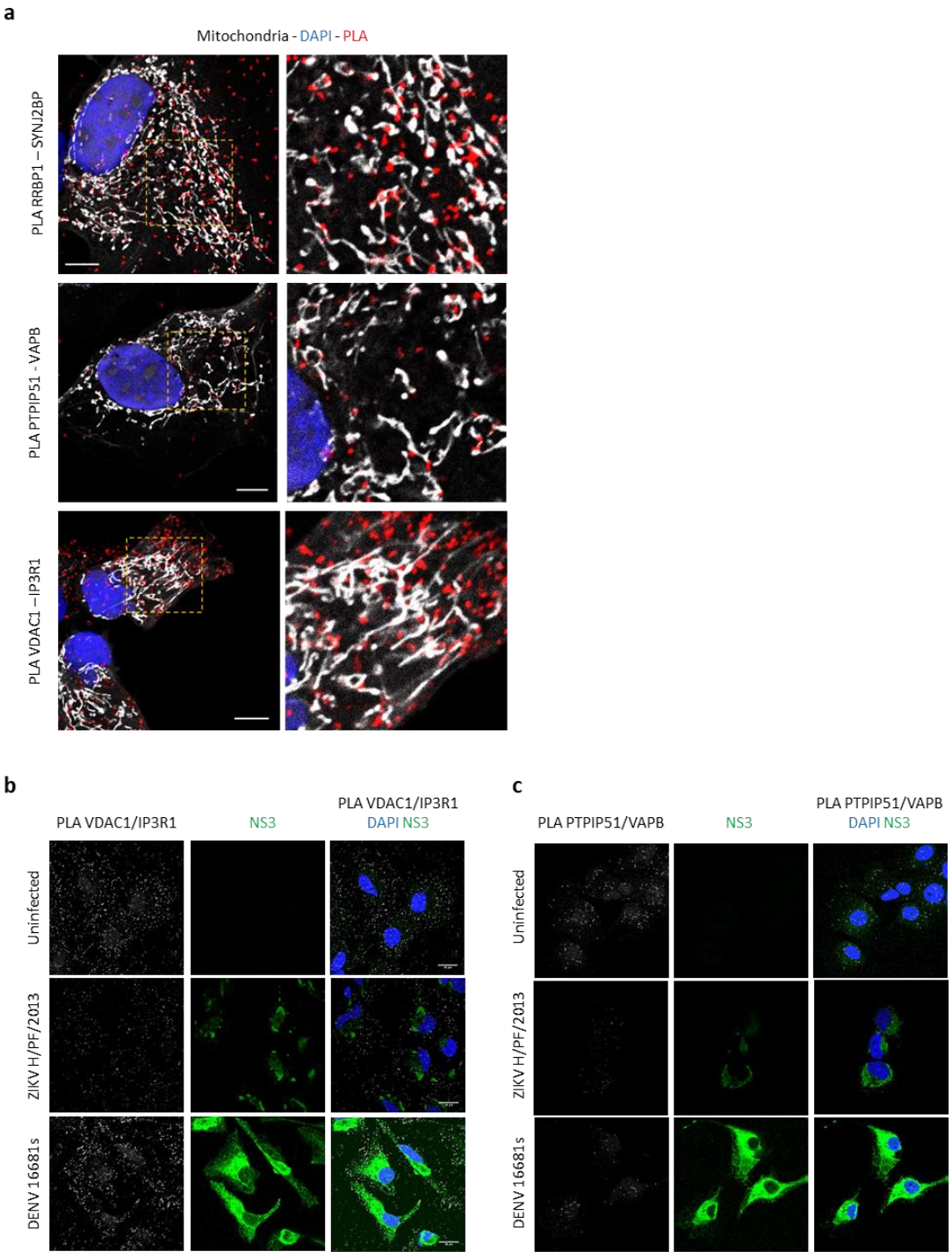

Suppl Figure 3.1

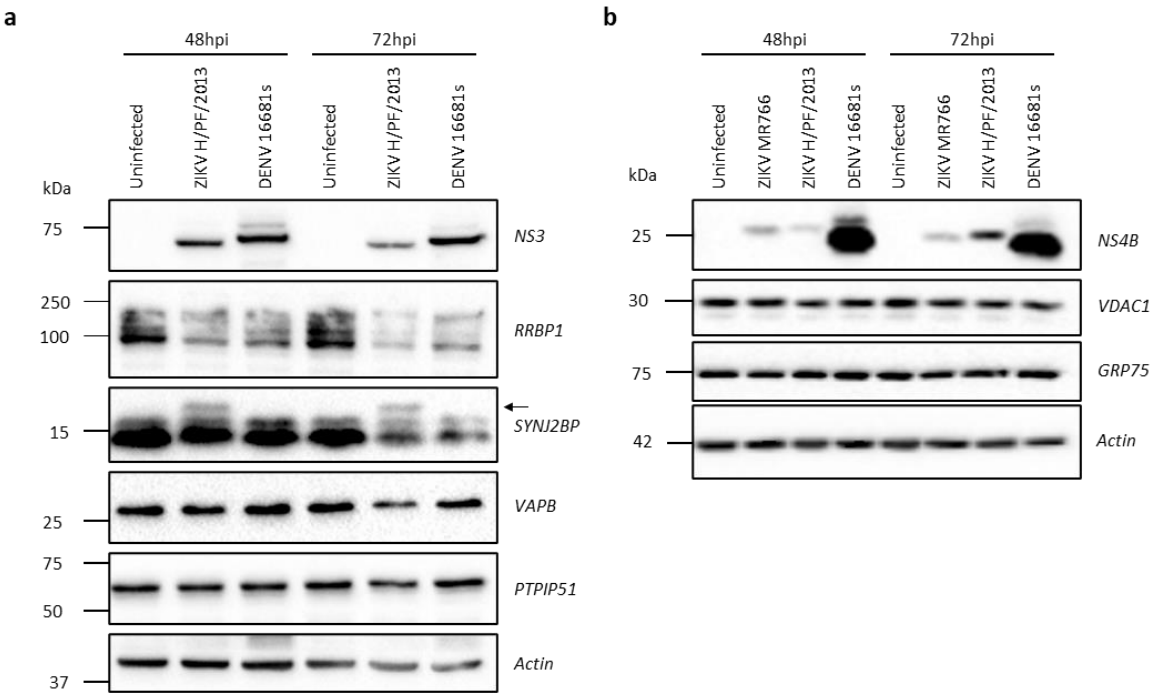

Suppl Figure 3.2

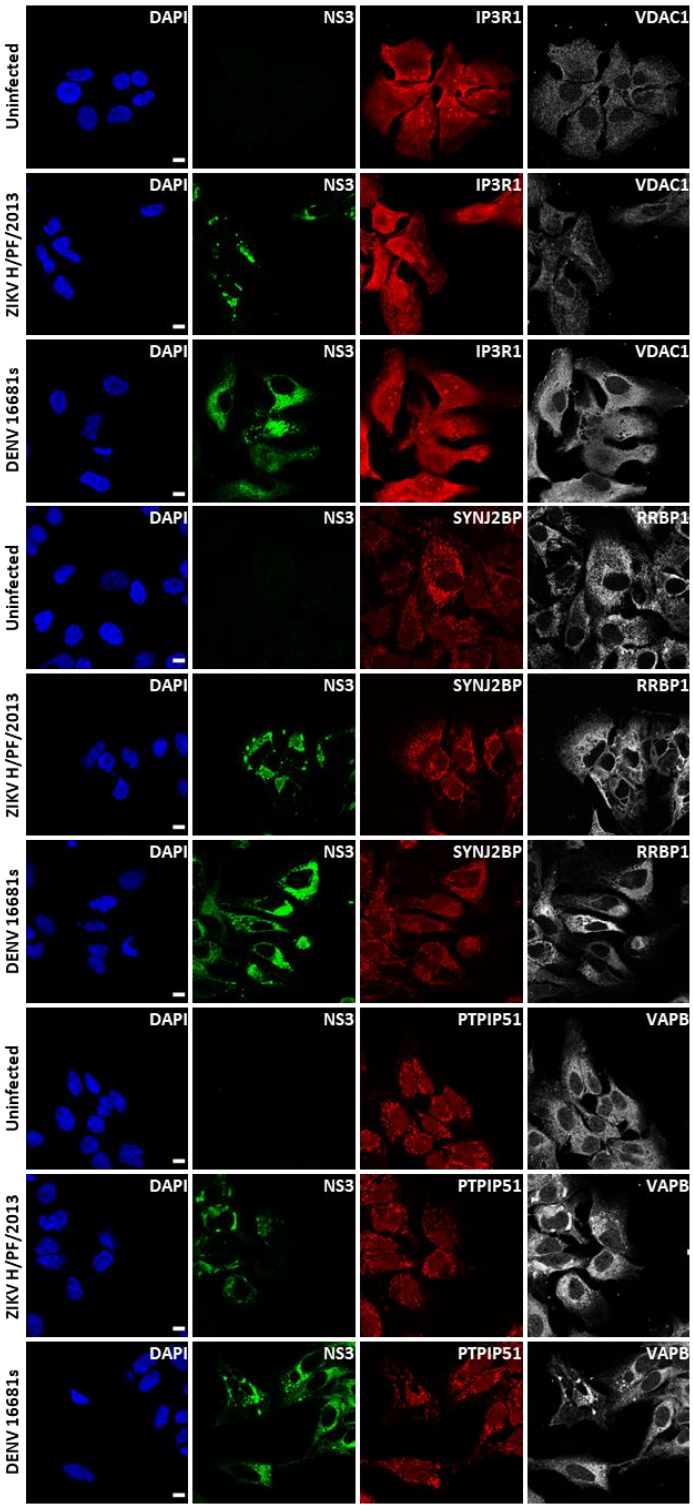

Suppl Figure 3.3

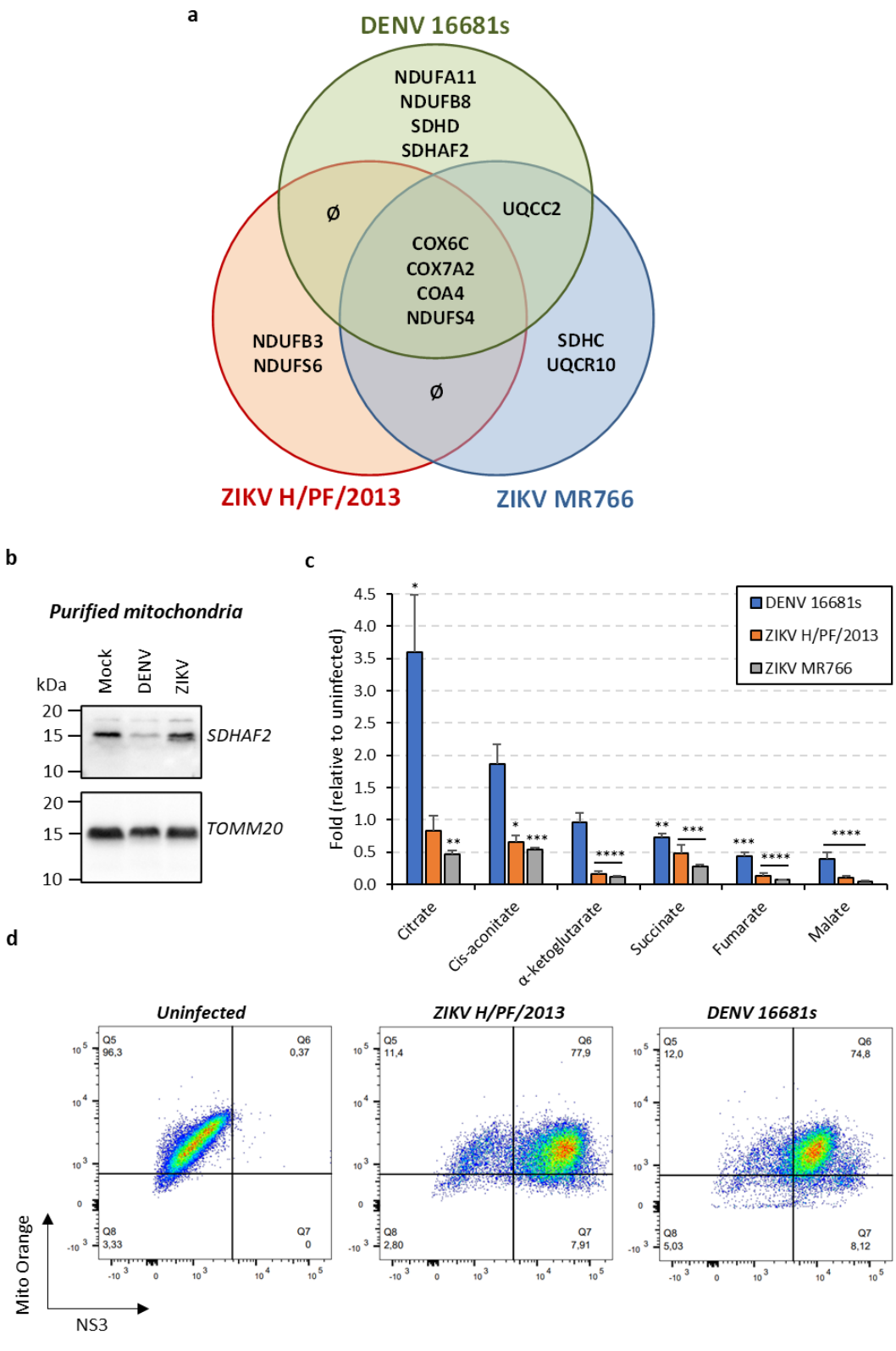

Suppl Figure 3.4

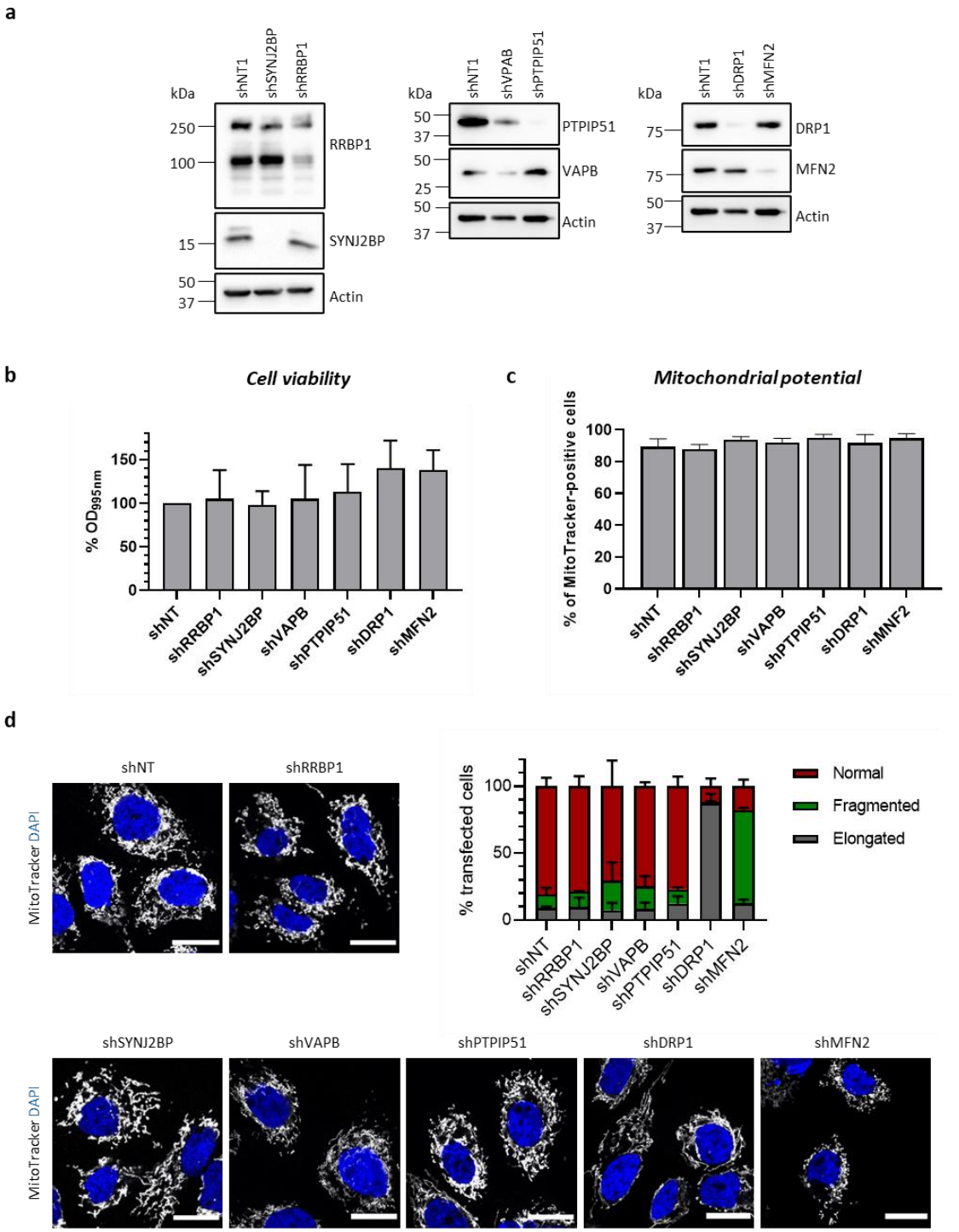

Suppl Figure 3.5

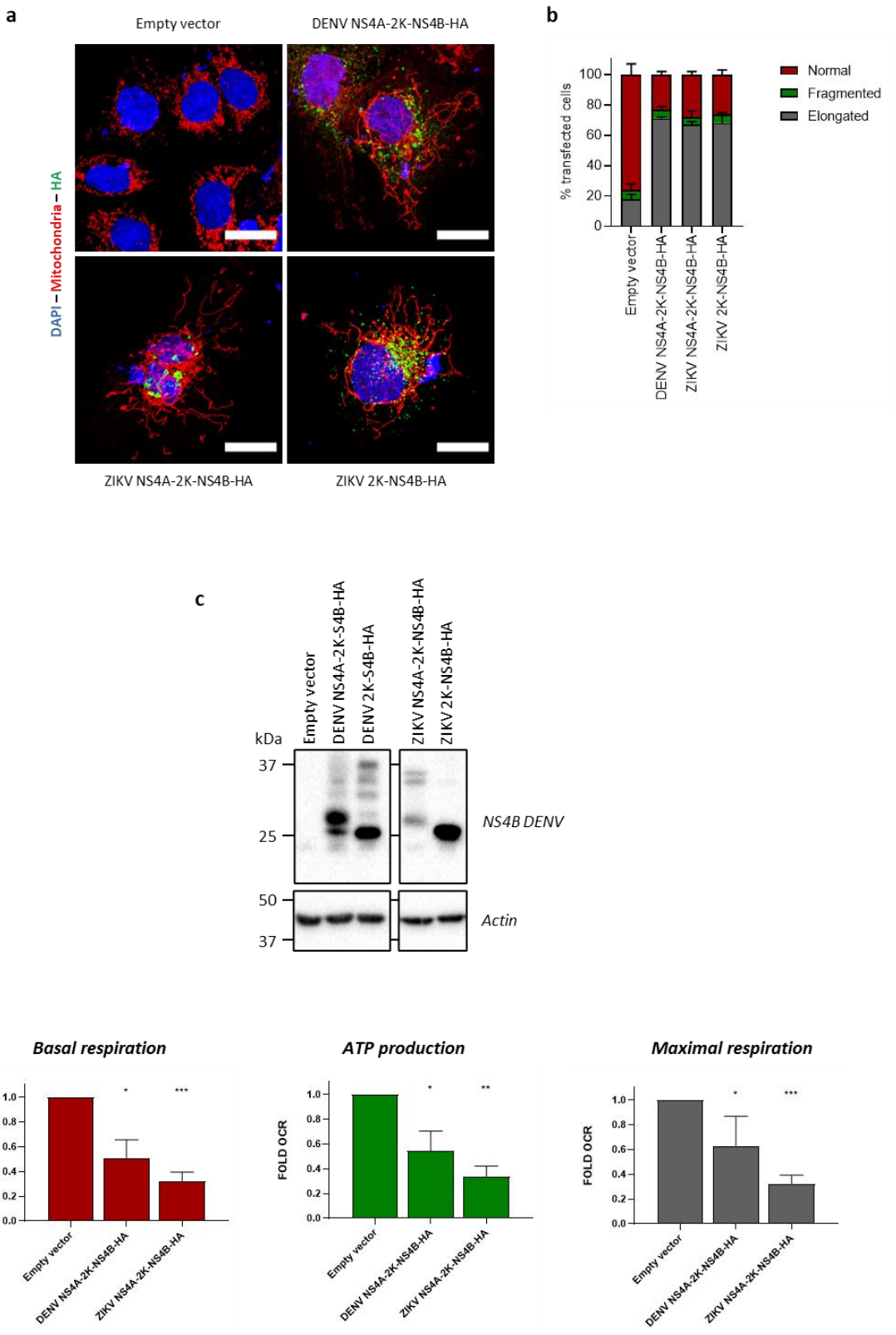

Suppl Figure 3.6

4 DISCUSSION GENERALE

L'article principal présent dans cette thèse a déjà discuté de la majorité des points clés concernant l'habilité des *Flavivirus* à manipuler l'interface réticulo-mitochondriale pour favoriser leur réplication et ne sera que brièvement repris pour discuter du contexte de nos résultats vis-à-vis de la littérature actuelle. Autrement dit, cette section discutera principalement d'autre horizons de recherche tels que, l'impact des *Flavivirus* dans la biologie cellulaire de son vecteur principale, le moustique, de la manipulation des mitochondries par d'autres virus et pour finir, de l'impact des *Flavivirus* sur d'autres interactions organite – organite.

4.1 Impact contradictoire des *Flavivirus* sur l'interface réticulo-mitochondriale

Nous avons montré dans ce projet l'importance pour les VDEN et VZIK de perturber la morphologie mitochondriale et l'IRM pour contrôler le fonctionnement de certaines activités métaboliques cellulaires. Notamment, nos découvertes montrent que VDEN et VZIK retardent le processus de mort cellulaire par voie apoptotique et module la respiration mitochondriale. Pour autant, nos données ne s'alignent pas parfaitement avec la littérature. En effet, d'autres équipes de recherche ont montré des données contradictoires qu'il est important de discuter.

Par exemple, l'équipe de Yu a démontré en 2015 que le VDEN provoque la fragmentation des mitochondries (Yu *et al.*, 2015). En effet dans cette étude, la protéase virale NS2B3 serait responsable du clivage des facteurs de fusion mitochondriale MFN1 et MFN2. Leurs résultats montrent également que MFN1 est important dans la réponse immunitaire antivirale médié par RIG-I et MFN2 dans le maintien du potentiel de membrane mitochondriale réduisant ainsi la mort cellulaire causé par le VDEN. Le clivage des deux MFN permettrait alors d'atténuer la réponse immunitaire antivirale par RIG-I et les effets cytopathiques causés par le virus. Ceci est intéressant car Chatel-Chaix et al., ont montré l'élongation mitochondriale que nous avons également confirmé dans cette thèse pour le VZIK et ceci par l'intermédiaire de NS4B. Par ailleurs, nous n'avons pas observé de différence dans l'expression des MFN1/2 en western blot lors de cette thèse (données non montrées). Cependant, nos observations montrent une élongation principalement à partir de 48h d'infection alors que Yu et al., ont étudié la morphologie à des temps précoces et surtout, dans des systèmes artificiels d'hétérocaryons et d'hyperfusion mitochondriale. De plus, ils ont utilisé des cellules stables n'exprimant plus les MFN1/2, ce qui pourrait favoriser la sélection de cellules ayant contourné la perte des MFN1/2 dans la fusion mitochondriale. En effet une autre étude contradictoire mais réalisée dans des cellules

neuronales appuie cette théorie (Yang *et al.*, 2020). Cette étude confirme la modulation négative de MFN2 par VZIK en faveur de la fragmentation mitochondriale. Il est important de préciser que les cellules neuronales sont généralement plus sensibles aux infections virales et agissent de manière différente tel que dans l'activation de l'apoptose ce qui pourrait expliquer la fragmentation mitochondriale observée.

Finalement, toutes ces études contradictoires suggèrent fortement que le temps d'infection, le type cellulaire infecté et la souche flavivirale jouent un rôle important dans la modulation de la morphologie mitochondriale et de l'IRM. Mais qu'en est-il chez les arthropodes ?

4.2 L'infection flavivirale chez les arthropodes

Tel que discuté dans l'introduction, le moustique est le principal vecteur des *Flavivirus.* Cependant, malgré l'importance que le moustique possède dans leur cycle de vie, nos connaissances actuelles portent principalement de l'étude des *Flavivirus* dans des cellules de mammifères. Pourtant, les moustiques, appartenant à l'embranchement des arthropodes, possèdent une biologie cellulaire différente des mammifères d'un point de vue de processus et possiblement de structure également.

En effet, lorsqu'un moustique femelle non-infecté prélève du sang infecté chez l'Humain, les *Flavivirus* présents vont se répliquer dans l'intestin, lieu de digestion du sang. La digestion ne neutralise pas les *Flavivirus* : au contraire, les virus vont se déplacer et atteindre des tissus secondaires, tels que les glandes salivaires, lieu de stockage des virus avant la transmission à l'humain. La période d'incubation extrinsèque, c'est-à-dire la période entre l'ingestion du virus par le moustique et la transmission du virus à l'humain lors d'une piqûre est d'environ de 8 à 12 jours si les conditions climatiques avoisinent les 28°C (Tjaden *et al.*, 2013; Watts *et al.*, 1987). Une fois infecté, le moustique ne guérira jamais du virus mais n'en mourra pas non plus. Ceci est particulièrement intéressant puisque l'humain développe des complications sévères très rapidement. Il est alors évident que la réponse cellulaire face à l'infection virale est différente chez le moustique.

Dans ce cas, il est intéressant de discuter de la possible différence de stratégie des *Flavivirus* dans la mise en place d'un environnement cytoplasmique adéquat à la réplication chez le moustique et également comment les *Flavivirus* contournent les réponses cellulaires face à l'infection, notamment, dans l'interférence des *Flavivirus* dans la morphologie et le métabolisme des mitochondries chez les arthropodes.

4.2.1 Remodelage du réticulum endoplasmique en usines de réplication

Les *Flavivirus* remodèlent la structure morphologique du RE en usines de réplication dans des cellules de mammifère et ceci même dans des cellules de moustique C6/36 (Grief *et al.*, 1997; Junjhon *et al.*, 2014; Ko *et al.*, 1979). Cependant, ce remodelage n'est pas identique à celui observé dans des cellules de mammifère. En effet, alors que des cellules de mammifère Huh7 infectées par le VDEN présentent les trois sous structures des usines de réplication, c'est-à-dire les paquets vésiculaires, les sacs de virus et les convolutions de membrane, les cellules de moustiques C6/36 ne présentent que les paquets vésiculaires et les sacs de virus, mais pas les CM. Le fait que les CM ne soient retrouvés que chez les mammifères suggère premièrement que la réplication de l'ARNv ne dépend pas des CM. En effet, les *Flavivirus* sont tout à fait capable de se répliquer dans les moustiques si ce n'est plus efficacement (Barreto-Vieira *et al.*, 2017; Chan *et al.*, 2016a). Ceci implique également que le mécanisme de la biogénèse des CM retrouvé chez les mammifères soit spécifique et nécessite probablement des facteurs ou des processus cellulaires qui ne sont pas retrouvés chez le moustique. Une autre hypothèse vraiment très intéressante est que toute la machinerie nécessaire à la biogénèse des CM soit présente chez le moustique, mais que le virus ne provoque pas la formation des CM dépendamment de leur nécessité face à la réponse immunitaire du moustique lors d'une infection virale.

Lorsque l'on compare toutes ces données, il est possible que les CM possèdent un rôle dans la protection de la réplication virale face aux processus cellulaires qui sont présents chez les mammifères et non chez les arthropodes. Dans ce contexte, la présence des protéines virales NS4A, NS4B, NS3 ou de la protéine cellulaire VCP dans les CM jouerait un rôle bien précis dans l'interférence des voies cellulaires spécifiques aux mammifères qui sont néfastes à la réplication virale telles que l'immunité antivirale (discuté à la section 1.1.4) ou l'apoptose (discuté à la section 1.1.5).

4.2.2 La morphologie mitochondriale

Un des phénotypes les plus remarquables lors d'une infection avec le VDEN ou VZIK est la manipulation morphologique mitochondriale. Chatel-Chaix et al., ont montré que le VDEN inhibe la phosphorylation de DRP1 en S616, empêchant ainsi sa translocation au niveau des mitochondries (Chatel-Chaix *et al.*, 2016). Cette inhibition équilibre la dynamique fission/fusion vers la fusion mitochondriale par les facteurs de fusion MFN1/2 et OPA1. Il est intéressant de noter que cette élongation soit spécifique au VDEN et VZIK puisque ce phénotype n'a jamais été observé avec aucun autre *Flavivirus* étudié en laboratoire. Cependant, ceci n'exclut pas la

possibilité que d'autres *Flavivirus* soient également capables de créer un tel phénotype tels que les *Flavivirus* dit rare (Murray Valley Encephalitis virus, Egde Hill virus, Kokobera virus ou encore le Stratford virus) qui ont été étudiés seulement au niveau clinique.

Jusqu'à présent, il n'y a pas de preuve visuelle en microscopie montrant une élongation mitochondriale chez le moustique. Bien que les mécanismes moléculaires de la morphodynamique mitochondriale chez le moustique soient peu connus, des évidences moléculaires similaires aux mammifères pourraient suggérer qu'il y a bien élongation des mitochondries. En effet, María E. Santana-Roman et al., ont montré très récemment dans des cellules de moustiques C6/36 infectées au VDEN, l'absence de la localisation de DRP1 au niveau des mitochondries (Santana-Roman *et al.*, 2021). L'hypothèse actuelle de la biogénèse des CM est basée sur l'enroulement de membranes du RE à la suite de l'altération de l'IRM chez les mammifères et dépendrait de la morphologie mitochondriale (Chatel-Chaix *et al.*, 2016). Pourtant chez le moustique, la forte présomption de l'élongation mitochondriale alors qu'il n'y a pas de CM suggère cette fois que l'élongation mitochondriale ne provoque pas forcément la formation des CM. Dans un tel contexte, il semblerait que l'élongation mitochondriale est importante et est un phénotype conservé par le VDEN et le VZIK notamment en interférant sur le métabolisme mitochondrial lipidique ou respiratoire propre aux mitochondries. En revanche, dépendamment de l'espèce, la biogénèse des CM par l'élongation mitochondriale quant à elle dépendrait plutôt d'un ensemble de processus cellulaires spécifiques aux cellules infectées qui ne sont pas retrouvés chez le moustique. Dans ce cas, la biogénèse des CM serait spécifique en fonction de son apport protectif proviral dans la cellule en interférant sur des processus cellulaires, tels que la réponse immunitaire antivirale par exemple qui diffère entre arthropodes et mammifères.

Finalement, dans un arthropode différent du moustique, une étude menée chez la drosophile a mis en évidence qu'une mutation du facteur de fusion OPA1 aboutit à la mort précoce de l'insecte en réduisant également l'activité de la phosphorylation oxydative (Tang *et al.*, 2009). Cette étude montre que l'inhibition de l'élongation mitochondriale impacte négativement le métabolisme respiratoire des mitochondries. Ainsi, la corrélation de cette étude et nos données suggèrent que les VDEN et VZIK pourraient favoriser l'élongation mitochondriale pour augmenter la phosphorylation oxydative.

4.2.3 L'interface réticulo-mitochondriale

L'IRM est importante dans la survie cellulaire en intervenant dans différents processus tels que les échanges calciques entre RE et mitochondries, dans les échanges lipidiques ou encore dans

l'activation de l'immunité innée précoce antivirale. Dans un contexte de survie virale dans un environnement cytoplasmique toxique pour les *Flavivirus*, nous avons montré dans cette thèse que le VDEN et le VZIK altèrent cette interface dans des cellules de mammifères. Nos données suggèrent fortement que cette altération non seulement retarde la mort cellulaire par apoptose, mais également aurait un impact sur la respiration mitochondriale en favorisant finalement la réplication virale. Malheureusement il n'y a pas de preuve dans la littérature d'une quelconque manipulation de l'IRM par les *Flavivirus* chez le moustique.

Une question importante se pose, y a-t-il présence d'une quelconque IRM chez les arthropodes ? Récemment, Paradis et al., ont montré une protéine importante chez l'humain impliquée dans la régulation de la dynamique de l'IRM, la protéine CRELD1 (Paradis *et al.*, 2022). CRELD1 appartient à la famille des facteurs de croissance épidermique riche en cystéine et possède un rôle dans la médiation des interactions protéine-protéine ou dans la régulation du stress du RE (Kern *et al.*, 2021; Oh-hashi *et al.*, 2009). Première observation importante, CRELD1 est présent au niveau de l'IRM suggérant un rôle dans son intégrité et/ou dans ses fonctions. Lorsque CRELD1 est atténuée par mutation dans des cellules cardiaques et musculaires provenant de mammifère ou d'amphibien (*Xenopus tropicalis)*, la distribution des mitochondries augmente et leur morphologie est allongée (Paradis *et al.*, 2022). Ce phénotype résulte de la diminution de la translocation de DRP1 aux mitochondries. Outre l'élongation mitochondriale, il est intéressant de noter que l'activité du complexe I de la phosphorylation oxydative est diminuée lorsque CRELD1 est inhibée et que cette diminution impacte négativement la structure de l'IRM. Il serait alors vraiment intéressant d'étudier si les *Flavivirus* interfèrent sur le rôle de CRELD1 par exemple par l'intermédiaire de NS4B qui pourrait être impliquée. L'interférence de CRELD1 par les *Flavivirus* pourrait alors favoriser le phénotype d'élongation mitochondriale, de l'altération de l'IRM et de la manipulation de la phosphorylation oxydative observée lors d'une infection par un *Flavivirus* chez les mammifères. Par ailleurs, CRELD1 est également retrouvée chez la drosophile montrant la grande conservation de cette protéine dans l'évolution (Paradis *et al.*, 2022). Bien que les protéines diffèrent au niveau structurale et en composition entre les mammifères et les arthropodes, le faite que la drosophile partage cette protéine avec l'humain laisse à penser qu'il y a interaction protéine-protéine entre le RE et les mitochondries chez les arthropodes qui pourrait être régulée par CRELD1. Une autre évidence provient de la GTPase rho mitochondriale (MIRO) qui chez la drosophile serait impliquée dans la régulation de l'IRM au niveau des échanges calciques (Lee *et al.*, 2018; Lee *et al.*, 2016). Ces résultats montrent que l'IRM serait également présente chez les arthropodes. Pour appuyer notre hypothèse que le moustique possède une IRM, une précédente étude a déterminé que 15% au minimum du répertoire lipidique est modifié

après une infection par le VDEN (Perera *et al.*, 2012). L'augmentation de l'abondance de plusieurs acides gras, tels que les sphingolipides ou la phosphatidylcholine qui sont impliqués dans le dynamisme mitochondrial de fusion/fission et dans les échanges lipidiques dans l'IRM chez les mammifères pourrait appuyer la possibilité de la présence d'une IRM chez le moustique.

Dans un contexte hypothétique où les cellules de moustiques possèderaient de l'IRM mais pas de CM en condition d'infection par un *Flavivirus* suggérerait que l'IRM n'est pas altérée chez le moustique et ce, malgré la possible élongation mitochondriale. Ceci pourrait appuyer notre hypothèse que les moustiques possèdent de l'IRM mais que les *Flavivirus* n'ont potentiellement pas la nécessité ou pas les moyens moléculaires de l'altérer. Puisque l'IRM est impliquée dans divers processus cellulaire, son altération chez le mammifère pourrait également expliquer pourquoi les dommages liés à l'infection sont plus sévères que chez l'arthropode.

Fait intéressant, il semblerait que le *Plasmodium falciparum*, parasite causant le Paludisme et appartenant à l'embranchement des *Apicomplexa* possède de l'IRM montrant ainsi l'origine lointaine et la grande conservation dans l'évolution de l'IRM (Anwar *et al.*, 2022).

4.2.4 L'immunité innée antivirale

L'immunité antivirale chez les arthropodes est particulièrement intéressante puisque contrairement aux mammifères, il n'existe pas d'immunité adaptative. Les pathogènes tels que les *Flavivirus* doivent alors contrecarrer uniquement l'immunité innée antivirale pour consolider une transmission efficace. Les arthropodes possèdent deux grandes voies antivirales principales, celle des ARN d'interférence (ARNi) et celles des récepteurs de type Toll (Campbell *et al.*, 2008; Clarke *et al.*, 2003; Sanchez-Vargas *et al.*, 2004). Rapidement, lors de la réplication virale chez les arthropodes, les ARNdb générés pendant la réplication vont être reconnus par le complexe Dicer2-R2D2 qui est une enzyme RNase III (Rand *et al.*, 2004). L'ARNdb viral est alors clivé en petits fragments appelés petit ARN interférent (siRNA) (Okamura *et al.*, 2004). Ces siRNA vont ensuite activer la machinerie ARNi en se liant au complexe RISC pour neutraliser l'ARNv (Fire *et al.*, 1998). La voie des récepteurs de type Toll est similaire à celle de NF-κB des mammifères. L'activation de la voie par reconnaissance de motifs moléculaires associés aux pathogènes aboutit à l'expression de facteurs immunitaires antimicrobiennes ou antiviraux (Xi *et al.*, 2008). Il n'est pas connu à ce jour si ces deux voies antivirales pourraient utiliser l'IRM puisque sa présence chez le moustique n'a pas encore été démontrée. Chez les mammifères, l'IRM fait intervenir le complexe protéiques MAVS impliqué dans l'expression des interférons, le complexe MAVS n'existe pas chez les arthropodes. Dans un contexte hypothétique où les *Flavivirus* altèrent

l'IRM chez les mammifères et non chez les arthropodes, on peut supposer que cette altération est éventuellement causée pour inhiber la réponse immunitaire liée à l'IRM par l'intermédiaire de MAVS. Cette possibilité appuie l'hypothèse que chez les mammifères, les *Flavivirus* altèrent l'IRM en enroulant la membrane du RE en CM afin de bloquer la voie de signalisation antivirale couplée à MAVS et potentiellement en le séquestrant dans les CM par l'intermédiaire de NS4B. Chez les arthropodes, l'absence d'une réponse immunitaire lié à l'IRM expliquerait la non-nécessité des *Flavivirus* à dégrader l'IRM et donc de produire des CM.

4.2.5 La mort cellulaire par apoptose

La mort cellulaire par apoptose est un processus cellulaire utilisé par les cellules comme moyen de défense antivirale en éliminant les cellules infectées. Comme les mammifères, les arthropodes sont également capables d'un tel processus. Chez les mammifères, les cellules activent rapidement l'apoptose en cas d'infection virale (Thomson, 2001). En revanche, nous avons récemment montré que le VZIK retardent l'activation de l'apoptose par l'intermédiaire de l'activité ATPase de VCP (Anton *et al.*, 2021) et dans cette thèse, par l'altération de l'IRM. Cette interférence de l'apoptose permet aux *Flavivirus* de mettre en place rapidement un environnement favorable à la réplication sur une courte période puisque les cellules étudiées dans cette thèse, les Huh7.5 finissent pas montrer des effets cytopathiques après trois jour d'infection. Chez le moustique, des évidences montrent que les cellules C6/36 peuvent être maintenues en culture sur de longues périodes malgré une infection virale suggérant une modulation de l'apoptose (Karpf *et al.*, 1997). Puisque les cellules survivent plus longtemps, ceci laisse penser que les virus retardent l'apoptose pour augmenter la survie cellulaire. En effet, l'activation de l'apoptose chez le moustique en condition d'infection est un phénomène rarement observé. Pour autant, l'étude d'une apoptose forcée dans des moustiques infectés avec le virus Sendai montre que l'apoptose est un mécanisme puissant contre une infection virale d'où l'intérêt du virus de bloquer la voie apoptotique (O'Neill *et al.*, 2015).

D'un côté, cette évidence suggère que les arbovirus ont développé des mécanismes neutralisant l'apoptose. Par exemple, la protéine C du VZIK interagit avec l'orthologue de VCP chez les arthropodes, TER94, en augmentant la réplication virale par favorisation de la libération de l'ARNv de l'endosome (Azuma *et al.*, 2014; Gestuveo *et al.*, 2021). TER94 a été corrélée à la modulation de la mort cellulaire intervenant dans la dégénération des neurones chez la drosophile (Azuma *et al.*, 2014). On peut supposer que les *Flavivirus* pourraient moduler l'apoptose chez les arthropodes par l'intermédiaire de TER94 tel qu'observé par l'intermédiaire de VCP chez les

mammifères (Anton *et al.*, 2021). Cependant, l'absence des CM chez le moustique impliquerait que la modulation de l'apoptose par TER94 se ferait indépendamment des CM contrairement à ce qui a été récemment observé (Anton *et al.*, 2021).

D'un autre côté, l'opposé est également observé. En effet, l'infection aux VDEN et VZIK chez le moustique stimule une rapide activation de l'apoptose favorisant la prolifération des virus au niveau de l'intestin et des glandes salivaires (Ayers *et al.*, 2021). Ceci est intéressant puisque chez la drosophile, l'immunité antivirale par ARNi est atténuée par la suractivation de l'apoptose (Xie *et al.*, 2011a). Ces données pourraient suggérer une éventuelle stimulation de la mort cellulaire par les arthropodes en début d'infection afin d'atténuer la réponse antivirale et favoriser la dissémination et la réplication virale puis une atténuation tardive dans l'infection pour favoriser la survie cellulaire et ainsi du virus.

4.3 Impact d'autres virus sur la mitochondrie et l'interface réticulo-mitochondriale

4.3.1 La morphologie mitochondriale

Les *Flavivirus* ne sont pas les seuls virus à modifier la morphologie et le métabolisme des mitochondries. Par ailleurs, nombreux sont ceux qui ont un impact sur le métabolisme lié aux mitochondries. Pour autant, cette section discutera des virus ayant un impact principalement sur la morphologie mitochondriale qui pourrait alors avoir un effet direct sur l'IRM et le métabolisme également (Tableau 5.1).

Les recherches menées sur la modification morphologique des mitochondries par des virus ont principalement montré une prédominance pour la fission mitochondriale. Par exemple, les virus d'Epstein-Barr (VEB), de la fièvre porcine classique (VFPC) et de l'Hépatite B (VHB), des virus à ADN, favorisent la fission. En effet, le VEB active la voie NOTCH augmentant alors l'expression de DRP1 (Young *et al.*, 2004). Le VFPC cause l'ubiquitination et la dégradation de MFN2 aboutissant à la fission mitochondriale (Gou *et al.*, 2017). De plus, le VFPC surexprime les protéines Parkin et PINK1 favorisant la mitophagie. Le VHB quant à lui favorise également la surexpression de DRP1 par l'intermédiaire de la protéine virale HBx (Kim *et al.*, 2013). Les virus de l'Influenza A (H1N1) et de l'Hépatite C (VHC), tous deux des virus à ARN favorisent également la fragmentation. En effet, la protéine PB1-F2 du H1N1 favorise la mitophagie et inhibe l'expression des IFN de type I (Wang *et al.*, 2021) alors que le VHC phosphoryle DRP1 en S616 favorisant la translocation de DRP1 aux mitochondries en faveur de la fission (Kim *et al.*, 2014b). Le VHC est intéressant puisque c'est un cousin des *Flavivirus*. La fragmentation mitochondriale

observée avec le VHC est également provoquée par l'association de la protéine virale NS5A avec la PI4KA permettant de favoriser les sites de pré constriction des mitochondries par le RE (Siu *et al.*, 2016). De plus, le VHC redistribue les mitochondries dans la région périnucléaire par l'intervention de NS4A qui s'accumule au niveau des mitochondries et les endommage. Ceci crée un stress mitochondriale favorisant le relargage accru de cytochrome C (Nomura-Takigawa *et al.*, 2006). Ces exemples de virus favorisant la fission mitochondriale montrent l'importance des protéines DRP1 et MFN2 dans la dynamique morphologique des mitochondries puisque ce sont les cibles principales des virus.

Par ailleurs, les virus favorisant la fusion mitochondriale utilisent également les facteurs DRP1 et MFN2. Par exemple, les virus à ARN tels que le H1N1, la Rougeole (VR) et SARS-CoV favorisent l'élongation mitochondriale. Le H1N1 surexprime OPA1 et diminue l'expression de DRP1 (Pila-Castellanos *et al.*, 2021). Le VR cause une hyperfusion mitochondriale (Sato *et al.*, 2021) tandis que le SARS-CoV dégrade DRP1 par le protéasome favorisant la fusion des mitochondries (Shi *et al.*, 2014).

Finalement, toutes ces différentes stratégies permettant la modification morphologique par les virus ont un seul même but commun, l'amélioration de la réplication virale dans la cellule en perturbant les mécanismes cellulaires néfastes ou avantageux pour les virus. Il est intéressant de voir qu'au cours de l'évolution, chaque virus a adopté un mécanisme similaire ou différent permettant le remodelage morphologique des mitochondries aboutissant à l'interférence de différent processus cellulaires. Leigh Van Valen a proposé en 1973 la théorie de la reine rouge, basé du livre de Lewis Carroll : De l'autre côté du miroir (deuxième volet d'Alice au pays des merveilles). Cette théorie se résume par : « l'évolution permanente d'une espèce est nécessaire pour maintenir son aptitude face aux évolutions des espèces avec lesquelles elle coévolue ». D'un point de vue coévolutif, il est vraiment intéressant de voir comment les virus ont chacun développé des stratégies différentes pour contrôler cet organite vraiment complexe et extraordinaire qu'est la mitochondrie après des milliers d'années d'évolution. Ceci n'est vraiment pas surprenant étant donné que la mitochondrie est l'un des organites les plus importants de la cellule puisqu'elle intervient dans de nombreux processus que les virus ont tout intérêt à contrôler pour créer un environnement cytoplasmique favorable à leur réplication.

4.3.2 L'interface réticulo-mitochondriale

L'IRM a malheureusement été très peu étudiée et commence à peine à faire son entrée dans le monde scientifique. En effet, après des décennies où la mitochondrie était considérée

principalement pour son rôle de productrice d'énergie, ses autres rôles dans les processus cellulaires et en relation avec le RE dans les infections virales restent encore un mystère.

Dans la littérature, deux exemples de virus altérant l'IRM sont intéressants à discuter. Par exemple, la surexpression de OPA1 et la diminution de l'expression de DRP1 par le H1N1 impactent négativement sur l'IRM dans des cellules humaines de poumon A549 (Pila-Castellanos *et al.*, 2021). Le cytomégalovirus humain (VCMH) restructure l'IRM différemment en fonction du temps de l'infection (Cook *et al.*, 2022). Tôt dans l'infection, le virus réduit les contacts ER mitochondries pour contourner la réponse immunitaire antivirale dépendante de STING, senseur d'ADN viral. Tard dans l'infection, le virus cette fois favorise les contacts ER mitochondries en recrutant le couple VAPB-PTPIP51 pour renforcer l'intégrité de l'IRM. Finalement, l'augmentation des protéines de l'IRM telles que VAPA/B, MFN1/2, des protéines de fission telles que DRP1, MFF ou des protéines de transfert de calcium telles que PTPIP51, VDAC1 favorisent la bioénergétique pour la production virale du VCMH en activant le flux de calcium et la fission mitochondriale. Il n'est pas connu dans la littérature si ces virus stimulent la formation des CM qui n'ont pour l'instant été observés qu'avec des *Flavivirus*. Dans un tel contexte d'altération de l'IRM sans formation hypothétique de CM, on peut se demander où et comment ces deux virus organisent la membrane du RE libre dans le cytosol. Dans ce cas, les virus altèrent l'IRM sans pour autant avoir la nécessité de former des CM pour contrecarrer certain processus cellulaires par séquestration de protéines. Ceci ouvre la possibilité que la formation des CM dépend de l'altération de l'IRM mais à l'inverse, l'altération de l'IRM ne provoquerait pas forcément la biogenèse des CM. Alors que l'altération de l'IRM semble être potentiellement conservée chez certains virus pour empêcher la réponse immunitaire antivirale liée à MAVS, il semblerait que la biogénèse des CM à partir de l'altération de l'IRM soit spécifique aux *Flavivirus*.

4.4 Modifications morphologiques et métaboliques d'autres interactions organite – organite par les *Flavivirus*

Les organites cellulaires possèdent une grande dynamique et plasticité qui leur permet d'interagir entre elles par l'intermédiaire d'interactions protéine-protéine (Chu *et al.*, 2015; Helle *et al.*, 2013 ; Raiborg *et al.*, 2015; Rowland *et al.*, 2014). Cette thèse a étudié l'impact des *Flavivirus* sur l'interaction entre la membrane du RE et des mitochondries. Pour autant, il est intéressant de discuter de l'impact des *Flavivirus* sur d'autres interactions organites – organites. Cette sections discutera de quelques exemples intéressants d'interactions organites – organites susceptibles d'être la cible des *Flavivirus*.

Famille	*Coronaviridae*	*Pneumoviridae*	*Orthomyxoviridae*	*Flaviviridae*	*Paramyxoviridae*	*Herpesviridae*	*Hepadnaviridae*	*Flaviviridae*	*Herpesviridae*
Genre	*Coronavirus*	*Orthopneumovirus*	*Alphainfluenzavirus*	*Hepacivirus*	*Morbillivirus*	*Cytomegalovirus*	*Orthohepadnavirus*	*Pestivirus*	*Lymphocryptovirus*
Espèce	SARS-CoV	Virus respiratoire syncytial	Virus Influenza A	Virus de l'Hépatite C	Virus de la Rougeole	Cytomegalovirus humain	Virus de l'hépatite B	Virus de la Peste porcine	Virus Epstein-Barr
Génome	ARNsb+	ARNsb-	ARNsb-	ARNsb+	ARNsb-	ADNdb	ADN circulaire	ARNsb+	ADNdb
IRM	n/a	n/a	Alltération	n/a	n/a	Altération puis Renforcement	n/a	n/a	n/a
Morphologie mitochondriale	Fusion	Fusion	Fission	Fission	Fusion	Fission	Fission	Fission	Fission
Immunité	Inhibe MAVS et RIG-I ↘ IFN	Inhibe MAVS ↘ IFN	Inhibe RIG-I ↘ IFN	Clive MAVS ↘ IFN	Inhibe MAVS ↘ IFN	Inhibe cGAS-STING ↘ IFN	↘ IFN	↘ IFN	Échappe aux senseurs d'ADN ↘ IFN
Apoptose	↗ Apoptose	↘ Apoptose	↗ Apoptose	↘ Apoptose	↗ Apoptose	↘ Apoptose	↘ Apoptose	↘ Apoptose	↘ Apoptose

Tableau 4.1 Impact viral sur la mitochondrie et l'IRM

SARS-CoV (Elesela *et al.*, 2021). Virus respiratoire syncytial (Elesela *et al.*, 2021). Influenza A (Elesela *et al.*, 2021; Sorouri *et al.*, 2022). Virus de l'hépatite C (Elesela *et al.*, 2021; Sorouri *et al.*, 2022). Virus de la Rougeole (Elesela *et al.*, 2021). Cytomegalovirus humain (Combs *et al.*, 2020; Ren *et al.*, 2022). Virus de l'hépatite B (Elesela *et al.*, 2021; Hossain *et al.*, 2020; Khan *et al.*, 2016; Sorouri *et al.*, 2022). Virus de la Peste porcine (Gou *et al.*, 2017; Hardy *et al.*, 2020; Ma *et al.*, 2019). Virus Epstein-Barr (Gilardini Montani *et al.*, 2019; Sorouri *et al.*, 2022).

4.4.1 L'interface gouttelette lipidique – mitochondrie

Les GL sont des organites intracellulaires ayant une structure unique, c'est-à-dire composées uniquement d'une membrane phospholipidique renfermant une quantité indéfinie de triglycérides (Olzmann *et al.*, 2019). De plus, la surface membranaire des GL possède des protéines membranaires permettant l'interaction organite – organite. Les GL sont très dynamiques morphologiquement en fonction des besoins cellulaires en lipides notamment par lipophagie. La lipophagie des GL va permettre la libération d'acides gras qui seront utilisés par les mitochondries pour nourrir la β-oxydation et le cycle de Krebs (Olzmann *et al.*, 2019). Ces échanges en lipides se font au niveau de l'interface gouttelette lipidique – mitochondrie (GLMI) reposant sur de nombreuses interactions protéine – protéine. Par exemple, la paire la plus connue dans la littérature, PLIN1 (protéine de surface des GL) et MFN2 (protéine de surface des mitochondries) confère à l'interface GLMI une proximité étroite (Boutant *et al.*, 2017; Olzmann *et al.*, 2019). Tel que discuté dans la section 1.8.2.1, le VDEN active la β-oxydation et la libération des acides gras libres provenant de l'autophagie des GL par un mécanisme d'induction de la lipophagie par les protéines virales C, NS4A et NS4B (Byk *et al.*, 2016; Heaton *et al.*, 2010b; Jordan *et al.*, 2017; Samsa *et al.*, 2009; Zhang *et al.*, 2018). De plus, le VZIK utilise également les GL pour favoriser la réplication virale (discuté dans la revue (Qin *et al.*, 2022)). Il n'y a à ce jour aucune preuve de l'altération de cette interface par les *Flavivirus.* Néanmoins, le fait que les *Flavivirus* stimulent l'altération des GL en faveur de la réplication suggère possiblement une modulation de l'interface GLMI. En effet, de nombreuses évidences montrent que les *Flavivirus* augmentent la quantité et taille des GL très tôt dans l'infection suivi finalement par une diminution importante accompagnée également par une diminution de la distribution des mitochondries (Garcia *et al.*, 2020).(Koh *et al.*, 2020; Zhang *et al.*, 2017). De tels résultats appuient la possible interférence des *Flavivirus* sur la GLMI ouvrent la porte à de nouvelles potentielles cibles thérapeutiques contre les *Flavivirus*.

4.4.2 L'interface lysosome – mitochondrie

Les lysosomes sont de petites structures dans le cytosol retrouvés chez les mammifères et arthropodes (Sandri, 2014). Principalement composés d'enzymes permettant la digestion de nombreux différents types de molécules telles que les peptides, les acides nucléiques, les carbohydrates ou encore les lipides, leur fonction est essentiellement la dégradation par digestion enzymatique. Les lysosomes ont également la capacité à fusionner avec d'autres organites pour digérer leur contenu par l'intermédiaire du processus cellulaire autophagique, notamment les

mitochondries avec la mitophagie. Pour autant, les deux organites forment une interface saine et dépendants de l'un et l'autre pour le maintien de la survie cellulaire. Par exemple, lorsque des protéines mitochondriales fonctionnelles ou la chaine de transport d'électrons sont inhibées, la fonction des lysosomes est compromise (Demers-Lamarche *et al.*, 2016). À l'inverse, le facteur TFEB lysosomial favorise la biogénèse mitochondriale et augmente l'expression des enzymes de la phosphorylation oxydative mitochondriale (Mansueto *et al.*, 2017). De plus, l'inhibition de l'acidification des lysosomes diminue la respiration basale et maximale mitochondriale (Monteleon *et al.*, 2018). L'interface lysosome – mitochondrie (ILYM) repose essentiellement sur l'interaction protéine-protéine de LAMP-1, protéines de surface lysosomial et MFN2 ou GADP1, toutes deux des protéines mitochondriales (Pijuan *et al.*, 2022). Par ailleurs, cette interaction est régulée par Rab7 qui recrute au niveau des lysosomes des protéines effectrices Rab (Wong *et al.*, 2018). Ces protéines effectrices vont favoriser le transport des lysosomes dans le cytosol, la fusion et l'interaction avec d'autres organites.

Il n'y a actuellement aucunes données sur l'interférence des *Flavivirus* sur l'ILYM. Cependant, en condition d'infection flavivirale, nous avons montré dans cette thèse l'impact des *Flavivirus* sur le métabolisme et la morphologie des mitochondries qui pourrait alors avoir un impact direct sur le bon fonctionnement des lysosomes. Pour appuyer cette hypothèse, il a déjà été montré que le VDEN impacte la voie autophagique par la diminution de l'activité des lysosomes (Metz *et al.*, 2015). Outre ces différents rôle tels que le transport du cholestérol ou du Fer, l'ILYM est impliquée dans la régulation positive de la fission mitochondriale (Abrisch *et al.*, 2020) ce qui va à l'encontre des données montrées dans cette thèse suggérant alors une possible altération de l'ILYM par les *Flavivirus*. Nous n'avons personnellement pas observé de lysosome en contact avec les mitochondries lors de l'analyse de l'impact des *Flavivirus* sur l'IRM en observation microscopique. Il serait alors intéressant d'étudier en parallèle l'impact de l'ILYM sur la réplication des *Flavivirus* notamment dans l'élongation mitochondriale.

4.4.3 L'interface RE – appareil de Golgi

Finalement, un dernier exemple d'interaction organite – organite intéressant pour les *Flavivirus* serait l'interface RE – appareil de Golgi (REGO). Cette interface est importante dans la synthèse et la sécrétion de protéines cellulaires et facilite le transfert de lipides (De Matteis *et al.*, 2015). L'interface REGO possède de nombreuses interactions protéine-protéine telles que PI4P (Golgi) avec OSBP1 ou ORP9/10/11 (RE) ou encore PI4P (Golgi) avec SAC1 ou VAP (RE) (Mesmin *et al.*, 2013; Venditti *et al.*, 2020; Venditti *et al.*, 2019; Weber-Boyvat *et al.*, 2015).

Lorsque l'on observe le cycle de vie des *Flavivirus,* l'appareil de Golgi possède un rôle clé puisque les virions nouvellement synthétisés vont traverser l'appareil de Golgi et subir leur maturation par un clivage orchestré par la furine (Elshuber *et al.*, 2003). Il n'y a pas non plus d'études de l'impact des *Flavivirus* sur l'interface REGO. En revanche, il est possible qu'il y ait un impact positif en favorisant l'interface REGO puisque les virions synthétisés et stockés dans les sacs de virus formés à partir de la membrane du RE sont ensuite relâchés en direction de l'appareil de Golgi.

Puisque les *Flavivirus* tels que VDEN et VZIK causent un stress au niveau de l'appareil de Golgi, tel que la dilatation des citernes chez les mammifères et les arthropodes (Viettri *et al.*, 2021), Il serait intéressant d'étudier si le remodelage morphologique du RE impacte l'interface REGO et par quelle manière ceci impacte le cycle viral des *Flavivirus* et possiblement les processus cellulaires impliquant l'appareil de Golgi.

4.5 Perspectives de recherche

Cette thèse soulève de nombreuses questions qu'il serait intéressant d'étudier. Par exemple, nous avons montré par diminution de l'expression des protéines de l'IRM que son altération forcée améliore la réplication virale (discuté à la section 4.3.4). Cependant, nous n'avons pas pu montrer si à l'inverse, la stabilisation forcée de l'IRM provoque une diminution de la réplication virale. Etudier ce point important par une construction moléculaire permettrait de confirmer nos résultats. Également, nous savons dans la littérature que l'élongation mitochondriale diminue la réponse immunitaire précoce antivirale en diminuant l'expression des interférons (Chatel-Chaix *et al.*, 2016). Dans un futur proche, il serait vraiment intéressant d'étudier si l'altération de l'IRM indépendamment de l'élongation mitochondriale a un impact sur l'expression des interférons. De plus, un point vraiment important et mentionné à la section 4.3.1 est l'apparition d'un sous-produit de SYNJ2BP observé en western blot seulement avec une infection virale au VZIK. Des études plus approfondies devraient être menées pour comprendre cette différence de mécanisme entre le VDEN et le VZIK. Par ailleurs, nous n'avons pas pu étudier l'aspect lipidique impliqué lors de la manipulation des mitochondries par les *Flavivirus*. En effet, des études complémentaires sur la β-oxydation et la libération d'acides gras provenant des gouttelettes lipidiques tôt dans l'infection devraient être menées pour appuyer notre hypothèse dans le remodelage morphologique membranaire.

Dans un futur et horizon plus large, il serait intéressant d'investiguer d'autres impacts possibles des *Flavivirus* sur des contacts organite – organite cellulaires. Par exemple, en dehors du contexte mitochondrial, les peroxysomes sont des organites cellulaires importants dans

l'oxydation de molécules et dans la production de plasmalogènes, ingrédients clés dans la myélinisation des cellules neuronales (da Silva *et al.*, 2014). De plus les peroxysomes sont également une plateforme immunitaire faisant intervenir le complexe MAVS (Dixit *et al.*, 2010). D'un point de vue interaction, les peroxysomes forme une interface avec les gouttelettes lipidiques (PXGL) (Schrader, 2001; Schuldiner *et al.*, 2017). Cette interface est importante dans la réalisation d'une β-oxydation efficace des acides gras longs et une défaillance de ce processus cellulaire dans l'interface PXGL aboutit à de sévères problèmes neurologiques (Chang *et al.*, 2019). Les *Flavivirus* modulent la dynamique et le métabolisme des peroxysomes afin de favoriser la réplication virale et la propagation (Ferreira *et al.*, 2022). En effet, ceci résulte en une perte significative des peroxysomes aboutissant en une réduction drastique de la production d'IFN de type III (Wong *et al.*, 2019; You *et al.*, 2015). De plus, tel que discuté dans l'introduction, les *Flavivirus* contrôle la lipophagie des gouttelettes lipidiques par l'intermédiaire de AUP1 (Zhang *et al.*, 2018). Finalement, toutes ces interférences sur ces deux organites pourraient également expliquer les complications neurologiques sévères causés par les *Flavivirus* neurotrophiques. Dans un contexte où les *Flavivirus* altèrent l'IRM pour limiter le rôle de MAVS dans la réponse immunitaire antivirale, il n'est pas surprenant qu'ils interfèrent également au niveau des peroxysomes, notamment dans la voie de signalisation de MAVS. Malgré la démonstration que les *Flavivirus* perturbent les peroxysomes ou les gouttelettes lipidiques, il n'y a à ce jour aucune preuve formelle de l'altération de l'interface PXGL. L'interface PXGL repose sur l'interaction de la protéine de surface spastin M1 des gouttelettes lipidiques et de la protéine de surface ABCD1 des peroxysomes (Chang *et al.*, 2019; Henne, 2019). Il serait vraiment intéressant d'étudier si les *Flavivirus* neurotrophiques interfèrent dans l'interface PXGL et quel serait l'impact dans l'activité cellulaire des deux organites, notamment dans la myélinisation des cellules neuronales liée aux maladies neurodégénératives, telles que le syndrome de Guillain-Barré causé par le VZIK chez l'adulte. Pour ceci, une approche par PLA entre spastin M1 et ABCD1 permettrait d'étudier la proximité entre les péroxysomes et les GL en condition d'infection. Par ailleurs, à la suite d'une infection flavivirale, des essais d'immunobuvardages indiqueraient l'impact d'une infection flavivirale dans l'intégrité de l'interface PXGL, notamment dans l'expression des protéines impliquées dans la voie de synthèse des plasmalogènes.

5 CONCLUSION

En conclusion, ce doctorat a permis de mieux comprendre l'impact des *Flavivirus* sur l'interface réticulo-mitochondriale *(Freppel et al., 2023).* En effet, il a déjà été montré que par l'intermédiaire de la protéine virale NS4B, les *Flavivirus* inhibent la translocation de DRP1 aux mitochondries favorisant leur élongation au détriment de la production d'IFN de type I et III (Chatel-Chaix *et al.*, 2016). Nos nouvelles données obtenues lors de ce doctorat montrent que ce phénotype est accompagné de l'altération structurelle de l'IRM. Notamment, nous avons également montré que l'altération de l'IRM a un impact négatif important dans la mort cellulaire par apoptose en réponse à l'infection virale. De plus, l'infection par les *Flavivirus* impacte la phosphorylation oxydative mitochondriale suggérant une augmentation d'ATP en début d'infection.

Nos résultats semblent appuyer l'hypothèse selon laquelle la modification de la phosphorylation oxydative tôt dans l'infection permettrait l'augmentation de production d'ATP servant au remodelage morphologique. L'altération de l'IRM pourrait alors permettre la biogénèse des CM et la perturbation des mécanismes cellulaires présents au niveau de l'IRM, tels que l'apoptose ou la réponse immunitaire antivirale précoce. Les CM, riches en NS3, NS4B et VCP (Anton *et al.*, 2021) pourraient jouer un rôle dans la séquestration de facteurs importants dans des mécanismes défavorables à la réplication virale permettant ainsi la mise en place d'un environnement cytoplasmique favorable à la réplication virale.

6 BIBLIOGRAPHIE

Abdulrahman BA, Abdelaziz D, Thapa S, Lu L, Jain S, Gilch S, Proniuk S, Zukiwski A, Schatzl HM (2017) The celecoxib derivatives AR-12 and AR-14 induce autophagy and clear prion-infected cells from prions. *Sci Rep* 7(1):17565.

Abrisch RG, Gumbin SC, Wisniewski BT, Lackner LL, Voeltz GK (2020) Fission and fusion machineries converge at ER contact sites to regulate mitochondrial morphology. *J Cell Biol* 219(4).

Acosta EG, Castilla V, Damonte EB (2008) Functional entry of dengue virus into Aedes albopictus mosquito cells is dependent on clathrin-mediated endocytosis. *J Gen Virol* 89(Pt 2):474-484.

Aguirre S, Luthra P, Sanchez-Aparicio MT, Maestre AM, Patel J, Lamothe F, Fredericks AC, Tripathi S, Zhu T, Pintado-Silva J, Webb LG, Bernal-Rubio D, Solovyov A, Greenbaum B, Simon V, Basler CF, Mulder LC, Garcia-Sastre A, Fernandez-Sesma A (2017) Dengue virus NS2B protein targets cGAS for degradation and prevents mitochondrial DNA sensing during infection. *Nat Microbiol* 2:17037.

Airo AM, Urbanowski MD, Lopez-Orozco J, You JH, Skene-Arnold TD, Holmes C, Yamshchikov V, Malik-Soni N, Frappier L, Hobman TC (2018) Expression of flavivirus capsids enhance the cellular environment for viral replication by activating Akt-signalling pathways. *Virology* 516:147-157.

Alabduladhem TO, Bordoni B (2022) Physiology, Krebs Cycle. *StatPearls,* Treasure Island (FL).

Allison SL, Schalich J, Stiasny K, Mandl CW, Kunz C, Heinz FX (1995) Oligomeric rearrangement of tick-borne encephalitis virus envelope proteins induced by an acidic pH. *J Virol* 69(2):695-700.

Allonso D, Andrade IS, Conde JN, Coelho DR, Rocha DC, da Silva ML, Ventura GT, Silva EM, Mohana-Borges R (2015) Dengue Virus NS1 Protein Modulates Cellular Energy Metabolism by Increasing Glyceraldehyde-3-Phosphate Dehydrogenase Activity. *J Virol* 89(23):11871-11883.

Anastasia I, Ilacqua N, Raimondi A, Lemieux P, Ghandehari-Alavijeh R, Faure G, Mekhedov SL, Williams KJ, Caicci F, Valle G, Giacomello M, Quiroga AD, Lehner R, Miksis MJ, Toth K, de Aguiar Vallim TQ, Koonin EV, Scorrano L, Pellegrini L (2021) Mitochondria-rough-ER contacts in the liver regulate systemic lipid homeostasis. *Cell Rep* 34(11):108873.

Antico Arciuch VG, Elguero ME, Poderoso JJ, Carreras MC (2012) Mitochondrial regulation of cell cycle and proliferation. *Antioxid Redox Signal* 16(10):1150-1180.

Anton A, Mazeaud C, Freppel W, Gilbert C, Tremblay N, Sow AA, Roy M, Rodrigue-Gervais IG, Chatel-Chaix L (2021) Valosin-containing protein ATPase activity regulates the morphogenesis of Zika virus replication organelles and virus-induced cell death. *Cell Microbiol* 10.1111/cmi.13302:e13302.

Anwar MO, Islam MM, Thakur V, Kaur I, Mohmmed A (2022) Defining ER-mitochondria contact dynamics in Plasmodium falciparum by targeting component of phospholipid synthesis pathway, phosphatidylserine synthase (PfPSS). *Mitochondrion* 65:124-138.

Aoyama-Ishiwatari S, Hirabayashi Y (2021) Endoplasmic Reticulum-Mitochondria Contact Sites-Emerging Intracellular Signaling Hubs. *Front Cell Dev Biol* 9:653828.

Arakawa M, Tabata K, Ishida K, Kobayashi M, Arai A, Ishikawa T, Suzuki R, Takeuchi H, Tripathi LP, Mizuguchi K, Morita E (2022) Flavivirus recruits the valosin-containing protein-NPL4 complex to induce stress granule disassembly for efficient viral genome replication. *J Biol Chem* 298(3):101597.

Araujo SC, Pereira LR, Alves RPS, Andreata-Santos R, Kanno AI, Ferreira LCS, Goncalves VM (2020) Anti-Flavivirus Vaccines: Review of the Present Situation and Perspectives of Subunit Vaccines Produced in Escherichia coli. *Vaccines (Basel)* 8(3).

Atkinson B, Hearn P, Afrough B, Lumley S, Carter D, Aarons EJ, Simpson AJ, Brooks TJ, Hewson R (2016) Detection of Zika Virus in Semen. *Emerg Infect Dis* 22(5):940.

Avirutnan P, Malasit P, Seliger B, Bhakdi S, Husmann M (1998) Dengue virus infection of human endothelial cells leads to chemokine production, complement activation, and apoptosis. *J Immunol* 161(11):6338-6346.

Ayers JB, Coatsworth HG, Kang S, Dinglasan RR, Zhou L (2021) Clustered rapid induction of apoptosis limits ZIKV and DENV-2 proliferation in the midguts of Aedes aegypti. *Commun Biol* 4(1):69.

Azuma Y, Tokuda T, Shimamura M, Kyotani A, Sasayama H, Yoshida T, Mizuta I, Mizuno T, Nakagawa M, Fujikake N, Ueyama M, Nagai Y, Yamaguchi M (2014) Identification of ter94, Drosophila VCP, as a strong modulator of motor neuron degeneration induced by knockdown of Caz, Drosophila FUS. *Hum Mol Genet* 23(13):3467-3480.

Barbier V, Lang D, Valois S, Rothman AL, Medin CL (2017) Dengue virus induces mitochondrial elongation through impairment of Drp1-triggered mitochondrial fission. *Virology* 500:149-160.

Barreto-Vieira DF, Jacome FC, da Silva MAN, Caldas GC, de Filippis AMB, de Sequeira PC, de Souza EM, Andrade AA, Manso PPA, Trindade GF, Lima SMB, Barth OM (2017) Structural investigation of C6/36 and Vero cell cultures infected with a Brazilian Zika virus. *PLoS One* 12(9):e0184397.

Bartenschlager R, Lohmann V, Penin F (2013) The molecular and structural basis of advanced antiviral therapy for hepatitis C virus infection. *Nat Rev Microbiol* 11(7):482-496.

Bartlett K, Eaton S (2004) Mitochondrial beta-oxidation. *Eur J Biochem* 271(3):462-469.

Bartok A, Weaver D, Golenar T, Nichtova Z, Katona M, Bansaghi S, Alzayady KJ, Thomas VK, Ando H, Mikoshiba K, Joseph SK, Yule DI, Csordas G, Hajnoczky G (2019) IP3 receptor isoforms differently regulate ER-mitochondrial contacts and local calcium transfer. *Nat Commun* 10(1):3726.

Bauer MF, Hofmann S, Neupert W, Brunner M (2000) Protein translocation into mitochondria: the role of TIM complexes. *Trends Cell Biol* 10(1):25-31.

Bayrhuber M, Meins T, Habeck M, Becker S, Giller K, Villinger S, Vonrhein C, Griesinger C, Zweckstetter M, Zeth K (2008) Structure of the human voltage-dependent anion channel. *Proc Natl Acad Sci U S A* 105(40):15370-15375.

Beau F, Mallet HP, Lastere S, Broult J, Laperche S (2020) Transfusion risk associated with recent arbovirus outbreaks in French Polynesia. *Vox Sang* 115(2):124-132.

Beauclair G, Streicher F, Chazal M, Bruni D, Lesage S, Gracias S, Bourgeau S, Sinigaglia L, Fujita T, Meurs EF, Tangy F, Jouvenet N (2020) Retinoic Acid Inducible Gene I and Protein Kinase R, but Not Stress Granules, Mediate the Proinflammatory Response to Yellow Fever Virus. *J Virol* 94(22).

Becker Z (2022) *Takeda's dengue fever vaccine picks up first global nod in Indonesia.*Fierce Pharma, https://www.takeda.com/newsroom/newsreleases/2022/takedas-qdenga-dengue-tetravalent-vaccine-live-attenuated-approved-in-indonesia-for-use-regardless-of-prior-dengue-exposure/

Bekerman E, Neveu G, Shulla A, Brannan J, Pu SY, Wang S, Xiao F, Barouch-Bentov R, Bakken RR, Mateo R, Govero J, Nagamine CM, Diamond MS, De Jonghe S, Herdewijn P, Dye JM, Randall G, Einav S (2017) Anticancer kinase inhibitors impair intracellular viral trafficking and exert broad-spectrum antiviral effects. *J Clin Invest* 127(4):1338-1352.

Bellot G, Garcia-Medina R, Gounon P, Chiche J, Roux D, Pouyssegur J, Mazure NM (2009) Hypoxia-induced autophagy is mediated through hypoxia-inducible factor induction of BNIP3 and BNIP3L via their BH3 domains. *Mol Cell Biol* 29(10):2570-2581.

Berridge MJ (2002) The endoplasmic reticulum: a multifunctional signaling organelle. *Cell Calcium* 32(5-6):235-249.

Bhatt S, Gething PW, Brady OJ, Messina JP, Farlow AW, Moyes CL, Drake JM, Brownstein JS, Hoen AG, Sankoh O, Myers MF, George DB, Jaenisch T, Wint GR, Simmons CP, Scott TW, Farrar JJ, Hay SI (2013) The global distribution and burden of dengue. *Nature* 496(7446):504-507.

Bhuvanakantham R, Cheong YK, Ng ML (2010) West Nile virus capsid protein interaction with importin and HDM2 protein is regulated by protein kinase C-mediated phosphorylation. *Microbes Infect* 12(8-9):615-625.

Biswal S, Borja-Tabora C, Martinez Vargas L, Velasquez H, Theresa Alera M, Sierra V, Johana Rodriguez-Arenales E, Yu D, Wickramasinghe VP, Duarte Moreira E, Jr., Fernando AD, Gunasekera D, Kosalaraksa P, Espinoza F, Lopez-Medina E, Bravo L, Tuboi S, Hutagalung Y, Garbes P, Escudero I, Rauscher M, Bizjajeva S, LeFevre I, Borkowski A, Saez-Llorens X, Wallace D, group Ts (2020) Efficacy of a tetravalent dengue vaccine in healthy children aged 4-16 years: a randomised, placebo-controlled, phase 3 trial. *Lancet* 395(10234):1423-1433.

Blaney JE, Jr., Durbin AP, Murphy BR, Whitehead SS (2006) Development of a live attenuated dengue virus vaccine using reverse genetics. *Viral Immunol* 19(1):10-32.

Blaney JE, Jr., Hanson CT, Firestone CY, Hanley KA, Murphy BR, Whitehead SS (2004) Genetically modified, live attenuated dengue virus type 3 vaccine candidates. *Am J Trop Med Hyg* 71(6):811-821.

Blaney JE, Jr., Manipon GG, Firestone CY, Johnson DH, Hanson CT, Murphy BR, Whitehead SS (2003) Mutations which enhance the replication of dengue virus type 4 and an antigenic chimeric dengue virus type 2/4 vaccine candidate in Vero cells. *Vaccine* 21(27-30):4317-4327.

Blaney JE, Jr., Sathe NS, Goddard L, Hanson CT, Romero TA, Hanley KA, Murphy BR, Whitehead SS (2008) Dengue virus type 3 vaccine candidates generated by introduction of deletions in the 3' untranslated region (3'-UTR) or by exchange of the DENV-3 3'-UTR with that of DENV-4. *Vaccine* 26(6):817-828.

Boutant M, Kulkarni SS, Joffraud M, Ratajczak J, Valera-Alberni M, Combe R, Zorzano A, Canto C (2017) Mfn2 is critical for brown adipose tissue thermogenic function. *EMBO J* 36(11):1543-1558.

Bowen JR, Quicke KM, Maddur MS, O'Neal JT, McDonald CE, Fedorova NB, Puri V, Shabman RS, Pulendran B, Suthar MS (2017) Zika Virus Antagonizes Type I Interferon Responses during Infection of Human Dendritic Cells. *Plos Pathogens* 13(2):e1006164.

Boyman L, Lederer WJ (2020) How the mitochondrial calcium uniporter complex (MCUcx) works. *Proc Natl Acad Sci U S A* 117(37):22634-22636.

Brady OJ, Hay SI (2019a) The first local cases of Zika virus in Europe. *Lancet* 394(10213):1991-1992.

Brady OJ, Osgood-Zimmerman A, Kassebaum NJ, Ray SE, de Araujo VEM, da Nobrega AA, Frutuoso LCV, Lecca RCR, Stevens A, Zoca de Oliveira B, de Lima JM, Jr., Bogoch, II, Mayaud P, Jaenisch T, Mokdad AH, Murray CJL, Hay SI, Reiner RC, Jr., Marinho F (2019b) The association between Zika virus infection and microcephaly in Brazil 2015-2017: An observational analysis of over 4 million births. *PLoS Med* 16(3):e1002755.

Brasil P, Pereira JP, Jr., Moreira ME, Ribeiro Nogueira RM, Damasceno L, Wakimoto M, Rabello RS, Valderramos SG, Halai UA, Salles TS, Zin AA, Horovitz D, Daltro P, Boechat M, Raja Gabaglia C, Carvalho de Sequeira P, Pilotto JH, Medialdea-Carrera R, Cotrim da Cunha D, Abreu de Carvalho LM, Pone M, Machado Siqueira A, Calvet GA, Rodrigues Baiao AE, Neves ES, Nassar de Carvalho PR, Hasue RH, Marschik PB, Einspieler C, Janzen C, Cherry JD, Bispo de Filippis AM, Nielsen-Saines K (2016) Zika Virus Infection in Pregnant Women in Rio de Janeiro. *N Engl J Med* 375(24):2321-2334.

Breckenridge DG, Stojanovic M, Marcellus RC, Shore GC (2003) Caspase cleavage product of BAP31 induces mitochondrial fission through endoplasmic reticulum calcium signals, enhancing cytochrome c release to the cytosol. *J Cell Biol* 160(7):1115-1127.

Brisse M, Ly H (2019) Comparative Structure and Function Analysis of the RIG-I-Like Receptors: RIG-I and MDA5. *Front Immunol* 10:1586.

Byk LA, Gamarnik AV (2016) Properties and Functions of the Dengue Virus Capsid Protein. *Annu Rev Virol* 3(1):263-281.

Cahour A, Falgout B, Lai CJ (1992) Cleavage of the dengue virus polyprotein at the NS3/NS4A and NS4B/NS5 junctions is mediated by viral protease NS2B-NS3, whereas NS4A/NS4B may be processed by a cellular protease. *J Virol* 66(3):1535-1542.

Cai X, Chiu YH, Chen ZJ (2014) The cGAS-cGAMP-STING pathway of cytosolic DNA sensing and signaling. *Mol Cell* 54(2):289-296.

Camara AKS, Zhou Y, Wen PC, Tajkhorshid E, Kwok WM (2017) Mitochondrial VDAC1: A Key Gatekeeper as Potential Therapeutic Target. *Front Physiol* 8:460.

Campbell CL, Keene KM, Brackney DE, Olson KE, Blair CD, Wilusz J, Foy BD (2008) Aedes aegypti uses RNA interference in defense against Sindbis virus infection. *BMC Microbiol* 8:47.

Carod-Artal FJ (2018) Neurological complications of Zika virus infection. *Expert Rev Anti Infect Ther* 16(5):399-410.

Carpio MA, Means RE, Brill AL, Sainz A, Ehrlich BE, Katz SG (2021) BOK controls apoptosis by Ca(2+) transfer through ER-mitochondrial contact sites. *Cell Rep* 34(10):108827.

Carroll J, Fearnley IM, Skehel JM, Shannon RJ, Hirst J, Walker JE (2006) Bovine complex I is a complex of 45 different subunits. *J Biol Chem* 281(43):32724-32727.

Carteaux G, Maquart M, Bedet A, Contou D, Brugieres P, Fourati S, Cleret de Langavant L, de Broucker T, Brun-Buisson C, Leparc-Goffart I, Mekontso Dessap A (2016) Zika Virus Associated with Meningoencephalitis. *N Engl J Med* 374(16):1595-1596.

Cassidy-Stone A, Chipuk JE, Ingerman E, Song C, Yoo C, Kuwana T, Kurth MJ, Shaw JT, Hinshaw JE, Green DR, Nunnari J (2008) Chemical inhibition of the mitochondrial division dynamin reveals its role in Bax/Bak-dependent mitochondrial outer membrane permeabilization. *Dev Cell* 14(2):193-204.

Castanier C, Garcin D, Vazquez A, Arnoult D (2010) Mitochondrial dynamics regulate the RIG-I-like receptor antiviral pathway. *EMBO Rep* 11(2):133-138.

Catteau A, Kalinina O, Wagner MC, Deubel V, Courageot MP, Despres P (2003) Dengue virus M protein contains a proapoptotic sequence referred to as ApoptoM. *J Gen Virol* 84(Pt 10):2781-2793.

CDC (2020) Congenital Zika Syndrome & Other Birth Defects. *CDC*.

Chan JF, Yip CC, Tsang JO, Tee KM, Cai JP, Chik KK, Zhu Z, Chan CC, Choi GK, Sridhar S, Zhang AJ, Lu G, Chiu K, Lo AC, Tsao SW, Kok KH, Jin DY, Chan KH, Yuen KY (2016a) Differential cell line susceptibility to the emerging Zika virus: implications for disease pathogenesis, non-vector-borne human transmission and animal reservoirs. *Emerg Microbes Infect* 5(8):e93.

Chan YK, Gack MU (2016b) A phosphomimetic-based mechanism of dengue virus to antagonize innate immunity. *Nat Immunol* 17(5):523-530.

Chang C, Ortiz K, Ansari A, Gershwin ME (2016) The Zika outbreak of the 21st century. *J Autoimmun* 68:1-13.

Chang CL, Weigel AV, Ioannou MS, Pasolli HA, Xu CS, Peale DR, Shtengel G, Freeman M, Hess HF, Blackstone C, Lippincott-Schwartz J (2019) Spastin tethers lipid droplets to peroxisomes and directs fatty acid trafficking through ESCRT-III. *J Cell Biol* 218(8):2583-2599.

Chang CR, Blackstone C (2007) Drp1 phosphorylation and mitochondrial regulation. *EMBO Rep* 8(12):1088-1089; author reply 1089-1090.

Chang TH, Liao CL, Lin YL (2006) Flavivirus induces interferon-beta gene expression through a pathway involving RIG-I-dependent IRF-3 and PI3K-dependent NF-kappaB activation. *Microbes Infect* 8(1):157-171.

Chao LH, Klein DE, Schmidt AG, Pena JM, Harrison SC (2015) Correction: Sequential conformational rearrangements in flavivirus membrane fusion. *Elife* 4.

Chatel-Chaix L, Bartenschlager R (2014) Dengue virus- and hepatitis C virus-induced replication and assembly compartments: the enemy inside--caught in the web. *J Virol* 88(11):5907-5911.

Chatel-Chaix L, Cortese M, Romero-Brey I, Bender S, Neufeldt CJ, Fischl W, Scaturro P, Schieber N, Schwab Y, Fischer B, Ruggieri A, Bartenschlager R (2016) Dengue Virus Perturbs Mitochondrial Morphodynamics to Dampen Innate Immune Responses. *Cell Host Microbe* 20(3):342-356.

Chatel-Chaix L, Fischl W, Scaturro P, Cortese M, Kallis S, Bartenschlager M, Fischer B, Bartenschlager R (2015) A Combined Genetic-Proteomic Approach Identifies Residues within Dengue Virus NS4B Critical for Interaction with NS3 and Viral Replication. *J Virol* 89(14):7170-7186.

Chaudhry R, Varacallo M (2021) Biochemistry, Glycolysis. *StatPearls,* © 2021, StatPearls Publishing LLC., Treasure Island FL.

Chen Q, Gouilly J, Ferrat YJ, Espino A, Glaziou Q, Cartron G, El Costa H, Al-Daccak R, Jabrane-Ferrat N (2020) Metabolic reprogramming by Zika virus provokes inflammation in human placenta. *Nat Commun* 11(1):2967.

Cheng Q, Chen J (2010) Mechanism of p53 stabilization by ATM after DNA damage. *Cell Cycle* 9(3):472-478.

Chin WX, Lee RCH, Kaur P, Lew TS, Yogarajah T, Kong HY, Teo ZY, Salim CK, Zhang RR, Li XF, Alonso S, Qin CF, Chu JJH (2021) A single-dose live attenuated chimeric vaccine candidate against Zika virus. *NPJ Vaccines* 6(1):20.

Cho DH, Nakamura T, Lipton SA (2010) Mitochondrial dynamics in cell death and neurodegeneration. *Cell Mol Life Sci* 67(20):3435-3447.

Choi SY, Gonzalvez F, Jenkins GM, Slomianny C, Chretien D, Arnoult D, Petit PX, Frohman MA (2007) Cardiolipin deficiency releases cytochrome c from the inner mitochondrial membrane and accelerates stimuli-elicited apoptosis. *Cell Death Differ* 14(3):597-606.

Chu BB, Liao YC, Qi W, Xie C, Du X, Wang J, Yang H, Miao HH, Li BL, Song BL (2015) Cholesterol transport through lysosome-peroxisome membrane contacts. *Cell* 161(2):291-306.

Chu CT, Ji J, Dagda RK, Jiang JF, Tyurina YY, Kapralov AA, Tyurin VA, Yanamala N, Shrivastava IH, Mohammadyani D, Wang KZQ, Zhu J, Klein-Seetharaman J, Balasubramanian K, Amoscato AA, Borisenko G, Huang Z, Gusdon AM, Cheikhi A, Steer EK, Wang R, Baty C, Watkins S, Bahar I, Bayir H, Kagan VE (2013) Cardiolipin externalization to the outer mitochondrial membrane acts as an elimination signal for mitophagy in neuronal cells. *Nat Cell Biol* 15(10):1197-1205.

Chu JJ, Ng ML (2004) Interaction of West Nile virus with alpha v beta 3 integrin mediates virus entry into cells. *J Biol Chem* 279(52):54533-54541.

Clapham DE (2007) Calcium signaling. *Cell* 131(6):1047-1058.

Clarke TE, Clem RJ (2003) Insect defenses against virus infection: the role of apoptosis. *Int Rev Immunol* 22(5-6):401-424.

Cohen S, Valm AM, Lippincott-Schwartz J (2018) Interacting organelles. *Curr Opin Cell Biol* 53:84-91.

Colombini M (2016) The VDAC channel: Molecular basis for selectivity. *Biochim Biophys Acta* 1863(10):2498-2502.

Combs JA, Norton EB, Saifudeen ZR, Bentrup KHZ, Katakam PV, Morris CA, Myers L, Kaur A, Sullivan DE, Zwezdaryk KJ (2020) Human Cytomegalovirus Alters Host Cell Mitochondrial Function during Acute Infection. *J Virol* 94(2).

Cook KC, Tsopurashvili E, Needham JM, Thompson SR, Cristea IM (2022) Restructured membrane contacts rewire organelles for human cytomegalovirus infection. *Nat Commun* 13(1):4720.

Cooper G, M. (2000) ***The Cell: A Molecular Approach. 2nd edition.*** Oxford University Press,

Cortese M, Goellner S, Acosta EG, Neufeldt CJ, Oleksiuk O, Lampe M, Haselmann U, Funaya C, Schieber N, Ronchi P, Schorb M, Pruunsild P, Schwab Y, Chatel-Chaix L, Ruggieri A, Bartenschlager R (2017) Ultrastructural Characterization of Zika Virus Replication Factories. *Cell Rep* 18(9):2113-2123.

Crill WD, Chang GJ (2004) Localization and characterization of flavivirus envelope glycoprotein cross-reactive epitopes. *J Virol* 78(24):13975-13986.

Crump A (2017) Ivermectin: enigmatic multifaceted 'wonder' drug continues to surprise and exceed expectations. *J Antibiot (Tokyo)* 70(5):495-505.

Csordas G, Renken C, Varnai P, Walter L, Weaver D, Buttle KF, Balla T, Mannella CA, Hajnoczky G (2006) Structural and functional features and significance of the physical linkage between ER and mitochondria. *J Cell Biol* 174(7):915-921.

da Silva IRF, Frontera JA, Bispo de Filippis AM, Nascimento O, Group R-G-ZR (2017) Neurologic Complications Associated With the Zika Virus in Brazilian Adults. *JAMA Neurol* 74(10):1190-1198.

da Silva TF, Eira J, Lopes AT, Malheiro AR, Sousa V, Luoma A, Avila RL, Wanders RJ, Just WW, Kirschner DA, Sousa MM, Brites P (2014) Peripheral nervous system plasmalogens regulate Schwann cell differentiation and myelination. *J Clin Invest* 124(6):2560-2570.

Dalrymple NA, Cimica V, Mackow ER (2015) Dengue Virus NS Proteins Inhibit RIG-I/MAVS Signaling by Blocking TBK1/IRF3 Phosphorylation: Dengue Virus Serotype 1 NS4A Is a Unique Interferon-Regulating Virulence Determinant. *mBio* 6(3):e00553-00515.

Davidson AD (2009) Chapter 2. New insights into flavivirus nonstructural protein 5. *Adv Virus Res* 74:41-101.

de Araujo TVB, Rodrigues LC, de Alencar Ximenes RA, de Barros Miranda-Filho D, Montarroyos UR, de Melo APL, Valongueiro S, de Albuquerque M, Souza WV, Braga C, Filho SPB, Cordeiro MT, Vazquez E, Di Cavalcanti Souza Cruz D, Henriques CMP, Bezerra LCA, da Silva Castanha PM, Dhalia R, Marques-Junior ETA, Martelli CMT, investigators from the Microcephaly Epidemic Research G, Brazilian Ministry of H, Pan American Health O, Instituto de Medicina Integral Professor Fernando F, State Health Department of P (2016) Association between Zika virus infection and microcephaly in Brazil, January to May, 2016: preliminary report of a case-control study. *Lancet Infect Dis* 16(12):1356-1363.

de Brito OM, Scorrano L (2008) Mitofusin 2 tethers endoplasmic reticulum to mitochondria. *Nature* 456(7222):605-610.

De Matteis MA, Rega LR (2015) Endoplasmic reticulum-Golgi complex membrane contact sites. *Curr Opin Cell Biol* 35:43-50.

De Vos KJ, Morotz GM, Stoica R, Tudor EL, Lau KF, Ackerley S, Warley A, Shaw CE, Miller CC (2012) VAPB interacts with the mitochondrial protein PTPIP51 to regulate calcium homeostasis. *Hum Mol Genet* 21(6):1299-1311.

de Wispelaere M, Lian W, Potisopon S, Li PC, Jang J, Ficarro SB, Clark MJ, Zhu X, Kaplan JB, Pitts JD, Wales TE, Wang J, Engen JR, Marto JA, Gray NS, Yang PL (2018) Inhibition of Flaviviruses by Targeting a Conserved Pocket on the Viral Envelope Protein. *Cell Chem Biol* 25(8):1006-1016 e1008.

Delvecchio R, Higa LM, Pezzuto P, Valadao AL, Garcez PP, Monteiro FL, Loiola EC, Dias AA, Silva FJ, Aliota MT, Caine EA, Osorio JE, Bellio M, O'Connor DH, Rehen S, de Aguiar RS,

Savarino A, Campanati L, Tanuri A (2016) Chloroquine, an Endocytosis Blocking Agent, Inhibits Zika Virus Infection in Different Cell Models. *Viruses* 8(12).
Demers-Lamarche J, Guillebaud G, Tlili M, Todkar K, Belanger N, Grondin M, Nguyen AP, Michel J, Germain M (2016) Loss of Mitochondrial Function Impairs Lysosomes. *J Biol Chem* 291(19):10263-10276.
Deng L, Adachi T, Kitayama K, Bungyoku Y, Kitazawa S, Ishido S, Shoji I, Hotta H (2008) Hepatitis C virus infection induces apoptosis through a Bax-triggered, mitochondrion-mediated, caspase 3-dependent pathway. *J Virol* 82(21):10375-10385.
Deng YQ, Zhang NN, Li CF, Tian M, Hao JN, Xie XP, Shi PY, Qin CF (2016) Adenosine Analog NITD008 Is a Potent Inhibitor of Zika Virus. *Open Forum Infect Dis* 3(4):ofw175.
Diamond DL, Syder AJ, Jacobs JM, Sorensen CM, Walters KA, Proll SC, McDermott JE, Gritsenko MA, Zhang Q, Zhao R, Metz TO, Camp DG, 2nd, Waters KM, Smith RD, Rice CM, Katze MG (2010) Temporal proteome and lipidome profiles reveal hepatitis C virus-associated reprogramming of hepatocellular metabolism and bioenergetics. *Plos Pathogens* 6(1):e1000719.
Dick GW, Kitchen SF, Haddow AJ (1952) Zika virus. I. Isolations and serological specificity. *Trans R Soc Trop Med Hyg* 46(5):509-520.
Ding Q, Gaska JM, Douam F, Wei L, Kim D, Balev M, Heller B, Ploss A (2018) Species-specific disruption of STING-dependent antiviral cellular defenses by the Zika virus NS2B3 protease. *Proc Natl Acad Sci U S A* 115(27):E6310-E6318.
Dionicio CL, Pena F, Constantino-Jonapa LA, Vazquez C, Yocupicio-Monroy M, Rosales R, Zambrano JL, Ruiz MC, Del Angel RM, Ludert JE (2018) Dengue virus induced changes in Ca(2+) homeostasis in human hepatic cells that favor the viral replicative cycle. *Virus Res* 245:17-28.
Dixit E, Boulant S, Zhang Y, Lee AS, Odendall C, Shum B, Hacohen N, Chen ZJ, Whelan SP, Fransen M, Nibert ML, Superti-Furga G, Kagan JC (2010) Peroxisomes are signaling platforms for antiviral innate immunity. *Cell* 141(4):668-681.
Duan X, Li S, Holmes JA, Tu Z, Li Y, Cai D, Liu X, Li W, Yang C, Jiao B, Schaefer EA, Fusco DN, Salloum S, Chen L, Lin W, Chung RT (2018) MicroRNA 130a Regulates both Hepatitis C Virus and Hepatitis B Virus Replication through a Central Metabolic Pathway. *J Virol* 92(7).
Duan Y, Wang X, Sun K, Lin Y, Wang X, Chen K, Yang G, Wang X, Du C (2022) SYNJ2BP Improves the Production of Lentiviral Envelope Protein by Facilitating the Formation of Mitochondrion-Associated Endoplasmic Reticulum Membrane. *J Virol* 96(20):e0054922.
Dupont-Rouzeyrol M, Biron A, O'Connor O, Huguon E, Descloux E (2016) Infectious Zika viral particles in breastmilk. *Lancet* 387(10023):1051.
Durbin AP, Karron RA, Sun W, Vaughn DW, Reynolds MJ, Perreault JR, Thumar B, Men R, Lai CJ, Elkins WR, Chanock RM, Murphy BR, Whitehead SS (2001) Attenuation and immunogenicity in humans of a live dengue virus type-4 vaccine candidate with a 30 nucleotide deletion in its 3'-untranslated region. *Am J Trop Med Hyg* 65(5):405-413.
Durbin AP, Whitehead SS, Shaffer D, Elwood D, Wanionek K, Thumar B, Blaney JE, Murphy BR, Schmidt AC (2011) A single dose of the DENV-1 candidate vaccine rDEN1Delta30 is strongly immunogenic and induces resistance to a second dose in a randomized trial. *PLoS Negl Trop Dis* 5(8):e1267.
Effler PV, Pang L, Kitsutani P, Vorndam V, Nakata M, Ayers T, Elm J, Tom T, Reiter P, Rigau-Perez JG, Hayes JM, Mills K, Napier M, Clark GG, Gubler DJ, Hawaii Dengue Outbreak Investigation T (2005) Dengue fever, Hawaii, 2001-2002. *Emerg Infect Dis* 11(5):742-749.
El-Bacha T, Midlej V, Pereira da Silva AP, Silva da Costa L, Benchimol M, Galina A, Da Poian AT (2007) Mitochondrial and bioenergetic dysfunction in human hepatic cells infected with dengue 2 virus. *Biochim Biophys Acta* 1772(10):1158-1166.
El Ghouzzi V, Bianchi FT, Molineris I, Mounce BC, Berto GE, Rak M, Lebon S, Aubry L, Tocco C, Gai M, Chiotto AMA, Sgro F, Pallavicini G, Simon-Loriere E, Passemard S, Vignuzzi M,

Gressens P, Di Cunto F (2018) Correction to: ZIKA virus elicits P53 activation and genotoxic stress in human neural progenitors similar to mutations involved in severe forms of genetic microcephaly. *Cell Death Dis* 9(12):1155.
Elesela S, Lukacs NW (2021) Role of Mitochondria in Viral Infections. *Life (Basel)* 11(3).
Ellenrieder L, Dieterle MP, Doan KN, Martensson CU, Floerchinger A, Campo ML, Pfanner N, Becker T (2019) Dual Role of Mitochondrial Porin in Metabolite Transport across the Outer Membrane and Protein Transfer to the Inner Membrane. *Mol Cell* 73(5):1056-1065 e1057.
Elmore S (2007) Apoptosis: a review of programmed cell death. *Toxicol Pathol* 35(4):495-516.
Elshuber S, Allison SL, Heinz FX, Mandl CW (2003) Cleavage of protein prM is necessary for infection of BHK-21 cells by tick-borne encephalitis virus. *J Gen Virol* 84(Pt 1):183-191.
Endo T, Yamano K (2010) Transport of proteins across or into the mitochondrial outer membrane. *Biochim Biophys Acta* 1803(6):706-714.
Eyer L, Zouharova D, Sirmarova J, Fojtikova M, Stefanik M, Haviernik J, Nencka R, de Clercq E, Ruzek D (2017) Antiviral activity of the adenosine analogue BCX4430 against West Nile virus and tick-borne flaviviruses. *Antiviral Res* 142:63-67.
Fanunza E, Grandi N, Quartu M, Carletti F, Ermellino L, Milia J, Corona A, Capobianchi MR, Ippolito G, Tramontano E (2021) INMI1 Zika Virus NS4B Antagonizes the Interferon Signaling by Suppressing STAT1 Phosphorylation. *Viruses* 13(12).
Farias KJ, Machado PR, Muniz JA, Imbeloni AA, da Fonseca BA (2015) Antiviral activity of chloroquine against dengue virus type 2 replication in Aotus monkeys. *Viral Immunol* 28(3):161-169.
Ferguson M, Shin J, Knezevic I, Minor P, Barrett A, Group WHOW (2010) WHO Working Group on Technical Specifications for Manufacture and Evaluation of Yellow Fever Vaccines, Geneva, Switzerland, 13-14 May 2009. *Vaccine* 28(52):8236-8245.
Ferreira AR, Marques M, Ramos B, Kagan JC, Ribeiro D (2022) Emerging roles of peroxisomes in viral infections. *Trends Cell Biol* 32(2):124-139.
Fibriansah G, Ibarra KD, Ng TS, Smith SA, Tan JL, Lim XN, Ooi JS, Kostyuchenko VA, Wang J, de Silva AM, Harris E, Crowe JE, Jr., Lok SM (2015) DENGUE VIRUS. Cryo-EM structure of an antibody that neutralizes dengue virus type 2 by locking E protein dimers. *Science* 349(6243):88-91.
Finol E, Ooi EE (2019) Evolution of Subgenomic RNA Shapes Dengue Virus Adaptation and Epidemiological Fitness. *iScience* 16:94-105.
Fire A, Xu S, Montgomery MK, Kostas SA, Driver SE, Mello CC (1998) Potent and specific genetic interference by double-stranded RNA in Caenorhabditis elegans. *Nature* 391(6669):806-811.
Fischer R, Baumert T, Blum HE (2007) Hepatitis C virus infection and apoptosis. *World J Gastroenterol* 13(36):4865-4872.
Fischl W, Bartenschlager R (2013) High-throughput screening using dengue virus reporter genomes. *Methods Mol Biol* 1030:205-219.
Fontaine KA, Sanchez EL, Camarda R, Lagunoff M (2015) Dengue virus induces and requires glycolysis for optimal replication. *J Virol* 89(4):2358-2366.
Frank S, Gaume B, Bergmann-Leitner ES, Leitner WW, Robert EG, Catez F, Smith CL, Youle RJ (2001) The role of dynamin-related protein 1, a mediator of mitochondrial fission, in apoptosis. *Dev Cell* 1(4):515-525.
Fredericksen BL, Keller BC, Fornek J, Katze MG, Gale M, Jr. (2008) Establishment and maintenance of the innate antiviral response to West Nile Virus involves both RIG-I and MDA5 signaling through IPS-1. *J Virol* 82(2):609-616.
Freppel W, Anton A, Nouhi Z, Mazeaud C, Gilbert C, Tremblay N, Torres VAB, Sow AA, Laulhé X, Lamarre A, Rodrigue-Gervais IG, Pichlmair A, Scaturro P, Hulea L, Chatel-Chaix L (2023) Flaviviruses alter endoplasmic reticulum-mitochondria contacts to regulate respiration and apoptosis. *bioRxiv* 10.1101/2023.03.09.531853:2023.2003.2009.531853.

Freppel W, Mazeaud C, Chatel-Chaix L (2018) Production, Titration and Imaging of Zika Virus in Mammalian Cells. *Bio-protocol* 8(24).

Freppel W, Roy M, Chatel-Chaix L (2022) Flaviviridae and mitochondria: Everything you always wanted to know about their relationship but were afraid to ask. *Virologie (Montrouge)* 10.1684/vir.2022.0926.

Friedman JR, Lackner LL, West M, DiBenedetto JR, Nunnari J, Voeltz GK (2011) ER tubules mark sites of mitochondrial division. *Science* 334(6054):358-362.

Fu M, St-Pierre P, Shankar J, Wang PT, Joshi B, Nabi IR (2013) Regulation of mitophagy by the Gp78 E3 ubiquitin ligase. *Mol Biol Cell* 24(8):1153-1162.

Fujimoto M, Hayashi T (2011) New insights into the role of mitochondria-associated endoplasmic reticulum membrane. *Int Rev Cell Mol Biol* 292:73-117.

Funk A, Truong K, Nagasaki T, Torres S, Floden N, Balmori Melian E, Edmonds J, Dong H, Shi PY, Khromykh AA (2010) RNA structures required for production of subgenomic flavivirus RNA. *J Virol* 84(21):11407-11417.

Gaburro J, Bhatti A, Harper J, Jeanne I, Dearnley M, Green D, Nahavandi S, Paradkar PN, Duchemin JB (2018) Neurotropism and behavioral changes associated with Zika infection in the vector Aedes aegypti. *Emerg Microbes Infect* 7(1):68.

Gack MU, Diamond MS (2016) Innate immune escape by Dengue and West Nile viruses. *Curr Opin Virol* 20:119-128.

Gack MU, Shin YC, Joo CH, Urano T, Liang C, Sun L, Takeuchi O, Akira S, Chen Z, Inoue S, Jung JU (2007) TRIM25 RING-finger E3 ubiquitin ligase is essential for RIG-I-mediated antiviral activity. *Nature* 446(7138):916-920.

Galluzzi L, Baehrecke EH, Ballabio A, Boya P, Bravo-San Pedro JM, Cecconi F, Choi AM, Chu CT, Codogno P, Colombo MI, Cuervo AM, Debnath J, Deretic V, Dikic I, Eskelinen EL, Fimia GM, Fulda S, Gewirtz DA, Green DR, Hansen M, Harper JW, Jaattela M, Johansen T, Juhasz G, Kimmelman AC, Kraft C, Ktistakis NT, Kumar S, Levine B, Lopez-Otin C, Madeo F, Martens S, Martinez J, Melendez A, Mizushima N, Munz C, Murphy LO, Penninger JM, Piacentini M, Reggiori F, Rubinsztein DC, Ryan KM, Santambrogio L, Scorrano L, Simon AK, Simon HU, Simonsen A, Tavernarakis N, Tooze SA, Yoshimori T, Yuan J, Yue Z, Zhong Q, Kroemer G (2017) Molecular definitions of autophagy and related processes. *EMBO J* 36(13):1811-1836.

Galluzzi L, Vitale I, Aaronson SA, Abrams JM, Adam D, Agostinis P, Alnemri ES, Altucci L, Amelio I, Andrews DW, Annicchiarico-Petruzzelli M, Antonov AV, Arama E, Baehrecke EH, Barlev NA, Bazan NG, Bernassola F, Bertrand MJM, Bianchi K, Blagosklonny MV, Blomgren K, Borner C, Boya P, Brenner C, Campanella M, Candi E, Carmona-Gutierrez D, Cecconi F, Chan FK, Chandel NS, Cheng EH, Chipuk JE, Cidlowski JA, Ciechanover A, Cohen GM, Conrad M, Cubillos-Ruiz JR, Czabotar PE, D'Angiolella V, Dawson TM, Dawson VL, De Laurenzi V, De Maria R, Debatin KM, DeBerardinis RJ, Deshmukh M, Di Daniele N, Di Virgilio F, Dixit VM, Dixon SJ, Duckett CS, Dynlacht BD, El-Deiry WS, Elrod JW, Fimia GM, Fulda S, Garcia-Saez AJ, Garg AD, Garrido C, Gavathiotis E, Golstein P, Gottlieb E, Green DR, Greene LA, Gronemeyer H, Gross A, Hajnoczky G, Hardwick JM, Harris IS, Hengartner MO, Hetz C, Ichijo H, Jaattela M, Joseph B, Jost PJ, Juin PP, Kaiser WJ, Karin M, Kaufmann T, Kepp O, Kimchi A, Kitsis RN, Klionsky DJ, Knight RA, Kumar S, Lee SW, Lemasters JJ, Levine B, Linkermann A, Lipton SA, Lockshin RA, Lopez-Otin C, Lowe SW, Luedde T, Lugli E, MacFarlane M, Madeo F, Malewicz M, Malorni W, Manic G, Marine JC, Martin SJ, Martinou JC, Medema JP, Mehlen P, Meier P, Melino S, Miao EA, Molkentin JD, Moll UM, Munoz-Pinedo C, Nagata S, Nunez G, Oberst A, Oren M, Overholtzer M, Pagano M, Panaretakis T, Pasparakis M, Penninger JM, Pereira DM, Pervaiz S, Peter ME, Piacentini M, Pinton P, Prehn JHM, Puthalakath H, Rabinovich GA, Rehm M, Rizzuto R, Rodrigues CMP, Rubinsztein DC, Rudel T, Ryan KM, Sayan E, Scorrano L, Shao F, Shi Y, Silke J, Simon HU, Sistigu A, Stockwell BR, Strasser A, Szabadkai G, Tait SWG,

Tang D, Tavernarakis N, Thorburn A, Tsujimoto Y, Turk B, Vanden Berghe T, Vandenabeele P, Vander Heiden MG, Villunger A, Virgin HW, Vousden KH, Vucic D, Wagner EF, Walczak H, Wallach D, Wang Y, Wells JA, Wood W, Yuan J, Zakeri Z, Zhivotovsky B, Zitvogel L, Melino G, Kroemer G (2018) Molecular mechanisms of cell death: recommendations of the Nomenclature Committee on Cell Death 2018. *Cell Death Differ* 25(3):486-541.

Galmes R, Houcine A, van Vliet AR, Agostinis P, Jackson CL, Giordano F (2016) ORP5/ORP8 localize to endoplasmic reticulum-mitochondria contacts and are involved in mitochondrial function. *EMBO Rep* 17(6):800-810.

Garcia-Blanco MA, Vasudevan SG, Bradrick SS, Nicchitta C (2016) Flavivirus RNA transactions from viral entry to genome replication. *Antiviral Res* 134:244-249.

Garcia CC, Vazquez CA, Giovannoni F, Russo CA, Cordo SM, Alaimo A, Damonte EB (2020) Cellular Organelles Reorganization During Zika Virus Infection of Human Cells. *Front Microbiol* 11:1558.

Garrido C, Galluzzi L, Brunet M, Puig PE, Didelot C, Kroemer G (2006) Mechanisms of cytochrome c release from mitochondria. *Cell Death Differ* 13(9):1423-1433.

Gaudinski MR, Houser KV, Morabito KM, Hu Z, Yamshchikov G, Rothwell RS, Berkowitz N, Mendoza F, Saunders JG, Novik L, Hendel CS, Holman LA, Gordon IJ, Cox JH, Edupuganti S, McArthur MA, Rouphael NG, Lyke KE, Cummings GE, Sitar S, Bailer RT, Foreman BM, Burgomaster K, Pelc RS, Gordon DN, DeMaso CR, Dowd KA, Laurencot C, Schwartz RM, Mascola JR, Graham BS, Pierson TC, Ledgerwood JE, Chen GL, Vrc, teams VRCs (2018) Safety, tolerability, and immunogenicity of two Zika virus DNA vaccine candidates in healthy adults: randomised, open-label, phase 1 clinical trials. *Lancet* 391(10120):552-562.

George SL, Wong MA, Dube TJ, Boroughs KL, Stovall JL, Luy BE, Haller AA, Osorio JE, Eggemeyer LM, Irby-Moore S, Frey SE, Huang CY, Stinchcomb DT (2015) Safety and Immunogenicity of a Live Attenuated Tetravalent Dengue Vaccine Candidate in Flavivirus-Naive Adults: A Randomized, Double-Blinded Phase 1 Clinical Trial. *J Infect Dis* 212(7):1032-1041.

Germi R, Crance JM, Garin D, Guimet J, Lortat-Jacob H, Ruigrok RW, Zarski JP, Drouet E (2002) Heparan sulfate-mediated binding of infectious dengue virus type 2 and yellow fever virus. *Virology* 292(1):162-168.

Gestuveo RJ, Royle J, Donald CL, Lamont DJ, Hutchinson EC, Merits A, Kohl A, Varjak M (2021) Analysis of Zika virus capsid-Aedes aegypti mosquito interactome reveals pro-viral host factors critical for establishing infection. *Nat Commun* 12(1):2766.

Ghosh Roy S, Sadigh B, Datan E, Lockshin RA, Zakeri Z (2014) Regulation of cell survival and death during Flavivirus infections. *World J Biol Chem* 5(2):93-105.

Ghouzzi VE, Bianchi FT, Molineris I, Mounce BC, Berto GE, Rak M, Lebon S, Aubry L, Tocco C, Gai M, Chiotto AM, Sgro F, Pallavicini G, Simon-Loriere E, Passemard S, Vignuzzi M, Gressens P, Di Cunto F (2016) ZIKA virus elicits P53 activation and genotoxic stress in human neural progenitors similar to mutations involved in severe forms of genetic microcephaly. *Cell Death Dis* 7(10):e2440.

Giacomello M, Pellegrini L (2016) The coming of age of the mitochondria-ER contact: a matter of thickness. *Cell Death Differ* 23(9):1417-1427.

Giamogante F, Poggio E, Barazzuol L, Covallero A, Cali T (2021) Apoptotic signals at the endoplasmic reticulum-mitochondria interface. *Adv Protein Chem Struct Biol* 126:307-343.

Gilardini Montani MS, Santarelli R, Granato M, Gonnella R, Torrisi MR, Faggioni A, Cirone M (2019) EBV reduces autophagy, intracellular ROS and mitochondria to impair monocyte survival and differentiation. *Autophagy* 15(4):652-667.

Gillespie LK, Hoenen A, Morgan G, Mackenzie JM (2010) The endoplasmic reticulum provides the membrane platform for biogenesis of the flavivirus replication complex. *J Virol* 84(20):10438-10447.

Giraldo MI, Vargas-Cuartas O, Gallego-Gomez JC, Shi PY, Padilla-Sanabria L, Castano-Osorio JC, Rajsbaum R (2018) K48-linked polyubiquitination of dengue virus NS1 protein inhibits its interaction with the viral partner NS4B. *Virus Res* 246:1-11.

Goethals O, Kaptein SJF, Kesteleyn B, Bonfanti JF, Van Wesenbeeck L, Bardiot D, Verschoor EJ, Verstrepen BE, Fagrouch Z, Putnak JR, Kiemel D, Ackaert O, Straetemans R, Lachau-Durand S, Geluykens P, Crabbe M, Thys K, Stoops B, Lenz O, Tambuyzer L, De Meyer S, Dallmeier K, McCracken MK, Gromowski GD, Rutvisuttinunt W, Jarman RG, Karasavvas N, Touret F, Querat G, de Lamballerie X, Chatel-Chaix L, Milligan GN, Beasley DWC, Bourne N, Barrett ADT, Marchand A, Jonckers THM, Raboisson P, Simmen K, Chaltin P, Bartenschlager R, Bogers WM, Neyts J, Van Loock M (2023) Blocking NS3-NS4B interaction inhibits dengue virus in non-human primates. *Nature* 615(7953):678-686.

Gomez-Suaga P, Paillusson S, Stoica R, Noble W, Hanger DP, Miller CCJ (2017) The ER-Mitochondria Tethering Complex VAPB-PTPIP51 Regulates Autophagy. *Curr Biol* 27(3):371-385.

Gou H, Zhao M, Xu H, Yuan J, He W, Zhu M, Ding H, Yi L, Chen J (2017) CSFV induced mitochondrial fission and mitophagy to inhibit apoptosis. *Oncotarget* 8(24):39382-39400.

Grabowski JM, Tsetsarkin KA, Long D, Scott DP, Rosenke R, Schwan TG, Mlera L, Offerdahl DK, Pletnev AG, Bloom ME (2017) Flavivirus Infection of Ixodes scapularis (Black-Legged Tick) Ex Vivo Organotypic Cultures and Applications for Disease Control. *mBio* 8(4).

Granata S, Dalla Gassa A, Tomei P, Lupo A, Zaza G (2015) Mitochondria: a new therapeutic target in chronic kidney disease. *Nutr Metab (Lond)* 12:49.

Grant D, Tan GK, Qing M, Ng JK, Yip A, Zou G, Xie X, Yuan Z, Schreiber MJ, Schul W, Shi PY, Alonso S (2011) A single amino acid in nonstructural protein NS4B confers virulence to dengue virus in AG129 mice through enhancement of viral RNA synthesis. *J Virol* 85(15):7775-7787.

Grief C, Galler R, Cortes LM, Barth OM (1997) Intracellular localisation of dengue-2 RNA in mosquito cell culture using electron microscopic in situ hybridisation. *Arch Virol* 142(12):2347-2357.

Gubler DJ (2011) Dengue, Urbanization and Globalization: The Unholy Trinity of the 21(st) Century. *Trop Med Health* 39(4 Suppl):3-11.

Guo Y, Gu R, Gan D, Hu F, Li G, Xu G (2020) Mitochondrial DNA drives noncanonical inflammation activation via cGAS-STING signaling pathway in retinal microvascular endothelial cells. *Cell Commun Signal* 18(1):172.

Guy B, Noriega F, Ochiai RL, L'Azou M, Delore V, Skipetrova A, Verdier F, Coudeville L, Savarino S, Jackson N (2017) A recombinant live attenuated tetravalent vaccine for the prevention of dengue. *Expert Rev Vaccines* 16(7):1-13.

Guzman A, Isturiz RE (2010) Update on the global spread of dengue. *Int J Antimicrob Agents* 36 Suppl 1:S40-42.

Hackett BA, Cherry S (2018) Flavivirus internalization is regulated by a size-dependent endocytic pathway. *Proc Natl Acad Sci U S A* 115(16):4246-4251.

Haddow AD, Schuh AJ, Yasuda CY, Kasper MR, Heang V, Huy R, Guzman H, Tesh RB, Weaver SC (2012) Genetic characterization of Zika virus strains: geographic expansion of the Asian lineage. *PLoS Negl Trop Dis* 6(2):e1477.

Hadinegoro SR, Arredondo-Garcia JL, Capeding MR, Deseda C, Chotpitayasunondh T, Dietze R, Muhammad Ismail HI, Reynales H, Limkittikul K, Rivera-Medina DM, Tran HN, Bouckenooghe A, Chansinghakul D, Cortes M, Fanouillere K, Forrat R, Frago C, Gailhardou S, Jackson N, Noriega F, Plennevaux E, Wartel TA, Zambrano B, Saville M,

Group C-TDVW (2015) Efficacy and Long-Term Safety of a Dengue Vaccine in Regions of Endemic Disease. *N Engl J Med* 373(13):1195-1206.
Halstead SB (2003) Neutralization and antibody-dependent enhancement of dengue viruses. *Adv Virus Res* 60:421-467.
Halstead SB, Nimmannitya S, Yamarat C, Russell PK (1967) Hemorrhagic fever in Thailand; recent knowledge regarding etiology. *Jpn J Med Sci Biol* 20 Suppl:96-103.
Hamasaki M, Furuta N, Matsuda A, Nezu A, Yamamoto A, Fujita N, Oomori H, Noda T, Haraguchi T, Hiraoka Y, Amano A, Yoshimori T (2013) Autophagosomes form at ER-mitochondria contact sites. *Nature* 495(7441):389-393.
Hamel R, Dejarnac O, Wichit S, Ekchariyawat P, Neyret A, Luplertlop N, Perera-Lecoin M, Surasombatpattana P, Talignani L, Thomas F, Cao-Lormeau VM, Choumet V, Briant L, Despres P, Amara A, Yssel H, Misse D (2015) Biology of Zika Virus Infection in Human Skin Cells. *J Virol* 89(17):8880-8896.
Hamilton AJ, Baulcombe DC (1999) A species of small antisense RNA in posttranscriptional gene silencing in plants. *Science* 286(5441):950-952.
Hardy S, Jackson B, Goodbourn S, Seago J (2020) Classical swine fever virus N(pro) antagonises IRF3 to prevent IFN-independent TLR3 and RIG-I-mediated apoptosis. *J Virol* 95(9).
Hartmann J, Verkhratsky A (1998) Relations between intracellular Ca2+ stores and store-operated Ca2+ entry in primary cultured human glioblastoma cells. *J Physiol* 513 (Pt 2):411-424.
Heaton NS, Perera R, Berger KL, Khadka S, Lacount DJ, Kuhn RJ, Randall G (2010a) Dengue virus nonstructural protein 3 redistributes fatty acid synthase to sites of viral replication and increases cellular fatty acid synthesis. *Proc Natl Acad Sci U S A* 107(40):17345-17350.
Heaton NS, Randall G (2010b) Dengue virus-induced autophagy regulates lipid metabolism. *Cell Host Microbe* 8(5):422-432.
Heinz FX, Stiasny K (2012) Flaviviruses and their antigenic structure. *J Clin Virol* 55(4):289-295.
Helle SC, Kanfer G, Kolar K, Lang A, Michel AH, Kornmann B (2013) Organization and function of membrane contact sites. *Biochim Biophys Acta* 1833(11):2526-2541.
Hemmings BA, Restuccia DF (2012) PI3K-PKB/Akt pathway. *Cold Spring Harb Perspect Biol* 4(9):a011189.
Henne WM (2019) Spastin joins LDs and peroxisomes in the interorganelle contact ballet. *J Cell Biol* 218(8):2439-2441.
Hernandez-Morales I, Geluykens P, Clynhens M, Strijbos R, Goethals O, Megens S, Verheyen N, Last S, McGowan D, Coesemans E, De Boeck B, Stoops B, Devogelaere B, Pauwels F, Vandyck K, Berke JM, Raboisson P, Simmen K, Lory P, Van Loock M (2017) Characterization of a dengue NS4B inhibitor originating from an HCV small molecule library. *Antiviral Res* 147:149-158.
Hirabayashi Y, Kwon SK, Paek H, Pernice WM, Paul MA, Lee J, Erfani P, Raczkowski A, Petrey DS, Pon LA, Polleux F (2017) ER-mitochondria tethering by PDZD8 regulates Ca(2+) dynamics in mammalian neurons. *Science* 358(6363):623-630.
Hoke CH, Nisalak A, Sangawhipa N, Jatanasen S, Laorakapongse T, Innis BL, Kotchasenee S, Gingrich JB, Latendresse J, Fukai K, et al. (1988) Protection against Japanese encephalitis by inactivated vaccines. *N Engl J Med* 319(10):608-614.
Holmes EC, Twiddy SS (2003) The origin, emergence and evolutionary genetics of dengue virus. *Infect Genet Evol* 3(1):19-28.
Holze C, Michaudel C, Mackowiak C, Haas DA, Benda C, Hubel P, Pennemann FL, Schnepf D, Wettmarshausen J, Braun M, Leung DW, Amarasinghe GK, Perocchi F, Staeheli P, Ryffel B, Pichlmair A (2018) Oxeiptosis, a ROS-induced caspase-independent apoptosis-like cell-death pathway. *Nat Immunol* 19(2):130-140.

Horner SM, Liu HM, Park HS, Briley J, Gale M, Jr. (2011) Mitochondrial-associated endoplasmic reticulum membranes (MAM) form innate immune synapses and are targeted by hepatitis C virus. *Proc Natl Acad Sci U S A* 108(35):14590-14595.

Horner SM, Wilkins C, Badil S, Iskarpatyoti J, Gale M, Jr. (2015) Proteomic analysis of mitochondrial-associated ER membranes (MAM) during RNA virus infection reveals dynamic changes in protein and organelle trafficking. *PLoS One* 10(3):e0117963.

Hossain MG, Akter S, Ohsaki E, Ueda K (2020) Impact of the Interaction of Hepatitis B Virus with Mitochondria and Associated Proteins. *Viruses* 12(2).

Hotta S (1952) Experimental studies on dengue. I. Isolation, identification and modification of the virus. *J Infect Dis* 90(1):1-9.

Houtkooper RH, Vaz FM (2008) Cardiolipin, the heart of mitochondrial metabolism. *Cell Mol Life Sci* 65(16):2493-2506.

Hsu TC, Chow LP, Wei HY, Chen CL, Hsu ST (1971) A controlled field trial for an evaluation of effectiveness of mouse-brain Japanese encephalitis vaccine. *Taiwan Yi Xue Hui Za Zhi* 70(2):55-62.

Huang CY, Kinney RM, Livengood JA, Bolling B, Arguello JJ, Luy BE, Silengo SJ, Boroughs KL, Stovall JL, Kalanidhi AP, Brault AC, Osorio JE, Stinchcomb DT (2013) Genetic and phenotypic characterization of manufacturing seeds for a tetravalent dengue vaccine (DENVax). *PLoS Negl Trop Dis* 7(5):e2243.

Huang WC, Abraham R, Shim BS, Choe H, Page DT (2016) Zika virus infection during the period of maximal brain growth causes microcephaly and corticospinal neuron apoptosis in wild type mice. *Sci Rep* 6:34793.

Hulea L, Gravel SP, Morita M, Cargnello M, Uchenunu O, Im YK, Lehuede C, Ma EH, Leibovitch M, McLaughlan S, Blouin MJ, Parisotto M, Papavasiliou V, Lavoie C, Larsson O, Ohh M, Ferreira T, Greenwood C, Bridon G, Avizonis D, Ferbeyre G, Siegel P, Jones RG, Muller W, Ursini-Siegel J, St-Pierre J, Pollak M, Topisirovic I (2018) Translational and HIF-1alpha-Dependent Metabolic Reprogramming Underpin Metabolic Plasticity and Responses to Kinase Inhibitors and Biguanides. *Cell Metab* 28(6):817-832 e818.

Hung V, Lam SS, Udeshi ND, Svinkina T, Guzman G, Mootha VK, Carr SA, Ting AY (2019) Correction: Proteomic mapping of cytosol-facing outer mitochondrial and ER membranes in living human cells by proximity biotinylation. *Elife* 8.

Ingerman E, Perkins EM, Marino M, Mears JA, McCaffery JM, Hinshaw JE, Nunnari J (2005) Dnm1 forms spirals that are structurally tailored to fit mitochondria. *J Cell Biol* 170(7):1021-1027.

Ishihara N, Eura Y, Mihara K (2004) Mitofusin 1 and 2 play distinct roles in mitochondrial fusion reactions via GTPase activity. *J Cell Sci* 117(Pt 26):6535-6546.

Ishikawa H, Ma Z, Barber GN (2009) STING regulates intracellular DNA-mediated, type I interferon-dependent innate immunity. *Nature* 461(7265):788-792.

Ishikawa T, Yamanaka A, Konishi E (2014) A review of successful flavivirus vaccines and the problems with those flaviviruses for which vaccines are not yet available. *Vaccine* 32(12):1326-1337.

Issur M, Geiss BJ, Bougie I, Picard-Jean F, Despins S, Mayette J, Hobdey SE, Bisaillon M (2009) The flavivirus NS5 protein is a true RNA guanylyltransferase that catalyzes a two-step reaction to form the RNA cap structure. *RNA* 15(12):2340-2350.

Iwamura T, Guzman-Holst A, Murray KA (2020) Accelerating invasion potential of disease vector Aedes aegypti under climate change. *Nat Commun* 11(1):2130.

Jackson LA, Rupp R, Papadimitriou A, Wallace D, Raanan M, Moss KJ (2018) A phase 1 study of safety and immunogenicity following intradermal administration of a tetravalent dengue vaccine candidate. *Vaccine* 36(27):3976-3983.

Jacobs JL, Coyne CB (2013) Mechanisms of MAVS regulation at the mitochondrial membrane. *J Mol Biol* 425(24):5009-5019.

Jastroch M, Divakaruni AS, Mookerjee S, Treberg JR, Brand MD (2010) Mitochondrial proton and electron leaks. *Essays Biochem* 47:53-67.
Jayaraman T, Marks AR (1997) T cells deficient in inositol 1,4,5-trisphosphate receptor are resistant to apoptosis. *Mol Cell Biol* 17(6):3005-3012.
Jenner A, Pena-Blanco A, Salvador-Gallego R, Ugarte-Uribe B, Zollo C, Ganief T, Bierlmeier J, Mund M, Lee JE, Ries J, Schwarzer D, Macek B, Garcia-Saez AJ (2022) DRP1 interacts directly with BAX to induce its activation and apoptosis. *EMBO J* 41(8):e108587.
Ji W, Luo G (2020) Zika virus NS5 nuclear accumulation is protective of protein degradation and is required for viral RNA replication. *Virology* 541:124-135.
Jiang R, Ye J, Zhu B, Song Y, Chen H, Cao S (2014) Roles of TLR3 and RIG-I in mediating the inflammatory response in mouse microglia following Japanese encephalitis virus infection. *J Immunol Res* 2014:787023.
Jin SM, Lazarou M, Wang C, Kane LA, Narendra DP, Youle RJ (2010) Mitochondrial membrane potential regulates PINK1 import and proteolytic destabilization by PARL. *J Cell Biol* 191(5):933-942.
Jitobaom K, Tongluan N, Smith DR (2016) Involvement of voltage-dependent anion channel (VDAC) in dengue infection. *Sci Rep* 6:35753.
Jonckheere AI, Smeitink JA, Rodenburg RJ (2012) Mitochondrial ATP synthase: architecture, function and pathology. *J Inherit Metab Dis* 35(2):211-225.
Jordan TX, Randall G (2017) Dengue Virus Activates the AMP Kinase-mTOR Axis To Stimulate a Proviral Lipophagy. *J Virol* 91(11).
Julander JG, Siddharthan V, Evans J, Taylor R, Tolbert K, Apuli C, Stewart J, Collins P, Gebre M, Neilson S, Van Wettere A, Lee YM, Sheridan WP, Morrey JD, Babu YS (2017) Efficacy of the broad-spectrum antiviral compound BCX4430 against Zika virus in cell culture and in a mouse model. *Antiviral Res* 137:14-22.
Jung GS, Jeon JH, Choi YK, Jang SY, Park SY, Kim SW, Byun JK, Kim MK, Lee S, Shin EC, Lee IK, Kang YN, Park KG (2016) Pyruvate dehydrogenase kinase regulates hepatitis C virus replication. *Sci Rep* 6:30846.
Jungmann P, Pires P, Araujo Junior E (2017) Early insights into Zika's microcephaly physiopathology from the epicenter of the outbreak: teratogenic apoptosis in the central nervous system. *Acta Obstet Gynecol Scand* 96(9):1039-1044.
Junjhon J, Pennington JG, Edwards TJ, Perera R, Lanman J, Kuhn RJ (2014) Ultrastructural characterization and three-dimensional architecture of replication sites in dengue virus-infected mosquito cells. *J Virol* 88(9):4687-4697.
Kagan VE, Tyurin VA, Jiang J, Tyurina YY, Ritov VB, Amoscato AA, Osipov AN, Belikova NA, Kapralov AA, Kini V, Vlasova, II, Zhao Q, Zou M, Di P, Svistunenko DA, Kurnikov IV, Borisenko GG (2005) Cytochrome c acts as a cardiolipin oxygenase required for release of proapoptotic factors. *Nat Chem Biol* 1(4):223-232.
Kaiser JA, Barrett ADT (2019) Twenty Years of Progress Toward West Nile Virus Vaccine Development. *Viruses* 11(9).
Kanesa-thasan N, Smucny JJ, Hoke CH, Marks DH, Konishi E, Kurane I, Tang DB, Vaughn DW, Mason PW, Shope RE (2000) Safety and immunogenicity of NYVAC-JEV and ALVAC-JEV attenuated recombinant Japanese encephalitis virus--poxvirus vaccines in vaccinia-nonimmune and vaccinia-immune humans. *Vaccine* 19(4-5):483-491.
Kaptein SJF, Goethals O, Kiemel D, Marchand A, Kesteleyn B, Bonfanti JF, Bardiot D, Stoops B, Jonckers THM, Dallmeier K, Geluykens P, Thys K, Crabbe M, Chatel-Chaix L, Munster M, Querat G, Touret F, de Lamballerie X, Raboisson P, Simmen K, Chaltin P, Bartenschlager R, Van Loock M, Neyts J (2021) Publisher Correction: A pan-serotype dengue virus inhibitor targeting the NS3-NS4B interaction. *Nature* 599(7883):E2.

Karpf AR, Lenches E, Strauss EG, Strauss JH, Brown DT (1997) Superinfection exclusion of alphaviruses in three mosquito cell lines persistently infected with Sindbis virus. *J Virol* 71(9):7119-7123.

Kato H, Takeuchi O, Sato S, Yoneyama M, Yamamoto M, Matsui K, Uematsu S, Jung A, Kawai T, Ishii KJ, Yamaguchi O, Otsu K, Tsujimura T, Koh CS, Reis e Sousa C, Matsuura Y, Fujita T, Akira S (2006) Differential roles of MDA5 and RIG-I helicases in the recognition of RNA viruses. *Nature* 441(7089):101-105.

Kelly EP, Puri B, Sun W, Falgout B (2010) Identification of mutations in a candidate dengue 4 vaccine strain 341750 PDK20 and construction of a full-length cDNA clone of the PDK20 vaccine candidate. *Vaccine* 28(17):3030-3037.

Kern P, Balzer NR, Blank N, Cygon C, Wunderling K, Bender F, Frolov A, Sowa JP, Bonaguro L, Ulas T, Homrich M, Kiermaier E, Thiele C, Schultze JL, Canbay A, Bauer R, Mass E (2021) Creld2 function during unfolded protein response is essential for liver metabolism homeostasis. *FASEB J* 35(10):e21939.

Ketkar H, Yang L, Wormser GP, Wang P (2019) Lack of efficacy of ivermectin for prevention of a lethal Zika virus infection in a murine system. *Diagn Microbiol Infect Dis* 95(1):38-40.

Khan AA, Soloski MJ, Sharp AH, Schilling G, Sabatini DM, Li SH, Ross CA, Snyder SH (1996) Lymphocyte apoptosis: mediation by increased type 3 inositol 1,4,5-trisphosphate receptor. *Science* 273(5274):503-507.

Khan M, Syed GH, Kim SJ, Siddiqui A (2016) Hepatitis B Virus-Induced Parkin-Dependent Recruitment of Linear Ubiquitin Assembly Complex (LUBAC) to Mitochondria and Attenuation of Innate Immunity. *Plos Pathogens* 12(6):e1005693.

Khongwichit S, Sornjai W, Jitobaom K, Greenwood M, Greenwood MP, Hitakarun A, Wikan N, Murphy D, Smith DR (2021) A functional interaction between GRP78 and Zika virus E protein. *Sci Rep* 11(1):393.

Khunchai S, Junking M, Suttitheptumrong A, Yasamut U, Sawasdee N, Netsawang J, Morchang A, Chaowalit P, Noisakran S, Yenchitsomanus PT, Limjindaporn T (2012) Interaction of dengue virus nonstructural protein 5 with Daxx modulates RANTES production. *Biochem Biophys Res Commun* 423(2):398-403.

Kim CR, Counotte M, Bernstein K, Deal C, Mayaud P, Low N, Broutet N, Sexual Transmission of Zika virus Expert Meeting p (2018) Investigating the sexual transmission of Zika virus. *Lancet Glob Health* 6(1):e24-e25.

Kim DS, Houillon G, Jang GC, Cha SH, Choi SH, Lee J, Kim HM, Kim JH, Kang JH, Kim JH, Kim KH, Kim HS, Bang J, Naimi Z, Bosch-Castells V, Boaz M, Bouckenooghe A (2014a) A randomized study of the immunogenicity and safety of Japanese encephalitis chimeric virus vaccine (JE-CV) in comparison with SA14-14-2 vaccine in children in the Republic of Korea. *Hum Vaccin Immunother* 10(9):2656-2663.

Kim H, Esser L, Hossain MB, Xia D, Yu C-A, Rizo J, van der Helm D, Deisenhofer J (1999) Structure of Antimycin A1, a Specific Electron Transfer Inhibitor of Ubiquinol−Cytochrome c Oxidoreductase. *Journal of the American Chemical Society* 121(20):4902-4903.

Kim SJ, Khan M, Quan J, Till A, Subramani S, Siddiqui A (2013) Hepatitis B virus disrupts mitochondrial dynamics: induces fission and mitophagy to attenuate apoptosis. *Plos Pathogens* 9(12):e1003722.

Kim SJ, Syed GH, Khan M, Chiu WW, Sohail MA, Gish RG, Siddiqui A (2014b) Hepatitis C virus triggers mitochondrial fission and attenuates apoptosis to promote viral persistence. *Proc Natl Acad Sci U S A* 111(17):6413-6418.

Kirkpatrick BD, Durbin AP, Pierce KK, Carmolli MP, Tibery CM, Grier PL, Hynes N, Diehl SA, Elwood D, Jarvis AP, Sabundayo BP, Lyon CE, Larsson CJ, Jo M, Lovchik JM, Luke CJ, Walsh MC, Fraser EA, Subbarao K, Whitehead SS (2015) Robust and Balanced Immune Responses to All 4 Dengue Virus Serotypes Following Administration of a Single Dose of

a Live Attenuated Tetravalent Dengue Vaccine to Healthy, Flavivirus-Naive Adults. *J Infect Dis* 212(5):702-710.
Kirkpatrick BD, Whitehead SS, Pierce KK, Tibery CM, Grier PL, Hynes NA, Larsson CJ, Sabundayo BP, Talaat KR, Janiak A, Carmolli MP, Luke CJ, Diehl SA, Durbin AP (2016) The live attenuated dengue vaccine TV003 elicits complete protection against dengue in a human challenge model. *Sci Transl Med* 8(330):330ra336.
Kittler J (2015) Regulation of mitochondrial trafficking, function and quality control by the mitochondrial GTPases Miro1 and Miro2. *Springerplus* 4(Suppl 1):L33.
Kloska A, Wesierska M, Malinowska M, Gabig-Ciminska M, Jakobkiewicz-Banecka J (2020) Lipophagy and Lipolysis Status in Lipid Storage and Lipid Metabolism Diseases. *Int J Mol Sci* 21(17).
Ko KK, Igarashi A, Fukai K (1979) Electron microscopic observations on Aedes albopictus cells infected with dengue viruses. *Arch Virol* 62(1):41-52.
Koh C, Islam MN, Ye YH, Chotiwan N, Graham B, Belisle JT, Kouremenos KA, Dayalan S, Tull DL, Klatt S, Perera R, McGraw EA (2020) Dengue virus dominates lipid metabolism modulations in Wolbachia-coinfected Aedes aegypti. *Commun Biol* 3(1):518.
Kornmann B, Currie E, Collins SR, Schuldiner M, Nunnari J, Weissman JS, Walter P (2009) An ER-mitochondria tethering complex revealed by a synthetic biology screen. *Science* 325(5939):477-481.
Kornmann B, Osman C, Walter P (2011) The conserved GTPase Gem1 regulates endoplasmic reticulum-mitochondria connections. *Proc Natl Acad Sci U S A* 108(34):14151-14156.
Koshiba T, Detmer SA, Kaiser JT, Chen H, McCaffery JM, Chan DC (2004) Structural basis of mitochondrial tethering by mitofusin complexes. *Science* 305(5685):858-862.
Kozik P, Hodson NA, Sahlender DA, Simecek N, Soromani C, Wu J, Collinson LM, Robinson MS (2013) A human genome-wide screen for regulators of clathrin-coated vesicle formation reveals an unexpected role for the V-ATPase. *Nat Cell Biol* 15(1):50-60.
Kraemer MU, Sinka ME, Duda KA, Mylne AQ, Shearer FM, Barker CM, Moore CG, Carvalho RG, Coelho GE, Van Bortel W, Hendrickx G, Schaffner F, Elyazar IR, Teng HJ, Brady OJ, Messina JP, Pigott DM, Scott TW, Smith DL, Wint GR, Golding N, Hay SI (2015) The global distribution of the arbovirus vectors Aedes aegypti and Ae. albopictus. *Elife* 4:e08347.
Kroemer G, Marino G, Levine B (2010) Autophagy and the integrated stress response. *Mol Cell* 40(2):280-293.
Kroschewski H, Lim SP, Butcher RE, Yap TL, Lescar J, Wright PJ, Vasudevan SG, Davidson AD (2008) Mutagenesis of the dengue virus type 2 NS5 methyltransferase domain. *J Biol Chem* 283(28):19410-19421.
Kuhn RJ, Zhang W, Rossmann MG, Pletnev SV, Corver J, Lenches E, Jones CT, Mukhopadhyay S, Chipman PR, Strauss EG, Baker TS, Strauss JH (2002) Structure of dengue virus: implications for flavivirus organization, maturation, and fusion. *Cell* 108(5):717-725.
Kumar A, Singh S, Singh P, Giri S (2019) Activation of AMPK restricts Zika virus replication in endothelial cells by potentiating antiviral response and inhibiting viral-induced glycolysis. *The Journal of Immunology* 202(1 Supplement):127.119-127.119.
Kurane I, Takasaki T (2000) Immunogenicity and protective efficacy of the current inactivated Japanese encephalitis vaccine against different Japanese encephalitis virus strains. *Vaccine* 18 Suppl 2:33-35.
La Ruche G, Souares Y, Armengaud A, Peloux-Petiot F, Delaunay P, Despres P, Lenglet A, Jourdain F, Leparc-Goffart I, Charlet F, Ollier L, Mantey K, Mollet T, Fournier JP, Torrents R, Leitmeyer K, Hilairet P, Zeller H, Van Bortel W, Dejour-Salamanca D, Grandadam M, Gastellu-Etchegorry M (2010) First two autochthonous dengue virus infections in metropolitan France, September 2010. *Euro Surveill* 15(39):19676.

Lafourcade C, Sobo K, Kieffer-Jaquinod S, Garin J, van der Goot FG (2008) Regulation of the V-ATPase along the endocytic pathway occurs through reversible subunit association and membrane localization. *PLoS One* 3(7):e2758.

Lahav G (2008) Oscillations by the p53-Mdm2 feedback loop. *Adv Exp Med Biol* 641:28-38.

Lai JH, Wang MY, Huang CY, Wu CH, Hung LF, Yang CY, Ke PY, Luo SF, Liu SJ, Ho LJ (2018) Infection with the dengue RNA virus activates TLR9 signaling in human dendritic cells. *EMBO Rep* 19(8).

Lambert AJ, Brand MD (2004) Inhibitors of the quinone-binding site allow rapid superoxide production from mitochondrial NADH:ubiquinone oxidoreductase (complex I). *J Biol Chem* 279(38):39414-39420.

Lanciotti RS, Lambert AJ, Holodniy M, Saavedra S, Signor Ldel C (2016) Phylogeny of Zika Virus in Western Hemisphere, 2015. *Emerg Infect Dis* 22(5):933-935.

Lazarou M, Sliter DA, Kane LA, Sarraf SA, Wang C, Burman JL, Sideris DP, Fogel AI, Youle RJ (2015) The ubiquitin kinase PINK1 recruits autophagy receptors to induce mitophagy. *Nature* 524(7565):309-314.

Lazzarini L, Barzon L, Foglia F, Manfrin V, Pacenti M, Pavan G, Rassu M, Capelli G, Montarsi F, Martini S, Zanella F, Padovan MT, Russo F, Gobbi F (2020) First autochthonous dengue outbreak in Italy, August 2020. *Euro Surveill* 25(36).

Leaman DW, Chawla-Sarkar M, Vyas K, Reheman M, Tamai K, Toji S, Borden EC (2002) Identification of X-linked inhibitor of apoptosis-associated factor-1 as an interferon-stimulated gene that augments TRAIL Apo2L-induced apoptosis. *J Biol Chem* 277(32):28504-28511.

Ledur PF, Karmirian K, Pedrosa C, Souza LRQ, Assis-de-Lemos G, Martins TM, Ferreira J, de Azevedo Reis GF, Silva ES, Silva D, Salerno JA, Ornelas IM, Devalle S, Madeiro da Costa RF, Goto-Silva L, Higa LM, Melo A, Tanuri A, Chimelli L, Murata MM, Garcez PP, Filippi-Chiela EC, Galina A, Borges HL, Rehen SK (2020) Zika virus infection leads to mitochondrial failure, oxidative stress and DNA damage in human iPSC-derived astrocytes. *Sci Rep* 10(1):1218.

Lee CJ, Liao CL, Lin YL (2005) Flavivirus activates phosphatidylinositol 3-kinase signaling to block caspase-dependent apoptotic cell death at the early stage of virus infection. *J Virol* 79(13):8388-8399.

Lee KS, Huh S, Lee S, Wu Z, Kim AK, Kang HY, Lu B (2018) Altered ER-mitochondria contact impacts mitochondria calcium homeostasis and contributes to neurodegeneration in vivo in disease models. *Proc Natl Acad Sci U S A* 115(38):E8844-E8853.

Lee S, Lee KS, Huh S, Liu S, Lee DY, Hong SH, Yu K, Lu B (2016) Polo Kinase Phosphorylates Miro to Control ER-Mitochondria Contact Sites and Mitochondrial Ca(2+) Homeostasis in Neural Stem Cell Development. *Dev Cell* 37(2):174-189.

Lee YJ, Jeong SY, Karbowski M, Smith CL, Youle RJ (2004) Roles of the mammalian mitochondrial fission and fusion mediators Fis1, Drp1, and Opa1 in apoptosis. *Mol Biol Cell* 15(11):5001-5011.

Legesse-Miller A, Massol RH, Kirchhausen T (2003) Constriction and Dnm1p recruitment are distinct processes in mitochondrial fission. *Mol Biol Cell* 14(5):1953-1963.

Leier HC, Weinstein JB, Kyle JE, Lee JY, Bramer LM, Stratton KG, Kempthorne D, Navratil AR, Tafesse EG, Hornemann T, Messer WB, Dennis EA, Metz TO, Barklis E, Tafesse FG (2020) A global lipid map defines a network essential for Zika virus replication. *Nat Commun* 11(1):3652.

Li C, Deng YQ, Wang S, Ma F, Aliyari R, Huang XY, Zhang NN, Watanabe M, Dong HL, Liu P, Li XF, Ye Q, Tian M, Hong S, Fan J, Zhao H, Li L, Vishlaghi N, Buth JE, Au C, Liu Y, Lu N, Du P, Qin FX, Zhang B, Gong D, Dai X, Sun R, Novitch BG, Xu Z, Qin CF, Cheng G (2017a) 25-Hydroxycholesterol Protects Host against Zika Virus Infection and Its Associated Microcephaly in a Mouse Model. *Immunity* 46(3):446-456.

Li C, Xu D, Ye Q, Hong S, Jiang Y, Liu X, Zhang N, Shi L, Qin CF, Xu Z (2016) Zika Virus Disrupts Neural Progenitor Development and Leads to Microcephaly in Mice. *Cell Stem Cell* 19(5):672.

Li C, Zhu X, Ji X, Quanquin N, Deng YQ, Tian M, Aliyari R, Zuo X, Yuan L, Afridi SK, Li XF, Jung JU, Nielsen-Saines K, Qin FX, Qin CF, Xu Z, Cheng G (2017b) Chloroquine, a FDA-approved Drug, Prevents Zika Virus Infection and its Associated Congenital Microcephaly in Mice. *EBioMedicine* 24:189-194.

Li PC, Jang J, Hsia CY, Groomes PV, Lian W, de Wispelaere M, Pitts JD, Wang J, Kwiatkowski N, Gray NS, Yang PL (2019) Small Molecules Targeting the Flavivirus E Protein with Broad-Spectrum Activity and Antiviral Efficacy in Vivo. *ACS Infect Dis* 5(3):460-472.

Li W, Brinton MA (2001) The 3' stem loop of the West Nile virus genomic RNA can suppress translation of chimeric mRNAs. *Virology* 287(1):49-61.

Li XB, Gu JD, Zhou QH (2015a) Review of aerobic glycolysis and its key enzymes - new targets for lung cancer therapy. *Thorac Cancer* 6(1):17-24.

Li XD, Ye HQ, Deng CL, Liu SQ, Zhang HL, Shang BD, Shi PY, Yuan ZM, Zhang B (2015b) Genetic interaction between NS4A and NS4B for replication of Japanese encephalitis virus. *J Gen Virol* 96(Pt 6):1264-1275.

Liang Q, Luo Z, Zeng J, Chen W, Foo SS, Lee SA, Ge J, Wang S, Goldman SA, Zlokovic BV, Zhao Z, Jung JU (2016) Zika Virus NS4A and NS4B Proteins Deregulate Akt-mTOR Signaling in Human Fetal Neural Stem Cells to Inhibit Neurogenesis and Induce Autophagy. *Cell Stem Cell* 19(5):663-671.

Liesa M, Palacin M, Zorzano A (2009) Mitochondrial dynamics in mammalian health and disease. *Physiol Rev* 89(3):799-845.

Lin DL, Cherepanova NA, Bozzacco L, MacDonald MR, Gilmore R, Tai AW (2017a) Dengue Virus Hijacks a Noncanonical Oxidoreductase Function of a Cellular Oligosaccharyltransferase Complex. *mBio* 8(4).

Lin MY, Wang YL, Wu WL, Wolseley V, Tsai MT, Radic V, Thornton ME, Grubbs BH, Chow RH, Huang IC (2017b) Zika Virus Infects Intermediate Progenitor Cells and Post-mitotic Committed Neurons in Human Fetal Brain Tissues. *Sci Rep* 7(1):14883.

Lindsey NP, Schroeder BA, Miller ER, Braun MM, Hinckley AF, Marano N, Slade BA, Barnett ED, Brunette GW, Horan K, Staples JE, Kozarsky PE, Hayes EB (2008) Adverse event reports following yellow fever vaccination. *Vaccine* 26(48):6077-6082.

Liu-Helmersson J, Quam M, Wilder-Smith A, Stenlund H, Ebi K, Massad E, Rocklov J (2016) Climate Change and Aedes Vectors: 21st Century Projections for Dengue Transmission in Europe. *EBioMedicine* 7:267-277.

Liu HM, Loo YM, Horner SM, Zornetzer GA, Katze MG, Gale M, Jr. (2012) The mitochondrial targeting chaperone 14-3-3epsilon regulates a RIG-I translocon that mediates membrane association and innate antiviral immunity. *Cell Host Microbe* 11(5):528-537.

Liu WJ, Wang XJ, Clark DC, Lobigs M, Hall RA, Khromykh AA (2006) A single amino acid substitution in the West Nile virus nonstructural protein NS2A disables its ability to inhibit alpha/beta interferon induction and attenuates virus virulence in mice. *J Virol* 80(5):2396-2404.

Liu Y, Liu H, Zou J, Zhang B, Yuan Z (2014) Dengue virus subgenomic RNA induces apoptosis through the Bcl-2-mediated PI3k/Akt signaling pathway. *Virology* 448:15-25.

Liu ZY, Shi WF, Qin CF (2019) The evolution of Zika virus from Asia to the Americas. *Nat Rev Microbiol* 17(3):131-139.

Long X, Li Y, Qi Y, Xu J, Wang Z, Zhang X, Zhang D, Zhang L, Huang J (2013) XAF1 contributes to dengue virus-induced apoptosis in vascular endothelial cells. *FASEB J* 27(3):1062-1073.

Loo YM, Gale M, Jr. (2011) Immune signaling by RIG-I-like receptors. *Immunity* 34(5):680-692.

Lopez-Camacho C, De Lorenzo G, Slon-Campos JL, Dowall S, Abbink P, Larocca RA, Kim YC, Poggianella M, Graham V, Findlay-Wilson S, Rayner E, Carmichael J, Dejnirattisai W, Boyd M, Hewson R, Mongkolsapaya J, Screaton GR, Barouch DH, Burrone OR, Patel AH, Reyes-Sandoval A (2020) Immunogenicity and Efficacy of Zika Virus Envelope Domain III in DNA, Protein, and ChAdOx1 Adenoviral-Vectored Vaccines. *Vaccines (Basel)* 8(2).

Lopez-Medina E, Biswal S, Saez-Llorens X, Borja-Tabora C, Bravo L, Sirivichayakul C, Vargas LM, Alera MT, Velasquez H, Reynales H, Rivera L, Watanaveeradej V, Rodriguez-Arenales EJ, Yu D, Espinoza F, Dietze R, Fernando LK, Wickramasinghe P, Duarte Moreira E, Fernando AD, Gunasekera D, Luz K, da Cunha RV, Tricou V, Rauscher M, Liu M, LeFevre I, Wallace D, Kosalaraksa P, Borkowski A (2022) Efficacy of a Dengue Vaccine Candidate (TAK-003) in Healthy Children and Adolescents 2 Years after Vaccination. *J Infect Dis* 225(9):1521-1532.

Lu H, Zhan Y, Li X, Bai X, Yuan F, Ma L, Wang X, Xie M, Wu W, Chen Z (2021) Novel insights into the function of an N-terminal region of DENV2 NS4B for the optimal helicase activity of NS3. *Virus Res* 295:198318.

Lu ZY, Cheng MH, Yu CY, Lin YS, Yeh TM, Chen CL, Chen CC, Wan SW, Chang CP (2020) Dengue Nonstructural Protein 1 Maintains Autophagy through Retarding Caspase-Mediated Cleavage of Beclin-1. *Int J Mol Sci* 21(24).

Lutmer H, Beall M, Bolt B, Felton C, Germann L, Gildersleeve N, Goode AL, Hall A, Kyral S, Lu K, Nguyen CN, Nguyen P, Ragan L, Reiter D, Robenson K, Sanchez CK, Sanchez JP (2022) *Stamaril Yellow Fever Vaccine.* Precision vaccinationsp

Ma SM, Mao Q, Yi L, Zhao MQ, Chen JD (2019) Apoptosis, Autophagy, and Pyroptosis: Immune Escape Strategies for Persistent Infection and Pathogenesis of Classical Swine Fever Virus. *Pathogens* 8(4).

Ma X, Qian H, Chen A, Ni HM, Ding WX (2021) Perspectives on Mitochondria-ER and Mitochondria-Lipid Droplet Contact in Hepatocytes and Hepatic Lipid Metabolism. *Cells* 10(9).

Malisheni M, Khaiboullina SF, Rizvanov AA, Takah N, Murewanhema G, Bates M (2017) Clinical Efficacy, Safety, and Immunogenicity of a Live Attenuated Tetravalent Dengue Vaccine (CYD-TDV) in Children: A Systematic Review with Meta-analysis. *Front Immunol* 8:863.

Mann TZ, Haddad LB, Williams TR, Hills SL, Read JS, Dee DL, Dziuban EJ, Perez-Padilla J, Jamieson DJ, Honein MA, Shapiro-Mendoza CK (2018) Breast milk transmission of flaviviruses in the context of Zika virus: A systematic review. *Paediatr Perinat Epidemiol* 32(4):358-368.

Manokaran G, Finol E, Wang C, Gunaratne J, Bahl J, Ong EZ, Tan HC, Sessions OM, Ward AM, Gubler DJ, Harris E, Garcia-Blanco MA, Ooi EE (2015) Dengue subgenomic RNA binds TRIM25 to inhibit interferon expression for epidemiological fitness. *Science* 350(6257):217-221.

Manor U, Bartholomew S, Golani G, Christenson E, Kozlov M, Higgs H, Spudich J, Lippincott-Schwartz J (2015) A mitochondria-anchored isoform of the actin-nucleating spire protein regulates mitochondrial division. *Elife* 4.

Mansueto G, Armani A, Viscomi C, D'Orsi L, De Cegli R, Polishchuk EV, Lamperti C, Di Meo I, Romanello V, Marchet S, Saha PK, Zong H, Blaauw B, Solagna F, Tezze C, Grumati P, Bonaldo P, Pessin JE, Zeviani M, Sandri M, Ballabio A (2017) Transcription Factor EB Controls Metabolic Flexibility during Exercise. *Cell Metab* 25(1):182-196.

Marchette NJ, Garcia R, Rudnick A (1969) Isolation of Zika virus from Aedes aegypti mosquitoes in Malaysia. *Am J Trop Med Hyg* 18(3):411-415.

Martin-Acebes MA, Blazquez AB, Jimenez de Oya N, Escribano-Romero E, Saiz JC (2011) West Nile virus replication requires fatty acid synthesis but is independent on phosphatidylinositol-4-phosphate lipids. *PLoS One* 6(9):e24970.

Martin-Acebes MA, Merino-Ramos T, Blazquez AB, Casas J, Escribano-Romero E, Sobrino F, Saiz JC (2014) The composition of West Nile virus lipid envelope unveils a role of sphingolipid metabolism in flavivirus biogenesis. *J Virol* 88(20):12041-12054.

Martinot AJ, Abbink P, Afacan O, Prohl AK, Bronson R, Hecht JL, Borducchi EN, Larocca RA, Peterson RL, Rinaldi W, Ferguson M, Didier PJ, Weiss D, Lewis MG, De La Barrera RA, Yang E, Warfield SK, Barouch DH (2018) Fetal Neuropathology in Zika Virus-Infected Pregnant Female Rhesus Monkeys. *Cell* 173(5):1111-1122 e1110.

Matsuda N, Sato S, Shiba K, Okatsu K, Saisho K, Gautier CA, Sou YS, Saiki S, Kawajiri S, Sato F, Kimura M, Komatsu M, Hattori N, Tanaka K (2010) PINK1 stabilized by mitochondrial depolarization recruits Parkin to damaged mitochondria and activates latent Parkin for mitophagy. *J Cell Biol* 189(2):211-221.

Mazeaud C, Anton A, Pahmeier F, Sow AA, Cerikan B, Freppel W, Cortese M, Bartenschlager R, Chatel-Chaix L (2021) The Biogenesis of Dengue Virus Replication Organelles Requires the ATPase Activity of Valosin-Containing Protein. *Viruses* 13(10).

Mazeaud C, Freppel W, Chatel-Chaix L (2018) The Multiples Fates of the Flavivirus RNA Genome During Pathogenesis. *Front Genet* 9:595.

McBride HM, Neuspiel M, Wasiak S (2006) Mitochondria: more than just a powerhouse. *Curr Biol* 16(14):R551-560.

McLean JE, Wudzinska A, Datan E, Quaglino D, Zakeri Z (2011) Flavivirus NS4A-induced autophagy protects cells against death and enhances virus replication. *J Biol Chem* 286(25):22147-22159.

Mears JA, Lackner LL, Fang S, Ingerman E, Nunnari J, Hinshaw JE (2011) Conformational changes in Dnm1 support a contractile mechanism for mitochondrial fission. *Nat Struct Mol Biol* 18(1):20-26.

Medlock JM, Hansford KM, Versteirt V, Cull B, Kampen H, Fontenille D, Hendrickx G, Zeller H, Van Bortel W, Schaffner F (2015) An entomological review of invasive mosquitoes in Europe. *Bull Entomol Res* 105(6):637-663.

Meertens L, Carnec X, Lecoin MP, Ramdasi R, Guivel-Benhassine F, Lew E, Lemke G, Schwartz O, Amara A (2012) The TIM and TAM families of phosphatidylserine receptors mediate dengue virus entry. *Cell Host Microbe* 12(4):544-557.

Meissner C, Lorenz H, Weihofen A, Selkoe DJ, Lemberg MK (2011) The mitochondrial intramembrane protease PARL cleaves human Pink1 to regulate Pink1 trafficking. *J Neurochem* 117(5):856-867.

Melo CF, de Oliveira DN, Lima EO, Guerreiro TM, Esteves CZ, Beck RM, Padilla MA, Milanez GP, Arns CW, Proenca-Modena JL, Souza-Neto JA, Catharino RR (2016) A Lipidomics Approach in the Characterization of Zika-Infected Mosquito Cells: Potential Targets for Breaking the Transmission Cycle. *PLoS One* 11(10):e0164377.

Mesmin B, Bigay J, Moser von Filseck J, Lacas-Gervais S, Drin G, Antonny B (2013) A four-step cycle driven by PI(4)P hydrolysis directs sterol/PI(4)P exchange by the ER-Golgi tether OSBP. *Cell* 155(4):830-843.

Messina JP, Brady OJ, Scott TW, Zou C, Pigott DM, Duda KA, Bhatt S, Katzelnick L, Howes RE, Battle KE, Simmons CP, Hay SI (2014) Global spread of dengue virus types: mapping the 70 year history. *Trends Microbiol* 22(3):138-146.

Metz P, Chiramel A, Chatel-Chaix L, Alvisi G, Bankhead P, Mora-Rodriguez R, Long G, Hamacher-Brady A, Brady NR, Bartenschlager R (2015) Dengue Virus Inhibition of Autophagic Flux and Dependency of Viral Replication on Proteasomal Degradation of the Autophagy Receptor p62. *J Virol* 89(15):8026-8041.

Miller JD, van der Most RG, Akondy RS, Glidewell JT, Albott S, Masopust D, Murali-Krishna K, Mahar PL, Edupuganti S, Lalor S, Germon S, Del Rio C, Mulligan MJ, Staprans SI, Altman JD, Feinberg MB, Ahmed R (2008a) Human effector and memory CD8+ T cell responses to smallpox and yellow fever vaccines. *Immunity* 28(5):710-722.

Miller JL, de Wet BJ, Martinez-Pomares L, Radcliffe CM, Dwek RA, Rudd PM, Gordon S (2008b) The mannose receptor mediates dengue virus infection of macrophages. *Plos Pathogens* 4(2):e17.

Miller S, Kastner S, Krijnse-Locker J, Buhler S, Bartenschlager R (2007) The non-structural protein 4A of dengue virus is an integral membrane protein inducing membrane alterations in a 2K-regulated manner. *J Biol Chem* 282(12):8873-8882.

Miller S, Sparacio S, Bartenschlager R (2006) Subcellular localization and membrane topology of the Dengue virus type 2 Non-structural protein 4B. *J Biol Chem* 281(13):8854-8863.

Miner JJ, Diamond MS (2017) Zika Virus Pathogenesis and Tissue Tropism. *Cell Host Microbe* 21(2):134-142.

Miorin L, Romero-Brey I, Maiuri P, Hoppe S, Krijnse-Locker J, Bartenschlager R, Marcello A (2013) Three-dimensional architecture of tick-borne encephalitis virus replication sites and trafficking of the replicated RNA. *J Virol* 87(11):6469-6481.

Mizushima N (2018) A brief history of autophagy from cell biology to physiology and disease. *Nat Cell Biol* 20(5):521-527.

Modhiran N, Kalayanarooj S, Ubol S (2010) Subversion of innate defenses by the interplay between DENV and pre-existing enhancing antibodies: TLRs signaling collapse. *PLoS Negl Trop Dis* 4(12):e924.

Mohamed B, Mazeaud C, Baril M, Poirier D, Sow AA, Chatel-Chaix L, Titorenko V, Lamarre D (2020) Very-long-chain fatty acid metabolic capacity of 17-beta-hydroxysteroid dehydrogenase type 12 (HSD17B12) promotes replication of hepatitis C virus and related flaviviruses. *Sci Rep* 10(1):4040.

Molino D, Pila-Castellanos I, Marjault HB, Dias Amoedo N, Kopp K, Rochin L, Karmi O, Sohn YS, Lines L, Hamai A, Joly S, Radreau P, Vonderscher J, Codogno P, Giordano F, Machin P, Rossignol R, Meldrum E, Arnoult D, Ruggieri A, Nechushtai R, de Chassey B, Morel E (2020) Chemical targeting of NEET proteins reveals their function in mitochondrial morphodynamics. *EMBO Rep* 21(12):e49019.

Monath TP, Nichols R, Archambault WT, Moore L, Marchesani R, Tian J, Shope RE, Thomas N, Schrader R, Furby D, Bedford P (2002) Comparative safety and immunogenicity of two yellow fever 17D vaccines (ARILVAX and YF-VAX) in a phase III multicenter, double-blind clinical trial. *Am J Trop Med Hyg* 66(5):533-541.

Monteleon CL, Agnihotri T, Dahal A, Liu M, Rebecca VW, Beatty GL, Amaravadi RK, Ridky TW (2018) Lysosomes Support the Degradation, Signaling, and Mitochondrial Metabolism Necessary for Human Epidermal Differentiation. *J Invest Dermatol* 138(9):1945-1954.

Montessuit S, Somasekharan SP, Terrones O, Lucken-Ardjomande S, Herzig S, Schwarzenbacher R, Manstein DJ, Bossy-Wetzel E, Basanez G, Meda P, Martinou JC (2010) Membrane remodeling induced by the dynamin-related protein Drp1 stimulates Bax oligomerization. *Cell* 142(6):889-901.

Moore CA, Staples JE, Dobyns WB, Pessoa A, Ventura CV, Fonseca EB, Ribeiro EM, Ventura LO, Neto NN, Arena JF, Rasmussen SA (2017) Characterizing the Pattern of Anomalies in Congenital Zika Syndrome for Pediatric Clinicians. *JAMA Pediatr* 171(3):288-295.

Moquin SA, Simon O, Karuna R, Lakshminarayana SB, Yokokawa F, Wang F, Saravanan C, Zhang J, Day CW, Chan K, Wang QY, Lu S, Dong H, Wan KF, Lim SP, Liu W, Seh CC, Chen YL, Xu H, Barkan DT, Kounde CS, Sim WLS, Wang G, Yeo HQ, Zou B, Chan WL, Ding M, Song JG, Li M, Osborne C, Blasco F, Sarko C, Beer D, Bonamy GMC, Sasseville VG, Shi PY, Diagana TT, Yeung BKS, Gu F (2021) NITD-688, a pan-serotype inhibitor of the dengue virus NS4B protein, shows favorable pharmacokinetics and efficacy in preclinical animal models. *Sci Transl Med* 13(579).

Moretton A, Morel F, Macao B, Lachaume P, Ishak L, Lefebvre M, Garreau-Balandier I, Vernet P, Falkenberg M, Farge G (2017) Selective mitochondrial DNA degradation following double-strand breaks. *PLoS One* 12(4):e0176795.

Motta IJ, Spencer BR, Cordeiro da Silva SG, Arruda MB, Dobbin JA, Gonzaga YB, Arcuri IP, Tavares RC, Atta EH, Fernandes RF, Costa DA, Ribeiro LJ, Limonte F, Higa LM, Voloch CM, Brindeiro RM, Tanuri A, Ferreira OC, Jr. (2016) Evidence for Transmission of Zika Virus by Platelet Transfusion. *N Engl J Med* 375(11):1101-1103.

Moura da Silva AA, Ganz JS, Sousa PD, Doriqui MJ, Ribeiro MR, Branco MD, Queiroz RC, Pacheco MJ, Vieira da Costa FR, Silva FS, Simoes VM, Pacheco MA, Lamy-Filho F, Lamy ZC, Soares de Britto EAMT (2016) Early Growth and Neurologic Outcomes of Infants with Probable Congenital Zika Virus Syndrome. *Emerg Infect Dis* 22(11):1953-1956.

Mousson L, Dauga C, Garrigues T, Schaffner F, Vazeille M, Failloux AB (2005) Phylogeography of Aedes (Stegomyia) aegypti (L.) and Aedes (Stegomyia) albopictus (Skuse) (Diptera: Culicidae) based on mitochondrial DNA variations. *Genet Res* 86(1):1-11.

Mukherjee S, Ghosh S, Nazmi A, Basu A (2015) RIG-I knockdown impedes neurogenesis in a murine model of Japanese encephalitis. *Cell Biol Int* 39(2):224-229.

Muller DA, Young PR (2013) The flavivirus NS1 protein: molecular and structural biology, immunology, role in pathogenesis and application as a diagnostic biomarker. *Antiviral Res* 98(2):192-208.

Munoz-Jordan JL, Laurent-Rolle M, Ashour J, Martinez-Sobrido L, Ashok M, Lipkin WI, Garcia-Sastre A (2005) Inhibition of alpha/beta interferon signaling by the NS4B protein of flaviviruses. *J Virol* 79(13):8004-8013.

Murphy E, Ardehali H, Balaban RS, DiLisa F, Dorn GW, 2nd, Kitsis RN, Otsu K, Ping P, Rizzuto R, Sack MN, Wallace D, Youle RJ, American Heart Association Council on Basic Cardiovascular Sciences CoCC, Council on Functional G, Translational B (2016) Mitochondrial Function, Biology, and Role in Disease: A Scientific Statement From the American Heart Association. *Circ Res* 118(12):1960-1991.

Narendra D, Tanaka A, Suen DF, Youle RJ (2008) Parkin is recruited selectively to impaired mitochondria and promotes their autophagy. *J Cell Biol* 183(5):795-803.

Nazmi A, Dutta K, Basu A (2011) RIG-I mediates innate immune response in mouse neurons following Japanese encephalitis virus infection. *PLoS One* 6(6):e21761.

Netsawang J, Noisakran S, Puttikhunt C, Kasinrerk W, Wongwiwat W, Malasit P, Yenchitsomanus PT, Limjindaporn T (2010) Nuclear localization of dengue virus capsid protein is required for DAXX interaction and apoptosis. *Virus Res* 147(2):275-283.

Ng WC, Soto-Acosta R, Bradrick SS, Garcia-Blanco MA, Ooi EE (2017) The 5' and 3' Untranslated Regions of the Flaviviral Genome. *Viruses* 9(6).

Niu J, Jiang Y, Xu H, Zhao C, Zhou G, Chen P, Cao R (2018) TIM-1 Promotes Japanese Encephalitis Virus Entry and Infection. *Viruses* 10(11).

Nivarthi UK, Swanstrom J, Delacruz MJ, Patel B, Durbin AP, Whitehead SS, Kirkpatrick BD, Pierce KK, Diehl SA, Katzelnick L, Baric RS, de Silva AM (2021) A tetravalent live attenuated dengue virus vaccine stimulates balanced immunity to multiple serotypes in humans. *Nat Commun* 12(1):1102.

Nomura-Takigawa Y, Nagano-Fujii M, Deng L, Kitazawa S, Ishido S, Sada K, Hotta H (2006) Non-structural protein 4A of Hepatitis C virus accumulates on mitochondria and renders the cells prone to undergoing mitochondria-mediated apoptosis. *J Gen Virol* 87(Pt 7):1935-1945.

O'Neill K, Olson BJ, Huang N, Unis D, Clem RJ (2015) Rapid selection against arbovirus-induced apoptosis during infection of a mosquito vector. *Proc Natl Acad Sci U S A* 112(10):E1152-1161.

Oettinghaus B, D'Alonzo D, Barbieri E, Restelli LM, Savoia C, Licci M, Tolnay M, Frank S, Scorrano L (2016) DRP1-dependent apoptotic mitochondrial fission occurs independently of BAX, BAK and APAF1 to amplify cell death by BID and oxidative stress. *Biochim Biophys Acta* 1857(8):1267-1276.

Oh-hashi K, Koga H, Ikeda S, Shimada K, Hirata Y, Kiuchi K (2009) CRELD2 is a novel endoplasmic reticulum stress-inducible gene. *Biochem Biophys Res Commun* 387(3):504-510.

Okamoto T, Suzuki T, Kusakabe S, Tokunaga M, Hirano J, Miyata Y, Matsuura Y (2017) Regulation of Apoptosis during Flavivirus Infection. *Viruses* 9(9).

Okamura K, Ishizuka A, Siomi H, Siomi MC (2004) Distinct roles for Argonaute proteins in small RNA-directed RNA cleavage pathways. *Genes Dev* 18(14):1655-1666.

Olzmann JA, Carvalho P (2019) Dynamics and functions of lipid droplets. *Nat Rev Mol Cell Biol* 20(3):137-155.

Orrenius S, Zhivotovsky B, Nicotera P (2003) Regulation of cell death: the calcium-apoptosis link. *Nat Rev Mol Cell Biol* 4(7):552-565.

Osman C, Voelker DR, Langer T (2011) Making heads or tails of phospholipids in mitochondria. *J Cell Biol* 192(1):7-16.

Osorio JE, Velez ID, Thomson C, Lopez L, Jimenez A, Haller AA, Silengo S, Scott J, Boroughs KL, Stovall JL, Luy BE, Arguello J, Beatty ME, Santangelo J, Gordon GS, Huang CY, Stinchcomb DT (2014) Safety and immunogenicity of a recombinant live attenuated tetravalent dengue vaccine (DENVax) in flavivirus-naive healthy adults in Colombia: a randomised, placebo-controlled, phase 1 study. *Lancet Infect Dis* 14(9):830-838.

Ott M, Robertson JD, Gogvadze V, Zhivotovsky B, Orrenius S (2002) Cytochrome c release from mitochondria proceeds by a two-step process. *Proc Natl Acad Sci U S A* 99(3):1259-1263.

Ott M, Zhivotovsky B, Orrenius S (2007) Role of cardiolipin in cytochrome c release from mitochondria. *Cell Death Differ* 14(7):1243-1247.

Palucka AK (2000) Dengue virus and dendritic cells. *Nat Med* 6(7):748-749.

Pandit PS, Doyle MM, Smart KM, Young CCW, Drape GW, Johnson CK (2018) Predicting wildlife reservoirs and global vulnerability to zoonotic Flaviviruses. *Nat Commun* 9(1):5425.

Papa S, Martino PL, Capitanio G, Gaballo A, De Rasmo D, Signorile A, Petruzzella V (2012) The oxidative phosphorylation system in mammalian mitochondria. *Adv Exp Med Biol* 942:3-37.

Paradies G, Paradies V, Ruggiero FM, Petrosillo G (2019) Role of Cardiolipin in Mitochondrial Function and Dynamics in Health and Disease: Molecular and Pharmacological Aspects. *Cells* 8(7).

Paradis M, Kucharowski N, Edwards Faret G, Maya Palacios SJ, Meyer C, Stumpges B, Jamitzky I, Kalinowski J, Thiele C, Bauer R, Paululat A, Sellin J, Bulow MH (2022) The ER protein Creld regulates ER-mitochondria contact dynamics and respiratory complex 1 activity. *Sci Adv* 8(29):eabo0155.

Pardi N, Hogan MJ, Pelc RS, Muramatsu H, Andersen H, DeMaso CR, Dowd KA, Sutherland LL, Scearce RM, Parks R, Wagner W, Granados A, Greenhouse J, Walker M, Willis E, Yu JS, McGee CE, Sempowski GD, Mui BL, Tam YK, Huang YJ, Vanlandingham D, Holmes VM, Balachandran H, Sahu S, Lifton M, Higgs S, Hensley SE, Madden TD, Hope MJ, Kariko K, Santra S, Graham BS, Lewis MG, Pierson TC, Haynes BF, Weissman D (2017) Zika virus protection by a single low-dose nucleoside-modified mRNA vaccination. *Nature* 543(7644):248-251.

Park JH, Ko J, Hwang J, Koh HC (2015) Dynamin-related protein 1 mediates mitochondria-dependent apoptosis in chlorpyrifos-treated SH-SY5Y cells. *Neurotoxicology* 51:145-157.

Patergnani S, Suski JM, Agnoletto C, Bononi A, Bonora M, De Marchi E, Giorgi C, Marchi S, Missiroli S, Poletti F, Rimessi A, Duszynski J, Wieckowski MR, Pinton P (2011) Calcium signaling around Mitochondria Associated Membranes (MAMs). *Cell Commun Signal* 9:19.

Patil V, Cuenin C, Chung F, Aguilera JRR, Fernandez-Jimenez N, Romero-Garmendia I, Bilbao JR, Cahais V, Rothwell J, Herceg Z (2019) Human mitochondrial DNA is extensively methylated in a non-CpG context. *Nucleic Acids Res* 47(19):10072-10085.

Paul D, Bartenschlager R (2015) Flaviviridae Replication Organelles: Oh, What a Tangled Web We Weave. *Annu Rev Virol* 2(1):289-310.
Paul P, Munz C (2016) Autophagy and Mammalian Viruses: Roles in Immune Response, Viral Replication, and Beyond. *Adv Virus Res* 95:149-195.
Paulke-Korinek M, Kollaritsch H (2008) Japanese encephalitis and vaccines: past and future prospects. *Wien Klin Wochenschr* 120(19-20 Suppl 4):15-19.
Paupy C, Delatte H, Bagny L, Corbel V, Fontenille D (2009) Aedes albopictus, an arbovirus vector: from the darkness to the light. *Microbes Infect* 11(14-15):1177-1185.
Pereira LHS, de Souza TPP, Camargos VN, de Oliveira Barbosa LA, Taranto AG, Junior MC, de Lima Santos H, de Oliveira Lopes D, Ferreira JMS, Dos Santos LL (2019) Assays with recombinant soluble isoforms of DC-SIGN, a dengue virus ligand, show variation in their ability to bind to mannose residues. *Arch Virol* 164(11):2793-2797.
Perera R, Riley C, Isaac G, Hopf-Jannasch AS, Moore RJ, Weitz KW, Pasa-Tolic L, Metz TO, Adamec J, Kuhn RJ (2012) Dengue virus infection perturbs lipid homeostasis in infected mosquito cells. *Plos Pathogens* 8(3):e1002584.
Pierson TC, Diamond MS (2013) Flaviviruses. *Fields Virology: Sixth Edition,* Wolters Kluwer Health Adis (ESP).
Pijlman GP, Funk A, Kondratieva N, Leung J, Torres S, van der Aa L, Liu WJ, Palmenberg AC, Shi PY, Hall RA, Khromykh AA (2008) A highly structured, nuclease-resistant, noncoding RNA produced by flaviviruses is required for pathogenicity. *Cell Host Microbe* 4(6):579-591.
Pijuan J, Cantarero L, Natera-de Benito D, Altimir A, Altisent-Huguet A, Diaz-Osorio Y, Carrera-Garcia L, Exposito-Escudero J, Ortez C, Nascimento A, Hoenicka J, Palau F (2022) Mitochondrial Dynamics and Mitochondria-Lysosome Contacts in Neurogenetic Diseases. *Front Neurosci* 16:784880.
Pila-Castellanos I, Molino D, McKellar J, Lines L, Da Graca J, Tauziet M, Chanteloup L, Mikaelian I, Meyniel-Schicklin L, Codogno P, Vonderscher J, Delevoye C, Moncorge O, Meldrum E, Goujon C, Morel E, de Chassey B (2021) Correction: Mitochondrial morphodynamics alteration induced by influenza virus infection as a new antiviral strategy. *Plos Pathogens* 17(3):e1009485.
Pilling AD, Horiuchi D, Lively CM, Saxton WM (2006) Kinesin-1 and Dynein are the primary motors for fast transport of mitochondria in Drosophila motor axons. *Mol Biol Cell* 17(4):2057-2068.
Plaszczyca A, Scaturro P, Neufeldt CJ, Cortese M, Cerikan B, Ferla S, Brancale A, Pichlmair A, Bartenschlager R (2019) A novel interaction between dengue virus nonstructural protein 1 and the NS4A-2K-4B precursor is required for viral RNA replication but not for formation of the membranous replication organelle. *Plos Pathogens* 15(5):e1007736.
Poirier Y, Antonenkov VD, Glumoff T, Hiltunen JK (2006) Peroxisomal beta-oxidation--a metabolic pathway with multiple functions. *Biochim Biophys Acta* 1763(12):1413-1426.
Ponia SS, Robertson SJ, McNally KL, Sturdevant GL, Lewis M, Jessop F, Bosio CM, Kendall C, Gallegos D, Hay A, Schwartz C, Rosenke R, Saturday G, Martens C, Best SM (2021) Mitophagy antagonism by Zika virus reveals Ajuba as a regulator of PINK1-Parkin signaling, PKR-dependent inflammation, and viral invasion of tissues. *bioRxiv* 10.1101/2021.01.29.428870:2021.2001.2029.428870.
Pourcelot M, Arnoult D (2014) Mitochondrial dynamics and the innate antiviral immune response. *FEBS J* 281(17):3791-3802.
Prikhod'ko GG, Prikhod'ko EA, Cohen JI, Pletnev AG (2001) Infection with Langat Flavivirus or expression of the envelope protein induces apoptotic cell death. *Virology* 286(2):328-335.
Prikhod'ko GG, Prikhod'ko EA, Pletnev AG, Cohen JI (2002) Langat flavivirus protease NS3 binds caspase-8 and induces apoptosis. *J Virol* 76(11):5701-5710.

Qian X, Nguyen HN, Song MM, Hadiono C, Ogden SC, Hammack C, Yao B, Hamersky GR, Jacob F, Zhong C, Yoon KJ, Jeang W, Lin L, Li Y, Thakor J, Berg DA, Zhang C, Kang E, Chickering M, Nauen D, Ho CY, Wen Z, Christian KM, Shi PY, Maher BJ, Wu H, Jin P, Tang H, Song H, Ming GL (2016) Brain-Region-Specific Organoids Using Mini-bioreactors for Modeling ZIKV Exposure. *Cell* 165(5):1238-1254.

Qin CF, Zhao H, Liu ZY, Jiang T, Deng YQ, Yu XD, Yu M, Qin ED (2011) Retinoic acid inducible gene-I and melanoma differentiation-associated gene 5 are induced but not essential for dengue virus induced type I interferon response. *Mol Biol Rep* 38(6):3867-3873.

Qin ZL, Yao QF, Ren H, Zhao P, Qi ZT (2022) Lipid Droplets and Their Participation in Zika Virus Infection. *Int J Mol Sci* 23(20).

Raiborg C, Wenzel EM, Pedersen NM, Olsvik H, Schink KO, Schultz SW, Vietri M, Nisi V, Bucci C, Brech A, Johansen T, Stenmark H (2015) Repeated ER-endosome contacts promote endosome translocation and neurite outgrowth. *Nature* 520(7546):234-238.

Ramchurn SK, Moheeput K, Goorah SS (2009) An analysis of a short-lived outbreak of dengue fever in Mauritius. *Euro Surveill* 14(34).

Ramière C, Rodriguez J, Enache LS, Lotteau V, André P, Diaz O (2014) Activity of hexokinase is increased by its interaction with hepatitis C virus protein NS5A. *J Virol* 88(6):3246-3254.

Rand TA, Ginalski K, Grishin NV, Wang X (2004) Biochemical identification of Argonaute 2 as the sole protein required for RNA-induced silencing complex activity. *Proc Natl Acad Sci U S A* 101(40):14385-14389.

Refolo G, Vescovo T, Piacentini M, Fimia GM, Ciccosanti F (2020) Mitochondrial Interactome: A Focus on Antiviral Signaling Pathways. *Front Cell Dev Biol* 8:8.

Ren Y, Wang A, Wu D, Wang C, Huang M, Xiong X, Jin L, Zhou W, Qiu Y, Zhou X (2022) Dual inhibition of innate immunity and apoptosis by human cytomegalovirus protein UL37x1 enables efficient virus replication. *Nat Microbiol* 7(7):1041-1053.

Reyes-Del Valle J, Chavez-Salinas S, Medina F, Del Angel RM (2005) Heat shock protein 90 and heat shock protein 70 are components of dengue virus receptor complex in human cells. *J Virol* 79(8):4557-4567.

Richard AS, Shim BS, Kwon YC, Zhang R, Otsuka Y, Schmitt K, Berri F, Diamond MS, Choe H (2017) AXL-dependent infection of human fetal endothelial cells distinguishes Zika virus from other pathogenic flaviviruses. *Proc Natl Acad Sci U S A* 114(8):2024-2029.

Richner JM, Himansu S, Dowd KA, Butler SL, Salazar V, Fox JM, Julander JG, Tang WW, Shresta S, Pierson TC, Ciaramella G, Diamond MS (2017) Modified mRNA Vaccines Protect against Zika Virus Infection. *Cell* 169(1):176.

Riedl W, Acharya D, Lee JH, Liu G, Serman T, Chiang C, Chan YK, Diamond MS, Gack MU (2019) Zika Virus NS3 Mimics a Cellular 14-3-3-Binding Motif to Antagonize RIG-I- and MDA5-Mediated Innate Immunity. *Cell Host Microbe* 26(4):493-503 e496.

Rivera L, Biswal S, Saez-Llorens X, Reynales H, Lopez-Medina E, Borja-Tabora C, Bravo L, Sirivichayakul C, Kosalaraksa P, Martinez Vargas L, Yu D, Watanaveeradej V, Espinoza F, Dietze R, Fernando L, Wickramasinghe P, Duarte MoreiraJr E, Fernando AD, Gunasekera D, Luz K, Venancioda Cunha R, Rauscher M, Zent O, Liu M, Hoffman E, LeFevre I, Tricou V, Wallace D, Alera M, Borkowski A (2022) Three-year Efficacy and Safety of Takeda's Dengue Vaccine Candidate (TAK-003). *Clin Infect Dis* 75(1):107-117.

Robinson LN, Tharakaraman K, Rowley KJ, Costa VV, Chan KR, Wong YH, Ong LC, Tan HC, Koch T, Cain D, Kirloskar R, Viswanathan K, Liew CW, Tissire H, Ramakrishnan B, Myette JR, Babcock GJ, Sasisekharan V, Alonso S, Chen J, Lescar J, Shriver Z, Ooi EE, Sasisekharan R (2015) Structure-Guided Design of an Anti-dengue Antibody Directed to a Non-immunodominant Epitope. *Cell* 162(3):493-504.

Roosendaal J, Westaway EG, Khromykh A, Mackenzie JM (2006) Regulated cleavages at the West Nile virus NS4A-2K-NS4B junctions play a major role in rearranging cytoplasmic membranes and Golgi trafficking of the NS4A protein. *J Virol* 80(9):4623-4632.

Rowland AA, Chitwood PJ, Phillips MJ, Voeltz GK (2014) ER contact sites define the position and timing of endosome fission. *Cell* 159(5):1027-1041.
Roy S (2016) Virus Zika, le nouveau fléau propagé par les moustiques. *Le Figaro Santé*
Rupp R, Luckasen GJ, Kirstein JL, Osorio JE, Santangelo JD, Raanan M, Smith MK, Wallace D, Gordon GS, Stinchcomb DT (2015) Safety and immunogenicity of different doses and schedules of a live attenuated tetravalent dengue vaccine (TDV) in healthy adults: A Phase 1b randomized study. *Vaccine* 33(46):6351-6359.
Ryan SJ, Carlson CJ, Mordecai EA, Johnson LR (2019) Global expansion and redistribution of Aedes-borne virus transmission risk with climate change. *PLoS Negl Trop Dis* 13(3):e0007213.
Said EA, Tremblay N, Al-Balushi MS, Al-Jabri AA, Lamarre D (2018) Viruses Seen by Our Cells: The Role of Viral RNA Sensors. *J Immunol Res* 2018:9480497.
Saito T, Owen DM, Jiang F, Marcotrigiano J, Gale M, Jr. (2008) Innate immunity induced by composition-dependent RIG-I recognition of hepatitis C virus RNA. *Nature* 454(7203):523-527.
Samsa MM, Mondotte JA, Iglesias NG, Assuncao-Miranda I, Barbosa-Lima G, Da Poian AT, Bozza PT, Gamarnik AV (2009) Dengue virus capsid protein usurps lipid droplets for viral particle formation. *Plos Pathogens* 5(10):e1000632.
Sanchez-Vargas I, Travanty EA, Keene KM, Franz AW, Beaty BJ, Blair CD, Olson KE (2004) RNA interference, arthropod-borne viruses, and mosquitoes. *Virus Res* 102(1):65-74.
Sandri M (2014) Atrophy and Hypertrophy: The Balance Between Removal and Synthesis of Proteins and Organelles. *Pathobiology of Human Disease*, Mcmanus LM, Mitchell RN (Édit.) Academic Press, San Diegohttps://doi.org/10.1016/B978-0-12-386456-7.01401-5. p 64-71.
Santana-Roman ME, Maycotte P, Uribe-Carvajal S, Uribe-Alvarez C, Alvarado-Medina N, Khan M, Siddiqui A, Pando-Robles V (2021) Monitoring Mitochondrial Function in Aedes albopictus C6/36 Cell Line during Dengue Virus Infection. *Insects* 12(10).
Sato H, Hoshi M, Ikeda F, Fujiyuki T, Yoneda M, Kai C (2021) Downregulation of mitochondrial biogenesis by virus infection triggers antiviral responses by cyclic GMP-AMP synthase. *Plos Pathogens* 17(10):e1009841.
Scaturro P, Stukalov A, Haas DA, Cortese M, Draganova K, Plaszczyca A, Bartenschlager R, Gotz M, Pichlmair A (2018) An orthogonal proteomic survey uncovers novel Zika virus host factors. *Nature* 561(7722):253-257.
Schaffner F, Medlock JM, Van Bortel W (2013) Public health significance of invasive mosquitoes in Europe. *Clin Microbiol Infect* 19(8):685-692.
Scherbik SV, Brinton MA (2010) Virus-induced Ca2+ influx extends survival of west nile virus-infected cells. *J Virol* 84(17):8721-8731.
Schioler KL, Samuel M, Wai KL (2007) Vaccines for preventing Japanese encephalitis. *Cochrane Database Syst Rev* 2007(3):CD004263.
Schmidt AG, Yang PL, Harrison SC (2010) Peptide inhibitors of dengue-virus entry target a late-stage fusion intermediate. *Plos Pathogens* 6(4):e1000851.
Schrader M (2001) Tubulo-reticular clusters of peroxisomes in living COS-7 cells: dynamic behavior and association with lipid droplets. *J Histochem Cytochem* 49(11):1421-1429.
Schuldiner M, Bohnert M (2017) A different kind of love - lipid droplet contact sites. *Biochim Biophys Acta Mol Cell Biol Lipids* 1862(10 Pt B):1188-1196.
Schultz V, Cumberworth SL, Gu Q, Johnson N, Donald CL, McCanney GA, Barrie JA, Da Silva Filipe A, Linington C, Willison HJ, Edgar JM, Barnett SC, Kohl A (2021) Zika Virus Infection Leads to Demyelination and Axonal Injury in Mature CNS Cultures. *Viruses* 13(1).
Schwarz DS, Blower MD (2016) The endoplasmic reticulum: structure, function and response to cellular signaling. *Cell Mol Life Sci* 73(1):79-94.

Scorrano L, Oakes SA, Opferman JT, Cheng EH, Sorcinelli MD, Pozzan T, Korsmeyer SJ (2003) BAX and BAK regulation of endoplasmic reticulum Ca2+: a control point for apoptosis. *Science* 300(5616):135-139.

Sebastian D, Palacin M, Zorzano A (2017) Mitochondrial Dynamics: Coupling Mitochondrial Fitness with Healthy Aging. *Trends Mol Med* 23(3):201-215.

Selisko B, Wang C, Harris E, Canard B (2014) Regulation of Flavivirus RNA synthesis and replication. *Curr Opin Virol* 9:74-83.

Serafin IL, Aaskov JG (2001) Identification of epitopes on the envelope (E) protein of dengue 2 and dengue 3 viruses using monoclonal antibodies. *Arch Virol* 146(12):2469-2479.

Serman TM, Gack MU (2019) Evasion of Innate and Intrinsic Antiviral Pathways by the Zika Virus. *Viruses* 11(10).

Shan C, Xie X, Muruato AE, Rossi SL, Roundy CM, Azar SR, Yang Y, Tesh RB, Bourne N, Barrett AD, Vasilakis N, Weaver SC, Shi PY (2016) An Infectious cDNA Clone of Zika Virus to Study Viral Virulence, Mosquito Transmission, and Antiviral Inhibitors. *Cell Host Microbe* 19(6):891-900.

Shen Y, White E (2001) p53-dependent apoptosis pathways. *Adv Cancer Res* 82:55-84.

Shepard DS, Undurraga EA, Halasa YA, Stanaway JD (2016) The global economic burden of dengue: a systematic analysis. *Lancet Infect Dis* 16(8):935-941.

Sheridan C, Martin SJ (2010) Mitochondrial fission/fusion dynamics and apoptosis. *Mitochondrion* 10(6):640-648.

Shi CS, Qi HY, Boularan C, Huang NN, Abu-Asab M, Shelhamer JH, Kehrl JH (2014) SARS-coronavirus open reading frame-9b suppresses innate immunity by targeting mitochondria and the MAVS/TRAF3/TRAF6 signalosome. *J Immunol* 193(6):3080-3089.

Shin DW (2020) Lipophagy: Molecular Mechanisms and Implications in Metabolic Disorders. *Mol Cells* 43(8):686-693.

Shiryaev SA, Farhy C, Pinto A, Huang CT, Simonetti N, Elong Ngono A, Dewing A, Shresta S, Pinkerton AB, Cieplak P, Strongin AY, Terskikh AV (2017) Characterization of the Zika virus two-component NS2B-NS3 protease and structure-assisted identification of allosteric small-molecule antagonists. *Antiviral Res* 143:218-229.

Simanjuntak Y, Liang JJ, Lee YL, Lin YL (2015) Repurposing of prochlorperazine for use against dengue virus infection. *J Infect Dis* 211(3):394-404.

Simmons CP, Farrar JJ, Nguyen v V, Wills B (2012) Dengue. *N Engl J Med* 366(15):1423-1432.

Siu GK, Zhou F, Yu MK, Zhang L, Wang T, Liang Y, Chen Y, Chan HC, Yu S (2016) Hepatitis C virus NS5A protein cooperates with phosphatidylinositol 4-kinase IIIalpha to induce mitochondrial fragmentation. *Sci Rep* 6:23464.

Slonchak A, Hugo LE, Freney ME, Hall-Mendelin S, Amarilla AA, Torres FJ, Setoh YX, Peng NYG, Sng JDJ, Hall RA, van den Hurk AF, Devine GJ, Khromykh AA (2020) Zika virus noncoding RNA suppresses apoptosis and is required for virus transmission by mosquitoes. *Nat Commun* 11(1):2205.

Sorouri M, Chang T, Hancks DC (2022) Mitochondria and Viral Infection: Advances and Emerging Battlefronts. *mBio* 13(1):e0209621.

Souza BS, Sampaio GL, Pereira CS, Campos GS, Sardi SI, Freitas LA, Figueira CP, Paredes BD, Nonaka CK, Azevedo CM, Rocha VP, Bandeira AC, Mendez-Otero R, Dos Santos RR, Soares MB (2016) Zika virus infection induces mitosis abnormalities and apoptotic cell death of human neural progenitor cells. *Sci Rep* 6:39775.

Spinelli JB, Haigis MC (2018) The multifaceted contributions of mitochondria to cellular metabolism. *Nat Cell Biol* 20(7):745-754.

Stern O, Hung YF, Valdau O, Yaffe Y, Harris E, Hoffmann S, Willbold D, Sklan EH (2013) An N-terminal amphipathic helix in dengue virus nonstructural protein 4A mediates oligomerization and is essential for replication. *J Virol* 87(7):4080-4085.

Stoica R, De Vos KJ, Paillusson S, Mueller S, Sancho RM, Lau KF, Vizcay-Barrena G, Lin WL, Xu YF, Lewis J, Dickson DW, Petrucelli L, Mitchell JC, Shaw CE, Miller CC (2014) ER-mitochondria associations are regulated by the VAPB-PTPIP51 interaction and are disrupted by ALS/FTD-associated TDP-43. *Nat Commun* 5:3996.

Suen DF, Norris KL, Youle RJ (2008) Mitochondrial dynamics and apoptosis. *Genes Dev* 22(12):1577-1590.

Sun B, Sundstrom KB, Chew JJ, Bist P, Gan ES, Tan HC, Goh KC, Chawla T, Tang CK, Ooi EE (2017) Dengue virus activates cGAS through the release of mitochondrial DNA. *Sci Rep* 7(1):3594.

Suresh SN (2019) Endoplasmic reticulum mitochondria contacts modulate apoptosis of renal cells and its implications in diabetic neuropathy. *EBioMedicine* 44:24-25.

Szargel R, Shani V, Abd Elghani F, Mekies LN, Liani E, Rott R, Engelender S (2016) The PINK1, synphilin-1 and SIAH-1 complex constitutes a novel mitophagy pathway. *Hum Mol Genet* 25(16):3476-3490.

Tabata T, Petitt M, Puerta-Guardo H, Michlmayr D, Harris E, Pereira L (2018) Zika Virus Replicates in Proliferating Cells in Explants From First-Trimester Human Placentas, Potential Sites for Dissemination of Infection. *J Infect Dis* 217(8):1202-1213.

Tajima S, Takasaki T, Kurane I (2011) Restoration of replication-defective dengue type 1 virus bearing mutations in the N-terminal cytoplasmic portion of NS4A by additional mutations in NS4B. *Arch Virol* 156(1):63-69.

Tamura Y, Kawano S, Endo T (2020) Lipid homeostasis in mitochondria. *Biol Chem* 401(6-7):821-833.

Tang H, Hammack C, Ogden SC, Wen Z, Qian X, Li Y, Yao B, Shin J, Zhang F, Lee EM, Christian KM, Didier RA, Jin P, Song H, Ming GL (2016a) Zika Virus Infects Human Cortical Neural Progenitors and Attenuates Their Growth. *Cell Stem Cell* 18(5):587-590.

Tang S, Le PK, Tse S, Wallace DC, Huang T (2009) Heterozygous mutation of Opa1 in Drosophila shortens lifespan mediated through increased reactive oxygen species production. *PLoS One* 4(2):e4492.

Tang WC, Lin RJ, Liao CL, Lin YL (2014) Rab18 facilitates dengue virus infection by targeting fatty acid synthase to sites of viral replication. *J Virol* 88(12):6793-6804.

Tang WW, Young MP, Mamidi A, Regla-Nava JA, Kim K, Shresta S (2016b) A Mouse Model of Zika Virus Sexual Transmission and Vaginal Viral Replication. *Cell Rep* 17(12):3091-3098.

Tangsongcharoen C, Roytrakul S, Smith DR (2019) Analysis of cellular proteome changes in response to ZIKV NS2B-NS3 protease expression. *Biochim Biophys Acta Proteins Proteom* 1867(2):89-97.

Taylor R, Kotian P, Warren T, Panchal R, Bavari S, Julander J, Dobo S, Rose A, El-Kattan Y, Taubenheim B, Babu Y, Sheridan WP (2016) BCX4430 - A broad-spectrum antiviral adenosine nucleoside analog under development for the treatment of Ebola virus disease. *J Infect Public Health* 9(3):220-226.

Thomas SJ, Yoon IK (2019) A review of Dengvaxia(R): development to deployment. *Hum Vaccin Immunother* 15(10):2295-2314.

Thomson BJ (2001) Viruses and apoptosis. *Int J Exp Pathol* 82(2):65-76.

Tigano M, Vargas DC, Tremblay-Belzile S, Fu Y, Sfeir A (2021) Nuclear sensing of breaks in mitochondrial DNA enhances immune surveillance. *Nature* 591(7850):477-481.

Tio PH, Jong WW, Cardosa MJ (2005) Two dimensional VOPBA reveals laminin receptor (LAMR1) interaction with dengue virus serotypes 1, 2 and 3. *Virol J* 2:25.

Tjaden NB, Thomas SM, Fischer D, Beierkuhnlein C (2013) Extrinsic Incubation Period of Dengue: Knowledge, Backlog, and Applications of Temperature Dependence. *PLoS Negl Trop Dis* 7(6):e2207.

Tremblay N, Freppel W, Sow AA, Chatel-Chaix L (2019) The Interplay between Dengue Virus and the Human Innate Immune System: A Game of Hide and Seek. *Vaccines (Basel)* 7(4).

Trotter PJ, Voelker DR (1995) Identification of a non-mitochondrial phosphatidylserine decarboxylase activity (PSD2) in the yeast Saccharomyces cerevisiae. *J Biol Chem* 270(11):6062-6070.

Turpin J, Frumence E, Despres P, Viranaicken W, Krejbich-Trotot P (2019) The ZIKA Virus Delays Cell Death Through the Anti-Apoptotic Bcl-2 Family Proteins. *Cells* 8(11).

Tyanova S, Temu T, Cox J (2016a) The MaxQuant computational platform for mass spectrometry-based shotgun proteomics. *Nat Protoc* 11(12):2301-2319.

Tyanova S, Temu T, Sinitcyn P, Carlson A, Hein MY, Geiger T, Mann M, Cox J (2016b) The Perseus computational platform for comprehensive analysis of (prote)omics data. *Nat Methods* 13(9):731-740.

Ubol S, Phuklia W, Kalayanarooj S, Modhiran N (2010) Mechanisms of immune evasion induced by a complex of dengue virus and preexisting enhancing antibodies. *J Infect Dis* 201(6):923-935.

Uhlemann AC, Krishna S (2005) Antimalarial multi-drug resistance in Asia: mechanisms and assessment. *Curr Top Microbiol Immunol* 295:39-53.

Umareddy I, Chao A, Sampath A, Gu F, Vasudevan SG (2006) Dengue virus NS4B interacts with NS3 and dissociates it from single-stranded RNA. *J Gen Virol* 87(Pt 9):2605-2614.

Urbanowski MD, Hobman TC (2013) The West Nile virus capsid protein blocks apoptosis through a phosphatidylinositol 3-kinase-dependent mechanism. *J Virol* 87(2):872-881.

van Cleef KW, Overheul GJ, Thomassen MC, Kaptein SJ, Davidson AD, Jacobs M, Neyts J, van Kuppeveld FJ, van Rij RP (2013) Identification of a new dengue virus inhibitor that targets the viral NS4B protein and restricts genomic RNA replication. *Antiviral Res* 99(2):165-171.

van den Berg B, Walgaard C, Drenthen J, Fokke C, Jacobs BC, van Doorn PA (2014) Guillain-Barre syndrome: pathogenesis, diagnosis, treatment and prognosis. *Nat Rev Neurol* 10(8):469-482.

van der Schaar HM, Rust MJ, Chen C, van der Ende-Metselaar H, Wilschut J, Zhuang X, Smit JM (2008) Dissecting the cell entry pathway of dengue virus by single-particle tracking in living cells. *Plos Pathogens* 4(12):e1000244.

Van Norman GA (2016) Drugs, Devices, and the FDA: Part 2: An Overview of Approval Processes: FDA Approval of Medical Devices. *JACC Basic Transl Sci* 1(4):277-287.

Van Rompay KKA, Keesler RI, Ardeshir A, Watanabe J, Usachenko J, Singapuri A, Cruzen C, Bliss-Moreau E, Murphy AM, Yee JL, Webster H, Dennis M, Singh T, Heimsath H, Lemos D, Stuart J, Morabito KM, Foreman BM, Burgomaster KE, Noe AT, Dowd KA, Ball E, Woolard K, Presicce P, Kallapur SG, Permar SR, Foulds KE, Coffey LL, Pierson TC, Graham BS (2019) DNA vaccination before conception protects Zika virus-exposed pregnant macaques against prolonged viremia and improves fetal outcomes. *Sci Transl Med* 11(523).

Vance JE (2014) MAM (mitochondria-associated membranes) in mammalian cells: lipids and beyond. *Biochim Biophys Acta* 1841(4):595-609.

Vance JE (2015) Phospholipid synthesis and transport in mammalian cells. *Traffic* 16(1):1-18.

Vance JE, Tasseva G (2013) Formation and function of phosphatidylserine and phosphatidylethanolamine in mammalian cells. *Biochim Biophys Acta* 1831(3):543-554.

Venditti R, Masone MC, De Matteis MA (2020) ER-Golgi membrane contact sites. *Biochem Soc Trans* 48(1):187-197.

Venditti R, Masone MC, Rega LR, Di Tullio G, Santoro M, Polishchuk E, Serrano IC, Olkkonen VM, Harada A, Medina DL, La Montagna R, De Matteis MA (2019) The activity of Sac1 across ER-TGN contact sites requires the four-phosphate-adaptor-protein-1. *J Cell Biol* 218(3):783-797.

Verfaillie T, Rubio N, Garg AD, Bultynck G, Rizzuto R, Decuypere JP, Piette J, Linehan C, Gupta S, Samali A, Agostinis P (2012) PERK is required at the ER-mitochondrial contact sites to convey apoptosis after ROS-based ER stress. *Cell Death Differ* 19(11):1880-1891.

Vidal J (2016) Zika forest: birthplace of virus that has spread fear across the world. *The Guardian*
Viettri M, Zambrano JL, Rosales R, Caraballo GI, Gutierrez-Escolano AL, Ludert JE (2021) Flavivirus infections induce a Golgi stress response in vertebrate and mosquito cells. *Sci Rep* 11(1):23489.
Villordo SM, Filomatori CV, Sanchez-Vargas I, Blair CD, Gamarnik AV (2015) Dengue virus RNA structure specialization facilitates host adaptation. *Plos Pathogens* 11(1):e1004604.
von Stockum S, Marchesan E, Ziviani E (2018) Mitochondrial quality control beyond PINK1/Parkin. *Oncotarget* 9(16):12550-12551.
Vratskikh O, Stiasny K, Zlatkovic J, Tsouchnikas G, Jarmer J, Karrer U, Roggendorf M, Roggendorf H, Allwinn R, Heinz FX (2013) Dissection of antibody specificities induced by yellow fever vaccination. *Plos Pathogens* 9(6):e1003458.
Wang Q, Xin X, Wang T, Wan J, Ou Y, Yang Z, Yu Q, Zhu L, Guo Y, Wu Y, Ding Z, Zhang Y, Pan Z, Tang Y, Li S, Kong L (2019) Japanese Encephalitis Virus Induces Apoptosis and Encephalitis by Activating the PERK Pathway. *J Virol* 93(17).
Wang QY, Dong H, Zou B, Karuna R, Wan KF, Zou J, Susila A, Yip A, Shan C, Yeo KL, Xu H, Ding M, Chan WL, Gu F, Seah PG, Liu W, Lakshminarayana SB, Kang C, Lescar J, Blasco F, Smith PW, Shi PY (2015) Discovery of Dengue Virus NS4B Inhibitors. *J Virol* 89(16):8233-8244.
Wang R, Zhu Y, Ren C, Yang S, Tian S, Chen H, Jin M, Zhou H (2021) Influenza A virus protein PB1-F2 impairs innate immunity by inducing mitophagy. *Autophagy* 17(2):496-511.
Wang T, Town T, Alexopoulou L, Anderson JF, Fikrig E, Flavell RA (2004) Toll-like receptor 3 mediates West Nile virus entry into the brain causing lethal encephalitis. *Nat Med* 10(12):1366-1373.
Warfield KL, Plummer E, Alonzi DS, Wolfe GW, Sampath A, Nguyen T, Butters TD, Enterlein SG, Stavale EJ, Shresta S, Ramstedt U (2015) A Novel Iminosugar UV-12 with Activity against the Diverse Viruses Influenza and Dengue (Novel Iminosugar Antiviral for Influenza and Dengue). *Viruses* 7(5):2404-2427.
Warfield KL, Plummer EM, Sayce AC, Alonzi DS, Tang W, Tyrrell BE, Hill ML, Caputo AT, Killingbeck SS, Beatty PR, Harris E, Iwaki R, Kinami K, Ide D, Kiappes JL, Kato A, Buck MD, King K, Eddy W, Khaliq M, Sampath A, Treston AM, Dwek RA, Enterlein SG, Miller JL, Zitzmann N, Ramstedt U, Shresta S (2016) Inhibition of endoplasmic reticulum glucosidases is required for in vitro and in vivo dengue antiviral activity by the iminosugar UV-4. *Antiviral Res* 129:93-98.
Watts DM, Burke DS, Harrison BA, Whitmire RE, Nisalak A (1987) Effect of temperature on the vector efficiency of Aedes aegypti for dengue 2 virus. *Am J Trop Med Hyg* 36(1):143-152.
Weaver SC (2013) Urbanization and geographic expansion of zoonotic arboviral diseases: mechanisms and potential strategies for prevention. *Trends Microbiol* 21(8):360-363.
Weber-Boyvat M, Kentala H, Peranen J, Olkkonen VM (2015) Ligand-dependent localization and function of ORP-VAP complexes at membrane contact sites. *Cell Mol Life Sci* 72(10):1967-1987.
Weinberg SE, Sena LA, Chandel NS (2015) Mitochondria in the regulation of innate and adaptive immunity. *Immunity* 42(3):406-417.
Welsch S, Miller S, Romero-Brey I, Merz A, Bleck CK, Walther P, Fuller SD, Antony C, Krijnse-Locker J, Bartenschlager R (2009) Composition and three-dimensional architecture of the dengue virus replication and assembly sites. *Cell Host Microbe* 5(4):365-375.
Wen Z, Song H, Ming GL (2017) How does Zika virus cause microcephaly? *Genes Dev* 31(9):849-861.
Westaway EG, Mackenzie JM, Kenney MT, Jones MK, Khromykh AA (1997) Ultrastructure of Kunjin virus-infected cells: colocalization of NS1 and NS3 with double-stranded RNA, and of NS2B with NS3, in virus-induced membrane structures. *J Virol* 71(9):6650-6661.

Westermann B (2010) Mitochondrial fusion and fission in cell life and death. *Nat Rev Mol Cell Biol* 11(12):872-884.
Westermann B (2012) Bioenergetic role of mitochondrial fusion and fission. *Biochim Biophys Acta* 1817(10):1833-1838.
Whitehorn J, Simmons CP (2011) The pathogenesis of dengue. *Vaccine* 29(42):7221-7228.
Wong CP, Xu Z, Hou S, Limonta D, Kumar A, Power C, Hobman TC (2019) Interplay between Zika Virus and Peroxisomes during Infection. *Cells* 8(7).
Wong YC, Ysselstein D, Krainc D (2018) Mitochondria-lysosome contacts regulate mitochondrial fission via RAB7 GTP hydrolysis. *Nature* 554(7692):382-386.
World Health Organisation (2018) Zika virus. Key facts. *20 July*.
World Health Organisation (2022) *Zika epidemiology update.* p
World Health Organization (2016) WHO statement on the first meeting of the International Health Regulations (2005) (IHR 2005): Emergency Committee on Zika virus and observed increase in neurological disorders and neonatal malformations.).
World Health Organization (2022) *Fact sheet : Dengue and severe dengue.* p
Wu C, Yao W, Kai W, Liu W, Wang W, Li S, Chen Y, Wu X, Wang L, Li Y, Tong J, Qian J, Zhang L, Hong Z, Yi C (2020) Mitochondrial Fusion Machinery Specifically Involved in Energy Deprivation-Induced Autophagy. *Front Cell Dev Biol* 8:221.
Xi Z, Ramirez JL, Dimopoulos G (2008) The Aedes aegypti toll pathway controls dengue virus infection. *Plos Pathogens* 4(7):e1000098.
Xiao B, Deng X, Lim GGY, Xie S, Zhou ZD, Lim KL, Tan EK (2017a) Superoxide drives progression of Parkin/PINK1-dependent mitophagy following translocation of Parkin to mitochondria. *Cell Death Dis* 8(10):e3097.
Xiao B, Goh JY, Xiao L, Xian H, Lim KL, Liou YC (2017b) Reactive oxygen species trigger Parkin/PINK1 pathway-dependent mitophagy by inducing mitochondrial recruitment of Parkin. *J Biol Chem* 292(40):16697-16708.
Xie W, Liang C, Birchler JA (2011a) Inhibition of RNA interference and modulation of transposable element expression by cell death in Drosophila. *Genetics* 188(4):823-834.
Xie X, Wang QY, Xu HY, Qing M, Kramer L, Yuan Z, Shi PY (2011b) Inhibition of dengue virus by targeting viral NS4B protein. *J Virol* 85(21):11183-11195.
Xie X, Zou J, Wang QY, Shi PY (2015) Targeting dengue virus NS4B protein for drug discovery. *Antiviral Res* 118:39-45.
Xu M, Lee EM, Wen Z, Cheng Y, Huang WK, Qian X, Tcw J, Kouznetsova J, Ogden SC, Hammack C, Jacob F, Nguyen HN, Itkin M, Hanna C, Shinn P, Allen C, Michael SG, Simeonov A, Huang W, Christian KM, Goate A, Brennand KJ, Huang R, Xia M, Ming GL, Zheng W, Song H, Tang H (2016) Identification of small-molecule inhibitors of Zika virus infection and induced neural cell death via a drug repurposing screen. *Nat Med* 22(10):1101-1107.
Yang S, Gorshkov K, Lee EM, Xu M, Cheng YS, Sun N, Soheilian F, de Val N, Ming G, Song H, Tang H, Zheng W (2020) Zika Virus-Induced Neuronal Apoptosis via Increased Mitochondrial Fragmentation. *Front Microbiol* 11:598203.
Yartsev A (2019) *Structure and function of the mitochondria.* https://derangedphysiology.com/main/cicm-primary-exam/required-reading/cellular-physiology/Chapter%20122/structure-and-function-mitochondria
Yeo HK, Park TH, Kim HY, Jang H, Lee J, Hwang GS, Ryu SE, Park SH, Song HK, Ban HS, Yoon HJ, Lee BI (2021) Phospholipid transfer function of PTPIP51 at mitochondria-associated ER membranes. *EMBO Rep* 22(6):e51323.
Yin Z, Chen YL, Schul W, Wang QY, Gu F, Duraiswamy J, Kondreddi RR, Niyomrattanakit P, Lakshminarayana SB, Goh A, Xu HY, Liu W, Liu B, Lim JY, Ng CY, Qing M, Lim CC, Yip A, Wang G, Chan WL, Tan HP, Lin K, Zhang B, Zou G, Bernard KA, Garrett C, Beltz K,

Dong M, Weaver M, He H, Pichota A, Dartois V, Keller TH, Shi PY (2009) An adenosine nucleoside inhibitor of dengue virus. *Proc Natl Acad Sci U S A* 106(48):20435-20439.
Yoon Y, McNiven MA (2001) Mitochondrial division: New partners in membrane pinching. *Curr Biol* 11(2):R67-70.
Yorimitsu T, Klionsky DJ (2005) Autophagy: molecular machinery for self-eating. *Cell Death Differ* 12 Suppl 2(Suppl 2):1542-1552.
You J, Hou S, Malik-Soni N, Xu Z, Kumar A, Rachubinski RA, Frappier L, Hobman TC (2015) Flavivirus Infection Impairs Peroxisome Biogenesis and Early Antiviral Signaling. *J Virol* 89(24):12349-12361.
Youn S, Li T, McCune BT, Edeling MA, Fremont DH, Cristea IM, Diamond MS (2012) Evidence for a genetic and physical interaction between nonstructural proteins NS1 and NS4B that modulates replication of West Nile virus. *J Virol* 86(13):7360-7371.
Young LS, Rickinson AB (2004) Epstein-Barr virus: 40 years on. *Nat Rev Cancer* 4(10):757-768.
Yu CY, Liang JJ, Li JK, Lee YL, Chang BL, Su CI, Huang WJ, Lai MM, Lin YL (2015) Dengue Virus Impairs Mitochondrial Fusion by Cleaving Mitofusins. *Plos Pathogens* 11(12):e1005350.
Yu IM, Zhang W, Holdaway HA, Li L, Kostyuchenko VA, Chipman PR, Kuhn RJ, Rossmann MG, Chen J (2008) Structure of the immature dengue virus at low pH primes proteolytic maturation. *Science* 319(5871):1834-1837.
Yu L, Takeda K, Markoff L (2013) Protein-protein interactions among West Nile non-structural proteins and transmembrane complex formation in mammalian cells. *Virology* 446(1-2):365-377.
Yu Y (2010) Phenotypic and genotypic characteristics of Japanese encephalitis attenuated live vaccine virus SA14-14-2 and their stabilities. *Vaccine* 28(21):3635-3641.
Yu Y, Deng YQ, Zou P, Wang Q, Dai Y, Yu F, Du L, Zhang NN, Tian M, Hao JN, Meng Y, Li Y, Zhou X, Fuk-Woo Chan J, Yuen KY, Qin CF, Jiang S, Lu L (2017) A peptide-based viral inactivator inhibits Zika virus infection in pregnant mice and fetuses. *Nat Commun* 8:15672.
Yuan S, Chan JF, den-Haan H, Chik KK, Zhang AJ, Chan CC, Poon VK, Yip CC, Mak WW, Zhu Z, Zou Z, Tee KM, Cai JP, Chan KH, de la Pena J, Perez-Sanchez H, Ceron-Carrasco JP, Yuen KY (2017) Structure-based discovery of clinically approved drugs as Zika virus NS2B-NS3 protease inhibitors that potently inhibit Zika virus infection in vitro and in vivo. *Antiviral Res* 145:33-43.
Zhang H, Bosch-Marce M, Shimoda LA, Tan YS, Baek JH, Wesley JB, Gonzalez FJ, Semenza GL (2008) Mitochondrial autophagy is an HIF-1-dependent adaptive metabolic response to hypoxia. *J Biol Chem* 283(16):10892-10903.
Zhang J, Lan Y, Li MY, Lamers MM, Fusade-Boyer M, Klemm E, Thiele C, Ashour J, Sanyal S (2018) Flaviviruses Exploit the Lipid Droplet Protein AUP1 to Trigger Lipophagy and Drive Virus Production. *Cell Host Microbe* 23(6):819-831 e815.
Zhang J, Lan Y, Sanyal S (2017) Modulation of Lipid Droplet Metabolism-A Potential Target for Therapeutic Intervention in Flaviviridae Infections. *Front Microbiol* 8:2286.
Zhang JZ, Liu Z, Liu J, Ren JX, Sun TS (2014) Mitochondrial DNA induces inflammation and increases TLR9/NF-kappaB expression in lung tissue. *Int J Mol Med* 33(4):817-824.
Zhang Q, Raoof M, Chen Y, Sumi Y, Sursal T, Junger W, Brohi K, Itagaki K, Hauser CJ (2010) Circulating mitochondrial DAMPs cause inflammatory responses to injury. *Nature* 464(7285):104-107.
Zhang X, Liang C, Wang H, Guo Z, Rong H, Pan J, Li W, Pei R, Chen X, Zhang Z, Zhang XE, Cui Z (2022) T-Cell Immunoglobulin and Mucin Domain 1 (TIM-1) Is a Functional Entry Factor for Tick-Borne Encephalitis Virus. *mBio* 13(1):e0286021.

Zhang Y, Corver J, Chipman PR, Zhang W, Pletnev SV, Sedlak D, Baker TS, Strauss JH, Kuhn RJ, Rossmann MG (2003) Structures of immature flavivirus particles. *EMBO J* 22(11):2604-2613.

Zhang Y, Kostyuchenko VA, Rossmann MG (2007) Structural analysis of viral nucleocapsids by subtraction of partial projections. *J Struct Biol* 157(2):356-364.

Zhang Z, Huang L, Shulmeister VM, Chi YI, Kim KK, Hung LW, Crofts AR, Berry EA, Kim SH (1998) Electron transfer by domain movement in cytochrome bc1. *Nature* 392(6677):677-684.

Zheng Y, Liu Q, Wu Y, Ma L, Zhang Z, Liu T, Jin S, She Y, Li YP, Cui J (2018) Zika virus elicits inflammation to evade antiviral response by cleaving cGAS via NS1-caspase-1 axis. *EMBO J* 37(18).

Zinser E, Sperka-Gottlieb CD, Fasch EV, Kohlwein SD, Paltauf F, Daum G (1991) Phospholipid synthesis and lipid composition of subcellular membranes in the unicellular eukaryote Saccharomyces cerevisiae. *J Bacteriol* 173(6):2026-2034.

Zmurko J, Marques RE, Schols D, Verbeken E, Kaptein SJ, Neyts J (2016) The Viral Polymerase Inhibitor 7-Deaza-2'-C-Methyladenosine Is a Potent Inhibitor of In Vitro Zika Virus Replication and Delays Disease Progression in a Robust Mouse Infection Model. *PLoS Negl Trop Dis* 10(5):e0004695.

Zmurko J, Neyts J, Dallmeier K (2015) Flaviviral NS4b, chameleon and jack-in-the-box roles in viral replication and pathogenesis, and a molecular target for antiviral intervention. *Rev Med Virol* 25(4):205-223.

Zong S, Wu M, Gu J, Liu T, Guo R, Yang M (2018) Structure of the intact 14-subunit human cytochrome c oxidase. *Cell Res* 28(10):1026-1034.

Zou J, Lee le T, Wang QY, Xie X, Lu S, Yau YH, Yuan Z, Geifman Shochat S, Kang C, Lescar J, Shi PY (2015a) Mapping the Interactions between the NS4B and NS3 proteins of dengue virus. *J Virol* 89(7):3471-3483.

Zou J, Xie X, Lee le T, Chandrasekaran R, Reynaud A, Yap L, Wang QY, Dong H, Kang C, Yuan Z, Lescar J, Shi PY (2014) Dimerization of flavivirus NS4B protein. *J Virol* 88(6):3379-3391.

Zou J, Xie X, Wang QY, Dong H, Lee MY, Kang C, Yuan Z, Shi PY (2015b) Characterization of dengue virus NS4A and NS4B protein interaction. *J Virol* 89(7):3455-3470.

Zucker J, Neu N, Chiriboga CA, Hinton VJ, Leonardo M, Sheikh A, Thakur K (2017) Zika Virus-Associated Cognitive Impairment in Adolescent, 2016. *Emerg Infect Dis* 23(6):1047-1048.

7 ANNEXE I

Received: 1 March 2020 | Revised: 1 December 2020 | Accepted: 15 December 2020
DOI: 10.1111/cmi.13302

WILEY

RESEARCH ARTICLE

Valosin-containing protein ATPase activity regulates the morphogenesis of Zika virus replication organelles and virus-induced cell death

Anaïs Anton[1] | Clément Mazeaud[1] | Wesley Freppel[1] | Claudia Gilbert[1] | Nicolas Tremblay[1] | Aïssatou Aïcha Sow[1] | Marie Roy[1] | Ian Gaël Rodrigue-Gervais[1] | Laurent Chatel-Chaix[1,2,3]

[1]Centre Armand-Frappier Santé Biotechnologie, Institut National de la Recherche Scientifique, Laval, Québec, Canada

[2]Center of Excellence in Research on Orphan Diseases-Courtois Foundation (CERMO-FC), Montreal, Québec, Canada

[3]Réseau Intersectoriel de Recherche en Santé de l'Université du Québec (RISUQ), Québec, Canada

Correspondence
Laurent Chatel-Chaix, Centre Armand-Frappier Santé Biotechnologie, Institut National de la Recherche Scientifique, Laval, QC, Canada.
Email: laurent.chatel-chaix@inrs.ca

Funding information
Fonds de la Recherche du Québec-Nature et Technologies, Grant/Award Number: 2018-NC-205593; Canadian Institutes of Health Research, Grant/Award Numbers: ICS154142, PJT153020; Natural Sciences and Engineering Research Council of Canada, Grant/Award Number: RGPIN-2016-05584

Abstract

With no available therapies, infections with Zika virus (ZIKV) constitute a major public health concern as they can lead to congenital microcephaly. In order to generate an intracellular environment favourable to viral replication, ZIKV induces endomembrane remodelling and the morphogenesis of replication factories via enigmatic mechanisms. In this study, we identified the AAA+ type ATPase valosin-containing protein (VCP) as a cellular interaction partner of ZIKV non-structural protein 4B (NS4B). Importantly, its pharmacological inhibition as well as the expression of a VCP dominant-negative mutant impaired ZIKV replication. In infected cells, VCP is relocalised to large ultrastructures containing both NS4B and NS3, which are reminiscent of dengue virus convoluted membranes. Moreover, short treatment with the VCP inhibitors NMS-873 or CB-5083 drastically decreased the abundance and size of ZIKV-induced convoluted membranes. Furthermore, NMS-873 treatment inhibited ZIKV-induced mitochondria elongation previously reported to be physically and functionally linked to convoluted membranes in case of the closely related dengue virus. Finally, VCP inhibition resulted in enhanced apoptosis of ZIKV-infected cells strongly suggesting that convoluted membranes limit virus-induced cytopathic effects. Altogether, this study identifies VCP as a host factor required for ZIKV life cycle and more precisely, for the maintenance of viral replication factories. Our data further support a model in which convoluted membranes regulate ZIKV life cycle by impacting on mitochondrial functions and ZIKV-induced death signals in order to create a cytoplasmic environment favourable to viral replication.

1 | INTRODUCTION

Following the recent outbreak of Zika virus (ZIKV) in the Americas, the World Health Organisation issued a global health emergency in 2016 and considers that this pathogen is now endemic (World Health Organization, 2016, 2017). As of January 2018, 100 million infection cases have been estimated in the Americas (Grubaugh, Faria, Andersen, & Pybus, 2018). While ZIKV is mainly transmitted through the bite of *Aedes* species mosquitoes, this pathogen brought a lot of concerns notably because of its extremely rapid spread within the Americas and of so-far-unsuspected modes-of-transmission. In addition to clinical features usually associated with other related viruses, unique symptoms were reported for ZIKV. Notably worrisome, infection of pregnant women with ZIKV can lead to congenital transmission and

Anaïs Anton, Clément Mazeaud and Wesley Freppel contributed equally to this study.

eventually to fetal brain development defects including (but not restricted to) neonate microcephaly, leaving surviving children with severe life-long disabilities. Following infection of pregnant women with ZIKV, this pathogen can cross the placental barrier and reach the developing brain to infect neural progenitor cells. This causes their death by apoptosis and the deregulation of their differentiation program via unknown mechanisms, resulting in severe defects in brain development (Cugola et al., 2016; Lazear & Diamond, 2016; Li, Saucedo-Cuevas, Shresta, & Gleeson, 2016; Li, Xu, et al., 2016; Miner et al., 2016; Pierson & Graham, 2016). ZIKV infection is generally not lethal in humans but this pathogen also reaches adult brain and can cause peripheral nervous system disorders such as the Guillain-Barré syndrome. Late-onset appearance of ZIKV-induced neurological disorders has never been reported in adults but should not be excluded given the relatively short history of the ZIKV contemporary pandemic. Unfortunately, neither antiviral therapies nor vaccines against this emerging neurotropic virus are currently available. Hence, to fight this spreading viral threat both therapeutically and prophylactically, there is an urgent need to develop antiviral strategies. Through repurposing screening campaigns, much research efforts are being deployed to identify 'ready-to-use' highly potent ZIKV inhibitors that are already approved by the US Food and Drug Administration (Barrows et al., 2016; Rausch et al., 2017; Xu et al., 2016; Zhou et al., 2017). Unfortunately, developing antivirals remains challenging partly because our knowledge of ZIKV biology and neuropathogenesis is very limited and mostly relies on the transposition of the state-of-the-art of related viruses. As a result, viral and host determinants governing the ZIKV life cycle and the severity of fetal brain defects remain poorly understood.

ZIKV belongs to the *Flavivirus* genus within the *Flaviviridae* family and is closely related to dengue virus (DENV). Following entry into a target cell, the genomic viral RNA is translated into one single polyprotein, which is further processed into 10 mature proteins by host and viral proteases. The non-structural proteins (NS) 1, 2A, 2B, 3, 4A, 4B and 5 are all essential to RNA replication (Neufeldt, Cortese, Acosta, & Bartenschlager, 2018). The structural proteins Capsid (C), prM and Envelope (E) assemble together with the RNA genome to form new virus particles. ZIKV, like other flaviviruses, induces massive rearrangements of the endoplasmic reticulum (ER) (Cortese et al., 2017) generically called 'viral replication factories' (vRF) or 'viral replication organelles'. vRFs include three sub-types of ultrastructures. Vesicle packets (VP) formed through invaginations of the ER, are believed to host the viral RNA synthesis process. Virus bags are dilated ER-derived cisternae and contain assembled viruses that accumulate in regular arrays. Lastly, ZIKV induces convoluted membranes (CM), which look like tight accumulations of smooth ER. CM precise function remains elusive and has been so far underestimated while it most probably involves the hijacking of specific cellular factors (Chatel-Chaix & Bartenschlager, 2014; Cortese et al., 2017). More generally, the host and viral determinants regulating the morphogenesis and/or stability of ZIKV vRF are mostly unknown.

Flaviviral NS4B is of particular interest since this transmembrane protein is strictly required for RNA replication via yet unknown mechanisms (Chatel-Chaix et al., 2015; Zou, Lee, et al., 2015; Zou et al., 2014). It is highly enriched in DENV CMs and has been hypothesised to regulate vRF morphogenesis (Chatel-Chaix et al., 2016; Miller, Sparacio, & Bartenschlager, 2006; Welsch et al., 2009). NS4B's critical role is further illustrated by the fact that it is the target of several antivirals under preclinical development (van Cleef et al., 2013; Wang et al., 2015; Xie et al., 2011; Xie, Zou, Wang, & Shi, 2015). Interestingly, in the case of DENV, NS4B-containing CMs make contacts with mitochondria whose morphology is elongated upon infection or NS4B expression (Barbier, Lang, Valois, Rothman, & Medin, 2017; Chatel-Chaix et al., 2016). These changes in mitochondrial morphodynamics impact on the morphogenesis of DENV CMs as well as on the efficiency of early innate immune signalling. Importantly, similar mitochondrial elongation was also observed in ZIKV-infected cells and favoured viral replication (Chatel-Chaix et al., 2016). Additionally, ZIKV NS4B was shown to inhibit neurogenesis in neural progenitor cells (Liang et al., 2016). This suggests that NS4B-enriched CMs might contribute to neuropathogenesis in the infected brain and hence, represent an attractive drug target. A mass spectrometry-based interactomic approach has recently showed that DENV NS4B associates with the host AAA+ ATPase valosin-containing protein (VCP or p97) in infected cells (Chatel-Chaix et al., 2016). However, this interaction was never validated and its potential relevance during the infection was not further investigated. Since DENV and ZIKV NS4B are genetically close, ZIKV NS4B might also interact with VCP. VCP is an ubiquitous, abundant and multifunctional protein, which is involved in maintaining protein homeostasis (proteostasis) by retrotranslocating ER or mitochondrial proteins to the cytosol, unfolding proteins for degradation and disassembling protein aggregates (Beskow et al., 2009; Bodnar & Rapoport, 2017; DeLaBarre, Christianson, Kopito, & Brunger, 2006; Jarosch et al., 2002; Ju, Miller, Hanson, & Weihl, 2008; Kim et al., 2013; Wojcik et al., 2006; Ye, Meyer, & Rapoport, 2001). VCP has also important functions in autophagy-associated mitochondrial morphology and oxidative respiration (Bartolome et al., 2013; Guo et al., 2016; Kim et al., 2013; Ludtmann et al., 2017; Zhang, Mishra, Hay, Chan, & Guo, 2017), two features modulated by DENV and/or ZIKV (Barbier et al., 2017; Chatel-Chaix et al., 2016; Ledur et al., 2020). VCP contains a N-terminus regulatory domain and two ATPase domains (D1 and D2), which mediate hexamerization to form the ring-shaped active enzyme (Banerjee et al., 2016). Interestingly, several missense mutations of VCP in patients are associated with important disorders of both central and peripheral nervous systems. Indeed, they cause a late-onset multisystem proteinopathy, also called IBMFPD/ALS, which manifests in patient as frontotemporal dementia, classical amyotrophic lateral sclerosis, inclusion body myopathy and Paget's disease of bone, alone or in combination (Halawani et al., 2009; Niwa et al., 2012; Watts et al., 2004; Weihl, Dalal, Pestronk, & Hanson, 2006). Several of these mutations are associated with distinct defects in VCP function. Accordingly, treatments with VCP inhibitors can rescue the defects associated to these mutants both in patient fibroblast and *in vivo* in insect models (Zhang et al., 2017). Finally, the knockdown of VCP zebrafish orthologue CDC48 impairs neuronal outgrowth and induces

neurodegeneration in the larva *in vivo* (Imamura, Yabu, & Yamashita, 2012). Considering the important roles of VCP in both peripheral and central nervous systems, two targets of ZIKV, we hypothesised here that ZIKV co-opts this host factor for the benefit of its replication.

In this study, we demonstrate that VCP interacts with ZIKV NS4B and regulates the viral replication cycle. In addition, we show that VCP is relocalised into ZIKV-induced large ultrastructures, which contain NS3 and NS4B, and are reminiscent of CMs. Strikingly, CM morphology and abundance are profoundly and rapidly altered upon pharmacological inhibition of VCP. Finally, we show that VCP inhibition results in the loss of ZIKV-induced elongation of mitochondria and is associated with increased ZIKV-induced apoptosis. Overall, this study identifies VCP as an important host factor during ZIKV replication, which considering its implication in several neurological diseases, may contribute to ZIKV pathogenesis.

2 | RESULTS

2.1 | VCP interacts with NS4B during ZIKV life cycle

Previous quantitative interactomic analyses in infectious conditions and NS4B-expressing cells identified VCP as a DENV NS4B interaction partner although this interaction was never validated or characterised (Chatel-Chaix et al., 2016; Shah et al., 2018). Considering that ZIKV NS4B and DENV NS4B are genetically close (54% identity between ZIKV H/PF/2013 NS4B and DENV2 16681 NS4B at the protein level), we hypothesised that ZIKV NS4B also interacts with VCP. To test this, Huh7.5 liver carcinoma cells were infected with ZIKV contemporary strain H/PF/2013 (isolated during the 2013 French Polynesia ZIKV outbreak). Seventy-two hours later, co-immunoprecipitation assays were performed and the resulting eluates were analysed using western blotting. NS4B was successfully detected when endogenous VCP was purified with anti-VCP antibodies (Figure 1a). As specificity controls, no NS4B was detected in the uninfected condition (mock) or when anti-HA antibodies were used while only marginal amounts of NS3 were non-specifically pulled-down. To confirm that NS4B and VCP associate during the life cycle, we performed proximity ligation assays (PLA), which allow the detection of protein–protein interactions (distance <40 nm) *in situ* using confocal microscopy. We used anti-VCP and cross-reactive anti-DENV NS4B antibodies for the assay and following amplification, VCP/NS4B interactions were visualised as white dots (Figure 1b). While very low abundance of positive signal was detected in the uninfected condition or when only one antibody was used in the assay, PLA signals were specifically visualised when cells were infected with ZIKV H/PF/2013 or the historical African strain MR766 (Figure 1c) confirming that NS4B and VCP associate in close proximity during the life cycle. Interestingly, the PLA dots were more abundant in MR766-infected cells than in the H/PF/2013 condition, implying an increased number of VCP/NS4B complexes. However, while both viruses produced comparable infectious titres after 2 days of infection (Figure S1A), such difference in VCP/NS4B interaction was not corroborated in co-immunoprecipitation assays with MR766 (Figure S1B). Of note, MR766 NS4B was not more expressed than H/PF/2013 NS4B in infected cells or than FSS13025 NS4B (sharing the same amino acid sequence as H/PF/2013 NS4B) in transiently transfected cells (Figure S1B,C). Importantly, we have also validated NS4B/VCP interaction with both strains using another anti-ZIKV NS4B in PLAs (Figure S1D). With this combination, no marked difference was observed between the two strains, highlighting that the sensitivity of PLA might be impacted by differences in the spatial organisation of the viral replication compartment (unpublished data). In contrast, no specific signal was detected in PLAs assessing VCP/NS1 association while weak but specific VCP/NS3 signal was detected (Figure S1E). Considering that NS3 was not co-immunoprecipitated with VCP (Figure 1a), this reflects that VCP/NS4B complexes may be located in the vicinity of NS3/NS4B complexes (Chatel-Chaix et al., 2015).

To determine whether NS4B/VCP interaction requires other ZIKV proteins, we transiently expressed HA-tagged NS4B with its 2K signal peptide (2K-NS4B-HA) or as a NS4A-NS4B precursor (NS4A-NS4B-HA) (Figure 1d) in Huh7.5-T7 cells (see Section 4). Overexpressed NS4B proteins were immunoprecipitated using anti-HA antibodies and resulting eluates were analysed using western blotting (Figure 1e). While no VCP was detected when the empty vector was transfected or untagged NS4A-NS4B protein was expressed, it specifically co-purified with 2K-NS4B-HA or NS4A-NS4B-HA demonstrating an interaction between transiently expressed proteins. Overall, these data demonstrate that NS4B and VCP associate even in the absence of other ZIKV proteins.

2.2 | VCP ATPase activity regulates ZIKV life cycle

To test whether VCP is a host dependency factor for ZIKV replication, we overexpressed an HA-tagged VCP dominant-negative mutant, which harbours E305Q and E578Q mutations in the ATPase domains D1 and D2 (VCP DN; Figure 2a), respectively, resulting in the impairment of VCP hexamer enzymatic activity (Tresse et al., 2010). To this end, Huh7.5 cells were transduced with lentiviruses whose delivered genome encoded either VCP DN or wild type VCP as control. VCP-HA expression was confirmed 4 days post-transduction using western blotting (Figure 2b). To monitor a potential impact on viral replication, 2-day transduced cells were infected with ZIKV H/PF/2013 and 48 hr later, extracellular infectious titres were determined using plaque assays. In these conditions, VCP overexpression did not induce any cytotoxicity regardless of low MOI ZIKV infection (Figure S2A). In contrast to VCP wt, when VCP DN was overexpressed, the production of infectious particles was reduced by about 70% (Figure 2c) indicating an impairment of ZIKV replication. To confirm that the ATPase activity of VCP was required for its regulatory role in ZIKV replication, we treated Huh7.5 cells infected with ZIKV H/PF/2013 for 24 hr with 50 nM of NMS-873, a selective allosteric non-ATP-competitive inhibitor of VCP ATPase activity (Magnaghi et al., 2013). A total of 48 hr

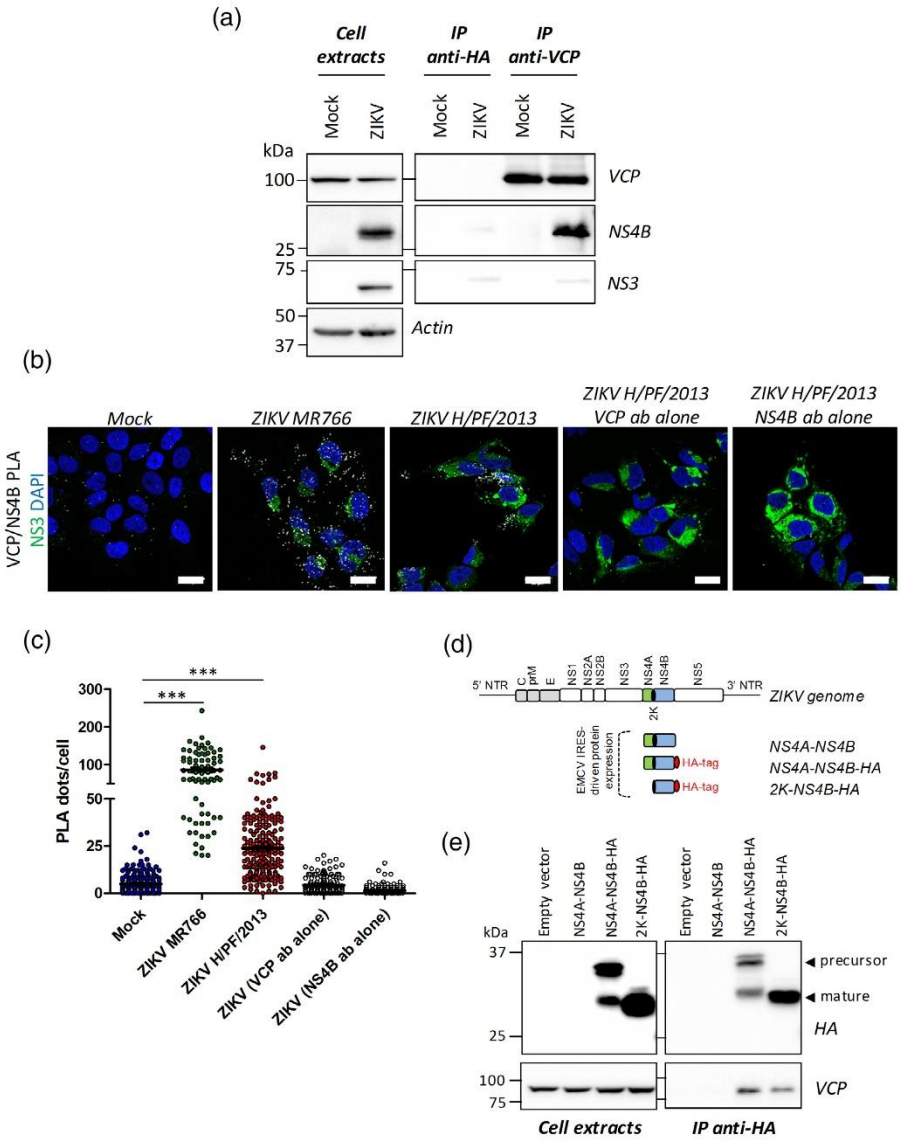

FIGURE 1 ZIKV NS4B interacts with valosin-containing protein (VCP). (a) Huh7.5 cells were infected with ZIKV H/PF/2013 (MOI = 10) or left uninfected. Seventy-two hours post-infection, cell extracts were prepared and subjected to immunoprecipitation with mouse anti-VCP antibodies or mouse anti-HA antibodies as specificity control. Resulting eluates and cell extracts were analysed by western blotting using the indicated antibodies. (b) Huh7.5 were infected with ZIKV H/PF/2013 (MOI = 5), ZIKV MR766 (MOI = 1) or left uninfected. Forty-eight hours post-infection, cells were fixed, subjected to proximity ligation assays (PLA) using ZIKV-cross-reactive rabbit anti-DENV NS4B and mouse anti-VCP antibodies and analysed using confocal microscopy. Single antibody PLA controls were performed with ZIKV H/PF/2013-infected cells. Infected cells were detected with rat anti-NS3 antibodies (green). Scale bars: 20 μm. (c) From two independent experiments, the amount of PLA puncta was quantified for each condition including single antibody staining controls. Mean with *SEM* are also indicated as black lines. ***p-value ≤ 0.001. (d) Schematic representation of different transfected EMCV IRES-driven ZIKV NS4B constructs used for the immunoprecipitation. The full-length polyprotein is shown as a reference. (e) Huh7.5-T7 cells were transfected with the indicated constructs. Eighteen hours post-transfection, cell extracts were prepared and subjected to immunoprecipitation with mouse anti-HA antibodies. Resulting eluates and cell extracts were analysed by western blotting using the indicated antibodies

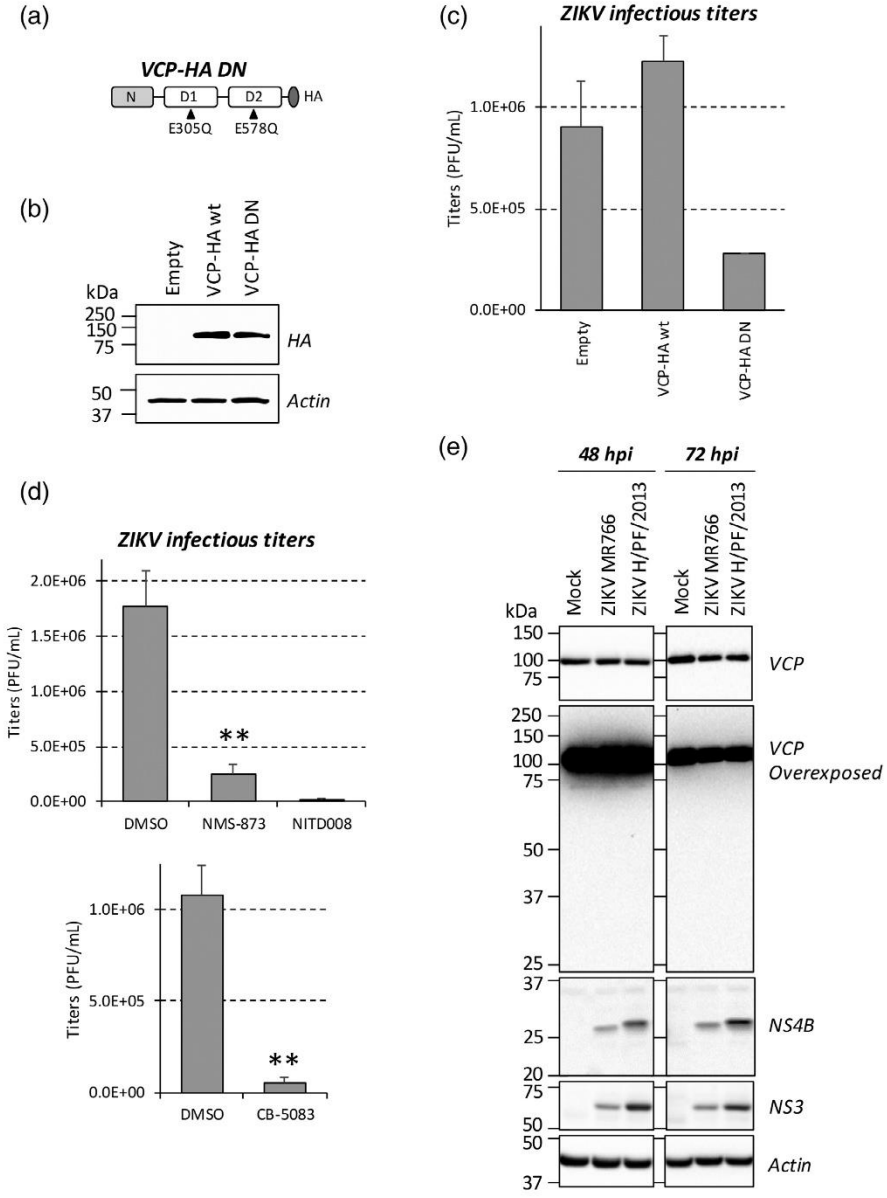

FIGURE 2 Valosin-containing protein (VCP) ATPase activity regulates ZIKV replication. (a) Schematic representation of the HA-tagged dominant-negative VCP mutant. (b) Huh7.5 cells were transduced with lentiviruses expressing VCP-HA wt or DN. Four days post-transduction, VCP-HA expression was analysed using western blotting. (c) Two days post-transduction, cells were infected with ZIKV H/PF/2013 (MOI = 0.1) and extracellular infectious titres were determined using plaque assays. (d) Huh7.5 cells were infected with ZIKV H/PF/2013 at a MOI of 0.1 and treated 24 hr later with 50 or 500 nM of the VCP ATPase inhibitors NMS-873 or CB-5083, respectively. Forty-eight hours post-infection (24-hr treatment), infectious viral titres were determined using plaque assays. Treatment with the NS5 polymerase inhibitor NITD008 was used as a positive control. $^{**}p$-value < 0.01. (e) Huh7.5 cells were infected with ZIKV MR766, ZIKV H/PF/2013 (MOI = 1) or left uninfected. Forty-eight and 72 hr post-infection, cell extracts were prepared and the expression of the indicated proteins was analysed by western blotting using the indicated antibodies. Anti-DENV NS3 and anti-DENV NS4B antibodies that are cross-reactive for ZIKV proteins were used

post-infection, infectious viral titres were determined by plaque assays (Figure 2d). The viability of uninfected cells or cells infected with ZIKV at low MOI was not impacted at this concentration of NMS-873 (Figure S2B). NMS-873-mediated VCP inhibition led to a significant decrease in ZIKV titres validating the important role of this host factor during viral replication. Confirming the specific VCP dependency of ZIKV replication, the same phenotype was obtained when infected cells were treated with CB-5083, an ATP-competitive highly selective inhibitor of VCP, which exhibits a different mode-of-action than NMS-873 and was recently challenged in patients for cancer treatment (Figure 2d; Anderson et al., 2015; Le Moigne et al., 2017; Zhou et al., 2015). As control, treatment with the flaviviral NS5 inhibitor NITD008 (Deng et al., 2016; Yin et al., 2009) almost completely abrogated viral replication. Finally, similar dependency phenotypes were observed when cells were infected with the historical ZIKV strain MR766 and treated with the VCP inhibitors (Figure S2C).

2.3 | VCP accumulates into NS4B-positive sub-structures in ZIKV-infected cells

We next evaluated whether ZIKV influences the cellular distribution of VCP during the infection using confocal microscopy. In uninfected cells, VCP showed a diffuse distribution throughout the cells without obvious accumulation in any specific compartment (Figure 3a). Strikingly, in ZIKV H/PF/2013-infected cells, a fraction of VCP did redistribute into large cytoplasmic NS4B-positive foci, which also contained NS3 (Figure 3a,b). This did not correlate with any changes in VCP expression or appearance of shorter byproducts (potentially generated by NS3 protease activity) over 3 days of infection as monitored by western blotting (Figure 2e). Importantly, VCP similarly colocalised with transiently expressed HA-tagged 2K-NS4B or NS4A-NS4B (Figure 4) suggesting that NS4B induces VCP redistribution in infected cells through their interaction independently of other viral proteins.

It is well accepted that large ultrastructures induced by flaviviruses observed by confocal microscopy are constituted of remodelled ER that contains viral replication organelles. In case of DENV, the large puncta visualised in Huh7 cells by fluorescence microscopy that contained both NS4B and NS3 were demonstrated to be CMs using correlative light-electron microscopy (Chatel-Chaix et al., 2016). This strongly supports that the large NS4B/NS3/VCP-positive ZIKV-induced structures actually are CMs.

2.4 | VCP ATPase activity is important for ZIKV replication factory stability

Considering that VCP accumulates into ZIKV RFs, we have tested the hypothesis that its ATPase activity regulates the biogenesis of these NS4B-rich cytoplasmic structures using a pharmacological inhibition approach. We chose this strategy instead of the 24-hr-long VCP downregulation approach since the latter resulted in a viral replication decrease (Figure 2d). Hence, in such context, we would not be able to rule out that any vRF-related phenotype would result from a decreased input of viral proteins. To test our hypothesis, Huh7.5 cells were infected with ZIKV H/PF/2013. At 48 hr post-infection, a time point in which RF are established (Cortese et al., 2017), cells were treated for only 4 hr with high concentrations of NMS-873. Cells were then fixed and prepared for imaging using confocal or transmission electron microscopy. While NS4B-positive cytoplasmic puncta were expectedly observed in DMSO-treated cells, they appeared to be less abundant and smaller upon NMS-873 treatment (Figure S3A). As control, viral dsRNA, the viral replication intermediate, was still readily detected in infected cells and a relatively short treatment with NMS-873 did not drastically decrease overall polyprotein expression as monitored by the detection of mature proteins by western blotting (Figure 5a). We also controlled that NMS-873 treatment did not decrease the levels of NS4B when either transiently or stably expressed by plasmid transfection or lentivirus transduction, respectively (Figure S3B,C). This indicates that 4 hr-long VCP inhibition seems to specifically impact NS4B puncta stability rather than on NS4B expression or overall replication. Most importantly, when analysed at the ultrastructural level using transmission electron microscopy, the architecture of ZIKV vRFs in NMS-873-treated cells was strikingly altered (Figure 5b). Indeed, CM size and abundance were significantly reduced in NMS-873-treated cells (Figure 5d,e). The remaining CM exhibited a relaxed morphology with less tightly packed ER membranes as compared to the DMSO control (Figure 5b, middle row, left panel). Upon NMS-873 treatment, we also observed accumulation of small vesicles often located in the perinuclear region (Figure 5b, middle row, middle and right panels), which might originate from disrupted CMs. We also observed an alteration of ZIKV CM morphology, size and abundance when VCP activity was inhibited with CB-5083 while NS4B expression remained unchanged upon treatment (Figures 5b,c,f,g and S3B,C). Interestingly, in this specific case, we could often detect residual CMs exhibiting a long and thin architecture with 'zipper-like' organised membranes (Figure 5b, bottom row, middle and right panels). While the stability of CMs was clearly impaired with either inhibitor treatment, these differences of morphology between NMS-873 and CB-5083 might reflect their different modes-of-action (allosteric vs. ATP-competitive). Finally, in contrast to the infected control condition (Figure 5b, upper right panel), we could not find any VPs in cells treated with NMS-873 or CB-5083. This phenotype was obvious but low preservation and occurrence of VPs in DMSO-treated cells did not allow for statistically reliable quantification. Altogether, these data show that VCP ATPase activity is important for ZIKV CM maintenance.

2.5 | ZIKV-induced mitochondria elongation depends on VCP ATPase activity

Both ZIKV and DENV induce the elongation of mitochondria (Barbier et al., 2017; Chatel-Chaix et al., 2016). In case of DENV, this

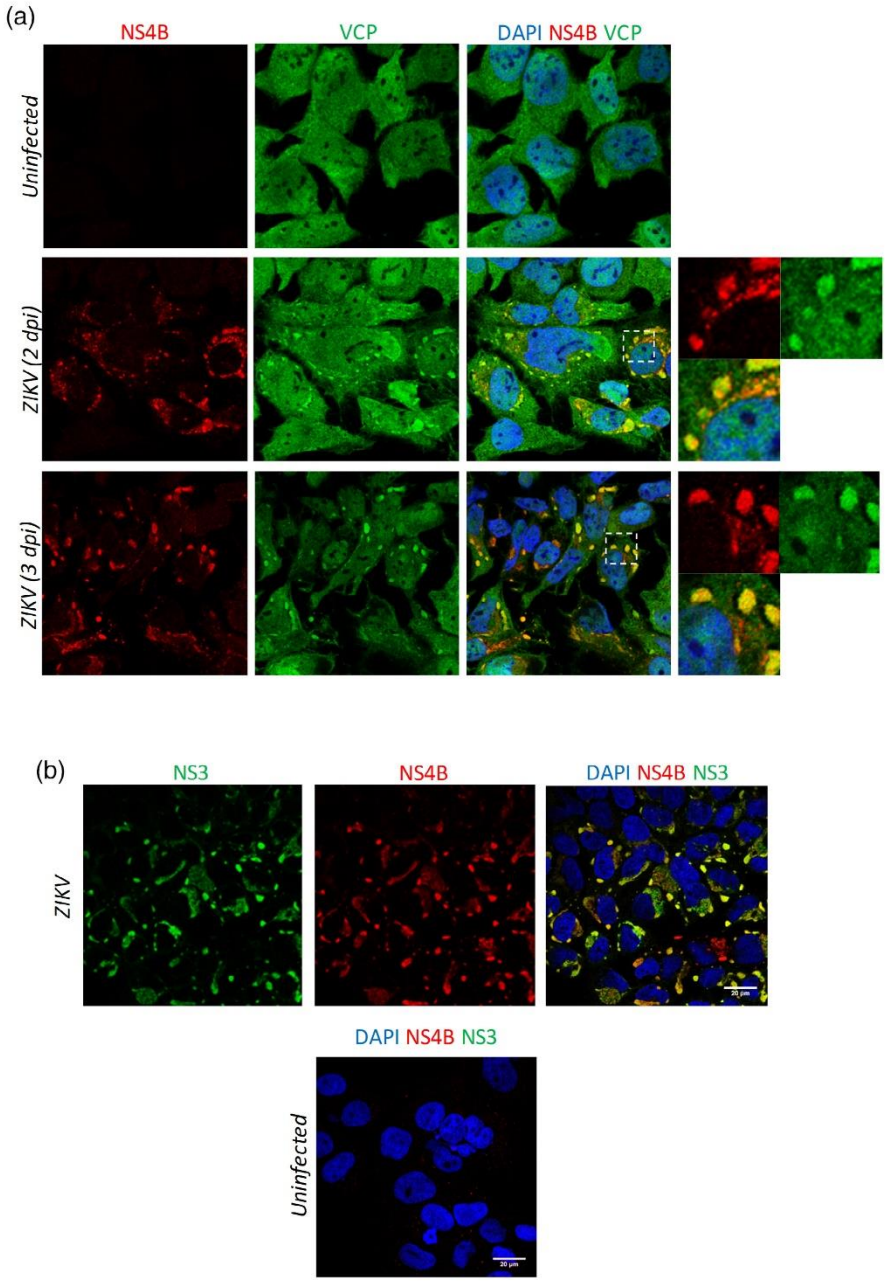

FIGURE 3 ZIKV NS4B induces the redistribution of valosin-containing protein (VCP) into large cytoplasmic structures. (a) Huh7.5 cells were infected with ZIKV H/PF/2013 (MOI = 1) or left uninfected. Forty-eight and 72 hr post-infection, cells were fixed, labelled with anti-VCP and anti-NS4B antibodies and observed by confocal microscopy. The right panels show a magnification of an infected cell. (b) Cells were treated as in (a) and labelled 3 days post-infection with anti-NS3 and anti-NS4B antibodies before imaging

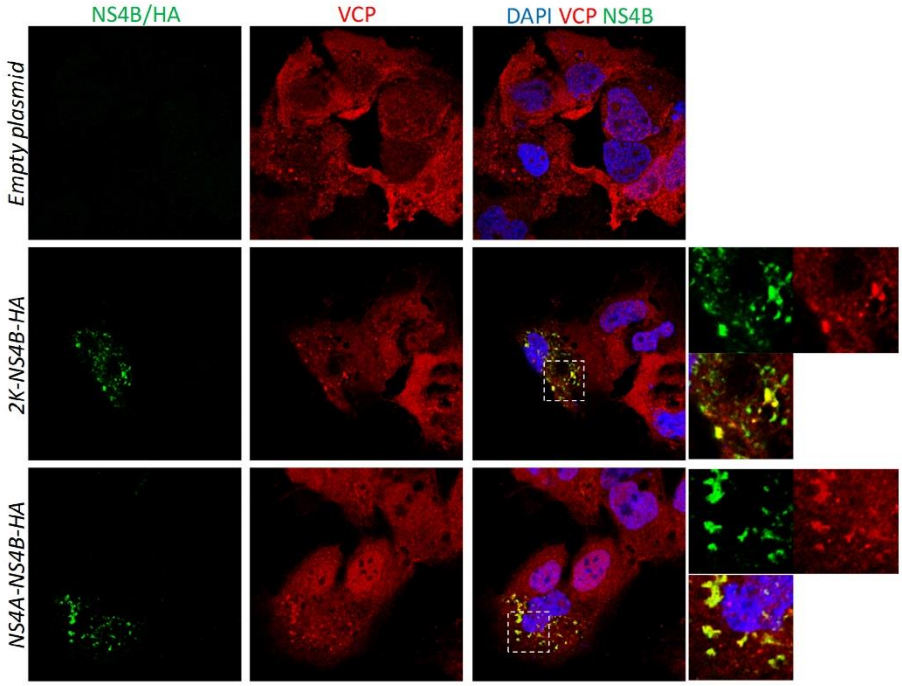

FIGURE 4 Valosin-containing protein (VCP) colocalises with ZIKV NS4B when expressed alone. Huh7.5-T7 cells were transfected with the indicated constructs. Eighteen hours post-transfection, cells were fixed, labelled with anti-VCP and anti-NS4B or anti-HA antibodies and observed by confocal microscopy. The right panels show a magnification of a transfected cell

phenotype is recapitulated upon NS4B transient expression while elongated mitochondria make physical contacts with CM and regulate their biogenesis. Moreover, it was showed that mitochondrial elongation favours ZIKV and DENV replication (Chatel-Chaix et al., 2016). Considering that VCP inhibition disrupts CMs and potentially the CM/mitochondria interface, we investigated whether this correlated with a loss of ZIKV-induced modulation of mitochondrial morphodynamics as well. ZIKV-infected cells were treated with NMS-873 exactly as above and analysed for mitochondrial morphology using antibodies directed against the mitochondrial heat shock protein GRP75 (Figure 6). As expected, when cells were treated with DMSO, ZIKV infection induced a marked elongation of mitochondria as compared to uninfected cells. When infected cells were treated with NMS-873, the NS4B/NS3 puncta were reduced in number and size consistent with the results described above. More importantly, the mitochondria elongation phenotype was lost in those cells since mitochondria morphology resembled the one observed in uninfected cells. This shows that VCP is important for ZIKV modulation of mitochondria morphodynamics and strongly supports the previously proposed model of a functional CM/mitochondria interface regulating ZIKV life cycle.

2.6 | VCP activity inhibits ZIKV-induced cell death by apoptosis

ZIKV is a cytopathic virus, which induces cell death at late time points of infection. On the one hand, mitochondria play a major role in apoptosis and their fragmentation has been often proposed to potentiate this process (Montessuit et al., 2010; Oettinghaus et al., 2016; Park, Ko, Hwang, & Koh, 2015). On the other hand, it was suggested that the communication between CMs and elongated mitochondria allows the attenuation of cellular processes potentially detrimental for optimal virus replication, such as innate immunity (Chatel-Chaix et al., 2016) or premature cell death. Considering that VCP inhibition resulted in CM destabilisation and loss of mitochondria elongation, we hypothesised that the disruption of this CM/mitochondria axis would result in enhanced cell death. To test this, we infected cells with ZIKV and treated them with NMS-873 for 4 hr as above. Cells were then labelled for NS3. Caspase 3/7 activity was detected using the CellEvent reagent and the % of cells with a ruptured plasma membrane (i.e. dead cells) was determined using LIVE/DEAD assays. All these parameters were quantified and analysed using flow cytometry. Using this NS3 detection assay, we

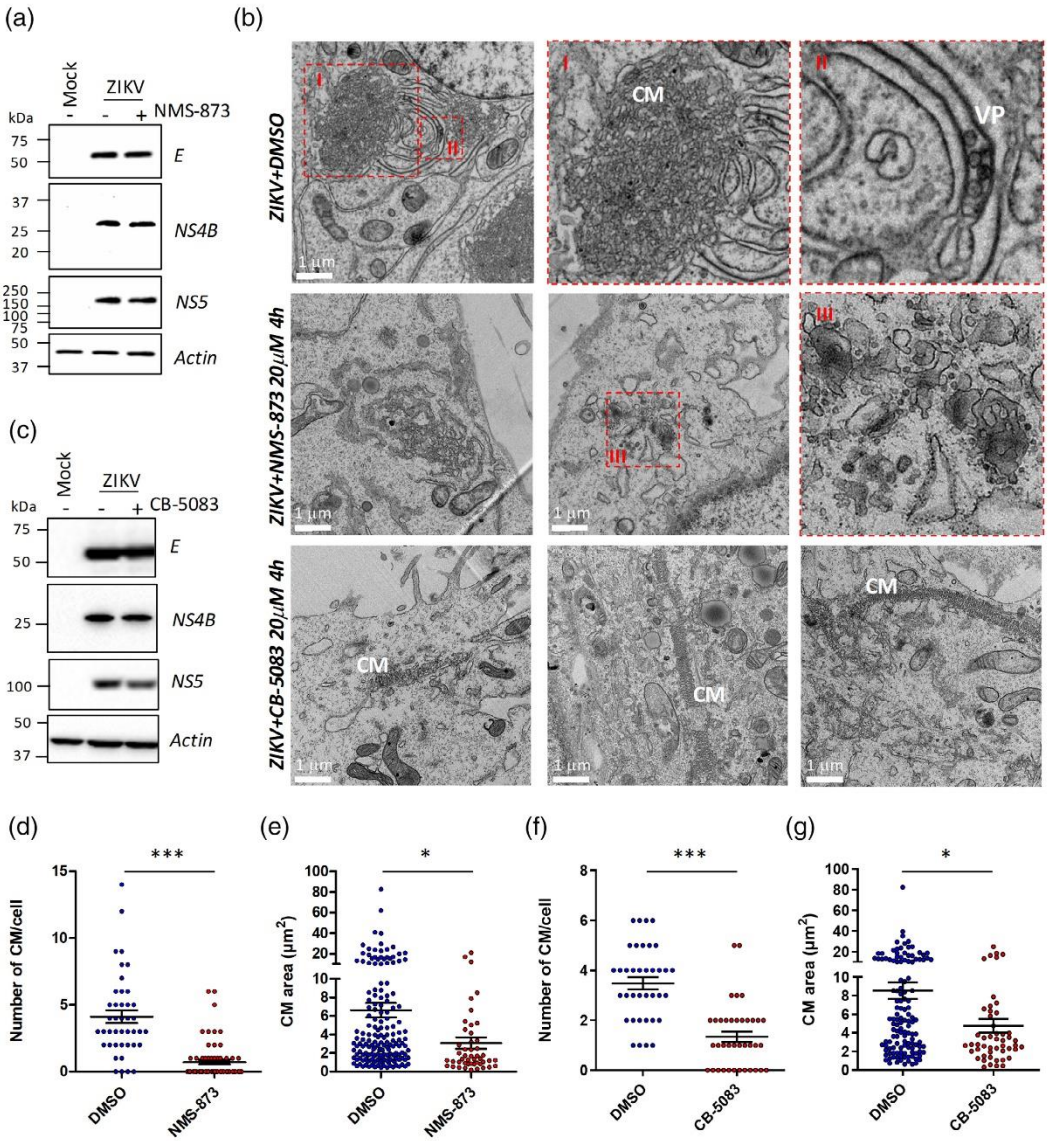

FIGURE 5 The inhibition of valosin-containing protein (VCP) ATPase activity alters ZIKV replication factories. (a,c) Huh7.5 cells were infected with ZIKV H/PF/2013 (MOI = 20) or left uninfected. Forty-eight hours post-infection, cells were treated with either DMSO, 20 μM NMS-873 (a) or 20 μM CB-5083 (c) for 4 hr. Viral protein content was analysed using western blotting. (b) Cells were treated exactly as in (a,c). After the 4-hr treatment with NMS-873 or CB-5083, cells were processed for transmission electron microscopy. Representative images for each condition are shown. From two independent experiments as in (b), the abundance (d) and size (e) of CMs of NMS-873-treated cells were analysed. Abundance (f) and size (g) of CMs in cells treated with CB-5083. Mean and *SEMs* were also determined and are indicated as black lines. **p*-value ≤ 0.05; ****p*-value ≤ 0.001. CM, convoluted membranes; VP, vesicle packets

determined that the infection efficiency was about 70% (Figure 7a). NMS-873 treatment of uninfected cells and ZIKV infection induced only minor cell death (Figure 7b). In a stark contrast, when the gating was performed on infected cells only (i.e. NS3+ cells), NMS-873 treatment increased the % of apoptotic dead cells (caspase 3/7+; live/dead+) from 0.4 to 4.26%. This VCP-dependent increase of

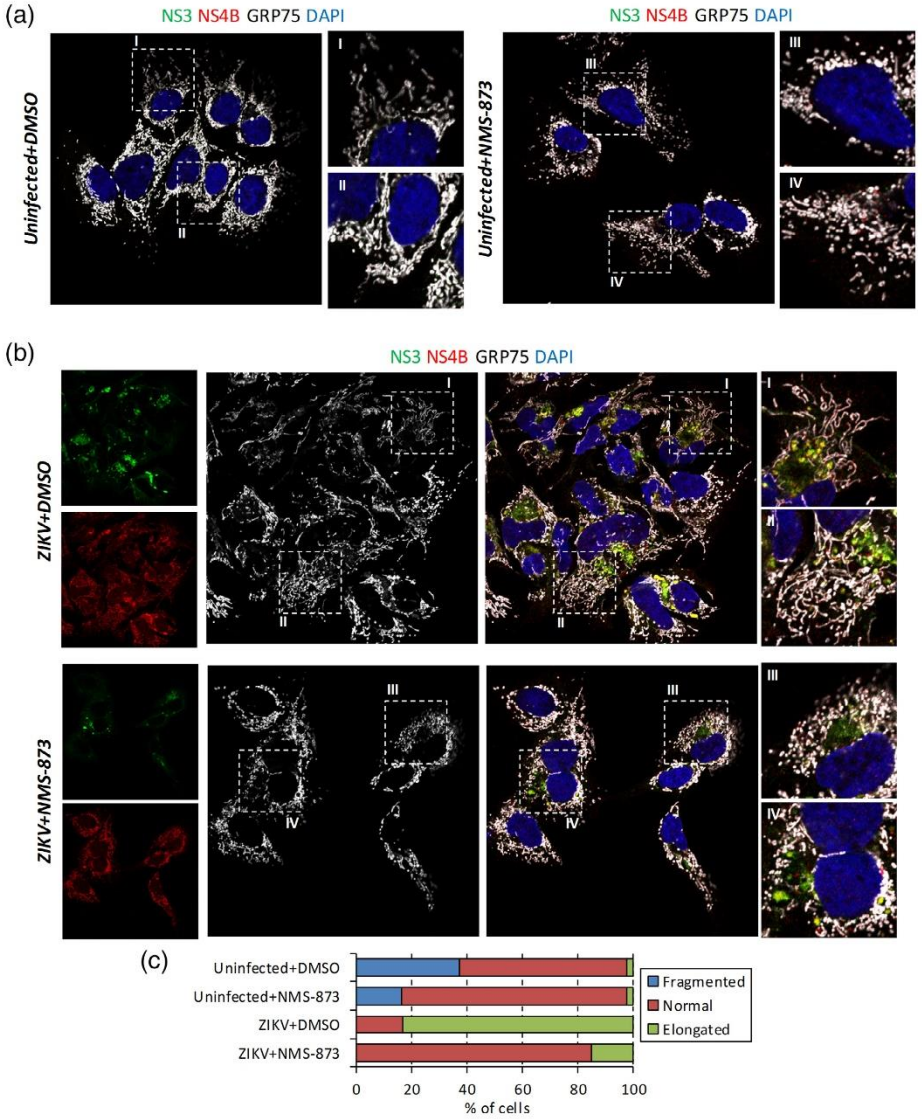

FIGURE 6 Valosin-containing protein (VCP) ATPase inhibition dampens ZIKV-dependent mitochondrial elongation. Huh7.5 cells were left uninfected (a) infected with ZIKV H/PF/2013 (MOI = 5; b). Forty-eight hours post-infection, cells were treated with either DMSO or 20 μM NMS-873 for 4 hr before fixation. Cells were then labelled with rabbit anti-ZIKV NS4B, rat anti-NS3 and mouse anti-GRP75 antibodies. GRP75 is used as a marker of mitochondria. Viral protein distribution and mitochondrial morphology were analysed using confocal microscopy. (c) Quantification of the mitochondria morphology phenotypes from (a,b)

caspase activation and of cell death in infected cells was representative of two experiments (Figure 7c,d). Consistently, when measured with a bioluminescent assay (Figure 7e), the ZIKV-dependent activity of caspase 3 was increased in 3-day infected cells that were treated with either NMS-873 or CB-5083 for 4 hr. In contrast, drug treatment resulted only on marginal induction of this activity in uninfected cells (1.6–1.9-fold as compared to DMSO). Overall, these results show that VCP activity is required to limit ZIKV-induced cytopathic effects, a process that most likely requires VCP-containing CMs.

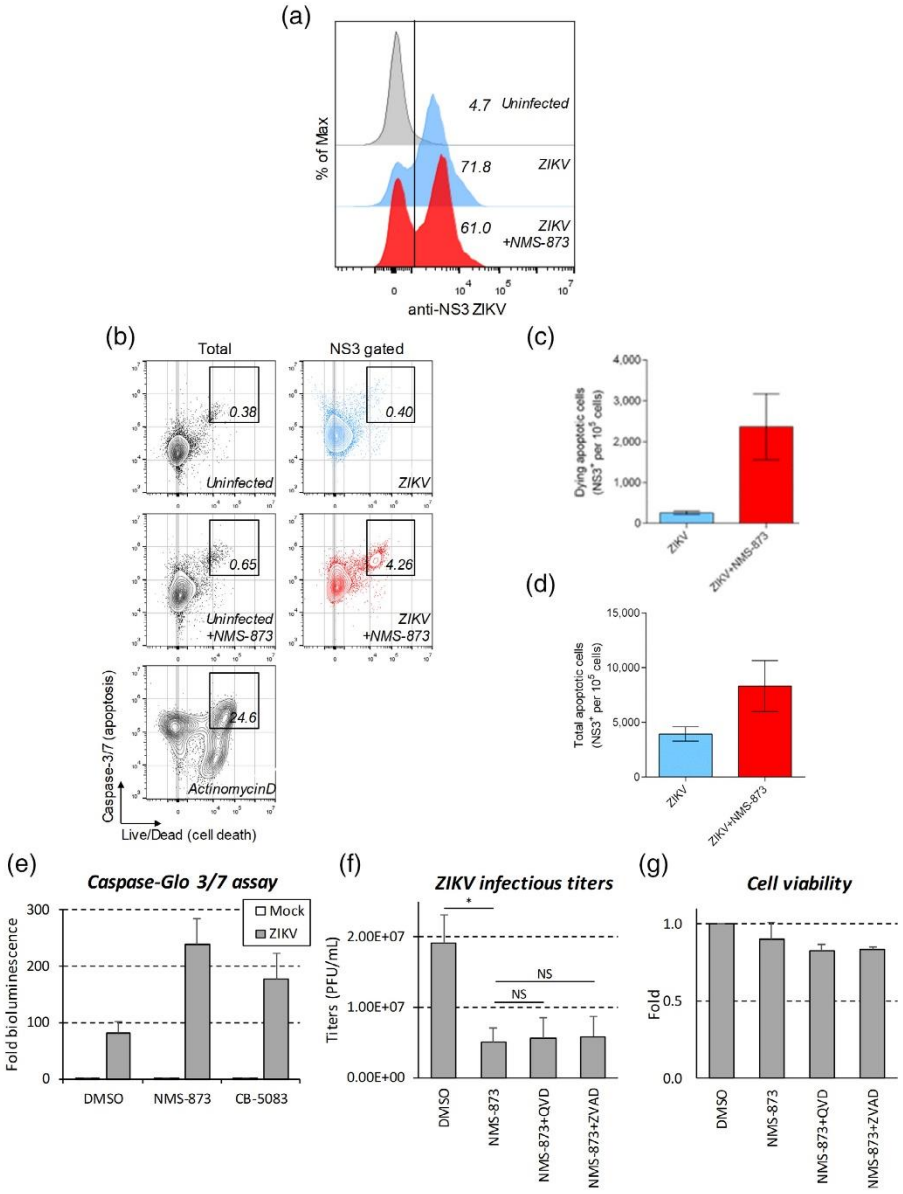

FIGURE 7 Valosin-containing protein (VCP) ATPase inhibition increases ZIKV-induced apoptosis. Huh7.5 cells were infected with ZIKV H/PF/2013 (MOI = 10) or left uninfected. Forty-eight hours post-infection, cells were treated with either DMSO or 20 μM NMS-873 for 4 hr. Cells were treated with LIVE/DEAD reagent and the CellEvent caspase-3/7 green before labelling with anti-NS3 antibodies and AlexaFluor secondary anti-rat antibodies. Fixed cells were then analysed by flow cytometry. A representative experiment is shown. (a) Analysis of the % of ZIKV-NS3 expressing cells. (b) Active caspase 3/7 and dead cell quantification. For the ZIKV infection condition, the analysis was performed on the NS3-positive cells. Actinomycin D treatment (2.5 μM, 24 hr) was performed as a positive control of apoptosis induction. (c,d) Determination of the abundance of (c) NS3-positive caspase 3/7+ dead cells and (d) total apoptotic infected cells compiled from two independent experiments. (e) Huh7.5 cells were infected with ZIKV H/PF/2013 (MOI = 10) or left uninfected. Seventy-two hours post-infection, cells were treated with DMSO, 20 μM NMS-873 or 20 μM CB-5083 for 4 hr and apoptosis induction was measured by measuring bioluminescence using the Caspase-Glo 3/7 assay kit. All values were normalised to the uninfected/DMSO condition. (f) Huh7.5 cells were infected with ZIKV H/PF/2013 at a MOI of 0.1 and treated 24 hr later with 50 nM NMS-873 alone or in combination with 20 μM VZAD or QVD (added 30 min before NMS-873). Forty-eight hours post-infection (24-hr treatment), infectious viral titres were determined using plaque assays. *p-value < 0.05; NS, not significant. (g) In parallel the impact of drug treatment on cell viability on uninfected cells was assessed using MTT assays

Finally, we investigated whether the reduction of ZIKV replication following the 24-hr treatment with NMS-873 (Figure 2d) was actually due to premature virus-induced apoptosis. We co-treated ZIKV-infected cells 24 hr post-infection with NMS-873 and pan-caspase inhibitors Z-VAD-FMK (ZVAD) or Q-VD-OPh (QVD). Twenty-four hours later (i.e. 2 days post-infection), ZIKV infectious titres levels were determined using plaque assays (Figure 7f). The combination of drugs was not toxic for the cells (Figure 7g). As expected from the results of Figure 2d, NMS-873 treatment reduced ZIKV production. Strikingly, treatments with caspase inhibitor did not rescue ZIKV replication, highlighting two independent roles of VCP in flaviviral replication and virus-induced cells death.

3 | DISCUSSION

In this study, we demonstrate that the AAA+ ATPase VCP/p97 is required for efficient ZIKV replication using both pharmacological inhibition and dominant-negative mutant expression approaches. VCP's main function is to target specific substrates to proteasome-mediated degradation. Hence, VCP dependency of ZIKV replication is consistent with the fact that proteasome activity is required for an efficient flavivirus life cycle *in cellulo* and *in vivo* (Choy, Sessions, Gubler, & Ooi, 2015; Gilfoy, Fayzulin, & Mason, 2009; Kanlaya, Pattanakitsakul, Sinchaikul, Chen, & Thongboonkerd, 2010; Xin et al., 2017).

We further show that VCP associates with ZIKV protein NS4B in both infected and NS4B-overexpressing cells. Such interaction appears to be conserved within the *Flavivirus* genus since it was previously identified in two independent large-scale DENV NS4B interactome analyses (Chatel-Chaix et al., 2016; Shah et al., 2018). However, before our study, VCP/NS4B interaction was never validated or characterised. Flaviviral NS4B is a crucial non-enzymatic viral replication co-factor although its precise functions during vRNA amplification remain enigmatic. It is believed that the expression and/or maturation of NS4B, as a transmembrane ER-resident protein, is important for the biogenesis of vRFs (Kaufusi, Kelley, Yanagihara, & Nerurkar, 2014; Miller et al., 2006; Miller, Kastner, Krijnse-Locker, Buhler, & Bartenschlager, 2007; Roosendaal, Westaway, Khromykh, & Mackenzie, 2006; Welsch et al., 2009). However, despite many attempts in the past, we could never clearly demonstrate that DENV NS4B expression alone induces CM biogenesis and such activity was never reported to our knowledge. This is most likely achieved through interactions between NS4B and host factors as well as NS3 and NS4A (Chatel-Chaix et al., 2015; Zou, Lee, et al., 2015; Zou, Xie, et al., 2015). Consistently, as shown for DENV in previous reports and for ZIKV in this study, both NS4B and NS3 colocalise in large cytoplasmic structures identified as CMs (Chatel-Chaix et al., 2016; Junjhon et al., 2014; Welsch et al., 2009). Hence, our data support the current model implicating NS4B in vRF biogenesis. Finally, the VCP/NS4B complex was detected upon single expression of 2K-NS4B, a condition in which CM were never reported. This suggests that complete CM morphogenesis is not required for this interaction.

VCP accumulation in large ultrastructures reminiscent of DENV CMs led to the hypothesis that this host factor might influence the stability of ZIKV CMs. To test this, we performed short treatments with NMS-873 or CB-5083, two different pharmacological inhibitors of VCP ATPase activity. In a 4-hr treatment set-up, no drastic effects on cell viability or in the levels of viral proteins were observed (Figure 5a,c). This indicates that the observed phenotypes on vRFs were not due to defects in overall replication or polyprotein input at that time point. Very interestingly, NMS-873 and CB-5083 treatments had drastic impacts on the morphology, size and abundance of CMs in ZIKV-infected cells as observed in TEM micrographs (Figure 5). This suggests that VCP ATPase activity is important for the stability and/or the biogenesis of CMs. Interestingly, live cell imaging of CMs in DENV-infected cells previously showed that the morphology of this vRF sub-structure is highly dynamic since their size can increase or decrease within a few hours. CM fusion and division events could also be observed (Chatel-Chaix et al., 2016). VCP was previously shown to be important for the replication of West Nile virus (WNV), another neurotropic *Flavivirus* and the *Hepacivirus* hepatitis C virus (HCV), both belonging to the *Flaviviridae* family like ZIKV (Phongphaew et al., 2017; Yi et al., 2016; Yi & Yuan, 2017). However, in the case of WNV, no viral partner was identified and the molecular functions of VCP were not deeply investigated. Pharmacological inhibition of VCP inhibits HCV replicase activity and induces an aggregation of VCP-interacting viral protein NS5A (Yi & Yuan, 2017). NS5A is a component of HCV vRF, namely double-membrane vesicles and is a crucial co-factor of their morphogenesis as well as of viral replication (Berger et al., 2014; Romero-Brey et al., 2012). Although potential contributions of VCP in HCV or WNV vRF fate were never reported, it is tempting to speculate based on our results that VCP contribution to the biogenesis of vRFs overlaps with several *Flaviviridae* family members. While this study was under evaluation, Ramanathan et al. (2020) reported a novel and nicely designed yellow fever virus (YFV) entry assay that they used to demonstrate that VCP inhibition impairs a post-fusion pre-translation step of the life cycle. Since NS4B is not expressed and vRFs are absent during flavivirus entry, this VCP function is not related to the one described here. This further suggests that flaviviruses co-opt VCP during multiple steps of the life cycle.

VCP was shown to be important for the maturation of autophagosomes, more precisely in their targeting to lysosome in which their cargo is degraded (Chou et al., 2011; Ju et al., 2009; Tresse et al., 2010). Several studies have shown that autophagy is induced during ZIKV and other flavivirus infection (Chiramel & Best, 2018; Hamel et al., 2015; Heaton & Randall, 2010; Ke, 2018; Lee et al., 2008; Metz et al., 2015). In the case of ZIKV, the combined expression of NS4B and NS4A or of the NS4A-NS4B precursor induces autophagy (Liang et al., 2016). In DENV-infected cells, the fusion between autophagosomes and lysosomes is inhibited resulting in the stabilisation of the cargo (Metz et al., 2015). If this is also true for ZIKV, one might hypothesise that VCP is hijacked to CM to modulate its activity in the late steps of autophagy and prevent the degradation of viral proteins by the autophagy machinery. In addition, using

a comparative proteomic analysis using VCP inhibitors, it was shown that the ER-shaping protein reticulon (RTN) 4 is a specific substrate of VCP (Heidelberger et al., 2018). More recently, one study has shown that another reticulon protein RTN3.1A is an important regulator of WNV, ZIKV and DENV vRF biogenesis and/or morphology (Aktepe, Liebscher, Prier, Simmons, & Mackenzie, 2017). Hence, it is conceivable that VCP implication in CM maintenance is linked to its activity towards host factors involved in ER membrane curvature.

The disruption of CMs upon VCP inhibition correlated with a loss of mitochondrial elongation usually induced by ZIKV. These data are in line with the model envisioning a morphological and functional interplay between CMs and mitochondria. Indeed, in the case of DENV, it was previously shown that ER-derived CMs and elongated mitochondria establish physical contacts. In addition, genetic or chemical induction of mitochondria fragmentation severely impacts the morphogenesis and the stability of DENV-induced ER-derived CMs (Chatel-Chaix et al., 2016). Interestingly, several studies have shown that VCP is important for mitophagy (i.e. autophagy of mitochondria) during which VCP is translocated to this organelle (Kim et al., 2013; Kimura et al., 2013; Zhang et al., 2017). This is generally associated with a global and massive fragmentation of mitochondria, which is attributed to the VCP-mediated retrotranslocation and degradation of mitofusin protein (MFN) 1 and 2. In addition, because MFN2 is also involved in ER/mitochondria contacts through dimerisation, VCP also alters the reticulo-mitochondrial interface during that process (McLelland et al., 2018). While we show that VCP partly redistributes to structures resembling CM in infected cells, we never noticed any recruitment to mitochondria, a hallmark of VCP action during mitophagy. Hence, VCP sequestration within CM might counteract its function in mitophagy in order to maintain mitochondria in an elongated state, which was shown to be favourable to ZIKV replication (Chatel-Chaix et al., 2016). In addition, such hijacking might favour the biogenesis of CMs given that they might partly originate from mitochondria-associated ER membranes. More importantly, we show here that VCP inhibition stimulates ZIKV-induced cell death. This supports the model that CMs, in contact with elongated mitochondria, allow to buffer death signals induced by the infection. We propose that upon VCP inhibition-induced CM destabilisation, mitochondrial elongation is not maintained, hence leading to fission, a context reported to favour cell death by apoptosis (Montessuit et al., 2010; Oettinghaus et al., 2016; Park et al., 2015). This is consistent with a recent study showing that ZIKV-infected cells delay chemically induced apoptosis as compared to uninfected cells (Turpin, Frumence, Despres, Viranaicken, & Krejbich-Trotot, 2019). Concomitantly with innate immunity dampening (Chatel-Chaix et al., 2015), the control of cell death by the CM/mitochondria functional unit would provide a cellular environment and a temporal window to the virus to optimally replicate. Finally, VCP is a multifunctional protein involved in protection during stress conditions but it is accepted that its co-factors drive the specificity of its activity (Bandau, Knebel, Gage, Wood, & Alexandru, 2012; den Besten, Verma, Kleiger, Oania, & Deshaies, 2012; Meyer & Weihl, 2014; Schuberth & Buchberger, 2008; Ye et al., 2001; Yeung et al., 2008). Hence, it will be interesting to investigate whether ZIKV infection modifies VCP interactome, which could reprogram its activity to delay virus-induced death signals.

Given that VCP has already been shown to be involved in neuronal development and several diseases of both peripheral and central nervous system (Halawani et al., 2009; Imamura et al., 2012; Meyer & Weihl, 2014; Niwa et al., 2012; Stach & Freemont, 2017; van den Boom & Meyer, 2018; Watts et al., 2004; Weihl et al., 2006), this suggests that ZIKV hijacks VCP functions to impair the differentiation of the infected neural progenitor cells and hence, fetal brain development. This raises the hypothesis that VCP might potentially represent a novel antiviral target to limit ZIKV neurovirulence. Interestingly, while most VCP inhibitors are not suitable for treatments in mammals due to low bioavailability and high clearance, CB-5083 is effective in mice and has been challenged in phase I clinical trials for treatment of cancer (in which VCP activity is increased) (Anderson et al., 2015; Le Moigne et al., 2017; Zhou et al., 2015). While this trial was stopped because CB-5083 caused visual loss, a more selective and bioavailable analog, CB-5339 is planned to be tested soon in patients (Doroshow, Parchment, & Moscow, 2018; Huryn, Kornfilt, & Wipf, 2019). It will be relevant in future studies to evaluate whether these VCP inhibitors alleviate ZIKV replication and congenital neuropathogenesis in murine models. If the new generation VCP inhibitor CB-5339 protects against ZIKV *in vivo* and is safe for humans, this drug may be considered for a repurposing for anti-ZIKV therapeutic or prophylactic treatments. In the same line of idea, it would be interesting to study the impact of familial pathological mutations of VCP on the severity of ZIKV-caused symptoms. In the case of a putative correlation between these two, it would be tantalising to speculate that genetic polymorphisms in infected foetuses may help to predict ZIKV neurovirulence as well as the appearance and the outcome of brain development defects.

4 | EXPERIMENTAL PROCEDURES

4.1 | DNA cloning

To generate NS4A/NS4B expression constructs, PCR was performed using as template the ZIKV molecular clone pFL-ZIKV-WT containing the sequence of the 2010 FSS13025 Cambodian strain (Shan et al., 2016). Resulting amplified DNA fragments were inserted into the NcoI/SpeI cassette of pTM1 plasmid (Chatel-Chaix et al., 2016). This plasmid expresses a RNA of interest under the control of the T7 RNA polymerase promoter (see below). In the absence of a cap and a poly-A tail, ZIKV protein expression is driven by an internal ribosome entry site. Primers encoding the HA-tag sequence were used for PCR to insert the tag at the C terminus of NS4B (NS4B-HA) or the N-terminus of NS4A. Of note, ZIKV FSS13025 NS4B and NS4A amino acid sequences are 100% similar to the ones of the ZIKV H/PF/2013 protein counterparts. 2K-NS4B-HA PCR products were also cloned into the AscI/SpeI cassette of pWPI lentiviral vector. To clone ZIKV MR766 2K-NS4B, viral RNA was extracted from 10^6 ZIKV MR766 infectious particles using the RNeasy mini kit (Qiagen) and subjected to RT-PCR using the SuperScript IV VILO Master Mix RT kit (Life

Technologies). Resulting cDNA was used as template for PCR to generate MR766 2K-NS4B-HA DNA, which was clone into the NcoI/SpeI cassette of pTM1 plasmid. Complete sequencing of the insert confirmed that the cloned sequence was 100% identical to the one expected (Genbank ID: DQ859059). VCP(wt)-EGFP and VCP(DKO)-EGFP plasmids, a gift from Nico Dantuma (Addgene plasmid # 23971 and 23974; http://n2t.net/addgene:23971; RRID:Addgene_23971; http://n2t.net/addgene:23974; RRID:Addgene_23974) (Tresse et al., 2010), were used as PCR templates to amplify VCP wt and DN coding sequences, respectively. To C-terminally fuse VCP with the HA-tag, the coding sequence of the latter was contained in the one of the primers. PCR product were cloned into the AscI/SpeI cassette of pWPI. Primers sequences are available upon request.

4.2 | Cells, viruses and reagents

293T, VeroE6 and hepatocarcinoma Huh7.5 cells (a kind gift from Patrick Labonté) were all cultured in DMEM (Thermo-Fisher) supplemented with 10% fetal bovine (Wisent), 1% non-essential amino acids (Thermo-Fisher) and 1% penicillin–streptomycin (Thermo-Fisher).

Huh7.5-T7 cells were generated by transduction of Huh7.5 with lentiviruses expressing T7 RNA polymerase and were cultured in the presence of 5 μg/mL blasticidin (Thermo-Fisher). This cell line allows for cytoplasmic transcription of genes under the control of the T7 promoter, hence avoiding a nuclear step, which is detrimental for the expression of ZIKV proteins because of cryptic splicing sites. Thus, this mimics normal protein expression from the viral genome.

ZIKV H/PF/2013 and ZIKV MR766 strains were provided by the European Virus Archive goes Global. Virus stocks were generated by amplification in Vero cells following inoculation with an MOI of 0.01. Virus aliquots were stored at −80°C until use. Infectious titres were determined by plaque assays.

NMS-873, Z-VAD-FMK and Q-VD-OPh were obtained from Millipore-Sigma. CB-5083 was purchased from Selleck Chemicals. Mouse monoclonal anti-VCP (ab11433) was purchased from Abcam. Rabbit anti-DENV NS4B (GTX124250; cross-reactive for ZIKV), rabbit anti-ZIKV NS4B (GTX133311), rabbit anti-ZIKV NS1 (GTX133307), rabbit anti-ZIKV NS3 (GTX133309) and mouse monoclonal anti-DENV NS3 (GTX629477; cross-reactive for ZIKV) were all obtained from Genetex. Rat polyclonal antibodies targeting DENV2 16681 NS3, which are cross-reactive with ZIKV NS3 were generated at Medimabs, Montréal, Canada. Four Wistar rats were immunised with RRGRIGRNPKNENDQY (residues 457–472) and REIPERSWNSGHEWV (residues 337–351) NS3 KLH-coupled peptides, which were designed by Medimabs to maximise immunogenicity and minimise the generation of nonspecific antibodies. Immunisation was performed according to the regulation of the CCAC. Rats were subjected to a first intraperitoneal injection with complete Freund's adjuvant followed by three intraperitoneal injections with incomplete Freund's adjuvant. After a final intravenous boost, rat sera were collected and pooled. Polyclonal antibodies were purified by immunogen affinity.

4.3 | Lentivirus production, titration and transduction

Overexpression of VCP was achieved through transduction with lentiviruses encoding wild type or dominant-negative HA-tagged VCP proteins. For production of lentivirus stocks, sub-confluent 293T cells were transfected with packaging plasmids pCMV-Gag-Pol, pMD2-VSV-G and VCP-HA-encoding pWPI using 25 kDa linear polyethylenimine (Polysciences Inc.). Two days post-transfection, lentivirus-containing medium was collected and filtered. Lentiviruses were titrated by transducing HeLa cells and subsequent treatment with 1 μg/mL puromycin. Five days later, cells were fixed and stained with 1% crystal violet/10% ethanol for 15–30 min. Stained cells were rinsed with water, colonies were counted and titres calculated taking into account inoculum dilution. Transductions were performed by using a MOI of 1 for Huh7.5 cells in the presence of 8 μg/mL polybrene. The same experimental procedure was performed to produce 2K-NS4B-HA-expressing lentiviruses.

4.4 | Cell viability assays

Cell viability was evaluated using MTT assays. Huh7.5 were plated in 96-well plates (7,500 cells per well) and transduced or drug-treated as indicated. Four days later, 20 μL of 3-(4,5-dimethylthiazol-2-yl)-2,5-diphenyltetrazolium bromide (MTT) at 5 mg/mL was added in the medium for 1 to 3 hr at 37°C medium was removed and 150 μL of 2% (v/v) of 0.1 M glycin in DMSO (pH 11) was added to dissolve the MTT precipitates. Absorbance at 570 nm was read with Spark multi-mode microplate reader (Tecan) with the reference at 650 nm.

4.5 | Plaque assays

2.10^5 VeroE6 cells were seeded in 24-well plaques. The day after, cells were infected in duplicates with 200 μL virus samples that had been serially diluted 10^1 to 10^6 fold in complete DMEM. Two hours post-infection, the media was removed and cells were cultured at 37°C with serum-free MEM (Life Technologies) containing 1.5% carboxymethylcellulose (Millipore-Sigma). After 5 days, cells were fixed during 2 hr in 5% formaldehyde. After several washes with tap water, cells were stained with 1% crystal violet/10% ethanol for 15–30 min. Stained cells were gently washed with tap water, plaques were counted and titres of infectious virus were calculated in PFU/mL.

4.6 | Transfection

For co-immunoprecipitation assays, Huh7.5-T7 cells were cultured in 10 cm petri dishes (2.10^6 cells per petri dish) and transfected with 12 μg of DNA and 36 μL of TransIT-LT1 Transfection Reagent (Mirus, Madison, WI, USA) according to the manufacturer's instructions. After 4 hr of transfection, the culture medium was changed. Cells were

collected 18–20 hr post-transfection. For immunofluorescence studies, Huh7.5-T7 cells were cultured on glass coverslips in a 24-well plates (25,000 cells per well) and transfected with 0.5 μg of pTM-based plasmid and, 1.5 μL TransIT-LT1 Transfection Reagent (Mirus, Madison, WI) according to the manufacturer's instructions. Cells were treated exactly as described above.

4.7 | Immunofluorescence-based confocal microscopy

Infected or transfected cells were grown on glass coverslips, washed twice with PBS, fixed with 4% paraformaldehyde in PBS and permeabilised with PBS-0.2% Triton X-100 for 15 min. After 1 hr of blocking with PBS containing 5% bovine serum albumin (BSA) and 10% goat serum (Thermo-Fisher), coverslips were incubated with primary antibodies for 2 hr at room temperature in the dark. The cells were washed three times in PBS and incubated with Alexa Fluor (488, 568 or 647)-conjugated secondary antibodies (Life Technologies) for 1 hr at room temperature in the dark. The coverslips were subjected to three 15-min washes with PBS, and the nuclei were stained with 4′, 6′-diamidino-2-phenylindole (DAPI; Life Technologies). After three rapid final washes with PBS, the coverslips were mounted on slides with FluoromountG (Southern Biotechnology Associates). The cells were examined, and images were acquired using a LSM780 confocal microscope (Carl Zeiss Microimaging) at the Confocal Microscopy Core Facility of the INRS-Centre Armand-Frappier Santé Biotechnologie. Images were processed with the Fiji software.

4.8 | Co-immunoprecipitation assays

For anti-HA immunoprecipitation, transfected cells were washed twice in phosphate-buffered saline (PBS), collected and lysed during a 20 min on ice in a buffer containing 0.5% Dodecyl-B-D-maltoside, 100 mM NaCl, 20 mM Tris (pH 7.5), 50 mM NaF and EDTA-free protease inhibitors (Roche). The lysates were centrifuged during 15 min at 13,000 rpm at 4°C and supernatants were collected. Resulting cell extracts were incubated with 50 μL of a 50/50 sLurry of mouse monoclonal anti-HA coupled to agarose beads (Millipore-Sigma) for 3 hr. The resin was washed twice with lysis buffer and twice with 50 mM Tris (pH 7.5), 150 mM NaCl. Immunocomplexes were collected by a first elution with PBS-5% SDS, followed by a second elution with PBS. The pooled eluates were precipitated overnight at −20°C by adding 4 volumes of acetone. The precipitated proteins were sedimented by centrifugation for 1 hr at 13000 rpm. The protein pellets were air-dried, dissolved in loading buffer, subjected to SDS PAGE and western blot analysis.

For immunoprecipitation following infection, washed cells were lysed during 20 min on ice in a buffer containing 50 mM Tris (pH 7.8–8), 150 mM NaCl, 0.5% NP40 and EDTA-free protease inhibitors. The lysates were centrifuged during 15 min at 13,000 rpm at 4°C. Cell lysates were incubated with the indicated antibodies over night at 4°C. Then, 50 μL of a 50/50 slurry of protein G-Sepharose (Millipore-Sigma) were added in the lysate. After 1 hr incubation at 4°C, the resin was washed four times with lysis buffer and the immunocomplexes were collected and precipitated as indicated above.

4.9 | Proximity ligation assays

Infected cells were grown on glass coverslips, washed twice with PBS, fixed with 4% paraformaldehyde/PBS and permeabilised with PBS-0.2% Triton X-100 during 20 min. Proximity ligation assays were performed using the Duolink PLA Kit (Millipore-Sigma) according to the manufacturer's protocol. Briefly, cells were blocked in a humidity chamber for 1 hr at 37°C then incubated with the primary antibodies for 2 hr at room temperature. Cells were washed twice and incubated with PLUS and MINUS PLA probes in a humidity chamber for 1 hr at 37°C. After two additional washes, cells were incubated in a humidity chamber with ligation solution for 30 min at 37°C and then with the amplification solution for 100 min at 37°C. After the final washes, the coverslips were prepared for imaging with the DAPI-containing Mounting Media and imaged with a LSM780 confocal microscope (Carl Zeiss Microimaging). Image analysis and PLA dot counting were performed with the Fiji software.

4.10 | Transmission electron microscopy

Huh7.5 were grown on Lab-tech chamber SlideTM (Thermo-Fisher) and infected with ZIKV H/PF/2013 at a MOI of 20. Forty-eight hours later, cells were treated with either 20 μM NMS-873, 20 μM CB-5083 or 0.2% DMSO for 4 hr. Samples were then washed three times with PBS and fixed overnight at 4°C in 2.5% glutaraldehyde in 0.1 M sodium cacodylate buffer, pH 7.4 and washed three times with washing buffer. Samples were postfixed with 1% aqueous OsO_4 + 1.5% aqueous potassium ferrocyanide for 1 hr and washed three times with washing buffer. Specimens were dehydrated in a graded ethanol-dH2O series until 70%, then block stained with 2% uranyl acetate in 70% ethanol for 1 hr. Samples were washed twice with 70% ethanol followed by continued dehydration to 100% ethanol. The samples were infiltrated with a graded Epon-ethanol series (1:1, 3:1), embedded in 100% Epon and polymerised in an oven at 60°C for 48 hr. Ultrathin serial sections (90–100 nm thick) were prepared from the polymerised blocks with a Diatome diamond knife using a Leica Microsystems EM UC7 ultramicrotome, transferred onto 200-mesh copper grids and stained with 4% uranyl acetate for 6 min and Reynold's lead for 5 min. TEM grids were imaged with a FEI Tecnai G2 Spirit 120 kV TEM equipped with a Gatan Ultrascan 4000 CCD Camera Model 895 (Gatan, Pleasanton, CA) located at the McGill University Facility for Electron Microscopy Research. ZIKV CM analysis was performed using the Fiji software.

4.11 | Flow cytometry assays

Huh7.5 cells were trypsinised and stained with the appropriate predetermined concentrations of CellEvent caspase-3/7 green and the

amine reactive viability dye LIVE/DEAD aqua fixable stain (ThermoFisher) for 30 min in the dark at room temperature. After fixation with 2% formaldehyde and permeabilisation with 0.1% Triton X100, intracellular staining for NS3 using a rat polyclonal anti-NS3 and detection with a goat anti-rat cross-adsorbed AlexaFluor 647-conjugated secondary antibody were performed. Cells were fixed again in PBS containing 1% formaldehyde and stored at 4°C in the dark until FACS analysis (performed within 12 hr). Data were acquired on a CytoFlex instrument (Beckman Coulter) equipped for the detection of nine fluorescent parameters. Data analysis was performed using FlowJo version 10.0 software. After setting of singlets, infected Huh7.5 were defined as NS3+ cells and analysed for active caspase-3/7 expression and plasma membrane integrity.

4.12 | Caspase-Glo 3/7 assays

Huh7.5 cells were infected in triplicates with ZIKV H/PF/2013 (MOI = 10) or left uninfected. 72 hr post-infection, cells were treated with DMSO, 20 μM NMS-873 or 20 μM CB-5083 for 4 hr. Cells were scraped in medium, collected and centrifuged 1 min at 10,000 rpm. Cell pellets were resuspended in 50 μL of Caspase-Glo 3/7 reagent (Promega; G8093), which was diluted twofold in PBS prior to addition. After a 2-hr incubation in the dark at room temperature, luminescence was read with a Spark multi-mode microplate reader (Tecan). All values were background-subtracted and normalised to the uninfected/DMSO condition.

4.13 | Ethics statement

The rats used for the generation of antibodies were entirely handled by the company Medimabs (Montréal, Canada) following the protocol #951 (entitled 'Production d'anticorps monoclonaux chez les rongeurs') approved by the 'Comité Institutionnel de Protection des Animaux' (CIPA, translated as Institutional Committee for Animal protection) of the Université du Québec à Montréal (UQÀM). This animal care and use protocol strictly adhered to the guidelines and regulations of the Canadian Council on Animal Care.

4.14 | Statistical analysis

All Student *t* tests were unpaired and two-tailed. * p-value < 0.5; ** p-value < 0.01; *** p-value < 0.001.

ACKNOWLEDGEMENTS

We thank Dr Alessia Ruggieri (University of Heidelberg), Dr Mirko Cortese (University of Heidelberg), Dr Pietro Scaturro (Technical University of Munich) and Dr Karine Boulay (University of Montréal) for technical advice and the critical reading of the manuscript. We are grateful to Dr Pei-Yong Shi and the World Reference Center for Emerging Viruses and Arboviruses (WRCEVA) for providing the ZIKV reporter system, and Dr Ralf Bartenschlager (University of Heidelberg) for the T7 polymerase-expressing lentiviral construct and pTM plasmids. We thank the European Virus Archive goes Global (EVAg) and Dr Xavier de Lamballerie (Emergence des Pathologies Virales, Aix-Marseille University) for providing ZIKV MR766 and H/PF/2013 original stocks. We are grateful to Dr Patrick Labonté (Institut National de la Recherche Scientifique), Dr Tom Hobman (University of Alberta) and Dr Anil Kumar (University of Alberta) for generously providing Huh7.5 and Vero E6 cells. We thank Jessy Tremblay at the Centre Armand-Frappier Confocal Microscopy Facility for help and training during imaging, Jeannie Mui at the McGill University Facility for Electron Microscopy Research for sample preparation and considerable assistance during imaging. We are thankful to Benoit Lacoste and Pierre-André Scott at Medimabs (Montréal, Canada) for generating rat anti-NS3 antibodies. Anaïs Anton is a recipient of a master's training fellowship from Fonds de la Recherche du Québec-Santé (FRQS). Nicolas Tremblay is supported by a postdoctoral scholarship and Laurent Chatel-Chaix is receiving a research scholar (Junior 2) salary support, both from FRQS. This research was supported by grants from Natural Sciences and Engineering Research Council of Canada (NSERC; RGPIN-2016-05584), the Canadian Institutes of Health Research (CIHR; PJT153020; ICS154142), Fonds de la Recherche du Québec-Nature et Technologies (FRQNT; 2018-NC-205593), Armand-Frappier Foundation and Institut National de la Recherche Scientifique to Laurent Chatel-Chaix.

CONFLICT OF INTEREST

The authors declare no conflicts of interest.

AUTHOR CONTRIBUTIONS

Laurent Chatel-Chaix designed and supervised the study and wrote the manuscript. Anaïs Anton, Clément Mazeaud, Wesley Freppel, Claudia Gilbert, Nicolas Tremblay, Aïssatou Aïcha Sow and Marie Roy conducted the experiments. Ian Gaël Rodrigue-Gervais designed and analysed the cell death-related experiments. Anaïs Anton, Clément Mazeaud, Wesley Freppel, Claudia Gilbert, Nicolas Tremblay, Aïssatou Aïcha Sow, Marie Roy and Ian Gaël Rodrigue-Gervais revised and edited the manuscript.

DATA AVAILABILITY STATEMENT

The data that support the findings of this study are available from the corresponding author upon reasonable request.

ORCID

Wesley Freppel https://orcid.org/0000-0003-3628-0465
Nicolas Tremblay https://orcid.org/0000-0003-4246-7189
Laurent Chatel-Chaix https://orcid.org/0000-0002-7390-8250

REFERENCES

Aktepe, T. E., Liebscher, S., Prier, J. E., Simmons, C. P., & Mackenzie, J. M. (2017). The host protein reticulon 3.1A is utilized by flaviviruses to facilitate membrane remodelling. *Cell Reports*, *21*(6), 1639–1654. https://doi.org/10.1016/j.celrep.2017.10.055

Anderson, D. J., Le Moigne, R., Djakovic, S., Kumar, B., Rice, J., Wong, S., … Rolfe, M. (2015). Targeting the AAA ATPase p97 as an approach to treat cancer through disruption of protein homeostasis. *Cancer Cell*, *28* (5), 653–665. https://doi.org/10.1016/j.ccell.2015.10.002

Bandau, S., Knebel, A., Gage, Z. O., Wood, N. T., & Alexandru, G. (2012). UBXN7 docks on neddylated cullin complexes using its UIM motif and causes HIF1alpha accumulation. *BMC Biology*, *10*, 36. https://doi.org/10.1186/1741-7007-10-36

Banerjee, S., Bartesaghi, A., Merk, A., Rao, P., Bulfer, S. L., Yan, Y., … Subramaniam, S. (2016). 2.3 Å resolution cryo-EM structure of human p97 and mechanism of allosteric inhibition. *Science*, *351*(6275), 871–875. https://doi.org/10.1126/science.aad7974

Barbier, V., Lang, D., Valois, S., Rothman, A. L., & Medin, C. L. (2017). Dengue virus induces mitochondrial elongation through impairment of Drp1-triggered mitochondrial fission. *Virology*, *500*, 149–160. https://doi.org/10.1016/j.virol.2016.10.022

Barrows, N. J., Campos, R. K., Powell, S. T., Prasanth, K. R., Schott-Lerner, G., Soto-Acosta, R., … Garcia-Blanco, M. A. (2016). A screen of FDA-approved drugs for inhibitors of Zika virus infection. *Cell Host & Microbe*, *20*(2), 259–270. https://doi.org/10.1016/j.chom.2016.07.004

Bartolome, F., Wu, H. C., Burchell, V. S., Preza, E., Wray, S., Mahoney, C. J., … Plun-Favreau, H. (2013). Pathogenic VCP mutations induce mitochondrial uncoupling and reduced ATP levels. *Neuron*, *78*(1), 57–64. https://doi.org/10.1016/j.neuron.2013.02.028

Berger, C., Romero-Brey, I., Radujkovic, D., Terreux, R., Zayas, M., Paul, D., … Bartenschlager, R. (2014). Daclatasvir-like inhibitors of NS5A block early biogenesis of hepatitis C virus-induced membranous replication factories, independent of RNA replication. *Gastroenterology*, *147*(5), 1094–1105 e1025. https://doi.org/10.1053/j.gastro.2014.07.019

Beskow, A., Grimberg, K. B., Bott, L. C., Salomons, F. A., Dantuma, N. P., & Young, P. (2009). A conserved unfoldase activity for the p97 AAA-ATPase in proteasomal degradation. *Journal of Molecular Biology*, *394* (4), 732–746. https://doi.org/10.1016/j.jmb.2009.09.050

Bodnar, N. O., & Rapoport, T. A. (2017). Molecular mechanism of substrate processing by the Cdc48 ATPase complex. *Cell*, *169*(4), 722–735 e729. https://doi.org/10.1016/j.cell.2017.04.020

Chatel-Chaix, L., & Bartenschlager, R. (2014). Dengue virus- and hepatitis C virus-induced replication and assembly compartments: The enemy inside—Caught in the web. *Journal of Virology*, *88*(11), 5907–5911. https://doi.org/10.1128/JVI.03404-13

Chatel-Chaix, L., Cortese, M., Romero-Brey, I., Bender, S., Neufeldt, C. J., Fischl, W., … Bartenschlager, R. (2016). Dengue virus perturbs mitochondrial morphodynamics to dampen innate immune responses. *Cell Host & Microbe*, *20*(3), 342–356. https://doi.org/10.1016/j.chom.2016.07.008

Chatel-Chaix, L., Fischl, W., Scaturro, P., Cortese, M., Kallis, S., Bartenschlager, M., … Bartenschlager, R. (2015). A combined genetic-proteomic approach identifies residues within dengue virus NS4B critical for interaction with NS3 and viral replication. *Journal of Virology*, *89* (14), 7170–7186. https://doi.org/10.1128/JVI.00867-15

Chiramel, A. I., & Best, S. M. (2018). Role of autophagy in Zika virus infection and pathogenesis. *Virus Research*, *254*, 34–40. https://doi.org/10.1016/j.virusres.2017.09.006

Chou, T. F., Brown, S. J., Minond, D., Nordin, B. E., Li, K., Jones, A. C., … Deshaies, R. J. (2011). Reversible inhibitor of p97, DBeQ, impairs both ubiquitin-dependent and autophagic protein clearance pathways. *Proceedings of the National Academy of Sciences of the United States of America*, *108*(12), 4834–4839. https://doi.org/10.1073/pnas.1015312108

Choy, M. M., Sessions, O. M., Gubler, D. J., & Ooi, E. E. (2015). Production of infectious dengue virus in *Aedes aegypti* is dependent on the ubiquitin proteasome pathway. *PLoS Neglected Tropical Diseases*, *9*(11), e0004227. https://doi.org/10.1371/journal.pntd.0004227

Cortese, M., Goellner, S., Acosta, E. G., Neufeldt, C. J., Oleksiuk, O., Lampe, M., … Bartenschlager, R. (2017). Ultrastructural characterization of Zika virus replication factories. *Cell Reports*, *18*(9), 2113–2123. https://doi.org/10.1016/j.celrep.2017.02.014

Cugola, F. R., Fernandes, I. R., Russo, F. B., Freitas, B. C., Dias, J. L., Guimaraes, K. P., … Beltrao-Braga, P. C. (2016). The Brazilian Zika virus strain causes birth defects in experimental models. *Nature*, *534*(7606), 267–271. https://doi.org/10.1038/nature18296

DeLaBarre, B., Christianson, J. C., Kopito, R. R., & Brunger, A. T. (2006). Central pore residues mediate the p97/VCP activity required for ERAD. *Molecular Cell*, *22*(4), 451–462. https://doi.org/10.1016/j.molcel.2006.03.036

den Besten, W., Verma, R., Kleiger, G., Oania, R. S., & Deshaies, R. J. (2012). NEDD8 links cullin-RING ubiquitin ligase function to the p97 pathway. *Nature Structural & Molecular Biology*, *19*(5), 511–516, S511. https://doi.org/10.1038/nsmb.2269

Deng, Y. Q., Zhang, N. N., Li, C. F., Tian, M., Hao, J. N., Xie, X. P., … Qin, C. F. (2016). Adenosine analog NITD008 is a potent inhibitor of Zika virus. *Open Forum Infectious Diseases*, *3*(4), ofw175. https://doi.org/10.1093/ofid/ofw175

Doroshow, J. H., Parchment, R., & Moscow, J. (2018, May 8). NCI experimental therapeutics (NExT) program. Retrieved from https://deainfo.nci.nih.gov/advisory/fac/0518/Doroshow.pdf

Gilfoy, F., Fayzulin, R., & Mason, P. W. (2009). West Nile virus genome amplification requires the functional activities of the proteasome. *Virology*, *385*(1), 74–84. https://doi.org/10.1016/j.virol.2008.11.034

Grubaugh, N. D., Faria, N. R., Andersen, K. G., & Pybus, O. G. (2018). Genomic insights into Zika virus emergence and spread. *Cell*, *172*(6), 1160–1162. https://doi.org/10.1016/j.cell.2018.02.027

Guo, X., Sun, X., Hu, D., Wang, Y. J., Fujioka, H., Vyas, R., … Qi, X. (2016). VCP recruitment to mitochondria causes mitophagy impairment and neurodegeneration in models of Huntington's disease. *Nature Communications*, *7*, 12646. https://doi.org/10.1038/ncomms12646

Halawani, D., LeBlanc, A. C., Rouiller, I., Michnick, S. W., Servant, M. J., & Latterich, M. (2009). Hereditary inclusion body myopathy-linked p97/VCP mutations in the NH2 domain and the D1 ring modulate p97/VCP ATPase activity and D2 ring conformation. *Molecular and Cellular Biology*, *29*(16), 4484–4494. https://doi.org/10.1128/MCB.00252-09

Hamel, R., Dejarnac, O., Wichit, S., Ekchariyawat, P., Neyret, A., Luplertlop, N., … Misse, D. (2015). Biology of Zika virus infection in human skin cells. *Journal of Virology*, *89*(17), 8880–8896. https://doi.org/10.1128/JVI.00354-15

Heaton, N. S., & Randall, G. (2010). Dengue virus-induced autophagy regulates lipid metabolism. *Cell Host & Microbe*, *8*(5), 422–432. https://doi.org/10.1016/j.chom.2010.10.006

Heidelberger, J. B., Voigt, A., Borisova, M. E., Petrosino, G., Ruf, S., Wagner, S. A., & Beli, P. (2018). Proteomic profiling of VCP substrates links VCP to K6-linked ubiquitylation and c-Myc function. *EMBO Reports*, *19*(4), e44754. https://doi.org/10.15252/embr.201744754

Huryn, D. M., Kornfilt, D. J. P., & Wipf, P. (2019). p97: An emerging target for cancer, neurodegenerative diseases, and viral infections. *Journal of Medicinal Chemistry*, *63*, 1892–1907. https://doi.org/10.1021/acs.jmedchem.9b01318

Imamura, S., Yabu, T., & Yamashita, M. (2012). Protective role of cell division cycle 48 (CDC48) protein against neurodegeneration via ubiquitin-proteasome system dysfunction during zebrafish development. *The Journal of Biological Chemistry*, *287*(27), 23047–23056. https://doi.org/10.1074/jbc.M111.332882

Jarosch, E., Taxis, C., Volkwein, C., Bordallo, J., Finley, D., Wolf, D. H., & Sommer, T. (2002). Protein dislocation from the ER requires polyubiquitination and the AAA-ATPase Cdc48. *Nature Cell Biology*, *4*(2), 134–139. https://doi.org/10.1038/ncb746

Ju, J. S., Fuentealba, R. A., Miller, S. E., Jackson, E., Piwnica-Worms, D., Baloh, R. H., & Weihl, C. C. (2009). Valosin-containing protein (VCP) is required for autophagy and is disrupted in VCP disease. *The Journal of Cell Biology*, *187*(6), 875–888. https://doi.org/10.1083/jcb.200908115

Ju, J. S., Miller, S. E., Hanson, P. I., & Weihl, C. C. (2008). Impaired protein aggregate handling and clearance underlie the pathogenesis of p97/VCP-associated disease. *The Journal of Biological Chemistry*, *283*(44), 30289–30299. https://doi.org/10.1074/jbc.M805517200

Junjhon, J., Pennington, J. G., Edwards, T. J., Perera, R., Lanman, J., & Kuhn, R. J. (2014). Ultrastructural characterization and three-dimensional architecture of replication sites in dengue virus-infected mosquito cells. *Journal of Virology*, *88*(9), 4687–4697. https://doi.org/10.1128/JVI.00118-14

Kanlaya, R., Pattanakitsakul, S. N., Sinchaikul, S., Chen, S. T., & Thongboonkerd, V. (2010). The ubiquitin-proteasome pathway is important for dengue virus infection in primary human endothelial cells. *Journal of Proteome Research*, *9*(10), 4960–4971. https://doi.org/10.1021/pr100219y

Kaufusi, P. H., Kelley, J. F., Yanagihara, R., & Nerurkar, V. R. (2014). Induction of endoplasmic reticulum-derived replication-competent membrane structures by West Nile virus non-structural protein 4B. *PLoS One*, *9*(1), e84040. https://doi.org/10.1371/journal.pone.0084040

Ke, P. Y. (2018). The multifaceted roles of autophagy in flavivirus-host interactions. *International Journal of Molecular Sciences*, *19*(12), 3940. https://doi.org/10.3390/ijms19123940

Kim, N. C., Tresse, E., Kolaitis, R. M., Molliex, A., Thomas, R. E., Alami, N. H., … Taylor, J. P. (2013). VCP is essential for mitochondrial quality control by PINK1/Parkin and this function is impaired by VCP mutations. *Neuron*, *78*(1), 65–80. https://doi.org/10.1016/j.neuron.2013.02.029

Kimura, Y., Fukushi, J., Hori, S., Matsuda, N., Okatsu, K., Kakiyama, Y., … Tanaka, K. (2013). Different dynamic movements of wild-type and pathogenic VCPs and their cofactors to damaged mitochondria in a Parkin-mediated mitochondrial quality control system. *Genes to Cells*, *18*(12), 1131–1143. https://doi.org/10.1111/gtc.12103

Lazear, H. M., & Diamond, M. S. (2016). Zika virus: New clinical syndromes and its emergence in the Western hemisphere. *Journal of Virology*, *90*(10), 4864–4875. https://doi.org/10.1128/JVI.00252-16

Le Moigne, R., Aftab, B. T., Djakovic, S., Dhimolea, E., Valle, E., Murnane, M., … Rolfe, M. (2017). The p97 inhibitor CB-5083 is a unique disrupter of protein homeostasis in models of multiple myeloma. *Molecular Cancer Therapeutics*, *16*(11), 2375–2386. https://doi.org/10.1158/1535-7163.MCT-17-0233

Ledur, P. F., Karmirian, K., Pedrosa, C., Souza, L. R. Q., Assis-de-Lemos, G., Martins, T. M., … Rehen, S. K. (2020). Zika virus infection leads to mitochondrial failure, oxidative stress and DNA damage in human iPSC-derived astrocytes. *Scientific Reports*, *10*(1), 1218. https://doi.org/10.1038/s41598-020-57914-x

Lee, Y. R., Lei, H. Y., Liu, M. T., Wang, J. R., Chen, S. H., Jiang-Shieh, Y. F., … Liu, H. S. (2008). Autophagic machinery activated by dengue virus enhances virus replication. *Virology*, *374*(2), 240–248. https://doi.org/10.1016/j.virol.2008.02.016

Li, C., Xu, D., Ye, Q., Hong, S., Jiang, Y., Liu, X., … Xu, Z. (2016). Zika virus disrupts neural progenitor development and leads to microcephaly in mice. *Cell Stem Cell*, *19*(5), 672. https://doi.org/10.1016/j.stem.2016.10.017

Li, H., Saucedo-Cuevas, L., Shresta, S., & Gleeson, J. G. (2016). The neurobiology of Zika virus. *Neuron*, *92*(5), 949–958. https://doi.org/10.1016/j.neuron.2016.11.031

Liang, Q., Luo, Z., Zeng, J., Chen, W., Foo, S. S., Lee, S. A., … Jung, J. U. (2016). Zika virus NS4A and NS4B proteins deregulate Akt-mTOR signaling in human fetal neural stem cells to inhibit neurogenesis and induce autophagy. *Cell Stem Cell*, *19*(5), 663–671. https://doi.org/10.1016/j.stem.2016.07.019

Ludtmann, M. H. R., Arber, C., Bartolome, F., de Vicente, M., Preza, E., Carro, E., … Abramov, A. Y. (2017). Mutations in valosin-containing protein (VCP) decrease ADP/ATP translocation across the mitochondrial membrane and impair energy metabolism in human neurons. *The Journal of Biological Chemistry*, *292*(21), 8907–8917. https://doi.org/10.1074/jbc.M116.762898

Magnaghi, P., D'Alessio, R., Valsasina, B., Avanzi, N., Rizzi, S., Asa, D., … Isacchi, A. (2013). Covalent and allosteric inhibitors of the ATPase VCP/p97 induce cancer cell death. *Nature Chemical Biology*, *9*(9), 548–556. https://doi.org/10.1038/nchembio.1313

McLelland, G. L., Goiran, T., Yi, W., Dorval, G., Chen, C. X., Lauinger, N. D., … Fon, E. A. (2018). Mfn2 ubiquitination by PINK1/parkin gates the p97-dependent release of ER from mitochondria to drive mitophagy. *eLife*, *7*, e32866. https://doi.org/10.7554/eLife.32866

Metz, P., Chiramel, A., Chatel-Chaix, L., Alvisi, G., Bankhead, P., Mora-Rodriguez, R., … Bartenschlager, R. (2015). Dengue virus inhibition of autophagic flux and dependency of viral replication on proteasomal degradation of the autophagy receptor p62. *Journal of Virology*, *89*(15), 8026–8041. https://doi.org/10.1128/JVI.00787-15

Meyer, H., & Weihl, C. C. (2014). The VCP/p97 system at a glance: Connecting cellular function to disease pathogenesis. *Journal of Cell Science*, *127*(Pt 18), 3877–3883. https://doi.org/10.1242/jcs.093831

Miller, S., Kastner, S., Krijnse-Locker, J., Buhler, S., & Bartenschlager, R. (2007). The non-structural protein 4A of dengue virus is an integral membrane protein inducing membrane alterations in a 2K-regulated manner. *The Journal of Biological Chemistry*, *282*(12), 8873–8882. https://doi.org/10.1074/jbc.M609919200

Miller, S., Sparacio, S., & Bartenschlager, R. (2006). Subcellular localization and membrane topology of the dengue virus type 2 non-structural protein 4B. *The Journal of Biological Chemistry*, *281*(13), 8854–8863. https://doi.org/10.1074/jbc.M512697200

Miner, J. J., Cao, B., Govero, J., Smith, A. M., Fernandez, E., Cabrera, O. H., … Diamond, M. S. (2016). Zika virus infection during pregnancy in mice causes placental damage and fetal demise. *Cell*, *165*(5), 1081–1091. https://doi.org/10.1016/j.cell.2016.05.008

Montessuit, S., Somasekharan, S. P., Terrones, O., Lucken-Ardjomande, S., Herzig, S., Schwarzenbacher, R., … Martinou, J. C. (2010). Membrane remodeling induced by the dynamin-related protein Drp1 stimulates Bax oligomerization. *Cell*, *142*(6), 889–901. https://doi.org/10.1016/j.cell.2010.08.017

Neufeldt, C. J., Cortese, M., Acosta, E. G., & Bartenschlager, R. (2018). Rewiring cellular networks by members of the Flaviviridae family. *Nature Reviews. Microbiology*, *16*(3), 125–142. https://doi.org/10.1038/nrmicro.2017.170

Niwa, H., Ewens, C. A., Tsang, C., Yeung, H. O., Zhang, X., & Freemont, P. S. (2012). The role of the N-domain in the ATPase activity of the mammalian AAA ATPase p97/VCP. *The Journal of Biological Chemistry*, *287*(11), 8561–8570. https://doi.org/10.1074/jbc.M111.302778

Oettinghaus, B., D'Alonzo, D., Barbieri, E., Restelli, L. M., Savoia, C., Licci, M., … Scorrano, L. (2016). DRP1-dependent apoptotic mitochondrial fission occurs independently of BAX, BAK and APAF1 to amplify cell death by BID and oxidative stress. *Biochimica et Biophysica Acta*, *1857*(8), 1267–1276. https://doi.org/10.1016/j.bbabio.2016.03.016

Park, J. H., Ko, J., Hwang, J., & Koh, H. C. (2015). Dynamin-related protein 1 mediates mitochondria-dependent apoptosis in chlorpyrifos-treated SH-SY5Y cells. *Neurotoxicology*, *51*, 145–157. https://doi.org/10.1016/j.neuro.2015.10.008

Phongphaew, W., Kobayashi, S., Sasaki, M., Carr, M., Hall, W. W., Orba, Y., & Sawa, H. (2017). Valosin-containing protein (VCP/p97) plays a role in the replication of West Nile virus. *Virus Research*, *228*, 114–123. https://doi.org/10.1016/j.virusres.2016.11.029

Pierson, T. C., & Graham, B. S. (2016). Zika virus: Immunity and vaccine development. *Cell*, *167*(3), 625–631. https://doi.org/10.1016/j.cell.2016.09.020

Ramanathan, H. N., Zhang, S., Douam, F., Mar, K. B., Chang, J., Yang, P. L., … Lindenbach, B. D. (2020). A sensitive yellow fever virus entry reporter identifies valosin-containing protein (VCP/p97) as an essential host factor for flavivirus uncoating. *mBio*, *11*(2), e00467–20. https://doi.org/10.1128/mBio.00467-20

Rausch, K., Hackett, B. A., Weinbren, N. L., Reeder, S. M., Sadovsky, Y., Hunter, C. A., … Cherry, S. (2017). Screening bioactives reveals nanchangmycin as a broad spectrum antiviral active against Zika virus. *Cell Reports*, *18*(3), 804–815. https://doi.org/10.1016/j.celrep.2016.12.068

Romero-Brey, I., Merz, A., Chiramel, A., Lee, J. Y., Chlanda, P., Haselman, U., … Bartenschlager, R. (2012). Three-dimensional architecture and biogenesis of membrane structures associated with hepatitis C virus replication. *PLoS Pathogens*, *8*(12), e1003056. https://doi.org/10.1371/journal.ppat.1003056

Roosendaal, J., Westaway, E. G., Khromykh, A., & Mackenzie, J. M. (2006). Regulated cleavages at the West Nile virus NS4A-2K-NS4B junctions play a major role in rearranging cytoplasmic membranes and Golgi trafficking of the NS4A protein. *Journal of Virology*, *80*(9), 4623–4632. https://doi.org/10.1128/JVI.80.9.4623-4632.2006

Schuberth, C., & Buchberger, A. (2008). UBX domain proteins: Major regulators of the AAA ATPase Cdc48/p97. *Cellular and Molecular Life Sciences*, *65*(15), 2360–2371. https://doi.org/10.1007/s00018-008-8072-8

Shah, P. S., Link, N., Jang, G. M., Sharp, P. P., Zhu, T., Swaney, D. L., … Krogan, N. J. (2018). Comparative flavivirus-host protein interaction mapping reveals mechanisms of dengue and Zika virus pathogenesis. *Cell*, *175*(7), 1931–1945 e1918. https://doi.org/10.1016/j.cell.2018.11.028

Shan, C., Xie, X., Muruato, A. E., Rossi, S. L., Roundy, C. M., Azar, S. R., … Shi, P. Y. (2016). An infectious cDNA clone of Zika virus to study viral virulence, mosquito transmission, and antiviral inhibitors. *Cell Host & Microbe*, *19*(6), 891–900. https://doi.org/10.1016/j.chom.2016.05.004

Stach, L., & Freemont, P. S. (2017). The AAA+ ATPase p97, a cellular multitool. *The Biochemical Journal*, *474*(17), 2953–2976. https://doi.org/10.1042/BCJ20160783

Tresse, E., Salomons, F. A., Vesa, J., Bott, L. C., Kimonis, V., Yao, T. P., … Taylor, J. P. (2010). VCP/p97 is essential for maturation of ubiquitin-containing autophagosomes and this function is impaired by mutations that cause IBMPFD. *Autophagy*, *6*(2), 217–227.

Turpin, J., Frumence, E., Despres, P., Viranaicken, W., & Krejbich-Trotot, P. (2019). The ZIKA virus delays cell death through the anti-apoptotic Bcl-2 family proteins. *Cells*, *8*(11), 1338. https://doi.org/10.3390/cells8111338

van Cleef, K. W., Overheul, G. J., Thomassen, M. C., Kaptein, S. J., Davidson, A. D., Jacobs, M., … van Rij, R. P. (2013). Identification of a new dengue virus inhibitor that targets the viral NS4B protein and restricts genomic RNA replication. *Antiviral Research*, *99*(2), 165–171. https://doi.org/10.1016/j.antiviral.2013.05.011

van den Boom, J., & Meyer, H. (2018). VCP/p97-mediated unfolding as a principle in protein homeostasis and signaling. *Molecular Cell*, *69*(2), 182–194. https://doi.org/10.1016/j.molcel.2017.10.028

Wang, Q. Y., Dong, H., Zou, B., Karuna, R., Wan, K. F., Zou, J., … Shi, P. Y. (2015). Discovery of dengue virus NS4B inhibitors. *Journal of Virology*, *89*(16), 8233–8244. https://doi.org/10.1128/JVI.00855-15

Watts, G. D., Wymer, J., Kovach, M. J., Mehta, S. G., Mumm, S., Darvish, D., … Kimonis, V. E. (2004). Inclusion body myopathy associated with Paget disease of bone and frontotemporal dementia is caused by mutant valosin-containing protein. *Nature Genetics*, *36*(4), 377–381. https://doi.org/10.1038/ng1332

Weihl, C. C., Dalal, S., Pestronk, A., & Hanson, P. I. (2006). Inclusion body myopathy-associated mutations in p97/VCP impair endoplasmic reticulum-associated degradation. *Human Molecular Genetics*, *15*(2), 189–199. https://doi.org/10.1093/hmg/ddi426

Welsch, S., Miller, S., Romero-Brey, I., Merz, A., Bleck, C. K., Walther, P., … Bartenschlager, R. (2009). Composition and three-dimensional architecture of the dengue virus replication and assembly sites. *Cell Host & Microbe*, *5*(4), 365–375. https://doi.org/10.1016/j.chom.2009.03.007

Wojcik, C., Rowicka, M., Kudlicki, A., Nowis, D., McConnell, E., Kujawa, M., & DeMartino, G. N. (2006). Valosin-containing protein (p97) is a regulator of endoplasmic reticulum stress and of the degradation of N-end rule and ubiquitin-fusion degradation pathway substrates in mammalian cells. *Molecular Biology of the Cell*, *17*(11), 4606–4618. https://doi.org/10.1091/mbc.e06-05-0432

World Health Organization. (2016). WHO statement on the first meeting of the International Health Regulations (2005) (IHR 2005): Emergency Committee on Zika virus and observed increase in neurological disorders and neonatal malformations. Retrieved from http://www.who.int/mediacentre/news/statements/2016/1st-emergency-committee-zika/en/

World Health Organization. (2017). Zika: We must be ready for the long haul. Retrieved from http://www.who.int/mediacentre/commentaries/2017/zika-long-haul/en/

Xie, X., Wang, Q. Y., Xu, H. Y., Qing, M., Kramer, L., Yuan, Z., & Shi, P. Y. (2011). Inhibition of dengue virus by targeting viral NS4B protein. *Journal of Virology*, *85*(21), 11183–11195. https://doi.org/10.1128/JVI.05468-11

Xie, X., Zou, J., Wang, Q. Y., & Shi, P. Y. (2015). Targeting dengue virus NS4B protein for drug discovery. *Antiviral Research*, *118*, 39–45. https://doi.org/10.1016/j.antiviral.2015.03.007

Xin, Q. L., Deng, C. L., Chen, X., Wang, J., Wang, S. B., Wang, W., … Zhang, L. K. (2017). Quantitative proteomic analysis of mosquito C6/36 cells reveals host proteins involved in Zika virus infection. *Journal of Virology*, *91*(12), e00554–17. https://doi.org/10.1128/JVI.00554-17

Xu, M., Lee, E. M., Wen, Z., Cheng, Y., Huang, W. K., Qian, X., … Tang, H. (2016). Identification of small-molecule inhibitors of Zika virus infection and induced neural cell death via a drug repurposing screen. *Nature Medicine*, *22*(10), 1101–1107. https://doi.org/10.1038/nm.4184

Ye, Y., Meyer, H. H., & Rapoport, T. A. (2001). The AAA ATPase Cdc48/p97 and its partners transport proteins from the ER into the cytosol. *Nature*, *414*(6864), 652–656. https://doi.org/10.1038/414652a

Yeung, H. O., Kloppsteck, P., Niwa, H., Isaacson, R. L., Matthews, S., Zhang, X., & Freemont, P. S. (2008). Insights into adaptor binding to the AAA protein p97. *Biochemical Society Transactions*, *36*(Pt 1), 62–67. https://doi.org/10.1042/BST0360062

Yi, Z., Fang, C., Zou, J., Xu, J., Song, W., Du, X., … Yuan, Z. (2016). Affinity purification of the hepatitis C virus Replicase identifies valosin-containing protein, a member of the ATPases associated with diverse cellular activities family, as an active virus replication modulator. *Journal of Virology*, *90*(21), 9953–9966. https://doi.org/10.1128/JVI.01140-16

Yi, Z., & Yuan, Z. (2017). Aggregation of a hepatitis C virus replicase module induced by ablation of p97/VCP. *The Journal of General Virology*, *98*(7), 1667–1678. https://doi.org/10.1099/jgv.0.000828

Yin, Z., Chen, Y. L., Schul, W., Wang, Q. Y., Gu, F., Duraiswamy, J., … Shi, P. Y. (2009). An adenosine nucleoside inhibitor of dengue virus. *Proceedings of the National Academy of Sciences of the United States of America*, *106*(48), 20435–20439. https://doi.org/10.1073/pnas.0907010106

Zhang, T., Mishra, P., Hay, B. A., Chan, D., & Guo, M. (2017). Valosin-containing protein (VCP/p97) inhibitors relieve Mitofusin-dependent

mitochondrial defects due to VCP disease mutants. *eLife*, *6*, e17834. https://doi.org/10.7554/eLife.17834

Zhou, H. J., Wang, J., Yao, B., Wong, S., Djakovic, S., Kumar, B., … Wustrow, D. (2015). Discovery of a first-in-class, potent, selective, and orally bioavailable inhibitor of the p97 AAA ATPase (CB-5083). *Journal of Medicinal Chemistry*, *58*(24), 9480–9497. https://doi.org/10.1021/acs.jmedchem.5b01346

Zhou, T., Tan, L., Cederquist, G. Y., Fan, Y., Hartley, B. J., Mukherjee, S., … Chen, S. (2017). High-content screening in hPSC-neural progenitors identifies drug candidates that inhibit Zika virus infection in fetal-like organoids and adult brain. *Cell Stem Cell*, *21*(2), 274–283 e275. https://doi.org/10.1016/j.stem.2017.06.017

Zou, J., Lee, L. T., Wang, Q. Y., Xie, X., Lu, S., Yau, Y. H., … Shi, P. Y. (2015). Mapping the interactions between the NS4B and NS3 proteins of dengue virus. *Journal of Virology*, *89*(7), 3471–3483. https://doi.org/10.1128/JVI.03454-14

Zou, J., Xie, X., Lee, L. T., Chandrasekaran, R., Reynaud, A., Yap, L., … Shi, P. Y. (2014). Dimerization of flavivirus NS4B protein. *Journal of Virology*, *88*(6), 3379–3391. https://doi.org/10.1128/JVI.02782-13

Zou, J., Xie, X., Wang, Q. Y., Dong, H., Lee, M. Y., Kang, C., … Shi, P. Y. (2015). Characterization of dengue virus NS4A and NS4B protein interaction. *Journal of Virology*, *89*(7), 3455–3470. https://doi.org/10.1128/JVI.03453-14

SUPPORTING INFORMATION

Additional supporting information may be found online in the Supporting Information section at the end of this article.

How to cite this article: Anton A, Mazeaud C, Freppel W, et al. Valosin-containing protein ATPase activity regulates the morphogenesis of Zika virus replication organelles and virus-induced cell death. *Cellular Microbiology*. 2021;e13302. https://doi.org/10.1111/cmi.13302

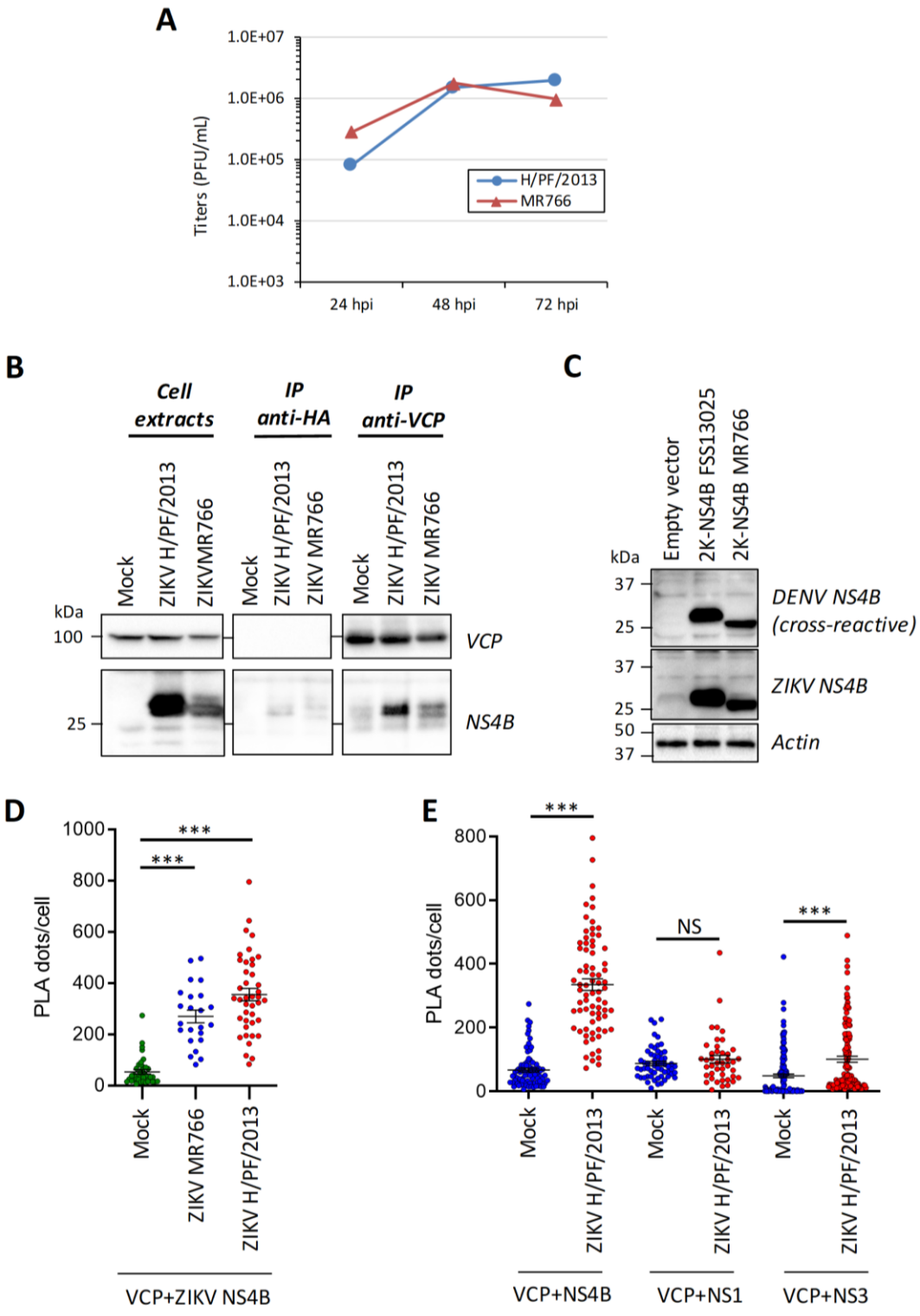

Suppl Figure 1

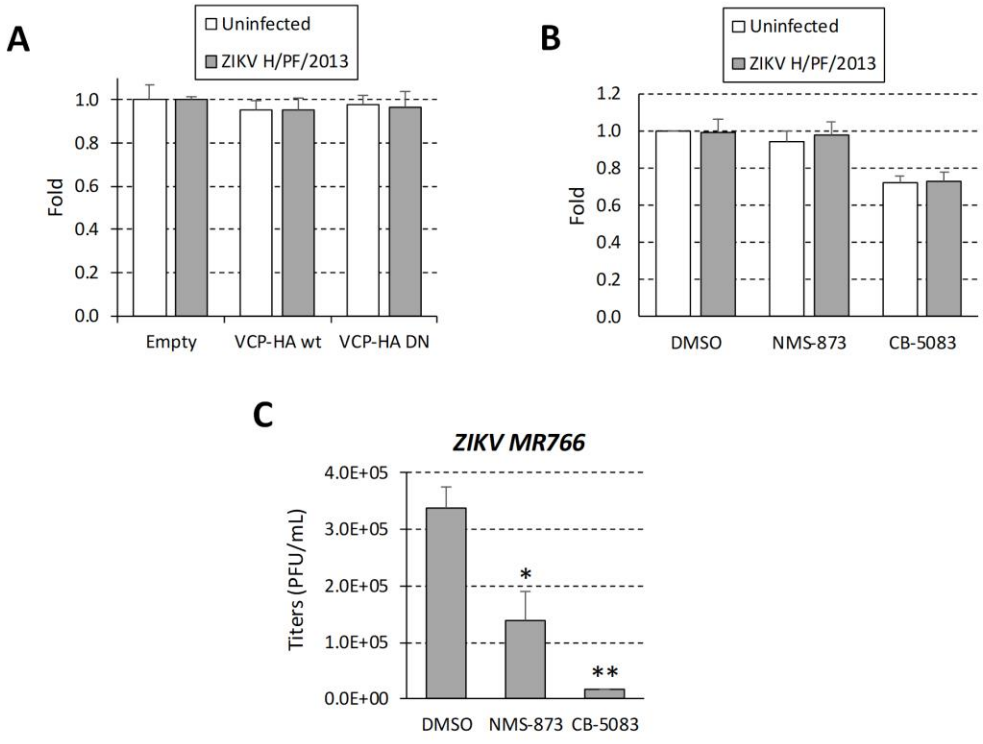

Suppl Figure 2

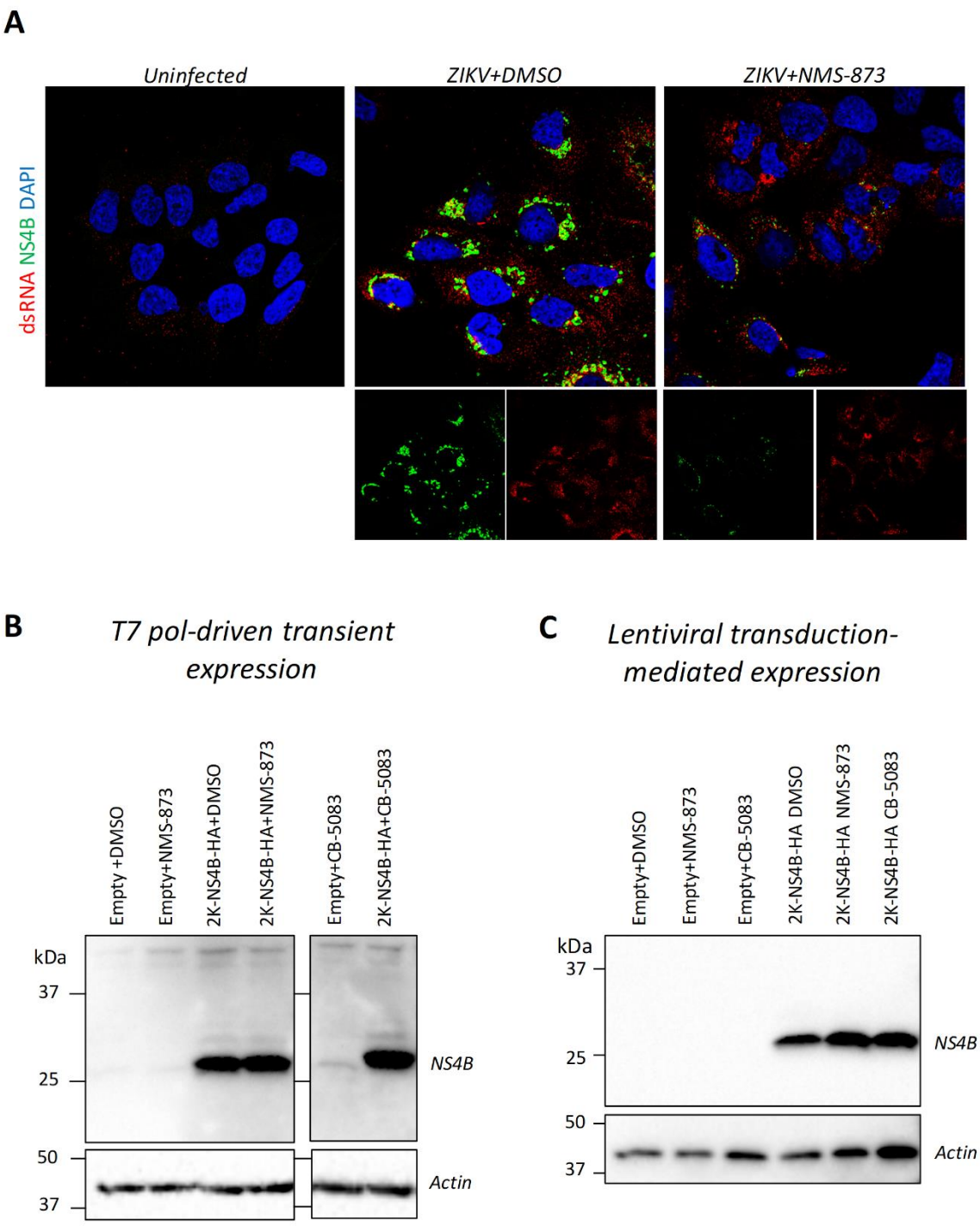

Suppl Figure 3

8 ANNEXE II

viruses

MDPI

Article

The Biogenesis of Dengue Virus Replication Organelles Requires the ATPase Activity of Valosin-Containing Protein

Clément Mazeaud [1,†], Anaïs Anton [1,†], Felix Pahmeier [2], Aïssatou Aïcha Sow [1], Berati Cerikan [2], Wesley Freppel [1], Mirko Cortese [2], Ralf Bartenschlager [2,3] and Laurent Chatel-Chaix [1,4,5,*]

[1] Centre Armand-Frappier Santé Biotechnologie, Institut National de la Recherche Scientifique, Laval, QC H7V 1B7, Canada; Clement.Mazeaud@inrs.ca (C.M.); Anais.Anton@inrs.ca (A.A.); Aicha.Sow@inrs.ca (A.A.S.); wesley.freppel@inrs.ca (W.F.)
[2] Center for Integrative Infectious Disease Research (CIID), Department of Infectious Diseases, Molecular Virology, Heidelberg University, D-69120 Heidelberg, Germany; felix.pahmeier@googlemail.com (F.P.); Berati.Cerikan@med.uni-heidelberg.de (B.C.); m.cortese@tigem.it (M.C.); Ralf.Bartenschlager@med.uni-heidelberg.de (R.B.)
[3] German Center for Infection Research (DZIF), Heidelberg Partner Site, D-69120 Heidelberg, Germany
[4] Center of Excellence in Research on Orphan Diseases-Fondation Courtois, Montreal, QC H7V 1B7, Canada
[5] Réseau Intersectoriel de Recherche en Santé de l'Université du Québec, Québec, QC H7V 1B7, Canada
* Correspondence: Laurent.Chatel-Chaix@inrs.ca; Tel.: +1-450-687-5010; Fax: +1-450-686-5566
† These authors contributed equally.

Abstract: The dengue virus (DENV) causes the most prevalent arthropod-borne viral disease worldwide. While its incidence is increasing in many countries, there is no approved antiviral therapy currently available. In infected cells, the DENV induces extensive morphological alterations of the endoplasmic reticulum (ER) to generate viral replication organelles (vRO), which include convoluted membranes (CM) and vesicle packets (VP) hosting viral RNA replication. The viral non-structural protein NS4B localizes to vROs and is absolutely required for viral replication through poorly defined mechanisms, which might involve cellular protein partners. Previous interactomic studies identified the ATPase valosin-containing protein (VCP) as a DENV NS4B-interacting host factor in infected cells. Using both pharmacological and dominant-negative inhibition approaches, we show, in this study, that VCP ATPase activity is required for efficient DENV replication. VCP associates with NS4B when expressed in the absence of other viral proteins while in infected cells, both proteins colocalize within large DENV-induced cytoplasmic structures previously demonstrated to be CMs. Consistently, VCP inhibition dramatically reduces the abundance of DENV CMs in infected cells. Most importantly, using a recently reported replication-independent plasmid-based vRO induction system, we show that *de novo* VP biogenesis is dependent on VCP ATPase activity. Overall, our data demonstrate that VCP ATPase activity is required for vRO morphogenesis and/or stability. Considering that VCP was shown to be required for the replication of other flaviviruses, our results argue that VCP is a pan-flaviviral host dependency factor. Given that new generation VCP-targeting drugs are currently evaluated in clinical trials for cancer treatment, VCP may constitute an attractive broad-spectrum antiviral target in drug repurposing approaches.

Keywords: dengue virus; valosin-containing protein; NS4B; viral replication organelles; endoplasmic reticulum

Citation: Mazeaud, C.; Anton, A.; Pahmeier, F.; Sow, A.A.; Cerikan, B.; Freppel, W.; Cortese, M.; Bartenschlager, R.; Chatel-Chaix, L. The Biogenesis of Dengue Virus Replication Organelles Requires the ATPase Activity of Valosin-Containing Protein. *Viruses* **2021**, *13*, 2092. https://doi.org/10.3390/v13102092

Academic Editor: Jaquelin Dudley

Received: 1 October 2021
Accepted: 13 October 2021
Published: 18 October 2021

1. Introduction

The dengue virus (DENV) causes the most prevalent arthropod-borne viral disease worldwide with approximately 100 million symptomatic infections annually. The DENV is endemic in 100 countries and its incidence has increased over 30-fold in the last 50 years. The DENV is transmitted to humans through the bite of *Aedes Aegypti* or *Aedes albopictus* female mosquitos. Infections can induce symptoms with a broad spectrum of severity,

which include hemorrhagic fever, shock syndrome, and death in some cases [1–3]. While the safety of the only approved dengue vaccine in seronegative individuals has been questioned [4], there are no antivirals currently available.

DENV is an enveloped positive single-stranded RNA virus that belongs to the genus *Flavivirus* within the family *Flaviviridae*. Following virus entry into the cell, the viral RNA genome (vRNA) is released in the cytosol and translated into a single large polyprotein, which is cleaved by host and viral proteases to generate 10 mature viral proteins. On one hand, structural proteins capsid (C), pre-membrane (prM), and envelope (E), together with vRNA, drive the assembly of viral particles. On the other hand, nonstructural proteins NS1, NS2A, NS2B, NS3, NS4A, NS4B, and NS5 are responsible for intracellular vRNA replication, a process which is believed to occur within endoplasmic reticulum (ER)-derived ultrastructures, called vesicle packets (VP) [5,6]. These ~90 nm-wide spherules are induced through the invagination of the ER, pack in plane in this organelle, and contain most (if not all) viral non-structural proteins, such as NS3, NS4B, and NS5, as well as double-stranded RNA (dsRNA), the vRNA replication intermediate [7,8]. In addition, the DENV induces the tight accumulation of smooth ER membranes, termed convoluted membranes (CM), which are structurally related to cubic membranes. These dsRNA-free ultrastructures are presumably not directly involved in the vRNA synthesis process. Since they are connected to VPs within the same ER network and are enriched in NS3 protease [8–10], it was proposed that they are involved in co-translational polyprotein maturation and VP biogenesis. However, it was never firmly demonstrated. More recently, their morphogenesis was functionally linked to the viral subversion of cellular processes, which are potentially detrimental to viral replication, such as innate immunity and apoptosis [9,11]. Finally, assembled virions accumulate in regular arrays within ER-derived enlarged cisternae [7,8]. These viral replication organelles (vROs) (or viral replication factories), generated through the extensive remodeling of the ER, constitute a cytoplasmic compartment that is favorable to vRNA amplification. Such virus-induced structures are also observed in cells infected with other flaviviruses, such as Zika virus (ZIKV), West Nile virus (WNV), Japanese encephalitis virus (JEV), and tick-borne encephalitis virus (TBEV) [10,12–16]. This strongly suggests that the molecular mechanisms governing vRO morphogenesis are conserved across the *Flavivirus* genus. However, the host and viral determinants of vRO biogenesis remain poorly defined. NS4B, an integral membrane protein, was proposed to be important for this process, since it is enriched in VPs and CMs, and is absolutely required for RNA replication [8,9,17–20]. Interestingly, NS4B was shown to be the viral target of several potent DENV inhibitors [21–25], illustrating the importance of this viral protein in the life cycle. Nevertheless, NS4B precise functions are poorly understood, while they may partly involve interactions with specific host factors.

Interactome studies have identified the AAA+ ATPase valosin-containing protein (VCP, also called p97) as a DENV NS4B protein partner, although such interaction was never validated [9,26]. We have recently reported that VCP also associates with ZIKV NS4B [11]. VCP is a ubiquitous protein with multiple roles related to proteostasis. Notably, it contributes to ER-associated degradation and mitochondria-associated degradation by retrotranslocating misfolded membrane proteins and targeting these substrates to the proteasome. It can also disassemble protein aggregates [27–34]. At the clinical level, multiple familial missense mutations are associated to severe genetic neurological diseases, such as frontotemporal dementia, classical amyotrophic lateral sclerosis, inclusion body myopathy, and Paget's disease of bone, alone or in combination [35–38]. Importantly, the inhibition of VCP ATPase activity impairs the replication of ZIKV, WNV, JEV, and yellow fever virus (YFV) in cell culture [11,39–43], demonstrating that this host factor regulates flavivirus replication, possibly through a conserved mechanism. In ZIKV-infected cells, we have shown that VCP and NS4B mostly colocalize in large structures, which presumably are the CMs [11]. Very interestingly, a four-hour treatment of ZIKV-infected cells with the selective VCP ATPase inhibitors CB-5083 or NMS-873 drastically reduced the abundance and size of the CMs, demonstrating that VCP is required for CM stability. This alteration

correlated with an increase of ZIKV-induced apoptosis, supporting that CMs regulate cellular processes. Whether this specific VCP function is conserved for all flaviviruses, including the DENV, is unknown. In such treatment conditions, ZIKV VPs could not be observed. While we could not quantify this phenotype and exclude that it was due to an indirect consequence of vRNA synthesis shutdown, this raised the hypothesis that VCP also regulates VP morphogenesis.

Using pharmacological and genetic inhibition approaches, we show in this study that VCP ATPase regulates DENV replication, similarly to other flaviviruses. VCP associates with NS4B when expressed alone or in infected cells, and these proteins colocalize within large DENV-induced cytoplasmic structures previously demonstrated to be CMs [9]. Consistently, VCP inhibition dramatically reduces the abundance of DENV CMs. Most importantly, using a recently reported replication-independent plasmid-based vRO induction system [44,45], we further show that *de novo* VP biogenesis requires VCP ATPase activity. This study supports that VCP is a pan-flaviviral host dependency factor and constitutes an attractive antiviral target, especially considering that new generation VCP drugs are currently evaluated in clinical trials for cancer treatment.

2. Materials and Methods

2.1. Cells, DNAs, Viruses, and Reagents

293T, HeLa, VeroE6 and Huh7.5 cells (kind gifts from Drs. Frédérick-Antoine Mallette, Tom Hobman, Anil Kumar, and Patrick Labonté) were cultured in a DMEM (Thermo-Fisher) supplemented with 10% fetal bovine serum (FBS; Wisent Inc., Saint-Jean-Baptiste, QC, Canada cat#098150), 1% penicillin-streptomycin (PS; Thermo-Fisher), and 1% non-essential amino acids (NEAA; Thermo-Fisher). The generation of Huh7.5-T7 and Huh7-Lunet-T7, which stably express the T7 RNA polymerase, was previously reported [11,44,45]. Huh7.5-T7 and Huh7-Lunet-T7 cells were cultured in DMEM/10% FBS/1% PS/1% NEAA, in the presence of 5 µg/mL blasticidin (Thermo-Fisher, Waltham, MA, USA) and 5 µg/mL zeocin (Invitrogen, Waltham, MA, USA), respectively.

The cloning of DENV2 16681s molecular clones (pFK-DVs and pFK-DVs-R2A), NS4B-encoding pTM constructs, pTM/DENV Δ5′ SLAB-3′ wt-Ribozyme (pIRO-D), and VCP-expressing lentiviral pWPI plasmids was previously reported [11,17,44,46].

Wild-type DENV2 16681s and Rluc-expressing reporter viruses were generated in VeroE6 cells following electroporation of in vitro transcribed RNA genomes. Briefly, following the linearization of pFK-DVs or pFK-DVs-R2A plasmids, in vitro transcription was performed using the mMESSAGE mMACHINE kit (Thermo-Fisher) with the SP6 RNA polymerase. RNAs were purified according to the manufacturer's instructions. Next, subconfluent VeroE6 cells were detached by trypsinization and collected in complete DMEM. The cells were washed once in PBS and resuspended in a cytomix buffer (120 mM KCl, 0.15 mM $CaCl_2$, 10 mM potassium phosphate buffer (pH 7.6), 25 mM HEPES (pH 7.6), 2 mM EGTA, 5 mM $MgCl_2$ (pH 7.6) freshly supplemented with 2 mM ATP, and 5 mM glutathione) at a density of 1.5×10^7 cells/mL. A total of 10 µg of in vitro-transcribed RNA were mixed with 400 µL of the cell suspension, transferred to an electroporation cuvette (0.4 cm gap width; Bio-Rad, Hercules, CA, USA), and pulsed once with a Gene Pulser Xcell Total System (Bio-Rad) at 975 µF and 270 V, typically resulting in time constants between 18 and 20 ms. Immediately after pulsing, the cells were transferred to pre-warmed complete DMEM and seeded in a 15 cm dish. On the next day, the cell culture medium was replaced with complete DMEM. Virus-containing cell culture supernatants were harvested once a day at 4, 5, 6, and 7 days post-electroporation, filtered through a 0.45 µm syringe filter, and supplemented with 10 mM HEPES (pH 7.5). DENV1 Hawaii, DENV2 New Guinea C, DENV3 H87, and DENV4 H241 were all generously provided by Professor Tom Hobman (University of Alberta) and amplified in VeroE6 cells for 4 to 7 days. Virus aliquots were stored at −80 °C until use. Infectious titers were determined by plaque assays.

NMS-873 and CB-5083 were obtained from Millipore-Sigma (Burlington, MA, USA) and Selleck Chemicals (Houston, TX, USA), respectively. Mouse monoclonal anti-VCP

(ab11433) was purchased from Abcam (Cambridge, United Kingdom). Rabbit anti-DENV NS4B (GTX124250) and mouse monoclonal anti-DENV NS3 (GTX629477) were obtained from Genetex (Irvine, CA, USA). The generation of rat polyclonal anti-DENV NS3 antibodies by Medimabs (Montréal, QC, Canada) was previously described [11].

2.2. Lentiviral Transduction

Lentiviruses encoding wild type or dominant negative HA-tagged VCP proteins were produced in 293T cells and titrated in HeLa cells exactly as previously described [11,45]. Huh7.5 cells were transduced with lentiviruses at a MOI of 1 in the presence of 8 µg/mL polybrene. A DENV infection was carried out 2 days post-transduction and viability, luciferase, and plaque assays were performed 4 days post-transduction.

2.3. Cell Viability Assays

For NMS-873 and CB-5083 CC_{50} values determination, cell viability was evaluated using the CellTiter-Glo Luminescent Cell Viability Assay kit (Promega, Madison, WI, USA) according to the manufacturer's instructions. Luminescence was measured with a Spark® multimode microplate reader (Tecan, Charlotte, NC, USA). Viability of transduced cells was assessed using MTT assays exactly as previously described [11].

2.4. Plaque Assays

200,000 VeroE6 cells were seeded in 24-well plates. Twenty-four hours later, cells were infected in duplicates with 200 µL virus samples that were subjected to 10-fold serial dilutions in a complete DMEM (10^1 to 10^6-fold dilution). Two hours post-infection, the inoculum was removed and a serum-free MEM (Life Technologies, Waltham, MA, USA) containing 1.5% carboxymethylcellulose (Millipore-Sigma, Burlington, MA, USA) was added. After 4 to 7 days, depending on the DENV strain, cells were fixed in 5% formaldehyde. Following washes with water, cells were stained with 1% crystal violet/10% ethanol for 15–30 min and then washed again with water. Plaques were counted and infectious titers were determined. The detection limit of this assay is 25 PFU/mL.

2.5. Luciferase Assays

Cells that were infected with the reporter virus DVs-R2A were lysed in 100–200 µL of lysis buffer (0.1% Triton X-100, 25 mM glycylglycine (pH 7.8), 15 mM MgSO4, 4 mM EGTA (pH 8), and 1 mM DTT). A total of 150 µL of assay buffer (25 mM glycylglycine (pH 7.8), 15 mM $MgSO_4$, 4 mM EGTA (pH 8), 15 mM K_2PO_4 (pH 7.8), and 1.43 µM benzylcoelenterazine (Prolume, Pinetop-Lakeside, AZ, USA) were injected to 30 µL of the lysate. Five seconds after this injection, the luminescence was measured for one second with a Spark® multimode microplate reader (Tecan).

2.6. Transfection

All cell transfections with NS4B-expressing pTM plasmids were carried out with the TransIT-LT1 Transfection Reagent (Mirus, Madison, WI, USA) according to the manufacturer's instructions and exactly as previously described [11,45]. Cells were subjected to co-immunoprecipitation assays or immuno-labelling for confocal microscopy 16 h post-transfection.

2.7. Immunofluorescence-Based Confocal Microscopy

Transfected or infected cells were grown on glass coverslips, washed twice with phosphate-buffered saline (PBS), fixed with 4% paraformaldehyde in PBS, and permeabilized with PBS-0.2% Triton X-100 for 15 min. Cells were blocked during 1 h with PBS containing 5% bovine serum albumin (BSA) and 10% goat serum (Thermo-Fisher), and then incubated with primary antibodies for 2 h at room temperature in the dark. Following three washes in PBS, the coverslips were incubated with Alexa Fluor-conjugated secondary antibodies (Life Technologies, Waltham, MA, USA) for 1 h at room temperature in the dark. The coverslips were then washed three times with PBS during 10 min, and the nuclei were

stained with 4′, 6′-diamidino-2-phenylindole (DAPI; Life Technologies). Following three final washes with PBS and one with water, the coverslips were mounted on slides with Fluoromount-G (Southern Biotechnology Associates, Birmingham, AL, USA). The cells were imaged with a LSM780 confocal microscope (Carl Zeiss Microimaging, Oberkochen, Germany) at the Confocal Microscopy Core Facility of the INRS-Centre Armand-Frappier Santé Biotechnologie.

2.8. Co-Immunoprecipitation Assays

Transfected cells were washed twice in PBS and incubated during 20 min on ice in a lysis buffer (0.5% Dodecyl-B-D-maltoside, 100 mM NaCl, 20 mM Tris (pH 7.5), 50 mM NaF, and EDTA-free protease inhibitors (Roche, Mannheim, Germany). Lysed cells were centrifuged during 15 min at 13,000 rpm at 4 °C, and supernatants were collected. Resulting cell extracts were incubated with 50 µL of a 50/50 slurry of mouse monoclonal anti-HA coupled to agarose beads (Millipore-Sigma) at 4 °C. Three hours later, the resin was washed twice with lysis buffer and twice with a solution containing 150 mM NaCl and 50 mM Tris (pH 7.5). Resin-associated proteins were collected by a first elution with PBS-5% SDS, and by a second one with PBS. The eluates were pooled and precipitated overnight at −20 °C by adding 4 volumes of acetone. The precipitated proteins were centrifuged during 1 h at 13,000 rpm. The resulting pellets were air-dried, resuspended in loading buffer, and subjected to Western blot analysis.

2.9. Transmission Electron Microscopy

Huh7.5 were grown on Lab-tech® chamber SlideTM (Thermo Fisher) and infected with DENV2 16681s at a MOI of 1. Two days post-infection, cells were treated with either 0.2% DMSO, 20 µM CB-5083, or 20 µM NMS-873 for 4 h. Following three washes with PBS, cells were fixed overnight at 4 °C in 2.5% glutaraldehyde in 0.1 M sodium cacodylate buffer (pH 7.4). Specimens were treated with osmium, dehydrated, and Epon-resin embedded at the McGill University Facility for Electron Microscopy Research exactly as previously described [11]. Ultrathin serial sections (90–100 nm thick) were prepared with a Diatome diamond knife using a Leica Microsystems EM UC7 ultramicrotome and transferred onto 200-mesh copper grids. The grids were stained with 4% uranyl acetate for 6 min and Reynold's lead for 5 min. Samples were imaged with a FEI Tecnai G2 Spirit 120 kV TEM equipped with a Gatan Ultrascan 4000 CCD Camera Model 895 (Gatan, Pleasanton, CA) located at the McGill University Facility for Electron Microscopy Research. The DENV CM analysis was performed using Fiji software.

For the replication-independent VP induction, Huh7-Lunet-T7 cells were transfected with pTM/DENV Δ5′ SLAB-3′ wt-Ribozyme (pIRO-D) plasmid exactly as previously described [44,45]. Four hours later, cells were treated with DMSO, 2.5 µM CB-5083 or 1 µM NMS-873 for 12 h. Sixteen hours post-transfection, the cells were fixed with an EM fixative (50 mM sodium cacodylate buffer, 50 mM KCl, 2.6 mM $MgCl_2$, 2.6 mM $CaCl_2$, 1% paraformaldehyde, 2.5% glutaraldehyde, and 2% sucrose (pH 7.4)) for 30 min at room temperature. In parallel to the EM samples, transfection efficiency was evaluated by immunofluorescence analysis as described above. After the fixation of the EM samples, they were washed 5 times with 50 mM sodium cacodylate and incubated with 2% osmium tetroxide in 50 mM cacodylate buffer for 40 min on ice. Following 3 additional washes with EM-grade water, samples were incubated for 30 min with 0.5% uranyl acetate in water, rinsed three times with water, and subject to dehydration in a graded ethanol series (from 40% to 100%). Samples were embedded in epoxy resin and the polymerized for 48 h at 60 °C. Ultrathin sections of 70 nm were produced by sectioning with a UC6 ultramicrotome (Leica Microsystems, Wetzlar, Germany) and sections were collected, counterstained with uranyl acetate and lead citrate, and examined with a JEOL JEM-1400 transmission electron microscope. For the VP measurements, the EM images were analyzed with Fiji software and the number and diameter of the VPs were measured. At least 15 cells were counted for each condition in 2 experiments.

3. Statistical Analysis

All Student t-tests were unpaired and two-tailed. In Figure 1A,E and Supplementary Materials Figure S1, because of variations in the reference titer absolute values (DMSO or Empty pWPI conditions) between independent experiments, t-tests challenging the significance of the phenotypes were performed with normalized values reflecting the percentage of replication as compared to the control.

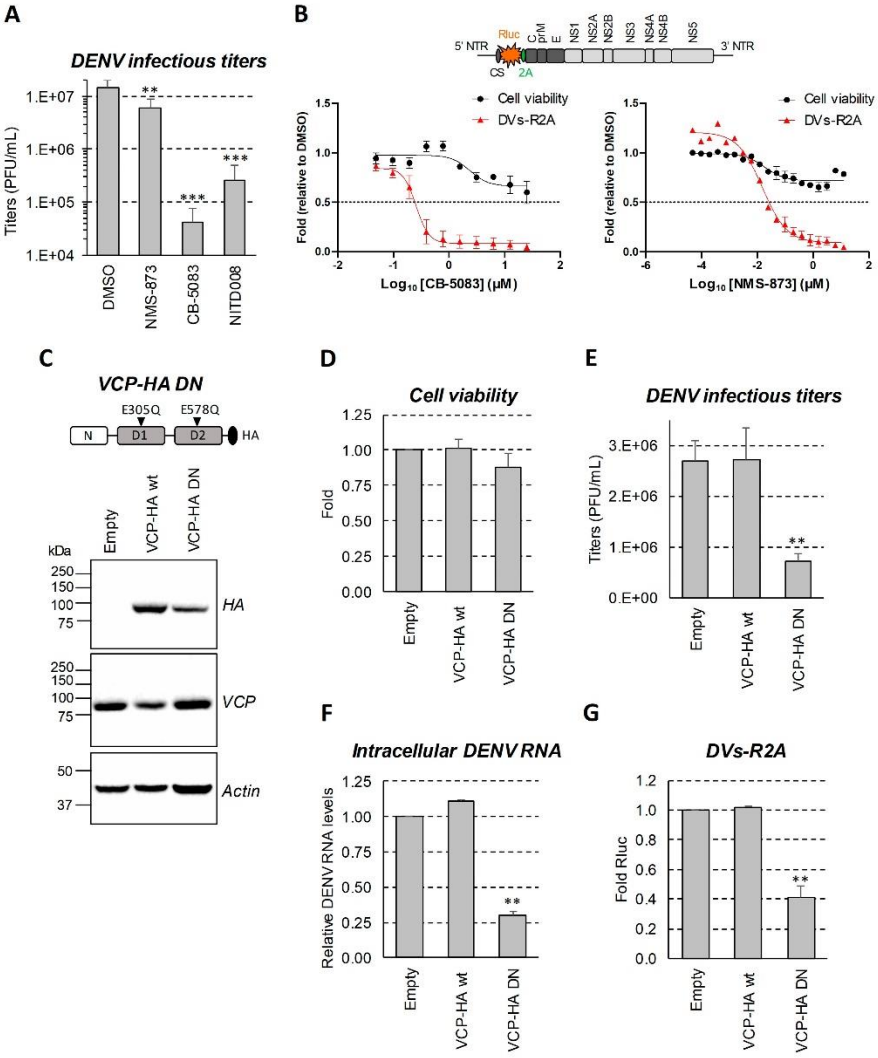

Figure 1. VCP ATPase inhibition impairs DENV replication. (**A**) Huh7.5 cells were infected with DENV2 16681s at a MOI of 0.05. The day after, the cells were treated with DMSO, 50 nM NMS-873, 0.5 μM CB-5083, or 10 μM NITD008 as positive control. After 24 h (2 days post-infection), cell supernatants were collected, and plaque assays were performed. (**B**) Huh7.5 cells were

infected with the DENV2 16681s Renilla luciferase (Rluc)-expressing reporter virus (DVs-R2A) at a MOI of 0.001. One day post-infection, the infected cells were treated with various concentration of CB-5083 or NMS-873. After 24 h (2 days post-infection), Rluc assays were performed. Cell viability was measured in uninfected cells by CellTiter-Glo luminescent assays. The plotted data are relative to the DMSO treatment control. The dot line is a marker of a 50% decrease in viability or replication. NTR: non-translated region; 5′ CS: 5′ cyclization sequence; 2A: *Tosea asigna* virus 2A cleavage site at the C-terminus of Rluc to ensure proper processing after polyprotein synthesis. (**C**,**D**) Huh7.5 cells were transduced with lentiviruses expressing wild-type VCP or the depicted dominant negative VCP E305Q/E578Q mutant (MOI = 1). Four days post-transduction, the cells were collected and analyzed by Western blotting using the indicated antibodies (**C**) or subjected to MTT assays (**D**). (**E**,**F**) The cells were transduced as in (**C**). Two days post-transduction, the cells were infected with DENV2 16681s at a MOI of 0.05. Two days post-infection (four days post-transduction), extracellular infectious titers and relative intracellular DENV RNA levels were determined using plaque assays (**E**) and RT-qPCR (**F**), respectively. (**G**) Cells were transduced as in (**C**). Two days post-transduction, cells were infected with DVs-R2A at a MOI of 0.001. Two days post-infection (4 days post-transduction), viral replication was measured using Rluc assays. All results are representative of two or three independent experiments. **: p-value ≤ 0.01; ***: p-value ≤ 0.001.

4. Results

4.1. VCP ATPase Activity Is Required for Efficient DENV Replication

To investigate whether VCP ATPase is required for DENV replication, Huh7.5 hepatocarcinoma cells were infected with the DENV (serotype 2, strain 16681s) at a multiplicity of infection (MOI) of 0.05, and treated for 24 h with 2 selective VCP ATPase inhibitors, namely CB-5083 or NMS-873, which exhibit 2 different modes of action (ATP-competitive vs. allosteric non-ATP-competitive, respectively) [47–50]. At concentrations previously shown to be non-toxic in this cell line [11], both treatments significantly reduced the production of infectious viruses (Figure 1A). Remarkably, DENV infectious titers were reduced by more than 100-fold following CB-5083 treatment at 0.5 μM. NMS-873 treatment reduced virus production by 60%. At this low MOI, the infection did not induce additional cell death (data not shown). Using a reporter DENV virus expressing the Renilla luciferase (Rluc) in frame with the polyprotein [46] and thus, allowing to indirectly measure intracellular viral replication in luciferase assays, we determined that the half maximal effective concentration (EC_{50}) of CB-5083 and NMS-873 were 0.25 μM and 0.02 μM, respectively (Figure 1B). In contrast, their 50% cytotoxic concentration CC_{50} were above 25 μM.

In order to confirm that DENV replication requires VCP ATPase activity, we expressed in Huh7.5 cells the VCP dominant-negative E305Q/E578Q mutant (VCP-HA DN) through lentiviral transduction (Figure 1C). In this set-up, VCP-HA DN was produced at sub-endogenous levels since the total VCP amounts (detected with anti-VCP antibodies) were not increased. This mutant was shown to impair the enzymatic activity of VCP hexamers [51]. In contrast to cells expressing HA-tagged wild-type VCP, virus production and vRNA intracellular levels were decreased when cells expressed VCP-HA-DN, while cell viability was not impacted (Figure 1D–F). The same phenotype was observed with DENV reporter virus using luciferase activity as a read-out of viral replication (Figure 1G).

Finally, we have confirmed the role of VCP in the DENV life cycle by extending our analysis to another serotype 2 strain, namely the DENV2 New Guinea C, as well as to DENV strains belonging to serotypes 1, 3, and 4. As shown in Supplementary Materials Figure S1, a 24 h treatment of infected cells with CB-5083 drastically decreased viral production in all cases. Overall, these results show that VCP ATPase activity is required for efficient DENV replication.

4.2. VCP Associates with DENV NS4B Independently of Other Viral Proteins

Our previous interactomic study has identified VCP as a protein partner of NS4B in infected cells [9]. To obtain more insight about a potential co-opting mechanism of VCP by the DENV through NS4B, VCP localization in DENV-infected Huh7.5 cells was analyzed using confocal microscopy. In uninfected conditions, VCP did exhibit a diffuse distribution throughout the cell. In contrast, two days post-infection, VCP distribution was drastically

altered (Figure 2A). Indeed, this protein accumulated in large NS4B-enriched structures (Figure 2A, white arrows), which we have previously demonstrated to be devoid of dsRNA and to be CMs using correlative light-electron microscopy (CLEM) (Figure 2B, white arrows) [9]. In addition, VCP relocalized to the NS4B-positive perinuclear area (Figure 2A) in which dsRNA (i.e., replication complexes) typically accumulates (Figure 2B) [9]. Although these phenotypes are consistent with the reported NS4B/VCP interaction in infected cells [9], we next assessed whether it required the contribution of other viral proteins. We transfected Huh7.5 cells stably expressing the T7 RNA polymerase (Huh7.5-T7) with a plasmid encoding NS4B as the HA-tagged NS4A-2K-NS4B precursor under the control of the T7 promoter, exactly as reported before [9,17]. We initially chose to express this precursor because it is readily detectable by confocal microscopy, with a much punctated distribution as compared to the one of the pseudo-mature 2K-NS4B [9,17]. Indeed, in transfected cells, NS4B localized in large punctae in which VCP partially redistributed (Figure 3A,C, white arrows). Although such punctae were less abundant in 2K-NS4B-HA-expressing cells, they were also enriched in VCP (Figure 3C, white arrows). In contrast, VCP distribution in HA-NS4A-expressing cells was comparable to that in control cells. This suggests that NS4B and VCP can interact in the absence of other proteins. To confirm this, we performed co-immunoprecipitations directed against the HA-tag with cells expressing HA-tagged NS4B proteins (Figure 3B). Endogenous VCP was readily detected in the eluates when immature or mature NS4B-HA was pulled-down, whereas very little, if any, was present in control conditions in which untagged NS4B proteins were expressed. These results demonstrate that VCP interaction with DENV NS4B does not absolutely require other viral proteins.

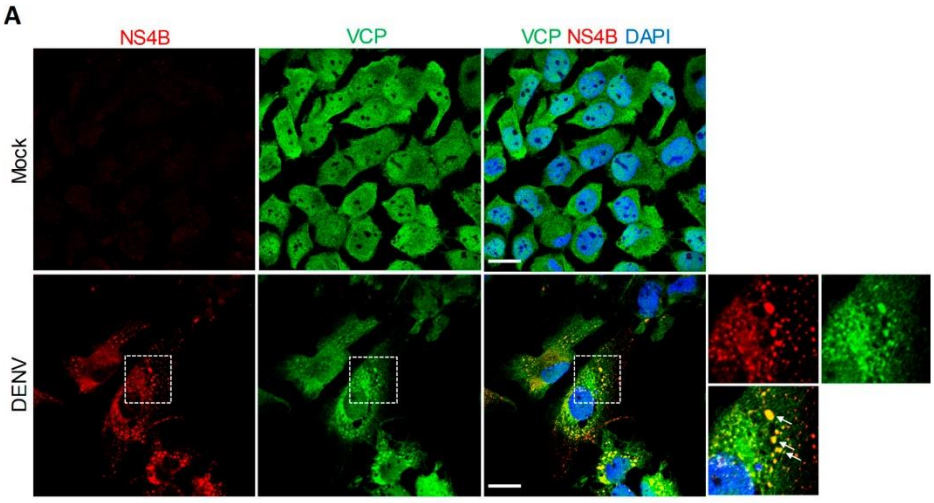

Figure 2. *Cont.*

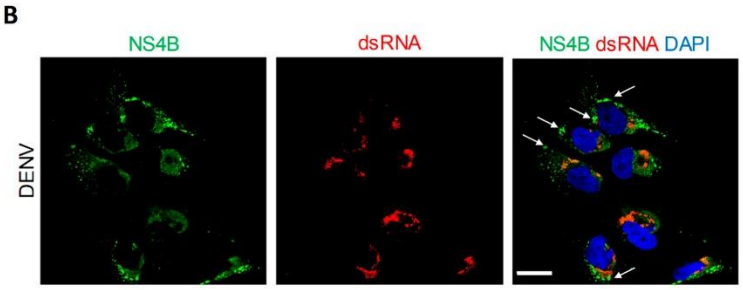

Figure 2. VCP associates with the DENV NS4B in infected cells. (**A**) Huh7.5 cells were infected with DENV2 16681s (MOI = 1) or left uninfected. Two days later, cells were fixed, immunolabeled with anti-VCP and anti-NS4B antibodies, and imaged by confocal microscopy. The bottom right panels show single channel and merged images of the magnified area indicated with the dashed square (~2.4-fold magnification). (**B**) Huh7.5 were prepared exactly as in (**A**) and labeled with anti-NS4B and anti-dsRNA antibodies. White arrows indicate colocalization foci.

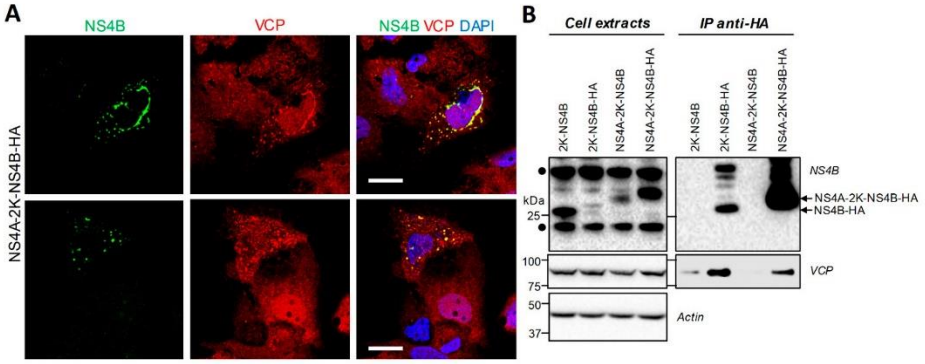

Figure 3. *Cont.*

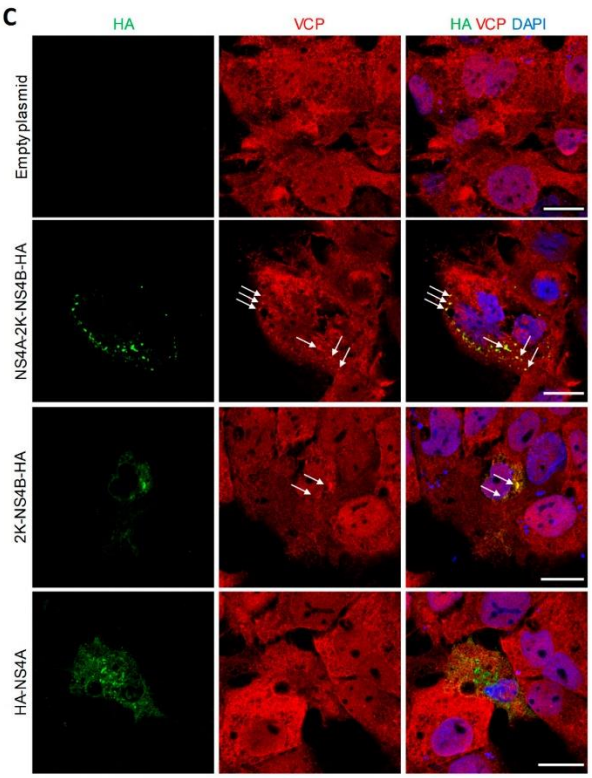

Figure 3. VCP associates with DENV NS4B when expressed alone as a precursor or a mature protein. (**A**) Huh7.5-T7 cells were transfected with a plasmid expressing DENV2 16681s NS4A-2K-NS4B-HA. Sixteen hours post-transfection, the cells were fixed, immunolabeled with anti-VCP and anti-NS4B antibodies, and imaged by confocal microscopy. Scale bar: 20 μm. (**B**) Huh7.5-T7 cells were transfected with the plasmids expressing the indicated viral proteins. Sixteen hours post-transfection, cells extracts were prepared and subjected to co-immunoprecipitation directed against HA. Resulting eluates and cell extracts were analyzed by Western blotting using the indicated antibodies. The DENV NS4A-2K-NS4B typically exhibits a lower molecular weight than expected because of a faster in-gel migration. The black dots indicate non-specific signals generated by the anti-NS4B antibodies. (**C**) Huh7.5-T7 cells were transfected with plasmids expressing the indicated DENV proteins. Sixteen hours post-transfection, the cells were fixed, immunolabeled with anti-VCP and anti-HA antibodies, and imaged by confocal microscopy. White arrows indicate colocalization foci. Scale bar: 20 μm.

4.3. The Abundance of DENV Convoluted Membranes in Infected Cells Depends on VCP ATPase Activity

Since VCP accumulates in large structures that are reminiscent of CMs in DENV-infected cells, we hypothesized that its ATPase activity is required for their stability and/or biogenesis. To test this, at 2 days post-infection, the cells were treated with high concentrations of NMS-873 or CB-5083 for 4 h and then prepared for CM imaging using transmission electron microscopy. In parallel, we controlled that the infection efficiency was 90–100% at this time post-infection and MOI. In control DMSO-treated infected cells, CMs as well as VPs were readily observed (Figure 4A). In stark contrast, following CB-5083 or NMS-873 treatment, the abundance of CMs was dramatically decreased with no CM detected at all in 33 CB-5083-treated analyzed cells (Figure 4B). While the few CMs detected in NMS-

873-treated cells did exhibit sizes in the range of those in control cells (Figure 4C), their appearance was different with a relaxed electron-dense morphology (Figure 4A, top-right panel). Upon either drug treatments, we noticed the accumulation of vesicles with irregular shapes that might result from CM destabilization (Figure 4A, bottom-right and middle panels). These phenotypes were not attributed to changes in viral protein stability since such short treatment did not impact overall levels of NS4B and NS3, the two components of the DENV CMs (Figure 4D) [8,9]. We and others have previously shown that DENV NS4B and NS3 interact in infected cells [17,18,52]. Considering this, we assessed whether the observed CM alteration correlates with an impairment of NS3/NS4B complexes. We performed co-immunoprecipitation assays with cells co-expressing NS2B/NS3 protease and NS4A-NS4B-HA (Supplementary Materials Figure S2). As previously reported [17], NS3/NS4B-HA interaction was specifically detected. As control, it was completely abrogated when we expressed a NS4B-HA mutant harboring the Q134A mutation in its cytosolic loop [17]. In contrast, neither the CB-5083 nor the NMS-873 four-hour treatment significantly impacted the extent of NS3/NS4B interaction. This strongly suggests that the alteration of CMs upon drug treatment is not due to a loss of NS3/NS4B interaction.

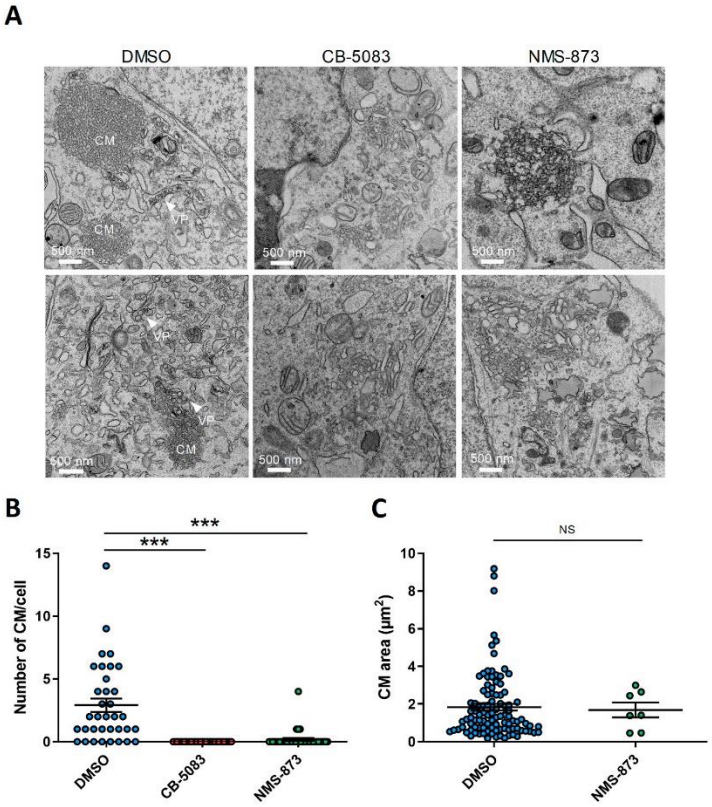

Figure 4. *Cont.*

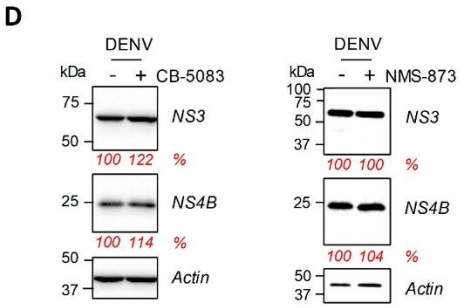

Figure 4. VCP ATPase activity is required for the stability of the DENV convoluted membranes. (**A**) Huh7.5 cells were infected with DENV2 16681s at a MOI of 1. Two days post-infection, cells were treated with DMSO, 20 μM CB-5083, or 20 μM NMS-873. After a 4 h treatment, the cells were prepared for imaging by transmission electron microscopy. CM: convoluted membranes; VP: vesicle packets. (**B**,**C**) More than 33 cells from each condition were analyzed for CM abundance (**B**) and size (**C**). ***: *p*-value $\leq$ 0.001; NS: not significant. (**D**) Huh7.5 cells were infected with DENV2 16681s at a MOI of 1. Two days post-transfection, cells were treated with DMSO, 20 μM CB-5083 for four hours, or 20 μM NMS-873 for one hour. Cell extracts were prepared and analyzed by Western blotting with the indicated antibodies. The relative abundance of NS3 and NS4B (shown in red) was quantified after normalization to actin levels using the ImageLab software (Bio-Rad).

4.4. VCP Inhibition Impedes the Biogenesis of the DENV VPs

In contrast to control cells, the VPs were completely undetectable in DENV-infected cells that were treated for 4 h with CB-5083 or NMS-873 (Figure 4A). This suggests that VCP ATPase activity is required for VP morphogenesis and/or stability. However, given that VCP inhibition impairs DENV replication, we could not rule out that this loss of the VPs was simply due to a potential shutdown of RNA replication (and, hence, viral protein synthesis) rather than a direct effect on VP morphogenesis. Considering this "chicken and egg" situation, an infection-based approach with longer drug treatments was not appropriate to challenge the hypothesis that VCP is involved in VP biogenesis. To tackle this and clearly evaluate whether VCP ATPase activity is required for *de novo* VP formation, we took advantage of a plasmid-induced DENV replication organelle formation system (pIRO-D) reported by us recently [44,45]. This system allows the expression of the DENV NS1-5 polyprotein under the transcriptional control of the T7 RNA polymerase promoter in a replication-independent context (Figure 5A). Following the plasmid transfection of Huh7-derived Lunet cells that stably express the T7 RNA polymerase (Lunet-T7) to allow cytoplasmic transcription, the IRES-driven synthesis of the polyprotein along with the presence of vRNA 5′ CS and 3′ non-translated region, as well as a ribozyme at the 3′ end of the RNA, is sufficient to induce the VPs with an authentic architecture in the absence of viral genome replication. Thus, this system allowed us to study the impact of VCP inhibitor treatments in VP morphogenesis. Lunet-T7 cells were transfected with the pIRO-D DNA construct and treated 4 h later with 2.5 μM CB-5083 or 1 μM NMS-873. Sixteen hours post-transfection, the cells were prepared for widefield and electron microscopy. Either drug treatment did not have a major impact on the transfection efficiency since the percentage of NS3-positive cells was comparable in all conditions (Figure 5B,C). Moreover, Western blot analysis of cell extracts showed that NS3 expression levels remained unchanged upon treatment (Figure 5D), supporting that VCP inhibition does not impact overall polyprotein synthesis. Interestingly, NS4B levels were decreased by both VCP inhibitor treatments suggesting that VCP ATPase activity is required for NS4B expression at the post-translational level through their interaction (Figure 5D). Very strikingly, transmission electron microscopy analysis of pIRO-D-transfected cells revealed that, despite unchanged polyprotein abundance, only 5–10% of drug-treated cells contained VPs as compared to 30% positive cells in the DMSO control condition (Figure 5E,F). Moreover, in that subset of

treated cells, we never detected more than two spherules per VP (Figure 5E, top middle and right panels). Notably, very few were observed in the CB-5083 condition (6 VPs vs. >40 VPs in DMSO-treated cells for 15 cells analyzed). Most importantly, in NMS-873-treated cells, VPs often exhibited an aberrant morphology in stark contrast with their usual circular shape observed in the DMSO control (Figure 5E, bottom right panel). However, the size of VPs in drug-treated cells remained unchanged (Figure 5G). Furthermore, the CB-5083 treatment also resulted in the aggregation of vesicular structures with irregular shapes in some cells (Figure 5E, bottom middle panel), but these structures were not classified as VPs in our quantification given their distinct morphology. Overall, these results unambiguously demonstrate that proper ER remodeling during VP biogenesis is dependent on the ATPase activity of VCP.

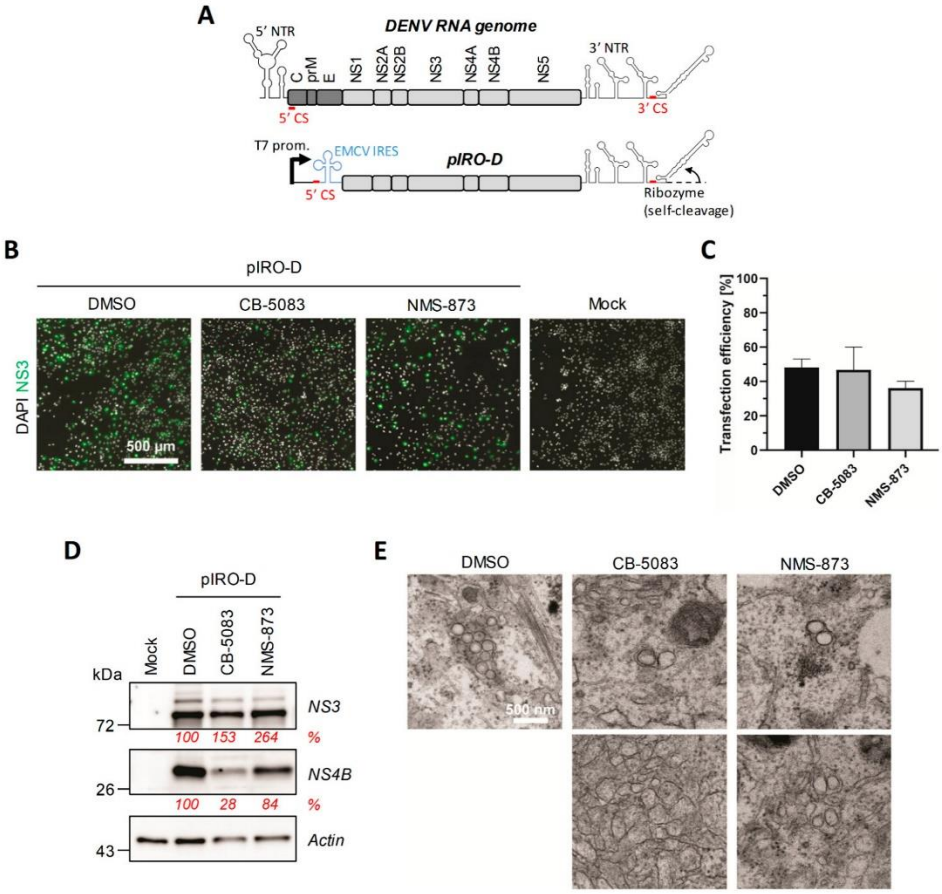

Figure 5. *Cont.*

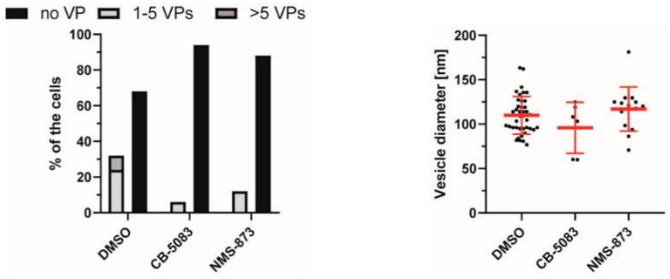

Figure 5. The DENV vesicle packet biogenesis requires VCP ATPase activity. (**A**) Schematic representation of the plasmid-induced DENV replication organelle system (pIRO-D) with a side-by-side comparison between the transcribed RNA with the DENV RNA genome. NTR: non-translated region; prom.: promoter; 5′ CS: 5′ cyclization sequence; IRES: internal ribosme entry site. (**B**–**D**) Huh7-Lunet-T7 cells were transfected with pIRO-D plasmid and, 4 h post-transfection, treated with DMSO, 2.5 μM CB-5083, or 1 μM NMS-873 for 12 h. (**B**) Fixed cells were labeled with anti-NS3 antibodies and imaged by widefield microscopy. (**C**) The transfection efficiency upon treatment with the different compounds was determined based on the % of NS3-positive cells. Mean and SD from two experiments are shown. (**D**) Total lysates of transfected and treated cells were analyzed by Western blotting using the indicated antibodies. The relative abundance of NS3 and NS4B (shown in red) was quantified after normalization to actin levels using the Fiji software. (**E**) Electron microscopy analysis of samples treated as in (**B**). (**F**) Quantification of the number of cells exhibiting the VPs. At least 15 cells from 2 different experiments have been analyzed for each condition. (**G**) The diameter of VPs was determined.

5. Discussion

Using both pharmacological and dominant-negative mutant overexpression approaches, we show in this study that VCP, through its ATPase activity, is required for DENV replication in cell culture. This is consistent with an important role of VCP in the homeostasis of the ER, an organelle that is morphologically altered by the DENV to generate vROs. Such viral dependency on this host factor was not surprising, since it is reminiscent to what was reported by us and others for several flaviviruses, such as the ZIKV, WNV, YFV, and JEV [11,39–43]. More specifically, similarly to the DENV, we had previously reported that VCP associates with ZIKV NS4B and that short inhibition of its ATPase activity destabilizes CMs in infected cells [11]. More recently, Sehrawat and colleagues showed that VCP is associated with JEV replication complexes [43]. An interaction with NS5 was detected in infected cells, but not when this viral protein was expressed alone. This is consistent with the idea that NS4B might recruit VCP to vROs. While we were preparing this manuscript, another study identified VCP as a protein partner of both JEV NS4B and DENV NS4B in overexpressing cells [41], confirming our results. Overall, this suggests that flaviviruses share conserved VCP co-opting mechanisms during intracellular viral replication.

Very importantly, neither VPs nor CMs were detected in infected cells following a 4-h treatment with VCP inhibitor CB-5083. In DENV-infected cells, a fraction of VCP did accumulate to large NS4B-containing punctae. Using CLEM, we had previously demonstrated that these dsRNA-free ultrastructures are CMs [9]. Moreover, a 4 h treatment with NMS-873 or CB-5083 induced a dramatic loss of DENV CMs while overall levels of both NS4B and NS3, two components of CMs, remained unchanged. Such rapid destabilization of CMs is consistent with the fact that CMs are very dynamic structures in terms of size, as previously observed in live-cell imaging of infected cells [9]. Overall, this supports a model in which VCP is physically recruited to CMs through its interaction with NS4B and regulates their stability and/or biogenesis. The exact role of CMs during flavivirus replication remains poorly understood. Since NS3 protease is enriched in this structure, it was for long believed that it is the site of polyprotein maturation. However, this process occurs post-translationally and CMs appear composed of smooth ER and devoid of ribo-

somes in electron microscopy. Being sometimes located in the same ER network as VPs [8], CMs might be required for VP biogenesis, or vice-versa. In addition, we favor a model in which CMs indirectly support intracellular replication by modulating cellular processes that are detrimental to the efficacy of the viral life cycle. For instance, we have recently shown that VCP ATPase inhibition-mediated CM destabilization stimulates ZIKV-induced apoptosis, supporting that CMs delay cytopathic effects potentially to maximize viral replication at the late time point of infection [11]. Moreover, this inhibition was associated with a loss of the elongated morphology of mitochondria, which are normally located in the vicinity of CMs. In the case of the DENV, mitochondria elongation was shown to promote viral replication while dampening early innate immune responses by decreasing RIG-I translocation to mitochondria-associated membranes [9]. Overall, this supports that flaviviral CMs contribute to replication by attenuating antiviral cellular responses. Very interestingly, Tabata and colleagues have recently reported that VCP inhibition by another drug, DBeQ, increased the half-life of JEV NS4B and increased the abundance of this viral protein in JEV CMs [41]. This is in contrast with what we observed for DENV NS4B in this study. Indeed, a 12 h treatment with VCP inhibitors reduced the levels of NS4B in a replication-independent DENV polyprotein expression set-up (Figure 5D). Such phenotype was not observed for NS3, supporting that VCP controls the stability of NS4B. Nevertheless, a shorter treatment destabilized CMs in infected cells without affecting NS4B abundance (Figure 4D). One possibility explaining the decrease in NS4B levels in longer treatments could be that the integrity of CMs is required for the stability of the NS4B molecules residing in these ultrastructures. This potential reciprocal functional relationship between NS4B and CMs as well as the apparent differences between DENV and JEV NS4B will have to be addressed in future studies. Regardless, this also raises the hypothesis that VCP also locally controls the proteostasis of specific host factors potentially "trapped" in CMs to modulate cellular pathways and promote viral replication.

It is noteworthy that, in contrast to the VPs, CMs were not detected in DENV-infected C6/36 mosquito cells when analyzed by electron microscopy [7], and VCP insect ortholog TER94 is required for the early steps of the ZIKV life cycle in AF5 mosquito cells [42]. While we cannot completely exclude that CMs are generated in the infected insect, this might reflect the difference between insect and mammals regarding virus-induced cellular responses, such as cytopathic effects and/or innate immunity. For instance, there are no RIG-I-like receptors in insects that instead, primarily use the Toll, Imd, and RNA interference pathways as innate immune systems [53]. Considering this, the reported CM functional interaction with the RIG-I pathway in human cells would be irrelevant and useless in insects.

By taking advantage of a novel replication-independent vRO-induction system, we further demonstrate in this study that VCP ATPase activity is required for VP biogenesis. Considering that DENV NS4B (1) is absolutely required for RNA replication [17–19]; (2) localizes to VPs as observed by transmission electron microscopy following immunogold labelling [8,9]; and (3) associates with VCP (this study and [41]), it is tantalizing to speculate that VCP directly regulates VP morphogenesis through its binding to NS4B. Future studies will determine whether VCP ATPase inhibition disrupts interactions between NS4B (or the NS4A-NS4B precursor) with other DENV proteins, which are believed to be important for vRNA replication and/or VP biogenesis. While our results show that the stability of the DENV NS4B/NS3 complex is not disrupted by a 4 h treatment with VCP inhibitors, VCP might regulate DENV NS4B *de novo* interactions with NS1 or NS4A [54,55]. Alternatively, one cannot exclude that VCP is required for VP morphogenesis because of its contribution to ER homeostasis, notably to the ER-associated degradation (ERAD) by retrotranslocating misfolded proteins from this organelle and targeting them to the proteasome [29,30,33]. It was recently reported that JEV replication is decreased upon knockdown of VCP co-factor UFD1, which confers substrate selectivity to the complex for proteasomal targeting [43]. Consistently, UFD1 was also identified as a protein partner of both JEV-NS4B and DENV NS4B [41]. However, JEV replication did not require the co-factor UBXD1 [43], suggesting

some selectivity regarding the flaviviral co-opting mechanism of VCP complexes and potentially the substrates targeted for degradation. It will be relevant to investigate in future studies whether DENV infection modulates VCP substrate selectivity and its interactome in terms of its 30 co-factors identified so far. More generally, it is tempting to hypothesize that VCP regulates the flavivirus life cycle in association with other known NS4B protein partners. For instance, transmembrane protein 41B (TMEM41B) was identified as a ZIKV NS4B protein partner, which is required for viral replication [56]. More recently, Hoffmann and colleagues showed that this protein is a pan-flaviviral host dependency factor [57]. Both studies showed that TMEM41B redistributed to NS4B-containing large punctae, similarly to VCP. Interestingly, while YFV replicated much less efficiently in TMEM41B-knock-out cells, interferon-stimulated genes and apoptosis were more induced than in wild-type cells. As an apparent ER resident protein, it was proposed that TMEM41B contributes to ER membrane remodeling during vRO biogenesis. All these data are relevant to the proposed role of VCP in this latter process (this study), as well as to the modulation of early innate immunity and cytopathic effects by CMs [9,11]. Thus, it is plausible that TMEM41B and VCP regulate the flavivirus life cycle within the same complex. Alternatively, VCP might also contribute to the NS4B-mediated downregulation of stress-associated ER protein 1 (SERP1), a reported DENV2 restriction factor [58].

Finally, it is noteworthy that several studies have also reported an additional role of VCP during the post-fusion steps of the YFV and ZIKV life cycles in both human and mosquito cells [40,42]. This highlights that VCP impacts the flavivirus life cycle at multiple levels and, hence, VCP-targeting inhibitors are expected to possess a high antiviral potency *in vivo*. In a murine JEV-infection model, administration of CB-5083 in infected mice reduces the viral load in the brain and significantly delays the mortality rate [43]. Unfortunately, the clinical trials assessing the anti-cancer activity of CB-5083 were stopped because of patients experiencing visual loss [59,60]. A more selective and bioavailable analog, CB-5339 is currently being challenged in phase I clinical trials for treatment of acute myeloid leukemia and myelodysplastic syndrome, as well as solid tumors and lymphomas (www.clinicaltrials.gov; identifiers NCT04372641 and NCT04402541) (accessed on 17 July 2021). If this second generation oral drug is safe in humans, it will be highly relevant to assess whether it can be repurposed for the treatment of infection with the DENV and, ideally, as a broad-spectrum antiflaviviral drug.

Supplementary Materials: The following are available online at https://www.mdpi.com/article/10.3390/v13102092/s1, Figure S1: VCP ATPase inhibition impairs the replication of DENV strains from all four serotypes; Figure S2: VCP ATPase inhibition does not impair NS4B/NS3 interaction.

Author Contributions: Conceptualization: writing—original draft preparation, and supervision: L.C.-C. and C.M.; analysis and infection experiments: C.M., A.A., A.A.S., and W.F.; pIRO-based VP analysis: F.P., M.C., and B.C.; writing—review and editing: L.C.-C., C.M., A.A., F.P., A.A.S., W.F., M.C., and R.B. All authors have read and agreed to the published version of the manuscript.

Funding: C.M received PhD fellowships from the Armand—Frappier Foundation and the Center of Excellence in Research on Orphan Diseases-Courtois Foundation (CERMO-FC). A.A was a recipient of a Master's training fellowship from Fonds de la Recherche du Québec-Santé (FRQS). W.F currently receives a Ph.D. training fellowship from FRQS. L.C.C is receiving a research scholar (Junior 2) salary support from FRQS. This research was supported by a project grant from the Canadian Institutes of Health Research (CIHR; PJT153020), awarded to L.C.C. The work of R.B was funded by the Deutsche Forschungsgemeinschaft (DFG, German Research Foundation)—project number 240245660—SFB 1129 and grant Ba1505/8-1.

Institutional Review Board Statement: Not applicable.

Informed Consent Statement: Not Applicable.

Acknowledgments: We are grateful to Jessy Tremblay at the Centre Armand—Frappier Confocal Microscopy Facility for technical assistance during imaging, and Jeannie Mui and Kelly Sears at the McGill University Facility for Electron Microscopy Research for sample preparation. We are

thankful to Uta Haselmann for excellent technical support. We thank the Electron Microscopy Core Facility at Heidelberg University, headed by Stefan Hillmer, and the Infectious Diseases Imaging Platform (IDIP) at the Center for Integrative Infectious Disease Research in Heidelberg, headed by Vibor Laketa, for their expert support and access to their equipment. We thank Frédérick-Antoine Mallette (Université de Montréal), Patrick Labonté (Institut National de la Recherche Scientifique), Tom Hobman (University of Alberta), and Anil Kumar (University of Saskatchewan) for generously providing cell lines and DENV strains.

Conflicts of Interest: The authors declare no conflict of interest.

References

1. Bhatt, S.; Gething, P.W.; Brady, O.J.; Messina, J.P.; Farlow, A.W.; Moyes, C.L.; Drake, J.M.; Brownstein, J.S.; Hoen, A.G.; Sankoh, O.; et al. The global distribution and burden of dengue. *Nature* **2013**, *496*, 504–507. [CrossRef] [PubMed]
2. Rajapakse, S. Dengue shock. *J. Emergencies Trauma Shock.* **2011**, *4*, 120–127. [CrossRef]
3. Stanaway, J.D.; Shepard, D.S.; Undurraga, E.A.; Halasa, Y.A.; Coffeng, L.E.; Brady, O.J.; Hay, S.I.; Bedi, N.; Bensenor, I.M.; Castaneda-Orjuela, C.A.; et al. The global burden of dengue: An analysis from the Global Burden of Disease Study 2013. *Lancet Infect. Dis.* **2016**, *16*, 712–723. [CrossRef]
4. Sridhar, S.; Luedtke, A.; Langevin, E.; Zhu, M.; Bonaparte, M.; Machabert, T.; Savarino, S.; Zambrano, B.; Moureau, A.; Khromava, A.; et al. Effect of Dengue Serostatus on Dengue Vaccine Safety and Efficacy. *N. Engl. J. Med.* **2018**, *379*, 327–340. [CrossRef]
5. Mazeaud, C.; Freppel, W.; Chatel-Chaix, L. The Multiples Fates of the Flavivirus RNA Genome During Pathogenesis. *Front. Genet.* **2018**, *9*, 595. [CrossRef]
6. Neufeldt, C.J.; Cortese, M.; Acosta, E.G.; Bartenschlager, R. Rewiring cellular networks by members of the Flaviviridae family. *Nat. Rev. Microbiol.* **2018**, *16*, 125–142. [CrossRef]
7. Junjhon, J.; Pennington, J.G.; Edwards, T.J.; Perera, R.; Lanman, J.; Kuhn, R.J. Ultrastructural characterization and three-dimensional architecture of replication sites in dengue virus-infected mosquito cells. *J. Virol.* **2014**, *88*, 4687–4697. [CrossRef]
8. Welsch, S.; Miller, S.; Romero-Brey, I.; Merz, A.; Bleck, C.K.; Walther, P.; Fuller, S.D.; Antony, C.; Krijnse-Locker, J.; Bartenschlager, R. Composition and three-dimensional architecture of the dengue virus replication and assembly sites. *Cell Host Microbe* **2009**, *5*, 365–375. [CrossRef] [PubMed]
9. Chatel-Chaix, L.; Cortese, M.; Romero-Brey, I.; Bender, S.; Neufeldt, C.J.; Fischl, W.; Scaturro, P.; Schieber, N.; Schwab, Y.; Fischer, B.; et al. Dengue Virus Perturbs Mitochondrial Morphodynamics to Dampen Innate Immune Responses. *Cell Host Microbe* **2016**, *20*, 342–356. [CrossRef] [PubMed]
10. Westaway, E.G.; Mackenzie, J.M.; Kenney, M.T.; Jones, M.K.; Khromykh, A.A. Ultrastructure of Kunjin virus-infected cells: Colocalization of NS1 and NS3 with double-stranded RNA, and of NS2B with NS3, in virus-induced membrane structures. *J. Virol.* **1997**, *71*, 6650–6661. [CrossRef] [PubMed]
11. Anton, A.; Mazeaud, C.; Freppel, W.; Gilbert, C.; Tremblay, N.; Sow, A.A.; Roy, M.; Rodrigue-Gervais, I.G.; Chatel-Chaix, L. Valosin-containing protein ATPase activity regulates the morphogenesis of Zika virus replication organelles and virus-induced cell death. *Cell. Microbiol.* **2021**, *23*, e13302. [CrossRef]
12. Cortese, M.; Goellner, S.; Acosta, E.G.; Neufeldt, C.J.; Oleksiuk, O.; Lampe, M.; Haselmann, U.; Funaya, C.; Schieber, N.; Ronchi, P.; et al. Ultrastructural Characterization of Zika Virus Replication Factories. *Cell Rep.* **2017**, *18*, 2113–2123. [CrossRef]
13. Bily, T.; Palus, M.; Eyer, L.; Elsterova, J.; Vancova, M.; Ruzek, D. Electron Tomography Analysis of Tick-Borne Encephalitis Virus Infection in Human Neurons. *Sci. Rep.* **2015**, *5*, 10745. [CrossRef]
14. Gillespie, L.K.; Hoenen, A.; Morgan, G.; Mackenzie, J.M. The endoplasmic reticulum provides the membrane platform for biogenesis of the flavivirus replication complex. *J. Virol.* **2010**, *84*, 10438–10447. [CrossRef]
15. Miorin, L.; Romero-Brey, I.; Maiuri, P.; Hoppe, S.; Krijnse-Locker, J.; Bartenschlager, R.; Marcello, A. Three-dimensional architecture of tick-borne encephalitis virus replication sites and trafficking of the replicated RNA. *J. Virol.* **2013**, *87*, 6469–6481. [CrossRef] [PubMed]
16. Tabata, K.; Arimoto, M.; Arakawa, M.; Nara, A.; Saito, K.; Omori, H.; Arai, A.; Ishikawa, T.; Konishi, E.; Suzuki, R.; et al. Unique Requirement for ESCRT Factors in Flavivirus Particle Formation on the Endoplasmic Reticulum. *Cell Rep.* **2016**, *16*, 2339–2347. [CrossRef]
17. Chatel-Chaix, L.; Fischl, W.; Scaturro, P.; Cortese, M.; Kallis, S.; Bartenschlager, M.; Fischer, B.; Bartenschlager, R. A Combined Genetic-Proteomic Approach Identifies Residues within Dengue Virus NS4B Critical for Interaction with NS3 and Viral Replication. *J. Virol.* **2015**, *89*, 7170–7186. [CrossRef] [PubMed]
18. Zou, J.; Lee, L.T.; Wang, Q.Y.; Xie, X.; Lu, S.; Yau, Y.H.; Yuan, Z.; Geifman Shochat, S.; Kang, C.; Lescar, J.; et al. Mapping the Interactions between the NS4B and NS3 proteins of dengue virus. *J. Virol.* **2015**, *89*, 3471–3483. [CrossRef] [PubMed]
19. Zou, J.; Xie, X.; Lee, L.T.; Chandrasekaran, R.; Reynaud, A.; Yap, L.; Wang, Q.Y.; Dong, H.; Kang, C.; Yuan, Z.; et al. Dimerization of flavivirus NS4B protein. *J. Virol.* **2014**, *88*, 3379–3391. [CrossRef]
20. Miller, S.; Sparacio, S.; Bartenschlager, R. Subcellular localization and membrane topology of the Dengue virus type 2 Non-structural protein 4B. *J. Biol. Chem.* **2006**, *281*, 8854–8863. [CrossRef] [PubMed]

21. Moquin, S.A.; Simon, O.; Karuna, R.; Lakshminarayana, S.B.; Yokokawa, F.; Wang, F.; Saravanan, C.; Zhang, J.; Day, C.W.; Chan, K.; et al. NITD-688, a pan-serotype inhibitor of the dengue virus NS4B protein, shows favorable pharmacokinetics and efficacy in preclinical animal models. *Sci. Transl. Med.* **2021**, *13*. [CrossRef]
22. van Cleef, K.W.; Overheul, G.J.; Thomassen, M.C.; Kaptein, S.J.; Davidson, A.D.; Jacobs, M.; Neyts, J.; van Kuppeveld, F.J.; van Rij, R.P. Identification of a new dengue virus inhibitor that targets the viral NS4B protein and restricts genomic RNA replication. *Antivir. Res.* **2013**, *99*, 165–171. [CrossRef] [PubMed]
23. Wang, Q.Y.; Dong, H.; Zou, B.; Karuna, R.; Wan, K.F.; Zou, J.; Susila, A.; Yip, A.; Shan, C.; Yeo, K.L.; et al. Discovery of Dengue Virus NS4B Inhibitors. *J. Virol.* **2015**, *89*, 8233–8244. [CrossRef]
24. Xie, X.; Wang, Q.Y.; Xu, H.Y.; Qing, M.; Kramer, L.; Yuan, Z.; Shi, P.Y. Inhibition of dengue virus by targeting viral NS4B protein. *J. Virol.* **2011**, *85*, 11183–11195. [CrossRef]
25. Xie, X.; Zou, J.; Wang, Q.Y.; Shi, P.Y. Targeting dengue virus NS4B protein for drug discovery. *Antivir. Res.* **2015**, *118*, 39–45. [CrossRef]
26. Shah, P.S.; Link, N.; Jang, G.M.; Sharp, P.P.; Zhu, T.; Swaney, D.L.; Johnson, J.R.; Von Dollen, J.; Ramage, H.R.; Satkamp, L.; et al. Comparative Flavivirus-Host Protein Interaction Mapping Reveals Mechanisms of Dengue and Zika Virus Pathogenesis. *Cell* **2018**, *175*, 1931–1945.e1918. [CrossRef] [PubMed]
27. Beskow, A.; Grimberg, K.B.; Bott, L.C.; Salomons, F.A.; Dantuma, N.P.; Young, P. A conserved unfoldase activity for the p97 AAA-ATPase in proteasomal degradation. *J. Mol. Biol.* **2009**, *394*, 732–746. [CrossRef]
28. Bodnar, N.O.; Rapoport, T.A. Molecular Mechanism of Substrate Processing by the Cdc48 ATPase Complex. *Cell* **2017**, *169*, 722–735.e729. [CrossRef]
29. DeLaBarre, B.; Christianson, J.C.; Kopito, R.R.; Brunger, A.T. Central pore residues mediate the p97/VCP activity required for ERAD. *Mol. Cell* **2006**, *22*, 451–462. [CrossRef]
30. Jarosch, E.; Taxis, C.; Volkwein, C.; Bordallo, J.; Finley, D.; Wolf, D.H.; Sommer, T. Protein dislocation from the ER requires polyubiquitination and the AAA-ATPase Cdc48. *Nat. Cell Biol.* **2002**, *4*, 134–139. [CrossRef]
31. Ju, J.S.; Miller, S.E.; Hanson, P.I.; Weihl, C.C. Impaired protein aggregate handling and clearance underlie the pathogenesis of p97/VCP-associated disease. *J. Biol. Chem.* **2008**, *283*, 30289–30299. [CrossRef] [PubMed]
32. Kim, N.C.; Tresse, E.; Kolaitis, R.M.; Molliex, A.; Thomas, R.E.; Alami, N.H.; Wang, B.; Joshi, A.; Smith, R.B.; Ritson, G.P.; et al. VCP is essential for mitochondrial quality control by PINK1/Parkin and this function is impaired by VCP mutations. *Neuron* **2013**, *78*, 65–80. [CrossRef] [PubMed]
33. Wojcik, C.; Rowicka, M.; Kudlicki, A.; Nowis, D.; McConnell, E.; Kujawa, M.; DeMartino, G.N. Valosin-containing protein (p97) is a regulator of endoplasmic reticulum stress and of the degradation of N-end rule and ubiquitin-fusion degradation pathway substrates in mammalian cells. *Mol. Biol. Cell* **2006**, *17*, 4606–4618. [CrossRef] [PubMed]
34. Ye, Y.; Meyer, H.H.; Rapoport, T.A. The AAA ATPase Cdc48/p97 and its partners transport proteins from the ER into the cytosol. *Nature* **2001**, *414*, 652–656. [CrossRef] [PubMed]
35. Watts, G.D.; Wymer, J.; Kovach, M.J.; Mehta, S.G.; Mumm, S.; Darvish, D.; Pestronk, A.; Whyte, M.P.; Kimonis, V.E. Inclusion body myopathy associated with Paget disease of bone and frontotemporal dementia is caused by mutant valosin-containing protein. *Nat. Genet.* **2004**, *36*, 377–381. [CrossRef] [PubMed]
36. Halawani, D.; LeBlanc, A.C.; Rouiller, I.; Michnick, S.W.; Servant, M.J.; Latterich, M. Hereditary inclusion body myopathy-linked p97/VCP mutations in the NH2 domain and the D1 ring modulate p97/VCP ATPase activity and D2 ring conformation. *Mol. Cell. Biol.* **2009**, *29*, 4484–4494. [CrossRef] [PubMed]
37. Niwa, H.; Ewens, C.A.; Tsang, C.; Yeung, H.O.; Zhang, X.; Freemont, P.S. The role of the N-domain in the ATPase activity of the mammalian AAA ATPase p97/VCP. *J. Biol. Chem.* **2012**, *287*, 8561–8570. [CrossRef]
38. Weihl, C.C.; Dalal, S.; Pestronk, A.; Hanson, P.I. Inclusion body myopathy-associated mutations in p97/VCP impair endoplasmic reticulum-associated degradation. *Hum. Mol. Genet.* **2006**, *15*, 189–199. [CrossRef]
39. Phongphaew, W.; Kobayashi, S.; Sasaki, M.; Carr, M.; Hall, W.W.; Orba, Y.; Sawa, H. Valosin-containing protein (VCP/p97) plays a role in the replication of West Nile virus. *Virus Res.* **2017**, *228*, 114–123. [CrossRef]
40. Ramanathan, H.N.; Zhang, S.; Douam, F.; Mar, K.B.; Chang, J.; Yang, P.L.; Schoggins, J.W.; Ploss, A.; Lindenbach, B.D. A Sensitive Yellow Fever Virus Entry Reporter Identifies Valosin-Containing Protein (VCP/p97) as an Essential Host Factor for Flavivirus Uncoating. *mBio* **2020**, *11*. [CrossRef]
41. Tabata, K.; Arakawa, M.; Ishida, K.; Kobayashi, M.; Nara, A.; Sugimoto, T.; Okada, T.; Mori, K.; Morita, E. Endoplasmic reticulum-associated degradation controls virus protein homeostasis that is required for the flavivirus propagation. *J. Virol.* **2021**. [CrossRef]
42. Gestuveo, R.J.; Royle, J.; Donald, C.L.; Lamont, D.J.; Hutchinson, E.C.; Merits, A.; Kohl, A.; Varjak, M. Analysis of Zika virus capsid-Aedes aegypti mosquito interactome reveals pro-viral host factors critical for establishing infection. *Nat. Commun.* **2021**, *12*, 2766. [CrossRef]
43. Sehrawat, S.; Khasa, R.; Deb, A.; Prajapat, S.K.; Mallick, S.; Basu, A.; Surjit, M.; Kalia, M.; Vrati, S. Valosin-containing protein/p97 plays critical roles in the Japanese encephalitis virus life cycle. *J. Virol.* **2021**. [CrossRef] [PubMed]
44. Cerikan, B.; Goellner, S.; Neufeldt, C.J.; Haselmann, U.; Mulder, K.; Chatel-Chaix, L.; Cortese, M.; Bartenschlager, R. A Non-Replicative Role of the 3′ Terminal Sequence of the Dengue Virus Genome in Membranous Replication Organelle Formation. *Cell Rep.* **2020**, *32*, 107859. [CrossRef] [PubMed]

45. Goellner, S.; Cerikan, B.; Cortese, M.; Neufeldt, C.J.; Haselmann, U.; Bartenschlager, R. Replication-Independent Generation and Morphological Analysis of Flavivirus Replication Organelles. *STAR Protoc.* **2020**, *1*, 100173. [CrossRef] [PubMed]
46. Fischl, W.; Bartenschlager, R. High-throughput screening using dengue virus reporter genomes. *Methods Mol. Biol.* **2013**, *1030*, 205–219. [CrossRef]
47. Anderson, D.J.; Le Moigne, R.; Djakovic, S.; Kumar, B.; Rice, J.; Wong, S.; Wang, J.; Yao, B.; Valle, E.; Kiss von Soly, S.; et al. Targeting the AAA ATPase p97 as an Approach to Treat Cancer through Disruption of Protein Homeostasis. *Cancer Cell* **2015**, *28*, 653–665. [CrossRef]
48. Le Moigne, R.; Aftab, B.T.; Djakovic, S.; Dhimolea, E.; Valle, E.; Murnane, M.; King, E.M.; Soriano, F.; Menon, M.K.; Wu, Z.Y.; et al. The p97 Inhibitor CB-5083 Is a Unique Disrupter of Protein Homeostasis in Models of Multiple Myeloma. *Mol. Cancer Ther.* **2017**, *16*, 2375–2386. [CrossRef]
49. Magnaghi, P.; D'Alessio, R.; Valsasina, B.; Avanzi, N.; Rizzi, S.; Asa, D.; Gasparri, F.; Cozzi, L.; Cucchi, U.; Orrenius, C.; et al. Covalent and allosteric inhibitors of the ATPase VCP/p97 induce cancer cell death. *Nat. Chem. Biol.* **2013**, *9*, 548–556. [CrossRef]
50. Zhou, H.J.; Wang, J.; Yao, B.; Wong, S.; Djakovic, S.; Kumar, B.; Rice, J.; Valle, E.; Soriano, F.; Menon, M.K.; et al. Discovery of a First-in-Class, Potent, Selective, and Orally Bioavailable Inhibitor of the p97 AAA ATPase (CB-5083). *J. Med. Chem.* **2015**, *58*, 9480–9497. [CrossRef]
51. Tresse, E.; Salomons, F.A.; Vesa, J.; Bott, L.C.; Kimonis, V.; Yao, T.P.; Dantuma, N.P.; Taylor, J.P. VCP/p97 is essential for maturation of ubiquitin-containing autophagosomes and this function is impaired by mutations that cause IBMPFD. *Autophagy* **2010**, *6*, 217–227. [CrossRef] [PubMed]
52. Umareddy, I.; Chao, A.; Sampath, A.; Gu, F.; Vasudevan, S.G. Dengue virus NS4B interacts with NS3 and dissociates it from single-stranded RNA. *J. Gen. Virol.* **2006**, *87*, 2605–2614. [CrossRef] [PubMed]
53. Kingsolver, M.B.; Huang, Z.; Hardy, R.W. Insect antiviral innate immunity: Pathways, effectors, and connections. *J. Mol. Biol.* **2013**, *425*, 4921–4936. [CrossRef]
54. Scaturro, P.; Cortese, M.; Chatel-Chaix, L.; Fischl, W.; Bartenschlager, R. Dengue Virus Non-structural Protein 1 Modulates Infectious Particle Production via Interaction with the Structural Proteins. *PLoS Pathog.* **2015**, *11*, e1005277. [CrossRef] [PubMed]
55. Zou, J.; Xie, X.; Wang, Q.Y.; Dong, H.; Lee, M.Y.; Kang, C.; Yuan, Z.; Shi, P.Y. Characterization of dengue virus NS4A and NS4B protein interaction. *J. Virol.* **2015**, *89*, 3455–3470. [CrossRef]
56. Scaturro, P.; Stukalov, A.; Haas, D.A.; Cortese, M.; Draganova, K.; Plaszczyca, A.; Bartenschlager, R.; Gotz, M.; Pichlmair, A. An orthogonal proteomic survey uncovers novel Zika virus host factors. *Nature* **2018**, *561*, 253–257. [CrossRef] [PubMed]
57. Hoffmann, H.H.; Schneider, W.M.; Rozen-Gagnon, K.; Miles, L.A.; Schuster, F.; Razooky, B.; Jacobson, E.; Wu, X.; Yi, S.; Rudin, C.M.; et al. TMEM41B Is a Pan-flavivirus Host Factor. *Cell* **2021**, *184*, 133–148.e120. [CrossRef]
58. Tian, J.N.; Yang, C.C.; Chuang, C.K.; Tsai, M.H.; Wu, R.H.; Chen, C.T.; Yueh, A. A Dengue Virus Type 2 (DENV-2) NS4B-Interacting Host Factor, SERP1, Reduces DENV-2 Production by Suppressing Viral RNA Replication. *Viruses* **2019**, *11*. [CrossRef]
59. Doroshow, J.H.; Parchment, R.; Moscow, J. NCI Experimental Therapeutics (NExT) Program May 8. Available online: https://deainfo.nci.nih.gov/advisory/fac/0518/Doroshow.pdf. (accessed on 1 July 2021).
60. Huryn, D.M.; Kornfilt, D.J.P.; Wipf, P. p97: An Emerging Target for Cancer, Neurodegenerative Diseases, and Viral Infections. *J. Med. Chem.* **2019**. [CrossRef]

Revue

Virologie

Virologie 2021, 25 (5) : 245-62

Flaviviridae et mitochondries : tout ce que vous avez toujours voulu savoir sur leur relation sans jamais oser le demander

Flaviviridae and mitochondria: Everything you always wanted to know about their relationship but were afraid to ask

Wesley Freppel
Marie Roy
Laurent Chatel-Chaix

Centre Armand-Frappier santé biotechnologie, Institut national de la recherche scientifique, Laval, Québec, Canada

Résumé. Les infections par les *Flaviviridae* constituent un enjeu majeur de santé publique dans le monde, surtout en l'absence ou en raison de l'accès limité à des traitements thérapeutiques et prophylactiques. En effet, les *Flaviviridae* ont beaucoup fait parler d'eux au cours des dernières décennies notamment avec l'émergence du virus Zika en Amérique lié à une augmentation importante de microcéphalies congénitales, ou avec le virus de l'hépatite C responsable du décès de 300 000 personnes environ par an à travers le globe. Au cours de l'évolution, ces différents virus ont évolué avec différents mécanismes de détournement de l'activité de certains organites et processus cellulaires qui promeuvent leur réplication et contribuent à leur pathogenèse. En effet, ces pathogènes restructurent morphologiquement le réticulum endoplasmique en compartiments impliqués dans la réplication du génome viral et l'assemblage de virions néosynthétisés. De plus, les *Flaviviridae* induisent des changements morphologiques des mitochondries, ce qui favorise leur réplication, notamment en régulant le métabolisme énergétique, la réponse immunitaire innée et l'apoptose. Cette revue décrit la relation étroite entre les *Flaviviridae* et les mitochondries, et explique comment elle contribue à instaurer un environnement cytoplasmique propice à leur réplication.

Mots clés : mitochondries, flavivirus, virus de l'hépatite C, morphodynamique mitochondriale, immunité innée, apoptose

Abstract. Infections with *Flaviviridae* constitute a major public health concern, especially considering the limited availability of prophylactic and therapeutic treatments. Most notably, the recent emergence of Zika virus in the Americas was associated with the dramatic increase of severe symptoms such as congenital microcephaly, while hepatitis C virus causes the death of approximately 300,000 individuals annually. *Flaviviridae* have evolved to hijack cellular organelles and to favor their replication, often by divergent molecular mechanisms. In addition to the remodeling of the endoplasmic reticulum, which is required for the replication of the viral genome and the assembly of the neosynthetized virions, *Flaviviridae* induce drastic morphological alterations of the mitochondria. This is associated with the viral co-opting of several key mitochondrial functions in apoptosis, innate immunity and metabolism. This review recapitulates the current knowledge about the morphological and functional relationship between *Flaviviridae* and mitochondria and explains how this contributes to the establishment of a cytoplasmic environment which is favorable to viral replication.

Key words: mitochondria, flavivirus, hepatitis C virus, mitochondria morphodynamics, innate immunity, apoptosis

Correspondance : L. Chatel-Chaix
<laurent.chatel-chaix@inrs.ca>

doi:10.1684/vir.2021.0920

Pour citer cet article : Freppel W, Roy M, Chatel-Chaix L. *Flaviviridae* et mitochondries : tout ce que vous avez toujours voulu savoir sur leur relation sans jamais oser le demander. *Virologie* 2021; 25(5) : 245-62 doi:10.1684/vir.2021.0920

Introduction

Il y a environ 1,5 à 2 milliards d'années, la vie unicellulaire a connu un tournant majeur grâce à l'intégration par endosymbiose d'une α-protéobactérie dans une protocellule eucaryote. Ce phénomène est à l'origine d'une composante intracellulaire complexe qui, au cours de l'évolution, est devenue un organite jouant un rôle central dans la vie des cellules eucaryotes : la mitochondrie. De taille avoisinant quelques micromètres, cet organite est composé d'une membrane externe, d'un espace intermembranaire et d'une membrane interne délimitant la matrice mitochondriale. Généralement présent en grande quantité dans la plupart des cellules eucaryotes supérieures, cet organite contribue au métabolisme énergétique de la cellule, notamment par l'intermédiaire du cycle de Krebs, de la phosphorylation oxydative ou encore de la β-oxydation [1]. Source principale d'ATP dans la cellule, la mitochondrie s'est vu attribuer le surnom de « centrale énergétique de la cellule ». Pourtant, depuis quelques décennies, nous savons qu'au-delà des fonctions métaboliques et respiratoires, les mitochondries jouent également des rôles importants dans l'apoptose et la sénescence cellulaire, le contrôle du cycle cellulaire ou encore la réponse antivirale [2-4] pour n'en citer que quelques-uns. Considérant que tous ces processus cellulaires influencent de façon positive ou néfaste les infections de la cellule hôte, il n'est pas surprenant que la mitochondrie constitue pour les virus une cible de prédilection à contrôler en priorité pour maximiser leur réplication intracellulaire. Les *Flaviviridae* ne font pas exception puisqu'ils interfèrent avec cet organite à plusieurs niveaux.

Dans le règne des virus, la famille des *Flaviviridae* est un groupe de virus enveloppés à ARN simple brin de polarité positive qui englobe beaucoup de pathogènes causants des maladies graves chez l'humain. Cette famille est sous-divisée en quatre genres, soit *Flavivirus*, *Hepacivirus*, *Pestivirus* et *Pegivirus*. Au cours des dernières décennies, les deux premiers groupes ont été plus étudiés que les deux autres puisqu'ils incluent des virus pathogènes pour les humains. Les infections par les flavivirus tels que le virus de la dengue (*dengue virus*, DENV), le virus Zika (*Zika virus*, ZIKV), le virus du Nil occidental (VNO), le virus de la fièvre jaune (*yellow fever virus*, YFV), le virus de la méningoencéphalite à tique (*tick-borne encephalitis virus*, TBEV) ou encore le virus de l'encéphalite japonaise (*Japanese encephalitis virus*, JEV) représentent un enjeu majeur de santé publique dans le monde. Par exemple, le DENV cause la maladie arbovirale la plus prévalente dans le monde avec environ 390 millions de personnes infectées annuellement dont 25 % présentent des symptômes qui peuvent être sévères et aboutir au décès [5]. Bien qu'identifié à la fin des années 1940, le ZIKV a, quant à lui, attiré beaucoup d'attention lors de son émergence et de sa dissémination rapide en Amérique latine en 2015-2016. Actuellement, le ZIKV est présent dans plus de 87 pays [6, 7]. La répartition des flavivirus à travers le globe repose essentiellement sur celle des vecteurs arthropodes les transmettant à la suite d'une piqûre, comme les moustiques de type *Aedes* pour le DENV, le ZIKV et le YFV, ou de type *Culex* pour le VNO [8]. Bien qu'il existe des vaccins contre certains flavivirus, il n'existe aucun traitement thérapeutique efficace à l'heure actuelle contre les virus de ce genre [9]. Le genre *Hepacivirus* comprend 14 virus dont le plus connu et mieux caractérisé est le virus de l'hépatite C (VHC). Ce virus est principalement transmis par voie sanguine et on estime qu'il est responsable de plus de 70 millions de cas avec environ 300 000 décès par an à la suite d'un cancer du foie ou d'une cirrhose viro-induits [10]. Dans la lutte contre le VHC, des traitements hautement efficaces à 95 % basés sur l'administration d'antiviraux à action directe (AAD) sont disponibles [11]. Malheureusement, le coût de ces traitements est très élevé, ce qui les rend peu accessibles à la majorité des patients atteints du VHC, notamment dans les pays en voie de développement et il n'existe pas de vaccins contre ce virus. Malgré les avancées cliniques des dernières décennies, le développement de vaccins et d'antiviraux est primordial. Cela constitue un défi qui repose en partie sur une meilleure compréhension des mécanismes moléculaires au centre du cycle de réplication et de la pathogenèse de ces virus.

À la suite de l'entrée d'un *Flaviviridae* dans une cellule hôte, le génome viral constitué par un ARN simple brin est décapsidé puis traduit par les ribosomes en une seule protéine virale. Cette polyprotéine est clivée de manière post-traductionnelle par des protéases virales et cellulaires, générant ainsi des protéines structurales (C, prM et E pour les flavivirus ; C, E1 et E2 pour les hépacivirus) et non-structurales (NS1, NS2A, NS2B, NS3, NS4A, NS4B et NS5 pour les flavivirus ; P7, NS2, NS3, NS4A, NS4B, NS5A et NS5B pour le VHC, prototype des hépacivirus) [12, 13]. À la suite d'une interaction entre l'ARN viral et la protéine de capside (C), les protéines structurales s'assemblent en nouveaux virions qui bourgeonnent dans le lumen du réticulum endoplasmique (RE). Les protéines E, E1 et E2 sont situées à la surface des virions et une fois ces derniers relâchés à l'extérieur de la cellule, ces protéines d'enveloppe sont responsables de l'entrée virale. Les protéines non structurales, incluant deux types d'enzymes virales, contrôlent la réplication du génome viral tout en établissant un environnement cytoplasmique favorable à la pathogenèse virale. La néosynthèse de l'ARN viral est catalysée par une ARN polymérase dépendante de l'ARN, soit NS5 pour les flavivirus et NS5B pour le VHC. Cette étape du cycle viral est assistée par l'activité hélicase des

protéines virales NS3 qui déroulent les ARN double brins générés lors de la réplication. NS3 possède également une activité protéase qui, avec les cofacteurs NS2B (flavivirus) ou NS4A (VHC) est requise pour cliver la polyprotéine virale en protéines virales matures. Les autres protéines non structurales ne possèdent pas d'activité enzymatique mais sont néanmoins indispensables à la réplication virale [12, 13]. Notamment, ces dernières induisent le remodelage du RE en ultrastructures membranaires appelées organites ou usines de réplication virale (URV). Les URV flavivirales se forment à partir des membranes du RE et incluent trois sous-structures singulières et facilement observables en microscopie électronique [14-17] :

1. « les paquets vésiculaires », résultant de l'invagination de la membrane du RE et dont l'intérieur est suspecté d'être le site où la réplication du génome viral s'effectue ;
2. les « sacs de virus » qui sont de larges citernes de RE où les virions assemblés s'accumulent de façon ordonnée, voire géométrique ; et
3. les « convolutions de membranes » (CM) dont les fonctions sont peu caractérisées.

Alors que les CM ne semblent pas contenir de complexes de réplication du génome viral, elles sont en revanche riches en protéines virales NS3, NS4B et NS4A [14, 18] et pourraient contribuer à atténuer des processus cellulaires potentiellement défavorables à un déroulement efficace du cycle viral, comme l'immunité innée antivirale précoce ou l'apoptose. Dans le cas des hépacivirus et plus particulièrement du VHC, le compartiment cytoplasmique contenant les URV est appelé toile membraneuse (TM) [19, 20]. La TM est composée d'URV avec une architecture différente de celles des flavivirus. En effet, le VHC induit des protubérances du RE, formant ainsi des vésicules à double membrane (VDM) au sein desquelles s'effectue la réplication du génome viral [21-23]. Comme les URV flavivirales, la TM a pour origine les membranes du RE ce qui en fait une particularité qui semble conservée chez les *Flaviviridae.* Ces différences d'architecture des URV illustrent que, bien que les propriétés générales du cycle viral des *Flaviviridae* soient très comparables, les flavivirus et les hépacivirus ont divergé lors de l'évolution au niveau des mécanismes viraux utilisant certains organites endo-membranaires et les processus qui y sont associés.

Intuitivement, on peut s'attendre à ce que ces processus de remodelage du RE et du maintien des URV au cours du temps soient extrêmement énergivores. Les mitochondries représentent donc d'excellentes sources d'énergie que l'évolution a permis aux *Flaviviridae* de contrôler pour répondre à leurs besoins indispensables à la réplication. Outre les besoins en ATP, la morphogenèse des URV implique d'autres processus normalement contrôlés par les mitochondries, alors que ce remodelage induit un stress potentiellement cytopathique dont la réponse dépend également de cet organite. Notamment, les mitochondries participent à des échanges moléculaires avec le RE par l'interface réticulo-mitochondriale (IRM), contribuant à de nombreux processus tels que l'homéostasie des lipides et du calcium, la réponse immunitaire antivirale précoce, l'apoptose, l'autophagie ainsi que la régulation de la morphologie mitochondriale [24-28]. Considérant l'impact de tous ces processus mitochondriaux sur le cycle viral, les *Flaviviridae* ont développé des mécanismes visant à les contrôler ou à les détourner afin de créer un environnement favorable à la réplication virale. Dans cette revue, nous discutons de l'impact de l'infection virale par les *Flaviviridae* sur les différentes fonctions mitochondriales.

Morphodynamique mitochondriale

Les mitochondries ont une longueur allant de 1 à 10 µm en moyenne pour un diamètre de 1 à 3 µm. Elles sont capables de se déplacer dans le cytoplasme le long du cytosquelette par des kinésines (transport antérograde) et des dynéines (transport rétrograde) [29]. Outre leur mobilité intracellulaire, lorsque l'on observe des mitochondries dans des cellules vivantes, il est évident que leur forme est en constante évolution. En effet, les mitochondries changent de longueur et peuvent se présenter sous forme allongée ou sphérique selon l'état de stress ou de croissance de la cellule. D'une manière générale, elles oscillent entre ces deux états très rapidement par un mécanisme de régulation dynamique qui permet de répondre rapidement aux besoins de la cellule. Plus généralement, la forme des mitochondries repose sur un équilibre entre leur fusion (menant à leur élongation) et leur fission (résultant en un aspect fragmenté). Par exemple, l'aspect allongé des mitochondries peut résulter soit d'une stimulation de leur fusion, soit d'une altération de leur fragmentation. Cette morphodynamique mitochondriale est régulée dans le temps et dans l'espace par des facteurs de fusion et de fission (*figure 1*). Les mitofusines MFN1 et MFN2 sont responsables de la fusion des membranes mitochondriales externes, et OPA1 (*optic atrophy 1*) de celles des membranes mitochondriales internes. Brièvement, lors de la fusion, l'ancrage de deux mitochondries est contrôlé par l'interaction entre deux molécules MFN1 ou MFN2 par l'intermédiaire de leur domaine HR2 et la fusion membranaire dépend de leur activité GTPase [30, 31]. Le transfert aux mitochondries du facteur de fission DRP1 (*dynamin-related protein 1*) par l'interaction avec ses récepteurs mitochondriaux MFF (*mitochondrial fission factor*), FIS1 (*mitochondrial fission 1 protein*), MID49 (*mitochondrial dynamics protein 49*) et MID51 (*mitochondrial dynamics protein 51*) régule la fragmentation des mitochondries [32]. Lors de la fission, la phosphorylation

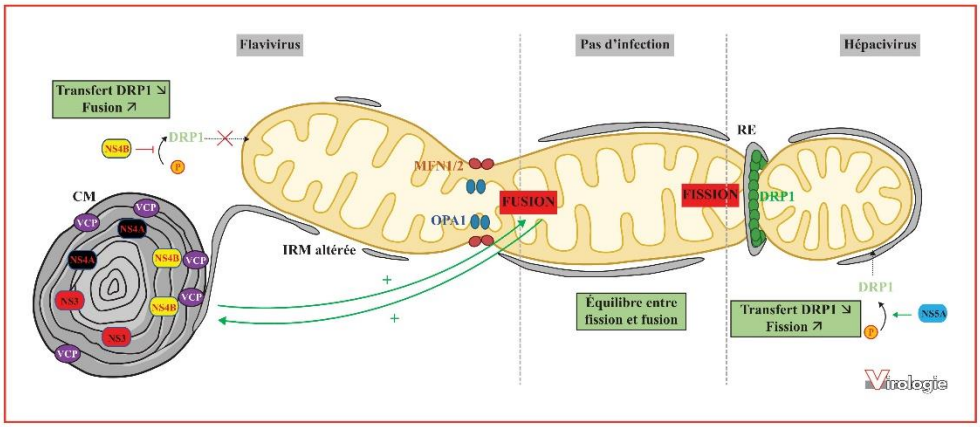

Figure 1. Altérations morphologiques de la mitochondrie par les flavivirus et le VHC. *Partie gauche :* représentation schématique de la fusion mitochondriale provoquée par les flavivirus par l'entremise de l'inhibition de l'activation du facteur de fission DRP1 (*dynamin-related protein 1*) par phosphorylation. Les convolutions de membranes (CM) riches en protéines flavivirales NS3, NS4B et NS4A sont connectées aux mitochondries par un tubule de réticulum endoplasmique (RE) alors que l'interface réticulo-mitochondriale (IRM) est altérée. *Section centrale :* représentation schématique de l'équilibre entre fusion et fission à l'état normal de la cellule. *Partie droite :* représentation schématique de la fission mitochondriale induite par le VHC. Le virus favorise le transfert du facteur de fission DRP1 vers la mitochondrie. Schéma réalisé à l'aide de la ressource en ligne BioRender (https://biorender.com/).

de DRP1 sur la sérine 616 active son transfert aux mitochondries et la formation d'une structure en hélice au niveau de sites de pré-constriction formés par le RE [26, 33]. Ainsi, l'IRM maintenue par des interactions protéine-protéine gardant une distance d'environ 10 à 25 nm entre les deux organites implique que le RE contrôle également la morphologie mitochondriale [34]. À l'inverse, la phosphorylation en sérine 637 de DRP1 inhibe le transfert de DRP1 favorisant ainsi indirectement la fusion [35]. Les mitochondries fusionnent ou se fragmentent constamment selon l'état fonctionnel et les besoins métaboliques de la cellule. En effet, il y a fusion si les mitochondries sont très mobiles avec une augmentation de la consommation en O_2, de la production d'ATP et du potentiel de membrane tandis qu'une situation inverse provoque la fission mitochondriale [36]. En considérant les besoins énergétiques requis par la réplication et la production virale, il n'est donc pas étonnant que les virus aient développé des moyens de réguler la morphologie des mitochondries afin d'interférer avec les fonctions cellulaires qui y sont associées.

Bien que le RE soit l'organite le plus étudié en ce qui concerne les altérations morphologiques du cytoplasme par les *Flaviviridae,* la morphodynamique mitochondriale est également une cible de ces pathogènes. En effet, lors d'une infection par le DENV ou le ZIKV, ces deux virus induisent une élongation mitochondriale marquée (*figure 1*, partie de gauche) [18, 37]. Dans le cas du DENV, cette élongation est attribuée à une inhibition de la phosphorylation du facteur de fission DRP1 sur la sérine 616 par la protéine virale NS4B empêchant ainsi son transfert aux mitochondries [18]. Une diminution de l'expression de DRP1 stimule la réplication du DENV et du ZIKV alors que celle du facteur de fusion MFN2 provoque le phénotype inverse. Cela soutient le modèle selon lequel les flavivirus induisent l'élongation au profit de la réplication virale. Cette étude montre également que l'IRM est largement altérée, suggérant une déstabilisation des sites de pré-fission des mitochondries par le RE, ce qui favoriserait en retour la fusion mitochondriale. Dans les cellules infectées par le DENV, le peu de tubules de RE encore en contact avec les mitochondries est connecté avec les CM. Ceci suggère fortement que la morphogenèse des CM est responsable de l'altération de l'IRM et donc contribue à l'élongation mitochondriale. En parfait accord avec ce modèle, nous avons récemment démontré que la déstabilisation des CM du ZIKV par l'inhibition pharmacologique de l'activité ATPase de la protéine cellulaire VCP (*valosin-containing protein*), une composante de cette ultrastructure, induit une perte rapide de la morphologie allongée des mitochondries [38]. Puisque la biogenèse des CM est réalisée à partir de la membrane du RE, il se pourrait qu'indirectement, VCP favorise la fusion mitochondriale par le biais de l'altération des contacts RE-mitochondries tel qu'observé avec le DENV. De façon

réciproque, l'élongation des mitochondries stimule la formation des CM puisque l'invalidation génique de DRP1 augmente leur taille. De plus, une fragmentation mitochondriale subite causée par la dépolarisation des mitochondries à la suite d'un traitement avec du carbonylcyanure m-chlorophénylhydrazone (CCCP) provoque la disparition des CM. Finalement, la réplication du DENV est diminuée dans des cellules traitées avec du Mito-C, un inhibiteur hétérocyclique ciblant les protéines de la famille des NEET, qui induit une augmentation des contacts RE-mitochondries et de la fragmentation mitochondriale dépendante de DRP1 [39].

Malgré les évidences d'un lien morphologique et fonctionnel entre les URV et les mitochondries allongées, une autre étude a montré récemment l'inverse, avec une induction de la fragmentation des mitochondries dans des cellules neuronales par le ZIKV [40]. Dans ce type cellulaire, le ZIKV modulerait la morphologie mitochondriale en favorisant la fission par la diminution de MFN2. De plus, l'inhibition pharmacologique de la fission avec la molécule Mdivi-1 (*mitochondrial division inhibitor 1*) réduit la mort cellulaire induite par le ZIKV, indiquant l'importance de la fusion mitochondriale dans la diminution de l'apoptose et la réplication du ZIKV. Les cellules neuronales sont en général sensibles aux infections virales et vont rapidement induire l'apoptose en réponse à l'infection et ce, même à des niveaux faibles de réplication. La fragmentation observée, dans ce cas, serait plutôt une conséquence de l'induction de la mort cellulaire, les deux processus étant généralement fonctionnellement reliés (*voir* section plus bas). Dans un autre contexte expérimental, une étude antérieure montre que le DENV peut interférer avec la fusion mitochondriale dans une certaine mesure par l'intermédiaire du clivage des deux facteurs de fusion MFN1/2 par la protéase virale NS2B/3 lorsque cette dernière est surexprimée [41]. Cependant, la fragmentation observée avec le ZIKV et le DENV dans cette étude a été étudiée à des temps précoces de l'infection dans des systèmes artificiels d'hétérocaryons et d'hyperfusion mitochondriale alors que l'élongation rapportée dans d'autres études est plutôt très marquée à des temps plus tardifs correspondant au pic de réplication. Par ailleurs, cette étude n'a pas rapporté que l'infection virale dans la lignée cellulaire d'étude (soit les cellules épithéliales pulmonaires humaines A549) induit une fragmentation mitochondriale, ce qui questionne l'impact d'un tel clivage des mitofusines sur la morphologie générale des mitochondries. Considérant ces résultats contradictoires en apparence, il est possible que la capacité de certains flavivirus à moduler la morphodynamique mitochondriale varie selon le temps d'infection, la souche utilisée, le type cellulaire et la sensibilité des cellules au stress produit par les infections. D'ailleurs, que le VNO ne semble pas induire l'élongation mitochondriale dans les hépatocytes humains Huh7, à l'inverse du ZIKV et du DENV lorsque ces derniers sont testés en parallèle [18]. Ceci suggère donc qu'il y a des différences parmi les flavivirus en ce qui concerne la régulation de la morphologie des mitochondries.

Fait intéressant, les *Flaviviridae* appartenant aux autres genres utilisent apparemment des mécanismes de subversion de morphologie mitochondriale différents de ceux observés avec les flavivirus puisque l'élongation mitochondriale induite par ces virus n'a jamais été rapportée à ce jour. À l'inverse, la fission des mitochondries est induite par le virus de la fièvre porcine classique, un pestivirus, suite à l'ubiquitination et à la dégradation de MFN2, favorisant ainsi la fission [42]. Cette fission est également observée chez les hépacivirus. En effet, le VHC stimule l'expression de DRP1 et de son récepteur MFF, et induit la phosphorylation de DRP1 sur la sérine 616, favorisant ainsi son transfert aux mitochondries et provoquant leur fission (*figure 1*, partie de droite) [43]. En association avec la PI4KA, la protéine virale NS5A est également impliquée dans la fission en favorisant l'association du RE aux mitochondries, favorisant ainsi la préconstriction des mitochondries [44]. Une autre particularité du VHC est sa capacité à modifier la distribution cytoplasmique des mitochondries. La protéine virale NS4A exprimée seule ou en tant que cofacteur de la protéase NS3 s'accumule au niveau des mitochondries et les endommage, aboutissant au relargage de cytochrome C et à leur redistribution avec NS4A dans la région périnucléaire [45]. Globalement, toutes ces données mettent en lumière l'impact des infections par les *Flaviviridae* sur le remodelage morphologique des mitochondries. Considérant que de nombreuses fonctions des mitochondries sont intimement liées à la morphologie de cet organite, ces altérations architecturales pourraient contribuer à leur contrôle fonctionnel par les *Flaviviridae* au profit de la réplication virale.

Métabolisme mitochondrial

Homéostasie calcique

Le calcium (Ca^{2+}) intracellulaire, impliqué dans de nombreux processus moléculaires, est un élément essentiel de la cellule. Il peut notamment servir de second messager dans plusieurs voies de signalisation, notamment celles impliquant la calmoduline [46]. Bien que le RE soit le principal réservoir de Ca^{2+}, les mitochondries en contiennent également et jouent donc un rôle important dans cette homéostasie. Les mitochondries ont une capacité de stockage du Ca^{2+} intracellulaire allant de 50 à 500 nM et en échangent avec le RE au niveau de l'IRM par l'intermédiaire des récepteurs de l'inositol 1,4,5-triphosphate (IP3R) de la membrane du RE, et de la VDAC1 (*voltage-dependent anion channel* 1), une

protéine transmembranaire de la membrane mitochondriale externe [47]. Ces protéines, avec l'aide de la chaperonne GRP75, forment un canal permettant le transfert direct du Ca^{2+} du RE vers l'espace intermembranaire des mitochondries [48]. Ce cation est ensuite transporté vers la matrice mitochondriale par la protéine transmembranaire MCU (*mitochondrial calcium uniporter*) [49]. Une surcharge en Ca^{2+} dans les mitochondries induit l'apoptose tandis qu'une diminution excessive conduit à la mort cellulaire par nécrose [50]. Ainsi, une altération de l'interface entre le RE et les mitochondries a un impact direct sur les fonctions mitochondriales et plus généralement sur l'homéostasie cellulaire du Ca^{2+} [51]. La maîtrise du flux calcique par un pathogène donné permet en théorie de contrôler indirectement des processus cellulaires qui pourraient nuire ou favoriser la multiplication de l'agent infectieux et contribuer à sa pathogenèse. Dans le cas des hépacivirus, les protéines Core et NS5A du VHC induisent une augmentation des niveaux du Ca^{2+} intramitochondrial [52, 53]. À la suite de la libération du Ca^{2+} par le RE en réponse aux stimulations avec la thapsigargine ou l'ATP, la protéine Core favorise l'entrée du Ca^{2+} dans les mitochondries en augmentant le Ca^{2+} pris en charge par la MCU bien que celle-ci contrôle les échanges calciques au niveau de la membrane mitochondriale interne. La protéine Core quant à elle est plutôt présente à l'interface cytoplasmique rendant une interaction directe entre ces deux protéines improbables compte-tenu de leur topologie respective. Bien que le mécanisme impliqué dans la perturbation du flux calcique par la protéine Core sur MCU soit inconnu, il se pourrait que le complexe IP3R1-VDAC de l'IRM constitue l'intermédiaire de ce processus. En effet, les inhibiteurs de MCU (rouge de ruthénium et Ru360) agissent par l'interaction avec le site de liaison du Ca^{2+} de VDAC1 [54], et une fraction de la protéine Core est retrouvée au niveau de l'IRM [55]. D'un point de vue général, puisque la biogenèse des URV implique le remodelage du RE, qui est le réservoir principal du Ca^{2+}, il est possible que ce processus soit associé à un contrôle par le virus de l'homéostasie du Ca^{2+}. Par la suite, le maintien des URV et l'altération de l'IRM pourraient influencer les échanges de Ca^{2+} entre le RE et les mitochondries et contrôler indirectement les différents processus qui en dépendent, comme l'apoptose (*voir* ci-dessous). Dans le cas des flavivirus, il n'y a pas d'évidence qui montre un lien direct entre le contrôle des concentrations calciques mitochondriales et l'infection virale. Cependant, la protéine E du DENV ou du ZIKV interagit avec des composants structuraux de l'IRM tels que GRP78 *(glucose-regulated protein 78)* au niveau du RE, qui elle-même lie VDAC à la surface des mitochondries [56, 57]. VDAC1 normalement distribuée de façon périnucléaire serait relocalisée de façon diffuse à la suite d'une infection par DENV sans être dégradée. Une autre étude a rapporté que VDAC1 est également relocalisée de l'IRM vers le cytosol par le complexe protéase NS2B3 sans pour autant modifier le niveau d'expression de VDAC1 [58]. Bien que ces données soient contradictoires avec une localisation mitochondriale de VDAC1, elles ouvrent la porte à l'hypothèse d'une altération de l'intégrité du module de transit calcique IP3R1-VDAC1 par le virus bien que cela n'ait pas été testé. Par ailleurs, une étude d'interactome a identifié VDAC2 comme partenaire de la protéine NS4B du DENV dans les cellules infectées [18]. Cependant, il reste à démontrer si ces interactions sont spécifiques ou si elles résultent plutôt d'une copurification de mitochondries entières avec les URV, les VDAC étant des composantes abondantes des mitochondries.

Finalement, en activant la voie SOCE (*store operated calcium entry*), le DENV perturbe la perméabilité de la membrane plasmique et augmente la concentration en Ca^{2+} cytoplasmique [59]. Ceci corrèle avec une diminution de la capacité du RE à relâcher du Ca^{2+}. De façon similaire, cet influx calcique dans la cellule est également observé lors des premières heures de l'infection par le VNO [60]. Ces changements de concentration cytoplasmique en Ca^{2+} sont importants pour le cycle viral puisque des traitements avec des inhibiteurs du flux calcique réduisent la réplication du DENV et du VNO. Au-delà de ces changements généraux sur VDAC1 et sur les flux de calcium au niveau du RE et de la membrane plasmique lors de l'infection par les flavivirus, il serait important d'évaluer dans le futur si cela induit des changements spécifiques du transport du calcium vers les mitochondries et dans quelle mesure cela influence la réplication et la pathogenèse.

Homéostasie lipidique

Les mitochondries ont la particularité d'être composées de deux membranes lipidiques, une interne et une externe, dont les compositions sont spécifiques à chacune et contribuent à leurs fonctions, leurs échanges et leurs modifications morphologiques. Ce lipidome repose sur la stœchiométrie entre les différentes classes de lipides importés du cytoplasme ou synthétisés localement dans la mitochondrie. En effet, elle synthétise elle-même deux principaux lipides qui constituent une signature moléculaire spécifique de cet organite, soit la phosphatidyléthanolamine et la cardiolipine [61]. Bien que la mitochondrie importe la plupart des lipides depuis d'autres compartiments intracellulaires, principalement le RE, elle est également capable d'interagir avec les gouttelettes lipidiques (GL) ou adiposomes, réservoir d'acides gras et de cholestérol [62]. Cette interaction pourrait être requise pour un meilleur catabolisme des acides gras [63]. D'autre part, la mitochondrie est également bien caractérisée pour son rôle primordial dans le processus de β-oxydation lipidique en aérobiose dans la matrice mitochondriale. En effet, le processus permet de dégrader les

acides gras en acétyl-CoA qui servira de substrat d'entrée dans le cycle de Krebs, et de fournir du NADH et du $FADH_2$, deux cofacteurs essentiels au bon fonctionnement de la chaîne respiratoire oxydative [64]. Finalement, les *Flaviviridae* posséderaient des mécanismes pour contrôler l'homéostasie lipidique afin de favoriser le remodelage morphologique des organites membranaires, mais aussi pour contrôler certains processus cellulaires dépendants des acides gras. Par exemple, une étude de spectrométrie de masse à haute résolution de cellules de moustique a permis de déterminer qu'au moins 15 % du répertoire lipidique est modifié à la suite d'une infection par le DENV [65]. L'ajout de C75, un inhibiteur de la distribution lipidique intracellulaire réduit la réplication virale. Cette étude montre aussi que l'abondance de plusieurs acides gras tels que les sphingolipides ou la phosphatidylcholine qui sont impliqués dans le dynamisme mitochondrial de fusion/fission et dans la régulation du cytosquelette est augmentée lors d'une infection virale, illustrant ainsi l'importance des lipides dans le cycle viral du DENV, mais également dans celui du VNO, du ZIKV et du VHC [66-68]. D'autre part, le DENV et le VNO augmentent la production locale de la synthèse des acides gras libres en recrutant FASN, la synthétase d'acides gras, vers les complexes de réplication du génome viral [69-72]. Dans le cas du DENV, cette redistribution s'effectue par l'intermédiaire de la protéase virale NS3 et de la protéine Rab18, une GTPase [70, 73]. Chez le VNO, des traitements avec deux inhibiteurs pharmacologiques de la synthèse des acides gras, soit la cérulénine et le C75, diminuent la réplication virale ce qui démontre que la réplication du VNO dépend de la synthèse des acides gras. Dans le cas du VHC, du DENV et du ZIKV, la synthèse des lipides à longue chaîne est importante pour la réplication puisque la diminution de l'expression ou l'inhibition de l'hydrostéroide β17 déhydrogénase de type 2 (HSD17B12) diminue l'abondance des GL et la production de particules infectieuses [72]. En aval de ces détournements des facteurs intervenant dans la lipogenèse, les *Flaviviridae* interfèrent également avec le catabolisme des acides gras au niveau des mitochondries. En effet, le DENV stimule la β-oxydation et la libération des acides gras libres provenant de l'autophagie des GL. La stimulation de cette lipophagie par le DENV dépend de l'activation d'AMPK qui en retour inhibe mTOR, le répresseur principal de l'autophagie [74]. Par ailleurs, la lipophagie est induite par les protéines virales C, NS4A et NS4B, ces deux dernières interagissant avec AUP1, une protéine membranaire de type III associée aux GL. L'interaction avec AUP1 a pour effet de détourner son activité acyltransférase et de cibler les GLs vers la machinerie autophagique [69, 75-77]. Finalement, dans le cas du VHC, la β-oxydation lipidique est atténuée. Cela corrèle avec une diminution de l'expression des sous-unités α et β de la protéine mitochondriale trifonctionnelle (responsable de la catalyse des trois dernières étapes de la β-oxydation) alors que ces protéines cellulaires interagissent avec NS5A [78, 79]. Par ailleurs, à l'inverse de DENV, la taille des GL dans les cellules infectées est augmentée alors que ces dernières servent de plate-forme d'assemblage viral, suggérant que dans ce cas, leur lipophagie est réprimée. Ainsi, les mécanismes moléculaires divergents employés par les *Flaviviridae* pour moduler les niveaux d'acides gras pourraient illustrer que les URV des flavivirus et des hépacivirus requièrent des classes de lipides différentes lors de leur morphogenèse lors du remodelage à partir du RE. Par ailleurs, la régulation de la β-oxydation influence indirectement le rendement en ATP fourni par la respiration cellulaire et pourrait également atténuer des processus potentiellement antiviraux qui dépendent des lipides.

Finalement, l'infection par le ZIKV et la surexpression de NS4B induisent une diminution des niveaux de cardiolipine [80]. Considérant le rôle de ce lipide mito-spécifique » dans la fission mitochondriale et l'apoptose [81, 82], il est possible qu'une telle perturbation de l'homéostasie lipidique des mitochondries favorise leur élongation virus-induite ainsi que l'atténuation des effets cytopathiques (*voir* la section « Apoptose » ci-dessous).

Respiration cellulaire

La respiration cellulaire est la principale voie de production d'ATP regroupant différents processus se passant dans plusieurs compartiments cellulaires. Dans le cytosol, la glycolyse métabolise le glucose en pyruvate en générant deux molécules d'ATP, le tout suivi par la décarboxylation du pyruvate en acétyl-CoA [83]. Ce dernier est pris en charge par le cycle de l'acide citrique (appelé également cycle de Krebs) qui s'effectue dans la matrice mitochondriale et libère deux molécules d'ATP, trois de $NADH^+$ et une de $FADH^{2+}$. Au sein de la membrane interne de la mitochondrie, le processus général de phosphorylation oxydative implique tout d'abord l'oxydation du NADH et du $FADH_2$ par la chaîne de transport d'électron. Le gradient de protons, généré par les différents complexes de la chaîne de transport d'électron permet à l'ATP synthase d'effectuer la phosphorylation de 34 ADP en ATP [84]. De plus, la respiration mitochondriale au sein de la phosphorylation oxydative va principalement consommer de l'oxygène au niveau de la réaction catalysée par le complexe IV réduisant le dioxygène en eau. L'ensemble de la respiration cellulaire aérobie permet de produire 38 molécules d'ATP qui serviront au fonctionnement de l'ensemble des processus cellulaires. Les différentes étapes de la respiration cellulaire constituent des cibles de choix pour les virus, afin de contrôler l'apport d'énergie sous forme d'ATP requis pour les différentes étapes du cycle viral. Bien que la glycolyse n'implique pas directement la mitochondrie, elle n'en reste

pas moins la voie de synthèse clé nourrissant le cycle de Krebs en acétyl-CoA. Plusieurs études ont démontré que la glycolyse est stimulée par plusieurs *Flaviviridae* (DENV, ZIKV, VHC) par divers mécanismes moléculaires et que ce processus métabolique est requis pour une réplication virale optimale [85-90].

Les flavivirus ont évolué pour s'approprier le cœur de la production d'énergie mitochondriale de masse (*figure 2*). En effet, des augmentations de la consommation en oxygène ont été observées dans des cellules hépatiques HepG2 infectées par le DENV [91]. Ces modifications bioénergétiques sont accompagnées d'une modification ultrastructurale des mitochondries où elles apparaissent gonflées, un phénotype typique de l'initiation du processus apoptotique. La technologie Seahorse mesurant de la consommation en oxygène en temps réel et sans marquage dans les cellules vivantes a confirmé ces résultats [37]. Cette étude montre que les cellules infectées par le DENV ayant des mitochondries allongées présentent une consommation cellulaire en oxygène augmentée. En effet, l'infection par le DENV augmente la respiration basale (soit la consommation « normale » d'oxygène des cellules à l'équilibre), la respiration maximale et la production en ATP. Ces résultats corrèlent avec une morphologie allongée des mitochondries dans les cellules infectées, suggérant que le virus favorise la fusion mitochondriale, ce qui augmente la production en ATP. À l'inverse des observations faites dans le cas des infections avec le DENV, le ZIKV inhibe les consommations basale et maximale en oxygène dans les trophoblastes infectés [92]. De plus, cette étude rapporte une fragmentation mitochondriale à la suite d'une infection par le ZIKV confirmant le lien fonctionnel entre la respiration et la morphologie mitochondriale. Une étude récente dans des cellules astrocytaires a montré une augmentation dans la consommation en oxygène et en production d'ATP suivant une infection précoce avec le ZIKV [93]. Cependant, à partir de 36 heures d'infection, la tendance s'inverse et la consommation diminue ce qui suggère un besoin massif en énergie dans les phases précoces de l'infection, durant lesquelles la biogenèse des URV s'effectue. Tel que mentionné plus haut pour la morphologie, la perturbation de la respiration mitochondriale pourrait également dépendre du type cellulaire, du temps d'infection, ou encore de l'état de stress tel que l'apoptose qui modifie la perméabilisation de la membrane externe mitochondriale et provoque l'arrêt de la phosphorylation oxydative. De plus, on ignore toujours quelles protéines virales régulent ce processus métabolique.

Dans le cas du VHC, des mitochondries de cellules de foie de souris exprimant les protéines virales Core, E1 et E2 présentent une diminution de la production de NADPH se traduisant par une réduction de l'activité du complexe I de la chaîne de transport d'électrons [94]. Cette observation est confirmée par une autre étude montrant la diminution de l'activité du complexe I suite à la dégradation des mitochondries par l'autophagie [95]. Bien que le mécanisme d'interférence ne soit pas clairement identifié, une étude d'interactome montre que plusieurs protéines impliquées dans la respiration mitochondriale interagissent avec la protéine Core du VHC [96]. Cependant, seuls les niveaux de la prohibitine augmentent quand la protéine Core est exprimée en l'absence d'autres protéines virales ou lors de l'infection. La prohibitine a un rôle de chaperonne des sous-unités de l'oxydase du cytochrome c, le complexe IV de la chaîne respiratoire mitochondriale. Ceci suggère que le VHC contrôle la chaîne de transport d'électrons par l'intermédiaire de cette protéine chaperonne. Il serait pertinent d'évaluer si ce contrôle du métabolisme mitochondrial peut contribuer à l'établissement de l'infection chronique dans le foie, ainsi qu'au développement des formes sévères de la maladie comme la cirrhose et le cancer du foie.

Réponse immunitaire antivirale

La surface mitochondriale, un carrefour de la réponse immunitaire innée

Outre les fonctions métaboliques décrites ci-dessus, la mitochondrie possède un rôle primordial dans la réponse immunitaire innée précoce. Notamment, sa surface, et plus précisément l'IRM constituent un carrefour permettant à de nombreux facteurs de l'immunité de déclencher une cascade de réactions aboutissant à l'activation de facteurs de transcription qui contrôlent l'expression d'interférons de types I et III. Par exemple, la protéine transmembranaire mitochondriale de signalisation antivirale (MAVS pour *mitochondrial antiviral-signaling protein*), sert de protéine adaptatrice pour les récepteurs cytosoliques de type RIG-I (RIG-I pour *retinoic acid-inducible gene I*, et MDA5 pour *melanoma differentiation-associated protein 5*). Suite à la reconnaissance par ces derniers d'un motif d'ARN étranger par leurs domaines hélicases « *DExD/H box* » [97, 98], ces détecteurs se déplacent vers l'IRM grâce à la liaison de leur motif CARD (*caspase activation and recruitment domains*) à MAVS. Il s'en suit alors la stimulation des voies de signalisation IKKα/β/γ (*inhibitor of nuclear factor kappa-B kinase subunits* α, β, *and* γ) ou IKKε/TBK1 (*TANK-binding kinase 1*) qui vont phosphoryler et activer les facteurs de transcription IRF3 (*interferon regulatory factor 3*), IRF7, NF-κB (*nuclear factor-kappa-B*). Suite à leur import nucléaire, ces derniers induisent la transcription d'interférons (IFN) de types I et III. RIG-I et MDA5 sont les récepteurs cytosoliques les plus étudiés dans la littérature. Ils jouent un rôle important dans la reconnaissance de génomes viraux sous forme d'ARN simple brin non coiffés, d'ARN double brin courts, d'ARN

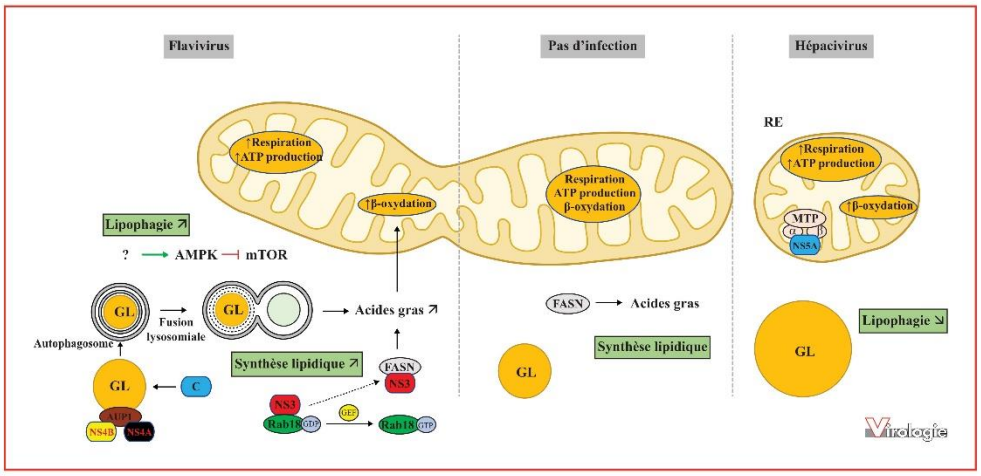

Figure 2. Impact des flavivirus et du VHC sur le métabolisme mitochondrial. *Partie gauche :* représentation schématique de la perturbation du métabolisme mitochondrial par les flavivirus. Les protéines virales stimulent la lipophagie des gouttelettes lipidiques (GL) et la synthèse des acides gras par la *fatty acid synthase* (FASN), aboutissant à l'augmentation de la β-oxydation et de la respiration mitochondriale. *Section centrale :* représentation schématique du métabolisme mitochondrial dans des conditions « normales » en l'absence d'infection. *Partie de droite :* représentation schématique de la régulation négative de la respiration mitochondriale par le VHC.
MTP : *mitochondrial trifunctional protein* ; AUP1 : *ancient ubiquitous protein* 1 ; AMPK : AMP-*activated protein kinase* ; mTOR : *mammalian target of rapamycin.*
Schéma réalisé à l'aide de la ressource en ligne BioRender (https://biorender.com/).

riches en U/A (poly U/A) et d'ARN double brin longs [99, 100]. RIG-I et MDA5 sont des facteurs-clés de la détection intracellulaire de la plupart des *Flaviviridae* tels que le DENV, le VNO, le ZIKV, le YFV, le JEV et le VHC [101-111]. Cependant, d'un point de vue coévolutif, ces virus sont capables d'atténuer l'induction de cette réponse antivirale par des mécanismes moléculaires variés (*figure 3*). Par exemple, l'ubiquitination de RIG-I par TRIM25 (*tripartite motif-containing protein 25*), une ligase d'ubiquitine de type E3 TRIM25 est requise pour son transfert vers les mitochondries [112]. Dans le cas du DENV, des petits ARN flaviviraux sous-génomiques (ARNsf) qui sont des sous-produits non codants issus de la dégradation intracellulaire de l'ARN viral [113, 114], inhibent l'activation de RIG-I en se liant à TRIM25, empêchant ainsi l'activation de RIG-I par ubiquitination [115]. 14-3-3ε, une autre protéine impliquée dans le recrutement de RIG-I et de MDA5 par MAVS par la reconnaissance de motifs sérine ou thréonine phosphorylés, est également ciblée par le DENV, ZIKV et VHC [116-118]. Au cours des infections avec le DENV et le ZIKV, la protéine virale NS3 inhibe le transfert mitochondrial de RIG-I en séquestrant 14-3-3ε par compétition grâce à un motif phosphomimétique conservé de type RxEP dans la protéine NS3 [116, 117].

Concernant le VHC, la protéase virale NS3/4A inactive la voie de production d'IFN-β en clivant MAVS au niveau de l'IRM [119]. Fait très important, ce phénotype a été validé dans des biopsies de foie de patients infectés avec le VHC de façon chronique, soutenant l'idée que cette interférence de l'immunité innée contribue à la persistance virale et à la pathogenèse chez l'humain [120-122].

Finalement, la régulation de la morphodynamique mitochondriale par les Flaviviridae joue également un rôle significatif dans l'interférence de l'immunité innée antivirale en régulant la voie dépendante de MAVS [123-125]. En effet, l'altération de l'IRM ou la perturbation de la dynamique fusion/fission mitochondriale peuvent avoir un impact sur les protéines pro-immunologiques présentes à l'IRM. Comme déjà mentionné plus haut, la fission mitochondriale est favorisée lors de l'infection par le VHC par la stimulation de l'expression de DRP1 chez le VHC [43]. Lorsque l'expression de DRP1 est inhibée pendant une infection par le VHC, l'induction d'IFN-β est augmentée, ce qui est en faveur d'une réponse immunitaire innée à ce virus dépendante de la morphologie mitochondriale. Par ailleurs, la stimulation de l'élongation mitochondriale dans les cellules infectées avec le DENV joue également un rôle dans l'atténuation de l'immunité innée précoce puisqu'elle

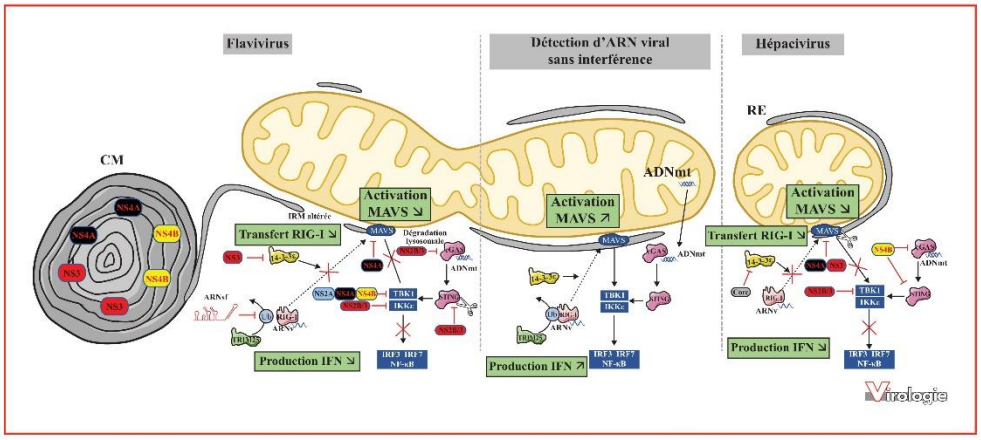

Figure 3. Interférence de l'immunité innée par les flavivirus et le VHC. *Partie gauche :* représentation schématique de l'interférence des voies de signalisation de l'immunité innée précoce par les flavivirus. *Section centrale :* représentation schématique des voies de signalisation de l'immunité innée précoce en condition classique d'infection avec un virus à ARN reconnu par *retinoic acid-inducible gene I* (RIG-I) sans interférence. L'effet indirect de l'infection sur la voie interféron (IFN) par l'entremise de la libération d'ADN mitochondrial (ADNmt) par les mitochondries et sa reconnaissance par la *cyclic GMP-AMP synthase* (cGAS) est également illustré. *Partie de droite :* représentation schématique de l'interférence négative par le VHC sur les mécanismes immunitaires antiviraux.
Ciseaux : clivage protéolytique ; MAVS : *mitochondrial antiviral-signaling protein* ; STING : *stimulator of interferon genes protein* ; TRIM25 : *tripartite motif-containing protein* 25 ; TBK1 : TANK-*binding kinase* 1 ; IKKε : *Inhibitor of nuclear factor kappa-B kinase subunit epsilon* ; IRF3, 7 : *Interferon regulatory factor* 3 and 7 ; ARNsf : petits ARN flaviviraux sous-génomiques ; Ub : ubiquitine ; CM : convolutions de membranes ; IRM : interface réticulo-mitochondriale ; RE : réticulum endoplasmique.
Schéma réalisé à l'aide de la ressource en ligne BioRender (https://biorender.com/).

régule négativement l'expression des IFN-λ et -β [18]. De plus, ceci corrèle avec une réduction du transfert de RIG-I vers l'IRM et une augmentation de la réplication virale. Des phénotypes inverses sont observés lorsqu'on favorise la fission mitochondriale par l'invalidation de MFN2. Finalement, l'IRM est altérée dans les cellules infectées par le DENV ce qui est consistant avec le fait que la voie de signalisation RIG-I/MAVS n'est pas activée de façon optimale. Dans l'ensemble, toutes ces données illustrent que les *Flaviviridae* exploitent la morphodynamique mitochondriale et l'IRM à leur avantage pour atténuer la réponse immunitaire innée et ainsi éviter un état cellulaire antiviral potentiellement préjudiciable à la réplication virale.

La mitochondrie et son matériel génétique, une boîte de Pandore cellulaire

Une des particularités de la mitochondrie est de contenir son propre génome sous forme d'ADN mitochondrial (ADNmt). Ce dernier possède de nombreux sites CpG et est hautement méthylé de façon similaire à l'ADN des procaryotes [126]. L'ADNmt peut être libéré dans le cytoplasme à la suite d'un stress tel qu'une infection virale. Dans une telle situation, cet acide nucléique est reconnu comme un ADN étranger par TLR9 (*Toll-like receptor 9*) [127] ou par cGAS (*cyclic GMP-AMP synthase*) [128, 129] aboutissant à la stimulation de la voie de signalisation dépendante de NF-κB, et donc à l'expression de protéines pro-inflammatoires [130]. Par exemple, dans des cellules dendritiques, le DENV induit la libération de l'ADNmt dans le cytosol suite à la production excessive de dérivés réactifs d'oxygène (ROS pour *reactive oxygen species*) et à l'activation de l'inflammasome, ce qui résulte en l'activation des TLR9 [131]. Par ailleurs, suite à la détection de l'ADNmt par cGAS, cette protéine par l'intermédiaire de la protéine adaptatrice STING (*stimulator of interferon genes protein*), partage l'information aux cellules voisines non infectées à travers les jonctions serrées intercellulaires [132]. Un mécanisme d'interférence développé par le DENV est d'induire la dégradation de cGAS par les lysosomes par la protéine virale NS2B (*figure 3*) [133]. Un tel mode d'évasion est aussi retrouvé pendant l'infection par le ZIKV. En effet, le ZIKV, par l'intermédiaire de la protéine virale NS1, recrute la deubiquitinase U8 pour cliver les chaînes de polyubiquitine sur la caspase 1, ce qui la stabilise. Ceci favorise le clivage de cGAS par cette dernière, empêchant ainsi la reconnaissance de l'ADNmt libéré [134]. De plus, STING est également soumis à un clivage par la protéase virale NS3

(avec son co-facteur NS2B). Ce mécanisme d'interférence est retrouvé lors de l'infection par plusieurs flavivirus tels que le DENV, le ZIKV et le VNO, mais pas par le YFV [135]. Enfin, le domaine transmembranaire de la protéine virale NS4B du VHC réduit la sensibilité des cellules à une stimulation avec le ligand de cGAS. Cette atténuation est due à une inhibition de l'interaction entre STING, TBK1 et MAVS par la portion aminoterminale de NS4B, ce qui résulte ultimement en une évasion du système immunitaire [136]. Tous ces mécanismes d'échappement développés par les *Flaviviridae* montrent l'ingéniosité de l'évolution de ces virus en parallèle de l'évolution du système immunitaire de l'humain.

Fait intéressant, lorsque des erreurs se produisent lors de la réplication de l'ADNmt à la suite de stress externes, l'ADNmt peut subir des cassures double brin pour former des ADNmt fragmentés [137]. Ces ADNmt fragmentés sont encore peu connus, mais leur production active la voie IFN de type I par la phosphorylation de STAT1 (*signal transducer and activator of transcription 1*) et l'activation des gènes stimulés par les interférons [138]. Ces ADNmt fragmentés peuvent également provoquer la perméabilisation des membranes mitochondriales par BAX (*Bcl-2–associated X protein*) et BAK (*Bcl-2 homologous antagonist/killer protein*») permettant l'échappement de l'ARN mitochondrial de la matrice et la reconnaissance par RIG-I et MAVS activant l'expression des IFN de types I et III. Cependant, un tel processus reste à démontrer expérimentalement lors d'infections par les *Flaviviridae*.

Apoptose

L'apoptose est une mort cellulaire programmée à la suite d'un stress permettant à la cellule de s'auto-détruire. Elle peut être activée par deux voies possibles, la voie extrinsèque impliquant des récepteurs de la superfamille des facteurs de croissance tumorale et la voie intrinsèque faisant intervenir la mitochondrie par le biais des protéines de la famille BCL-2 [139]. En effet, cette dernière est notamment activée lorsque les cellules sont soumises à un stress modifiant la perméabilité membranaire des mitochondries provoquée par les facteurs pro-apoptotiques BAX et BAK. Ceci a pour effet de libérer dans le cytosol du cytochrome C et MCL1 (*induced myeloid leukemia cell differentiation protein*), ce qui conduit à l'activation de APAF1 (*apoptotic protease-activating factor 1*) puis des caspases 9 et 3 qui en retour, activent des facteurs apoptotiques et engagent la phase d'exécution de l'apoptose. Il y a beaucoup d'évidences que les *Flaviviridae* induisent les deux voies de l'apoptose *in vivo* comme *in vitro* [140-146]. Notamment, les protéines virales NS2, NS3, C, E et M des virus DENV, VNO et JEV activent individuellement la voie intrinsèque [147, 148]. De plus, l'apoptose résultant du stress oxydatif, du stress du RE et/ou de la dérégulation des homéostasies du Ca^{2+} et des lipides contribue aux effets cytopathiques observés en culture cellulaire suite à l'infection [149]. En réponse à cette réponse cellulaire, ces pathogènes possèdent des mécanismes d'atténuation qui vont retarder la mort cellulaire et maximiser la production virale (*figure 4*). La voie PI3K/PKB/mTOR (*phosphoinositide 3-kinase/protein kinase B*, appelée aussi AKT/*mammalian target of rapamycin*), particulièrement importante dans la régulation de la croissance et la survie cellulaire a un rôle central dans le contrôle de l'apoptose induite par les infections aux *Flaviviridae* [150]. En effet, une fois PKB phosphorylée, cette dernière inhibe les facteurs pro-apoptotiques tels que BAD (*Bcl2-associated agonist of cell death*) et la caspase 9, ainsi que le relargage du cytochrome C par les mitochondries. Lors de l'infection par les virus DENV, JEV, VNO et VHC, cette voie est stimulée, ce qui favorise la survie cellulaire et retarde l'apoptose. Par exemple, la voie PI3K/PKB/mTOR impliquée dans l'inhibition de l'apoptose est soit activée lors d'une infection par le DENV ou JEV favorisant ainsi le relargage de Bcl-2 [151], soit intervient dans l'inhibition des caspases 3 et 8 suite à son activation par la protéine C du VNO [152]. L'infection par le ZIKV entraîne également un retard de l'apoptose, ce qui favorise sa réplication. En effet, le virus contrôle la voie anti-apoptotique au moyen d'une stabilisation de Bcl-2 [153]. Finalement ? dans l'infection par le VHC, la protéine virale NS5A limite l'apoptose en activant la voie PI3K/PKB/mTOR, ce qui favorise la persistance virale [154]. D'un point de vue morphologique, la dynamique mitochondriale joue également un rôle dans l'apoptose. En effet, la fragmentation altère la morphologie des crêtes de la membrane mitochondriale interne et rend les membranes de cet organite plus perméables, résultant en un relargage accru de cytochrome C et à la potentialisation de l'apoptose [155-160]. Même si cela reste débattu, la fragmentation augmenterait la surface membranaire des mitochondries, permettant ainsi d'accommoder plus de pores qui libèrent des molécules pro-apoptotiques. Ce modèle est soutenu par le fait que l'infection de neurones par le ZIKV induit l'apoptose neuronale à la suite de la fragmentation des mitochondries par une réduction de l'abondance du facteur de fusion MFN2 dans ce type cellulaire [40]. Un traitement avec le Mdivi-1, un inhibiteur de DRP1 et donc, de la fragmentation mitochondriale, atténue la mort cellulaire lors d'une infection par le ZIKV, suggérant que la dynamique mitochondriale a un impact direct sur l'apoptose. À l'opposé, certains types cellulaires tolèrent mieux le stress de l'infection virale et les effets cytopathiques apparaissent à des temps tardifs de l'infection. La production virale dans ces conditions est généralement élevée et corrèle avec un aspect allongé des mitochondries

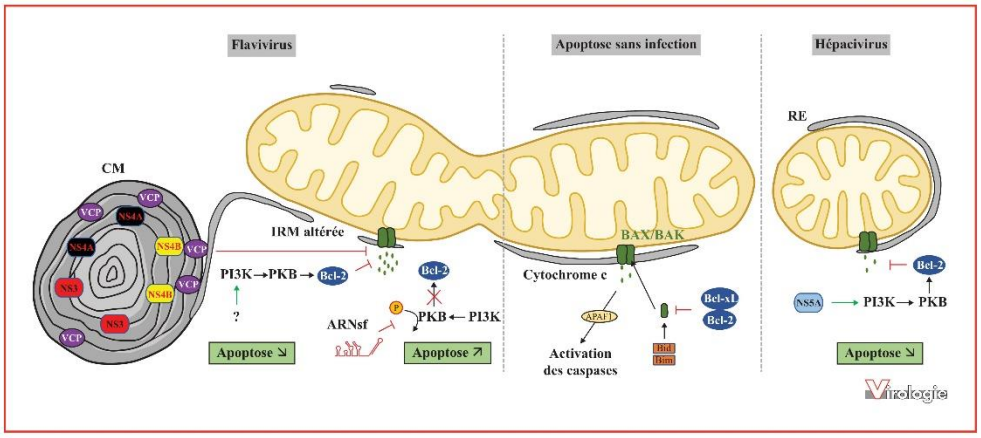

Figure 4. Perturbations de l'apoptose par les flavivirus et le VHC. *Section centrale :* représentation de la voie intrinsèque d'induction de l'apoptose dans des conditions sans infection. *Partie de gauche :* représentation schématique de la perturbation négative ou positive de l'induction de l'apoptose par les flavivirus. *Partie de droite :* représentation schématique de la perturbation négative de l'apoptose par le VHC.
IRM : Interface réticulo-mitochondriale ; CM : convolutions de membranes ; RE : réticulum endoplasmique. PI3K : *Phosphatidylinositol 3-kinase* ; ARNsf : petits ARN flaviviraux sous-génomiques ; VCP : *valosin-containing protein.*
Schéma réalisé à l'aide de la ressource en ligne BioRender (https://biorender.com/).

tel que discuté plus haut. Notamment, l'activité ATPase de VCP est requise pour maintenir l'élongation mitochondriale et la formation des CM. Ceci corrèle avec une atténuation des effets cytopathiques puisque l'inhibition de VCP induit une apoptose prématurée dépendante du ZIKV [38]. Ceci suggère que la diminution de l'apoptose par VCP serait accompagnée par la fusion mitochondriale et l'altération de l'IRM lors de la biogénèse des CM [38]. L'activité du facteur de fission DRP1, une cible inhibée par le DENV, est intimement liée à la régulation de l'apoptose. En effet, suite à sa déplétion par interférence par l'ARN, on constate un délai dans la fission mitochondriale, la sortie du cytochrome C et dans l'activation des caspases ce qui décroît l'induction de l'apoptose [161-163]. L'hypothèse la plus probable serait donc que les flavivirus modulent la morphodynamique mitochondriale ce qui retarderait la mort cellulaire due au stress de l'infection et maximiserait la réplication du génome et la production de virions.

Dans le cas du VHC, c'est, au contraire, la fragmentation des mitochondries observée lors de l'infection, qui atténue l'apoptose et favorise la persistance virale par le biais de DRP1 [43]. Lorsque DRP1 est atténué par l'interférence par ARN, il y a une diminution de la fission induite par le VHC aboutissant à l'augmentation de la voie de signalisation de l'apoptose et de l'inhibition du relargage de nouveaux virions suggérant que la fission est importante non seulement pour réduire l'apoptose mais également pour la dissémination du virus. Suivant le même principe, le virus de la fièvre porcine, membre du genre *Pestivirus* induit la fission et la mitophagie, ce qui atténue aussi l'apoptose [42].

Fait très intéressant, les ARNsf régulent l'apoptose et ce, de façon divergente selon l'espèce. En effet, des souches de ZIKV mutées qui ne produisent pas d'ARNsf, induisent de l'apoptose dans des moustiques infectés, à l'inverse de la souche sauvage [164]. Cette étude démontre donc un rôle anti-apoptotique de l'ARNsf, soulevant l'hypothèse que cet ARN non codant constituerait un facteur clé dans la transmission du ZIKV du moustique à l'humain. Pourtant à l'inverse, dans les cellules de mammifères, l'ARNsf joue également un rôle stimulateur dans l'activation de l'apoptose et des effets cytopathiques, notamment en inhibant la phosphorylation de PKB et l'activation de Bcl-2, ce qui finalement promeut le relargage de cytochrome C [114, 144].

Enfin, on ne peut pas exclure que la diminution des niveaux de cardiolipine dans les cellules infectées par le ZIKV [80] contribue aux effets cytopathiques, puisque ce lipide mitochondrial lie le cytochrome C au sein de la membrane mitochondriale interne et limite donc son relargage lors de l'apoptose [165-167]. À l'inverse, et de façon paradoxale (et controversée), la cardiolipine serait requise pour la perméabilisation de la membrane mitochondriale externe et donc, pour la libération du cytochrome C. Il serait très intéressant

d'évaluer comment cette altération des niveaux de cardiolipine influence la réplication et surtout, si cela potentialise ou atténue l'apoptose induite par le ZIKV.

Mitophagie

La mitophagie consiste en la dégradation sélective des mitochondries par autophagie. Cette dernière est la conséquence de différents types de stress tels que l'hypoxie [168, 169], la dépolarisation mitochondriale [170, 171] ou encore l'accumulation des ROS [172, 173] permettant le recyclage des mitochondries par voie lysosomale [174-176]. La voie d'activation de la mitophagie impliquant les protéines PINK1 (*PTEN-induced putative kinase 1*) et Parkin est la mieux caractérisée [177-179]. Brièvement, PINK1 détecte l'endommagement des mitochondries, souvent fragmentées, par l'entremise de la phosphorylation de l'ubiquitine. Cela conduit au transfert mitochondrial et à l'activation de Parkin, une ligase d'ubiquitine de type E3. Le complexe PINK1/Parkin mitochondrial va alors induire le recrutement du phagophore, la membrane isolée à l'origine de la formation de l'autophagosome. De nombreuses études ont montré que la réplication des *Flaviviridae* dépend des protéines impliquées dans l'autophagie induite dans les cellules infectées [180]. Le VHC stimule l'expression de PINK1 et de Parkin et favorise le transfert de Parkin aux mitochondries pour initier la mitophagie, ce qui corrèle avec la fission mitochondriale provoquée par le virus [43, 95]. L'induction de la mitophagie a été confirmée suite à l'observation de la colocalisation entre le récepteur autophagique LC3 (*light chain 3*), les lysosomes et les mitochondries associées à Parkin. Finalement, l'inhibition de PINK1 et Parkin réduit la réplication du virus montrant l'importance de la mitophagie dans l'infection par le VHC. Chez les flavivirus, il semblerait que la mitophagie ne soit pas induite. En effet, l'inhibition du transfert de Ajuba aux mitochondries, une protéine cellulaire impliquée dans l'activation de PINK1, par la protéine virale NS5 du ZIKV bloque la mitophagie [181]. De plus, le fait que la fusion mitochondriale soit favorisée lors d'une infection avec le DENV et ZIKV favorise le modèle selon lequel la mitophagie n'a pas lieu dans les cellules infectées [18, 37]. En effet, la majorité des mitochondries prises en charge par la machinerie autophagique sont fragmentées dans la plupart des cas. L'élongation mitochondriale, à l'inverse, est plutôt associée à une protection de ces organites vis-à-vis de l'autophagie ce qui favoriserait la production d'énergie et la survie cellulaire lors d'un stress de privation en sérum [182]. Finalement, on ne peut pour l'instant pas exclure l'hypothèse que la réplication des *Flaviviridae* dépende aussi de perturbations des processus mitophagiques indépendants de Parkin, tels que ceux impliquant la cardiolipine ou les ligases d'ubiquitine Gp78 et SIAH1 [183-186]. Notamment, le fait que les niveaux de cardiolipine diminuent dans les cellules infectées par le ZIKV laisse supposer que cela contribuerait à inhiber la mitophagie [80].

Conclusion & perspectives

La compréhension du rôle de la mitochondrie dans la cellule s'est considérablement complexifiée dans les quinze dernières années. Cet organite est passé du simple statut de « centrale énergétique de la cellule » à celui de carrefour fonctionnel où convergent de nombreux processus cellulaires importants au maintien de l'homéostasie, à la survie et à la réponse à divers stress (pathogéniques ou non). Il n'est donc pas surprenant que lors d'infections par des pathogènes tels que les *Flaviviridae,* cet organite soit ciblé, ce qui favorise leur multiplication et contribue à la pathogenèse que ce soit en régulant la production d'énergie ou en s'évadant du système immunitaire. Il reste encore beaucoup d'énigmes à résoudre dans la plupart des cas, notamment au niveau des mécanismes moléculaires impliqués dans ces détournements fonctionnels, incluant l'identification des déterminants viraux impliqués. Dans le cas des flavivirus, il apparaît que les usines de réplication virales dérivées du RE sont impliquées dans ce détournement par l'intermédiaire de contacts physiques. Cela illustre que le remodelage du RE par ces virus n'est pas seulement responsable de l'hébergement des complexes de réplication du génome viral mais aussi de l'établissement d'un contexte cytoplasmique proviral. Considérant qu'un de leurs constituants, la protéine NS4B régule au moins en partie ces processus, l'interface entre les URV et les mitochondries pourrait constituer une cible thérapeutique attractive et plusieurs inhibiteurs de cette protéine virale sont en cours de développement.

Malgré l'appartenance des flavivirus et des hépacivirus à la même famille, ces virus ont divergé significativement lors de l'évolution en ce qui concerne leurs mécanismes de contrôle de la morphologie et des fonctions mitochondriales. En effet, les architectures respectives des URV sont complètement différentes avec des invaginations flavivirales et des protubérances hépacivirales du RE. Ces deux modes de remodelage du RE requièrent probablement des besoins distincts en énergie, calcium et lipides, ce qui pourrait se traduire par des contributions mitochondriales différentes. Au-delà des connaissances en virologie moléculaire et en biologie des mitochondries, mieux comprendre la relation étroite entre les *Flaviviridae* et les mitochondries pourrait contribuer à identifier des stratégies thérapeutiques ciblant spécifiquement la cytopathogenèse virale sans pour autant perturber l'homéostasie cellulaire globale.

Remerciements. Nous remercions Clément Mazeaud et Anaïs Anton pour leurs commentaires et suggestions lors de la relecture de ce manuscrit. Nous sommes également reconnaissants envers la Fondation Armand-Frappier et le Fond de recherche du Québec-Santé pour les bourses d'études doctorales allouées à WF. Le Fonds de recherche du Québec-Santé fournit également un appui salarial à LCC en tant que chercheur-boursier junior 2. Le programme de recherche sur la relation entre les flavivirus et les mitochondries est financé par une subvention des Instituts de recherche en santé du Canada (PJT153020).

Liens d'intérêt : Les auteurs déclarent ne pas avoir de lien d'intérêt en rapport avec cet article.

Références

1. Spinelli JB, Haigis MC. The multifaceted contributions of mitochondria to cellular metabolism. *Nat Cell Biol* 2018 ; 20(7) : 745-54.

2. McBride HM, Neuspiel M, Wasiak S. Mitochondria: more than just a powerhouse. *Curr Biol* 2006 ; 16(14) : R551-60.

3. Antico Arciuch VG, Elguero ME, Poderoso JJ, Carreras MC. Mitochondrial regulation of cell cycle and proliferation. *Antioxid Redox Signal* 2012 ; 16(10) : 1150-80.

4. Weinberg SE, Sena LA, Chandel NS. Mitochondria in the regulation of innate and adaptive immunity. *Immunity* 2015 ; 42(3) : 406-17.

5. World Health Organisation (WHO). *Dengue and severe dengue*. Key facts. WHO, 2020.

6. Lowe R, Barcellos C, Brasil P, *et al*. The Zika virus epidemic in Brazil: from discovery to future implications. *Int J Environ Res Public Health* 2018 ; 15(1) : e02020-2116.

7. World Health Organisation (WHO). *Zika virus*. Key facts. WHO, 2018.

8. Pandit PS, Doyle MM, Smart KM, Young CCW, Drape GW, Johnson CK. Predicting wildlife reservoirs and global vulnerability to zoonotic Flaviviruses. *Nat Commun* 2018 ; 9(1) : 5425.

9. Araujo SC, Pereira LR, Alves RPS, *et al*. Anti-flavivirus vaccines: review of the present situation and perspectives of subunit vaccines produced in *Escherichia coli*. *Vaccines (Basel)* 2020 ; 8(3) : 492.

10. World Health Organisation (WHO). *Heptitis C*. Key facts. WHO, 2020.

11. Das D, Pandya M. Recent advancement of direct-acting antiviral agents (DAAs) in hepatitis C therapy. *Mini Rev Med Chem* 2018 ; 18(7) : 584-96.

12. Mazeaud C, Freppel W, Chatel-Chaix L. The multiples fates of the Flavivirus RNA genome during pathogenesis. *Front Genet* 2018 ; 9 : 595.

13. Bartenschlager R, Lohmann V, Penin F. The molecular and structural basis of advanced antiviral therapy for hepatitis C virus infection. *Nat Rev Microbiol* 2013 ; 11(7) : 482-96.

14. Welsch S, Miller S, Romero-Brey I, *et al*. Composition and three-dimensional architecture of the dengue virus replication and assembly sites. *Cell Host Microbe* 2009 ; 5(4) : 365-75.

15. Westaway EG, Mackenzie JM, Kenney MT, Jones MK, Khromykh AA. Ultrastructure of Kunjin virus-infected cells: colocalization of NS1 and NS3 with double-stranded RNA, and of NS2B with NS3, in virus-induced membrane structures. *J Virol* 1997 ; 71(9) : 6650-61.

16. Cortese M, Goellner S, Acosta EG, *et al*. Ultrastructural characterization of Zika virus replication factories. *Cell Rep* 2017 ; 18(9) : 2113-23.

17. Gillespie LK, Hoenen A, Morgan G, Mackenzie JM. The endoplasmic reticulum provides the membrane platform for biogenesis of the flavivirus replication complex. *J Virol* 2010 ; 84(20) : 10438-47.

18. Chatel-Chaix L, Cortese M, Romero-Brey I, *et al*. Dengue virus perturbs mitochondrial morphodynamics to dampen innate immune responses. *Cell Host Microbe* 2016 ; 20(3) : 342-56.

19. Romero-Brey I, Bartenschlager R. Membranous replication factories induced by plus-strand RNA viruses. *Viruses* 2014 ; 6(7) : 2826-57.

20. Chatel-Chaix L, Bartenschlager R. Dengue virus- and hepatitis C virus-induced replication and assembly compartments: the enemy inside–caught in the web. *J Virol* 2014 ; 88(11) : 5907-11.

21. Ferraris P, Blanchard E, Roingeard P. Ultrastructural and biochemical analyses of hepatitis C virus-associated host cell membranes. *J Gen Virol* 2010 ; 91(Pt 9) : 2230-7.

22. Ferraris P, Beaumont E, Uzbekov R, *et al*. Sequential biogenesis of host cell membrane rearrangements induced by hepatitis C virus infection. *Cell Mol Life Sci* 2013 ; 70(7) : 1297-306.

23. Paul D, Hoppe S, Saher G, Krijnse-Locker J, Bartenschlager R. Morphological and biochemical characterization of the membranous hepatitis C virus replication compartment. *J Virol* 2013 ; 87(19) : 10612-27.

24. Schwarz DS, Blower MD. The endoplasmic reticulum: structure, function and response to cellular signaling. *Cell Mol Life Sci* 2016 ; 73(1) : 79-94.

25. Pourcelot M, Arnoult D. Mitochondrial dynamics and the innate antiviral immune response. *FEBS J* 2014 ; 281(17) : 3791-802.

26. Friedman JR, Lackner LL, West M, DiBenedetto JR, Nunnari J, Voeltz GK. ER tubules mark sites of mitochondrial division. *Science* 2011 ; 334(6054) : 358-62.

27. Hamasaki M, Furuta N, Matsuda A, *et al*. Autophagosomes form at ER-mitochondria contact sites. *Nature* 2013 ; 495(7441) : 389-93.

28. Anastasia I, Ilacqua N, Raimondi A, *et al*. Mitochondria-rough-ER contacts in the liver regulate systemic lipid homeostasis. *Cell Rep* 2021 ; 34(11) : 108873.

29. Pilling AD, Horiuchi D, Lively CM, Saxton WM. Kinesin-1 and Dynein are the primary motors for fast transport of mitochondria in Drosophila motor axons. *Mol Biol Cell* 2006 ; 17(4) : 2057-68.

30. Ishihara N, Eura Y, Mihara K. Mitofusin 1 and 2 play distinct roles in mitochondrial fusion reactions *via* GTPase activity. *J Cell Sci* 2004 ; 117(Pt 26) : 6535-46.

31. Koshiba T, Detmer SA, Kaiser JT, Chen H, McCaffery JM, Chan DC. Structural basis of mitochondrial tethering by mitofusin complexes. *Science* 2004 ; 305(5685) : 858-62.

32. Westermann B. Mitochondrial fusion and fission in cell life and death. *Nat Rev Mol Cell Biol* 2010 ; 11(12) : 872-84.

33. Yoon Y, McNiven MA. Mitochondrial division: new partners in membrane pinching. *Curr Biol* 2001 ; 11(2) : R67-70.

34. Giacomello M, Pellegrini L. The coming of age of the mitochondria-ER contact: a matter of thickness. *Cell Death Differ* 2016 ; 23(9) : 1417-27.

35. Chang CR, Blackstone C. Drp1 phosphorylation and mitochondrial regulation. *EMBO Rep* 2007 ; 8(12) : 1088-9.

36. Westermann B. Bioenergetic role of mitochondrial fusion and fission. *Biochim Biophys Acta* 2012 ; 1817(10) : 1833-8.

37. Barbier V, Lang D, Valois S, Rothman AL, Medin CL. Dengue virus induces mitochondrial elongation through impairment of Drp1-triggered mitochondrial fission. *Virology* 2017 ; 500 : 149-60.

38. Anton A, Mazeaud C, Freppel W, *et al*. Valosin-containing protein ATPase activity regulates the morphogenesis of Zika virus replication organelles and virus-induced cell death. *Cell Microbiol* 2021 ; 23(4) : e13302.

39. Molino D, Pila-Castellanos I, Marjault HB, *et al*. Chemical targeting of NEET proteins reveals their function in mitochondrial morphodynamics. *EMBO Rep* 2020 ; 21(12) : e49019.

40. Yang S, Gorshkov K, Lee EM, *et al*. Zika virus-induced neuronal apoptosis *via* increased mitochondrial fragmentation. *Front Microbiol* 2020 ; 11 : 598203.

41. Yu CY, Liang JJ, Li JK, *et al*. Dengue virus impairs mitochondrial fusion by cleaving mitofusins. *PLoS Pathog* 2015 ; 11(12) : e1005350.

42. Gou H, Zhao M, Xu H, *et al*. CSFV induced mitochondrial fission and mitophagy to inhibit apoptosis. *Oncotarget* 2017 ; 8(24) : 39382-400.

43. Kim SJ, Syed GH, Khan M, *et al*. Hepatitis C virus triggers mitochondrial fission and attenuates apoptosis to promote viral persistence. *Proc Natl Acad Sci U S A* 2014 ; 111(17) : 6413-8.

44. Siu GK, Zhou F, Yu MK, *et al*. Hepatitis C virus NS5A protein cooperates with phosphatidylinositol 4-kinase IIIalpha to induce mitochondrial fragmentation. *Sci Rep* 2016 ; 6 : 23464.

45. Nomura-Takigawa Y, Nagano-Fujii M, Deng L, *et al*. Non-structural protein 4A of Hepatitis C virus accumulates on mitochondria and renders the cells prone to undergoing mitochondria-mediated apoptosis. *J Gen Virol* 2006 ; 87(Pt 7) : 1935-45.

46. Clapham DE. Calcium signaling. *Cell* 2007 ; 131(6) : 1047-58.

47. Hartmann J, Verkhratsky A. Relations between intracellular Ca^{2+} stores and store-operated Ca^{2+} entry in primary cultured human glioblastoma cells. *J Physiol* 1998 ; 513(Pt 2) : 411-24.

48. Bartok A, Weaver D, Golenar T, *et al*. IP3 receptor isoforms differently regulate ER-mitochondrial contacts and local calcium transfer. *Nat Commun* 2019 ; 10(1) : 3726.

49. Boyman L, Lederer WJ. How the mitochondrial calcium uniporter complex (MCUcx) works. *Proc Natl Acad Sci U S A* 2020 ; 117(37) : 22634-6.

50. Orrenius S, Zhivotovsky B, Nicotera P. Regulation of cell death: the calcium-apoptosis link. *Nat Rev Mol Cell Biol* 2003 ; 4(7) : 552-65.

51. Lee KS, Huh S, Lee S, *et al*. Altered ER-mitochondria contact impacts mitochondria calcium homeostasis and contributes to neurodegeneration *in vivo* in disease models. *Proc Natl Acad Sci U S A* 2018 ; 115(38) : E8844-53.

52. Li Y, Boehning DF, Qian T, Popov VL, Weinman SA. Hepatitis C virus core protein increases mitochondrial ROS production by stimulation of Ca^{2+} uniporter activity. *FASEB J* 2007 ; 21(10) : 2474-85.

53. Dionisio N, Garcia-Mediavilla MV, Sanchez-Campos S, *et al*. Hepatitis C virus NS5A and core proteins induce oxidative stress-mediated calcium signalling alterations in hepatocytes. *J Hepatol* 2009 ; 50(5) : 872-82.

54. Gincel D, Zaid H, Shoshan-Barmatz V. Calcium binding and translocation by the voltage-dependent anion channel: a possible regulatory mechanism in mitochondrial function. *Biochem J* 2001 ; 358(Pt 1) : 147-55.

55. Schwer B, Ren S, Pietschmann T, *et al*. Targeting of hepatitis C virus core protein to mitochondria through a novel C-terminal localization motif. *J Virol* 2004 ; 78(15) : 7958-68.

56. Jitobaom K, Tongluan N, Smith DR. Involvement of voltage-dependent anion channel (VDAC) in dengue infection. *Sci Rep* 2016 ; 6 : 35753.

57. Khongwichit S, Sornjai W, Jitobaom K, *et al*. A functional interaction between GRP78 and Zika virus E protein. *Sci Rep* 2021 ; 11(1) : 393.

58. Tangsongcharoen C, Roytrakul S, Smith DR. Analysis of cellular proteome changes in response to ZIKV NS2B-NS3 protease expression. *Biochim Biophys Acta Proteins Proteom* 2019 ; 1867(2) : 89-97.

59. Dionicio CL, Pena F, Constantino-Jonapa LA, *et al*. Dengue virus induced changes in Ca $(^{2+})$ homeostasis in human hepatic cells that favor the viral replicative cycle. *Virus Res* 2018 ; 245 : 17-28.

60. Scherbik SV, Brinton MA. Virus-induced Ca^{2+} influx extends survival of west nile virus-infected cells. *J Virol* 2010 ; 84(17) : 8721-31.

61. Tamura Y, Kawano S, Endo T. Lipid homeostasis in mitochondria. *Biol Chem* 2020 ; 401(6-7) : 821-33.

62. Martin S, Parton RG. Lipid droplets: a unified view of a dynamic organelle. *Nat Rev Mol Cell Biol* 2006 ; 7(5) : 373-8.

63. Barbosa AD, Siniossoglou S. Function of lipid droplet-organelle interactions in lipid homeostasis. *Biochim Biophys Acta Mol Cell Res* 2017 ; 1864(9) : 1459-68.

64. Calder PC. Fatty acids: metabolism. In : Caballero B, Finglas PM, Toldrá F, eds. *Encyclopedia of Food and Health*. Oxford : Academic Press, 2016, pp. 632-44.

65. Perera R, Riley C, Isaac G, *et al*. Dengue virus infection perturbs lipid homeostasis in infected mosquito cells. *PLoS Pathog* 2012 ; 8(3) : e1002584.

66. Martin-Acebes MA, Merino-Ramos T, Blazquez AB, *et al*. The composition of West Nile virus lipid envelope unveils a role of sphingolipid metabolism in flavivirus biogenesis. *J Virol* 2014 ; 88(20) : 12041-54.

67. Melo CF, de Oliveira DN, Lima EO, *et al*. A lipidomics approach in the characterization of Zika-infected mosquito cells: potential targets for breaking the transmission cycle. *PLoS One* 2016 ; 11(10) : e0164377.

68. Diamond DL, Syder AJ, Jacobs JM, *et al*. Temporal proteome and lipidome profiles reveal hepatitis C virus-associated reprogramming of hepatocellular metabolism and bioenergetics. *PLoS Pathog* 2010 ; 6(1) : e1000719.

69. Heaton NS, Randall G. Dengue virus-induced autophagy regulates lipid metabolism. *Cell Host Microbe* 2010 ; 8(5) : 422-32.

70. Tang WC, Lin RJ, Liao CL, Lin YL. Rab18 facilitates dengue virus infection by targeting fatty acid synthase to sites of viral replication. *J Virol* 2014 ; 88(12) : 6793-804.

71. Martin-Acebes MA, Blazquez AB, Jimenez de Oya N, Escribano-Romero E, Saiz JC. West Nile virus replication requires fatty acid synthesis but is independent on phosphatidylinositol-4-phosphate lipids. *PLoS One* 2011 ; 6(9) : e24970.

72. Mohamed B, Mazeaud C, Baril M, *et al*. Very-long-chain fatty acid metabolic capacity of 17-beta-hydroxysteroid dehydrogenase type 12 (HSD17B12) promotes replication of hepatitis C virus and related flaviviruses. *Sci Rep* 2020 ; 10(1) : 4040.

73. Heaton NS, Perera R, Berger KL, *et al*. Dengue virus nonstructural protein 3 redistributes fatty acid synthase to sites of viral replication and increases cellular fatty acid synthesis. *Proc Natl Acad Sci U S A* 2010 ; 107(40) : 17345-50.

74. Jordan TX, Randall G. Dengue virus activates the AMP Kinase-mTOR axis to stimulate a proviral lipophagy. *J Virol* 2017 ; 91(11) : e02020-2116.

75. Samsa MM, Mondotte JA, Iglesias NG, *et al*. Dengue virus capsid protein usurps lipid droplets for viral particle formation. *Plos Pathog* 2009 ; 5(10) : e1000632.

76. Byk LA, Gamarnik AV. Properties and functions of the Dengue virus capsid protein. *Annu Rev Virol* 2016 ; 3(1) : 263-81.

77. Zhang J, Lan Y, Li MY, *et al*. Flaviviruses exploit the lipid droplet protein AUP1 to trigger lipophagy and drive virus production. *Cell Host Microbe* 2018 ; 23(6) : 819-31 e5.

78. Amako Y, Munakata T, Kohara M, Siddiqui A, Peers C, Harris M. Hepatitis C virus attenuates mitochondrial lipid beta-oxidation by downregulating mitochondrial trifunctional-protein expression. *J Virol* 2015 ; 89(8) : 4092-101.

79. Amako Y, Sarkeshik A, Hotta H, Yates 3rd H, Siddiqui A. Role of oxysterol binding protein in hepatitis C virus infection. *J Virol* 2009 ; 83(18) : 9237-46.

80. Leier HC, Weinstein JB, Kyle JE, *et al*. A global lipid map defines a network essential for Zika virus replication. *Nat Commun* 2020 ; 11(1) : 3652.

81. Ott M, Zhivotovsky B, Orrenius S. Role of cardiolipin in cytochrome C release from mitochondria. *Cell Death Differ* 2007 ; 14(7) : 1243-7.

82. Paradies G, Paradies V, Ruggiero FM, Petrosillo G. Role of cardiolipin in mitochondrial function and dynamics in health and disease: molecular and pharmacological aspects. *Cells* 2019 ; 8(7) : 728.

83. Li XB, Gu JD, Zhou QH. Review of aerobic glycolysis and its key enzymes – new targets for lung cancer therapy. *Thorac Cancer* 2015 ; 6(1) : 17-24.

84. Papa S, Martino PL, Capitanio G, Gaballo A, De Rasmo D, Signorile A, *et al*. The oxidative phosphorylation system in mammalian mitochondria. *Adv Exp Med Biol* 2012 ; 942 : 3-37.

85. Fontaine KA, Sanchez EL, Camarda R, Lagunoff M. Dengue virus induces and requires glycolysis for optimal replication. *J Virol* 2015 ; 89(4) : 2358-66.

86. Allonso D, Andrade IS, Conde JN, *et al*. Dengue Virus NS1 protein modulates cellular energy metabolism by increasing glyceraldehyde-3-phosphate dehydrogenase activity. *J Virol* 2015 ; 89(23) : 11871-83.

87. Kumar A, Singh S, Singh P, Giri S. Activation of AMPK restricts Zika virus replication in endothelial cells by potentiating antiviral response and inhibiting viral-induced glycolysis. *J Immunol* 2019 ; 202(1) : 127.19.

88. Ramière C, Rodriguez J, Enache LS, Lotteau V, André P, Diaz O. Activity of hexokinase is increased by its interaction with hepatitis C virus protein NS5A. *J Virol* 2014 ; 88(6) : 3246-54.

89. Duan X, Li S, Holmes JA, *et al*. MicroRNA 130a regulates both hepatitis C virus and hepatitis B virus replication through a central metabolic pathway. *J Virol* 2018 ; 92(7) : e02009-2017.

90. Jung GS, Jeon JH, Choi YK, *et al*. Pyruvate dehydrogenase kinase regulates hepatitis C virus replication. *Sci Rep* 2016 ; 6 : 30846.

91. El-Bacha T, Midlej V, Pereira da Silva AP, *et al*. Mitochondrial and bioenergetic dysfunction in human hepatic cells infected with dengue 2 virus. *Biochim Biophys Acta* 2007 ; 1772(10) : 1158-66.

92. Chen Q, Gouilly J, Ferrat YJ, *et al*. Metabolic reprogramming by Zika virus provokes inflammation in human placenta. *Nat Commun* 2020 ; 11(1) : 2967.

93. Ledur PF, Karmirian K, Pedrosa C, *et al*. Zika virus infection leads to mitochondrial failure, oxidative stress and DNA damage in human iPSC-derived astrocytes. *Sci Rep* 2020 ; 10(1) : 1218.

94. Korenaga M, Wang T, Li Y, *et al*. Hepatitis C virus core protein inhibits mitochondrial electron transport and increases reactive oxygen species (ROS) production. *J Biol Chem* 2005 ; 280(45) : 37481-8.

95. Kim SJ, Syed GH, Siddiqui A. Hepatitis C virus induces the mitochondrial translocation of Parkin and subsequent mitophagy. *PLoS Pathog* 2013 ; 9(3) : e1003285.

96. Tsutsumi T, Matsuda M, Aizaki H, *et al*. Proteomics analysis of mitochondrial proteins reveals overexpression of a mitochondrial protein chaperon, prohibitin, in cells expressing hepatitis C virus core protein. *Hepatology* 2009 ; 50(2) : 378-86.

97. Loo YM, Gale Jr. M. Immune signaling by RIG-I-like receptors. *Immunity* 2011 ; 34(5) : 680-92.

98. Refolo G, Vescovo T, Piacentini M, Fimia GM, Ciccosanti F. Mitochondrial interactome: a focus on antiviral signaling pathways. *Front Cell Dev Biol* 2020 ; 8 : 8.

99. Brisse M, Ly H. Comparative structure and function analysis of the RIG-I-like receptors: RIG-I and MDA5. *Front Immunol* 2019 ; 10 : 1586.

100. Said EA, Tremblay N, Al-Balushi MS, Al-Jabri AA, Lamarre D. Viruses seen by our cells: the role of viral RNA sensors. *J Immunol Res* 2018 ; 2018 : 9480497.

101. Chang TH, Liao CL, Lin YL. Flavivirus induces interferon-beta gene expression through a pathway involving RIG-I-dependent IRF-3 and PI3K-dependent NF-kappaB activation. *Microbes Infect* 2006 ; 8(1) : 157-71.

102. Fredericksen BL, Keller BC, Fornek J, Katze MG, Gale Jr. M. Establishment and maintenance of the innate antiviral response to West Nile Virus involves both RIG-I and MDA5 signaling through IPS-1. *J Virol* 2008 ; 82(2) : 609-16.

103. Hamel R, Dejarnac O, Wichit S, *et al*. Biology of Zika virus infection in human skin cells. *J Virol* 2015 ; 89(17) : 8880-96.

104. Bowen JR, Quicke KM, Maddur MS, *et al*. Zika virus antagonizes type I interferon responses during infection of human dendritic cells. *PLoS Pathog* 2017 ; 13(2) : e1006164.

105. Mukherjee S, Ghosh S, Nazmi A, Basu A. RIG-I knockdown impedes neurogenesis in a murine model of Japanese encephalitis. *Cell Biol Int* 2015 ; 39(2) : 224-9.

106. Nazmi A, Dutta K, Basu A. RIG-I mediates innate immune response in mouse neurons following Japanese encephalitis virus infection. *PLoS One* 2011 ; 6(6) : e21761.

107. Kato H, Takeuchi O, Sato S, *et al*. Differential roles of MDA5 and RIG-I helicases in the recognition of RNA viruses. *Nature* 2006 ; 441(7089) : 101-5.

108. Jiang R, Ye J, Zhu B, Song Y, Chen H, Cao S. Roles of TLR3 and RIG-I in mediating the inflammatory response in mouse microglia following Japanese encephalitis virus infection. *J Immunol Res* 2014 ; 2014 : 787023.

109. Beauclair G, Streicher F, Chazal M, *et al*. Retinoic acid inducible gene I and protein kinase R, but not stress granules, mediate the proinflammatory response to yellow fever virus. *J Virol* 2020 ; 94(22) : e00403-420.

110. Saito T, Owen DM, Jiang F, Marcotrigiano J, Gale Jr. M. Innate immunity induced by composition-dependent RIG-I recognition of hepatitis C virus RNA. *Nature* 2008 ; 454(7203) : 523-7.

111. Qin CF, Zhao H, Liu ZY, *et al*. Retinoic acid inducible gene-I and melanoma differentiation-associated gene 5 are induced but not essential for dengue virus induced type I interferon response. *Mol Biol Rep* 2011 ; 38(6) : 3867-73.

112. Gack MU, Shin YC, Joo CH, *et al*. TRIM25 RING-finger E3 ubiquitin ligase is essential for RIG-I-mediated antiviral activity. *Nature* 2007 ; 446(7138) : 916-20.

113. Finol E, Ooi EE. Evolution of subgenomic RNA shapes dengue virus adaptation and epidemiological fitness. *iScience* 2019 ; 16 : 94-105.

114. Pijlman GP, Funk A, Kondratieva N, *et al*. A highly structured, nuclease-resistant, noncoding RNA produced by flaviviruses is required for pathogenicity. *Cell Host Microbe* 2008 ; 4(6) : 579-91.

115. Manokaran G, Finol E, Wang C, *et al*. Dengue subgenomic RNA binds TRIM25 to inhibit interferon expression for epidemiological fitness. *Science* 2015 ; 350(6257) : 217-21.

116. Riedl W, Acharya D, Lee JH, *et al*. Zika virus NS3 mimics a cellular 14-3-3-binding motif to antagonize RIG-I- and MDA5-mediated innate immunity. *Cell Host Microbe* 2019 ; 26(4) : 493-503 e6.

117. Chan YK, Gack MU. A phosphomimetic-based mechanism of dengue virus to antagonize innate immunity. *Nat Immunol* 2016 ; 17(5) : 523-30.

118. Liu HM, Loo YM, Horner SM, Zornetzer GA, Katze MG, Gale Jr. M. The mitochondrial targeting chaperone 14-3-3epsilon regulates a RIG-I translocon that mediates membrane association and innate antiviral immunity. *Cell Host Microbe* 2012 ; 11(5) : 528-37.

119. Sumpter Jr. R, Loo YM, Foy E, *et al*. Regulating intracellular antiviral defense and permissiveness to hepatitis C virus RNA replication through a cellular RNA helicase, RIG-I. *J Virol* 2005 ; 79(5) : 2689-99.

120. Bellecave P, Sarasin-Filipowicz M, Donze O, *et al*. Cleavage of mitochondrial antiviral signaling protein in the liver of patients with chronic hepatitis C correlates with a reduced activation of the endogenous interferon system. *Hepatology* 2010 ; 51(4) : 1127-36.

121. Jouan L, Chatel-Chaix L, Melancon P, *et al*. Targeted impairment of innate antiviral responses in the liver of chronic hepatitis C patients. *J Hepatol* 2012 ; 56(1) : 70-7.

122. Jouan L, Melancon P, Rodrigue-Gervais IG, *et al*. Distinct antiviral signaling pathways in primary human hepatocytes and their differential disruption by HCV NS3 protease. *J Hepatol* 2010 ; 52(2) : 167-75.

123. Castanier C, Garcin D, Vazquez A, Arnoult D. Mitochondrial dynamics regulate the RIG-I-like receptor antiviral pathway. *EMBO Rep* 2010 ; 11(2) : 133-8.

124. Jacobs JL, Coyne CB. Mechanisms of MAVS regulation at the mitochondrial membrane. *J Mol Biol* 2013 ; 425(24) : 5009-19.

125. Horner SM, Liu HM, Park HS, Briley J, Gale Jr. M. Mitochondrial-associated endoplasmic reticulum membranes (MAM) form innate immune synapses and are targeted by hepatitis C virus. *Proc Natl Acad Sci U S A* 2011 ; 108(35) : 14590-5.

126. Patil V, Cuenin C, Chung F, *et al*. Human mitochondrial DNA is extensively methylated in a non-CpG context. *Nucleic Acids Res* 2019 ; 47(19) : 10072-85.

127. Zhang Q, Raoof M, Chen Y, *et al*. Circulating mitochondrial DAMPs cause inflammatory responses to injury. *Nature* 2010 ; 464(7285) : 104-7.

128. Guo Y, Gu R, Gan D, Hu F, Li G, Xu G. Mitochondrial DNA drives noncanonical inflammation activation *via* cGAS-STING signaling pathway in retinal microvascular endothelial cells. *Cell Commun Signal* 2020 ; 18(1) : 172.

129. Cai X, Chiu YH, Chen ZJ. The cGAS-cGAMP-STING pathway of cytosolic DNA sensing and signaling. *Mol Cell* 2014 ; 54(2) : 289-96.

130. Zhang JZ, Liu Z, Liu J, Ren JX, Sun TS. Mitochondrial DNA induces inflammation and increases TLR9/NF-kappaB expression in lung tissue. *Int J Mol Med* 2014 ; 33(4) : 817-24.

131. Lai JH, Wang MY, Huang CY, *et al*. Infection with the dengue RNA virus activates TLR9 signaling in human dendritic cells. *EMBO Rep* 2018 ; 19(8) : e46182.

132. Sun B, Sundstrom KB, Chew JJ, *et al*. Dengue virus activates cGAS through the release of mitochondrial DNA. *Sci Rep* 2017 ; 7(1) : 3594.

133. Aguirre S, Luthra P, Sanchez-Aparicio MT, *et al*. Dengue virus NS2B protein targets cGAS for degradation and prevents mitochondrial DNA sensing during infection. *Nat Microbiol* 2017 ; 2 : 17037.

134. Zheng Y, Liu Q, Wu Y, *et al*. Zika virus elicits inflammation to evade antiviral response by cleaving cGAS via NS1-caspase-1 axis. *EMBO J* 2018 ; 37(18) : e99347.

135. Ding Q, Gaska JM, Douam F, *et al*. Species-specific disruption of STING-dependent antiviral cellular defenses by the Zika virus NS2B3 protease. *Proc Natl Acad Sci U S A* 2018 ; 115(27) : E6310-8.

136. Yi G, Wen Y, Shu C, *et al*. Hepatitis C virus NS4B can suppress STING accumulation to evade innate immune responses. *J Virol* 2016 ; 90(1) : 254-65.

137. Moretton A, Morel F, Macao B, *et al*. Selective mitochondrial DNA degradation following double-strand breaks. *PLoS One* 2017 ; 12(4) : e0176795.

138. Tigano M, Vargas DC, Tremblay-Belzile S, Fu Y, Sfeir A. Nuclear sensing of breaks in mitochondrial DNA enhances immune surveillance. *Nature* 2021 ; 591(7850) : 477-81.

139. Elmore S. Apoptosis: a review of programmed cell death. *Toxicol Pathol* 2007 ; 35(4) : 495-516.

140. Ghosh Roy S, Sadigh B, Datan E, Lockshin RA, Zakeri Z. Regulation of cell survival and death during Flavivirus infections. *World J Biol Chem* 2014 ; 5(2) : 93-105.

141. Souza BS, Sampaio GL, Pereira CS, *et al*. Zika virus infection induces mitosis abnormalities and apoptotic cell death of human neural progenitor cells. *Sci Rep* 2016 ; 6 : 39775.

142. Li C, Xu D, Ye Q, *et al*. Zika virus disrupts neural progenitor development and leads to microcephaly in mice. *Cell Stem Cell* 2016 ; 19(5) : 672.

143. Ghouzzi VE, Bianchi FT, Molineris I, *et al*. ZIKA virus elicits P53 activation and genotoxic stress in human neural progenitors similar to mutations involved in severe forms of genetic microcephaly. *Cell Death Dis* 2016 ; 7(10) : e2440.

144. Liu Y, Liu H, Zou J, Zhang B, Yuan Z. Dengue virus subgenomic RNA induces apoptosis through the Bcl-2-mediated PI3k/Akt signaling pathway. *Virology* 2014 ; 448 : 15-25.

145. Fischer R, Baumert T, Blum HE. Hepatitis C virus infection and apoptosis. *World J Gastroenterol* 2007 ; 13(36) : 4865-72.

146. Deng L, Adachi T, Kitayama K, *et al*. Hepatitis C virus infection induces apoptosis through a Bax-triggered, mitochondrion-mediated, caspase 3-dependent pathway. *J Virol* 2008 ; 82(21) : 10375-85.

147. Catteau A, Kalinina O, Wagner MC, Deubel V, Courageot MP, Despres P. Dengue virus M protein contains a proapoptotic sequence referred to as ApoptoM. *J Gen Virol* 2003 ; 84(Pt 10) : 2781-93.

148. Bhuvanakantham R, Cheong YK, Ng ML. West Nile virus capsid protein interaction with importin and HDM2 protein is regulated by protein kinase C-mediated phosphorylation. *Microbes Infect* 2010 ; 12(8-9) : 615-25.

149. Okamoto T, Suzuki T, Kusakabe S, *et al*. Regulation of apoptosis during flavivirus infection. *Viruses* 2017 ; 9(9) : 243.

150. Hemmings BA, Restuccia DF. PI3K-PKB/Akt pathway. *Cold Spring Harb Perspect Biol* 2012 ; 4(9) : a011189.

151. Lee CJ, Liao CL, Lin YL. Flavivirus activates phosphatidylinositol 3-kinase signaling to block caspase-dependent apoptotic cell death at the early stage of virus infection. *J Virol* 2005 ; 79(13) : 8388-99.

152. Urbanowski MD, Hobman TC. The West Nile virus capsid protein blocks apoptosis through a phosphatidylinositol 3-kinase-dependent mechanism. *J Virol* 2013 ; 87(2) : 872-81.

153. Turpin J, Frumence E, Despres P, Viranaicken W, Krejbich-Trotot P. The Zika virus delays cell death through the anti-apoptotic Bcl-2 family proteins. *Cells* 2019 ; 8(11) : 1338.

154. He Y, Nakao H, Tan SL, *et al*. Subversion of cell signaling pathways by hepatitis C virus nonstructural 5A protein *via* interaction with Grb2 and P85 phosphatidylinositol 3-kinase. *J Virol* 2002 ; 76(18) : 9207-17.

155. Montessuit S, Somasekharan SP, Terrones O, *et al*. Membrane remodeling induced by the dynamin-related protein Drp1 stimulates Bax oligomerization. *Cell* 2010 ; 142(6) : 889-901.

156. Oettinghaus B, D'Alonzo D, Barbieri E, *et al*. DRP1-dependent apoptotic mitochondrial fission occurs independently of BAX, BAK and APAF1 to amplify cell death by BID and oxidative stress. *Biochim Biophys Acta* 2016 ; 1857(8) : 1267-76.

157. Park JH, Ko J, Hwang J, Koh HC. Dynamin-related protein 1 mediates mitochondria-dependent apoptosis in chlorpyrifos-treated SH-SY5Y cells. *Neurotoxicology* 2015 ; 51 : 145-57.

158. Sheridan C, Martin SJ. Mitochondrial fission/fusion dynamics and apoptosis. *Mitochondrion* 2010 ; 10(6) : 640-8.

159. Liesa M, Palacin M, Zorzano A. Mitochondrial dynamics in mammalian health and disease. *Physiol Rev* 2009 ; 89(3) : 799-845.

160. Suen DF, Norris KL, Youle RJ. Mitochondrial dynamics and apoptosis. *Genes Dev* 2008 ; 22(12) : 1577-90.

161. Frank S, Gaume B, Bergmann-Leitner ES, *et al*. The role of dynamin-related protein 1, a mediator of mitochondrial fission, in apoptosis. *Dev Cell* 2001 ; 1(4) : 515-25.

162. Breckenridge DG, Stojanovic M, Marcellus RC, Shore GC. Caspase cleavage product of BAP31 induces mitochondrial fission through endoplasmic reticulum calcium signals, enhancing cytochrome c release to the cytosol. *J Cell Biol* 2003 ; 160(7) : 1115-27.

163. Lee YJ, Jeong SY, Karbowski M, Smith CL, Youle RJ. Roles of the mammalian mitochondrial fission and fusion mediators Fis1, Drp1 and Opa1 in apoptosis. *Mol Biol Cell* 2004 ; 15(11) : 5001-11.

164. Slonchak A, Hugo LE, Freney ME, *et al*. Zika virus noncoding RNA suppresses apoptosis and is required for virus transmission by mosquitoes. *Nat Commun* 2020 ; 11(1) : 2205.

165. Choi SY, Gonzalvez F, Jenkins GM, *et al*. Cardiolipin deficiency releases cytochrome c from the inner mitochondrial membrane and accelerates stimuli-elicited apoptosis. *Cell Death Differ* 2007 ; 14(3) : 597-606.

166. Kagan VE, Tyurin VA, Jiang J, *et al*. Cytochrome c acts as a cardiolipin oxygenase required for release of proapoptotic factors. *Nat Chem Biol* 2005 ; 1(4) : 223-32.

167. Ott M, Robertson JD, Gogvadze V, Zhivotovsky B, Orrenius S. Cytochrome c release from mitochondria proceeds by a two-step process. *Proc Natl Acad Sci U S A* 2002 ; 99(3) : 1259-63.

168. Bellot G, Garcia-Medina R, Gounon P, *et al*. Hypoxia-induced autophagy is mediated through hypoxia-inducible factor induction of BNIP3 and BNIP3L *via* their BH3 domains. *Mol Cell Biol* 2009 ; 29(10) : 2570-81.

169. Zhang H, Bosch-Marce M, Shimoda LA, *et al*. Mitochondrial autophagy is an HIF-1-dependent adaptive metabolic response to hypoxia. *J Biol Chem* 2008 ; 283(16) : 10892-903.

170. Narendra D, Tanaka A, Suen DF, Youle RJ. Parkin is recruited selectively to impaired mitochondria and promotes their autophagy. *J Cell Biol* 2008 ; 183(5) : 795-803.

171. Matsuda N, Sato S, Shiba K, *et al*. PINK1 stabilized by mitochondrial depolarization recruits Parkin to damaged mitochondria and activates latent Parkin for mitophagy. *J Cell Biol* 2010 ; 189(2) : 211-21.

172. Xiao B, Goh JY, Xiao L, Xian H, Lim KL, Liou YC. Reactive oxygen species trigger Parkin/PINK1 pathway-dependent mitophagy by inducing mitochondrial recruitment of Parkin. *J Biol Chem* 2017 ; 292(40) : 16697-708.

173. Xiao B, Deng X, Lim GGY, *et al*. Superoxide drives progression of Parkin/PINK1-dependent mitophagy following translocation of Parkin to mitochondria. *Cell Death Dis* 2017 ; 8(10) : e3097.

174. Mizushima N. A brief history of autophagy from cell biology to physiology and disease. *Nat Cell Biol* 2018 ; 20(5) : 521-7.

175. Galluzzi L, Baehrecke EH, Ballabio A, *et al*. Molecular definitions of autophagy and related processes. *EMBO J* 2017 ; 36(13) : 1811-36.

176. Kroemer G, Marino G, Levine B. Autophagy and the integrated stress response. *Mol Cell* 2010 ; 40(2) : 280-93.

177. Jin SM, Lazarou M, Wang C, Kane LA, Narendra DP, Youle RJ. Mitochondrial membrane potential regulates PINK1 import and proteolytic destabilization by PARL. *J Cell Biol* 2010 ; 191(5) : 933-42.

178. Meissner C, Lorenz H, Weihofen A, Selkoe DJ, Lemberg MK. The mitochondrial intramembrane protease PARL cleaves human Pink1 to regulate Pink1 trafficking. *J Neurochem* 2011 ; 117(5) : 856-67.

179. Lazarou M, Sliter DA, Kane LA, *et al*. The ubiquitin kinase PINK1 recruits autophagy receptors to induce mitophagy. *Nature* 2015 ; 524(7565) : 309-14.

180. Paul P, Munz C. Autophagy and mammalian viruses: roles in immune response, viral replication, and beyond. *Adv Virus Res* 2016 ; 95 : 149-95.

181. Ponia SS, Robertson SJ, McNally KL, *et al*. Mitophagy antagonism by Zika virus reveals Ajuba as a regulator of PINK1-Parkin signaling, PKR-dependent inflammation, and viral invasion of tissues. *Cell Rep* 2021 ; 37 (4) : 109888. doi: 10.1016/j.celrep.2021.109888.

182. Wu C, Yao W, Kai W, *et al*. Mitochondrial fusion machinery specifically involved in energy deprivation-induced autophagy. *Front Cell Dev Biol* 2020 ; 8 : 221.

183. Chu CT, Ji J, Dagda RK, *et al*. Cardiolipin externalization to the outer mitochondrial membrane acts as an elimination signal for mitophagy in neuronal cells. *Nat Cell Biol* 2013 ; 15(10) : 1197-205.

184. von Stockum S, Marchesan E, Ziviani E. Mitochondrial quality control beyond PINK1/Parkin. *Oncotarget* 2018 ; 9(16) : 12550-1.

185. Fu M, St-Pierre P, Shankar J, Wang PT, Joshi B, Nabi IR. Regulation of mitophagy by the Gp78 E3 ubiquitin ligase. *Mol Biol Cell* 2013 ; 24(8) : 1153-62.

186. Szargel R, Shani V, Abd Elghani F, *et al*. The PINK1, synphilin-1 and SIAH-1 complex constitutes a novel mitophagy pathway. *Hum Mol Genet* 2016 ; 25(16) : 3476-90.

10 ANNEXE IV

vaccines

MDPI

Review

The Interplay between Dengue Virus and the Human Innate Immune System: A Game of Hide and Seek

Nicolas Tremblay, Wesley Freppel, Aïssatou Aïcha Sow and Laurent Chatel-Chaix *

Institut national de la recherche scientifique, Centre Armand-Frappier Santé Biotechnologie, Laval, QC H7V 1B4, Canada; Nicolas.Tremblay@iaf.inrs.ca (N.T.); Wesley.Freppel@iaf.inrs.ca (W.F.); Aicha.Sow@iaf.inrs.ca (A.A.S.)

* Correspondence: laurent.chatel-chaix@iaf.inrs.ca

Received: 31 July 2019; Accepted: 8 October 2019; Published: 10 October 2019

check for updates

Abstract: With 40% of the world population at risk, infections with dengue virus (DENV) constitute a serious threat to public health. While there is no antiviral therapy available against this potentially lethal disease, the efficacy of the only approved vaccine is not optimal and its safety has been recently questioned. In order to develop better vaccines based on attenuated and/or chimeric viruses, one must consider how the human immune system is engaged during DENV infection. The activation of the innate immunity through the detection of viruses by cellular sensors is the first line of defence against those pathogens. This triggers a cascade of events which establishes an antiviral state at the cell level and leads to a global immunological response. However, DENV has evolved to interfere with the innate immune signalling at multiple levels, hence dampening antiviral responses and favouring viral replication and dissemination. This review elaborates on the interplay between DENV and the innate immune system. A special focus is given on the viral countermeasure mechanisms reported over the last decade which should be taken into consideration during vaccine development.

Keywords: dengue virus; innate immunity; viral evasion; interferon; MAVS; RIG-I; mitochondria

1. Introduction

1.1. Disease Burden

Dengue is a neglected tropical disease caused by the dengue virus (DENV) that is transmitted to humans by *Aedes aegypti* or *Aedes albopictus* mosquitoes. In the recent years, it has become a public health concern, given that its global incidence has dramatically increased over the last 20 years and that no effective antiviral therapies are currently available. A dengue vaccine developed by Sanofi Pasteur, Dengvaxia, has been recently approved in over 20 countries around the globe. However, while the efficacy of this vaccine is not optimal for all DENV serotypes, its safety has been seriously questioned, especially for seronegative individuals. Epidemiological models estimate that about 390 million out of the 3.9 billion people living in endemic or epidemic areas contract the disease each year, making it the most prevalent arbovirus infection [1,2]. About 60 million infected individuals per year will develop symptomatic dengue fever, resulting in 10 to 20 thousand fatalities and 1.14 million Disability-Adjusted Life Years (DALY) [3]. This increase in the disease burden is not evenly distributed across the globe, with Latin America and the Caribbean ending up since 1990 with an increase in dengue-related DALY of about 250% or 4-fold above the global average and with Southeast Asia accounting for 596,000 DALY. This might be due to the simultaneous occurrence of multiple factors in these low-to-middle income emerging countries which affect the complex balance of DENV transmission dynamics, leading to a rapid endemic–epidemic cycle. For instance, this includes an optimal climate for *Aedes* life cycle, a rapid increase in population density in urban centres, and the concomitant circulation of all DENV

serotypes (1–4) in one given restricted geographic area [4,5]. While there is an unmet medical need regarding strategies against dengue, the incidence of this disease is expected to geographically expand in the future considering that the arthropod vector is colonizing northern European and American territories with temperate climates.

1.2. Clinical Manifestation

DENV infection is characterized by a mixed clinical presentation that ranges from an asymptomatic disease to a mild febrile prodrome all the way to a severe hemorrhagic fever and shock syndrome. All infected individuals, asymptomatic or not, can transmit DENV to *Aedes* mosquitoes during a blood meal, making it difficult to precisely estimate the actual size of the reservoir at any given time. DENV infection severity is classified according to the World Health Organization (WHO) 1997 and 2009 guidelines [6]. Dengue "without warning signs" (or dengue fever) regroups at-risk individuals with fever and at least two of the following signs and symptoms: nausea/vomiting, rash, headaches, eye pain, muscle aches, joint pain, leukopenia, or positivity at the tourniquet test. Dengue "with warning signs of severe infection" (or dengue hemorrhagic fever) includes in addition to the previous signs and symptoms abdominal pain, persistent vomiting, ascites, pleural effusion, mucosal bleeding, lethargy or restlessness, hepatomegaly, and an increase in hematocrit paired with rapid decrease in platelet count. Lastly, severe dengue (or dengue shock) occurs when the infection leads to severe plasma leakage, massive bleeding, and multiple organ failures. As of now, the therapeutic arsenal against DENV infection is fairly limited and only consists of supportive care and intravenous fluid therapy.

From a host–pathogen interaction point of view, it is interesting to note that, in the majority of DENV-infected individuals, viremia is controlled by the innate and adaptive immune systems within three to seven days, independently of the clinical manifestation [7]. However, in some cases, the infection is not properly handled and symptoms aggravate. A higher peak in viral titres seems to be predictive of disease severity [8,9]. While the pathophysiology behind severe dengue is not fully understood, it is accepted that dengue hemorrhagic fever and severe dengue result from a cytokine-mediated pathology (cytokine storm) that occurs because of the unbalanced production of various soluble and short-lived immune factors, such as TNF-α, VEGF-A, IL-6, IL-8, IL-10, CCL2, and CXCL10, that are produced by immune cells [10].

1.3. Dengue Virus Life Cycle

DENV is an enveloped, positive-stranded RNA virus and belongs to the *Flavivirus* genus within the Flaviviridae family. Flaviviruses also include genetically related and/or medically relevant arthropod-borne pathogens such as yellow fever virus (YFV), Zika virus (ZIKV), West Nile virus (WNV), and Japanese encephalitis virus (JEV). The enveloped virion is constituted of prM/M (precursor membrane/membrane) and E (envelope) structural proteins at the surface while C nucleocapsid protein surrounds the 11 kilobase-long non-segmented viral RNA genome (vRNA). Following virus entry into the target cell, vRNA is translated into one polyprotein, which is subsequently processed by host and viral proteases to generate the structural proteins C, prM, and E and the seven nonstructural (NS) proteins NS1, NS2A, NS2B, NS3, NS4A, NS4B, and NS5. NS proteins are responsible for vRNA replication that occurs exclusively in the cytoplasm of infected cells. This involves the specific enzymatic activity of several NS proteins. The NS5 RNA-dependent RNA polymerase is responsible for vRNA synthesis and possesses a methyltransferase activity which is absolutely required for vRNA 5′ capping and 2′-*O*-methylation. The processing of the DENV polyprotein involves the serine protease activity of the NS2B/NS3 complex (or NS2B3). NS3 is also essential for vRNA synthesis and capping through its helicase, NTPase, and triphosphatase activities. Assembled virions bud into the endoplasmic reticulum (ER) and are taken in charge by the cellular secretion machinery. In the Golgi apparatus, they undergo a final round of furin-mediated maturation and acquire infectivity before their release via exocytosis [11–13]. In order to create a cytoplasmic environment that can sustain an optimal life cycle, DENV, much like other flaviviruses, induces within the infected cell the biogenesis of specific

membranous replication organelles or replication factories (RF) with unique morphologies [14,15]. These RFs are formed by altering the curvature and composition of cellular endomembranes. They have been characterized as ER-derived ultrastructures that include (1) vesicle packets (VP) which result from membrane invaginations and contain the vRNA replication components; (2) convoluted membranes (CM) which are enriched in NS3, NS4A, and NS4B and of which the exact role(s) remain poorly defined; and (3) virus bags which contain immature virions organized in regular arrays [16–18]. In addition, DENV also manipulates the architecture of other organelles (such as mitochondria or peroxisomes) to modulate specific cellular functions, including innate immunity, in favour of replication (see below). While DENV is genetically simple with only 10 viral protein expressed, its life cycle relies on highly coordinated machineries that offer various points of intervention and research interests.

Following the entry of the virus inside the cell, it is rapidly sensed as a foreign "intruder" by the cell surveillance machinery, which triggers innate immunity. Strikingly, in response to these defence mechanisms, DENV has evolved to efficiently hide and mask its foreign molecular signatures, hence, avoiding the establishment of an antiviral environment that is detrimental for replication. In addition to these "cloak-and-dagger" operations, many viral proteins are able to directly hit the host antiviral machinery to shutdown innate immune signalling. Thus, antiviral immunity and DENV life cycle are dynamically interconnected events which balance each other; on one hand, the virus is trying to hijack the functions of the cellular machinery to its own benefit, while, on the other hand, the host factors are trying to control the viral infection while minimizing damages to cell homeostasis.

In this review, we elaborate on the interplay between DENV and innate immunity. More precisely, it brings into focus how DENV is detected inside an infected cell as well as how it can hide to avoid detection. A better understanding of how DENV circumvents and/or attenuates innate immunity can provide critical information for rational vaccine development.

2. Recognition of DENV by Pathogen Recognition Receptors

Innate antiviral immunity is the first line of defence against viral pathogens and participates in the establishment of the adaptive immune response. It engages complex networks of proteins that are able to detect, control, and defeat viral threats. Virus detection is done by specialized proteins called Pattern Recognition Receptors (PRR), which can recognize various virus-specific conserved molecular signatures known as Pathogen-Associated Molecular Patterns (PAMP). This detection signal is transduced by adaptor proteins to ultimately activate various transcription factors (e.g., Interferon Regulatory Factors (IRF) 3 and 7) that drive the production of antiviral proteins including type I and type III interferons (IFN) (Figure 1, upper panel) [19–22]. Once secreted, these cytokines activate the Janus Kinase-Signal Transducer and Activator of Transcription (JAK-STAT) pathway, leading to the production of many Interferon-Stimulated Genes (ISG), which contribute to sustained paracrine and autocrine antiviral responses. Briefly, following the binding of type I IFN to the Interferon-α/β Receptors (IFNAR) 1/2, signalling through the JAK-STAT pathway results in the amplification of the antiviral response via the activation of STAT1, STAT2, and IRF9, a transcription factor complex known as IFN-stimulated gene factor 3 (ISGF3) [23,24]. All in all, innate antiviral immunity is a crucial cellular system that provides a quick reaction force against a given pathogen infection and can eventually lead to the establishment of a more focused yet costly effector response [25,26].

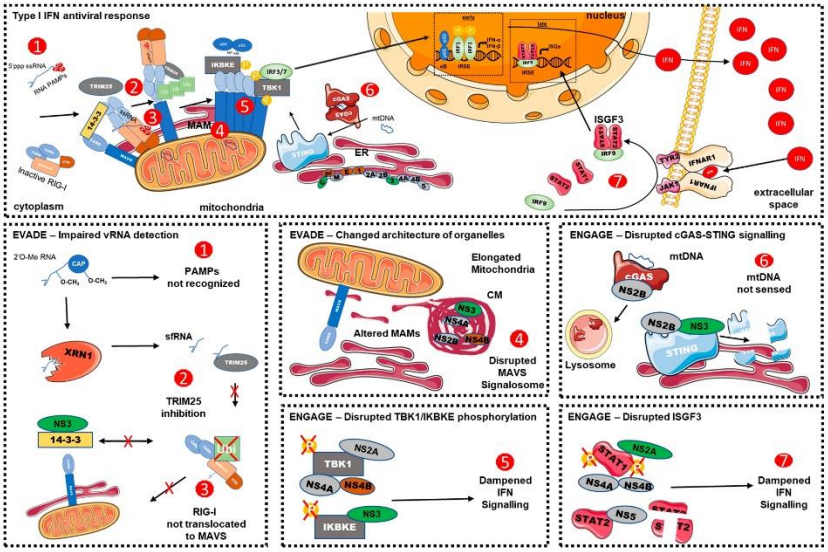

Figure 1. The sensing of Dengue virus by the innate immune responses and multiple evasion strategies to hinder the production of type I interferons (IFN).The upper panel shows the sensing of viral infection by RIG-I and cGAS. DENV-derived PAMPs are recognized by various pathogen recognition receptors like RIG-I. Upon recognition of pathogenic RNA, RIG-I is translocated to the mitochondria-associated MAVS adaptor protein with the help of the 14-3-3 and TRIM25 proteins. This induces the formation of MAVS aggregates that serve as an immune signalosome to activate through phosphorylation transcription factors IRF3 and NF-κB. In turn, these transcription factors translocate to the nucleus and elicit the transactivation of type I IFN. Once produced, type I IFN is secreted into the extracellular space and activates, in paracrine and autocrine fashions, the JAK-STAT pathway, leading to the amplification of the antiviral response via the activation of STAT1, STAT2, and IRF9, a transcription factor complex known as ISGF3. Infection also leads to mitochondrial stress and the release of mtDNA into the cytosol. mtDNA is recognized by cGAS, which activates STING, leading to the activation of IRF3/NF-κB and IFN production. DENV has developed various countermeasures to evade and/or engage the RLR and cGAS/STING pathways and to hinder innate immune signalling. These evasion mechanisms include (**1**) posttranscriptional modification of vRNA; (**2**) inhibition of 14-3-3ε or TRIM25 to hinder RIG-I activation; (**3**) MAVS aggregation; (**4**) alterations in endomembrane architecture to disrupt the MAVS signalosome; (**5**) the inhibition of TBK1 and IKBKE kinase activation, preventing the activation of transcription factors like IRF3; (**6**) the disruption of cGAS/STING signalling; and (**7**) the dampening of ISGF3 complex activation that is required for late innate antiviral responses.

2.1. DENV vRNA-Recognition

The RIG-I-Like Receptor (RLR) pathway has been classically studied for its role in the detection of viral ribonucleic acids and involves Retinoic Acid-Inducible gene I (RIG-I or DDX58), Melanoma Differentiation-Associated protein 5 (MDA5), and Laboratory of Genetics and Physiology 2 (LGP2/DHX58) as cytosolic sensors of an infection. They are ubiquitously expressed and are able to sense specific viral RNA moieties such as short uncapped 5′ triphosphorylated single-stranded (ss) RNA, short double-stranded (ds) RNA, U/A-rich 3′ regions of viral RNA, or long dsRNA [27]. Upon binding to vRNA, RIG-I and MDA5 are activated and translocated to the surface of the mitochondria where they interact with an adaptor protein, Mitochondrial Antiviral-Signalling Protein (MAVS), via their

respective caspase activation and recruitment domains (CARD) (Figure 1, upper panel). This triggers MAVS oligomerization and the formation of prion-like structures required to transduce the signal to downstream effector proteins. This signalling platform, often called MAVS signalosome is believed to bring together to the mitochondrial surface both upstream PRRs and downstream regulatory subunits (TRAF2, TRAF5, TRAF6, and NEMO) and protein kinases (TBK1 and IKBKE, also known as IKKε). Once activated, this signalosome orchestrates the phosphorylation of the transcription factors IRF3 and NF-κB, resulting in their nuclear translocation and the induction of type 1 IFN [28–34]. Remarkably, the activity of the MAVS regulome is tightly regulated by the morphodynamics of mitochondria as well as their contacts with the ER (see below) [35–38]. To sum up, mitochondria outer membrane is the scaffold of RLR signalling and, thus, plays an essential role in the initiation, the propagation, and the amplification of innate immunity against RNA viruses.

To date, there are several lines of evidence suggesting that that DENV is preferentially and directly sensed by the RLR pathway. An early study using RIG-I dominant-negative mutants showed that RIG-I is required to trigger IRF-3-dependent antiviral immunity against DENV in A549 lung cancer cells [39]. This observation was then recapitulated in various cell types (Huh7 hepatocarcinoma cells, endothelial cells, and primary monocytes) and experimental settings [17,40–42]. Combining affinity purification and next-generation sequencing, Chazal and colleagues recently showed that RIG-I is able to recognize 5′-ppp uncapped DENV vRNA, suggesting that detection of DENV nucleic acids occurs before the 5′-end maturation by capping is completed and that vRNA is afterwards hidden from PRR [43]. In stark contrast, the putative role of MDA5 in the detection of DENV nucleic acids remains unclear. Several groups have shown that silencing or interfering with MDA5 results in increased viral susceptibility and an altered innate immune response, but no clear mechanism of direct vRNA sensing has emerged despite this body of evidence. This might be due to the fact that all of these studies addressed the role of MDA5 in the early detection of vRNA. Strikingly, in the case of WNV, RIG-I and MDA5 have nonredundant roles at various stages of infection *in vitro* and *in vivo* [44]. Indeed, it was shown that MDA5 signalling to rely on the presence of WNV RNA PAMPs processed by cellular factors to become immunostimulatory but not on virion RNA that is initially uncoated upon viral entry. Overall, these studies support the view that RIG-I is a major player of the early detection of DENV RNA and of the initiation of the immune response. These further highlight that additional work is required to define the role of MDA5 during DENV infection.

Toll-like receptors (TLR) constitute another important family of PRR. They are located at the plasma membrane or within late endosomes and can sense a variety of PAMPs such as bacterial lipopolysaccharide, dsDNA, ssRNA, and dsRNA [45,46]. For DENV infection, TLR3 can recognize vRNA and its stimulation or overexpression dampens DENV replication *in cellulo* [47,48]. Both TLR and RLR pathways converge to MAVS and stimulate IRF3, NF-κB, and type I IFN production. While it remains unknown whether DENV stimulates TLR3 in vivo, a study in rhesus macaques showed that the combined agonist-mediated stimulation of both TLR3 and TLR7/8 following DENV infection resulted in a decrease in viral replication and enhanced pro-inflammatory responses [49]. This highlights the antiviral potential of the TLR3 pathway against DENV *in vivo*.

2.2. The DNA Sensing Pathway and DENV Infection

Converging to the same downstream effector molecules as the RLR pathway, that is, the TBK1/IRF3/IFN-β axis, the foreign DNA-sensing pathway relies on various intracellular DNA sensors, such as cyclic GMP-AMP Synthase (cGAS), which detect dsDNA danger signals from self or pathogen [50]. Upon binding, cGAS produces the second messenger cyclic GMP-AMP (cGAMP), which in turn activates Stimulator of Interferon Genes (STING). The engagement of the STING/cGAS pathway leads to the stimulation of TBK1 and ultimately to the production of type I IFN. Since its discovery, this pathway has been at the centre of many research interests in the fields of cancer, autoimmunity, inflammation, senescence, cell death, and viral infection, among others. Interestingly, while sensing DNA, the cGAS/STING pathway has been reported to be essential for the optimal innate

immune response against RNA viruses [51–53]. Not surprisingly, several viruses such as influenza virus, hepatitis C virus, and coronavirus [52,54–56] have developed targeted evasion mechanisms to interfere with this pathway. The involvement of cGAS and STING in the innate immune response against DENV has become evident over the last few years, with several reports showing that DENV actually modulates this pathway (see below) [54,57–59]. While it remains unclear how a DNA-binding protein, like cGAS, can detect viral RNA, it was recently suggested that the sensing of DENV infection rather occurs indirectly. Indeed, virus-induced mitochondrial stress leads to the leakage of mitochondrial DNA (mtDNA) into the cytosol. It is subsequently sensed by cGAS, which in turn activates the type I IFN response [60]. More recently, it was shown that following inflammasome activation, secreted Interleukin (IL)-1β can induce mtDNA release, leading to the stimulation of the cGAS pathway and IFN production [61]. Considering that DENV infection triggers the activation of the inflammasome in human platelets and macrophages [62,63], it is plausible that this indirectly contributes to the mtDNA-dependent induction of early innate immunity.

Lastly, the emerging concept of a cross talk between the RIG-I/MAVS and cGAS/STING pathways is surely interesting to understand DENV biology. Indeed, there is an accumulating literature that shows that the RLR pathway is able to potentiate the cGAS/STING pathway and vice versa during RNA virus infection [64]. This seems to occur through the physical connection between RIG, MAVS, and STING during viral infection [51,65,66], the coactivation of both pathways [52,53,67], or a transcriptional feedback loops [66,68,69]. For flaviviral infections, a study has shown that STING potentiates the RLR signalling via the assembly of a RIG-I/MAVS/STING complex following JEV nucleic acid recognition [66]. In addition, another study in mice has shown that cGAS is required for the optimal RLR-dependent IFN response against WNV. Indeed, cGAS mice had a higher viral load and lower ISG expression, resulting in a higher mortality when compared to wild-type controls [53]. Future studies will be required to assess the role of the cross talk between the RIG-I/MAVS and cGAS/STING during DENV infection.

More generally, it will be required to investigate the exact nature, role, and distribution of the immunomodulatory molecules and signalling adaptors that are produced and expressed as a result of the pathogenesis of DENV infection. This will ultimately provide mechanistic insights on the exact contribution of the cGAS/STING pathway during DENV infection.

3. Viral Countermeasures

3.1. Interference with RLR-Dependent Signalling

DENV RNA synthesis and capping are believed to occur within the VPs since the viral replication dsRNA intermediate localizes within this ER-derived ultrastructure as shown by imaging studies using immunogold labelling and electron microscopy [16]. This confined environment is most probably important not only to concentrate the metabolites and proteins required for replication but also to exclude potentially inhibitory host factors. Considering this, it is tempting to speculate that neo-synthesized uncapped DENV RNAs "hide" from RIG-I in VPs although this model remains to be experimentally validated.

The replicated DENV RNA molecule possesses several intrinsic features that allow its evasion from detection by the innate immune system. These sensing interference strategies rely on two specific modifications of vRNA: its 2′-*O*-methylation and its partial degradation by host nucleases (Figure 1, bottom left panel). In addition to its RNA polymerase function, DENV NS5 has a methyltransferase (MTase) activity that generates the 5′ 7-methyl-guanosine cap and also methylates the 2′-*O*H position on the first nucleotide, forming a type 1 cap (m7GpppNm) structure [70,71]. The 2′-*O*-methylated vRNAs mimic cellular mRNAs, thus evading the host immune system [72–76] (Figure 1). Surprisingly, this mechanism is not necessarily strictly dependent on the capping of the vRNA since internal 2′-*O*-methylation can occur on vRNA lacking the 5′ cap structure during infections with DENV and other flavivirus such as WNV [72]. The 2′-*O*-methylation has been shown to be important to avoid coronavirus infection recognition by MDA5 in mouse and human cells. Indeed, a DENV2

mutant deficient in the 2′-*O* MTase activity (NS5 E217A mutation) leads to an attenuated viral spread in IFN-competent cells [73,74]. Consistent with this, it was later shown that the replication of the 2′-*O*-MTase mutant is attenuated at the very early stages of the life cycle, i.e. during the first 16 h of infection. As shown by a transcriptome kinetic analysis, this resulted in an increase in ISG transcription at the early time points postinfection with an enrichment in PRR genes (RIG-I, MDA5, and IFIT1). Altogether, these studies strongly support that DENV 2′-*O*-methylation aims to hide viral nucleic acids from early recognition by RLRs [76]. Importantly, a 2′-*O*-MTase mutant DENV2 strain was identified as a vaccine candidate since immunization with it conferred protection against subsequent DENV infection in mice and rhesus macaques [75]. However, it was proposed that exacerbated immune response might be due rather to a 2′-*O*-methylation-mediated evasion of the antiviral action of specific ISGs that enact downstream RLR and IFN signalling (see below).

Another vRNA-related evasion mechanism relies on the partial degradation of vRNA by host factors, resulting in the generation of the subgenomic flavivirus RNA (sfRNA), a small noncoding RNA (Figure 1). sfRNAs are produced as byproducts of an incomplete degradation of flaviviral RNA due to unique secondary structures in the 3′ UTR that causes XRN1, a 5′–3′ exoribonuclease, to stall and cut the vRNA prematurely [77,78]. Produced by all tested flaviviruses, the accumulation of biologically active sfRNA can contribute to virus-induced cytopathic effects [78,79]; to hijack mRNA processing machinery [80,81]; to promote optimal viral replication [82]; and most relevant here, to help the virus to circumvent antiviral signalling [83–85]. Indeed, in the case of DENV, one study showed that DENV sfRNAs are able to inhibit TRIM25 deubiquitylation by USP15 [86]. This prevents the K63 polyubiquitylation of RIG-I, its dimerization via its CARD domains; and its subsequent interaction with downstream adaptor protein MAVS, resulting in hindered interferon signalling [31,87,88]. On the whole, vRNA methylation and degradation into sfRNA consist of two evolutionarily conserved flaviviral strategies to counteract innate antiviral immunity.

In addition to interfering with RLR sensing of vRNA, DENV has developed other evasion strategies to inhibit the signalling cascade following RLR activation. Several DENV proteins modulate the pathway both upstream and downstream from MAVS. Notably, DENV NS3, through a conserved phosphomimetic RxEP motif, is able to prevent RIG-I translocation to the mitochondria by sequestering 14-3-3ε [89] (Figure 1). 14-3-3ε is required for efficient RIG-I/TRIM25 association and subsequent recruitment to mitochondria and interaction with MAVS [90]. Importantly, viruses expressing a mutated NS3 unable to associate with 14-3-3ε elicited a stronger immune response and replicated less efficiently in immune-competent cells [89]. Moreover, DENV NS4A is able to bind to MAVS CARD domains and to effectively prevent RIG-I/MAVS interaction through an unknown mechanism [91].

In order to sustain and maintain the immune synapse, MAVS needs to be physically accessible and at the proper position on the surface of the mitochondria; otherwise, antiviral signalling and response may not be optimal. Targeting this aspect of RLR-dependent innate immune signalling, DENV is also able to change the architecture of mitochondria in terms of morphodynamics and contacts with the endoplasmic reticulum (Figure 1). First, mitochondria show an elongated morphology in DENV-infected cells and make contacts with DENV convoluted membranes [17,92]. Interestingly, mitochondrial morphodynamics were reported to modulate antiviral signalling [35–37]. The morphology of mitochondria relies on an equilibrium between their fusion and fission regulated by dynamin-like GTPases. Briefly, these key players are mitofusins (MFN1 and MFN2) and Optic Atrophy 1 (OPA1), which mediate fusion (leading to elongation), and Dynamin-Related Protein 1 (DRP1), which mediates mitochondrial fission [93]. DENV-induced mitochondria elongation was attributed to NS4B since its overexpression alone recapitulated the phenotype. Furthermore, an inhibition of the phosphorylation-dependent activation of DRP1 was observed in both infected and NS4B-expressing cells, thus favouring mitochondrial elongation over fission [17].

Second, DENV infection resulted in a drastic disruption of the contacts between mitochondria and the ER (ERMC) [17]. Interestingly, the residual Mitochondria-Associated Membranes (MAM) appeared to be connected to CMs, suggesting that the biogenesis of this DENV RF substructure was

responsible for ERMC disruption. Notably, MAMs are important for normal RLR signalling since they favour the tethering of MAVS required for optimal antiviral signalling [35–38]. This suggests that the alteration of the reticulo-mitochondrial interface by DENV would contribute to the dampening of RLR signalling. In strong support to this, upon enforced mitochondria elongation via DRP1 expression knockdown in DENV-infected Huh7 cells, RIG-I was barely recruited to the MAMs, correlating with a dampened type I and III IFN mRNA transcription and an increased viral replication. This highlights the functional interplay between mitochondria morphodynamics and contact with ER. In another study, Yu and colleagues showed that DENV NS2B3 protease cleaves MFN1 and MFN2 [94]. Interestingly, MFN1 overexpression-mediated hyperfusion of mitochondria in the perinuclear region resulted in a decreased viral replication. Moreover, independent expression knockdown of MFN1 or MFN2 led to different phenotypes in viral replication, IFN-β induction, and cell death, illustrating the divergent roles of mitofusins despite their similarity. This is consistent with the different assumed functions of MFN1 in docking and fusion of the mitochondria and of MFN2 in the stabilization of the interactions between mitochondria [95,96]. Furthermore, MFN2 localizes to MAMs and as an ER-resident protein tethers mitochondria to ER through homodimerization and heterotypic interactions with MFN1 [97]. This suggests that DENV might alter ERMCs by directly targeting MFN2 through NS2B3 protease activity without necessarily impacting on mitochondria fusion and elongation. Overall, these studies support the model that antiviral signalling is dependent on various spatiotemporal events and that alterations of the mitochondrial morphology and cytosolic interface regulate MAVS signalosome function. This concept of viral subversion of mitochondrial morphodynamics is not unique to DENV since related strategies have been observed for other viruses such as hepatitis B virus, hepatitis C virus, Severe acute respiratory syndrome-related coronavirus (SARS–CoV), and alphaherpesvirus [98–101].

In addition to ER and mitochondria, DENV impairs the morphology of another membranous organelle functionally linked to MAVS-related signalling. Indeed, DENV as well as WNV and ZIKV induce a loss of cellular peroxisomes [102,103], which contain MAVS at their surface and constitute a transduction platform for innate signalling [104–106]. Notably, the expression knockdown of the peroxin Pex19, which is essential for peroxisome biogenesis [107], led to a significant decrease in type III IFN gene transcription following the activation of RLR signalling with a synthetic dsRNA [102]. This highlights the importance of peroxisome integrity in innate immune signalling and the benefit for DENV of depleting them upon infection. Overall, these changes in cellular endomembrane morphology are believed to create a cytoplasmic microenvironment in which viral proteins are able to engage cellular host factors that are crucial to mount an adequate antiviral response.

Finally, downstream of MAVS, DENV is also able to evade RLR signalling by interfering with the activity of effector proteins (Figure 1). Indeed, NS2A, NS2B3, and NS4B are able to block IRF3 phosphorylation by interfering with serine kinase activity of TBK1 and IKBKE, which leads to a suboptimal type I IFN response [108,109].

All these evasion strategies are consistent with the idea that DENV physically targets the MAVS signalosome in its entirety when it brings together upstream and downstream factors to the cytosolic side of the mitochondria. Interestingly, several DENV proteins involved in this co-opting, namely NS2B3, NS4A, and NS4B, all interact and partly localize within CMs [16–18,110–113]. Furthermore, CMs make with elongated mitochondria and there is strong evidence that they originate from MAMs, an important compartment for MAVS-dependent signalling [17]. Altogether, this supports a model in which CMs constitute a "hijacking" unit, which targets the whole MAVS signalosome at multiple levels. Rather than directly regulating vRNA replication, this viral substructure would instead "shutoff" potentially antiviral responses to infection, including early innate immunity, hence creating a cytoplasmic environment favourable to viral replication. The close spatial relationship between CMs and mitochondria would help to "trap" host targets inside CMs or to concentrate them near viral proteins in order to very efficiently downregulate the MAVS signalosome and maximize viral evasion. Nevertheless, this model requires experimental challenging.

3.2. Interference with the cGAS/STING Pathway

DENV also has the capacity to directly interfere with IFN induction that is triggered by the activated cGAS/STING pathway as a result of the release of mtDNA into the cytoplasm following DENV infection [114] (Figure 1). Indeed, DENV NS2B marks cGAS for lysosomal degradation and DENV NS2B-NS3 protease cleaves STING to suppress type I IFN induction [54,58,114,115]. Interestingly, DENV NS2B3 cannot process either mouse or nonhuman primate STING orthologs, suggesting that this pathogen has evolved towards an optimal pathogenicity in its natural hosts [54,59]. Very recently, it has been reported that DRP1-mediated mitochondrial fission results in mitochondrial stress and the release of mtDNA in the cytosol [116]. Considering this, it will be interesting to investigate in the future whether DENV-induced mitochondrial elongation through DRP1 inhibition actually dampens not only RIG-I signal but also the activation of the STING/cGAS pathway and/or its cross talk with RLR signalling. In the same line of ideas, STING is a resident protein of MAMs [117], and the alteration of these structures during DENV infection might contribute to targeting STING to NS2B3-rich CMs for degradation or spatiotemporal sequestration.

3.3. Interference with the IFN Signalling

In addition to the primary virus sensing pathway, DENV is also able to target several components of the downstream interferon-induced JAK-STAT signalling cascade that normally leads to the sustained expression of various ISGs following the secretion of IFN-α and -β (Figure 1). Early *in vitro* assays demonstrated that DENV NS4B is able to prevent STAT1 activation by a mechanism conserved in WNV and YFV that is yet to be elucidated [118,119]. However, it can be rationalized that STAT1 inhibition most likely occurs either through prevention of its activation or by its dephosphorylation or by degradation of activated STAT1. On the matter of another STAT protein, DENV NS5 is able to bind STAT2 and to promote its E3 ubiquitin ligase UBR4-dependent degradation. This results in a drastic decrease of STAT2 basal expression level and, hence, to a hindered JAK-STAT signalling [120–122]. Interestingly, this STAT2-related evasion strategy is also conserved in other flaviviruses, such as ZIKV. Indeed, ZIKV is able to bind to STAT2 and to promote its proteasomal degradation but in an UBR4-independent manner [123,124].

3.4. Interference with Other Mechanisms

In addition to its role in STAT2 degradation, DENV NS5 protein is also able to interfere with ISG expression. First, both DENV and ZIKV NS5 selectively inhibit ISG expression by binding to and antagonizing the transcription factor PAF1C [125]. Second, DENV NS5 hijacks core components of the spliceosomal machinery, namely CD2BP2 and DDX23, resulting in an alteration of isoform abundance and stoichiometry of many antiviral factors such as RIG-I, ISG15, or IL-8, hence contributing to an environment favourable to viral replication [126]. At the posttranscriptional level, sfRNA has been shown to interfere with the translation of ISGs. Indeed, DENV sfRNA associates with the host RNA-binding proteins G3BP1, G3BP2, and CAPRIN1, which, as a result, are unable to stimulate as efficiently the translation of many ISGs such as PKR and IFITM2 for instance [127]. Consistently, sfRNA binding to these host factors protects DENV replication from IFN-β treatment. Interestingly, the 2′-*O*-methylation mechanism described above as a way to downregulate PRR early IFN response is also able to interfere with the functions of specific ISGs. Indeed, the replication of the NS5 E217A 2′-*O*-MTase DENV2 mutant is significantly more sensitive to IFN-β treatment than wt virus [75], demonstrating that this modification may contribute to immunity evasion downstream of PRR signalling. More specifically for DENV but also for WNV, poxvirus, coronavirus, and JEV, the 2′-*O*-methylation of vRNA cap enables the viral nucleic acids to be marked as "self-RNA" and to evade from the antiviral function of IFN-Induced Protein with Tetratricopeptide Repeat (IFIT) proteins [128–131]. Notably, IFIT1 was shown to associate with non-methylated RNAs with a higher affinity than the other IFITs. It was proposed that translation initiation factor eIF4E and IFIT1 compete for cap binding [129]. Hence,

IFIT1 senses virus infection through the binding to foreign RNAs lacking 2′-*O*-methyls and inhibits the translation of viral RNA via the displacement of eIF4E. Consistently, IFIT1 overexpression in HEK293-DC-SIGN cells significantly decreases DENV2 replication in contrast to other IFITs [75]. In the case of WNV, the pathogenesis of the E218A MTase mutant is greatly attenuated in wt mice. Very interestingly, intracranial infection of *Ifit1* knockout C57BL/6 mice with the E218A MTase mutant WNV restored lethality, highlighting the critical role of this IFIT in the sensing of the "2′-*O*-methyl-free" vRNA *in vivo* [128]. Considering the genetic and biological proximity with WNV, it is tantalizing to speculate that DENV RNA is able to evade IFIT antiviral activity *in vivo* by mimicking cellular mRNAs through the addition of 2′-*O*-methyls, one of the most common posttranscriptional modifications of RNA allowing vRNA to hide in plain sight among host mRNAs.

As explained above, DENV sfRNA targets innate immune signalling in human cells at multiple levels (i.e. RIG-I activation and ISG expression). Of significant interest, several recent studies have highlighted the important role of sfRNA in the dissemination of DENV among infected insects [81,132–134]. In fact, the DENV and YFV subgenomic RNAs are able to interfere with the *Aedes* mosquito innate system as well by targeting both Toll receptor and RNA interference (RNAi) pathways to favour optimal replication. In the mosquitoes, viral double-stranded RNA is processed into small siRNAs by RNase III DICER and is processed into viral siRNAs (vsiRNAs) by AGO2, which are able to target viral RNA for silencing [135,136]. This shows that sfRNA plays two distinct roles, albeit using the same cellular factors, in the evasion of the innate immune response in mammalian hosts or arthropod vectors. This concept of different roles of host factors between the mammalian hosts or arthropod vectors will most likely be explored in depth in the future considering that a recent system biology study identified more than 45 shared pathway interactions between DENV–human and DENV–mosquito interactomes in the context of innate immune evasion and viral pathogenesis [125].

4. Importance for Vaccine Development

Multiple tetravalent vaccine candidates are being developed. These include live-attenuated vaccines, whole virus inactivated vaccines, protein-based vaccines, chimeric vaccines, and mRNA-based and synthetic virus-like particle vaccines [137–142]. Among these vaccines, Dengvaxia (also called CYD-TDV), developed by Sanofi Pasteur, is the only one licensed for use in about 20 dengue-endemic countries in Asia, Latin America, and Oceania as well as in Europe. CYD-TDV is a tetravalent dengue chimeric live-attenuated vaccine which is based on the YFV 17D strain as a backbone. This vaccine is typically indicated for individuals aged from 9 to 45 years living in an endemic country and, hence, is not accessible to the population that is the most at risk to develop severe dengue-related symptoms. Unfortunately, the vaccine confers less protection against serotypes 1 and 2 than with serotypes 3 and 4 [143,144]. Importantly, CYD-TDV efficacy was higher than pooled estimates in seropositive individuals but extremely low for seronegative children with risks of severe complications due to the vaccine. As a probable consequence of this, a global vaccination campaign in schools of the Philippines has resulted in the death of many children and the suspension of the program by the Department of Health in late 2017 [145]. As such, a pre-vaccination screening of previous exposure is now recommended prior to vaccination [146]. Lastly, a study shows that the CYD-TDV-elicited memory response decreases over time, as measured by low antibody titres in blood samples 5 years following an initial three-dose vaccine regimen. This suggests that a booster dose might be needed for sustained long-term immunological protection [147].

The development of new dengue vaccines which are safe and highly efficacious against all serotypes faces many challenges, including some involving the interplay between the virus and the immune system. Seminal studies by Albert Sabin, dating from the WWII era [148], have demonstrated that volunteers exposed to DENV showed long-lived homotypic immunity but short-lived cross-protection against viruses of a different serotype. However, the mechanisms behind these observations are still not fully understood and prospective studies at the population level show that these conclusions cannot be generalized to inform rational vaccine design [149]. While a majority of DENV infections

go unnoticed, some infected individuals progress along the disease spectrum and develop dengue hemorrhagic fever or dengue shock. Although no consensus exists about the pathophysiology behind this progression, it is most likely due to host-specific factors related to the presence of preexisting immunity such as antibody-dependent enhancements (ADE) and immune-mediated cytokine storm related to the antigenic sin phenomenon that occurs even past the peak in viremia in symptomatic individuals [10,150]. Indeed, a second heterologous DENV infection is expected to elicit a strong memory recall of DENV-specific T and B cells that will produce an enhanced level of cytokines and neutralizing antibodies. However, this adaptive immune response might not lead to the control of viremia but rather quite the opposite, resulting in an antibody-dependent enhanced infection (virus opsonization and increased replication), mast cell activation (vascular permeability), and cellular cytotoxicity (cytokine storm) [151]. With this in mind, an effective antiviral therapy would need to be taken as a prophylactic treatment and would most likely be highly expensive given the number of individuals living in endemic areas. Thus, the only way to eradicate dengue worldwide would be to develop a safe, effective, and pan-serotypic vaccine that confers long-term sterilizing immunity.

In summary, while CYD-TDV constitutes a safe and efficacious tool in the therapeutic arsenal against DENV when properly administered, it is plagued by shortcomings and controversies and does not completely meet the need for an effective dengue vaccine, especially in seronegative individuals. Thus, many challenges remain to be addressed to develop the "holy grail" of DENV vaccines and a better understanding of host–pathogen interactions is warranted to set up new vaccinal strategies or relevant animal models. In the following section, we discuss three examples illustrating how innate immunity research can inform vaccine design.

4.1. DENVΔ30 Recombinant Dengue Virus

The DENVΔ30 is a live attenuated vaccine candidate that was engineered by deleting 30 nucleotides of the 3'UTR vRNA using reverse genetics and by subsequently creating modified dengue viruses for all four serotypes [152,153]. Proof-of-concept studies showed that, despite attenuation, the DENVΔ30 is highly immunogenic in both humans and rhesus monkeys for all tested serotypes and confers protection upon homologous rechallenge [153–161]. In addition, DENVΔ30 appears to be less virulent in mosquitoes, limiting the risk of transmission from a vaccinated human to the *Aedes* vector [162]. For long, the molecular mechanism conferring attenuation of this vaccine candidate was largely unknown. However, it was shown that DENV4Δ30-infected cells accumulated less sfRNA, resulting in an increased sensitivity to type I IFN [163]. Further studies will be required to assess if other evasion mechanisms are in play in DENVΔ30 attenuation to fully understand how this strain is able to create a balanced environment that is favourable to antigen presentation and cytokine production. However, given the reported roles of sfRNA in both IFN production and response (see above), it is likely that the attenuation of DENVΔ30 results from an increased innate immune response.

4.2. 2'-O-methyltransferase-Deficient Dengue Vaccine

As explained above, 2'-*O*-methylation is a modification that allows the vRNA to mimic cellular mRNAs and to evade the host innate immune system. Using reverse genetics, Züst and colleagues have generated DENV clones from serotypes 1 and 2 that harbour a single point mutation in the conserved KDKE motif of the NS5 methyltransferase catalytic site. These mutants (E216A for DENV1 or E217A for DENV2) are impaired in 2'-*O*-methylation but are still able to perform the N7-methylation of the cap. Importantly, they are more susceptible to IFN treatment or human IFIT1 overexpression than wild-type DENV, which is consistent with the idea that they are impaired in IFIT inhibition. Importantly, treatment of mice competent for T-cell responses with these viruses alone or in serotype combination conferred protection against a subsequent infection with a lethal mouse-adapted DENV strain. Remarkably, a single low dose of the DENV2 E217A mutant in monkeys was enough for a complete seroconversion and protection [75]. This approach was also applied to develop a JEV vaccine candidate. A E218A mutant JEV was attenuated and more sensitive to a type I IFN treatment

as well [164]. A single dose of this live attenuated vaccine was sufficient to elicit a strong humoral response that conferred protection and survival following heterologous rechallenge in BALB/c mice. Ongoing studies are now trying to implement this vaccine rational design towards the development of a tetravalent, non-chimeric vaccine with therapeutic relevance.

4.3. Immunocompetent Mouse Model for Denv Vaccine research

Vaccine development studies usually rely on large animal models during nonclinical and preclinical studies [165]. The use of small animal models such as mice usually requires genetic modifications that dampen their immune system in order to increase viral permissiveness and, thus, do not reflect the reality of an infection in the natural host with an intact immune response. In most of the cases, *in vivo* DENV studies classically involve immunodeficient mouse strains such as AG129 which do not express IFN-α/β and IFN-γ receptors. These mice are highly susceptible to DENV infection and generally die within two weeks after injection [166–168]. Following advancement of the knowledge about host–pathogen interactions and the advent of novel technologies (e.g., by CRISPR/Cas9 gene editing), a paradigm shift can be anticipated. As an example of this, using a gene knock-in approach and a mouse-adapted virus strain, Gorman and colleagues recently developed an immunocompetent transgenic mouse model of ZIVK infection by replacing the mouse STAT2 by the human STAT2 [169]. This genetic engineering was conceptually made possible thanks to previous studies which showed that ZIKV induces the degradation of human STAT2 but not of the mouse ortholog [123,124,170]. While it will be interesting to see if the use of humanized immunocompetent mouse model can be expanded to DENV studies, it definitely opens up many future research opportunities.

5. Conclusions and Perspectives

DENV research will most likely remain a challenging and exciting field in times to come. In recent years, DENV infection has taken a front seat in the realm of global health concerns as it spreads outside the Western Pacific region and is now threatening more than 4 billion individuals. With no effective antiviral therapies or prophylactic vaccine, DENV is expected to cause disease and to inflict harm that amounts to more than 1.14 million DALY. As extensively discussed in this review, DENV is well equipped to evade the innate antiviral immune system through various antagonizing functions of viral NS proteins and RNA. From being able to hide in plain sight due to the 2′-*O*-methylation of the viral genome and to the disruption of MAVS signalosome activity and of the IFN signalling, it can be acknowledged that, despite a simple viral genome organization, DENV pathogenesis relies on a complex network of host–pathogen interactions. It is conceivable that better understanding this complexity will contribute to solving the puzzle of dengue control and/or eradication. Indeed, the interplay between DENV and the immune system can lead to rational vaccine design by providing attractive targets for antigen and adjuvant development and by filling the gaps in knowledge regarding how the innate immune system can be harnessed to support a long-lasting protective immune response.

Author Contributions: Conceptualization and supervision: N.T. and L.C.-C.; original draft preparation: N.T., A.A.S. and W.F.; review and editing: N.T. and L.C.-C.

Funding: This work was supported by a postdoctoral scholarship to N.T. and a research scholarship to L.C.-C from Fonds de la Recherche du Québec-Santé. W.F. and A.A.S. salaries are funded by Institut National de la Recherche Scientifique and the Canadian Institutes of Health Research.

Acknowledgments: We are grateful to Karine Boulay (Université de Montréal, Canada) for critical reading of the manuscript and helpful comments.

Conflicts of Interest: The authors declare no conflict of interest. The funders had no role in the writing of the manuscript or in the decision to publish this review.

References

1. Bhatt, S.; Gething, P.W.; Brady, O.J.; Messina, J.P.; Farlow, A.W.; Moyes, C.L.; Drake, J.M.; Brownstein, J.S.; Hoen, A.G.; Sankoh, O.; et al. The global distribution and burden of dengue. *Nature* **2013**, *496*, 504–507. [CrossRef] [PubMed]
2. Brady, O.J.; Gething, P.W.; Bhatt, S.; Messina, J.P.; Brownstein, J.S.; Hoen, A.G.; Moyes, C.L.; Farlow, A.W.; Scott, T.W.; Hay, S.I. Refining the Global Spatial Limits of Dengue Virus Transmission by Evidence-Based Consensus. *PLoS Negl. Trop. Dis.* **2012**, *6*, e1760. [CrossRef] [PubMed]
3. Stanaway, J.D.; Shepard, D.S.; Undurraga, E.A.; Halasa, Y.A.; Coffeng, L.E.; Brady, O.J.; Hay, S.I.; Bedi, N.; Bensenor, I.M.; Castañeda-Orjuela, C.A.; et al. The global burden of dengue: An analysis from the Global Burden of Disease Study 2013. *Lancet Infect. Dis.* **2016**, *16*, 712–723. [PubMed]
4. Ramos-Castañeda, J.; Barreto Dos Santos, F.; Martínez-Vega, R.; Galvão de Araujo, J.M.; Joint, G.; Sarti, E. Dengue in Latin America: Systematic Review of Molecular Epidemiological Trends. *PLoS Negl. Trop. Dis.* **2017**, *11*, e0005224. [CrossRef] [PubMed]
5. San Martín, J.L.; Brathwaite, O.; Zambrano, B.; Solórzano, J.O.; Bouckenooghe, A.; Dayan, G.H.; Guzmán, M.G. The epidemiology of dengue in the americas over the last three decades: A worrisome reality. *Am. J. Trop. Med. Hyg.* **2010**, *82*, 128–135. [CrossRef] [PubMed]
6. World Health Organization. *Dengue: Guidelines for Diagnosis, Treatment, Prevention and Control*; World Health Organization: Geneva, Switzerland, 2009; ISBN 9789241547871.
7. Gubler, D.J.; Suharyono, W.; Tan, R.; Abidin, M.; Sie, A. Viraemia in patients with naturally acquired dengue infection. *Bull. World Health Organ.* **1981**, *59*, 623–630. [PubMed]
8. Gómez-Ochoa, S.A. Viremia en plasma como factor asociado a gravedad en la infección por el virus del dengue: Revisión sistemática de la literatura. *Revista Chilena de Infectología* **2018**, *35*, 176–183. [PubMed]
9. Vaughn, D.W.; Green, S.; Kalayanarooj, S.; Innis, B.L.; Nimmannitya, S.; Suntayakorn, S.; Endy, T.P.; Raengsakulrach, B.; Rothman, A.L.; Ennis, F.A.; et al. Dengue viremia titer, antibody response pattern, and virus serotype correlate with disease severity. *J. Infect. Dis.* **2000**, *181*, 2–9. [CrossRef] [PubMed]
10. Srikiatkhachorn, A.; Mathew, A.; Rothman, A.L. Immune-mediated cytokine storm and its role in severe dengue. *Semin. Immunopathol.* **2017**, *39*, 563–574. [CrossRef]
11. Apte-Sengupta, S.; Sirohi, D.; Kuhn, R.J. Coupling of replication and assembly in flaviviruses. *Curr. Opin. Virol.* **2014**, *9*, 134–142. [CrossRef]
12. Neufeldt, C.J.; Cortese, M.; Acosta, E.G.; Bartenschlager, R. Rewiring cellular networks by members of the Flaviviridae family. *Nat. Rev. Microbiol.* **2018**, *16*, 125–142. [CrossRef] [PubMed]
13. Mazeaud, C.; Freppel, W.; Chatel-Chaix, L. The Multiples Fates of the Flavivirus RNA Genome During Pathogenesis. *Front. Genet.* **2018**, *9*, 595. [CrossRef] [PubMed]
14. Paul, D.; Bartenschlager, R. Flaviviridae Replication Organelles: Oh, What a Tangled Web We Weave. *Annu. Rev. Virol.* **2015**, *2*, 289–310. [CrossRef] [PubMed]
15. Chatel-Chaix, L.; Bartenschlager, R. Dengue virus- and hepatitis C virus-induced replication and assembly compartments: The enemy inside–caught in the web. *J. Virol.* **2014**, *88*, 5907–5911. [CrossRef] [PubMed]
16. Welsch, S.; Miller, S.; Romero-Brey, I.; Merz, A.; Bleck, C.K.E.; Walther, P.; Fuller, S.D.; Antony, C.; Krijnse-Locker, J.; Bartenschlager, R. Composition and three-dimensional architecture of the dengue virus replication and assembly sites. *Cell Host Microbe* **2009**, *5*, 365–375. [CrossRef] [PubMed]
17. Chatel-Chaix, L.; Cortese, M.; Romero-Brey, I.; Bender, S.; Neufeldt, C.J.; Fischl, W.; Scaturro, P.; Schieber, N.; Schwab, Y.; Fischer, B.; et al. Dengue Virus Perturbs Mitochondrial Morphodynamics to Dampen Innate Immune Responses. *Cell Host Microbe* **2016**, *20*, 342–356. [CrossRef] [PubMed]
18. Miller, S.; Kastner, S.; Krijnse-Locker, J.; Bühler, S.; Bartenschlager, R. The non-structural protein 4A of dengue virus is an integral membrane protein inducing membrane alterations in a 2K-regulated manner. *J. Biol. Chem.* **2007**, *282*, 8873–8882. [CrossRef] [PubMed]
19. Yoneyama, M.; Suhara, W.; Fukuhara, Y.; Fukuda, M.; Nishida, E.; Fujita, T. Direct triggering of the type I interferon system by virus infection: Activation of a transcription factor complex containing IRF-3 and CBP/p300. *EMBO J.* **1998**, *17*, 1087–1095. [CrossRef]
20. Wathelet, M.G.; Lin, C.H.; Parekh, B.S.; Ronco, L.V.; Howley, P.M.; Maniatis, T. Virus infection induces the assembly of coordinately activated transcription factors on the IFN-beta enhancer in vivo. *Mol. Cell* **1998**, *1*, 507–518. [CrossRef]

21. Lin, R.; Heylbroeck, C.; Pitha, P.M.; Hiscott, J. Virus-dependent phosphorylation of the IRF-3 transcription factor regulates nuclear translocation, transactivation potential, and proteasome-mediated degradation. *Mol. Cell. Biol.* **1998**, *18*, 2986–2996. [CrossRef]
22. Yang, H.; Lin, C.H.; Ma, G.; Baffi, M.O.; Wathelet, M.G. Interferon regulatory factor-7 synergizes with other transcription factors through multiple interactions with p300/CBP coactivators. *J. Biol. Chem.* **2003**, *278*, 15495–15504. [CrossRef] [PubMed]
23. Darnell, J.E., Jr.; Kerr, I.M.; Stark, G.R. Jak-STAT pathways and transcriptional activation in response to IFNs and other extracellular signaling proteins. *Science* **1994**, *264*, 1415–1421. [CrossRef] [PubMed]
24. Kessler, D.S.; Veals, S.A.; Fu, X.Y.; Levy, D.E. Interferon-alpha regulates nuclear translocation and DNA-binding affinity of ISGF3, a multimeric transcriptional activator. *Genes Dev.* **1990**, *4*, 1753–1765. [CrossRef] [PubMed]
25. McDonald, D.R.; Levy, O. 3—Innate immunity. In *Clinical Immunology*, 4th ed.; Rich, R.R., Fleisher, T.A., Shearer, W.T., Schroeder, H.W., Frew, A.J., Weyand, C.M., Eds.; Content Repository Only: London, UK, 2013; pp. 35–46. ISBN 9780723436911.
26. Chow, K.T.; Gale, M., Jr.; Loo, Y.-M. RIG-I and Other RNA Sensors in Antiviral Immunity. *Annu. Rev. Immunol.* **2018**, *36*, 667–694. [CrossRef] [PubMed]
27. Said, E.A.; Tremblay, N.; Al-Balushi, M.S.; Al-Jabri, A.A.; Lamarre, D. Viruses Seen by Our Cells: The Role of Viral RNA Sensors. *J. Immunol. Res.* **2018**, *2018*, 9480497. [CrossRef] [PubMed]
28. Hou, F.; Sun, L.; Zheng, H.; Skaug, B.; Jiang, Q.-X.; Chen, Z.J. MAVS forms functional prion-like aggregates to activate and propagate antiviral innate immune response. *Cell* **2011**, *146*, 448–461. [CrossRef] [PubMed]
29. Kawai, T.; Takahashi, K.; Sato, S.; Coban, C.; Kumar, H.; Kato, H.; Ishii, K.J.; Takeuchi, O.; Akira, S. IPS-1, an adaptor triggering RIG-I- and Mda5-mediated type I interferon induction. *Nat. Immunol.* **2005**, *6*, 981–988. [CrossRef]
30. Meylan, E.; Curran, J.; Hofmann, K.; Moradpour, D.; Binder, M.; Bartenschlager, R.; Tschopp, J. Cardif is an adaptor protein in the RIG-I antiviral pathway and is targeted by hepatitis C virus. *Nature* **2005**, *437*, 1167–1172. [CrossRef]
31. Seth, R.B.; Sun, L.; Ea, C.-K.; Chen, Z.J. Identification and characterization of MAVS, a mitochondrial antiviral signaling protein that activates NF-kappaB and IRF 3. *Cell* **2005**, *122*, 669–682. [CrossRef]
32. Xu, H.; He, X.; Zheng, H.; Huang, L.J.; Hou, F.; Yu, Z.; de la Cruz, M.J.; Borkowski, B.; Zhang, X.; Chen, Z.J.; et al. Correction: Structural basis for the prion-like MAVS filaments in antiviral innate immunity. *Elife* **2015**, *4*. [CrossRef]
33. Xu, L.-G.; Wang, Y.-Y.; Han, K.-J.; Li, L.-Y.; Zhai, Z.; Shu, H.-B. VISA is an adapter protein required for virus-triggered IFN-beta signaling. *Mol. Cell* **2005**, *19*, 727–740. [CrossRef] [PubMed]
34. Liu, S.; Cai, X.; Wu, J.; Cong, Q.; Chen, X.; Li, T.; Du, F.; Ren, J.; Wu, Y.T.; Grishin, N.V.; et al. Phosphorylation of innate immune adaptor proteins MAVS, STING, and TRIF induces IRF3 activation. *Science* **2015**, *347*, aaa2630. [CrossRef] [PubMed]
35. Castanier, C.; Garcin, D.; Vazquez, A.; Arnoult, D. Mitochondrial dynamics regulate the RIG-I-like receptor antiviral pathway. *EMBO Rep.* **2010**, *11*, 133–138. [CrossRef] [PubMed]
36. Jacobs, J.L.; Coyne, C.B. Mechanisms of MAVS regulation at the mitochondrial membrane. *J. Mol. Biol.* **2013**, *425*, 5009–5019. [CrossRef]
37. Onoguchi, K.; Onomoto, K.; Takamatsu, S.; Jogi, M.; Takemura, A.; Morimoto, S.; Julkunen, I.; Namiki, H.; Yoneyama, M.; Fujita, T. Virus-Infection or 5′ppp-RNA Activates Antiviral Signal through Redistribution of IPS-1 Mediated by MFN1. *PLoS Pathog.* **2010**, *6*, e1001012. [CrossRef] [PubMed]
38. Horner, S.M.; Liu, H.M.; Park, H.S.; Briley, J.; Gale, M., Jr. Mitochondrial-associated endoplasmic reticulum membranes (MAM) form innate immune synapses and are targeted by hepatitis C virus. *Proc. Natl. Acad. Sci. USA* **2011**, *108*, 14590–14595. [CrossRef] [PubMed]
39. Chang, T.-H.; Liao, C.-L.; Lin, Y.-L. Flavivirus induces interferon-beta gene expression through a pathway involving RIG-I-dependent IRF-3 and PI3K-dependent NF-kappaB activation. *Microbes Infect.* **2006**, *8*, 157–171. [CrossRef] [PubMed]
40. Nasirudeen, A.M.A.; Wong, H.H.; Thien, P.; Xu, S.; Lam, K.-P.; Liu, D.X. RIG-I, MDA5 and TLR3 synergistically play an important role in restriction of dengue virus infection. *PLoS Negl. Trop. Dis.* **2011**, *5*, e926. [CrossRef] [PubMed]

41. da Conceição, T.M.; Rust, N.M.; Berbel, A.C.E.R.; Martins, N.B.; do Nascimento Santos, C.A.; Da Poian, A.T.; de Arruda, L.B. Essential role of RIG-I in the activation of endothelial cells by dengue virus. *Virology* **2013**, *435*, 281–292. [CrossRef] [PubMed]
42. Olagnier, D.; Scholte, F.E.M.; Chiang, C.; Albulescu, I.C.; Nichols, C.; He, Z.; Lin, R.; Snijder, E.J.; van Hemert, M.J.; Hiscott, J. Inhibition of dengue and chikungunya virus infections by RIG-I-mediated type I interferon-independent stimulation of the innate antiviral response. *J. Virol.* **2014**, *88*, 4180–4194. [CrossRef] [PubMed]
43. Chazal, M.; Beauclair, G.; Gracias, S.; Najburg, V.; Simon-Lorière, E.; Tangy, F.; Komarova, A.V.; Jouvenet, N. RIG-I Recognizes the 5′ Region of Dengue and Zika Virus Genomes. *Cell Rep.* **2018**, *24*, 320–328. [CrossRef]
44. Errett, J.S.; Suthar, M.S.; McMillan, A.; Diamond, M.S.; Gale, M. The Essential, Nonredundant Roles of RIG-I and MDA5 in Detecting and Controlling West Nile Virus Infection. *J. Virol.* **2013**, *87*, 11416–11425. [CrossRef]
45. Leifer, C.A.; Medvedev, A.E. Molecular mechanisms of regulation of Toll-like receptor signaling. *J. Leukoc. Biol.* **2016**, *100*, 927–941. [CrossRef]
46. Gao, D.; Li, W. Structures and recognition modes of toll-like receptors. *Proteins* **2017**, *85*, 3–9. [CrossRef]
47. Tsai, Y.-T.; Chang, S.-Y.; Lee, C.-N.; Kao, C.-L. Human TLR3 recognizes dengue virus and modulates viral replication in vitro. *Cell. Microbiol.* **2009**, *11*, 604–615. [CrossRef]
48. Liang, Z.; Wu, S.; Li, Y.; He, L.; Wu, M.; Jiang, L.; Feng, L.; Zhang, P.; Huang, X. Activation of Toll-like receptor 3 impairs the dengue virus serotype 2 replication through induction of IFN-β in cultured hepatoma cells. *PLoS ONE* **2011**, *6*, e23346. [CrossRef]
49. Sariol, C.A.; Martínez, M.I.; Rivera, F.; Rodríguez, I.V.; Pantoja, P.; Abel, K.; Arana, T.; Giavedoni, L.; Hodara, V.; White, L.J.; et al. Decreased dengue replication and an increased anti-viral humoral response with the use of combined Toll-like receptor 3 and 7/8 agonists in macaques. *PLoS ONE* **2011**, *6*, e19323. [CrossRef]
50. Dhanwani, R.; Takahashi, M.; Sharma, S. Cytosolic sensing of immuno-stimulatory DNA, the enemy within. *Curr. Opin. Immunol.* **2018**, *50*, 82–87. [CrossRef]
51. Ishikawa, H.; Barber, G.N. STING is an endoplasmic reticulum adaptor that facilitates innate immune signalling. *Nature* **2008**, *455*, 674–678. [CrossRef]
52. Holm, C.K.; Rahbek, S.H.; Gad, H.H.; Bak, R.O.; Jakobsen, M.R.; Jiang, Z.; Hansen, A.L.; Jensen, S.K.; Sun, C.; Thomsen, M.K.; et al. Influenza A virus targets a cGAS-independent STING pathway that controls enveloped RNA viruses. *Nat. Commun.* **2016**, *7*, 10680. [CrossRef]
53. Schoggins, J.W.; MacDuff, D.A.; Imanaka, N.; Gainey, M.D.; Shrestha, B.; Eitson, J.L.; Mar, K.B.; Richardson, R.B.; Ratushny, A.V.; Litvak, V.; et al. Pan-viral specificity of IFN-induced genes reveals new roles for cGAS in innate immunity. *Nature* **2014**, *505*, 691–695. [CrossRef]
54. Aguirre, S.; Maestre, A.M.; Pagni, S.; Patel, J.R.; Savage, T.; Gutman, D.; Maringer, K.; Bernal-Rubio, D.; Shabman, R.S.; Simon, V.; et al. DENV inhibits type I IFN production in infected cells by cleaving human STING. *PLoS Pathog.* **2012**, *8*, e1002934. [CrossRef]
55. Sun, L.; Xing, Y.; Chen, X.; Zheng, Y.; Yang, Y.; Nichols, D.B.; Clementz, M.A.; Banach, B.S.; Li, K.; Baker, S.C.; et al. Coronavirus papain-like proteases negatively regulate antiviral innate immune response through disruption of STING-mediated signaling. *PLoS ONE* **2012**, *7*, e30802. [CrossRef]
56. Ding, Q.; Cao, X.; Lu, J.; Huang, B.; Liu, Y.-J.; Kato, N.; Shu, H.-B.; Zhong, J. Hepatitis C virus NS4B blocks the interaction of STING and TBK1 to evade host innate immunity. *J. Hepatol.* **2013**, *59*, 52–58. [CrossRef]
57. Yu, C.-Y.; Chang, T.-H.; Liang, J.-J.; Chiang, R.-L.; Lee, Y.-L.; Liao, C.-L.; Lin, Y.-L. Dengue virus targets the adaptor protein MITA to subvert host innate immunity. *PLoS Pathog.* **2012**, *8*, e1002780. [CrossRef]
58. Aguirre, S.; Luthra, P.; Sanchez-Aparicio, M.T.; Maestre, A.M.; Patel, J.; Lamothe, F.; Fredericks, A.C.; Tripathi, S.; Zhu, T.; Pintado-Silva, J.; et al. Dengue virus NS2B protein targets cGAS for degradation and prevents mitochondrial DNA sensing during infection. *Nat. Microbiol.* **2017**, *2*, 17037. [CrossRef]
59. Stabell, A.C.; Meyerson, N.R.; Gullberg, R.C.; Gilchrist, A.R.; Webb, K.J.; Old, W.M.; Perera, R.; Sawyer, S.L. Dengue viruses cleave STING in humans but not in nonhuman primates, their presumed natural reservoir. *Elife* **2018**, *7*, e31919. [CrossRef]
60. West, A.P.; Khoury-Hanold, W.; Staron, M.; Tal, M.C.; Pineda, C.M.; Lang, S.M.; Bestwick, M.; Duguay, B.A.; Raimundo, N.; MacDuff, D.A.; et al. Mitochondrial DNA stress primes the antiviral innate immune response. *Nature* **2015**, *520*, 553–557. [CrossRef]

61. Aarreberg, L.D.; Esser-Nobis, K.; Driscoll, C.; Shuvarikov, A.; Roby, J.A.; Gale, M., Jr. Interleukin-1β Induces mtDNA Release to Activate Innate Immune Signaling via cGAS-STING. *Mol. Cell* **2019**, *74*, 801–815.e6. [CrossRef]
62. Wu, M.-F.; Chen, S.-T.; Yang, A.-H.; Lin, W.-W.; Lin, Y.-L.; Chen, N.-J.; Tsai, I.-S.; Li, L.; Hsieh, S.-L. CLEC5A is critical for dengue virus-induced inflammasome activation in human macrophages. *Blood* **2013**, *121*, 95–106. [CrossRef]
63. Hottz, E.D.; Lopes, J.F.; Freitas, C.; Valls-de-Souza, R.; Oliveira, M.F.; Bozza, M.T.; Da Poian, A.T.; Weyrich, A.S.; Zimmerman, G.A.; Bozza, F.A.; et al. Platelets mediate increased endothelium permeability in dengue through NLRP3-inflammasome activation. *Blood* **2013**, *122*, 3405–3414. [CrossRef]
64. Zevini, A.; Olagnier, D.; Hiscott, J. Crosstalk between Cytoplasmic RIG-I and STING Sensing Pathways. *Trends Immunol.* **2017**, *38*, 194–205. [CrossRef]
65. Zhong, B.; Yang, Y.; Li, S.; Wang, Y.-Y.; Li, Y.; Diao, F.; Lei, C.; He, X.; Zhang, L.; Tien, P.; et al. The adaptor protein MITA links virus-sensing receptors to IRF3 transcription factor activation. *Immunity* **2008**, *29*, 538–550. [CrossRef]
66. Nazmi, A.; Mukhopadhyay, R.; Dutta, K.; Basu, A. STING mediates neuronal innate immune response following Japanese encephalitis virus infection. *Sci. Rep.* **2012**, *2*, 347. [CrossRef]
67. Thompson, M.R.; Sharma, S.; Atianand, M.; Jensen, S.B.; Carpenter, S.; Knipe, D.M.; Fitzgerald, K.A.; Kurt-Jones, E.A. Interferon γ-inducible Protein (IFI) 16 Transcriptionally Regulates Type I Interferons and Other Interferon-stimulated Genes and Controls the Interferon Response to both DNA and RNA Viruses. *J. Biol. Chem.* **2014**, *289*, 23568–23581. [CrossRef]
68. Härtlova, A.; Erttmann, S.F.; Raffi, F.A.; Schmalz, A.M.; Resch, U.; Anugula, S.; Lienenklaus, S.; Nilsson, L.M.; Kröger, A.; Nilsson, J.A.; et al. DNA damage primes the type I interferon system via the cytosolic DNA sensor STING to promote anti-microbial innate immunity. *Immunity* **2015**, *42*, 332–343. [CrossRef]
69. Liu, Y.; Goulet, M.-L.; Sze, A.; Hadj, S.B.; Belgnaoui, S.M.; Lababidi, R.R.; Zheng, C.; Fritz, J.H.; Olagnier, D.; Lin, R. RIG-I-Mediated STING Upregulation Restricts Herpes Simplex Virus 1 Infection. *J. Virol.* **2016**, *90*, 9406–9419. [CrossRef]
70. Bradrick, S.S. Causes and Consequences of Flavivirus RNA Methylation. *Front. Microbiol.* **2017**, *8*, 2374. [CrossRef]
71. Furuichi, Y.; Shatkin, A.J. Viral and cellular mRNA capping: Past and prospects. *Adv. Virus Res.* **2000**, *55*, 135–184.
72. Dong, H.; Chang, D.C.; Hua, M.H.C.; Lim, S.P.; Chionh, Y.H.; Hia, F.; Lee, Y.H.; Kukkaro, P.; Lok, S.-M.; Dedon, P.C.; et al. 2′-*O* methylation of internal adenosine by flavivirus NS5 methyltransferase. *PLoS Pathog.* **2012**, *8*, e1002642. [CrossRef]
73. Schmid, B.; Rinas, M.; Ruggieri, A.; Acosta, E.G.; Bartenschlager, M.; Reuter, A.; Fischl, W.; Harder, N.; Bergeest, J.-P.; Flossdorf, M.; et al. Live Cell Analysis and Mathematical Modeling Identify Determinants of Attenuation of Dengue Virus 2′-*O*-Methylation Mutant. *PLoS Pathog.* **2015**, *11*, e1005345. [CrossRef]
74. Züst, R.; Cervantes-Barragan, L.; Habjan, M.; Maier, R.; Neuman, B.W.; Ziebuhr, J.; Szretter, K.J.; Baker, S.C.; Barchet, W.; Diamond, M.S.; et al. Ribose 2′-*O*-methylation provides a molecular signature for the distinction of self and non-self mRNA dependent on the RNA sensor Mda5. *Nat. Immunol.* **2011**, *12*, 137–143. [CrossRef]
75. Züst, R.; Dong, H.; Li, X.-F.; Chang, D.C.; Zhang, B.; Balakrishnan, T.; Toh, Y.-X.; Jiang, T.; Li, S.-H.; Deng, Y.-Q.; et al. Rational Design of a Live Attenuated Dengue Vaccine: 2′-*O*-Methyltransferase Mutants Are Highly Attenuated and Immunogenic in Mice and Macaques. *PLoS Pathog.* **2013**, *9*, e1003521. [CrossRef]
76. Chang, D.C.; Hoang, L.T.; Naim, A.N.M.; Dong, H.; Schreiber, M.J.; Hibberd, M.L.; Tan, M.J.A.; Shi, P.-Y. Evasion of early innate immune response by 2′- O -methylation of dengue genomic RNA. *Virology* **2016**, *499*, 259–266. [CrossRef]
77. Clarke, B.D.; Roby, J.A.; Slonchak, A.; Khromykh, A.A. Functional non-coding RNAs derived from the flavivirus 3′ untranslated region. *Virus Res.* **2015**, *206*, 53–61. [CrossRef]
78. Pijlman, G.P.; Funk, A.; Kondratieva, N.; Leung, J.; Torres, S.; van der Aa, L.; Liu, W.J.; Palmenberg, A.C.; Shi, P.-Y.; Hall, R.A.; et al. A highly structured, nuclease-resistant, noncoding RNA produced by flaviviruses is required for pathogenicity. *Cell Host Microbe* **2008**, *4*, 579–591. [CrossRef]
79. Liu, Y.; Liu, H.; Zou, J.; Zhang, B.; Yuan, Z. Dengue virus subgenomic RNA induces apoptosis through the Bcl-2-mediated PI3k/Akt signaling pathway. *Virology* **2014**, *448*, 15–25. [CrossRef]

80. Moon, S.L.; Anderson, J.R.; Kumagai, Y.; Wilusz, C.J.; Akira, S.; Khromykh, A.A.; Wilusz, J. A noncoding RNA produced by arthropod-borne flaviviruses inhibits the cellular exoribonuclease XRN1 and alters host mRNA stability. *RNA* **2012**, *18*, 2029–2040. [CrossRef]
81. Schnettler, E.; Sterken, M.G.; Leung, J.Y.; Metz, S.W.; Geertsema, C.; Goldbach, R.W.; Vlak, J.M.; Kohl, A.; Khromykh, A.A.; Pijlman, G.P. Noncoding flavivirus RNA displays RNA interference suppressor activity in insect and Mammalian cells. *J. Virol.* **2012**, *86*, 13486–13500. [CrossRef]
82. Fan, Y.-H.; Nadar, M.; Chen, C.-C.; Weng, C.-C.; Lin, Y.-T.; Chang, R.-Y. Small noncoding RNA modulates Japanese encephalitis virus replication and translation in trans. *Virol. J.* **2011**, *8*, 492. [CrossRef]
83. Chang, R.-Y.; Hsu, T.-W.; Chen, Y.-L.; Liu, S.-F.; Tsai, Y.-J.; Lin, Y.-T.; Chen, Y.-S.; Fan, Y.-H. Japanese encephalitis virus non-coding RNA inhibits activation of interferon by blocking nuclear translocation of interferon regulatory factor 3. *Vet. Microbiol.* **2013**, *166*, 11–21. [CrossRef] [PubMed]
84. Schuessler, A.; Funk, A.; Lazear, H.M.; Cooper, D.A.; Torres, S.; Daffis, S.; Jha, B.K.; Kumagai, Y.; Takeuchi, O.; Hertzog, P.; et al. West Nile virus noncoding subgenomic RNA contributes to viral evasion of the type I interferon-mediated antiviral response. *J. Virol.* **2012**, *86*, 5708–5718. [CrossRef] [PubMed]
85. Donald, C.L.; Brennan, B.; Cumberworth, S.L.; Rezelj, V.V.; Clark, J.J.; Cordeiro, M.T.; Freitas de Oliveira França, R.; Pena, L.J.; Wilkie, G.S.; Da Silva Filipe, A.; et al. Full Genome Sequence and sfRNA Interferon Antagonist Activity of Zika Virus from Recife, Brazil. *PLoS Negl. Trop. Dis.* **2016**, *10*, e0005048. [CrossRef] [PubMed]
86. Manokaran, G.; Finol, E.; Wang, C.; Gunaratne, J.; Bahl, J.; Ong, E.Z.; Tan, H.C.; Sessions, O.M.; Ward, A.M.; Gubler, D.J.; et al. Dengue subgenomic RNA binds TRIM25 to inhibit interferon expression for epidemiological fitness. *Science* **2015**, *350*, 217–221. [CrossRef] [PubMed]
87. Gack, M.U.; Albrecht, R.A.; Urano, T.; Inn, K.-S.; Huang, I.-C.; Carnero, E.; Farzan, M.; Inoue, S.; Jung, J.U.; García-Sastre, A. Influenza A virus NS1 targets the ubiquitin ligase TRIM25 to evade recognition by the host viral RNA sensor RIG-I. *Cell Host Microbe* **2009**, *5*, 439–449. [CrossRef] [PubMed]
88. Gack, M.U.; Shin, Y.C.; Joo, C.-H.; Urano, T.; Liang, C.; Sun, L.; Takeuchi, O.; Akira, S.; Chen, Z.; Inoue, S.; et al. TRIM25 RING-finger E3 ubiquitin ligase is essential for RIG-I-mediated antiviral activity. *Nature* **2007**, *446*, 916–920. [CrossRef] [PubMed]
89. Chan, Y.K.; Gack, M.U. A phosphomimetic-based mechanism of dengue virus to antagonize innate immunity. *Nat. Immunol.* **2016**, *17*, 523–530. [CrossRef] [PubMed]
90. Liu, H.M.; Loo, Y.-M.; Horner, S.M.; Zornetzer, G.A.; Katze, M.G.; Gale, M., Jr. The mitochondrial targeting chaperone 14-3-3ε regulates a RIG-I translocon that mediates membrane association and innate antiviral immunity. *Cell Host Microbe* **2012**, *11*, 528–537. [CrossRef] [PubMed]
91. He, Z.; Zhu, X.; Wen, W.; Yuan, J.; Hu, Y.; Chen, J.; An, S.; Dong, X.; Lin, C.; Yu, J.; et al. Dengue Virus Subverts Host Innate Immunity by Targeting Adaptor Protein MAVS. *J. Virol.* **2016**, *90*, 7219–7230. [CrossRef]
92. Barbier, V.; Lang, D.; Valois, S.; Rothman, A.L.; Medin, C.L. Dengue virus induces mitochondrial elongation through impairment of Drp1-triggered mitochondrial fission. *Virology* **2017**, *500*, 149–160. [CrossRef]
93. Lee, H.; Yoon, Y. Mitochondrial fission: Regulation and ER connection. *Mol. Cells* **2014**, *37*, 89–94. [CrossRef] [PubMed]
94. Yu, C.-Y.; Liang, J.-J.; Li, J.-K.; Lee, Y.-L.; Chang, B.-L.; Su, C.-I.; Huang, W.-J.; Lai, M.M.C.; Lin, Y.-L. Dengue Virus Impairs Mitochondrial Fusion by Cleaving Mitofusins. *PLoS Pathog.* **2015**, *11*, e1005350. [CrossRef] [PubMed]
95. Ishihara, N.; Eura, Y.; Mihara, K. Mitofusin 1 and 2 play distinct roles in mitochondrial fusion reactions via GTPase activity. *J. Cell Sci.* **2004**, *117*, 6535–6546. [CrossRef] [PubMed]
96. Koshiba, T.; Detmer, S.A.; Kaiser, J.T.; Chen, H.; McCaffery, J.M.; Chan, D.C. Structural basis of mitochondrial tethering by mitofusin complexes. *Science* **2004**, *305*, 858–862. [CrossRef] [PubMed]
97. de Brito, O.M.; Scorrano, L. Mitofusin 2 tethers endoplasmic reticulum to mitochondria. *Nature* **2008**, *456*, 605–610. [CrossRef] [PubMed]
98. Kim, S.-J.; Khan, M.; Quan, J.; Till, A.; Subramani, S.; Siddiqui, A. Hepatitis B virus disrupts mitochondrial dynamics: Induces fission and mitophagy to attenuate apoptosis. *PLoS Pathog.* **2013**, *9*, e1003722. [CrossRef] [PubMed]
99. Kim, S.-J.; Syed, G.H.; Khan, M.; Chiu, W.-W.; Sohail, M.A.; Gish, R.G.; Siddiqui, A. Hepatitis C virus triggers mitochondrial fission and attenuates apoptosis to promote viral persistence. *Proc. Natl. Acad. Sci. USA* **2014**, *111*, 6413–6418. [CrossRef] [PubMed]

100. Kramer, T.; Enquist, L.W. Alphaherpesvirus infection disrupts mitochondrial transport in neurons. *Cell Host Microbe* **2012**, *11*, 504–514. [CrossRef] [PubMed]
101. Shi, C.-S.; Qi, H.-Y.; Boularan, C.; Huang, N.-N.; Abu-Asab, M.; Shelhamer, J.H.; Kehrl, J.H. SARS-coronavirus open reading frame-9b suppresses innate immunity by targeting mitochondria and the MAVS/TRAF3/TRAF6 signalosome. *J. Immunol.* **2014**, *193*, 3080–3089. [CrossRef] [PubMed]
102. You, J.; Hou, S.; Malik-Soni, N.; Xu, Z.; Kumar, A.; Rachubinski, R.A.; Frappier, L.; Hobman, T.C. Flavivirus Infection Impairs Peroxisome Biogenesis and Early Antiviral Signaling. *J. Virol.* **2015**, *89*, 12349–12361. [CrossRef]
103. Wong, C.P.; Xu, Z.; Hou, S.; Limonta, D.; Kumar, A.; Power, C.; Hobman, T.C. Interplay between Zika Virus and Peroxisomes during Infection. *Cells* **2019**, *8*, 725. [CrossRef] [PubMed]
104. Dixit, E.; Boulant, S.; Zhang, Y.; Lee, A.S.Y.; Odendall, C.; Shum, B.; Hacohen, N.; Chen, Z.J.; Whelan, S.P.; Fransen, M.; et al. Peroxisomes are signaling platforms for antiviral innate immunity. *Cell* **2010**, *141*, 668–681. [CrossRef] [PubMed]
105. Odendall, C.; Dixit, E.; Stavru, F.; Bierne, H.; Franz, K.M.; Durbin, A.F.; Boulant, S.; Gehrke, L.; Cossart, P.; Kagan, J.C. Diverse intracellular pathogens activate type III interferon expression from peroxisomes. *Nat. Immunol.* **2014**, *15*, 717–726. [CrossRef] [PubMed]
106. Bender, S.; Reuter, A.; Eberle, F.; Einhorn, E.; Binder, M.; Bartenschlager, R. Activation of Type I and III Interferon Response by Mitochondrial and Peroxisomal MAVS and Inhibition by Hepatitis C Virus. *PLoS Pathog.* **2015**, *11*, e1005264. [CrossRef] [PubMed]
107. Götte, K.; Girzalsky, W.; Linkert, M.; Baumgart, E.; Kammerer, S.; Kunau, W.H.; Erdmann, R. Pex19p, a farnesylated protein essential for peroxisome biogenesis. *Mol. Cell. Biol.* **1998**, *18*, 616–628. [CrossRef] [PubMed]
108. Angleró-Rodríguez, Y.I.; Pantoja, P.; Sariol, C.A. Dengue virus subverts the interferon induction pathway via NS2B/3 protease-IκB kinase epsilon interaction. *Clin. Vaccine Immunol.* **2014**, *21*, 29–38. [CrossRef] [PubMed]
109. Dalrymple, N.A.; Cimica, V.; Mackow, E.R. Dengue Virus NS Proteins Inhibit RIG-I/MAVS Signaling by Blocking TBK1/IRF3 Phosphorylation: Dengue Virus Serotype 1 NS4A Is a Unique Interferon-Regulating Virulence Determinant. *mBio* **2015**, *6*. [CrossRef]
110. Chatel-Chaix, L.; Fischl, W.; Scaturro, P.; Cortese, M.; Kallis, S.; Bartenschlager, M.; Fischer, B.; Bartenschlager, R. A Combined Genetic-Proteomic Approach Identifies Residues within Dengue Virus NS4B Critical for Interaction with NS3 and Viral Replication. *J. Virol.* **2015**, *89*, 7170–7186. [CrossRef]
111. Zou, J.; Lee, L.T.; Wang, Q.Y.; Xie, X.; Lu, S.; Yau, Y.H.; Yuan, Z.; Geifman Shochat, S.; Kang, C.; Lescar, J.; et al. Mapping the Interactions between the NS4B and NS3 proteins of dengue virus. *J. Virol.* **2015**, *89*, 3471–3483. [CrossRef] [PubMed]
112. Zou, J.; Xie, X.; Wang, Q.-Y.; Dong, H.; Lee, M.Y.; Kang, C.; Yuan, Z.; Shi, P.-Y. Characterization of dengue virus NS4A and NS4B protein interaction. *J. Virol.* **2015**, *89*, 3455–3470. [CrossRef] [PubMed]
113. Umareddy, I.; Chao, A.; Sampath, A.; Gu, F.; Vasudevan, S.G. Dengue virus NS4B interacts with NS3 and dissociates it from single-stranded RNA. *J. Gen. Virol.* **2006**, *87*, 2605–2614. [CrossRef] [PubMed]
114. Sun, B.; Sundström, K.B.; Chew, J.J.; Bist, P.; Gan, E.S.; Tan, H.C.; Goh, K.C.; Chawla, T.; Tang, C.K.; Ooi, E.E. Dengue virus activates cGAS through the release of mitochondrial DNA. *Sci. Rep.* **2017**, *7*, 3594. [CrossRef] [PubMed]
115. Yu, C.-Y.; Chang, T.-H.; Liang, J.-J.; Chiang, R.-L.; Lee, Y.-L.; Liao, C.-L.; Lin, Y.-L. P122 Dengue virus targets the adaptor protein MITA to subvert host innate immunity. *Cytokine* **2012**, *59*, 558. [CrossRef]
116. Bao, D.; Zhao, J.; Zhou, X.; Yang, Q.; Chen, Y.; Zhu, J.; Yuan, P.; Yang, J.; Qin, T.; Wan, S.; et al. Mitochondrial fission-induced mtDNA stress promotes tumor-associated macrophage infiltration and HCC progression. *Oncogene* **2019**, *38*, 5007–5020. [CrossRef] [PubMed]
117. Ishikawa, H.; Ma, Z.; Barber, G.N. STING regulates intracellular DNA-mediated, type I interferon-dependent innate immunity. *Nature* **2009**, *461*, 788–792. [CrossRef]
118. Muñoz-Jordan, J.L.; Sánchez-Burgos, G.G.; Laurent-Rolle, M.; García-Sastre, A. Inhibition of interferon signaling by dengue virus. *Proc. Natl. Acad. Sci. USA* **2003**, *100*, 14333–14338. [CrossRef]
119. Muñoz-Jordán, J.L.; Laurent-Rolle, M.; Ashour, J.; Martínez-Sobrido, L.; Ashok, M.; Lipkin, W.I.; García-Sastre, A. Inhibition of alpha/beta interferon signaling by the NS4B protein of flaviviruses. *J. Virol.* **2005**, *79*, 8004–8013. [CrossRef]

120. Morrison, J.; Laurent-Rolle, M.; Maestre, A.M.; Rajsbaum, R.; Pisanelli, G.; Simon, V.; Mulder, L.C.F.; Fernandez-Sesma, A.; García-Sastre, A. Dengue virus co-opts UBR4 to degrade STAT2 and antagonize type I interferon signaling. *PLoS Pathog.* **2013**, *9*, e1003265. [CrossRef]
121. Ashour, J.; Laurent-Rolle, M.; Shi, P.-Y.; García-Sastre, A. NS5 of dengue virus mediates STAT2 binding and degradation. *J. Virol.* **2009**, *83*, 5408–5418. [CrossRef]
122. Jones, M.; Davidson, A.; Hibbert, L.; Gruenwald, P.; Schlaak, J.; Ball, S.; Foster, G.R.; Jacobs, M. Dengue virus inhibits alpha interferon signaling by reducing STAT2 expression. *J. Virol.* **2005**, *79*, 5414–5420. [CrossRef]
123. Kumar, A.; Hou, S.; Airo, A.M.; Limonta, D.; Mancinelli, V.; Branton, W.; Power, C.; Hobman, T.C. Zika virus inhibits type-I interferon production and downstream signaling. *EMBO Rep.* **2016**, *17*, 1766–1775. [CrossRef] [PubMed]
124. Grant, A.; Ponia, S.S.; Tripathi, S.; Balasubramaniam, V.; Miorin, L.; Sourisseau, M.; Schwarz, M.C.; Sánchez-Seco, M.P.; Evans, M.J.; Best, S.M.; et al. Zika Virus Targets Human STAT2 to Inhibit Type I Interferon Signaling. *Cell Host Microbe* **2016**, *19*, 882–890. [CrossRef] [PubMed]
125. Shah, P.S.; Link, N.; Jang, G.M.; Sharp, P.P.; Zhu, T.; Swaney, D.L.; Johnson, J.R.; Von Dollen, J.; Ramage, H.R.; Satkamp, L.; et al. Comparative Flavivirus-Host Protein Interaction Mapping Reveals Mechanisms of Dengue and Zika Virus Pathogenesis. *Cell* **2018**, *175*, 1931–1945.e18. [CrossRef] [PubMed]
126. De Maio, F.A.; Risso, G.; Iglesias, N.G.; Shah, P.; Pozzi, B.; Gebhard, L.G.; Mammi, P.; Mancini, E.; Yanovsky, M.J.; Andino, R.; et al. The Dengue Virus NS5 Protein Intrudes in the Cellular Spliceosome and Modulates Splicing. *PLoS Pathog.* **2016**, *12*, e1005841. [CrossRef] [PubMed]
127. Bidet, K.; Dadlani, D.; Garcia-Blanco, M.A. G3BP1, G3BP2 and CAPRIN1 Are Required for Translation of Interferon Stimulated mRNAs and Are Targeted by a Dengue Virus Non-coding RNA. *PLoS Pathog.* **2014**, *10*, e1004242. [CrossRef]
128. Daffis, S.; Szretter, K.J.; Schriewer, J.; Li, J.; Youn, S.; Errett, J.; Lin, T.-Y.; Schneller, S.; Zust, R.; Dong, H.; et al. 2′-*O* methylation of the viral mRNA cap evades host restriction by IFIT family members. *Nature* **2010**, *468*, 452. [CrossRef]
129. Habjan, M.; Hubel, P.; Lacerda, L.; Benda, C.; Holze, C.; Eberl, C.H.; Mann, A.; Kindler, E.; Gil-Cruz, C.; Ziebuhr, J.; et al. Sequestration by IFIT1 impairs translation of 2′ O-unmethylated capped RNA. *PLoS Pathog.* **2013**, *9*, e1003663. [CrossRef]
130. Kimura, T.; Katoh, H.; Kayama, H.; Saiga, H.; Okuyama, M.; Okamoto, T.; Umemoto, E.; Matsuura, Y.; Yamamoto, M.; Takeda, K. Ifit1 Inhibits Japanese Encephalitis Virus Replication through Binding to 5′ Capped 2′-*O* Unmethylated RNA. *J. Virol.* **2013**, *87*, 9997–10003. [CrossRef]
131. Kumar, P.; Sweeney, T.R.; Skabkin, M.A.; Skabkina, O.V.; Hellen, C.U.T.; Pestova, T.V. Inhibition of translation by IFIT family members is determined by their ability to interact selectively with the 5′-terminal regions of cap0-, cap1- and 5′ppp- mRNAs. *Nucleic Acids Res.* **2014**, *42*, 3228–3245. [CrossRef]
132. Pompon, J.; Manuel, M.; Ng, G.K.; Wong, B.; Shan, C.; Manokaran, G.; Soto-Acosta, R.; Bradrick, S.S.; Ooi, E.E.; Missé, D.; et al. Dengue subgenomic flaviviral RNA disrupts immunity in mosquito salivary glands to increase virus transmission. *PLoS Pathog.* **2017**, *13*, e1006535. [CrossRef]
133. Moon, S.L.; Dodd, B.J.T.; Brackney, D.E.; Wilusz, C.J.; Ebel, G.D.; Wilusz, J. Flavivirus sfRNA suppresses antiviral RNA interference in cultured cells and mosquitoes and directly interacts with the RNAi machinery. *Virology* **2015**, *485*, 322–329. [CrossRef] [PubMed]
134. Göertz, G.P.; Fros, J.J.; Miesen, P.; Vogels, C.B.F.; van der Bent, M.L.; Geertsema, C.; Koenraadt, C.J.M.; van Rij, R.P.; van Oers, M.M.; Pijlman, G.P. Noncoding Subgenomic Flavivirus RNA Is Processed by the Mosquito RNA Interference Machinery and Determines West Nile Virus Transmission by Culex pipiens Mosquitoes. *J. Virol.* **2016**, *90*, 10145–10159. [CrossRef] [PubMed]
135. Gammon, D.B.; Mello, C.C. RNA interference-mediated antiviral defense in insects. *Curr Opin Insect Sci* **2015**, *8*, 111–120. [CrossRef]
136. Siomi, H.; Siomi, M.C. On the road to reading the RNA-interference code. *Nature* **2009**, *457*, 396–404. [CrossRef] [PubMed]
137. Hu, H.-M.; Chen, H.-W.; Hsiao, Y.-J.; Wu, S.-H.; Chung, H.-H.; Hsieh, C.-H.; Chong, P.; Leng, C.-H.; Pan, C.-H. The successful induction of T-cell and antibody responses by a recombinant measles virus-vectored tetravalent dengue vaccine provides partial protection against dengue-2 infection. *Hum. Vaccin. Immunother.* **2016**, *12*, 1678–1689. [CrossRef] [PubMed]

138. Tripathi, N.K.; Shrivastava, A. Recent Developments in Recombinant Protein-Based Dengue Vaccines. *Front. Immunol.* **2018**, *9*, 1919. [CrossRef]
139. McArthur, M.A.; Sztein, M.B.; Edelman, R. Dengue vaccines: Recent developments, ongoing challenges and current candidates. *Expert Rev. Vaccines* **2013**, *12*, 933–953. [CrossRef]
140. Shukla, R.; Ramasamy, V.; Rajpoot, R.K.; Arora, U.; Poddar, A.; Ahuja, R.; Beesetti, H.; Swaminathan, S.; Khanna, N. Next generation designer virus-like particle vaccines for dengue. *Expert Rev. Vaccines* **2019**, *18*, 105–117. [CrossRef]
141. Fahimi, H.; Mohammadipour, M.; Haddad Kashani, H.; Parvini, F.; Sadeghizadeh, M. Dengue viruses and promising envelope protein domain III-based vaccines. *Appl. Microbiol. Biotechnol.* **2018**, *102*, 2977–2996. [CrossRef]
142. Lazo, L.; Valdes, I.; Guillén, G.; Hermida, L.; Gil, L. Aiming at the heart: The capsid protein of dengue virus as a vaccine candidate. *Expert Rev. Vaccines* **2019**, *18*, 161–173. [CrossRef]
143. Hadinegoro, S.R.; Arredondo-García, J.L.; Capeding, M.R.; Deseda, C.; Chotpitayasunondh, T.; Dietze, R.; Muhammad Ismail, H.I.H.; Reynales, H.; Limkittikul, K.; Rivera-Medina, D.M.; et al. Efficacy and Long-Term Safety of a Dengue Vaccine in Regions of Endemic Disease. *N. Engl. J. Med.* **2015**, *373*, 1195–1206. [CrossRef] [PubMed]
144. Malisheni, M.; Khaiboullina, S.F.; Rizvanov, A.A.; Takah, N.; Murewanhema, G.; Bates, M. Clinical Efficacy, Safety, and Immunogenicity of a Live Attenuated Tetravalent Dengue Vaccine (CYD-TDV) in Children: A Systematic Review with Meta-analysis. *Front. Immunol.* **2017**, *8*, 863. [CrossRef] [PubMed]
145. Diseases, T.L.I. The Lancet Infectious Diseases The dengue vaccine dilemma. *Lancet Infect. Dis.* **2018**, *18*, 123. [CrossRef]
146. Dengue vaccine: WHO position paper, September 2018—Recommendations. *Vaccine* **2019**, *37*, 4848–4849. [CrossRef] [PubMed]
147. Velumani, S.; Toh, Y.X.; Balasingam, S.; Archuleta, S.; Leo, Y.S.; Gan, V.C.; Thein, T.L.; Wilder-Smith, A.; Fink, K. Low antibody titers 5 years after vaccination with the CYD-TDV dengue vaccine in both pre-immune and naïve vaccinees. *Hum. Vaccines Immunother.* **2016**, *12*, 1265–1273. [CrossRef] [PubMed]
148. Sabin, A.B. Research on dengue during World War II. *Am. J. Trop. Med. Hyg.* **1952**, *1*, 30–50. [CrossRef]
149. Snow, G.E.; Haaland, B.; Ooi, E.E.; Gubler, D.J. Review article: Research on dengue during World War II revisited. *Am. J. Trop. Med. Hyg.* **2014**, *91*, 1203–1217. [CrossRef] [PubMed]
150. Kuczera, D.; Assolini, J.P.; Tomiotto-Pellissier, F.; Pavanelli, W.R.; Silveira, G.F. Highlights for Dengue Immunopathogenesis: Antibody-Dependent Enhancement, Cytokine Storm, and Beyond. *J. Interferon Cytokine Res.* **2018**, *38*, 69–80. [CrossRef]
151. St John, A.L.; Rathore, A.P.S. Adaptive immune responses to primary and secondary dengue virus infections. *Nat. Rev. Immunol.* **2019**, *19*, 218–230. [CrossRef]
152. Blaney, J.E., Jr.; Durbin, A.P.; Murphy, B.R.; Whitehead, S.S. Development of a live attenuated dengue virus vaccine using reverse genetics. *Viral Immunol.* **2006**, *19*, 10–32. [CrossRef]
153. Durbin, A.P.; Karron, R.A.; Sun, W.; Vaughn, D.W.; Reynolds, M.J.; Perreault, J.R.; Thumar, B.; Men, R.; Lai, C.J.; Elkins, W.R.; et al. Attenuation and immunogenicity in humans of a live dengue virus type-4 vaccine candidate with a 30 nucleotide deletion in its 3′-untranslated region. *Am. J. Trop. Med. Hyg.* **2001**, *65*, 405–413. [CrossRef] [PubMed]
154. Blaney, J.E.; Sathe, N.S.; Goddard, L.; Hanson, C.T.; Romero, T.A.; Hanley, K.A.; Murphy, B.R.; Whitehead, S.S. Dengue virus type 3 vaccine candidates generated by introduction of deletions in the 3′ untranslated region (3′-UTR) or by exchange of the DENV-3 3′-UTR with that of DENV-4. *Vaccine* **2008**, *26*, 817–828. [CrossRef] [PubMed]
155. Durbin, A.P.; Whitehead, S.S.; Shaffer, D.; Elwood, D.; Wanionek, K.; Thumar, B.; Blaney, J.E.; Murphy, B.R.; Schmidt, A.C. A single dose of the DENV-1 candidate vaccine rDEN1Δ30 is strongly immunogenic and induces resistance to a second dose in a randomized trial. *PLoS Negl. Trop. Dis.* **2011**, *5*, e1267. [CrossRef] [PubMed]
156. Blaney, J.E., Jr.; Hanson, C.T.; Firestone, C.-Y.; Hanley, K.A.; Murphy, B.R.; Whitehead, S.S. Genetically modified, live attenuated dengue virus type 3 vaccine candidates. *Am. J. Trop. Med. Hyg.* **2004**, *71*, 811–821. [CrossRef] [PubMed]

157. Durbin, A.P.; McArthur, J.; Marron, J.A.; Blaney, J.E., Jr.; Thumar, B.; Wanionek, K.; Murphy, B.R.; Whitehead, S.S. The Live Attenuated Dengue Serotype 1 Vaccine rDEN1Δ30 is Safe and Highly Immunogenic in Healthy Adult Volunteers. *Hum. Vaccin.* **2006**, *2*, 167–173. [CrossRef] [PubMed]
158. Durbin, A.P.; McArthur, J.H.; Marron, J.A.; Blaney, J.E.; Thumar, B.; Wanionek, K.; Murphy, B.R. rDEN2/4Δ30 (ME), a live attenuated chimeric dengue serotype 2 vaccine, is safe and highly immunogenic in healthy dengue-naïve adults. *Hum. Vaccin.* **2006**, *2*, 255–260. [CrossRef] [PubMed]
159. Durbin, A.P.; Whitehead, S.S.; McArthur, J.; Perreault, J.R.; Blaney, J.E., Jr.; Thumar, B.; Murphy, B.R.; Karron, R.A. rDEN4delta30, a live attenuated dengue virus type 4 vaccine candidate, is safe, immunogenic, and highly infectious in healthy adult volunteers. *J. Infect. Dis.* **2005**, *191*, 710–718. [CrossRef] [PubMed]
160. Blaney, J.E.; Matro, J.M.; Murphy, B.R.; Whitehead, S.S. Recombinant, Live-Attenuated Tetravalent Dengue Virus Vaccine Formulations Induce a Balanced, Broad, and Protective Neutralizing Antibody Response against Each of the Four Serotypes in Rhesus Monkeys. *J. Virol.* **2005**, *79*, 5516–5528. [CrossRef]
161. Kirkpatrick, B.D.; Whitehead, S.S.; Pierce, K.K.; Tibery, C.M.; Grier, P.L.; Hynes, N.A.; Larsson, C.J.; Sabundayo, B.P.; Talaat, K.R.; Janiak, A.; et al. The live attenuated dengue vaccine TV003 elicits complete protection against dengue in a human challenge model. *Sci. Transl. Med.* **2016**, *8*, 330ra36. [CrossRef]
162. Troyer, J.M.; Durbin, A.P.; Strickman, D.; Hanley, K.A.; Karron, R.A.; Murphy, B.R.; Whitehead, S.S. A live attenuated recombinant dengue-4 virus vaccine candidate with restricted capacity for dissemination in mosquitoes and lack of transmission from vaccinees to mosquitoes. *Am. J. Trop. Med. Hyg.* **2001**, *65*, 414–419. [CrossRef]
163. Bustos-Arriaga, J.; Gromowski, G.D.; Tsetsarkin, K.A.; Firestone, C.-Y.; Castro-Jiménez, T.; Pletnev, A.G.; Cedillo-Barrón, L.; Whitehead, S.S. Decreased accumulation of subgenomic RNA in human cells infected with vaccine candidate DEN4Δ30 increases viral susceptibility to type I interferon. *Vaccine* **2018**, *36*, 3460–3467. [CrossRef]
164. Li, S.-H.; Dong, H.; Li, X.-F.; Xie, X.; Zhao, H.; Deng, Y.-Q.; Wang, X.-Y.; Ye, Q.; Zhu, S.-Y.; Wang, H.-J.; et al. Rational design of a flavivirus vaccine by abolishing viral RNA 2′-*O* methylation. *J. Virol.* **2013**, *87*, 5812–5819. [CrossRef] [PubMed]
165. Gerdts, V.; Wilson, H.L.; Meurens, F.; van Drunen Littel-van den Hurk, S.; Wilson, D.; Walker, S.; Wheler, C.; Townsend, H.; Potter, A.A. Large animal models for vaccine development and testing. *ILAR J.* **2015**, *56*, 53–62. [CrossRef] [PubMed]
166. Johnson, A.J.; Roehrig, J.T. New mouse model for dengue virus vaccine testing. *J. Virol.* **1999**, *73*, 783–786.
167. Sarathy, V.V.; White, M.; Li, L.; Gorder, S.R.; Pyles, R.B.; Campbell, G.A.; Milligan, G.N.; Bourne, N.; Barrett, A.D.T. A lethal murine infection model for dengue virus 3 in AG129 mice deficient in type I and II interferon receptors leads to systemic disease. *J. Virol.* **2015**, *89*, 1254–1266. [CrossRef] [PubMed]
168. Shresta, S.; Kyle, J.L.; Snider, H.M.; Basavapatna, M.; Beatty, P.R.; Harris, E. Interferon-Dependent Immunity Is Essential for Resistance to Primary Dengue Virus Infection in Mice, Whereas T- and B-Cell-Dependent Immunity Are Less Critical. *J. Virol.* **2004**, *78*, 2701–2710. [CrossRef]
169. Gorman, M.J.; Caine, E.A.; Zaitsev, K.; Begley, M.C.; Weger-Lucarelli, J.; Uccellini, M.B.; Tripathi, S.; Morrison, J.; Yount, B.L.; Dinnon, K.H., 3rd; et al. An Immunocompetent Mouse Model of Zika Virus Infection. *Cell Host Microbe* **2018**, *23*, 672–685.e6. [CrossRef]
170. Bowen, J.R.; Quicke, K.M.; Maddur, M.S.; O'Neal, J.T.; McDonald, C.E.; Fedorova, N.B.; Puri, V.; Shabman, R.S.; Pulendran, B.; Suthar, M.S. Zika Virus Antagonizes Type I Interferon Responses during Infection of Human Dendritic Cells. *PLoS Pathog.* **2017**, *13*, e1006164. [CrossRef]

11 ANNEXE V

frontiers in Genetics

REVIEW
published: 04 December 2018
doi: 10.3389/fgene.2018.00595

Check for updates

The Multiples Fates of the Flavivirus RNA Genome During Pathogenesis

*Clément Mazeaud†, Wesley Freppel† and Laurent Chatel-Chaix**

Institut National de la Recherche Scientifique, Centre INRS-Institut Armand-Frappier, Laval, QC, Canada

The *Flavivirus* genus comprises many viruses (including dengue, Zika, West Nile and yellow fever viruses) which constitute important public health concerns worldwide. For several of these pathogens, neither antivirals nor vaccines are currently available. In addition to this unmet medical need, flaviviruses are of particular interest since they constitute an excellent model for the study of spatiotemporal regulation of RNA metabolism. Indeed, with no DNA intermediate or nuclear step, the flaviviral life cycle entirely relies on the cytoplasmic fate of a single RNA species, namely the genomic viral RNA (vRNA) which contains all the genetic information necessary for optimal viral replication. From a single open reading frame, the vRNA encodes a polyprotein which is processed to generate the mature viral proteins. In addition to coding for the viral polyprotein, the vRNA serves as a template for RNA synthesis and is also selectively packaged into newly assembled viral particles. Notably, vRNA translation, replication and encapsidation must be tightly coordinated in time and space via a fine-tuned equilibrium as these processes cannot occur simultaneously and hence, are mutually exclusive. As such, these dynamic processes involve several vRNA secondary and tertiary structures as well as RNA modifications. Finally, the vRNA can be detected as a foreign molecule by cytosolic sensors which trigger upon activation antiviral signaling pathways and the production of antiviral factors such as interferons and interferon-stimulated genes. However, to create an environment favorable to infection, flaviviruses have evolved mechanisms to dampen these antiviral processes, notably through the production of a specific vRNA degradation product termed subgenomic flavivirus RNA (sfRNA). In this review, we discuss the current understanding of the fates of flavivirus vRNA and how this is regulated at the molecular level to achieve an optimal replication within infected cells.

Keywords: flavivirus, dengue virus, Zika virus, West Nile virus, viral RNA replication, translation, RNA encapsidation, innate immunity

OPEN ACCESS

Edited by:
Chiara Gamberi,
Concordia University, Canada

Reviewed by:
Susann Friedrich,
Martin Luther University of Halle-Wittenberg, Germany
Fatah Kashanchi,
George Mason University, United States

****Correspondence:***
Laurent Chatel-Chaix
Laurent.Chatel-Chaix@iaf.inrs.ca

† These authors have contributed equally to this work

Specialty section:
This article was submitted to RNA, a section of the journal Frontiers in Genetics

Received: *10 August 2018*
Accepted: *15 November 2018*
Published: *04 December 2018*

Citation:
Mazeaud C, Freppel W and Chatel-Chaix L (2018) The Multiples Fates of the Flavivirus RNA Genome During Pathogenesis. Front. Genet. 9:595. doi: 10.3389/fgene.2018.00595

INTRODUCTION

Infections with flaviviruses constitute a major public health concern worldwide since they cause several human diseases with a wide range of symptoms that can potentially lead to lifelong impairment or even death. The genus *Flavivirus* within the *Flaviviridae* virus family comprises almost 70 reported species including the most studied yellow fever virus (YFV), dengue virus (DENV), Zika virus (ZIKV), West Nile virus (WNV), Japanese encephalitis virus (JEV), and tick-borne encephalitis virus (TBEV). The vast majority of flaviviral infections in humans occur through

the biting by arthropods such as *Aedes*-type mosquitoes (mostly *Aedes aegypti* and *Aedes albopictus*) in the case of YFV, DENV, and ZIKV or *Culex pipiens* mosquitoes in the case of WNV. Vaccines do exist for YFV, DENV and TBEV. However, in the case of DENV, the cause of the most prevalent arthropod-borne viral disease, the only available vaccine shows limited efficacy against all DENV serotypes and safety concerns have recently arisen in the Philippines in vaccinated children (Dyer, 2017). Importantly, no antivirals against flaviviruses are currently available partly because of our limited understanding of their life cycle and pathogenesis when compared to other virus groups. Interestingly, it appears that the general features of the life cycle are conserved across flaviviruses. Hence, there have been tremendous efforts by both industry and academia to identify or engineer antiviral drugs with a panflaviviral spectrum. This illustrates the importance of deciphering the molecular mechanisms underlying the flavivirus life cycle in order to identify novel antiviral targets.

The flavivirus life cycle is completely dependent on the cytoplasmic fate of only one RNA species, namely the genomic viral RNA (vRNA) whose replication entirely occurs in the cytoplasm and does not generate any DNA intermediates. Most notably, vRNA contains all the genetic information necessary for optimal virus replication. Hence, targeting vRNA or viral processes involved in its metabolism constitutes an attractive strategy for the development of novel antivirals. Moreover, fundamental virology often provides crucial insight into cellular machinery and processes at the molecular level. In this respect, flavivirus vRNA constitutes an exciting and excellent model for investigating the spatiotemporal regulation of RNA metabolism. With that in mind, we focus this review on our current understanding of the multiple fates of vRNA and how it orchestrates the viral life cycle and creates a cellular environment favorable to infection.

Flaviviruses are enveloped positive-strand RNA viruses that presumably contain a single copy of the genome RNA. Following receptor-mediated endocytosis of the virion and fusion with the endosomal membrane (reviewed in Perera-Lecoin et al., 2013), the vRNA is uncoated and released into the cytosol. The flaviviral vRNA genome contains all the genetic information required for efficient viral replication by hijacking the intracellular resources. With a single open reading frame, vRNA encodes an endoplasmic reticulum (ER)-associated transmembrane polyprotein (**Figure 1A**) (Garcia-Blanco et al., 2016; Neufeldt et al., 2018).

Upon translation, the polyprotein is subsequently processed by both cellular and viral proteases to generate 10 mature viral proteins. Structural proteins Capsid (C), Envelop (E) and prM assemble new viral particles while non-structural (NS) proteins NS1, NS2A, NS2B, NS3, NS4A, NS4B, and NS5 are responsible for vRNA replication (**Figure 1A**). vRNA synthesis relies on NS5, the RNA-dependent RNA polymerase as well as on critical vRNA secondary and tertiary structures. NS5 is also responsible for the capping of the neosynthetized vRNA. NS3 is a protease which, together with its co-factor NS2B, participates to the processing of the viral polyprotein. It also possesses helicase, NTPase and triphosphatase activities, all required for efficient vRNA synthesis and capping. vRNA is then encapsidated into assembling viral particles which bud into the ER. Assembled viruses egress through the secretory pathway where they undergo furin-mediated maturation in the Golgi apparatus, allowing fully infectious virions to be released via exocytosis (Apte-Sengupta et al., 2014; Neufeldt et al., 2018).

In order to efficiently complete the flaviviral life cycle, vRNA translation, synthesis and encapsidation must be tightly coordinated in both time and space since these processes cannot occur simultaneously and hence, are mutually exclusive. However, the molecular mechanisms underlying orchestration of these events remain mostly enigmatic. To achieve such a tight spatiotemporal regulation, flaviviruses, like the vast majority (if not all) of positive-strand RNA viruses, induce massive rearrangements of ER membranes to create a replication-favorable microenvironment that is generically called "replication factories (RF)" (Chatel-Chaix and Bartenschlager, 2014; Paul and Bartenschlager, 2015). These organelle-like ultrastructures host vRNA synthesis among other functions (discussed in more detail below). They are believed to spatially segregate the different steps of the viral life cycle although this model is primarily based on descriptive ultrastructural studies using electron microscopy (Welsch et al., 2009; Gillespie et al., 2010; Miorin et al., 2013; Junjhon et al., 2014; Bily et al., 2015; Cortese et al., 2017). However, there remains a knowledge gap regarding the fate of the vRNA in the cytoplasm of the infected cell. The majority of imaging studies have relied on antibody-based detection of the viral double-stranded (ds) RNA, the positive strand/negative strand hybrid replication intermediate and hence, do not take into consideration vRNA populations engaged in translation or encapsidated into virions. In addition, no detailed fluorescence *in situ* hybridization (FISH)-based sub-cellular distribution analyses of flaviviral vRNA and negative strand intermediate RNA have been reported to date in contrast with those of hepatitis C virus, a non-flavivirus member of the *Flaviviridae* family (Shulla and Randall, 2015).

The 10–11 kb-long flavivirus vRNA genome is composed of one open reading frame (ORF) flanked by highly structured 5′ and 3′ untranslated regions (UTR) (Selisko et al., 2014; Ng et al., 2017). The viral 5′UTR and 3′UTR have been demonstrated to engage in interactions with both host and viral proteins. The 3′UTR can be sub-divided into three sub-domains: (1) a highly variable region located immediately after the stop codon, which is implicated in viral adaptation to the host (Villordo et al., 2015); (2) the moderately conserved region and (3) a highly conserved region (**Figure 1A**). Most importantly, the vRNA shows a high structural plasticity, as it must undergo conformational changes implicated in the different steps of the viral life cycle. For instance, for efficient genome replication, the genome adopts a "pan-handle"-like circularized structure, which is achieved through long range RNA-RNA interactions between 5′ and 3′ termini. Several circularization motifs (discussed in more detail below) have been identified and are depicted in **Figure 1**. Interestingly, several sequences and structures in the 5′ and 3′UTRs can harbor multiple functions during distinct steps of the life cycle.

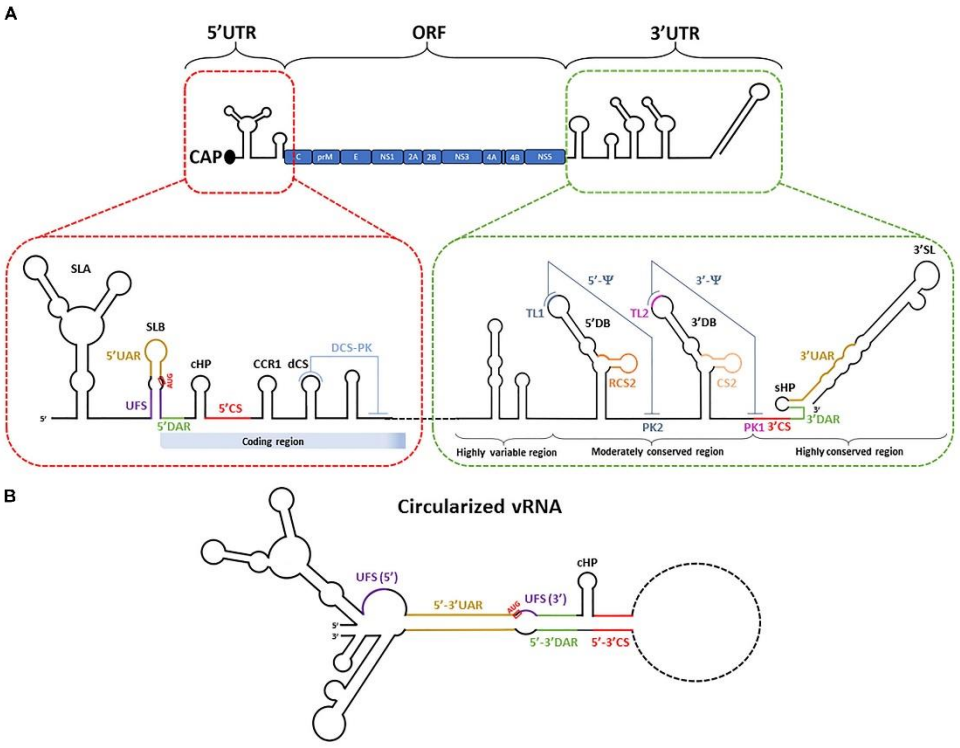

FIGURE 1 | Schematic representation of flavivirus vRNA. **(A)** vRNA is composed of a 5′UTR, one single open reading frame and a 3′UTR. The position of the sequences encoding for the viral proteins within the polyprotein is indicated. The bottom part of the figure shows in details the secondary structures of 5′UTR, capsid-coding region and 3′UTR. The different regions engaged in local pseudoknots and long-range RNA–RNA interactions are indicated and described in detail in the text. **(B)** Predicted structure of vRNA in its circularized conformation. The coding sequence (except 5′ capsid coding region) is depicted with a dashed line.

VIRAL TRANSLATION

Translation of the vRNA occurs at the surface of the ER and results in the synthesis of a highly membrane-associated polyprotein product. This polyprotein is further processed by host and cellular proteases co- and post-translationally through an ordered process that presumably dictates the ER topology of the mature viral proteins. Following the entry of the virion into the target cell, the first round of translation must take place in order to produce all viral proteins (including the viral RNA polymerase), which are absent from the infectious virus particle. Hence, vRNA translation is a critical step for the initiation of vRNA synthesis and subsequent amplification. The flaviviral genome, like cellular messenger RNAs (mRNA), contains a cap structure at the 5′ end which enables translation through canonical cap-dependent translation initiation (Garcia-Blanco et al., 2016). The addition of the cap is mediated by NS5 protein's methyltransferase activity in combination with the nucleotide triphosphatase activity of NS3. NS3 removes a phosphate from the 5′ terminus of the vRNA and NS5 catalyzes the addition of guanosine monophosphate (GMP) as well as the methylation of both this guanine on N-7 and the ribose-2′ OH of the first adenosine to form a type 1 5′ cap structure (m^7GpppAm2) (Egloff et al., 2002; Ray et al., 2006; Klema et al., 2016; Wang et al., 2018). Remarkably, in contrast to cellular mRNAs, vRNA lacks a 3′ poly-A tail. The poly-A tail is typically important for stability and to stimulate translation initiation of cellular mRNAs due to its strong association with poly-A-binding protein (PABP), which interacts with the cap-binding complex eIF4F and mediates the circularization of the mRNA. Despite the lack of a poly-A tail, the 3′ end of DENV RNA can associates with PABP *in vitro* (Polacek et al., 2009). This interaction appears to be specific for A-rich sequences flanking the DB structures upstream the terminal 3′SL motif of the 3′UTR (**Figure 1A**). Moreover, in *in vitro* translation assays using cell extracts, treatment with Paip2, an inhibitor of PABP, repressed translation of a reporter mRNA containing the DENV2 5′UTR, the first 72 nt of capsid coding sequence and the 3′UTR in a dose-dependent manner. This suggests that

PABP/3′UTR interaction mimics the role of mRNA poly-A tail and presumably stimulates translation initiation. In addition, the 3′SL structure also modulates DENV translation. However, since this motif is functional *in vitro* within mRNAs containing either an internal ribosome entry site (IRES) or a non-functional cap, it was proposed that the 3′SL independently influences translation after cap binding by the small 40S ribosomal subunit (Holden and Harris, 2004).

Another stem loop structure in 5′UTR named "capsid-coding region hairpin" (cHP) is also implicated in flaviviral translation (Clyde and Harris, 2006). Mutations in the cHP sequence which abrogate its secondary structure decreased initiation from the first AUG codon resulting in the production of shorter capsid protein products expressed from reporter RNAs in human hepatoma Hep3B and mosquito C6/36 cells. This highlights that cHP is important for initiating translation from the correct start codon and for generation of a functional capsid protein. Moreover, viral translation also relies on two pseudoknot motifs within the 3′UTR called 5′ψ and 3′ψ. They involve two identical dumbbells structures termed 5′-DB and 3′-DB (or DB1 and DB2, respectively) which are both flanked by A-rich regions. Their formation is promoted by the presence of "conserved sequences" RCS2 and CS2 in 5′-DB and 3′-DB, as well as their respective terminal loops which both contain five nucleotide sequences named TL1 and TL2 (**Figure 1A**). TL1 and TL2 are complementary to pentanucleotide sequences PK1 and PK2 downstream of each DB. TL1/PK2 and TL2/PK1 tertiary interactions constitute the 5′ψ and 3′ψ pseudoknots, respectively (Olsthoorn and Bol, 2001; Manzano et al., 2011). Similar structures have also been reported for other flaviviruses such as JEV and YFV (Olsthoorn and Bol, 2001). Manzano and colleagues have also reported that the TL1 and TL2 are important for flavivirus translation in BHK-21 cells, but their respective contributions to translation appear unequal (Manzano et al., 2011). Indeed the deletion of TL2 impaired translation only modestly while disruption of TL1 had no effect. However, the deletion of both sequences resulted in a more severe phenotype strongly suggesting that TL1 and TL2 act synergistically to enhance translation from the DENV vRNA. A similar phenotype was observed when TL1 and TL2 were swapped. Importantly, mutations abrogating TL/PK complementarity impeded translation, which returned to wild-type levels by mutations that restored base pairing, highlighting the importance of these tertiary interactions. However, in contrast to TL1 and TL2, PK1 and PK2 are not absolutely necessary for translation suggesting that alternative TL receptors within the vRNA might exist. For instance, when the PK1 sequence is mutated, TL2 might interact with the top loop of 3′-SL. Taken together, these observations highlight that this core RNA region is crucial for the regulation of efficient viral translation.

In addition to canonical initiation of translation, cap-independent mechanisms of translation have also been described for DENV. Indeed, DENV can achieve vRNA translation and wild-type production of infectious viral particles when cap-dependent translation is inhibited by treating the cells with drugs that impair the phosphoinositol-3 kinase (PI3K) pathway. Moreover, expression knockdown of eIF4E (a component of the eiF4F cap-binding complex) in hamster BHK-21 or monkey Vero cells led to a 60% decrease in total cellular protein synthesis, whereas DENV NS5 protein levels decreased by just 10% (Edgil et al., 2006). This data suggests that DENV translation initiation can also occur in a cap-independent manner. DENV cap-independent translation appears to be regulated by both 5′ and 3′UTRs. Nonetheless, no IRES has been identified for flaviviruses in contrast to virus from other genus within the *Flaviviridae* such as hepatitis C virus (HCV) (Perard et al., 2013).

Using polysome profiling, Roth and coworkers have demonstrated that all tested flaviruses (namely all DENV serotypes, pathogenic WNV, historical and contemporary ZIKV strains) induce a general shut-off of host cell translation early following infection in human hepatocarcinoma Huh7 cells (Roth et al., 2017). This DENV-induced translation inhibition occurs at the initiation step. Interestingly, another group has recently shown that DENV infection in Huh7 cells negatively regulates the translation of host mRNAs that are associated with the ER without impacting the synthesis cytosolic proteins (Reid et al., 2018). In contrast, translation of vRNA appears to be unaffected by this global inhibition strongly supporting that flaviviruses specifically divert host protein synthesis for the benefit of viral translation and/or other steps of the life cycle. Importantly, cellular stresses such as infection or oxidative stress induce perturbations in cell translation (Anderson and Kedersha, 2008). More specifically, such stresses can induce translational arrest associated with polysome disassembly, and a concomitant appearance of stress granules (SG). SGs are cytoplasmic granules composed of untranslated mRNAs and the translation initiation machinery comprising proteins of the 48S preinitiation complex including eIF3, eIF4A, eIF4G, PABP1 and small ribosomal subunits (Anderson and Kedersha, 2008). In most of the cases, the formation of SGs requires the phosphorylation of eIF2α by protein kinase R (PKR) or PKR-like endoplasmic reticulum kinase (PERK). In its phosphorylated form, eIF2α inhibits global protein translation by reducing levels of the eIF2α-GTP-$tRNA^{Met}$ ternary complex, which is absolutely required for translation initiation. Surprisingly, it appears that DENV-mediated repression of translation initiation is not functionally linked to PKR, infection-associated eIF2α phosphorylation or SG induction. These observations are consistent with several studies that have reported that DENV, ZIKV and WNV infection inhibits the formation of SGs, especially when cells are under oxidative stress following treatment with the SG inducer sodium arsenite (Emara and Brinton, 2007; Amorim et al., 2017; Roth et al., 2017). In such conditions, reductions in the number of formed SGs and a decrease of phospho-eIF2α levels are observed in infected cells. This inhibition seems to be specific to eIF2α-specific SGs since ZIKV infection did not impact of the formation of SGs upon pateamine A or sodium selenite treatments which do not require prior eIF2α phosphorylation and are devoid of the SG marker TIA-1-related protein (TIAR) (Amorim et al., 2017). Interestingly, eIF2α-specific SG components T cell internal antigen-1 (TIA-1) and TIAR, which are known to induce translational silencing (Anderson and Kedersha, 2008) are diverted by flaviviruses to regulate replication

(Li et al., 2002; Emara and Brinton, 2007). Indeed, in infected BHK-21 cells, these factors colocalize with viral proteins and dsRNA within the replication complex. Such relocalization has also been observed in TBEV-infected cells and it was proposed that these host factors inhibit the translation of the TBEV vRNA (Albornoz et al., 2014). Overall, these studies support the idea that flaviviruses manipulate host cell gene expression at the translational level to favor viral protein production and generate a cellular state which is favorable to replication.

vRNA REPLICATION

Overview of the vRNA Synthesis Process

vRNA replication is the core step leading to virus amplification and consists of *de novo* RNA synthesis (i.e., without initiation from a preexisting primer). Within RFs (see below), it generates a pool of neosynthesized vRNA molecules that are subsequently used for the formation of new replication complexes, for translation-driven production of viral proteins and for packaging into assembling virus particles. vRNA replication relies on the RNA-dependent RNA polymerase (RdRp) activity of flaviviral NS5 protein, through an asymmetric process. vRNA synthesis is initiated by binding of NS5 to a secondary structure located at the 5′ terminus of the genome called "stem loop A" (SLA) which is critical for the initiation of vRNA synthesis (Filomatori et al., 2006). NS5 synthesizes first one molecule of negative-strand intermediate RNA using the positive-strand vRNA as a template. Subsequently, new copies of vRNA are made from this negative strand RNA, with a higher proportion of positive-strand vRNAs produced (You and Padmanabhan, 1999; Guyatt et al., 2001). NS5 requires both 5′ and 3′UTRs to initiate negative-strand RNA synthesis (Filomatori et al., 2006; Hodge et al., 2016). For the synthesis of this antigenome, the vRNA must adopt a circularized panhandle-shaped structure formed through long range interactions between the 5′ and 3′UTRs. This conformation allows to position the 5′ and 3′UTR in close proximity and to transfer SLA-bound NS5 from the 5′UTR to the 3′ stem loop (3′SL) located at the terminus of the 3′UTR. More specifically, NS5 interacts with the top loop of the 3′SL which is highly conserved across the *Flavivirus* genus (Hodge et al., 2016). This configuration of NS5 enables the initiation of negative-strand synthesis using a pppAG dinucleotide as a primer. Following antigenome synthesis, NS5 can polymerize many copies of the positive-strand vRNA from the negative-strand intermediate. NS5 is optimized to specifically use the pppAG dinucleotide as a primer. As a result, 3′ CU and 5′ AG (3′ CU in the antigenome) termini of vRNA are strictly conserved among flaviviruses (Selisko et al., 2012). The reasons why the flavivirus RNA synthesis is asymmetric in favor of the positive-strand RNA (i.e., vRNA) are still unclear. However, it has been proposed that in the double-stranded RNA state (vRNA/antigenome hybrid), vRNA SLA-bound NS5 molecules would be directly transferred from neosynthetized vRNA to the 3′ end of the negative-strand (instead of vRNA 3′SL) to directly reinitiate positive-strand synthesis (Garcia-Blanco et al., 2016). This is consistent with a JEV study that indicated a greater affinity of NS5 for the 3′ end of the negative-strand RNA than for vRNA 3′UTR (Kim et al., 2007). This model of asymmetric viral RNA replication supports the idea that the negative-strand would not be free in the cell but rather annealed with both template and/or neosynthesized vRNA molecules.

Other RNA secondary structures in the 3′UTR have also been reported to influence replication. For instance, in addition to their role in translation (as discussed above), the 5′ψ and 3′ψ tertiary structures in the DENV vRNA regulate RNA synthesis (Olsthoorn and Bol, 2001; Manzano et al., 2011). Indeed, mutations in PK or TL sequences disrupting the pseudoknots result in a decrease of viral replication. Similarly to the translation phenotype, the contributions of TL1 and TL2 to viral RNA replication are not equivalent. However, in contrast to what has been observed for translation, restoration of base pairing between the TL and PK sequences does not rescue the replication defects caused by individual mutations. This pinpoints that there are differences between the roles of 5′ψ and 3′ψ in translation and replication, in line with the idea that changes in the conformation of the vRNA modulate the different steps of the viral life cycle.

It is believed that NS3 helicase assists vRNA synthesis presumably through direct interactions with NS5 (Johansson et al., 2001; Takahashi et al., 2012). Although this helicase activity is absolutely required for flavivirus life cycle, it remains unclear which exact step of vRNA synthesis it regulates in infected cells. Nevertheless, based on *in vitro* analyses, several models have been proposed. NS3 helicase activity is most likely involved in vRNA synthesis from the negative strand. According to the model described above in which vRNA synthesis is initiated from dsRNA, NS3 would be required to unwind this molecule and displace the original vRNA molecule in favor of the nascent genome. Moreover, it cannot be excluded that NS3 also contributes to the synthesis of the antigenome by unwinding secondary and tertiary structures in vRNA. Finally, NS3 might unwind the RNA duplex so that neosynthesized positive-strands can be translated or packaged into assembling viral particles.

Genome Circularization

As discussed above, the cyclization of the vRNA is critical for the initiation of genome replication through the recruitment of NS5 to SLA in the 5′UTR. vRNA shows a high structural plasticity with ample evidence to suggest that several sub-domains act as riboswitches to regulate the different steps of the viral life cycle, including initiation of RNA synthesis (**Figure 1B**). Firstly, DENV vRNA can adopt different conformations during infection, and switching from circular to linear conformations modulates negative and positive-strand RNA synthesis (Villordo et al., 2010). This structural plasticity relies on the highly structured 5′ and 3′UTRs, with the presence of a variety of stem loop structures termed "cyclization sequences" (or elements). Through sequence complementarity, they contribute to long range RNA-RNA interactions and hence, promote the circularization of the flaviviral genome. Notably, evidence of individual molecules of circularized DENV vRNA has been provided *in vitro* using atomic force microscopy (Alvarez et al., 2005). One of the main cyclization elements involved in this process are the "conserved sequences" (CS). They are constituted of 8 or more nucleotides

located in the 5′ region of the capsid-coding sequence and in the 3′UTR. CSs were first identified in WNV and have been demonstrated to be essential for flaviviral replication in BHK-21 cells (Khromykh et al., 2001a). However, Alvarez and colleagues later demonstrated that the base pairing between the 5′ and 3′ CS alone was necessary, but not sufficient for vRNA circularization *in vitro*. They demonstrated that other cyclization motifs contribute to this long range RNA-RNA interaction (Alvarez et al., 2005). Indeed, the "upstream AUG regions" (5′ UAR) located before the polyprotein start codon in "stem loop B" (SLB) interacts with the 3′ UAR which overlaps with the "small hairpin" (sHP) in the highly conserved 3′SL at the terminus of 3′UTR (**Figure 1**). The "downstream AUG region" (DAR) long range interaction is also an important determinant of genome circularization. Of note, DAR are not very conserved among flaviviruses and while DENV show only one DAR interaction, WNV and YFV seem to rather possess a bipartite element (named DAR1 and DAR2) (Friebe et al., 2011; Brinton and Basu, 2015). In the case of DENV, a region of 6 nucleotides identified in the 5′ region of the genome (5′DAR) is involved in DENV replication and possibly also RNA cyclization. The 3′DAR sequence mapping to the 5′ stem of sHP is complementary to the 5′DAR (Friebe and Harris, 2010; Villordo et al., 2010). Consistently, sHP has been demonstrated to be implicated in long-range RNA–RNA interactions, with a major contribution from the UAR-containing stem. Moreover, DENV harboring mutations in the stem of this structure replicates less efficiently than wild-type virus. However, while mutations in the 3′ DAR sequence impact viral replication, its role in genome circularization through interactions with 5′ DAR is less clear. In fact, 3′ DAR mutations would rather influence the stability and/or the formation of sHP and this may explain their overall impact on viral genome replication. Friebe and Harris have hypothesized that the 5′-3′ DAR interaction might not be needed to make the 3′UAR accessible to the 5′ UAR. Instead, they propose that the UAR, CS, DAR and cHP sequences constitute a functional unit essential for the circularization of vRNA (Friebe and Harris, 2010). In addition to its role in start codon selection during translation (see above), the cHP structure has also been shown to be important for DENV and WNV vRNA synthesis in a sequence-independent manner. How cHP influences vRNA synthesis remains to be determined; however, one possibility is that, within this functional unit, it contributes to the formation and/or stabilization of the vRNA panhandle structure (Clyde et al., 2008).

A sequence present downstream of the 5′ CS element in the capsid-coding sequence called "downstream CS" (dCS) is important for flavivirus replication and this sequence impacts genome circularization by modulating the topology of the 5′ end. In line with this, changes in the dCS sequence composition affects the formation of the 5′-3′ long range RNA-RNA interactions (Friebe et al., 2012). Moreover, an RNA motif termed "downstream of 5′ CS pseudoknot" (DCS-PK) also enhances replication in BHK-21 cells by regulating circularization (Liu et al., 2013). This tertiary interaction localizes to the capsid-coding region and appears to be constituted by a three-stem pseudoknot structure. Disruption of the DCS-PK structure hinders the ability of the 5′ RNA to bind 3′ RNA, while the rescue of DCS-PK structure recovered the formation of this 5′-3′ interaction. It was proposed that both dCS and DCS-PK contribute to the function of the cyclization unit containing 5′UAR, 5′CS, 5′DAR, and cHP. In this model, the DCS-PK sequence might help this unit to adopt specific conformations which favor genome circularization.

A structure present downstream SLA in the 5′UTR has been recently identified as an important riboswitch, which controls the equilibrium between NS5 recruitment to SLA and the circularization of the vRNA. This motif named "5′ UAR-flanking stem" (UFS) is a U-rich region located in SLB that promotes the formation of a conserved duplex RNA (Liu et al., 2016). The conformation of UFS is critical for the recruitment of NS5 to SLA and the SLA-dependent initiation of RNA synthesis. Indeed, mutations disrupting UFS result in a decrease in NS5 binding to the 5′UTR *in vitro* and consequently of replication. In contrast, increasing the stability of the UFS does impede vRNA circularization. If UFS is too stable, this could result in a "locked-up" conformation of the UAR sequence which is known to be implicated in long range RNA-RNA interactions. Consistently, the circularization of vRNA induced the melting of the UFS structure resulting in a decrease in affinity of NS5 for the 5′ end of the vRNA. These data support a model in which the UFS functions as a riboswitch during RNA replication, which dictates vRNA circularization and NS5 recruitment. Following the binding of NS5 to SLA, the circularization of the vRNA would induce a disruption of the UFS structure, leading to a decrease in the affinity between NS5 and the 5′UTR. This would favor NS5 transfer to the 3′UTR, hence properly positioning the polymerase for negative-strand RNA synthesis.

Viral Replication Factories

A striking feature of flaviviral infections is the appearance of organelle-like membranous replication factories (RF) resulting from severe alterations of ER membranes. The detailed tridimensional architecture of RFs from several flaviviruses has been reconstructed using electron tomography (Welsch et al., 2009; Gillespie et al., 2010; Miorin et al., 2013; Junjhon et al., 2014; Bily et al., 2015; Cortese et al., 2017). RFs are constituted of several sub-structures namely vesicle packets (VP), convoluted membranes (CM), and virus bags (VB) which are morphologically different and can be found within the same ER network.

Vesicle packets are spherical vesicles which are induced by invaginations of the ER (**Figure 2**). They show similar morphology in both mosquito and mammalian cells suggesting that their biogenesis relies on evolutionary conserved host machineries and pathways. In mammalian cells, their diameter is approximately 90 nm and they are connected to the cytoplasm by a 10 nm-wide pore. Interestingly, it was shown that in the case of WNV and TBEV, vesicles within the same ER cisternae are also connected to each other by pore-like openings suggesting that they exchange material (Gillespie et al., 2010; Offerdahl et al., 2012; Miorin et al., 2013). The determinants of both types of pores are completely unknown. Immunogold labeling combined with electron microscopy has revealed that VPs contain dsRNA, the replication intermediate as well as

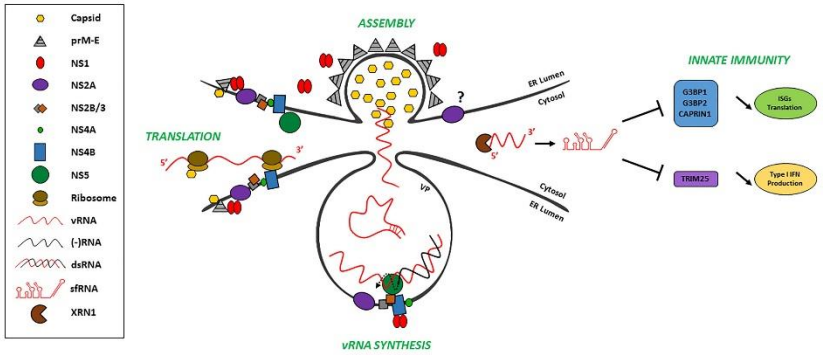

FIGURE 2 | A model of the different fates of vRNA. vRNA is replicated by NS5 within the vesicle packets (VP) with the assistance of other nonstructural proteins. Using vRNA, the positive strand (red), as a template, the synthesis of the negative strand (black) by NS5 is depicted. Subsequently, several new copies of vRNA are produced from the dsRNA replication intermediate (not shown). Translation presumably occurs outside of VPs since ribosomes can be visualized adjacent to these structures. vRNA is proposed to exit VPs through a pore to be directly encapsidated and enveloped into juxtaposed ER budding structures. Finally, vRNA is partially degraded by cellular XRN1 which generate sfRNA. sfRNA regulates several host responses including innate immunity at the levels of signal transduction and ISG translation.

several viral non-structural proteins absolutely required for replication such as NS5, NS3, NS1, NS4A and NS4B (Welsch et al., 2009; Miorin et al., 2013; Junjhon et al., 2014). Hence, it is strongly believed that vRNA synthesis takes place in this compartment. Nevertheless, it remains unclear if VPs are absolutely required for replication or if other ER sub-compartments can support replication. Furthermore, it is also thought that VPs constitute an environment favorable to vRNA synthesis. Indeed, they may play a role in protecting the vRNA from degradation by nucleases or recognition by cytosolic sensors of RNA, dampening the activation of antiviral signaling pathways. Finally, VPs would allow the concentration of metabolites, as well as cellular and viral factors required for efficient vRNA synthesis. However, these models remain to be experimentally validated.

Convoluted membranes are large reticular structures enriched in NS2B/3, NS4A and NS4B that are induced by membrane curvature and morphologically resemble tight accumulations of smooth ER membranes (Westaway et al., 1997; Miller et al., 2007; Welsch et al., 2009; Chatel-Chaix et al., 2016). The exact role of CMs is not well understood; however, they have been recently proposed to modulate cellular processes such as innate immunity or inter-organellar communication in order to create a proviral cytoplasmic environment rather than to directly regulate vRNA synthesis *per se* (Chatel-Chaix et al., 2016).

Newly assembled virions accumulate in regular arrays into VBs which are dilated ER cisternae (Welsch et al., 2009; Cortese et al., 2017). VPs and VBs may be found in close proximity within the same ER network, which contains ribosomes on its cytosolic side. This suggests that RFs provide a platform for the transfer of viral genomes between replication complexes, ribosomes and assembling virus particles. Moreover, this confers a spatial segregation of the different vRNA-containing complexes allowing the coordination of vRNA translation, replication and encapsidation in both space and time.

Trans Co-factors Involved in vRNA Replication

All flaviviral NS viral proteins are absolutely required for vRNA synthesis (Apte-Sengupta et al., 2014; Selisko et al., 2014); yet, only NS5 and NS3 possess enzymatic activities. The transmembrane proteins NS1, NS4A and NS4B are believed to be implicated in the formation of RFs. Notably, when transiently expressed alone, DENV and WNV NS4A are able to induce to some extent the formation of CMs in Huh7 and Vero cells, respectively (Roosendaal et al., 2006; Miller et al., 2007). NS1 was shown to alter liposome membrane *in vitro* (Akey et al., 2014). Considering that all of the NS proteins physically and/or genetically interact, it is tempting to speculate that they synergistically act to coordinate the different steps of vRNA replication. For instance, the interaction between NS5 and NS3 seems to be important to functionally couple vRNA synthesis and dsRNA unwinding (Yu et al., 2013; Tay et al., 2015). Moreover, the DENV NS3 helicase domain associates with the cytosolic loop of the NS4B transmembrane protein (Umareddy et al., 2006; Chatel-Chaix et al., 2015; Zou et al., 2015a). NS4B mutants that lose the capacity to interact with NS3 are defective in replication suggesting that the integrity of this complex is critical for DENV life cycle. Interestingly, NS4B was shown to promote the dissociation of NS3 from single-stranded RNA (Umareddy et al., 2006) implying that it would indirectly stimulate the recruitment of the helicase toward newly formed replication intermediates and would promote their unwinding. Finally, NS4B homodimerizes and interacts with both NS1 and NS4A (Youn et al., 2012; Zou et al., 2014, 2015b; Chatel-Chaix et al., 2015; Li et al., 2015). This further supports that protein-protein

interactions coordinate the activity of the replication complexes with a precise ER membrane topology within VPs.

Finally, numerous cellular RNA-binding proteins have been reported to interact with flaviviral vRNA and to modulate genome replication. Some examples are listed in **Table 1**. While vRNA binding motifs have been identified in some studies, the precise molecular mechanisms by which these proteins modulate the viral life cycle remain unclear in most cases. Some proteins show specificity for vRNA motifs. For example, TIA-1 and TIAR interact with negative-strand RNA 3′ SL of WNV and the knockout of these proteins decreases viral titers implicating these interactions in efficient viral replication (Li et al., 2002). In contrast, DDX6 and NF90 modulate DENV replication presumably through their interaction with the DB and 3′ SL structures in the 3′UTR of the vRNA, respectively (Gomila et al., 2011; Ward et al., 2011). Finally, the isoform p45 of host protein AUF1 (also named hnRNP D) was reported to positively regulate the replication of WNV, DENV and ZIKV in Huh7 cells by promoting vRNA circularization. Indeed, AUF1 destabilizes SLB and the 3′ SL thereby exposing the UAR circularization elements (Friedrich et al., 2014, 2018) (**Figure 1B**). This illustrates that host factors are able to impact viral genome plasticity and to regulate important riboswitches in the flaviviral vRNA.

vRNA PACKAGING

During virus assembly, the vRNA genome must be encapsidated into neosynthetized viral particles. This step of the flavivirus life cycle which is a prerequisite for full infectivity is one of the least characterized and understood at the molecular level. Our understanding of the vRNA packaging process remains limited due to the lack of identification of (presumably short-lived) assembly intermediates. Moreover, comprehensive studies about

TABLE 1 | Host RNA-binding proteins involved in flavivirus life cycle.

Host factor	Virus	Role	Regulated step(s)	vRNA binding site	Reference
CSDE1	DENV	Proviral	Translation/replication?	UTR	Phillips et al., 2016
DDX3	JEV	Proviral	Translation	5′UTR + 3′UTR	Li et al., 2014
DDX5	JEV	Proviral	Translation/replication?	3′UTR	Li C. et al., 2013
DDX6	DENV	Proviral	?	3′UTR (5′and 3′ DB)	Ward et al., 2011
eEF1α	DENV/WNV	proviral	Replication	DENV 3′UTR (between 3′CS and 3′ end)/WNV 3′ SL	Blackwell and Brinton, 1997; De Nova-Ocampo et al., 2002; Davis et al., 2007
ERI3	DENV/YFV	Proviral	Replication	3′UTR (DB)	Ward et al., 2016
FBP1	JEV	Antiviral	Translation	5′UTR + 3′UTR	Chien et al., 2011
hnRNP A2/B1	DENV/JEV	Proviral	?	DENV 3′UTR/JEV 5′ end of (-) RNA	Paranjape and Harris, 2007; Katoh et al., 2011
hnRNP C1/C2	DENV	Proviral	Replication? (not translation)	?	Dechtawewat et al., 2015; Phillips et al., 2016
hnRNP D/AUF-1	ZIKV/DENV/WNV	Proviral	Replication	5′UTR (SLB) + 3′UTR (3′SL)	Friedrich et al., 2014; Friedrich et al., 2018
hnRNP G/RBMX	DENV	Proviral	Translation/replication?	?	Viktorovskaya et al., 2016
La	JEV	Proviral	?	5′UTR + 3′UTR (3′ SL)	Vashist et al., 2009; Vashist et al., 2011
LSm1	DENV	Proviral	?	3′UTR	Dong et al., 2015
Musashi-1	ZIKV	Proviral	Translation/replication?	3′UTR	Chavali et al., 2017
NF90	DENV	Proviral	Translation/ replication?	3′UTR (3′SL)	Gomila et al., 2011
p100	DENV	Proviral	Translation	3′UTR (between 3′ CS and 3′ end)	Lei et al., 2011
PABP	DENV	Proviral	Translation	3′UTR (3′SL)	Polacek et al., 2009; Phillips et al., 2016
PTB	DENV/JEV	Proviral (DENV)/antiviral (JEV)	Translation/replication	DENV 3′UTR/JEV 5′UTR+(-) RNA	De Nova-Ocampo et al., 2002; Agis-Juarez et al., 2009; Bhullar et al., 2014
QKI	DENV (DENV4 only)	Antiviral	Translation?	3′UTR	Liao et al., 2018
RPLP1/2	DENV/YFV/ZIKV	Proviral	Translation	?	Campos et al., 2017
TIA1/TIAR	WNV	Proviral	Replication	3′SL of (-) RNA	Li et al., 2002; Emara et al., 2008
YBX1	DENV	Antiviral/proviral?	Translation (antiviral)/virus production (proviral)	3′UTR (3′SL)	Paranjape and Harris, 2007; Phillips et al., 2016
ZAP	JEV	Antiviral	?	3′UTR (DB)	Chiu et al., 2018

For each cellular co-factor, the virus(es), the known RNA-binding site(s) and the step(s) of its life cycle which is regulated are indicated. For simplification purposes, an indicated role in translation does not exclude an impact on vRNA stability. (-)RNA, Minus strand viral RNA.

the intracellular distribution of the different vRNA populations are lacking.

The vRNA encapsidation process must face several "challenges" that intuitively, have to be tightly regulated. First, this process must be specific. Only vRNA is encapsidated while cellular RNA and viral negative-strand intermediate RNA must be excluded from the capsid. Second, the stoichiometry of the viral genome inside the virion (i.e., vRNA copy number per virion) is important for optimal infectivity (Kuhn et al., 2002; Byk and Gamarnik, 2016). The highly basic viral capsid protein binds with high affinity to the negatively charged vRNA in what is presumed to be a rather non-specific manner through electrostatic interactions (Pong et al., 2011; Byk and Gamarnik, 2016). However, as capsid molecules far outnumber the copies of vRNA in the virion, vRNA packaging must be regulated to achieve optimal vRNA intraviral stoichiometry (presumably one genome copy per virion) and full infectivity. In contrast to several other viruses like HIV-1 (Comas-Garcia et al., 2016), no *bona fide* RNA packaging signal has been identified for members of the *Flavivirus* genus. If packaging signal do exist, they are most likely to be located within the highly structured untranslated regions. Indeed, in the case of the related *Hepacivirus* HCV, the 3′UTR was shown to be important for RNA *trans*-encapsidation while mechanistic details are still being characterized (Shi et al., 2016). Identifying putative flaviviral packaging signals remains challenging because, if located in the UTRs, they are likely to overlap with motifs important for translation and vRNA synthesis. Hence, mutation of these putative motifs may also potentially affect viral replication (and indirectly downstream virus assembly), making it difficult to functionally segregate replication from vRNA packaging. Nevertheless, one study has identified a *cis*-acting RNA motif that influences virus assembly. Using a silent mutagenesis approach, Groat-Carmona and colleagues demonstrated that the conserved DENV "capsid-coding region 1" (CCR1) influences the production of infectious particles in both insect C6/36 and mammalian BHK-21 cells without affecting vRNA stability, translation and synthesis (Groat-Carmona et al., 2012). Importantly, DENV replication as well as dissemination from the mid-gut to the salivary glands in the mosquito vector relied on the integrity of the CCR1 structure, highlighting the importance of this RNA motif *in vivo*. Since CCR1 mutations resulted in a drastic reduction in infectious titers without affecting the levels of extracellular vRNA, a contribution of CCR1 in vRNA packaging was ruled out by the authors and its exact role in virus assembly is still unknown. Nevertheless, a putative reduction of vRNA packaging may have been masked by the presence of non-encapsidated newly synthesized vRNA in the cell supernatants, which could have been released from the cell within exosomes in a viral assembly independent manner. Hence, a possible role of CCR1 in vRNA packaging should likely be re-evaluated. As discussed above (see vRNA replication), the structural dynamics of the vRNA itself allow it to orchestrate the different steps of vRNA replication including vRNA circularization, NS5 binding and RNA synthesis. Considering that some vRNA domains can function as riboswitches, it is tantalizing to speculate that conformational changes in vRNA secondary and tertiary structures drive vRNA transfer from replication complexes in VPs to assembling virions. Moreover, the methylation status of the vRNA might contribute determining its fate. Indeed, it was recently shown that DENV, WNV, YFV, ZIKV and HCV vRNAs are N^6-methylated on adenosines by the host methyltransferases METTL3 and METTL14 in infected cells (Gokhale et al., 2016; Lichinchi et al., 2016). Very interestingly, N^6A-methylated ZIKV vRNA is associated with cellular YTHDF proteins that inhibit infectious particle production (Lichinchi et al., 2016). In the case of HCV, the same inhibition is observed and it correlates with the redistribution of YTHDF proteins to lipid droplets (the virus assembly site) while this did not influence the vRNA replication process. Thus, this strongly suggests that N^6A methylation specifically regulates virus assembly (Gokhale et al., 2016). Based on these results and the possible conservation across the *Flaviviridae* family, one might hypothesize that only vRNA molecules that are not N^6A-methylated are packaged into assembling viruses. In addition, it is reasonable to consider that the methylation of vRNA influences its folding and hence, its functions during the different steps of the viral life cycle. Such hypotheses will likely be challenged in future studies.

Although no vRNA packaging signal has been identified, it is well established that *trans*-encapsidation is possible for flaviviruses. Indeed, when structural proteins are expressed in *trans*, they form virus-like particles that can encapsidate sub-genomic replicons, i.e., replication-competent genomes that express only NS proteins (Khromykh et al., 1998; Ansarah-Sobrinho et al., 2008; Qing et al., 2010; Suzuki et al., 2014; Scaturro et al., 2015). The resulting *trans*-complemented particles are infectious and are able to undergo a single round of infection. Interestingly, the structural proteins are able to encapsidate genomes from other flaviviruses (Yoshii et al., 2008; Shustov and Frolov, 2010; Suzuki et al., 2014). This strongly suggests that the *cis* RNA and *trans* protein determinants of the vRNA packaging process are conserved across the *Flavivirus* genus. However, it remains elusive how the flaviviral genome is specifically selected for encapsidation. Like HCV core protein, flaviviral C protein accumulation on lipid droplets is important for the generation of infectious virus particles (Miyanari et al., 2007; Samsa et al., 2009; Carvalho et al., 2012; Martins et al., 2012; Iglesias et al., 2015). However, this pool of structural proteins may represent a storage compartment for assembly competent capsid rather than the actual site of genome selection and particle assembly. Interestingly, early studies on YFV and Murray Valley encephalitis virus (MVEV), another flavivirus, have highlighted that polyprotein processing and virus morphogenesis are functionally linked (Lobigs, 1993; Lee et al., 2000; Lobigs and Lee, 2004; Lobigs et al., 2010). Indeed, uncoupling these two processes by introducing mutations altering the processing kinetics of the signal peptide between capsid and prM, critically impaired nucleocapsid envelopment and the production of infectious viral particles. Most strikingly, several independent ultrastructural studies on DENV and ZIKV based on 3D reconstruction of replication factories revealed structures budding into the ER and juxtaposed to the pore of the VPs, the presumed site of vRNA replication (see above and **Figure 2**) (Welsch et al., 2009; Junjhon et al., 2014; Cortese et al., 2017). This pore

was observed in 90% of DENV VPs and is homogenous in size (diameter of ∼10 nm) (Welsch et al., 2009). In the case of WNV, the RNA inside the VP is aligned with the pore (Gillespie et al., 2010). However, nothing is known about its morphogenesis and dynamics, and the viroporin activity of VP-associated NS2A, NS2B and NS4B transmembrane proteins might participate to this process (Chang et al., 1999; Leon-Juarez et al., 2016; Shrivastava et al., 2017). In addition, the juxtaposed budding structures have the size of assembled virions and contain an electron dense core which may correspond to a vRNA-containing capsid. Based on this observation, it is tempting to speculate that the vRNA replication and packaging processes are coordinated in time and space. The newly synthesized positive-strand genome molecule would exit the VP through the pore and be directly encapsidated into budding virions, hence conferring the selectivity of genome encapsidation. Such a coordinated model implies that the replication process and/or the presence of VPs would be required for vRNA encapsidation and envelopment by the ER membrane. This is further supported by early studies showing that replication is required for virus production in BHK-21 cells (Khromykh et al., 2001b). Indeed, DNA-launched WNV replication-deficient genomes fail to generate extracellular viral particles despite the presence of vRNA and structural proteins. It should be noted that replication is not required for the formation of sub-viral particles (i.e., devoid of the viral genome and non-infectious) whose budding can occur upon expression of prM/E alone (Schalich et al., 1996; Wang et al., 2009). Thus, it would be interesting to analyze the cellular RNA content of sub-viral particles since it is not known if they contain non-specifically enveloped cellular RNA or if they are free of nucleic acids. Importantly, it remains unclear how budding structures are physically juxtaposed to VPs and whether this event is absolutely required for the production of fully infectious virus. In addition to its critical function in replication, ZIKV and DENV NS1 were recently demonstrated to be important for both virus assembly and release (Scaturro et al., 2015; Yang et al., 2017). Consistently, ultrastructural studies have demonstrated that a fraction of DENV NS1 is associated with virions. Interestingly, mutants of the NS1 β-ladder domain lost their ability to indirectly associate with capsid while their interaction with glycoproteins E and prM was maintained (Scaturro et al., 2015). This suggests that NS1 might assist the specific envelopment of capsid/vRNA complexes in structures budding into the ER (**Figure 2**). Additionally, the expression level of WNV NS1', an alternative larger form of NS1 resulting from a translational frameshift was shown to influence the specific infectivity in *trans*-complementation experiments in BHK-21 cells (Winkelmann et al., 2011). In addition, NS2A also has an influence on both RNA replication and viral particle production (Liu et al., 2003; Leung et al., 2008; Vossmann et al., 2015; Wu et al., 2015; Xie et al., 2015; Yang et al., 2017). Finally, NS3 has specific functions during particle assembly independently from its enzymatic functions. Indeed the W349A mutation in YFV NS3 impacted infectious particle production while vRNA replication and the release of sub-viral particles remained unaffected (Patkar and Kuhn, 2008). Very interestingly, DENV NS3 helicase domain was shown to possess an RNA annealing activity *in vitro* (Gebhard et al., 2012), implying that it can influence the conformation of vRNA in infected cells. This suggests that through specific interactions with the vRNA (Swarbrick et al., 2017), NS3 might promote the exposure of a putative packaging motif and directly regulate genome encapsidation and/or capsid envelopment. This regulation might also involve a contribution of assembling virions since WNV capsid protein, similarly to NS3, possesses an RNA chaperoning activity *in vitro* (Ivanyi-Nagy and Darlix, 2012). Taken together, all these findings support the idea that viral proteins bring together replication and assembly complexes to orchestrate an efficient and selective vRNA encapsidation process.

Host factors may also play a role in the tight regulation of vRNA packaging during virus assembly. Several cellular RNA-binding proteins have been reported to associate with the flaviviral genome mostly through the UTRs, and to be important for the viral life cycle (**Table 1**). In most studies, the authors did not identify the exact step controlled by their candidate protein or may not have considered vRNA packaging in the analyses. Interestingly, the RNA-binding protein DDX56 appears to be important for the production of infectious WNV particles, but not for vRNA replication, strongly suggesting that it acts during vRNA selection for encapsidation (Xu et al., 2011; Xu and Hobman, 2012; Reid and Hobman, 2017). Nevertheless, while virions released from DDX56 depleted cells contained less encapsidated vRNA, a DDX56-vRNA interaction remains to be demonstrated.

Several of the identified flaviviral replication co-factors such as YBX1, hnRNP K, DDX6 or DDX3 were reported to also associate with the genome of HCV (Ariumi et al., 2007; Paranjape and Harris, 2007; Jangra et al., 2010; Chatel-Chaix et al., 2011; Chahar et al., 2013; Chatel-Chaix et al., 2013; Li et al., 2014; Brunetti et al., 2015; Poenisch et al., 2015; Phillips et al., 2016). Those host factors are components of the same ribonucleoprotein complex (RNP) (Vashist et al., 2012; Chatel-Chaix et al., 2013; Upadhyay et al., 2013) and some of them have been reported to regulate the equilibrium between HCV RNA replication and the production of infectious viral particles suggesting that they control the transfer of vRNA from replication to assembly complexes (Chatel-Chaix et al., 2011; Chatel-Chaix et al., 2013). Whether the viral co-opting of this host RNP is conserved across the *Flaviviridae* family will have to be evaluated in the future. Nonetheless, it is likely that flaviviruses, as obligatory intracellular parasites, hijack the function of several host RNA-binding proteins during vRNA encapsidation. One can envisage that such co-opting would influence or be modulated by the various 3D structures and modifications of the vRNA. Interestingly, several of *Flaviviridae* vRNA-binding proteins, such as hnRNP C, hnRNP A2/B1 and RBMX (see **Table 1**) were showed to have enhanced affinity for N^6A methylated RNAs whose local conformation is changed by this modification (Alarcon et al., 2015; Liu et al., 2015, 2017). This suggests a functional link between vRNA modifications, riboswitches and riboproteomic profiles. Thus, integration of all currently known models will likely help to provide a clearer understanding of how flaviviruses control genome selection for encapsidation.

FLAVIVIRAL RNA AND INNATE IMMUNITY

vRNA and Pattern Recognition Receptors

During viral entry or RNA amplification, flaviviral RNA can be sensed as foreign RNA by the cell and trigger antiviral innate immunity in mammalian cells. This first line of defense involves RNA sensors that, once activated, trigger a signaling cascade leading to the production of interferons (IFN) and interferon-stimulated genes (ISG). ISGs are antiviral effectors that in some cases, specifically target vRNA, may be secreted as proinflammatory cytokines or generate an overall antiviral state to impede virus replication (Adachi et al., 1998). Pattern recognition receptors (PRR) such as Toll-like receptor 3 (TLR3), retinoic acid-inducible gene I (RIG-I) as well as melanoma differentiation-associated protein 5 (MDA5) are expert sensors of highly structured viral RNAs or dsRNA, and consequently, are implicated in antiflaviviral host responses (Loo et al., 2008; Nasirudeen et al., 2011; Sprokholt et al., 2017).

TLR3 is a member of the Toll-like receptor family and plays a crucial role in activation of the immune response by recognition of dsRNA in endosomes, presumably during viral entry (Leifer and Medvedev, 2016; Gao and Li, 2017). TLR3 recognizes DENV RNA in infected cells and its overexpression or stimulation reduces viral replication (Tsai et al., 2009; Liang et al., 2011). In a pathological context, TLR3 knockout mice are more susceptible to lethal WNV infection (Daffis et al., 2008).

RIG-I belongs to the RIG-I-like receptor (RLR) family and possesses a dsRNA helicase activity. It is a cytosolic PRR that targets specifically dsRNA and the 5′ tri/diphosphate moiety of short structured uncapped RNAs (Yoneyama et al., 2004; Pichlmair et al., 2006; Takahasi et al., 2008; Goubau et al., 2014). It also has been shown to have affinity for the polyuridine tract of HCV 3′UTR (Schnell et al., 2012). Such sequences are very unusual in cellular RNAs and hence, constitute foreign signatures. Interestingly, treatment of cells or mice with U-rich 5′ppp-based RIG-I agonists protect from infection with variety of viruses (Chiang et al., 2015). MDA5 is another RLR family member related to the RIG-I protein. MDA5 targets long viral dsRNAs and activates the same innate antiviral response as RIG-I (Schlee, 2013). Once activated by RNA recognition, RIG-I and MDA5 interact with "mitochondrial antiviral-signaling protein" (MAVS) at the surface of mitochondria through their CARD domains. This interaction results in a signaling cascade to the nucleus via transcription factors NF-κB and IRF3. This ultimately leads to the induction of type I IFN, proinflammatory cytokines and ISGs expression (Gack and Diamond, 2016).

More recently, it has been shown that the cyclic GMP-AMP synthase (cGAS)/stimulator of IFN genes (STING) pathway, which normally senses DNA virus infection and mitochondrial DNA damage, is also activated upon RNA virus infection (including DENV and WNV) and induces type I IFN production (Schoggins et al., 2014). The vRNA sensing mechanism is still not well understood but DENV-induced mitochondrial damage may be involved in this process (Aguirre et al., 2017; Sun et al., 2017). Moreover, the relevance of this pathway to flavivirus infection is further highlighted by several evidence that DENV NS2B and NS3 are able to counteract the functions of cGAS and STING, respectively (Aguirre et al., 2012, 2017; Yu et al., 2012).

Flaviviral RNA-Based Evasion From the Innate Immune System

From a virus-host co-evolution viewpoint, the mammalian innate immune response has evolved to counteract viral infection. Of course, this also implies an adaptation from the pathogens in order to evade innate immunity to the benefit of replication. To this end, several interference mechanisms involving flaviviral proteins have been described over the last decade. Indeed, these viruses can dampen the antiviral signaling pathways by inhibiting for instance, cGAS, STING, RIG-I, MAVS, TBK1 and STAT1/2 functions through interactions with NS5, NS3, NS2B or NS4B (Chatel-Chaix et al., 2016; Gack and Diamond, 2016; Aguirre et al., 2017; Miorin et al., 2017). In addition, the viral genome itself and its degradation by-products also contribute to the efficient evasion of innate immunity. Firstly, as mentioned above, vRNA most likely replicates within VPs, constituting a confined environment providing limited access to cytosolic vRNA sensors. Hence, from an ultrastructural perspective, it is tempting to speculate that VPs "hide" vRNA and the dsRNA replication intermediate from the innate immune detection machinery. Nevertheless, such models remain to be addressed specifically.

vRNA Methylation and Innate Immunity

Interestingly, several studies have shown that vRNA modifications may confer the vRNA with the ability to be marked as "self" and evade recognition by host sensors of foreign RNA. Indeed, in addition to vRNA capping, NS5 also possesses a 2′-*O*-methyltransferase activity (Bradrick, 2017). 2′-*O*-methylation is an RNA modification on the first and second nucleotides of the mRNA cap structures in which the ribose is methylated at the 2′-OH position by cellular nucleoside 2′-O-methyltransferases (MTase) contributing to form cap 1 (m^7GpppNm) or cap 2 (m^7GpppNmNm) structures (Furuichi and Shatkin, 2000). Hence, through NS5-mediated 2′-*O* methylation of its cap, the flaviviral vRNA mimics cellular mRNAs. Moreover, DENV and WNV NS5 proteins were demonstrated to also perform internal RNA methylation on vRNAs that lack the 5′ cap structure (Dong et al., 2012). In this case, these modifications occur specifically at the 2′-OH position of adenosine residues.

By mimicking cellular mRNA, modified vRNAs appear to evade the host immune response during infection. Indeed, DENV 2′ O-MTase deficient viruses are severely attenuated and do not properly spread in cell lines that possess a functional IFN response system (like lung carcinoma A549 cells) (Schmid et al., 2015; Chang et al., 2016). In the case of WNV, a virus expressing the NS5 E218A mutant which lacks the 2′-O MTase activity is attenuated in primary cells and mice with a strongly reduced pathogenicity including the complete loss of virus-induced lethality (Daffis et al., 2010). Importantly, the pathogenicity of this mutant virus *in vivo* was restored in

mice harboring a deficiency in type I interferon signaling. This strongly supports the idea that 2′-*O*-methylation is crucial to evade the type I IFN-dependent antiviral response. Notably, mutant and wild-type viruses induce comparable levels of IFNs suggesting that WNV vRNA sensing by RLR or TLR3 is not involved in this evasion strategy. Importantly, this methylation-dependent antiviral effect was attributed to IFN-induced proteins with tetratricopeptide repeats (IFIT). More specifically, replication and pathogenicity of WNV E218A mutant virus was rescued and comparable to wild-type virus in *Ifit1* knockout mice demonstrating the key role of this ISG in antiviral immunity (Daffis et al., 2010). As compared to other IFITs, IFIT1 recognizes with high specificity RNAs lacking a 2′-O methylated cap. This results in the sequestration of these RNAs from translation initiation factors and consequently, in the inhibition of their translation (Habjan et al., 2013; Kimura et al., 2013; Kumar et al., 2014). Nevertheless, *Ifit1* deficiency did not rescue the replication WNV E218A in brain endothelial cells in contrast to other cell types of the central nervous system (Szretter et al., 2012). Consistently, overexpression of IFIT1 in 293-DC-SIGN cells only partially inhibited the replication of DENV2 2′-O MTase mutant (Zust et al., 2013). This highlights that the 2-*O*-methylation of vRNA allows evasion from innate immunity and relies on both IFIT1-dependent and independent mechanisms according to the cell type.

Interestingly, the role of virus-mediated 2′-*O*-methylation as a countermeasure against innate immunity has also been recognized in mouse and human coronaviruses. In this case, 2′-O MTase-deficient viruses induced a stronger type I IFN response resulting in attenuation of viral replication (Zust et al., 2011; Schmid et al., 2015). However, coronaviral replication was restored upon suppression of type I IFN receptor (IFNAR) or cytosolic RNA sensor MDA5 expression suggesting that 2′-O methylation of the coronavirus RNA directly evades early RNA sensing by MDA5. Whether the same strategy is also employed by flaviviruses (other than WNV) remains to be elucidated. Interestingly, a recent study has demonstrated that a DENV E216A 2′-O MTase-deficient mutant induced an early innate immune response after just a few hours of infection, consistent with a putative detection of unmethylated vRNA by RLRs such as MDA5 or RIG-I (Chang et al., 2016).

Since 2′-O-methylation is important for optimal viral replication and also has structural similarities among flaviviruses, it was proposed that 2′-O MTase-deficient viruses could be exploited as attenuated vaccines. Indeed, several groups have engineered attenuated DENV or JEV that lack 2′-*O*-methylation activity and are thus more sensitive to IFN inhibition than parental viruses (Li S.H. et al., 2013; Zust et al., 2013). Robust humoral and cellular immune responses protecting against both viruses were obtained after inoculation of mice with these attenuated viruses. In the case of DENV, protection was also achieved in rhesus macaques after a single administration of the vaccine candidate (Zust et al., 2013). These results pinpoint the potential success of such attenuated vaccine-based approach, which may be efficacious against a wide range of flaviviruses.

The Action of sfRNA Against Innate Immunity

During the infection, the accumulation of viral genome generates several by-products which do not encode any viral proteins. Three classes of non-coding RNAs have been described to date: viral small RNAs (vsRNAs) (Hamilton and Baulcombe, 1999), defective interfering genomes (DIGs) (Li and Brinton, 2001; Pesko et al., 2012; Juarez-Martinez et al., 2013) and most relevant to this review, the subgenomic flavivirus RNA (sfRNA) (Urosevic et al., 1997; Pijlman et al., 2008). DIGs and vsRNAs are not well described yet and remain to be characterized in detail. In contrast, the sfRNA has been comprehensively investigated during the last decade, especially with regards to its role in modulating host biological processes.

Produced by all tested members of the *Flavivirus* genus, sfRNA is a highly structured 0.3–0.7 kb-long non-coding RNA and apparently is the most abundant viral RNA species in the infected cell (Pijlman et al., 2008; Bidet et al., 2014; Manokaran et al., 2015; Akiyama et al., 2016; Donald et al., 2016; Bidet et al., 2017). It is well established that sfRNA is produced by an incomplete 5′-3′ degradation of the viral genome by the cellular XRN1/Pacman exonuclease. During RNA degradation, XRN1 is stalled at the 3′UTR extremity, more precisely at stem-loops/pseudoknots of the highly variable region upstream the DB structures causing the accumulation of different species of sfRNA (Pijlman et al., 2008; Funk et al., 2010; Silva et al., 2010; Chapman et al., 2014a,b; Akiyama et al., 2016). While XRN1 is required for sfRNA production, sfRNA is also able to sequester this cellular protein and to inhibit its endogenous functions (Silva et al., 2010; Moon et al., 2012; Chapman et al., 2014a). In 293T cells, this results in the accumulation of uncapped cellular mRNAs in the cytosol (Moon et al., 2012). However, the consequences of such inhibition are still unclear and remain to be further deciphered.

Despite its high levels in the cytosol, sfRNA does not appear to play a direct role in replication since mutations impairing sfRNA production do not affect vRNA synthesis in WNV-, YFV-, and DENV-infected cells (Funk et al., 2010; Schuessler et al., 2012; Szretter et al., 2012). Rather, sfRNA contributes to viral cytopathicity both *in cellulo* and *in vivo* partly by interfering with innate immune responses. For instance, in the case of WNV and DENV infection, mutations inhibiting sfRNA production lead to a decrease in the viral replication in cells that possess functional type I IFN responses, supporting the idea that sfRNA aids in evasion of the IFN response (Schuessler et al., 2012; Bidet et al., 2014, 2017). Moreover, a recent study shows that DENV sfRNA negatively impacts IFN induction through the inhibition of TRIM25, an E3 ubiquitin ligase required for RIG-I activation (Manokaran et al., 2015). Indeed, the interaction of sfRNA with TRIM25 in a sequence-dependent manner prevents its deubiquitylation. As a result, the decrease in IFN induction is consistent with an impairment in TRIM25-mediated polyubiquitylation and subsequent activation of RIG-I. Consistent with a conservation of this evasion strategy among flaviviruses, it was shown that JEV sfRNA overexpression in infected A549 cells inhibits IRF3 phosphorylation and its nuclear translocation that are required for type I IFN transcription (Chang et al., 2013). Finally, the RLR-dependent IFN induction

pathway was also inhibited upon ZIKV sfRNA overexpression in stimulated cells (Donald et al., 2016).

Downstream of IFN production and signaling, the sfRNA also plays a role in ISG expression at the post-transcriptional level. Indeed, host RNA-binding proteins G3BP1, G3PB2 and CAPRIN, which are involved in ISG translation are inhibited by their association with DENV sfRNA in Huh7 cells (Bidet et al., 2014). G3BP proteins are core components of SGs (Anderson and Kedersha, 2006) whose formation and functions are modulated by flavivirus infection, as discussed above. Hence, it is tempting to speculate that, through the hijacking of SG components, flaviviruses remodel the host proteome by positively or negatively regulating the expression of pro- and anti-viral host proteins, respectively.

Interestingly, several studies have shown that sfRNA also plays an important role in flaviviral life cycle and dissemination in infected insects (Schnettler et al., 2012; Moon et al., 2015; Pompon et al., 2017). The determinants of the viral genome governing the abundance of sfRNA appear to be the same in insect and mammalian cells; however, in mosquitos, the sfRNA causes disruption of the innate immune response in salivary glands by inhibiting the Toll receptor pathway (Pompon et al., 2017). Furthermore, sfRNA downregulates the RNA interference (RNAi) machinery, the main mediator of innate immunity in insects (Schnettler et al., 2012; Moon et al., 2015). Mutations in DENV and WNV decreasing the production of sfRNA showed an impairment in RNAi suppression (Moon et al., 2015). This appears to be mediated by the association of sfRNA with Dicer and Ago2, two essential proteins of the RNAi machinery. Taken together, these data suggest that the sfRNA crucially contributes at multiple levels to viral evasion from innate immunity in both arthropod and mammalian hosts.

sfRNA-MEDIATED MODULATION OF PATHOGENESIS

In addition to its roles in innate immune evasion, the sfRNA was shown to be important for WNV and DENV pathogenicity. WNV or DENV genomes harboring mutations that disrupt the formation of full-length sfRNA produced much smaller plaques in cell culture (Pijlman et al., 2008; Liu et al., 2014). Consistently, drastic decreases in overall cell death and apoptosis were observed. These phenotypes were rescued by the expression of the sfRNA in *trans*. However, sfRNA overexpression alone did not induce any cell death implying that its action requires flavivirus replication. Importantly, viral translation, vRNA synthesis and particle production were not significantly affected by the loss of sfRNA expression. Overall, this strongly suggests that sfRNA is not essential for flavivirus replication but rather modulates cytopathic effects in addition to innate immunity. Interestingly, DENV sfRNA-mutated viruses were unable to inhibit Bcl2 and the AKT/PI3K pro-survival pathways suggesting that flavivirus-induced cytopathic effects rely on the modulation of these signaling cascades (Liu et al., 2014). Most importantly, mice infected with full length sfRNA-deficient WNV all survive in contrast to the usual 100% mortality rate with wild-type WNV (Pijlman et al., 2008). This did not correlate with defects in virus dissemination in the brain and spleen confirming that sfRNA is crucial for pathogenicity *in vivo* without directly regulating viral replication. In stark contrast, overexpression of JEV sfRNA decreased virus-induced apoptosis in infected A549 cells (Chang et al., 2013). While it is clear that sfRNA is crucial for WNV pathogenicity and that all tested flaviviruses produce sfRNA (Pijlman et al., 2008; Bidet et al., 2014, 2017; Manokaran et al., 2015; Akiyama et al., 2016; Donald et al., 2016), their respective contributions to pathogenesis remain to be addressed. Finally, how sfRNA modulates the flavivirus-induced cytopathic effects at the molecular level is completely unknown. It will be interesting to determine if sfRNA acts at the gene expression level or rather post-translationally through direct interactions with factors involved in cell survival and/or cell death.

OPEN QUESTIONS AND CONCLUSION

The tremendous work on flaviviruses during the last decade highlights the complexity of the molecular mechanisms governing the fate and functions of the vRNA. This includes dynamic RNA secondary and tertiary structures, RNA modifications such as 2′-*O* and N^6A methylation, the formation of functional vRNA sub-products (like sfRNA) and the participation of viral proteins as well as host RNA-binding proteins. This intricate network is most likely hosted within viral RFs. Future studies will be needed to explore how all these regulated processes are interconnected to generate a precise integrated model of vRNA metabolism. For instance, does vRNA methylation on specific nucleotides impact vRNA tertiary structure formation, cyclization and/or affinity for host RNA-binding proteins, and vice-versa? Do these structural changes impact the efficiency of vRNA packaging into assembling virions? Importantly, when compared with HCV RFs, little is known about how flaviviruses regulate the morphogenesis of VPs that are very homogenous in size and shape. The same applies to the formation and maintenance of the VP pore that is believed to play a pivotal role in the transfer of vRNA from replication complexes to assembling particles. How is it functionally coordinated with budding viruses? Is this a dynamic structure oscillating between open and closed states? What is its viral and cellular protein composition? Finally, these considerations should ideally always take into account that flaviviruses infect both insects and mammals. Indeed, subtle differences between hosts in the life cycle (especially with regards to host factor dependency) may be observed and of great interest.

Overall, this review highlights how flaviviruses have evolved to confer upon a single RNA species and one viral polyprotein product all the information required for optimal infection in both insect and mammalian hosts. More generally, all of these open questions regarding the vRNA perfectly illustrate the importance of flaviviruses as an exquisite model to study spatio-temporal control of RNA metabolism. Finally, a precise

understanding of the dynamic control of vRNA in the flavivirus life cycle will hopefully identify potential therapeutic targets for the development of antivirals, ideally with a broad pan-flaviviral spectrum.

AUTHOR CONTRIBUTIONS

CM and WF contributed equally to this work. CM and WF wrote the manuscript and made the figures. LC-C edited the final version of the manuscript.

FUNDING

LC-C is receiving a research scholar (Junior 2) salary support from Fonds de la Recherche du Québec-Santé (FRQS). LC-C's research is supported by grants from Natural Sciences and Engineering Research Council of Canada (NSERC; RGPIN-2016-05584), the Canadian Institutes of Health Research (CIHR; PJT153020; ICS154142), Fonds de la Recherche du Québec-Nature et Technologies (FRQNT; 2018-NC-205593), Armand-Frappier Foundation, and Institut National de la Recherche Scientifique (INRS).

ACKNOWLEDGMENTS

We are grateful to Dr. Selena M. Sagan (McGill University, Canada) and Dr. Karine Boulay (Université de Montréal, Canada) for critical reading of the manuscript and helpful comments. We apologize to colleagues whose work could not be mentioned or referenced in this review due to space limitations.

REFERENCES

Adachi, O., Kawai, T., Takeda, K., Matsumoto, M., Tsutsui, H., Sakagami, M., et al. (1998). Targeted disruption of the MyD88 gene results in loss of IL-1- and IL-18-mediated function. *Immunity* 9, 143–150.

Agis-Juarez, R. A., Galvan, I., Medina, F., Daikoku, T., Padmanabhan, R., Ludert, J. E., et al. (2009). Polypyrimidine tract-binding protein is relocated to the cytoplasm and is required during dengue virus infection in Vero cells. *J. Gen. Virol.* 90(Pt 12), 2893–2901. doi: 10.1099/vir.0.013433-0

Aguirre, S., Luthra, P., Sanchez-Aparicio, M. T., Maestre, A. M., Patel, J., Lamothe, F., et al. (2017). Dengue virus NS2B protein targets cGAS for degradation and prevents mitochondrial DNA sensing during infection. *Nat. Microbiol.* 2:17037. doi: 10.1038/nmicrobiol.2017.37

Aguirre, S., Maestre, A. M., Pagni, S., Patel, J. R., Savage, T., Gutman, D., et al. (2012). DENV inhibits type I IFN production in infected cells by cleaving human STING. *PLoS Pathog.* 8:e1002934. doi: 10.1371/journal.ppat.1002934

Akey, D. L., Brown, W. C., Dutta, S., Konwerski, J., Jose, J., Jurkiw, T. J., et al. (2014). Flavivirus NS1 structures reveal surfaces for associations with membranes and the immune system. *Science* 343, 881–885. doi: 10.1126/science.1247749

Akiyama, B. M., Laurence, H. M., Massey, A. R., Costantino, D. A., Xie, X., Yang, Y., et al. (2016). Zika virus produces noncoding RNAs using a multi-pseudoknot structure that confounds a cellular exonuclease. *Science* 354, 1148–1152. doi: 10.1126/science.aah3963

Alarcon, C. R., Goodarzi, H., Lee, H., Liu, X., Tavazoie, S., and Tavazoie, S. F. (2015). HNRNPA2B1 is a mediator of m(6)A-dependent nuclear RNA processing events. *Cell* 162, 1299–1308. doi: 10.1016/j.cell.2015.08.011

Albornoz, A., Carletti, T., Corazza, G., and Marcello, A. (2014). The stress granule component TIA-1 binds tick-borne encephalitis virus RNA and is recruited to perinuclear sites of viral replication to inhibit viral translation. *J. Virol.* 88, 6611–6622. doi: 10.1128/JVI.03736-13

Alvarez, D. E., Lodeiro, M. F., Luduena, S. J., Pietrasanta, L. I., and Gamarnik, A. V. (2005). Long-range RNA-RNA interactions circularize the dengue virus genome. *J. Virol.* 79, 6631–6643. doi: 10.1128/JVI.79.11.6631-6643.2005

Amorim, R., Temzi, A., Griffin, B. D., and Mouland, A. J. (2017). Zika virus inhibits eIF2alpha-dependent stress granule assembly. *PLoS Negl. Trop. Dis.* 11:e0005775. doi: 10.1371/journal.pntd.0005775

Anderson, P., and Kedersha, N. (2006). RNA granules. *J. Cell Biol.* 172, 803–808. doi: 10.1083/jcb.200512082

Anderson, P., and Kedersha, N. (2008). Stress granules: the Tao of RNA triage. *Trends Biochem. Sci.* 33, 141–150. doi: 10.1016/j.tibs.2007.12.003

Ansarah-Sobrinho, C., Nelson, S., Jost, C. A., Whitehead, S. S., and Pierson, T. C. (2008). Temperature-dependent production of pseudoinfectious dengue reporter virus particles by complementation. *Virology* 381, 67–74. doi: 10.1016/j.virol.2008.08.021

Apte-Sengupta, S., Sirohi, D., and Kuhn, R. J. (2014). Coupling of replication and assembly in flaviviruses. *Curr. Opin. Virol.* 9, 134–142. doi: 10.1016/j.coviro.2014.09.020

Ariumi, Y., Kuroki, M., Abe, K., Dansako, H., Ikeda, M., Wakita, T., et al. (2007). DDX3 DEAD-box RNA helicase is required for hepatitis C virus RNA replication. *J. Virol.* 81, 13922–13926. doi: 10.1128/JVI.01517-07

Bhullar, D., Jalodia, R., Kalia, M., and Vrati, S. (2014). Cytoplasmic translocation of polypyrimidine tract-binding protein and its binding to viral RNA during Japanese encephalitis virus infection inhibits virus replication. *PLoS One* 9:e114931. doi: 10.1371/journal.pone.0114931

Bidet, K., Dadlani, D., and Garcia-Blanco, M. A. (2014). G3BP1, G3BP2 and CAPRIN1 are required for translation of interferon stimulated mRNAs and are targeted by a dengue virus non-coding RNA. *PLoS Pathog.* 10:e1004242. doi: 10.1371/journal.ppat.1004242

Bidet, K., Dadlani, D., and Garcia-Blanco, M. A. (2017). Correction: G3BP1, G3BP2 and CAPRIN1 are required for translation of interferon stimulated mRNAs and are targeted by a dengue virus non-coding RNA. *PLoS Pathog.* 13:e1006295. doi: 10.1371/journal.ppat.1006295

Bily, T., Palus, M., Eyer, L., Elsterova, J., Vancova, M., and Ruzek, D. (2015). Electron tomography analysis of tick-borne encephalitis virus infection in human neurons. *Sci. Rep.* 5:10745. doi: 10.1038/srep10745

Blackwell, J. L., and Brinton, M. A. (1997). Translation elongation factor-1 alpha interacts with the 3′ stem-loop region of West Nile virus genomic RNA. *J. Virol.* 71, 6433–6444.

Bradrick, S. S. (2017). Causes and consequences of flavivirus RNA methylation. *Front. Microbiol.* 8:2374. doi: 10.3389/fmicb.2017.02374

Brinton, M. A., and Basu, M. (2015). Functions of the 3′ and 5′ genome RNA regions of members of the genus Flavivirus. *Virus Res.* 206, 108–119. doi: 10.1016/j.virusres.2015.02.006

Brunetti, J. E., Scolaro, L. A., and Castilla, V. (2015). The heterogeneous nuclear ribonucleoprotein K (hnRNP K) is a host factor required for dengue virus and Junin virus multiplication. *Virus Res.* 203, 84–91. doi: 10.1016/j.virusres.2015.04.001

Byk, L. A., and Gamarnik, A. V. (2016). Properties and functions of the dengue virus capsid protein. *Annu. Rev. Virol.* 3, 263–281. doi: 10.1146/annurev-virology-110615-042334

Campos, R. K., Wong, B., Xie, X., Lu, Y. F., Shi, P. Y., Pompon, J., et al. (2017). RPLP1 and RPLP2 are essential flavivirus host factors that promote early viral protein accumulation. *J. Virol.* 91:e01706-16. doi: 10.1128/JVI.01706-16

Carvalho, F. A., Carneiro, F. A., Martins, I. C., Assuncao-Miranda, I., Faustino, A. F., Pereira, R. M., et al. (2012). Dengue virus capsid protein binding to hepatic lipid droplets (LD) is potassium ion dependent and is mediated by LD surface proteins. *J. Virol.* 86, 2096–2108. doi: 10.1128/JVI.06796-11

Chahar, H. S., Chen, S., and Manjunath, N. (2013). P-body components LSM1, GW182, DDX3, DDX6 and XRN1 are recruited to WNV replication sites and

positively regulate viral replication. *Virology* 436, 1–7. doi: 10.1016/j.virol.2012.09.041

Chang, D. C., Hoang, L. T., Mohamed Naim, A. N., Dong, H., Schreiber, M. J., Hibberd, M. L., et al. (2016). Evasion of early innate immune response by 2′-O-methylation of dengue genomic RNA. *Virology* 499, 259–266. doi: 10.1016/j.virol.2016.09.022

Chang, R. Y., Hsu, T. W., Chen, Y. L., Liu, S. F., Tsai, Y. J., Lin, Y. T., et al. (2013). Japanese encephalitis virus non-coding RNA inhibits activation of interferon by blocking nuclear translocation of interferon regulatory factor 3. *Vet. Microbiol.* 166, 11–21. doi: 10.1016/j.vetmic.2013.04.026

Chang, Y. S., Liao, C. L., Tsao, C. H., Chen, M. C., Liu, C. I., Chen, L. K., et al. (1999). Membrane permeabilization by small hydrophobic nonstructural proteins of Japanese encephalitis virus. *J. Virol.* 73, 6257–6264.

Chapman, E. G., Costantino, D. A., Rabe, J. L., Moon, S. L., Wilusz, J., Nix, J. C., et al. (2014a). The structural basis of pathogenic subgenomic flavivirus RNA (sfRNA) production. *Science* 344, 307–310. doi: 10.1126/science.1250897

Chapman, E. G., Moon, S. L., Wilusz, J., and Kieft, J. S. (2014b). RNA structures that resist degradation by Xrn1 produce a pathogenic Dengue virus RNA. *eLife* 3:e01892. doi: 10.7554/eLife.01892

Chatel-Chaix, L., and Bartenschlager, R. (2014). Dengue virus- and hepatitis C virus-induced replication and assembly compartments: the enemy inside–caught in the web. *J. Virol.* 88, 5907–5911. doi: 10.1128/JVI.03404-13

Chatel-Chaix, L., Cortese, M., Romero-Brey, I., Bender, S., Neufeldt, C. J., Fischl, W., et al. (2016). Dengue virus perturbs mitochondrial morphodynamics to dampen innate immune responses. *Cell Host Microbe* 20, 342–356. doi: 10.1016/j.chom.2016.07.008

Chatel-Chaix, L., Fischl, W., Scaturro, P., Cortese, M., Kallis, S., Bartenschlager, M., et al. (2015). A combined genetic-proteomic approach identifies residues within dengue virus NS4B critical for interaction with NS3 and viral replication. *J. Virol.* 89, 7170–7186. doi: 10.1128/Jvi.00867-15

Chatel-Chaix, L., Germain, M. A., Motorina, A., Bonneil, E., Thibault, P., Baril, M., et al. (2013). A host YB-1 ribonucleoprotein complex is hijacked by hepatitis C virus for the control of NS3-dependent particle production. *J. Virol.* 87, 11704–11720. doi: 10.1128/JVI.01474-13

Chatel-Chaix, L., Melancon, P., Racine, M. E., Baril, M., and Lamarre, D. (2011). Y-box-binding protein 1 interacts with hepatitis C virus NS3/4A and influences the equilibrium between viral RNA replication and infectious particle production. *J. Virol.* 85, 11022–11037. doi: 10.1128/JVI.00719-11

Chavali, P. L., Stojic, L., Meredith, L. W., Joseph, N., Nahorski, M. S., Sanford, T. J., et al. (2017). Neurodevelopmental protein Musashi-1 interacts with the Zika genome and promotes viral replication. *Science* 357, 83–88. doi: 10.1126/science.aam9243

Chiang, C., Beljanski, V., Yin, K., Olagnier, D., Ben Yebdri, F., Steel, C., et al. (2015). Sequence-specific modifications enhance the broad-spectrum antiviral response activated by RIG-I agonists. *J. Virol.* 89, 8011–8025. doi: 10.1128/JVI.00845-15

Chien, H. L., Liao, C. L., and Lin, Y. L. (2011). FUSE binding protein 1 interacts with untranslated regions of Japanese encephalitis virus RNA and negatively regulates viral replication. *J. Virol.* 85, 4698–4706. doi: 10.1128/JVI.01950-10

Chiu, H. P., Chiu, H., Yang, C. F., Lee, Y. L., Chiu, F. L., Kuo, H. C., et al. (2018). Inhibition of Japanese encephalitis virus infection by the host zinc-finger antiviral protein. *PLoS Pathog.* 14:e1007166. doi: 10.1371/journal.ppat.1007166

Clyde, K., Barrera, J., and Harris, E. (2008). The capsid-coding region hairpin element (cHP) is a critical determinant of dengue virus and West Nile virus RNA synthesis. *Virology* 379, 314–323. doi: 10.1016/j.virol.2008.06.034

Clyde, K., and Harris, E. (2006). RNA secondary structure in the coding region of dengue virus type 2 directs translation start codon selection and is required for viral replication. *J. Virol.* 80, 2170–2182. doi: 10.1128/JVI.80.5.2170-2182.2006

Comas-Garcia, M., Davis, S. R., and Rein, A. (2016). On the selective packaging of genomic RNA by HIV-1. *Viruses* 8:E246. doi: 10.3390/v8090246

Cortese, M., Goellner, S., Acosta, E. G., Neufeldt, C. J., Oleksiuk, O., Lampe, M., et al. (2017). Ultrastructural characterization of zika virus replication factories. *Cell Rep.* 18, 2113–2123. doi: 10.1016/j.celrep.2017.02.014

Daffis, S., Samuel, M. A., Suthar, M. S., Gale, M. Jr., and Diamond, M. S. (2008). Toll-like receptor 3 has a protective role against West Nile virus infection. *J. Virol.* 82, 10349–10358. doi: 10.1128/JVI.00935-08

Daffis, S., Szretter, K. J., Schriewer, J., Li, J., Youn, S., Errett, J., et al. (2010). 2′-O methylation of the viral mRNA cap evades host restriction by IFIT family members. *Nature* 468, 452–456. doi: 10.1038/nature09489

Davis, W. G., Blackwell, J. L., Shi, P. Y., and Brinton, M. A. (2007). Interaction between the cellular protein eEF1A and the 3′-terminal stem-loop of West Nile virus genomic RNA facilitates viral minus-strand RNA synthesis. *J. Virol.* 81, 10172–10187. doi: 10.1128/JVI.00531-07

De Nova-Ocampo, M., Villegas-Sepulveda, N., and del Angel, R. M. (2002). Translation elongation factor-1alpha, La, and PTB interact with the 3′ untranslated region of dengue 4 virus RNA. *Virology* 295, 337–347. doi: 10.1006/viro.2002.1407

Dechtawewat, T., Songprakhon, P., Limjindaporn, T., Puttikhunt, C., Kasinrerk, W., Saitornuang, S., et al. (2015). Role of human heterogeneous nuclear ribonucleoprotein C1/C2 in dengue virus replication. *Virol J.* 12:14. doi: 10.1186/s12985-014-0219-7

Donald, C. L., Brennan, B., Cumberworth, S. L., Rezelj, V. V., Clark, J. J., Cordeiro, M. T., et al. (2016). Full genome sequence and sfRNA interferon antagonist activity of zika virus from recife, Brazil. *PLoS Negl. Trop. Dis.* 10:e0005048. doi: 10.1371/journal.pntd.0005048

Dong, H., Chang, D. C., Hua, M. H., Lim, S. P., Chionh, Y. H., Hia, F., et al. (2012). 2′-O methylation of internal adenosine by flavivirus NS5 methyltransferase. *PLoS Pathog.* 8:e1002642. doi: 10.1371/journal.ppat.1002642

Dong, Y., Yang, J., Ye, W., Wang, Y., Miao, Y., Ding, T., et al. (2015). LSm1 binds to the Dengue virus RNA 3′ UTR and is a positive regulator of Dengue virus replication. *Int. J. Mol. Med.* 35, 1683–1689. doi: 10.3892/ijmm.2015.2169

Dyer, O. (2017). Philippines halts dengue immunisation campaign owing to safety risk. *BMJ* 359:j5759. doi: 10.1136/bmj.j5759

Edgil, D., Polacek, C., and Harris, E. (2006). Dengue virus utilizes a novel strategy for translation initiation when cap-dependent translation is inhibited. *J. Virol.* 80, 2976–2986. doi: 10.1128/JVI.80.6.2976-2986.2006

Egloff, M. P., Benarroch, D., Selisko, B., Romette, J. L., and Canard, B. (2002). An RNA cap (nucleoside-2′-O-)-methyltransferase in the flavivirus RNA polymerase NS5: crystal structure and functional characterization. *EMBO J.* 21, 2757–2768. doi: 10.1093/emboj/21.11.2757

Emara, M. M., and Brinton, M. A. (2007). Interaction of TIA-1/TIAR with West Nile and dengue virus products in infected cells interferes with stress granule formation and processing body assembly. *Proc. Natl. Acad. Sci. U.S.A.* 104, 9041–9046. doi: 10.1073/pnas.0703348104

Emara, M. M., Liu, H., Davis, W. G., and Brinton, M. A. (2008). Mutation of mapped TIA-1/TIAR binding sites in the 3′ terminal stem-loop of West Nile virus minus-strand RNA in an infectious clone negatively affects genomic RNA amplification. *J. Virol.* 82, 10657–10670. doi: 10.1128/JVI.00991-08

Filomatori, C. V., Lodeiro, M. F., Alvarez, D. E., Samsa, M. M., Pietrasanta, L., and Gamarnik, A. V. (2006). A 5′ RNA element promotes dengue virus RNA synthesis on a circular genome. *Genes Dev.* 20, 2238–2249. doi: 10.1101/gad.1444206

Friebe, P., and Harris, E. (2010). Interplay of RNA elements in the dengue virus 5′ and 3′ ends required for viral RNA replication. *J. Virol.* 84, 6103–6118. doi: 10.1128/JVI.02042-09

Friebe, P., Pena, J., Pohl, M. O., and Harris, E. (2012). Composition of the sequence downstream of the dengue virus 5′ cyclization sequence (dCS) affects viral RNA replication. *Virology* 422, 346–356. doi: 10.1016/j.virol.2011.10.025

Friebe, P., Shi, P. Y., and Harris, E. (2011). The 5′ and 3′ downstream AUG region elements are required for mosquito-borne flavivirus RNA replication. *J. Virol.* 85, 1900–1905. doi: 10.1128/JVI.02037-10

Friedrich, S., Engelmann, S., Schmidt, T., Szczepankiewicz, G., Bergs, S., Liebert, U. G., et al. (2018). The host factor AUF1 p45 supports flavivirus propagation by triggering the RNA switch required for viral genome cyclization. *J. Virol.* 92:e01647-17. doi: 10.1128/JVI.01647-17

Friedrich, S., Schmidt, T., Geissler, R., Lilie, H., Chabierski, S., Ulbert, S., et al. (2014). AUF1 p45 promotes West Nile virus replication by an RNA chaperone activity that supports cyclization of the viral genome. *J. Virol.* 88, 11586–11599. doi: 10.1128/JVI.01283-14

Funk, A., Truong, K., Nagasaki, T., Torres, S., Floden, N., Balmori Melian, E., et al. (2010). RNA structures required for production of subgenomic flavivirus RNA. *J. Virol.* 84, 11407–11417. doi: 10.1128/JVI.01159-10

Furuichi, Y., and Shatkin, A. J. (2000). Viral and cellular mRNA capping: past and prospects. *Adv. Virus Res.* 55, 135–184.

Gack, M. U., and Diamond, M. S. (2016). Innate immune escape by Dengue and West Nile viruses. *Curr. Opin. Virol.* 20, 119–128. doi: 10.1016/j.coviro.2016.09.013

Gao, D., and Li, W. (2017). Structures and recognition modes of toll-like receptors. *Proteins* 85, 3–9. doi: 10.1002/prot.25179

Garcia-Blanco, M. A., Vasudevan, S. G., Bradrick, S. S., and Nicchitta, C. (2016). Flavivirus RNA transactions from viral entry to genome replication. *Antiviral Res.* 134, 244–249. doi: 10.1016/j.antiviral.2016.09.010

Gebhard, L. G., Kaufman, S. B., and Gamarnik, A. V. (2012). Novel ATP-independent RNA annealing activity of the dengue virus NS3 helicase. *PLoS One* 7:e36244. doi: 10.1371/journal.pone.0036244

Gillespie, L. K., Hoenen, A., Morgan, G., and Mackenzie, J. M. (2010). The endoplasmic reticulum provides the membrane platform for biogenesis of the flavivirus replication complex. *J. Virol.* 84, 10438–10447. doi: 10.1128/JVI.00986-10

Gokhale, N. S., McIntyre, A. B. R., McFadden, M. J., Roder, A. E., Kennedy, E. M., Gandara, J. A., et al. (2016). N6-methyladenosine in flaviviridae viral RNA genomes regulates infection. *Cell Host Microbe* 20, 654–665. doi: 10.1016/j.chom.2016.09.015

Gomila, R. C., Martin, G. W., and Gehrke, L. (2011). NF90 binds the dengue virus RNA 3′ terminus and is a positive regulator of dengue virus replication. *PLoS One* 6:e16687. doi: 10.1371/journal.pone.0016687

Goubau, D., Schlee, M., Deddouche, S., Pruijssers, A. J., Zillinger, T., Goldeck, M., et al. (2014). Antiviral immunity via RIG-I-mediated recognition of RNA bearing 5′-diphosphates. *Nature* 514, 372–375. doi: 10.1038/nature13590

Groat-Carmona, A. M., Orozco, S., Friebe, P., Payne, A., Kramer, L., and Harris, E. (2012). A novel coding-region RNA element modulates infectious dengue virus particle production in both mammalian and mosquito cells and regulates viral replication in Aedes aegypti mosquitoes. *Virology* 432, 511–526. doi: 10.1016/j.virol.2012.06.028

Guyatt, K. J., Westaway, E. G., and Khromykh, A. A. (2001). Expression and purification of enzymatically active recombinant RNA-dependent RNA polymerase (NS5) of the flavivirus Kunjin. *J. Virol. Methods* 92, 37–44.

Habjan, M., Hubel, P., Lacerda, L., Benda, C., Holze, C., Eberl, C. H., et al. (2013). Sequestration by IFIT1 impairs translation of 2′O-unmethylated capped RNA. *PLoS Pathog.* 9:e1003663. doi: 10.1371/journal.ppat.1003663

Hamilton, A. J., and Baulcombe, D. C. (1999). A species of small antisense RNA in posttranscriptional gene silencing in plants. *Science* 286, 950–952.

Hodge, K., Tunghirun, C., Kamkaew, M., Limjindaporn, T., Yenchitsomanus, P. T., and Chimnaronk, S. (2016). Identification of a conserved RNA-dependent RNA polymerase (RdRp)-RNA interface required for flaviviral replication. *J. Biol. Chem.* 291, 17437–17449. doi: 10.1074/jbc.M116.724013

Holden, K. L., and Harris, E. (2004). Enhancement of dengue virus translation: role of the 3′ untranslated region and the terminal 3′ stem-loop domain. *Virology* 329, 119–133. doi: 10.1016/j.virol.2004.08.004

Iglesias, N. G., Mondotte, J. A., Byk, L. A., De Maio, F. A., Samsa, M. M., Alvarez, C., et al. (2015). Dengue virus uses a non-canonical function of the host GBF1-Arf-COPI system for capsid protein accumulation on lipid droplets. *Traffic* 16, 962–977. doi: 10.1111/tra.12305

Ivanyi-Nagy, R., and Darlix, J. L. (2012). Core protein-mediated 5′-3′ annealing of the West Nile virus genomic RNA in vitro. *Virus Res.* 167, 226–235. doi: 10.1016/j.virusres.2012.05.003

Jangra, R. K., Yi, M., and Lemon, S. M. (2010). DDX6 (Rck/p54) is required for efficient hepatitis C virus replication but not for internal ribosome entry site-directed translation. *J. Virol.* 84, 6810–6824. doi: 10.1128/JVI.00397-10

Johansson, M., Brooks, A. J., Jans, D. A., and Vasudevan, S. G. (2001). A small region of the dengue virus-encoded RNA-dependent RNA polymerase, NS5, confers interaction with both the nuclear transport receptor importin-beta and the viral helicase, NS3. *J. Gen. Virol.* 82(Pt 4), 735–745. doi: 10.1099/0022-1317-82-4-735

Juarez-Martinez, A. B., Vega-Almeida, T. O., Salas-Benito, M., Garcia-Espitia, M., De Nova-Ocampo, M., Del Angel, R. M., et al. (2013). Detection and sequencing of defective viral genomes in C6/36 cells persistently infected with dengue virus 2. *Arch. Virol.* 158, 583–599. doi: 10.1007/s00705-012-1525-2

Junjhon, J., Pennington, J. G., Edwards, T. J., Perera, R., Lanman, J., and Kuhn, R. J. (2014). Ultrastructural characterization and three-dimensional architecture of replication sites in dengue virus-infected mosquito cells. *J. Virol.* 88, 4687–4697. doi: 10.1128/JVI.00118-14

Katoh, H., Mori, Y., Kambara, H., Abe, T., Fukuhara, T., Morita, E., et al. (2011). Heterogeneous nuclear ribonucleoprotein A2 participates in the replication of Japanese encephalitis virus through an interaction with viral proteins and RNA. *J. Virol.* 85, 10976–10988. doi: 10.1128/JVI.00846-11

Khromykh, A. A., Meka, H., Guyatt, K. J., and Westaway, E. G. (2001a). Essential role of cyclization sequences in flavivirus RNA replication. *J. Virol.* 75, 6719–6728. doi: 10.1128/JVI.75.14.6719-6728.2001

Khromykh, A. A., Varnavski, A. N., Sedlak, P. L., and Westaway, E. G. (2001b). Coupling between replication and packaging of flavivirus RNA: evidence derived from the use of DNA-based full-length cDNA clones of Kunjin virus. *J. Virol.* 75, 4633–4640. doi: 10.1128/JVI.75.10.4633-4640.2001

Khromykh, A. A., Varnavski, A. N., and Westaway, E. G. (1998). Encapsidation of the flavivirus kunjin replicon RNA by using a complementation system providing Kunjin virus structural proteins in trans. *J. Virol.* 72, 5967–5977.

Kim, Y. G., Yoo, J. S., Kim, J. H., Kim, C. M., and Oh, J. W. (2007). Biochemical characterization of a recombinant Japanese encephalitis virus RNA-dependent RNA polymerase. *BMC Mol. Biol.* 8:59. doi: 10.1186/1471-2199-8-59

Kimura, T., Katoh, H., Kayama, H., Saiga, H., Okuyama, M., Okamoto, T., et al. (2013). Ifit1 inhibits Japanese encephalitis virus replication through binding to 5′ capped 2′-O unmethylated RNA. *J. Virol.* 87, 9997–10003. doi: 10.1128/JVI.00883-13

Klema, V. J., Ye, M., Hindupur, A., Teramoto, T., Gottipati, K., Padmanabhan, R., et al. (2016). Dengue virus nonstructural protein 5 (NS5) assembles into a dimer with a unique methyltransferase and polymerase interface. *PLoS Pathog.* 12:e1005451. doi: 10.1371/journal.ppat.1005451

Kuhn, R. J., Zhang, W., Rossmann, M. G., Pletnev, S. V., Corver, J., Lenches, E., et al. (2002). Structure of dengue virus: implications for flavivirus organization, maturation, and fusion. *Cell* 108, 717–725.

Kumar, P., Sweeney, T. R., Skabkin, M. A., Skabkina, O. V., Hellen, C. U., and Pestova, T. V. (2014). Inhibition of translation by IFIT family members is determined by their ability to interact selectively with the 5′-terminal regions of cap0-, cap1- and 5′ppp- mRNAs. *Nucleic Acids Res.* 42, 3228–3245. doi: 10.1093/nar/gkt1321

Lee, E., Stocks, C. E., Amberg, S. M., Rice, C. M., and Lobigs, M. (2000). Mutagenesis of the signal sequence of yellow fever virus prM protein: enhancement of signalase cleavage In vitro is lethal for virus production. *J. Virol.* 74, 24–32.

Lei, Y., Huang, Y., Zhang, H., Yu, L., Zhang, M., and Dayton, A. (2011). Functional interaction between cellular p100 and the dengue virus 3′ UTR. *J. Gen. Virol.* 92(Pt 4), 796–806. doi: 10.1099/vir.0.028597-0

Leifer, C. A., and Medvedev, A. E. (2016). Molecular mechanisms of regulation of Toll-like receptor signaling. *J. Leukoc. Biol.* 100, 927–941. doi: 10.1189/jlb.2MR0316-117RR

Leon-Juarez, M., Martinez-Castillo, M., Shrivastava, G., Garcia-Cordero, J., Villegas-Sepulveda, N., Mondragon-Castelan, M., et al. (2016). Recombinant Dengue virus protein NS2B alters membrane permeability in different membrane models. *Virol. J.* 13:1. doi: 10.1186/s12985-015-0456-4

Leung, J. Y., Pijlman, G. P., Kondratieva, N., Hyde, J., Mackenzie, J. M., and Khromykh, A. A. (2008). Role of nonstructural protein NS2A in flavivirus assembly. *J. Virol.* 82, 4731–4741. doi: 10.1128/JVI.00002-08

Li, C., Ge, L. L., Li, P. P., Wang, Y., Dai, J. J., Sun, M. X., et al. (2014). Cellular DDX3 regulates Japanese encephalitis virus replication by interacting with viral un-translated regions. *Virology* 449, 70–81. doi: 10.1016/j.virol.2013.11.008

Li, C., Ge, L. L., Li, P. P., Wang, Y., Sun, M. X., Huang, L., et al. (2013). The DEAD-box RNA helicase DDX5 acts as a positive regulator of Japanese encephalitis virus replication by binding to viral 3′ UTR. *Antiviral Res.* 100, 487–499. doi: 10.1016/j.antiviral.2013.09.002

Li, S. H., Dong, H., Li, X. F., Xie, X., Zhao, H., Deng, Y. Q., et al. (2013). Rational design of a flavivirus vaccine by abolishing viral RNA 2′-O methylation. *J. Virol.* 87, 5812–5819. doi: 10.1128/JVI.02806-12

Li, W., and Brinton, M. A. (2001). The 3′ stem loop of the West Nile virus genomic RNA can suppress translation of chimeric mRNAs. *Virology* 287, 49–61. doi: 10.1006/viro.2001.1015

Li, W., Li, Y., Kedersha, N., Anderson, P., Emara, M., Swiderek, K. M., et al. (2002). Cell proteins TIA-1 and TIAR interact with the 3′ stem-loop of the West Nile

virus complementary minus-strand RNA and facilitate virus replication. *J. Virol.* 76, 11989–12000.

Li, X. D., Ye, H. Q., Deng, C. L., Liu, S. Q., Zhang, H. L., Shang, B. D., et al. (2015). Genetic interaction between NS4A and NS4B for replication of Japanese encephalitis virus. *J. Gen. Virol.* 96(Pt 6), 1264–1275. doi: 10.1099/vir.0.000044

Liang, Z., Wu, S., Li, Y., He, L., Wu, M., Jiang, L., et al. (2011). Activation of Toll-like receptor 3 impairs the dengue virus serotype 2 replication through induction of IFN-beta in cultured hepatoma cells. *PLoS One* 6:e23346. doi: 10.1371/journal.pone.0023346

Liao, K. C., Chuo, V., Ng, W. C., Neo, S. P., Pompon, J., Gunaratne, J., et al. (2018). Identification and characterization of host proteins bound to dengue virus 3′ UTR reveal an antiviral role for quaking proteins. *RNA* 24, 803–814. doi: 10.1261/rna.064006.117

Lichinchi, G., Zhao, B. S., Wu, Y., Lu, Z., Qin, Y., He, C., et al. (2016). Dynamics of human and viral RNA methylation during zika virus infection. *Cell Host Microbe* 20, 666–673. doi: 10.1016/j.chom.2016.10.002

Liu, N., Dai, Q., Zheng, G., He, C., Parisien, M., and Pan, T. (2015). N(6)-methyladenosine-dependent RNA structural switches regulate RNA-protein interactions. *Nature* 518, 560–564. doi: 10.1038/nature14234

Liu, N., Zhou, K. I., Parisien, M., Dai, Q., Diatchenko, L., and Pan, T. (2017). N6-methyladenosine alters RNA structure to regulate binding of a low-complexity protein. *Nucleic Acids Res.* 45, 6051–6063. doi: 10.1093/nar/gkx141

Liu, W. J., Chen, H. B., and Khromykh, A. A. (2003). Molecular and functional analyses of Kunjin virus infectious cDNA clones demonstrate the essential roles for NS2A in virus assembly and for a nonconservative residue in NS3 in RNA replication. *J. Virol.* 77, 7804–7813.

Liu, Y., Liu, H., Zou, J., Zhang, B., and Yuan, Z. (2014). Dengue virus subgenomic RNA induces apoptosis through the Bcl-2-mediated PI3k/Akt signaling pathway. *Virology* 448, 15–25. doi: 10.1016/j.virol.2013.09.016

Liu, Z. Y., Li, X. F., Jiang, T., Deng, Y. Q., Ye, Q., Zhao, H., et al. (2016). Viral RNA switch mediates the dynamic control of flavivirus replicase recruitment by genome cyclization. *eLife* 5:e17636. doi: 10.7554/eLife.17636

Liu, Z. Y., Li, X. F., Jiang, T., Deng, Y. Q., Zhao, H., Wang, H. J., et al. (2013). Novel cis-acting element within the capsid-coding region enhances flavivirus viral-RNA replication by regulating genome cyclization. *J. Virol.* 87, 6804–6818. doi: 10.1128/JVI.00243-13

Lobigs, M. (1993). Flavivirus premembrane protein cleavage and spike heterodimer secretion require the function of the viral proteinase NS3. *Proc. Natl. Acad. Sci. U.S.A.* 90, 6218–6222.

Lobigs, M., and Lee, E. (2004). Inefficient signalase cleavage promotes efficient nucleocapsid incorporation into budding flavivirus membranes. *J. Virol.* 78, 178–186.

Lobigs, M., Lee, E., Ng, M. L., Pavy, M., and Lobigs, P. (2010). A flavivirus signal peptide balances the catalytic activity of two proteases and thereby facilitates virus morphogenesis. *Virology* 401, 80–89. doi: 10.1016/j.virol.2010.02.008

Loo, Y. M., Fornek, J., Crochet, N., Bajwa, G., Perwitasari, O., Martinez-Sobrido, L., et al. (2008). Distinct RIG-I and MDA5 signaling by RNA viruses in innate immunity. *J. Virol.* 82, 335–345. doi: 10.1128/JVI.01080-07

Manokaran, G., Finol, E., Wang, C., Gunaratne, J., Bahl, J., Ong, E. Z., et al. (2015). Dengue subgenomic RNA binds TRIM25 to inhibit interferon expression for epidemiological fitness. *Science* 350, 217–221. doi: 10.1126/science.aab3369

Manzano, M., Reichert, E. D., Polo, S., Falgout, B., Kasprzak, W., Shapiro, B. A., et al. (2011). Identification of cis-acting elements in the 3′-untranslated region of the dengue virus type 2 RNA that modulate translation and replication. *J. Biol. Chem.* 286, 22521–22534. doi: 10.1074/jbc.M111.234302

Martins, I. C., Gomes-Neto, F., Faustino, A. F., Carvalho, F. A., Carneiro, F. A., Bozza, P. T., et al. (2012). The disordered N-terminal region of dengue virus capsid protein contains a lipid-droplet-binding motif. *Biochem. J.* 444, 405–415. doi: 10.1042/BJ20112219

Miller, S., Kastner, S., Krijnse-Locker, J., Buhler, S., and Bartenschlager, R. (2007). The non-structural protein 4A of dengue virus is an integral membrane protein inducing membrane alterations in a 2K-regulated manner. *J. Biol. Chem.* 282, 8873–8882. doi: 10.1074/jbc.M609919200

Miorin, L., Maestre, A. M., Fernandez-Sesma, A., and Garcia-Sastre, A. (2017). Antagonism of type I interferon by flaviviruses. *Biochem. Biophys. Res. Commun.* 492, 587–596. doi: 10.1016/j.bbrc.2017.05.146

Miorin, L., Romero-Brey, I., Maiuri, P., Hoppe, S., Krijnse-Locker, J., Bartenschlager, R., et al. (2013). Three-dimensional architecture of tick-borne encephalitis virus replication sites and trafficking of the replicated RNA. *J. Virol.* 87, 6469–6481. doi: 10.1128/JVI.03456-12

Miyanari, Y., Atsuzawa, K., Usuda, N., Watashi, K., Hishiki, T., Zayas, M., et al. (2007). The lipid droplet is an important organelle for hepatitis C virus production. *Nat. Cell Biol.* 9, 1089–1097. doi: 10.1038/ncb1631

Moon, S. L., Anderson, J. R., Kumagai, Y., Wilusz, C. J., Akira, S., Khromykh, A. A., et al. (2012). A noncoding RNA produced by arthropod-borne flaviviruses inhibits the cellular exoribonuclease XRN1 and alters host mRNA stability. *RNA* 18, 2029–2040. doi: 10.1261/rna.034330.112

Moon, S. L., Dodd, B. J., Brackney, D. E., Wilusz, C. J., Ebel, G. D., and Wilusz, J. (2015). Flavivirus sfRNA suppresses antiviral RNA interference in cultured cells and mosquitoes and directly interacts with the RNAi machinery. *Virology* 485, 322–329. doi: 10.1016/j.virol.2015.08.009

Nasirudeen, A. M., Wong, H. H., Thien, P., Xu, S., Lam, K. P., and Liu, D. X. (2011). RIG-I, MDA5 and TLR3 synergistically play an important role in restriction of dengue virus infection. *PLoS Negl. Trop. Dis.* 5:e926. doi: 10.1371/journal.pntd.0000926

Neufeldt, C. J., Cortese, M., Acosta, E. G., and Bartenschlager, R. (2018). Rewiring cellular networks by members of the Flaviviridae family. *Nat. Rev. Microbiol.* 16, 125–142. doi: 10.1038/nrmicro.2017.170

Ng, W. C., Soto-Acosta, R., Bradrick, S. S., Garcia-Blanco, M. A., and Ooi, E. E. (2017). The 5′ and 3′ untranslated regions of the flaviviral genome. *Viruses* 9:E137. doi: 10.3390/v9060137

Offerdahl, D. K., Dorward, D. W., Hansen, B. T., and Bloom, M. E. (2012). A three-dimensional comparison of tick-borne flavivirus infection in mammalian and tick cell lines. *PLoS One* 7:e47912. doi: 10.1371/journal.pone.0047912

Olsthoorn, R. C., and Bol, J. F. (2001). Sequence comparison and secondary structure analysis of the 3′ noncoding region of flavivirus genomes reveals multiple pseudoknots. *RNA* 7, 1370–1377.

Paranjape, S. M., and Harris, E. (2007). Y box-binding protein-1 binds to the dengue virus 3′-untranslated region and mediates antiviral effects. *J. Biol. Chem.* 282, 30497–30508. doi: 10.1074/jbc.M705755200

Patkar, C. G., and Kuhn, R. J. (2008). Yellow Fever virus NS3 plays an essential role in virus assembly independent of its known enzymatic functions. *J. Virol.* 82, 3342–3352. doi: 10.1128/JVI.02447-07

Paul, D., and Bartenschlager, R. (2015). Flaviviridae replication organelles: oh, what a tangled web we weave. *Annu. Rev. Virol.* 2, 289–310. doi: 10.1146/annurev-virology-100114-055007

Perard, J., Leyrat, C., Baudin, F., Drouet, E., and Jamin, M. (2013). Structure of the full-length HCV IRES in solution. *Nat. Commun.* 4:1612. doi: 10.1038/ncomms2611

Perera-Lecoin, M., Meertens, L., Carnec, X., and Amara, A. (2013). Flavivirus entry receptors: an update. *Viruses* 6, 69–88. doi: 10.3390/v6010069

Pesko, K. N., Fitzpatrick, K. A., Ryan, E. M., Shi, P. Y., Zhang, B., Lennon, N. J., et al. (2012). Internally deleted WNV genomes isolated from exotic birds in New Mexico: function in cells, mosquitoes, and mice. *Virology* 427, 10–17. doi: 10.1016/j.virol.2012.01.028

Phillips, S. L., Soderblom, E. J., Bradrick, S. S., and Garcia-Blanco, M. A. (2016). Identification of proteins bound to dengue viral RNA in vivo reveals new host proteins important for virus replication. *mBio* 7:e01865-15. doi: 10.1128/mBio.01865-15

Pichlmair, A., Schulz, O., Tan, C. P., Naslund, T. I., Liljestrom, P., Weber, F., et al. (2006). RIG-I-mediated antiviral responses to single-stranded RNA bearing 5′-phosphates. *Science* 314, 997–1001. doi: 10.1126/science.1132998

Pijlman, G. P., Funk, A., Kondratieva, N., Leung, J., Torres, S., van der Aa, L., et al. (2008). A highly structured, nuclease-resistant, noncoding RNA produced by flaviviruses is required for pathogenicity. *Cell Host Microbe* 4, 579–591. doi: 10.1016/j.chom.2008.10.007

Poenisch, M., Metz, P., Blankenburg, H., Ruggieri, A., Lee, J. Y., Rupp, D., et al. (2015). Identification of HNRNPK as regulator of hepatitis C virus particle production. *PLoS Pathog.* 11:e1004573. doi: 10.1371/journal.ppat.1004573

Polacek, C., Friebe, P., and Harris, E. (2009). Poly(A)-binding protein binds to the non-polyadenylated 3′ untranslated region of dengue virus and modulates translation efficiency. *J. Gen. Virol.* 90(Pt 3), 687–692. doi: 10.1099/vir.0.007021-0

Pompon, J., Manuel, M., Ng, G. K., Wong, B., Shan, C., Manokaran, G., et al. (2017). Dengue subgenomic flaviviral RNA disrupts immunity in mosquito salivary glands to increase virus transmission. *PLoS Pathog.* 13:e1006535. doi: 10.1371/journal.ppat.1006535

Pong, W. L., Huang, Z. S., Teoh, P. G., Wang, C. C., and Wu, H. N. (2011). RNA binding property and RNA chaperone activity of dengue virus core protein and other viral RNA-interacting proteins. *FEBS Lett.* 585, 2575–2581. doi: 10.1016/j.febslet.2011.06.038

Qing, M., Liu, W., Yuan, Z., Gu, F., and Shi, P. Y. (2010). A high-throughput assay using dengue-1 virus-like particles for drug discovery. *Antiviral Res.* 86, 163–171. doi: 10.1016/j.antiviral.2010.02.313

Ray, D., Shah, A., Tilgner, M., Guo, Y., Zhao, Y. W., Dong, H. P., et al. (2006). West nile virus 5′-cap structure is formed by sequential guanine N-7 and ribose 2′-O methylations by nonstructural protein 5. *J. Virol.* 80, 8362–8370. doi: 10.1128/Jvi.00814-06

Reid, C. R., and Hobman, T. C. (2017). The nucleolar helicase DDX56 redistributes to West Nile virus assembly sites. *Virology* 500, 169–177. doi: 10.1016/j.virol.2016.10.025

Reid, D. W., Campos, R. K., Child, J. R., Zheng, T., Chan, K. W. K., Bradrick, S. S., et al. (2018). Dengue virus selectively annexes endoplasmic reticulum-associated translation machinery as a strategy for co-opting host cell protein synthesis. *J. Virol.* 92:e01766-17. doi: 10.1128/JVI.01766-17

Roosendaal, J., Westaway, E. G., Khromykh, A., and Mackenzie, J. M. (2006). Regulated cleavages at the West Nile virus NS4A-2K-NS4B junctions play a major role in rearranging cytoplasmic membranes and Golgi trafficking of the NS4A protein. *J. Virol.* 80, 4623–4632. doi: 10.1128/JVI.80.9.4623-4632.2006

Roth, H., Magg, V., Uch, F., Mutz, P., Klein, P., Haneke, K., et al. (2017). Flavivirus infection uncouples translation suppression from cellular stress responses. *mBio* 8:e02150-16. doi: 10.1128/mBio.02150-16

Samsa, M. M., Mondotte, J. A., Iglesias, N. G., Assuncao-Miranda, I., Barbosa-Lima, G., Da Poian, A. T., et al. (2009). Dengue virus capsid protein usurps lipid droplets for viral particle formation. *PLoS Pathog.* 5:e1000632. doi: 10.1371/journal.ppat.1000632

Scaturro, P., Cortese, M., Chatel-Chaix, L., Fischl, W., and Bartenschlager, R. (2015). Dengue virus non-structural protein 1 modulates infectious particle production via interaction with the structural proteins. *PLoS Pathog.* 11:e1005277. doi: 10.1371/journal.ppat.1005277

Schalich, J., Allison, S. L., Stiasny, K., Mandl, C. W., Kunz, C., and Heinz, F. X. (1996). Recombinant subviral particles from tick-borne encephalitis virus are fusogenic and provide a model system for studying flavivirus envelope glycoprotein functions. *J. Virol.* 70, 4549–4557.

Schlee, M. (2013). Master sensors of pathogenic RNA - RIG-I like receptors. *Immunobiology* 218, 1322–1335. doi: 10.1016/j.imbio.2013.06.007

Schmid, B., Rinas, M., Ruggieri, A., Acosta, E. G., Bartenschlager, M., Reuter, A., et al. (2015). Live cell analysis and mathematical modeling identify determinants of attenuation of dengue virus 2′-O-methylation mutant. *PLoS Pathog.* 11:e1005345. doi: 10.1371/journal.ppat.1005345

Schnell, G., Loo, Y. M., Marcotrigiano, J., and Gale, M. Jr. (2012). Uridine composition of the poly-U/UC tract of HCV RNA defines non-self recognition by RIG-I. *PLoS Pathog.* 8:e1002839. doi: 10.1371/journal.ppat.1002839

Schnettler, E., Sterken, M. G., Leung, J. Y., Metz, S. W., Geertsema, C., Goldbach, R. W., et al. (2012). Noncoding flavivirus RNA displays RNA interference suppressor activity in insect and Mammalian cells. *J. Virol.* 86, 13486–13500. doi: 10.1128/JVI.01104-12

Schoggins, J. W., MacDuff, D. A., Imanaka, N., Gainey, M. D., Shrestha, B., Eitson, J. L., et al. (2014). Pan-viral specificity of IFN-induced genes reveals new roles for cGAS in innate immunity. *Nature* 505, 691–695. doi: 10.1038/nature12862

Schuessler, A., Funk, A., Lazear, H. M., Cooper, D. A., Torres, S., Daffis, S., et al. (2012). West Nile virus noncoding subgenomic RNA contributes to viral evasion of the type I interferon-mediated antiviral response. *J. Virol.* 86, 5708–5718. doi: 10.1128/JVI.00207-12

Selisko, B., Potisopon, S., Agred, R., Priet, S., Varlet, I., Thillier, Y., et al. (2012). Molecular basis for nucleotide conservation at the ends of the dengue virus genome. *PLoS Pathog.* 8:e1002912. doi: 10.1371/journal.ppat.1002912

Selisko, B., Wang, C., Harris, E., and Canard, B. (2014). Regulation of Flavivirus RNA synthesis and replication. *Curr. Opin. Virol.* 9, 74–83. doi: 10.1016/j.coviro.2014.09.011

Shi, G., Ando, T., Suzuki, R., Matsuda, M., Nakashima, K., Ito, M., et al. (2016). Involvement of the 3′ untranslated region in encapsidation of the hepatitis C virus. *PLoS Pathog.* 12:e1005441. doi: 10.1371/journal.ppat.1005441

Shrivastava, G., Garcia-Cordero, J., Leon-Juarez, M., Oza, G., Tapia-Ramirez, J., Villegas-Sepulveda, N., et al. (2017). NS2A comprises a putative viroporin of Dengue virus 2. *Virulence* 8, 1450–1456. doi: 10.1080/21505594.2017.1356540

Shulla, A., and Randall, G. (2015). Spatiotemporal analysis of hepatitis C virus infection. *PLoS Pathog.* 11:e1004758. doi: 10.1371/journal.ppat.1004758

Shustov, A. V., and Frolov, I. (2010). Efficient, trans-complementing packaging systems for chimeric, pseudoinfectious dengue 2/yellow fever viruses. *Virology* 400, 8–17. doi: 10.1016/j.virol.2009.12.015

Silva, P. A., Pereira, C. F., Dalebout, T. J., Spaan, W. J., and Bredenbeek, P. J. (2010). An RNA pseudoknot is required for production of yellow fever virus subgenomic RNA by the host nuclease XRN1. *J. Virol.* 84, 11395–11406. doi: 10.1128/JVI.01047-10

Sprokholt, J. K., Kaptein, T. M., van Hamme, J. L., Overmars, R. J., Gringhuis, S. I., and Geijtenbeek, T. B. H. (2017). RIG-I-like receptor triggering by dengue virus drives dendritic cell immune activation and TH1 differentiation. *J. Immunol.* 198, 4764–4771. doi: 10.4049/jimmunol.1602121

Sun, B., Sundstrom, K. B., Chew, J. J., Bist, P., Gan, E. S., Tan, H. C., et al. (2017). Dengue virus activates cGAS through the release of mitochondrial DNA. *Sci. Rep.* 7:3594. doi: 10.1038/s41598-017-03932-1

Suzuki, R., Ishikawa, T., Konishi, E., Matsuda, M., Watashi, K., Aizaki, H., et al. (2014). Production of single-round infectious chimeric flaviviruses with DNA-based Japanese encephalitis virus replicon. *J. Gen. Virol.* 95(Pt 1), 60–65. doi: 10.1099/vir.0.058008-0

Swarbrick, C. M. D., Basavannacharya, C., Chan, K. W. K., Chan, S. A., Singh, D., Wei, N., et al. (2017). NS3 helicase from dengue virus specifically recognizes viral RNA sequence to ensure optimal replication. *Nucleic Acids Res.* 45, 12904–12920. doi: 10.1093/nar/gkx1127

Szretter, K. J., Daniels, B. P., Cho, H., Gainey, M. D., Yokoyama, W. M., Gale, M., et al. (2012). 2′-O methylation of the viral mRNA cap by West Nile virus evades ifit1-dependent and -independent mechanisms of host restriction in vivo. *PLoS Pathog.* 8:e1002698. doi: 10.1371/journal.ppat.1002698

Takahashi, H., Takahashi, C., Moreland, N. J., Chang, Y. T., Sawasaki, T., Ryo, A., et al. (2012). Establishment of a robust dengue virus NS3-NS5 binding assay for identification of protein-protein interaction inhibitors. *Antiviral Res.* 96, 305–314. doi: 10.1016/j.antiviral.2012.09.023

Takahasi, K., Yoneyama, M., Nishihori, T., Hirai, R., Kumeta, H., Narita, R., et al. (2008). Nonself RNA-sensing mechanism of RIG-I helicase and activation of antiviral immune responses. *Mol. Cell* 29, 428–440. doi: 10.1016/j.molcel.2007.11.028

Tay, M. Y., Saw, W. G., Zhao, Y., Chan, K. W., Singh, D., Chong, Y., et al. (2015). The C-terminal 50 amino acid residues of dengue NS3 protein are important for NS3-NS5 interaction and viral replication. *J. Biol. Chem.* 290, 2379–2394. doi: 10.1074/jbc.M114.607341

Tsai, Y. T., Chang, S. Y., Lee, C. N., and Kao, C. L. (2009). Human TLR3 recognizes dengue virus and modulates viral replication in vitro. *Cell Microbiol.* 11, 604–615. doi: 10.1111/j.1462-5822.2008.01277.x

Umareddy, I., Chao, A., Sampath, A., Gu, F., and Vasudevan, S. G. (2006). Dengue virus NS4B interacts with NS3 and dissociates it from single-stranded RNA. *J. Gen. Virol.* 87(Pt 9), 2605–2614. doi: 10.1099/vir.0.81844-0

Upadhyay, A., Dixit, U., Manvar, D., Chaturvedi, N., and Pandey, V. N. (2013). Affinity capture and identification of host cell factors associated with hepatitis C virus (+) strand subgenomic RNA. *Mol. Cell. Proteomics* 12, 1539–1552. doi: 10.1074/mcp.M112.017020

Urosevic, N., van Maanen, M., Mansfield, J. P., Mackenzie, J. S., and Shellam, G. R. (1997). Molecular characterization of virus-specific RNA produced in the brains of flavivirus-susceptible and -resistant mice after challenge with Murray Valley encephalitis virus. *J. Gen. Virol.* 78(Pt 1), 23–29. doi: 10.1099/0022-1317-78-1-23

Vashist, S., Anantpadma, M., Sharma, H., and Vrati, S. (2009). La protein binds the predicted loop structures in the 3′ non-coding region of Japanese encephalitis virus genome: role in virus replication. *J. Gen. Virol.* 90(Pt 6), 1343–1352. doi: 10.1099/vir.0.010850-0

Vashist, S., Bhullar, D., and Vrati, S. (2011). La protein can simultaneously bind to both 3′- and 5′-noncoding regions of Japanese encephalitis virus genome. *DNA Cell Biol.* 30, 339–346. doi: 10.1089/dna.2010.1114

Vashist, S., Urena, L., Chaudhry, Y., and Goodfellow, I. (2012). Identification of RNA-protein interaction networks involved in the norovirus life cycle. *J. Virol.* 86, 11977–11990. doi: 10.1128/JVI.00432-12

Viktorovskaya, O. V., Greco, T. M., Cristea, I. M., and Thompson, S. R. (2016). Identification of RNA binding proteins associated with dengue virus RNA in infected cells reveals temporally distinct host factor requirements. *PLoS Negl. Trop. Dis.* 10:e0004921. doi: 10.1371/journal.pntd.0004921

Villordo, S. M., Alvarez, D. E., and Gamarnik, A. V. (2010). A balance between circular and linear forms of the dengue virus genome is crucial for viral replication. *RNA* 16, 2325–2335. doi: 10.1261/rna.2120410

Villordo, S. M., Filomatori, C. V., Sanchez-Vargas, I., Blair, C. D., and Gamarnik, A. V. (2015). Dengue virus RNA structure specialization facilitates host adaptation. *PLoS Pathog.* 11:e1004604. doi: 10.1371/journal.ppat.1004604

Vossmann, S., Wieseler, J., Kerber, R., and Kummerer, B. M. (2015). A basic cluster in the N terminus of yellow fever virus NS2A contributes to infectious particle production. *J. Virol.* 89, 4951–4965. doi: 10.1128/JVI.03351-14

Wang, B., Thurmond, S., Hai, R., and Song, J. (2018). Structure and function of Zika virus NS5 protein: perspectives for drug design. *Cell. Mol. Life Sci.* 75, 1723–1736. doi: 10.1007/s00018-018-2751-x

Wang, P. G., Kudelko, M., Lo, J., Siu, L. Y., Kwok, K. T., Sachse, M., et al. (2009). Efficient assembly and secretion of recombinant subviral particles of the four dengue serotypes using native prM and E proteins. *PLoS One* 4:e8325. doi: 10.1371/journal.pone.0008325

Ward, A. M., Bidet, K., Yinglin, A., Ler, S. G., Hogue, K., Blackstock, W., et al. (2011). Quantitative mass spectrometry of DENV-2 RNA-interacting proteins reveals that the DEAD-box RNA helicase DDX6 binds the DB1 and DB2 3′ UTR structures. *RNA Biol.* 8, 1173–1186. doi: 10.4161/rna.8.6.17836

Ward, A. M., Calvert, M. E., Read, L. R., Kang, S., Levitt, B. E., Dimopoulos, G., et al. (2016). The Golgi associated ERI3 is a Flavivirus host factor. *Sci. Rep.* 6:34379. doi: 10.1038/srep34379

Welsch, S., Miller, S., Romero-Brey, I., Merz, A., Bleck, C. K., Walther, P., et al. (2009). Composition and three-dimensional architecture of the dengue virus replication and assembly sites. *Cell Host Microbe* 5, 365–375. doi: 10.1016/j.chom.2009.03.007

Westaway, E. G., Mackenzie, J. M., Kenney, M. T., Jones, M. K., and Khromykh, A. A. (1997). Ultrastructure of Kunjin virus-infected cells: colocalization of NS1 and NS3 with double-stranded RNA, and of NS2B with NS3, in virus-induced membrane structures. *J. Virol.* 71, 6650–6661.

Winkelmann, E. R., Widman, D. G., Suzuki, R., and Mason, P. W. (2011). Analyses of mutations selected by passaging a chimeric flavivirus identify mutations that alter infectivity and reveal an interaction between the structural proteins and the nonstructural glycoprotein NS1. *Virology* 421, 96–104. doi: 10.1016/j.virol.2011.09.007

Wu, R. H., Tsai, M. H., Chao, D. Y., and Yueh, A. (2015). Scanning mutagenesis studies reveal a potential intramolecular interaction within the C-terminal half of dengue virus NS2A involved in viral RNA replication and virus assembly and secretion. *J. Virol.* 89, 4281–4295. doi: 10.1128/JVI.03011-14

Xie, X., Zou, J., Puttikhunt, C., Yuan, Z., and Shi, P. Y. (2015). Two distinct sets of NS2A molecules are responsible for dengue virus RNA synthesis and virion assembly. *J. Virol.* 89(2), 1298-1313. doi: 10.1128/JVI.02882-14

Xu, Z., Anderson, R., and Hobman, T. C. (2011). The capsid-binding nucleolar helicase DDX56 is important for infectivity of West Nile virus. *J. Virol.* 85, 5571–5580. doi: 10.1128/JVI.01933-10

Xu, Z., and Hobman, T. C. (2012). The helicase activity of DDX56 is required for its role in assembly of infectious West Nile virus particles. *Virology* 433, 226–235. doi: 10.1016/j.virol.2012.08.011

Yang, Y., Shan, C., Zou, J., Muruato, A. E., Bruno, D. N., de Almeida Medeiros Daniele, B., et al. (2017). A cDNA clone-launched platform for high-yield production of inactivated zika vaccine. *EBioMedicine* 17, 145–156. doi: 10.1016/j.ebiom.2017.02.003

Yoneyama, M., Kikuchi, M., Natsukawa, T., Shinobu, N., Imaizumi, T., Miyagishi, M., et al. (2004). The RNA helicase RIG-I has an essential function in double-stranded RNA-induced innate antiviral responses. *Nat. Immunol.* 5, 730–737. doi: 10.1038/ni1087

Yoshii, K., Goto, A., Kawakami, K., Kariwa, H., and Takashima, I. (2008). Construction and application of chimeric virus-like particles of tick-borne encephalitis virus and mosquito-borne Japanese encephalitis virus. *J. Gen. Virol.* 89(Pt 1), 200–211. doi: 10.1099/vir.0.82824-0

You, S., and Padmanabhan, R. (1999). A novel in vitro replication system for Dengue virus. Initiation of RNA synthesis at the 3′-end of exogenous viral RNA templates requires 5′- and 3′-terminal complementary sequence motifs of the viral RNA. *J. Biol. Chem.* 274, 33714–33722.

Youn, S., Li, T., McCune, B. T., Edeling, M. A., Fremont, D. H., Cristea, I. M., et al. (2012). Evidence for a genetic and physical interaction between nonstructural proteins NS1 and NS4B that modulates replication of West Nile virus. *J. Virol.* 86, 7360–7371. doi: 10.1128/JVI.00157-12

Yu, C. Y., Chang, T. H., Liang, J. J., Chiang, R. L., Lee, Y. L., Liao, C. L., et al. (2012). Dengue virus targets the adaptor protein MITA to subvert host innate immunity. *PLoS Pathog.* 8:e1002780. doi: 10.1371/journal.ppat.1002780

Yu, L., Takeda, K., and Markoff, L. (2013). Protein-protein interactions among West Nile non-structural proteins and transmembrane complex formation in mammalian cells. *Virology* 446, 365–377. doi: 10.1016/j.virol.2013.08.006

Zou, J., Lee le, T., Wang, Q. Y., Xie, X., Lu, S., Yau, Y. H., et al. (2015a). Mapping the Interactions between the NS4B and NS3 proteins of dengue virus. *J. Virol.* 89, 3471–3483. doi: 10.1128/JVI.03454-14

Zou, J., Xie, X., Wang, Q. Y., Dong, H., Lee, M. Y., Kang, C., et al. (2015b). Characterization of dengue virus NS4A and NS4B protein interaction. *J. Virol.* 89, 3455–3470. doi: 10.1128/JVI.03453-14

Zou, J., Xie, X., Lee le, T., Chandrasekaran, R., Reynaud, A., Yap, L., et al. (2014). Dimerization of flavivirus NS4B protein. *J. Virol.* 88, 3379–3391. doi: 10.1128/JVI.02782-13

Zust, R., Cervantes-Barragan, L., Habjan, M., Maier, R., Neuman, B. W., Ziebuhr, J., et al. (2011). Ribose 2′-O-methylation provides a molecular signature for the distinction of self and non-self mRNA dependent on the RNA sensor Mda5. *Nat. Immunol.* 12, 137–143. doi: 10.1038/ni.1979

Zust, R., Dong, H., Li, X. F., Chang, D. C., Zhang, B., Balakrishnan, T., et al. (2013). Rational design of a live attenuated dengue vaccine: 2′-o-methyltransferase mutants are highly attenuated and immunogenic in mice and macaques. *PLoS Pathog.* 9:e1003521. doi: 10.1371/journal.ppat.1003521

Conflict of Interest Statement: The authors declare that the research was conducted in the absence of any commercial or financial relationships that could be construed as a potential conflict of interest.

12 ANNEXE VI

bio-protocol www.bio-protocol.org/e3115 Vol 8, Iss 24, Dec 20, 2018
DOI:10.21769/BioProtoc.3115

Production, Titration and Imaging of Zika Virus in Mammalian Cells

Wesley Freppel[#], Clément Mazeaud[#] and Laurent Chatel-Chaix*

Institut National de la Recherche Scientifique – Institut Armand-Frappier, H7V 1B7, Laval, QC, Canada
*For correspondence: Laurent.Chatel-Chaix@iaf.inrs.ca
[#]Contributed equally to this work

[Abstract] Since the outbreak of Zika virus (ZIKV) in Latin America and the US in 2016, this flavivirus has emerged as a major threat for public health. Indeed, it is now clear that ZIKV is vertically transmitted from the infected mother to the fetus and this may lead to severe neurological development defects including (but not restricted to) neonate microcephaly. Although ZIKV has been identified in the late 1940s, very little was known about its epidemiology, symptoms and molecular biology before its reemergence 60 years later. Recently, tremendous efforts have been made to develop molecular clones and tools as well as cell culture and animal models to better understand ZIKV fundamental biology and pathogenesis and to develop so-far-unavailable antiviral drugs and vaccines. This bio-protocol describes basic experimental procedures to produce ZIKV stocks and to quantify their concentration in infectious virus particles as well as to image and study this pathogen within infected cells using confocal microscopy-based imaging.

Keywords: Zika virus, NS4B, Double-stranded RNA, Virus titration, Immunofluorescence microscopy, Plaque assay

[Background] Zika virus (ZIKV), a mosquito-borne *Flavivirus* within the *Flaviviridae* virus family, was first isolated from a sentinel Rhesus monkey in 1947 in the Ziika Forest in Uganda and is closely related to dengue virus (DENV) (World Health Organization, 2018). Since then, it became famous in the last decade for its outbreaks in some Pacific islands (2007 and 2013) and in the Americas (2015). Symptomatic patients (25%-20% of the cases) may usually show rather mild clinical manifestations such as fevers, rashes, conjunctivitis, muscle/joint pains and/or headaches. However, since ZIKV re-emergence, severe neurological symptoms including (but not restricted to) Guillain-Barre syndrome in adults and congenitally transmitted newborn microcephaly were identified in infected individuals (Lazear and Diamond, 2016; Grubaugh *et al.*, 2018). Unfortunately, there are currently no available treatments or vaccines against Zika virus, and this is partly due to our poor understanding of its biology.

In terms of phylogeny, there are 2 distinct lineages of Zika virus (Haddow *et al.*, 2012). The so-called "historical" African lineage including the prototype strain MR766 and the "contemporary" Asian lineage derived from the African lineage after decades of mutations. For instance, the Asian strain H/PF/2013 is responsible for the outbreak in French Polynesia in 2013. Similarly, the virus strain responsible for the Brazilian outbreak also phylogenetically derives from the Asian lineage. Indeed, experiments in mouse and mosquito infection models support the idea that the Asian strain has acquired several key mutations which led to microcephaly in infected newborns in Brazil (Yuan *et al.*, 2017) and to enhanced

Vol 8, Iss 24, Dec 20, 2018
DOI:10.21769/BioProtoc.3115

viral infectivity in the arthropod transmission vector *Aedes aegypti* (Liu *et al.*, 2017).

Upon entry in the host cell, the viral genome, a positive single-stranded RNA, is translated into a single polyprotein at the endoplasmic reticulum (ER), which is subsequently cleaved into 3 structural proteins and 7 non-structural proteins by host and viral proteases. After replication, the genome is encapsidated into neosynthesized virions which are subsequently released from the cell (Neufeldt *et al.*, 2018). Like all other tested flaviviruses, ZIKV remodels the endomembranes of the infected cell to generate a cytoplasmic environment which is favorable to ZIKV life cycle (Cortese *et al.*, 2017). These membranous compartments, called viral replication factories are all ER-derived and can be sub-divided into three classes of ultrastructures (Cortese *et al.*, 2017): 1. vesicle packets, which are ER invaginations believed to be the site of viral RNA replication, 2. virus bags in which assembled immature viruses accumulate in regular arrays, and 3. convoluted membranes whose roles remain unclear although it was proposed for DENV that they modulate host processes for the benefit of replication (Chatel-Chaix *et al.*, 2016).

Before 2016, little was known about the general biology of ZIKV, and most of our knowledge relied on a direct transposition of fundamental discoveries about other flaviviruses closely related to this pathogen like DENV. However, it remains unclear what makes ZIKV so unique in terms of neuropathogenesis as compared to the other members of the *Flavivirus* genus. Hence, since ZIKV re-emergence and the recent outbreaks, the scientific community around the world has begun to decipher the mysteries surrounding this virus and to develop tools such as molecular clones as well as cell culture and animal models (Schwarz *et al.*, 2016; Shan *et al.*, 2016; Xie *et al.*, 2016; Morrison and Diamond, 2017; Mutso *et al.*, 2017; Munster *et al.*, 2018). Knowing how to culture ZIKV and to measure its infectivity constitutes key methods to perform any descriptive or functional studies about this virus both *in cellulo* and *in vivo*. Moreover, given that Asian and African lineages may differ in terms of symptom severity in infected mouse fetuses (Cugola *et al.*, 2016), it is sometimes relevant to compare model strains of these two lineages. In this bio-protocol, we describe basic cell culture methods to produce ZIKV stocks from Asian and African lineages and to quantify their concentration in infectious virus particles (more generally referred to as “titer”) as well as to image this pathogen inside infected cells using immunofluorescence-based microscopy.

Materials and Reagents

A. Materials
1. 1.5 ml microtubes (Ultident Scientific, catalog number: 87-B150-C)
2. 10 cm cell culture dishes (Falcon, Fisher Scientific, catalog number: 08-772-E)
3. 15 cm cell culture dishes (Falcon, Fisher Scientific, catalog number: 08-772-6)
4. 24-well polystyrene culture plates (Corning Life Sciences, Fisher Scientific, catalog number: 08-772-1)
5. MCE 0.45 µm filters, 30 mm diameter (Ultident Scientific, catalog number: 229753)
6. 20 ml sterile syringes (Ultident Scientific, catalog number: BD-302830)

7. 15 ml sterile conical tubes (Falcon, Fisher Scientific, catalog number: 352096)
8. Coverslips No. 1 (diameter: 12 mm, thickness: 0.13 to 0.17 mm), sterilized by autoclaving (Fisher Scientific, catalog number: 12-545-80)
9. Microscope glass slides, frosted clear glass 26 mm x 76 mm, 1-1.2 mm thick (Ultident Scientific, catalog number: 170-8105-W)
10. Absorbent paper
11. Parafilm
12. Aluminum foil

B. Viruses
1. ZIKV MR766 (African lineage) (EVAg, catalog number: 001v-EVA143) (under material and transfer agreement. Passage history: P5. Store original desiccated stocks at -80 °C)
2. ZIKV H/PF/2013 (Asian lineage) (EVAg, catalog number: 001v-EVA1545) (under material and transfer agreement. Passage history: P6. Store original desiccated stocks at -80 °C)

C. Cell lines
1. Vero E6 monkey epithelial cells (a kind gift from Drs. Tom Hobman and Anil Kumar, University of Alberta) (ATCC, catalog number: CRL-1586)
2. Huh7 hepatocarcinoma cells (a kind gift from Dr. Patrick Labonté, INRS) (Creative Bioarray, catalog number: CSC-C9441L)
   Alternatively, this cell line is typically available from most laboratories working on hepatitis C virus or DENV.

D. Reagents
1. UltraPure distilled water (Life Technologies, catalog number: 10977-015)
2. Dulbecco's modified Eagle medium (DMEM) (Life Technologies, catalog number: 111965-092)
3. Fetal bovine serum (FBS) performance (Wisent, catalog number: 098150)
4. Penicillin-streptomycin (Life Technologies, catalog number: 15140-122)
5. MEM non essential amino acids solution (100x) (Life Technologies, catalog number: 11140-050)
6. Phosphate buffered saline (PBS) (Life Technologies, catalog number: 14190-144)
7. 1 M HEPES buffer, pH range: 7.2-7.5 (Life Technologies, catalog number: 15630-080)
8. 0.25% Trypsin-EDTA (Life Technologies, catalog number: 25200-072)
9. Minimum Essential Medium (MEM) with L-Glutamine (Life Technologies, catalog number: 11095-080)
10. Carboxymethylcellulose (CMC) sodium salt, medium viscosity (Sigma-Aldrich, catalog number: 21902-100G)
11. 37% formaldehyde (Fisher Scientific, catalog number: BP531-500)
12. Crystal violet (Fisher Scientific, catalog number: C581-100)

13. 95% ethanol (Commercial Alcohols, catalog number: 1011C)
14. Triton X-100 (Mallinktrot, catalog number: 3555)
15. 4% paraformaldehyde (Sigma-Aldrich, catalog number: P6148-1KG)
16. Normal goat serum (Thermo-Fisher, catalog number: 01-6201)
17. Bovine serum albumin (BSA) (Sigma-Aldrich, catalog number: A-9647)
18. Sodium azide (Fisher Scientific, catalog number: BP922I-500)
19. Rabbit polyclonal anti-ZIKV NS4B (GeneTex, catalog number: GTX133311; dilution 1:200)
20. Mouse monoclonal anti-dsRNA, clone J2 (Scicons, catalog number: 10010200; dilution 1:400)
21. Rabbit polyclonal anti-DENV NS4B (GeneTex, catalog number: GTX124250; dilution 1:1,000)
22. Mouse monoclonal anti-DENV NS3, clone GT2811 (GeneTex, catalog number: GTX629477; dilution 1:100)
23. Mouse monoclononal panflaviviral anti-E, clone 4G2 (Sigma-Aldrich, catalog number: MAB10216, dilution 1:200)
24. Goat anti-Rabbit AlexaFluor 488 (Life Technologies, catalog number: A11034)
25. Goat anti-Mouse AlexaFluor 568 (Life Technologies, catalog number: A11004)
26. 4',6-Diamidino-2-Phenylindole (DAPI) (Life Technologies, catalog number: D1306)
27. Fluoromount G (Southern Biotech, catalog number: 0100-01)
28. Complete DMEM (see Recipes)
29. Plaquing medium (MEM-CMC) (see Recipes)
30. Formaldehyde fixative (see Recipes)
31. Paraformaldehyde fixative (see Recipes)
32. Crystal violet staining solution (see Recipes)
33. Triton X-100 permeabilization solution (see Recipes)
34. BSA Blocking solution (see Recipes)

Equipment

1. -80 °C freezer
2. Vortexer
3. Pipette
4. Beaker
5. CO_2 incubator
6. Hemacytometer
7. Magnetic stirrer
8. BSL2 cell culture cabinet
9. 2D rocking platform shaker
10. Zeiss LSM780 confocal microscope
11. Chemical hood
12. Tweezers

13. 4 °C refrigerator
14. Autoclavable glass bottle
15. Autoclave

Procedure

IMPORTANT NOTE: All experiments with live viruses (i.e., all pre-fixation steps) should be performed inside a biosafety level 2 (BSL2) or a BSL2+ tissue culture laboratory according to the country and institution regulations and required permits regarding Zika virus handling and storage.

A. Virus stock production
   1. Virus preparation
      a. Resuspend with 200 µl ultraPure sterile water the desiccated virus stocks by pipetting up and down, at room temperature in a BSL2 cell culture cabinet.
      b. Aliquot 50 µl of virus in sterile microtubes and store at -80 °C.
   2. Virus amplification

      Day -1: Preparation of cells for infection

      a. Prepare cells from 15 cm culture stock dishes of Vero E6 cells showing 80%-100% confluence. PBS, complete DMEM and trypsin-EDTA should be pre-warmed at 37 °C. It is worth mentioning that we never use Vero E6 cells "older" than 50 passages since this may affect cell permissiveness to ZIKV and yields of virus production.
      b. Remove the culture medium.
      c. Wash the cells with 10 ml PBS.
      d. Remove PBS and add 7 ml trypsin-EDTA.
      e. Incubate for 2 min at 37 °C in the CO_2 incubator.
      f. Remove trypsin-EDTA.
      g. Thoroughly tap the cell culture dish in order to detach the cells.
      h. Resuspend the cells in 10 ml complete DMEM (see Recipes section for composition).
      i. Transfer the cells into a 15 ml sterile tube.
      j. Using a hemacytometer, determine the number of cells per ml.
      k. Seed 2 x 10^6 Vero E6 cells in 8 ml of complete DMEM in 10 cm cell culture dishes and incubate overnight in the 37 °C incubator.

      Day 0: Infection

      a. In a 15 ml sterile tube, dilute 50 µl of virus stock in 6 ml of complete DMEM.
      b. Remove by aspiration the medium of Vero E6 cells. Cells should show a confluence of approximately 70%-80%).

      Note: Gently add the virus dilution on the cells and slowly shake the cell culture dish. Especially for the first pilot experiments, we recommend including a control dish of uninfected cells (mock

infection) that will be cultured in parallel (see important note below).

c. Incubate for 2 h at 37 °C.
d. After incubation, remove the virus inoculum.
e. Add 8 ml of pre-warmed complete DMEM.
f. Incubate for 3 days at 37 °C.

Days 3, 4, 5, 6 and 7 post-infection: virus harvest

a. At each day, harvest the supernatant with a sterile 20 ml syringe directly from the cell culture dish. Place an MCE 0.45 µm filter at the tip of the syringe.
b. Filter the supernatant into a sterile 15 ml tube.
c. Add 8 ml of complete DMEM in the cell culture dish and place it back into the incubator.
d. Add 80 µl HEPES buffer 1 M, pH 7.2-7.5 (final concentration of 10 mM) in the filtered supernatant. This will prevent acidification of virus stocks following freeze/thawing and contribute maintaining optimal viral infectivity.
e. Aliquot virus supernatants into sterile 1.5 ml microtubes (1 ml per tube).
f. Store aliquots at -80 °C.
g. Proceed with viral titration of each harvest using plaque assays.

IMPORTANT NOTE: During viral amplification, ZIKV-induced cytopathic effects which lead to cell death can be observed and increase over time. This is generally a good indication that virus infection and production was successful. As a reference for healthy cells, the mock infection control dish may be observed in parallel.

B. Viral titration using plaque assays

Day -1: Preparation of cells for infection

Notes:

a. Cells should be prepared from 15 cm dishes of Vero E6 with 80%-100% confluence.
b. One confluent 15-cm dish of cells is generally enough to prepare five 24-well plates corresponding to 10 samples to titer. PBS, trypsin-EDTA and culture media should be pre-warmed at 37 °C.

1. Remove by aspiration the medium from the culture dishes.
2. Wash the cells with 10 ml of PBS.
3. Remove PBS and add 7 ml trypsin-EDTA.
4. Incubate for 2 min in the incubator.
5. Remove the trypsin by aspiration.
6. Thoroughly tap the cell culture dish in order to detach the cells.
7. Resuspend the cell in 10 ml complete DMEM.
8. Transfer the cells into a sterile 15 ml tube.
9. Determine cell concentration with a hemacytometer.
10. Dilute the cells with complete DMEM to a final concentration of 4 x 10^5 Vero E6 cells/ml.

Vol 8, Iss 24, Dec 20, 2018
DOI:10.21769/BioProtoc.3115

11. Seed 24-well plates with 500 µl diluted cells per well. One 24-well plate allows the titration of two virus samples.
12. Incubate overnight at 37 °C.

Day 0: Infection

Note: The day of infection, the cells should show a confluence of 90%-100%.

1. Prepare 6 microtubes per sample to titer and identify them (10^{-1} to 10^{-6}). Add 450 µl complete DMEM in each microtube.
2. Dilute 10 times the sample in series:
   a. Add 50 µl of virus sample in the first microtube (dilution 10^{-1}). Vortex the tube for 5 s.
   b. Change the tip to avoid any cross-contamination between samples. Pipet 50 µl of the 10^{-1} dilution and transfer into the second tube (dilution 10^{-2}). Vortex the tube for 5 s.
   c. Repeat these steps for the other dilutions (10^{-3} to 10^{-6}).
3. Remove medium from rows A and B of one 24-well plate (Figure 1).
4. Pipet up-and-down twice the 10^{-6} dilution and add 200 µl with the same tip on the side of the last wells of rows A and B according to the plate layout shown in Figure 1. Thus, infection is performed in duplicates.
5. Proceed similarly with other sample dilutions (10^{-5} to 10^{-1} dilutions) according to the plate layout (Figure 1).

   IMPORTANT NOTE: It is critical to change used tips between each dilution to avoid cross-contamination between wells. Moreover, always start dispensing the samples into the plate starting with the most diluted samples. To avoid that cells dry, always wait to have processed one sample before aspirating the medium for another dilution series (e.g., rows C and D).

Vol 8, Iss 24, Dec 20, 2018
DOI:10.21769/BioProtoc.3115

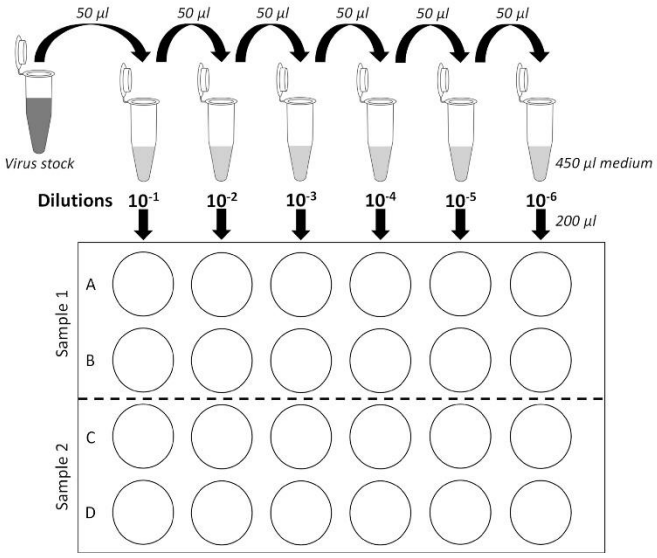

Figure 1. Serial dilution plan and plate layout for plaque assays. Schematic representation of the virus stock 10-fold dilutions and of 24-well plates used for plaque assays. Two samples per plate can be titered. Each dilution is assessed in biological duplicates.

6. Once a 24-well plate has been entirely processed, put it back to the incubator and proceed with the next plate and two new samples to titer.
7. Incubate all plates with gentle agitation at 37 °C for at least one hour using a 2D rocking platform shaker. Incubation period can be extended up to several hours without impacting titers.
8. After this incubation, take the first plate and aspirate the supernatant of the row A and B starting by the 10^{-6} dilution to avoid cross-contamination.
9. Add on the side of wells, starting from the highest dilutions, 1 ml of MEM-CMC (see Recipes) with a 10 ml pipette. Discard the pipette. It is important to change the pipette between each sample series to avoid contamination of the stock bottle of MEM-CMC with virus. Especially, contamination with fast-growing viruses may result in future experiments in the appearance of very large plaques in the wells which will render impossible to count smaller expected plaques.
10. Repeat for rows C and D and then for all plates.
11. Incubate for 5 days at 37 °C.
    IMPORTANT NOTE: Do not move the plates during the 5-day incubation since this will result in the formation of "comet-shaped" plaques which might render them difficult to count.

Day 5 post-infection: Fixation and staining

1. Add 1 ml 10% formaldehyde per well.
2. Incubate for at least 2 h at room temperature in the BSL2 laboratory. Incubation period can be extended up to several days.
3. Discard the liquid by inversion in a large beaker in a chemical hood. Formaldehyde-containing liquid wastes should be handled according to the chemical safety regulations of the research institution.
4. Wash plates by vigorously rinsing them with tap water to remove all the methylcellulose. Remove the excess of water by taping the plates on an absorbent paper.
5. Add 500 µl crystal violet-containing staining solution (see Recipes) on cell monolayers.
6. Incubate for 15 min at room temperature. Incubation period can be extended up to several hours.
7. Remove crystal violet solution by inversion in a reusable plastic container. Collected crystal violet solution can be transferred back to the stock bottle and be reused for future staining.
8. Wash the plates extensively with tap water to remove the excess of staining solution.
9. Dry the plates on absorbent paper to remove excess of water.
10. Count the number of plaques in the appropriate dilution and determine infectious titers (see Figure 2 and Data analysis).

C. Typical infection experiments for imaging

Day -1: Preparation of cells for infection

1. Using tweezers which have been cleaned with 70% ethanol, transfer sterile coverslips in each well of a 24-well culture dish.
2. Seed Huh7 cells (or any cell line of interest to be tested): 20,000 cells in 500 µl complete DMEM. Vigorously shake the plate to homogenously disperse the cells throughout the well. Of note, we never use Huh7 cells “older” than 50 passages since we have noticed a significant change of morphology and growth properties beyond this passage.
3. Incubate overnight at 37 °C with 5% CO_2.

Day 0: Viral infection

1. For infection, appropriate multiplicity of infection (MOI) and virus dilution must be chosen according to stock infectious titers (see Procedure B and Data analysis). For immunofluorescence purposes, MOI of 1 is typically used. MOI of 1 means that on average, each target cell is inoculated with 1 infectious virus particle.
2. In this case (20,000 cells) with an MOI of 1, 20,000 viruses must be diluted in a final volume of 500 µl DMEM in each well. Prepare a master mix for all the wells.
3. Remove culture medium and add gently on the side of each well 500 µl of the ZIKV/DMEM master mix.
4. Incubate for at least 2 h at 37 °C with 5% CO_2 and gentle agitation.

Vol 8, Iss 24, Dec 20, 2018
DOI:10.21769/BioProtoc.3115

5. Remove virus inoculum and add 1 ml complete DMEM per well.
6. Incubate for 48 or 72 h at 37 °C with 5% CO_2.

Day 2 or 3: Fixation

1. Remove media.
2. Wash the cells twice with cold PBS.
3. Add in each well 500 µl 4% paraformaldehyde/PBS solution.
4. Incubate for 20 min at room temperature with gentle shaking.
5. Wash once with 500 µl PBS and add 1 ml PBS.
6. Seal the plate with parafilm to avoid that cells dry because of PBS evaporation. Store fixed cells at 4 °C protected from light with an aluminum foil. The cells can be stored at 4 °C for a few months if no staining is immediately planned.

D. Immunofluorescence staining for confocal microscopy
   1. Remove PBS.
   2. Add 500 µl PBS/Triton X-100 permeabilization solution (see Recipes) and incubate for 15 min at room temperature with gentle shaking.
   3. Wash the cells once with PBS.
   4. During permeabilization, freshly prepare a premix of blocking solution (see Recipes). Plan 300 µl of blocking solution per coverslip to be labeled.
   5. Add 300 µl complete blocking solution per well.
   6. Incubate for 1 h at room temperature with gentle shaking.
   7. Quickly wash the cells three times with 500 µl PBS.
   8. Prepare the primary antibodies
      a. Dilute rabbit anti-ZIKV NS4B and mouse anti-dsRNA in PBS/5% BSA/0.05% sodium azide (*i.e.,* blocking solution without normal goat serum) with dilution of 1/200 and 1/400, respectively. Plan 30 µl antibody solution per coverslip.
      b. Alternatively, antibodies against dengue virus NS4B and NS3 may also be used to detect ZIKV since there is a cross-reaction between these two flaviviruses for the antibody epitopes. Using panflaviviral antibodies against E protein is also an option to be considered (see antibody reference and dilutions in the Materials and Reagents).
   9. To avoid coverslips to dry and maintain a sufficient level of humidity, prepare an airtight container with wet pieces of paper at the bottom.
   10. On a plastic support inside the box, place a piece of parafilm cleaned with 70% ethanol.
   11. For each coverslip to label, add 30 µl of primary antibody as drops.
   12. With tweezers, remove the excess of liquid on a piece of absorbent paper and put each coverslip on the antibody drop, with the cells facing parafilm.
   13. Incubate for at least 2 h at room temperature, protected from light.

14. Take back coverslips and transfer them in a sterile 24-well plate which contains 500 µl PBS per well. Cells must face the top of the plate.
15. Wash the coverslips three times for 5 min with 500 µl PBS.
16. During the last wash, prepare the secondary fluorescently labeled antibodies at a dilution of 1:1,000 in PBS/5% BSA/0.05% sodium azide. Plan 300 µl per coverslip.
17. Cover the coverslips with 300 µl of the secondary antibody solution. Alternatively, in order to spare reagents, coverslips may be incubated on an antibody drop exactly as the primary antibody incubation.
18. Incubate for 1 h at room temperature protected from light on a 2D rocking shaker.
19. Quickly wash once and then, three times for at least 10 min with gentle agitation with 500 µl PBS.
20. Dilute 10,000 fold the DAPI stock into PBS. Plan 500 µl per coverslip.
21. Remove PBS from the plate and add 500 µl DAPI/PBS per well.
22. Incubate for 10 min with gentle agitation at room temperature protected from light.
23. Quickly wash three times each with 500 µl PBS.
24. Wash once with 500 µl sterile water.
25. Clean a microscope glass slide with 70% ethanol. Add a 5 µl drop of Fluoromount G per coverslip. Depending on the microscope used for imaging, each slide can accommodate 3-4 coverslips.
26. Remove the excess of water on coverslip to-be-mounted by touching its side with a piece of absorbent paper. Place the coverslip on a Fluoromount G drop on the glass slide, with cells facing the drop.
27. Keep slides protected from light at 4 °C overnight before imaging.
28. Image the cells with a confocal or epifluorescence microscope in order to determine the % of infection, *i.e.,* the % of NS4B- or dsRNA-positive cells.

Data analysis

A. Infectious titer determination for virus stocks using plaque assays
   1. Count the number of plaques in the well where they can be discriminated. Select the well duplicate showing the highest number of individual plaques. See Figure 2 for a typical example.
   2. Calculate the infectious viral titers according to the following formula:

$$\left(\frac{plaques\ in\ first\ well + plaques\ in\ second\ well}{2}\right) \times \left(\frac{1}{dilution}\right) \times 5 = ZIKV\ titer\ (PFU/ml)$$

   3. Values are multiplied by 5 because the virus inoculum is 200 µl and the titers are normalized to 1 ml of the corresponding ZIKV stock.

   The unit of the viral titers is plaque forming units (PFU) per ml of virus stock. One PFU corresponds to one viral particle which has initially infected one target cell on Day 0. During the 5-day incubation,

newly produced viruses have only locally spread because of the semi-solid CMC-containing medium. At its late time points, virus infection ultimately leads to cell death in Vero E6 cells resulting in the formation of a plaque. Plaques are not stained by the crystal violet because dead cells have been washed off. It is important to note that in Vero E6 cells, plaque size is larger for ZIKV H/PF/2013 than for MR766 because of higher cytopathic effects (see Figure 2). If the plaques are so big that they overlap and are not distinguishable for counting, one may fix the cells one day earlier to reduce plaque size. Another alternative is to use 6- or 12-well plates to increase the cell culture area and to better separate the plaques, hence facilitating the counting.

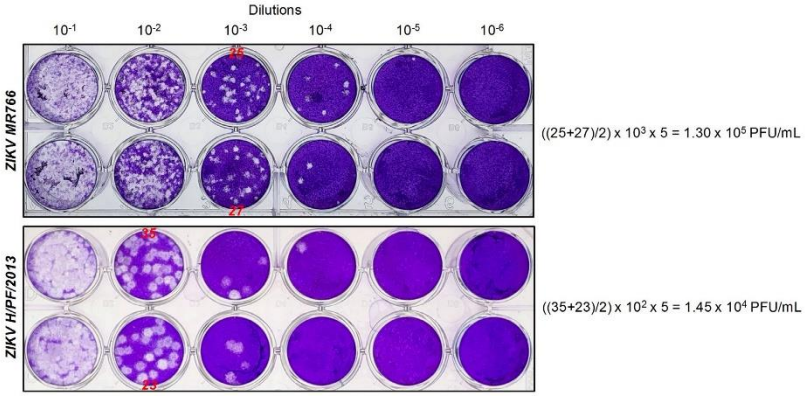

Figure 2. Typical plaque assay for ZIKV MR766 and H/PF/2013. Vero E6 cells were infected with 10-fold serial dilutions of ZIKV MR766 or H/PF/2013 stocks (Day 3 harvests). Five days post-infection, cells were fixed and stained with crystal violet. In this specific example, plaques can be counted in the 10^{-3} and 10^{-4} dilution well of ZIKV MR766 and H/PF/2013 (indicated in red), respectively. According to the formula described above, infectious titers are 1.3 x 10^5 PFU/ml for MR766 and 1.45 x 10^4 PFU/ml for H/PF/2013.

Typically, starting from ~10^4-10^5 PFU/ml depending on the experiment to ~10^7 PFU/ml (Figure 3), infectious titers for both strains logarithmically increase during the five first days of amplification and then reach a plateau. We never collect viruses at 1 and 2 days post-infection because titers are too low to perform subsequent experiments. In our hands, infectious titers over 5 x 10^7 PFU/ml were never achieved, even if the amplification period is extended beyond 7 days. It is worth mentioning that plaque morphology, and the profiles of amplification kinetics may change if high passages of viruses as well as of cells are used for virus stock production. This should be carefully considered and addressed if relevant.

Vol 8, Iss 24, Dec 20, 2018
DOI:10.21769/BioProtoc.3115

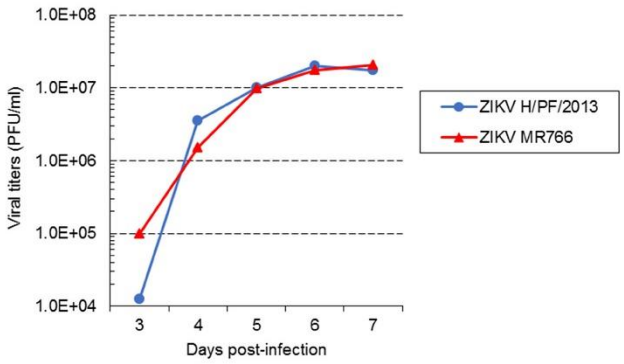

Figure 3. Virus amplification kinetics of ZIKV strains MR 766 and H/PF/2013 in Vero E6 cells. Vero E6 cells were infected with ZIKV MR766 or H/PF/2013 strains at an MOI of 0.01. Virus supernatants were collected at 3, 4, 5, 6 and 7 days post-infection. Infectious virus titers were determined using plaque assays in Vero E6 cells.

B. Imaging

Observe slides at a confocal microscope and set up the detection parameters with the “uninfected” condition coverslip. Any signal observed in this condition is non-specific. For NS4B antibody, it may be diffuse while it generally appears for anti-dsRNA as small dots with a very weak signal throughout the cell. Although anti-dsRNA is not supposed to recognize RNA helixes smaller than 40 base pairs (which are presumably inexistent or rare in cells), it most likely detects cellular highly structured RNAs with low affinity, explaining the observed background in uninfected cells. If non-specific signals are too high, detergent concentration in permeabilization buffer and/or primary antibody dilution may be increased. The ZIKV-specific signal for dsRNA (corresponding to the ZIKV RNA replication intermediate), typically shows a perinuclear accumulation of small intense puncta which presumably correspond to replication complexes within ER-derived vesicle packets (Chatel-Chaix *et al.*, 2016; Cortese *et al.*, 2017) (Figure 4). It was recently shown that dsRNA is localized in the vicinity of the microtubule organization center (MTOC) surrounded by a "cage-like” structure constituted of rearranged cytoskeleton (Cortese *et al.*, 2017). NS4B labeling for both ZIKV strains shows a diffuse distribution, which colocalizes with dsRNA signal (Figure 4), consistent with the fact that DENV NS4B was shown to be a component of vesicle packets as shown by immunogold labeling followed by electron microscopy (Welsch *et al.*, 2009). In addition, ZIKV H/PF/2013 NS4B also accumulates at the periphery of dsRNA clusters within large and intense punctated structure (diameter of ~1-5 µm) which by analogy with DENV NS4B most likely correspond to convoluted membranes, another replication factory sub-structure (Chatel-Chaix *et al.*, 2016).

To estimate the infection rate, count at least a hundred cells in five different fields of the coverslip and count how many are infected, *i.e.,* NS4B- and dsRNA-positive.

Vol 8, Iss 24, Dec 20, 2018
DOI:10.21769/BioProtoc.3115

$$\%\ of\ infection = \frac{100 \times\ infected\ (NS4B\ or\ dsRNA\ positive)\ cell\ number}{Total\ cell\ number\ (DAPI\ positive)}$$

A 100% infection rate is reproducibly achieved within 48 h with ZIKV MR766 in Huh7 cells at an MOI of 1. At 72 h post-infection, cells show obvious signs of cytopathic effect. In contrast, with the same infection conditions, ZIKV H/PF/2013 is generally detected in only 10% of the cells (in infected clusters of 10-20 cells) with no signs of cell death at 48 h post-infection. This infection rate can be improved by fixing the cells one day later. Moreover, we regularly achieve ~100% infection with this strain in Huh7 cells when we increase the MOI to 50. No obvious signs of cytopathic effects were noticed in Huh7 cells in these conditions.

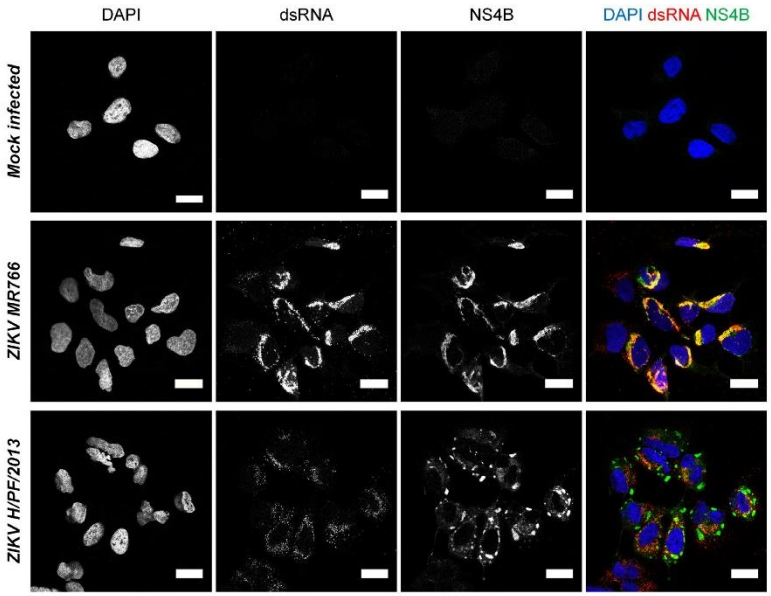

Figure 4. Imaging of Zika virus infection in Huh7 cells. Huh7 cells were infected with ZIKV MR766 or H/PF/2013 strains at an MOI of 1 or left uninfected. Forty-eight hours post-infection, cells were fixed, permeabilized and labeled with anti-dsRNA and anti-ZIKV NS4B antibodies. Nuclei were visualized with DAPI staining. Cells were observed with a Zeiss LSM780 confocal microscope. For ZIKV H/PF/2013, an infected cluster is shown. Scale bars: 20 µm.

C. Relevant remarks

It is important to note that the infection procedure may be adapted for other end-point readouts such as Western blotting, qPCR or RNA interference combined to any functional assay. For those

Vol 8, Iss 24, Dec 20, 2018
DOI:10.21769/BioProtoc.3115

purposes, the number of cells and volume may be up- or down-scaled according to dish or plate format. Cell density for microscopy experiments is kept rather low so that cells are well individualized for imaging. Hence, it is worth mentioning that more cells may be used as compared to microscopy experiments so that sufficient biological material is available. Typically, those ratios/formats may be used:

1. 10 cm dish: 1,000,000 Huh7 cells. Infection in 5 ml
2. 6-well plate: 200,000 Huh7 cells. Infection in 1 ml
3. 12-well plate: 100,000 Huh7 cells. Infection in 500 µl
4. 24-well plate: 50,000 Huh7 cells. Infection in 250-300 µl
5. 96-well plate: 10,000 Huh7 cells. Infection in 50 µl

When performing functional assays such as evaluating the impact of a drug or host gene expression modulation on ZIKV titers, a low MOI (typically between 0.01 and 0.1 for Huh7 cells) should be selected. Indeed, some phenotypes may be masked by the fact that titers are saturated over 10^6 PFU/ml if a high MOI is used. Using low MOI ensures that virus replication is in its logarithmic dynamic window when samples are collected.

Finally, any cell line or primary cells may theoretically be permissive to ZIKV infection. To test this, we typically perform replication kinetics experiments in which we infect cells with ZIKV at an MOI of 1. Cell supernatants are collected and filtered 1, 2, 3 and 4 days post-infection similarly to ZIKV stock harvest. Putative supernatant-associated infectivity is then assessed using plaques assays. The % of infection may be determined using the protocol described in this manuscript. Of note, it should be always kept in mind that the infectious titers determined using plaque assays are relative to Vero E6 cells permissiveness to ZIKV. For many possible reasons that are intrinsic to a given tested cell line (*e.g.*, virus receptor availability/expression, high induction of antiviral responses…) and/or virus strain, the infection rate may be low even with an MOI of 1. To circumvent this limitation, the MOI may be increased up to 10-50 and the infection procedure optimized (*e.g.*, time of infection, presence of serum in the inoculum…) in future experiment to eventually reach values close to 100%.

Recipes

1. Complete DMEM
   500 ml DMEM
   50 ml FBS Performance
   5 ml penicillin/streptomycin
   5 ml non essential amino acids solution
   Store at 4 °C
2. Plaquing medium (MEM-CMC)
   a. Put 7.5 g CMC in an autoclavable glass bottle which contains a magnetic bar
   b. Autoclave the bottle to sterilize the powder and stirrer (121 °C, 30 min, 20 bars; drying for

25 min)

c. Add into the bottle 500 ml MEM within the sterile environment of a cell culture cabinet. Close the bottle without touching the bottlenecks with the hands. Mix by inversion. Keep at 4 °C the original MEM bottle for further use (see below)
d. Incubate the MEM/CMC bottle at 4 °C above a magnetic stirring plate until complete solubilization of CMC. This generally takes between two and three days.
e. Transfer the reconstituted medium from the glass bottle into the original MEM plastic bottle inside the sterile environment of a cell culture cabinet. This will avoid introducing into the BSL2 area any glass-made material
f. Store at 4 °C. The final concentration of CMC is 1.5%

3. Formaldehyde fixative
   270 ml distilled water
   100 ml 37% formaldehyde (10% final concentration)
   Store at room temperature
4. Paraformaldehyde fixative
   1 L 1x PBS
   40 g paraformaldehyde (4% final concentration)
   Facilitate dissolving the paraformaldehyde by heating (~60-70 °C) the preparation inside a chemical hood for ~30 min
   Prepare 12 ml aliquots in 15 ml tubes and store at -20 °C
5. Crystal violet staining solution
   5 g crystal violet
   Dissolve in 52.6 ml of 95% ethanol
   Add 445 ml of double-distilled water
   Final concentrations of crystal violet and ethanol are 1% and 10%, respectively
   Store at room temperature
6. Triton X-100 permeabilization solution
   500 ml PBS
   1 ml Triton X-100 (final concentration 0.2%)
   Store at room temperature
7. BSA Blocking solution
   a. Dissolve 10 g BSA in 200 ml PBS (5% [w/v] final concentration)
   b. Add 1 ml 10% (w/v) sodium azide solution (NaN_3; final concentration: 0.05%)
   c. Store at 4 °C

   Notes:

   a. OPTIONAL: The solution can be sterilized by filtration in order to avoid contamination and to maintain the quality of the solution over several months.
   b. The day of immunofluorescence staining, supplement the solution with normal goat serum to a final concentration of 10% (v/v).

Acknowledgments

LCC is receiving a research scholar (Junior 2) salary support from Fonds de la Recherche du Québec-Santé (FRQS). LCC's research is supported by grants from Natural Sciences and Engineering Research Council of Canada (NSERC; RGPIN-2016-05584), the Canadian Institutes of Health Research (CIHR; PJT153020; ICS154142), Fonds de la Recherche du Québec-Nature et Technologies (FRQNT; 2018-NC-205593), Armand-Frappier Foundation and Institut National de la Recherche Scientifique. This protocol is mostly adapted from the experimental procedures used in our previous work (Chatel-Chaix *et al.*, 2016) in which we have optimized the production and detection of ZIKV. We thank the European Virus Archive goes Global (EVAg) and Dr. Xavier de Lamballerie (Emergence des Pathologies Virales, Aix-Marseille University) for providing ZIKV MR766 and H/PF/2013 original stocks. We are grateful to Drs Patrick Labonté (Institut National de la Recherche Scientifique), Tom Hobman (University of Alberta) and Anil Kumar (University of Alberta) for generously providing Huh7 and Vero E6 cells.

Competing interests

The authors declare that they do not have any conflicts of interests or competing interests.

References

1. Chatel-Chaix, L., Cortese, M., Romero-Brey, I., Bender, S., Neufeldt, C. J., Fischl, W., Scaturro, P., Schieber, N., Schwab, Y., Fischer, B., Ruggieri, A. and Bartenschlager, R. (2016). Dengue virus perturbs mitochondrial morphodynamics to dampen innate immune responses. *Cell Host Microbe* 20(3): 342-356.
2. Cortese, M., Goellner, S., Acosta, E. G., Neufeldt, C. J., Oleksiuk, O., Lampe, M., Haselmann, U., Funaya, C., Schieber, N., Ronchi, P., Schorb, M., Pruunsild, P., Schwab, Y., Chatel-Chaix, L., Ruggieri, A. and Bartenschlager, R. (2017). Ultrastructural characterization of Zika virus replication factories. *Cell Rep* 18(9): 2113-2123.
3. Cugola, F. R., Fernandes, I. R., Russo, F. B., Freitas, B. C., Dias, J. L., Guimaraes, K. P., Benazzato, C., Almeida, N., Pignatari, G. C., Romero, S., Polonio, C. M., Cunha, I., Freitas, C. L., Brandao, W. N., Rossato, C., Andrade, D. G., Faria Dde, P., Garcez, A. T., Buchpigel, C. A., Braconi, C. T., Mendes, E., Sall, A. A., Zanotto, P. M., Peron, J. P., Muotri, A. R. and Beltrao-Braga, P. C. (2016). The Brazilian Zika virus strain causes birth defects in experimental models. *Nature* 534(7606): 267-271.
4. Grubaugh, N. D., Faria, N. R., Andersen, K. G. and Pybus, O. G. (2018). Genomic insights into Zika virus emergence and spread. *Cell* 172(6): 1160-1162.
5. Haddow, A. D., Schuh, A. J., Yasuda, C. Y., Kasper, M. R., Heang, V., Huy, R., Guzman, H., Tesh, R. B. and Weaver, S. C. (2012). Genetic characterization of Zika virus strains:

geographic expansion of the Asian lineage. *PLoS Negl Trop Dis* 6(2): e1477.

6. Lazear, H. M. and Diamond, M. S. (2016). Zika Virus: new clinical syndromes and its emergence in the Western Hemisphere. *J Virol* 90(10): 4864-4875.
7. Liu, Y., Liu, J., Du, S., Shan, C., Nie, K., Zhang, R., Li, X. F., Zhang, R., Wang, T., Qin, C. F., Wang, P., Shi, P. Y. and Cheng, G. (2017). Evolutionary enhancement of Zika virus infectivity in *Aedes aegypti* mosquitoes. *Nature* 545(7655): 482-486.
8. Morrison, T. E. and Diamond, M. S. (2017). Animal models of Zika virus infection, pathogenesis, and immunity. *J Virol* 91(8): e00009-17.
9. Munster, M., Plaszczyca, A., Cortese, M., Neufeldt, C. J., Goellner, S., Long, G. and Bartenschlager, R. (2018). A reverse genetics system for Zika virus based on a simple molecular cloning strategy. *Viruses* 10(7): E368.
10. Mutso, M., Saul, S., Rausalu, K., Susova, O., Zusinaite, E., Mahalingam, S. and Merits, A. (2017). Reverse genetic system, genetically stable reporter viruses and packaged subgenomic replicon based on a Brazilian Zika virus isolate. *J Gen Virol* 98(11): 2712-2724.
11. Neufeldt, C. J., Cortese, M., Acosta, E. G. and Bartenschlager, R. (2018). Rewiring cellular networks by members of the *Flaviviridae* family. *Nat Rev Microbiol* 16(3): 125-142.
12. Schwarz, M. C., Sourisseau, M., Espino, M. M., Gray, E. S., Chambers, M. T., Tortorella, D. and Evans, M. J. (2016). Rescue of the 1947 Zika virus prototype strain with a cytomegalovirus promoter-driven cDNA clone. *mSphere* 1(5): e00246-16.
13. Shan, C., Xie, X., Muruato, A. E., Rossi, S. L., Roundy, C. M., Azar, S. R., Yang, Y., Tesh, R. B., Bourne, N., Barrett, A. D., Vasilakis, N., Weaver, S. C. and Shi, P. Y. (2016). An infectious cDNA clone of Zika virus to study viral virulence, mosquito transmission, and antiviral inhibitors. *Cell Host Microbe* 19(6): 891-900.
14. Welsch, S., Miller, S., Romero-Brey, I., Merz, A., Bleck, C. K., Walther, P., Fuller, S. D., Antony, C., Krijnse-Locker, J. and Bartenschlager, R. (2009). Composition and three-dimensional architecture of the dengue virus replication and assembly sites. *Cell Host Microbe* 5(4): 365-375.
15. World Health Organization. *Fact sheets-Zika virus*. 2018; Available from: http://www.who.int/news-room/fact-sheets/detail/zika-virus.
16. Xie, X., Zou, J., Shan, C., Yang, Y., Kum, D. B., Dallmeier, K., Neyts, J. and Shi, P. Y. (2016). Zika virus replicons for drug discovery. *EBioMedicine* 12: 156-160.
17. Yuan, L., Huang, X. Y., Liu, Z. Y., Zhang, F., Zhu, X. L., Yu, J. Y., Ji, X., Xu, Y. P., Li, G., Li, C., Wang, H. J., Deng, Y. Q., Wu, M., Cheng, M. L., Ye, Q., Xie, D. Y., Li, X. F., Wang, X., Shi, W., Hu, B., Shi, P. Y., Xu, Z. and Qin, C. F. (2017). A single mutation in the prM protein of Zika virus contributes to fetal microcephaly. *Science* 358(6365): 933-936.

